# *Carbonate facies, sequences and associated diagenesis, upper cretaceous, tremp basin, Spanish pyrenees*

Jonathan Paul Booler

# Carbonate Facies, Sequences and Associated Diagenesis, Upper Cretaceous, Tremp Basin, Spanish Pyrenees.

**Jonathan Paul Booler, B.A. Oxon.**

A thesis submitted to the University of Durham for the degree of Doctor of Philosophy



Department of Geological Sciences

October, 1994.

## Declaration

The contents of this thesis is the original work of the author and has not previously been submitted for a degree at this or any other university. The work of other people is acknowledged by reference.

Jonathan Paul Booler, B.A. Oxon.
Department of Geological Sciences,
University of Durham.

## Copyright

# Carbonate Facies, Sequences and Associated Diagenesis, Upper Cretaceous, Tremp basin, Spanish Pyrenees.

Jonathan Paul Booler,
PhD thesis, University of Durham, 1994.

This thesis details the results of an integrated study of carbonate platform sedimentology, geometry, evolution and diagenesis within a sequence stratigraphic framework. This study has been based on the Upper Cretaceous carbonates within the Tremp basin of the Spanish Pyrenees, which, through the effects of minor tectonic deformation during the later parts of the Pyrenean orogeny, are exceptionally well exposed and can be studied in the form of a platform to basin cross-section upon a scale that is comparable to that of a seismic section.

This study concentrates on the mid-Turonian to Coniacian-aged Congost platform and its associated basinal succession, whose sedimentology and geometrical features, in particular cyclic progradational cycles, and evidence of repeated flooding and exposure of the platform-top are interpreted in terms of fluctuations in relative sea-level and associated variations in available accommodation space. These interpretations, together with evidence of subaerial exposure in the form of karst features, intensive dissolution and the presence of speleo-cements, are used to propose a dynamic 'forced regression' model for the evolution of the Congost platform, which involves two phases of platform development, separated by a period of forced regression. The primary and secondary porosity afforded by the abundant bi-mineralic rudists within the platform-top sediments allows for a detailed and comprehensive diagenetic study of these carbonates, in the form of a case study for a number of interesting diagenetic features. In addition to standard petrography, cathodoluminescence and stable isotope studies have been employed and have allowed the identification of such features as botryoidal calcitic marine cements, neomorphism which occurred in lagoonal waters and speleo-cements. This study also provides a detailed investigation of the diagenesis associated with subaerial exposure and the development of sequence boundaries. Differences in the early diagenesis of these carbonates from different parts of the Congost platform suggest that two separate phases of platform development experienced: 1) differing pore-fluid regimes; 2) differing frequencies and duration of subaerial exposure events; and 3) different magnitudes of relative sea-level fall. These features are considered in terms of variations in accommodation space during platform development and are used to develop the dynamic 'forced regression' model for the evolution of the Congost platform.

A succession of Cenomanian to Santonian-aged basinal and slope sediments which can be correlated with the contemporaneous Santa Fe, Congost and Sant Corneli platforms and contain a large amount of allochthonous debris, much of which is derived from underlying units, are described and interpreted in terms of local tectonic activity and relative sea-level change.

The final part of this thesis presents a new sequence stratigraphic model for the mid-Turonian to Coniacian-aged Congost platform which is compatible with the observations and conclusions of this study. This new sequence stratigraphic model suggests that the Congost platform developed within two separate depositional sequences, albeit with one being on a much larger scale than the other. Sequence boundaries are characterised by subaerial exposure on the platform top which can be correlated with hardgrounds and/or glauconite accumulations within the more basinal locations, overlain by deeper-water facies. The presence of submarine onlap surfaces and down-slope slide deposits immediately above the sequence boundaries suggests that the major transgressive events which followed sequence boundary development were brought about by local extensional tectonic activity, while the stratigraphic cyclicity within the sequences and major falls in sea-level which produced the sequence boundaries are interpreted to have resulted largely from eustatic processes.

## Acknowledgements.

- Firstly I must thank my parents, who through their support and encouragement have made my passage through higher education a much easier one.

- Maurice Tucker is thanked for his help and advice during the last three years.

- Toni Simo contributed greatly to the field work part of this project. He is thanked for introducing me to the Upper Cretaceous of the Tremp basin and for his helpful advice and discussion both in and out of the field.

- Helen Vincent is thanked for keeping me company in Durham, providing me with rent free accommodation and for her patience in the field whilst I studied the rocks.

- Both Peter Drzewiecki and Debora Rodrigues-de-Miranda are thanked for their company and numerous discussions during the summer months in La Pobla.

- Esmeralda Caus is thanked for her time spent identifying small creatures within my samples.

- I am most grateful to all the technical staff at the Department of Geology in Durham, all of whom have helped me during the last three years. Julie Harrison, George Randall and Ron Lambert deserve a special mention for their time and effort spent cutting and polishing the 100's of large thin sections, which were essential to this project.

- Hilary Sloane, Melanie Leng, Baruch Spiro, Carolyn Chenery and Pete Greenwood (NIGL, Keyworth) are all thanked for their time spent helping with the stable isotope analyses.

- Lastly, I must thank all other staff and students of the Department of Geology in Durham, who have made my time in Durham an enjoyable one.

**Thanks!**

# Contents

## References

# Chapter 1
# Introduction and thesis outline

## 1.1 Introduction

Carbonate platforms and their diagenesis have been a major topic of research for many years. In the past, studies of carbonate platforms were based on facies associations and depositional profiles which were compared with present day platforms (eg. Wilson, 1975; Bathurst, 1975; Sellwood, 1978, amongst others), while their diagenesis was explored in the form of case histories (reviewed in: Moore, 1989; McIlreath & Morrow 1990; Tucker & Bathurst 1990; Tucker & Wright 1990 & Tucker 1991). With the development of sequence stratigraphy in the last decade (eg. Vail et al., 1977; Haq et al., 1987; 1988; Van-Wagoner et al., 1990 etc) and more recently its applications to carbonate depositonal systems (eg. Sarg, 1988; Calvet et al., 1990; Schlager, 1991; 1992; 1993; 1994; Hunt & Tucker, 1993 & Tucker et al., 1993) it has been possible to interpret the geometry and evolution of carbonate platforms in terms of their response to fluctuations in relative sea-level.

As sequence stratigraphy has become an increasingly widespread tool for basin analysis within the hydrocarbon industry, understanding the relationship between carbonate diagenesis and relative sea-level variations is clearly important, because of the possibilities it provides for porosity prediction, which is a major factor in reservoir potential. Diagenetic patterns associated with the sequence stratigraphic development of carbonate platforms have been explored recently by Tucker (1993).

Moderate structural deformation within the Tremp basin has caused the Upper Cretaceous carbonates to be so well exposed that they can be studied in the form of a platform to basin cross-section upon a scale that is comparible to that of a seismic section. Such excellent exposure means that the Upper Cretaceous carbonates of the Tremp basin provide an ideal opportunity for an integrated study of carbonate platform sedimentology, geometry, evolution and diagenesis within a sequence stratigraphic framework.

This thesis details the results of such an integrated case study, and concentrates in particular upon the mid-Turonian to mid-Coniacian-aged Congost platform.

The main aims of this thesis are: 1) to describe the geological context of the Congost platform; 2) to describe the microfacies and interpret the depositonal environment and evolution of the Congost platform; 3) to document the early diagenesis of the Congost platform, especially that related to the sequence boundaries; 4) to describe the slope and basinal facies of the Congost, Santa Fe, and Sant Corneli

platforms and interpret their origin in terms of local tectonics and relative sea-level changes; and 5) to present a sequence stratigraphic model for the Congost platform.

## 1.2 Thesis outline

### 1.2.1 Chapter 2

This chapter introduces the regional geology of the study area. Firstly the structural evolution of the Pyrenean chain is reviewed, and this is followed by a more detailed description of the structural geology of the southern Pyrenees and the Tremp basin. Next the stratigraphy is introduced; firstly on a regional scale with a description of the Mesozoic and Tertiary tectono-sedimentary cycles which can be recognised across the Pyrenees; and then on a more local scale with a description of the Mesozoic stratigraphy and palaeogeography of the Tremp basin.

### 1.2.2 Chapter 3

Here the Cenomanian to mid-Turonian carbonates of the Tremp basin, comprising the the Santa Fe and Pardina Limestones, are described and discussed in terms of their sedimentology, facies patterns, geometry and evolution. Correlation between the inner platform areas and the more basinal locations has been made possible by the detailed biostratigraphic and geochemical work of Soriano (1992) and Caus et al. (1993). This has allowed the construction of a detailed platform to basin cross section through the Santa Fe and Pardina Limestones which serves to set the scene for the detailed study, in the following chapters, of the overlying mid-Turonian to Coniacian-aged Congost platform.

### 1.2.3 Chapter 4

In this chapter the mid-Turonian to Coniacian-aged carbonates of the Congost platform and associated basinal succession are described and discussed in terms of sedimentology, facies patterns and geometry. Sedimentological and geometrical features are interpreted in terms of fluctuations in relative sea-level and associated variations in available accommodation space. These interpretations are considered together with evidence of subaerial exposure to propose a dynamic model for the evolution of the Congost platform.

### 1.2.4 Chapter 5

This chapter, after introducing carbonate diagenesis and the use of stable isotopes in such studies, describes and discusses the diagenesis of the Congost platform-top sediments. A succession of diagenetic events which have effected the Congost platform-top is presented on the basis of field observations, standard petrography, cathodoluminescence studies and stable isotope analyses. In addition to providing a case study for a number of interesting diagenetic features, including those associated with subaerial exposure and sequence boundary development, differences in the early diagenesis of these carbonates from different parts of the platform are considered in terms of variations in accommodation space change during platform development and are used to develop the dynamic model for the evolution of the Congost platform which was presented in chapter 4.

### 1.2.5 Chapter 6

In this chapter a complete stratigraphic section through over 1200 metres of the Cenomanian to Santonian-aged basinal and slope facies sediments of the Tremp basin are described and interpreted. These sediments can be correlated with contemporaneous carbonate platforms and contain a large amount of allochthonous debris in the form of megabreccia sheets and conglomeratic deposits. The sedimentology, depositonal geometry and inter-unit relationships within this succession are interpreted in terms of tectonic activity and relative sea-level variations.

### 1.2.6 Chapter 7

This chapter utilises the information that has been provided in earlier chapters to build upon the sequence stratigraphic framework which was proposed for the mid-Turonian to Coniacian-aged Congost platform as part of a broader sequence stratigraphic framework established for the entire Upper Cretaceous of the Tremp basin by Simo (1986; 1989 & 1992). A new sequence stratigraphic model is presented for the Congost platform which is compatible with the observations, interpretations and conclusions that are provided within the earlier chapters of this thesis.

### 1.2.7 Chapter 8

This chapter outlines the main conclusions presented within this thesis.

# Chapter 2
# Regional setting

## 2.1 Introduction

The study area is the Tremp basin which lies within the Montsec thrust sheet (Williams, 1985) of the south-central Pyrenees Upper Thrust Sheet unit (Munoz, 1985)(see Figs. 2.1 & 2.2). Geographically the sediments of the Tremp basin outcrop within an area approximately 40km wide which runs parallel to, and is bounded to the south by, the mountains of the Sierra del Montsec (between approximately 42.00°N and 42.20°N latitude). The western boundary of this area roughly corresponds to the path of the River Esera, while the River Segre runs along its eastern margin (between approximately 0.20°E and 1.20°E longitude). Figure 2.1 shows a simplified structural map of the Pyrenees upon which the location of the Tremp basin has been marked (modified from ECORS Pyrenees team, 1988), together with a geological map of the study area (modified from Institut Cartographic de Catalunya, 1990).

As can be seen from the geological map in Fig. 2.1 the Upper Cretaceous sediments are well exposed in the south, east and north, but are covered in the central and western parts of the study area by Tertiary sediments. This chapter introduces the structural geology and Mesozoic stratigraphy of this area of the south-central Pyrenees.

## 2.2 Structural evolution

The Pyrenees are an Alpine-aged chain of mountains which extend for approximately 1000km from the Cantabrians in northwest Spain to the Mediteranean Sea in the east and were created as a result of a multi-phase orogenic episode which has been reviewed by Banda and Wickham (1986).

The earliest phase of the Pyrenean orogeny is believed to have begun towards the end of the Lower Cretaceous when the extensional tectonic regime of the Lower Cretaceous became one of sinistral strike slip movement as a result of an anticlockwise rotation of Iberia with respect to the European plate (Fischer, 1984; Le Pichon et al., 1970; Masson & Miles, 1984). This period of sinistral-wrenching is interpreted to have been followed by a further extensional episode during the mid-Cenomanian to mid-Santonian prior to the final northwest-southeast orientated

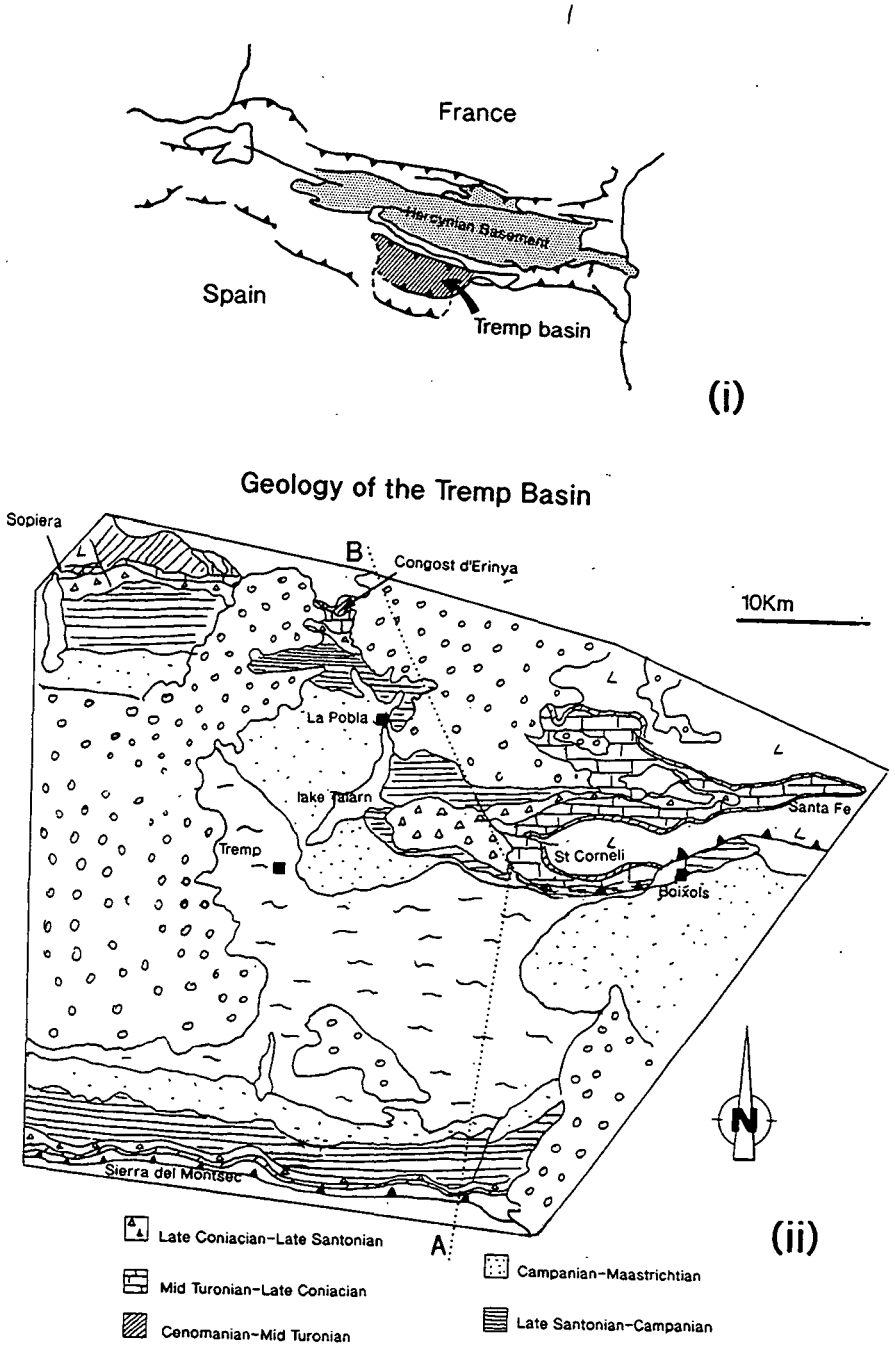


**Fig. 2.1.** Simplified structural map of the Pyrenean belt, showing the location of the Tremp basin (i), together with a geological map of the study area (ii).

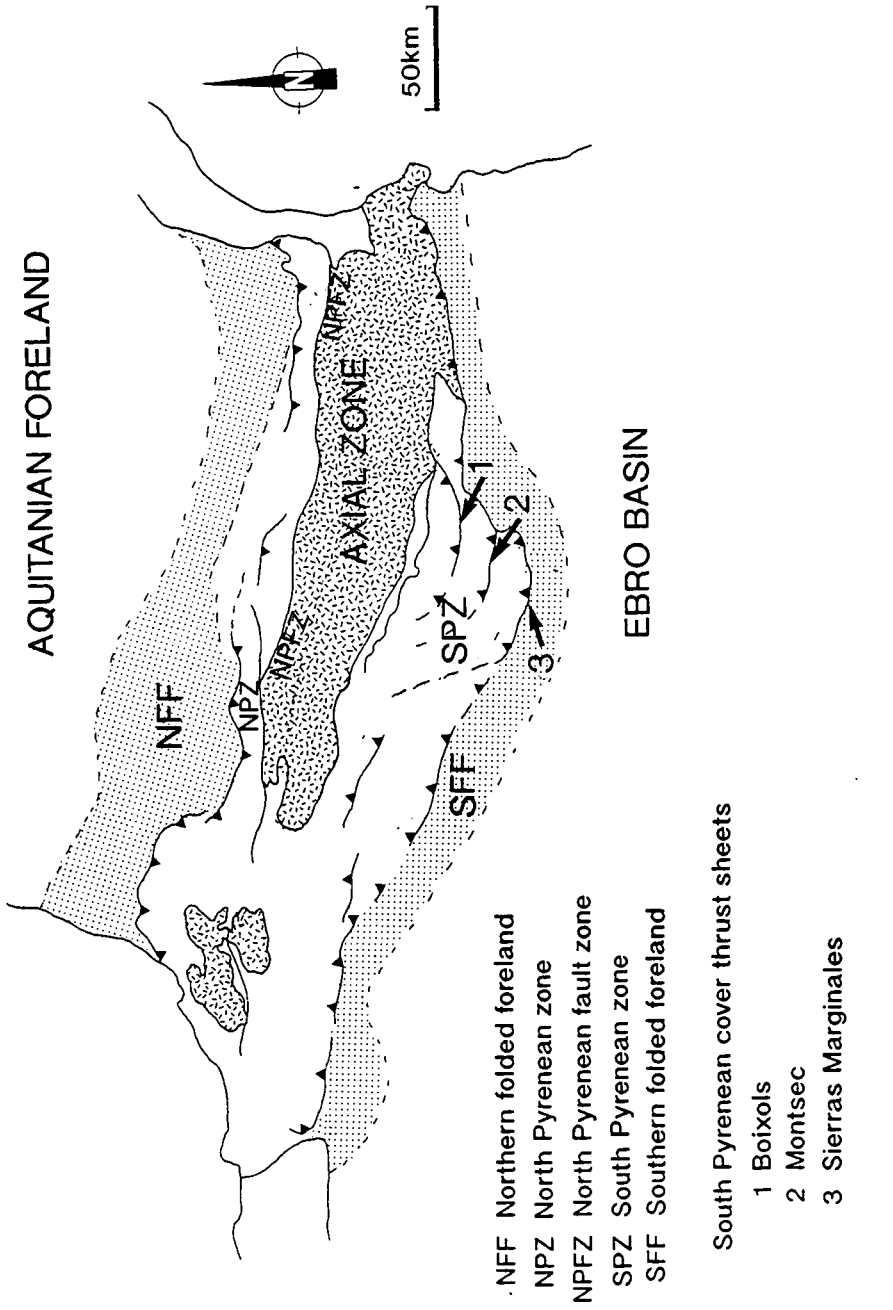


**Fig. 2.2.** Main structural units of the Pyrenean belt, showing the location of the south Pyrenean cover thrust sheets. Adapted from Puigdefabregas & Souquet (1986), and Farrel et al. (1987).

contractional episode of the Late Santonian and Cenozoic when the Iberian plate was displaced northwestward and impacted against the European plate (Grimaud et al., 1982). The Cenozoic contractional episode is interpreted to have resulted in the compressional thrust tectonics which produced the elevated Pyrenean mountain belt and triggered the development of foreland basins in the front of both northward and southward advancing thrust sheets (see below together with Figs. 2.1, 2.2 & 2.3). Field evidence for these phases of tectonic activity together with their relationship to sedimentary cycles have been documented by Souquet (1984) and Puigdefabregas & Souquet (1986)(see section 2.3 together with Fig. 2.5).

Structurally the Pyrenees can be divided into a series of zones, which are symmetrical about a central Axial Zone composed of Palaeozoic and possibly Precambrian rocks (see Fig. 2.2)(Mattauer, 1968; Choukroune & Seguret, 1973). In the northern part of the Pyrenean belt, the Aquitanian molassic foreland has been overthrust from the south by the post-Hercynian rocks of the North Pyrenean Zone and Northern Folded Foreland which are typified by north-verging asymmetric folds (Choukroune, 1969). The North Pyrenean zone is bounded to the south by the vertically faulted North Pyrenean Fault Zone which runs east-west along the Pyrenean belt, and locally contains highly strained Mesozoic metamorphic rocks and slices of mantle material (Choukroune, 1976a; 1976b). On the southern side of the Palaeozoic Axial Zone, the South Pyrenean Zone and Southern Folded Foreland have undergone south-directed thrusting over the Ebro molassic basin. The study area is located in the central part of the south Pyrenean zone (see Figs. 2.1 & 2.2)

The general fan-like geometry of the Pyrenean belt, with northward thrusting in the north and southward thrusting in the south, ~~which was~~ produced during Tertiary compression (see Figs. 2.1, 2.2 & 2.3), has been interpreted in a variety of ways (eg. Mattauer, 1968; Choukroune & Seguret, 1973; Choukroune, 1976b; Boillot & Lapdevila, 1977; Daignieres et al., 1982; Williams & Fischer, 1984; Deramond et al., 1985; Seguret & Daignieres, 1986). Many interpretations have emphasised the importance of the North Pyrenean Fault Zone as the central feature of the fan shaped structural geometry, which is generally believed to represent the locus of mid-Cretaceous crustal thinning and sinistral strike-slip motion between the Iberian and European plates. The geometry of the North Pyrenean Fault Zone and its relationship to the surrounding thrust faults at depth has been a subject of controversy. However, the ECORS seismic profile, which covers a roughly north-south orientated transect across the central Pyrenees and was completed in 1988, supports a thin-skinned thrusting model in which the North Pyrenean Fault Zone is truncated by both northward and southward moving thrusts (see Fig. 2.3)(Williams & Fischer, 1984; ECORS Pyrenees team, 1988; McCaig, 1988).

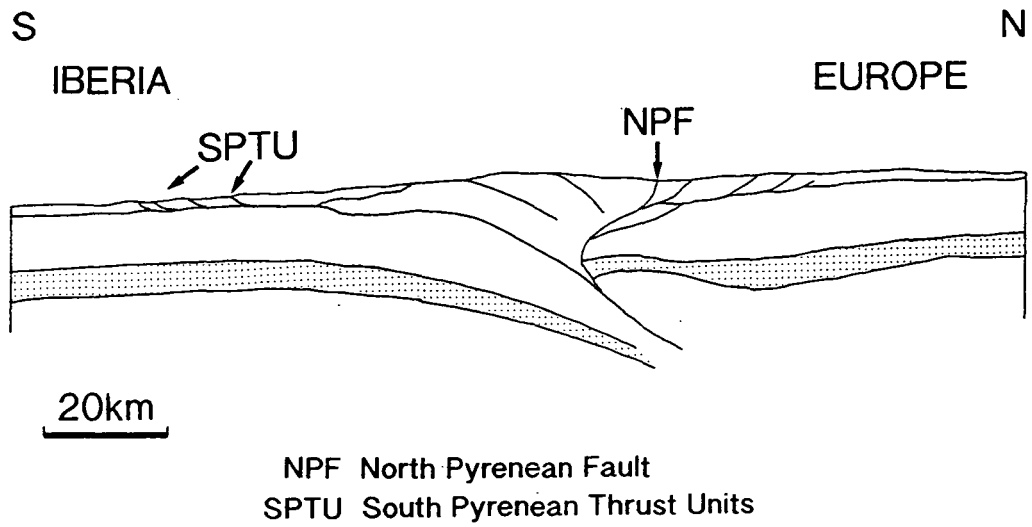


**Fig. 2.3.** Cross-section through the Pyrenees, showing a possible geometrical solution which is consistent with the ECORS data: the NPF is considered to be a Lower Cretaceous transform fault which was active during the earlier stages of the evolution of the chain, and deformed later during the orogeny. Modified from ECORS Pyrenean team (1988).

The allochthonous thrust units within the South Pyrenean Zone contain Mesozoic and Tertiary strata which became detached from their basement and moved upon a décollement zone of Upper Triassic evaporites (Sole-Sugranes, 1978)(see Fig. 2.4). These thrust units which developed through a sequence of piggy-back style thrusting events between the Late Cretaceous and Miocene are, from north to south (earliest to latest emplaced), Boixols, Montsec and Sierras Marginales (see Figs. 2.2 & 2.4)(Farrel et al., 1987; Verges & Munoz, 1990).

Figure 2.4 shows a north-south cross-section through part of the South Pyrenean zone (adapted from Soriano, 1992 after Hispanoil, 1985). The path of this cross-section corresponds approximately to the central part of the field area for this study (see Fig. 2.1) and includes the Upper Cretaceous stratigraphy of the Tremp basin which is incorporated within the Montsec and Boixols thrust sheets.

The Boixols thrust unit incorporates over 4000 metres of Mesozoic stratigraphy and possesses a well developed hanging wall anticline (the Sant Corneli anticline) which has created a topographic high and provides a superb exposure of the

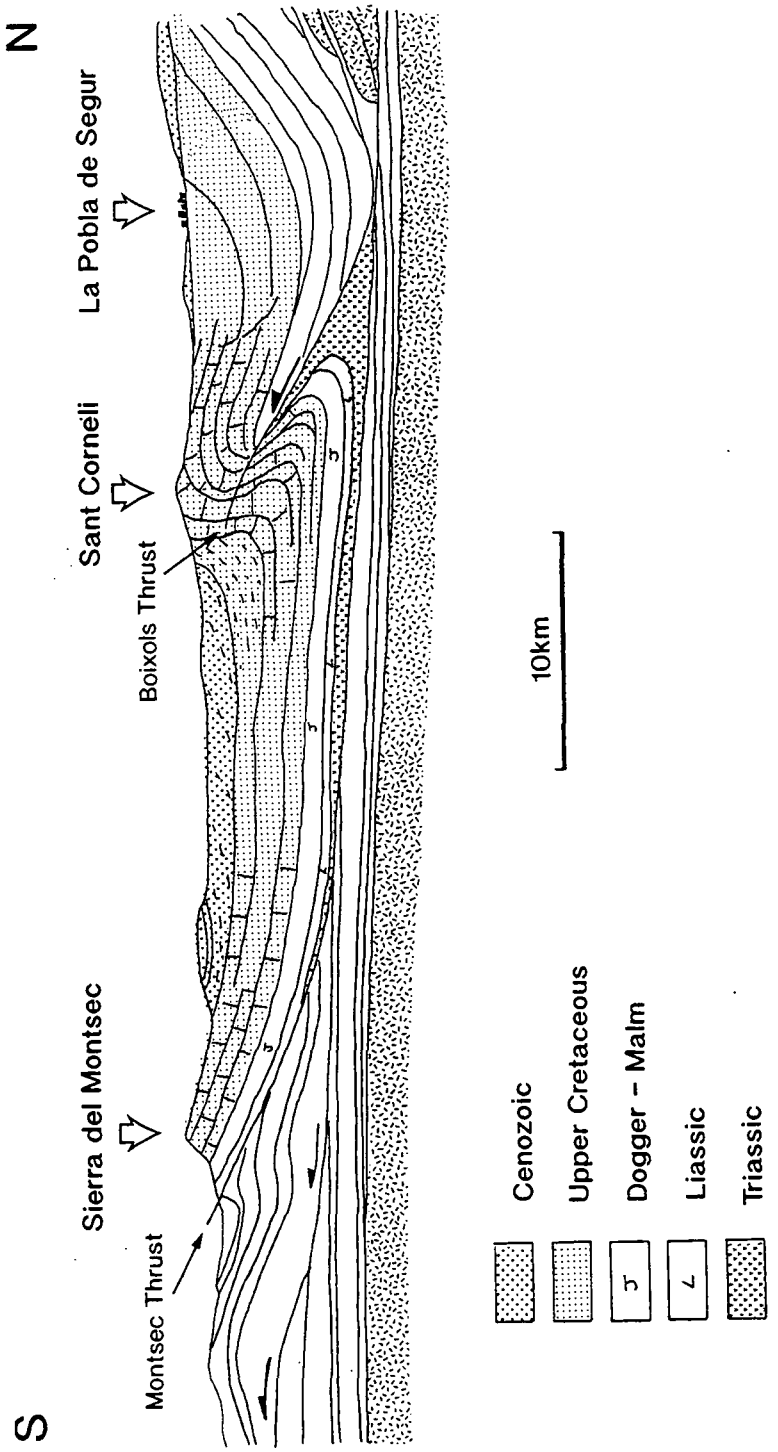


**Fig. 2.4.** Cross-section through the central part of the study area (locus shown in Fig. 2.1(ii)). The Boixols and Montsec thrust sheets moved along Triassic evaporites. Modified from Soriano (1992), after Hispanoil Exploracion (1985).

Upper Cretaceous succession (see sections 3.3 & 4.2 together with Figs. 2.1, 2.4 & 4.6). Movement along the Boixols thrust began during the Upper Campanian, as evidenced by thickness variations and facies changes within Upper Campanian and Maastrichtian sediments which onlap the southern limb of the Sant Corneli anticline (Simo, 1986).

The Montsec thrust unit incorporates over 6000 metres of Mesozoic and Cenozoic stratigraphy and was emplaced during the lower Eocene (Ypresian)(Williams & Fischer, 1984; Farrel et al., 1987). The Montsec thrust has created a topographic high in the form of the Sierra del Montsec, which is an east west trending chain of mountains with topographic heights in the order of 1400 to 1700 metres (a.s.l.) and steep south-facing slopes in which complete stratigraphic sections through the upthrown Jurassic and Cretaceous strata are exposed (see section 3.2atogether with Figs. 2.1, 2.2, 2.4 & 3.2b).

## 2.3 Mesozoic and Tertiary tectono-sedimentary cycles

Tectonic activity during the Mesozoic and Tertiary which was due to sea-floor spreading in the Ligurian Tethys, central North Atlantic and the Bay of Biscay, and the anticlockwise rotation of the Iberian plate and its related wrenching in the North Pyrenean fault zone has resulted in tecto-sedimentary discontinuities which can be recognised on regional scale within the Mesozoic and Tertiary stratigraphy of the Pyrenees (Puigdefabregas & Souquet, 1986).

Puigdefabregas and Souquet (1986) have distinguished 10 tectono-sedimentary cycles within the Mesozoic and Tertiary stratigraphy of the Pyrenees which can be loosely grouped together according to the prevailing basin-forming and basin-modifying tectonics at the time of deposition (see Fig. 2.5). Cycles 1 through 4, which include Permian to early Aptian-aged strata, are interpreted to be related to episodic rifting. Cycle 5, which includes middle Albian to early Cenomanian-aged strata is interpreted to be related to a period of sinistral extension during the opening of the north Atlantic and a change in the rotation of Iberia, which led to the final break up between the Iberian and European plates and the development of a deep wrench basin along the North Pyrenean fault zone. During deposition of Cycle 6 which includes middle Cenomanian to middle Santonian-aged strata the prevailing tectonic regime appears to have been one of extension, while, during the deposition of late Santonian to Maastrichtian-aged strata (cycle 7) it became one of progressive oblique convergence as the Iberian plate began to impact into the European plate. Cycles 8, 9 and 10 are interpreted to correspond to the general convergence during

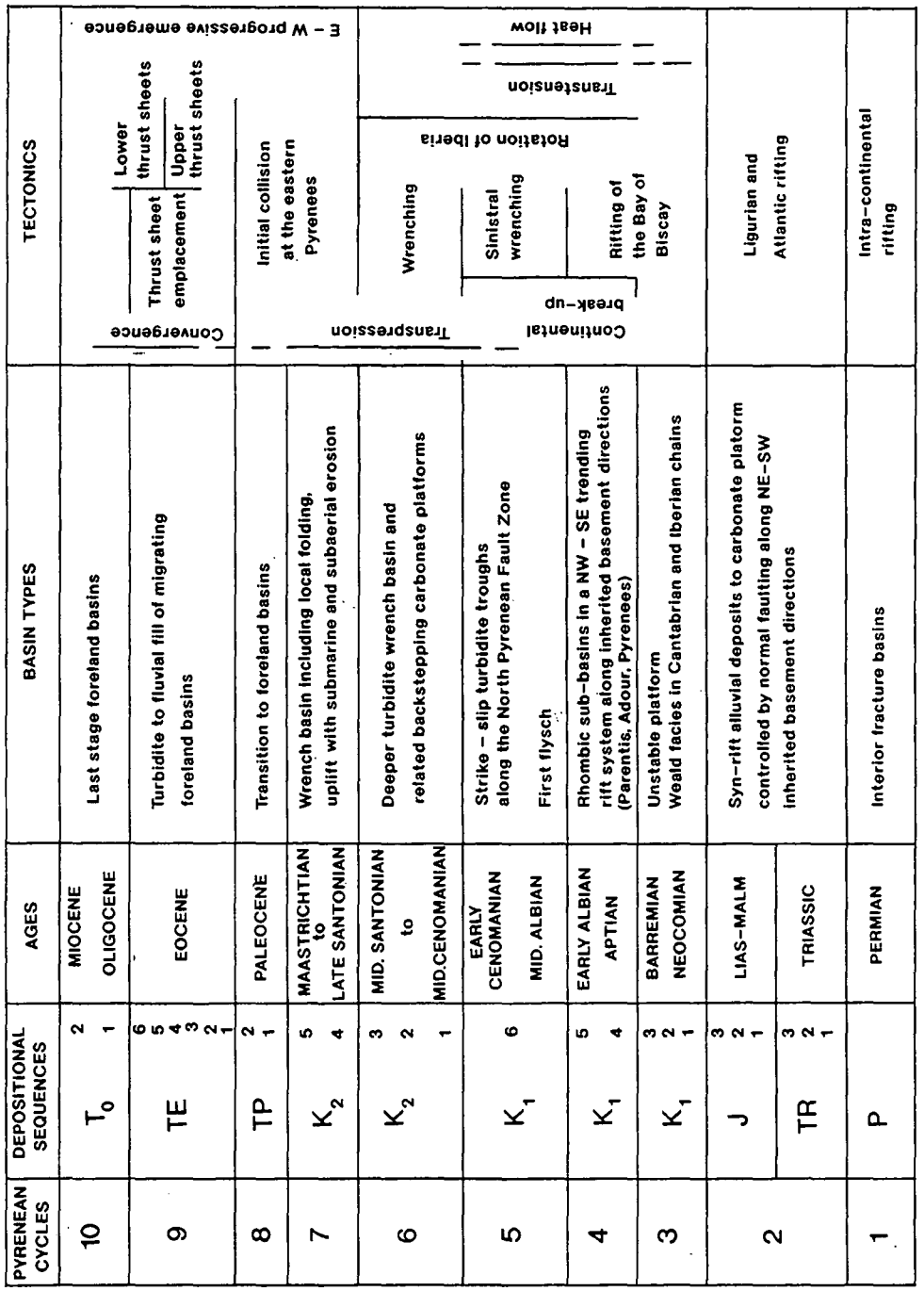


**Fig. 2.5.** Correlation chart of basin cycles and Pyrenean tectono-sedimentary events. From Puigdefabregas & Souquet (1986).

the Palaeocene through to Miocene and record the transition from wrench basin to foreland basin.

Two of the Pyrenean tectono-sedimentary cycle groups of Puigdefabregas and Souquet (1986) can be recognised within the Upper Cretaceous sediments of the south-central Pyrenees. The Cenomanian to Lower Campanian-aged sediments within the south-central Pyrenees consist of a series of 6 carbonate platforms which progressively backstep as a result of them having developed against a tectonic background of basin widening and deepening during the spreading apart of the Iberian and European plates (see Fig. 2.8b). By way of contrast, the Upper Campanian and Maastrichtian-aged sediments within the south-central Pyrenees record a story of regression and siliciclastic infill of the basin which resulted from a switch to compressional tectonics and the continent-continent collision of the Iberian and European plates (Simo, 1989).

## 2.4 Upper Cretaceous palaeogeography and climate

The palaeolatitude of the Tremp basin during the Upper Cretaceous is thought to have been between 30° and 40° north (Owen, 1983). Studies by Simo (1986; 1989) together with that of Caus et al. (1993), have shown the Upper Cretaceous palaeogeography of the Tremp basin to have been one of an expanding and subsiding basin in the north-northwest and a more stable platform in the south (see section 7.2.1). The restored isopach map for the Upper Cretaceous sediments from Simo (1992; his fig. 1) clearly shows their increasing thickness towards the north-northwest (see Fig. 2.6). The expanded nature of the basinal succession towards the north-northwest is also shown in the stratigraphic cross-section, adapted from Simo (1992), which can be seen in Fig. 2.8b.

A study of clay mineral assemblages within the sedimentary fill of the Upper Cretaceous basin in the south-central Pyrenees by Nagtegaal (1972) suggested that the palaeoclimate was sub-tropical to tropical but could have been either arid or humid. A subtropical to temperate palaeoclimate is suggested by the Upper Cretaceous carbonate grain assemblages (Caus et al., 1993). Diagenetic studies, which are described and discussed in this thesis, strongly suggest that the Tremp basin was experiencing humid climatic conditions during the Upper Cretaceous (see sections 5.1.3.2, 5.4.4, 5.5.4, 5.5.5, 5.6.4, 5.6.5 & 6.6.3.3(i)).

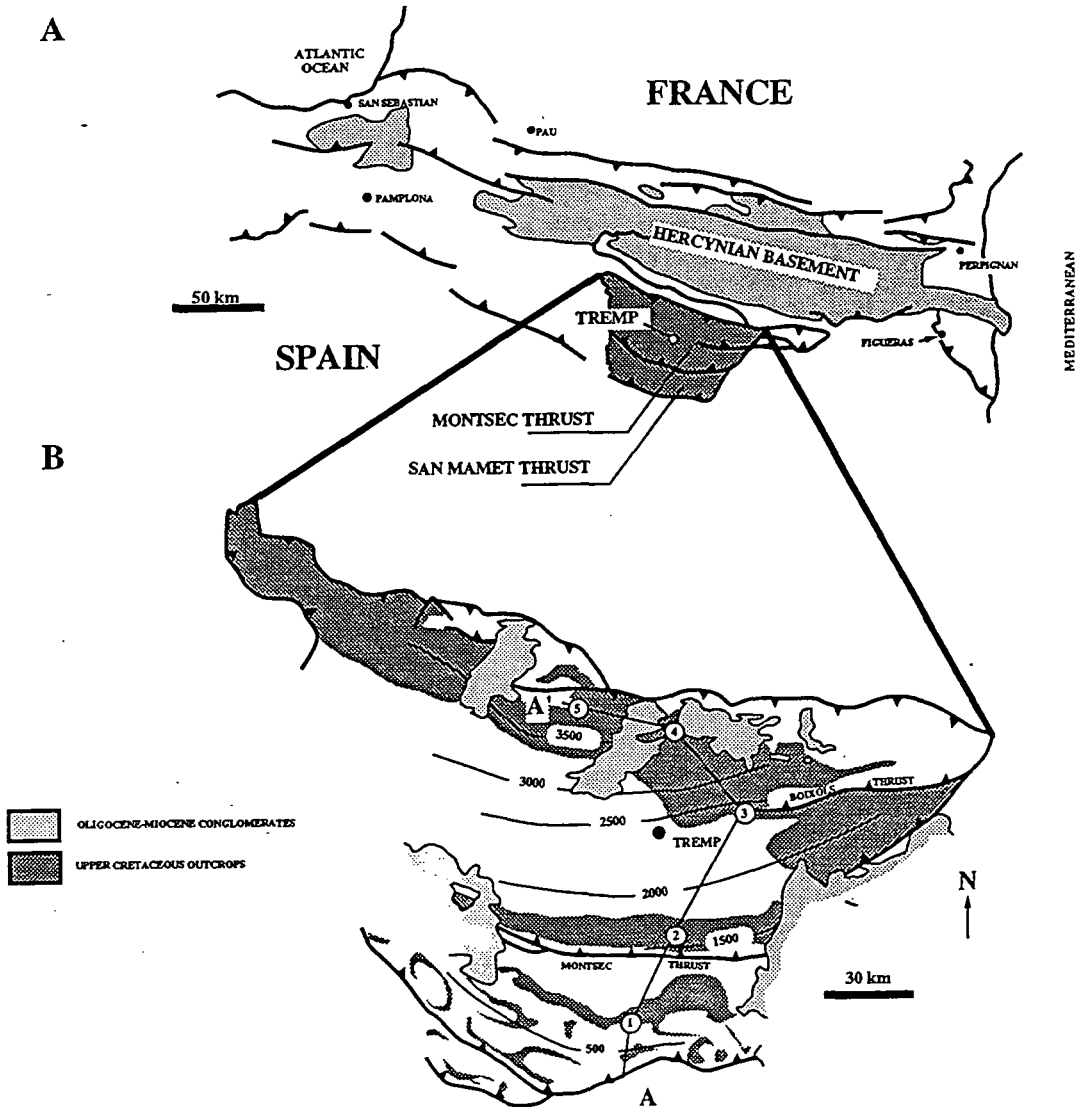


**Fig. 2.6.** A) Structure map of the Pyrenees and location of the south-central Pyrenees. B) Structure map of the south-central Pyrenees, and isopach map of the Upper Cretaceous strata. A - A' is the line of section shown in Fig. 2.8b. From Simo (1992).

## 2.5 Mesozoic stratigraphy

The Mesozoic stratigraphy of the southern Pyrenees was first reported by Rosell (1967), Souquet (1967), Garrido-Mejias & Rios (1972) and Garrido-Mejias (1973). The main lithostratigraphic units of the area were established by Mey et al. (1968) who based their informal lithostratigraphic divisions upon physical characteristics which were recognisable in the field (see Fig. 2.7). Further studies by Van Hoorn (1970), Rosell et al. (1972) and Nagtegaal (1972) provided palaeoenvironmental information, while that of Gallemi et al. (1983) involved a detailed stratigraphic study in the Sant Corneli area which resulted in the further division of the units of Mey et al. (1968)(see Fig. 2.7). Although the study of Gallemi et al. (1983) was very detailed it was based upon a small area of study and so is of limited use for regional correlation. Simo (1986), after a detailed regional mapping project of the Upper Cretaceous in the Tremp basin, devised a lithostratigraphic framework with a depositional sequential character which can be used on a regional basis (see Fig. 2.7).

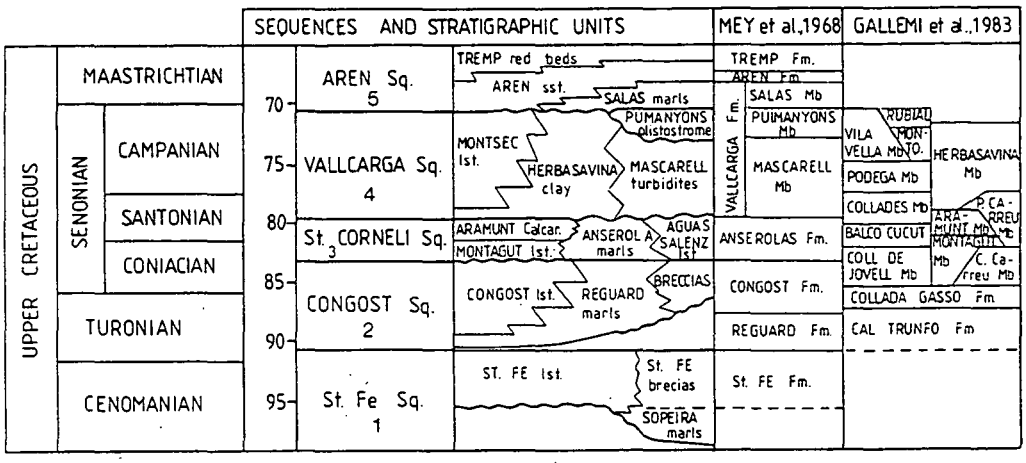


Fig. 2. Upper Cretaceous stratigraphic units and depositional sequences.

**Fig. 2.7.** Upper Cretaceous stratigraphic units and depositional sequences within the Tremp basin of Simo (1986), compared to those of Mey et al. (1968) and Gallemi et al. (1983). From Simo (1986).

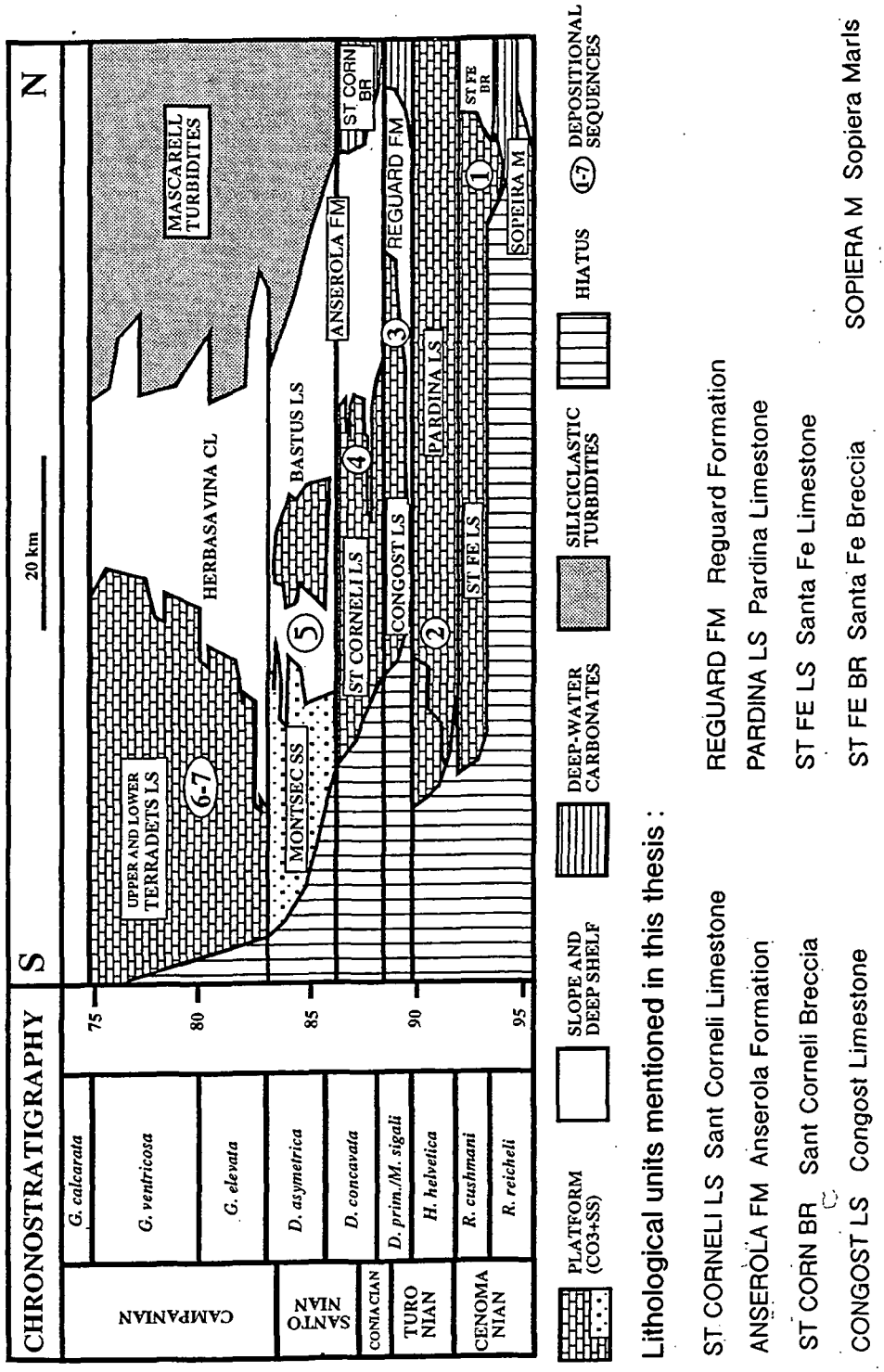


**Fig. 2.8a** Chronostratigraphic framework for the Cenomanian to Campanian-aged strata within the Tremp basin. Modified from Simo (1992).

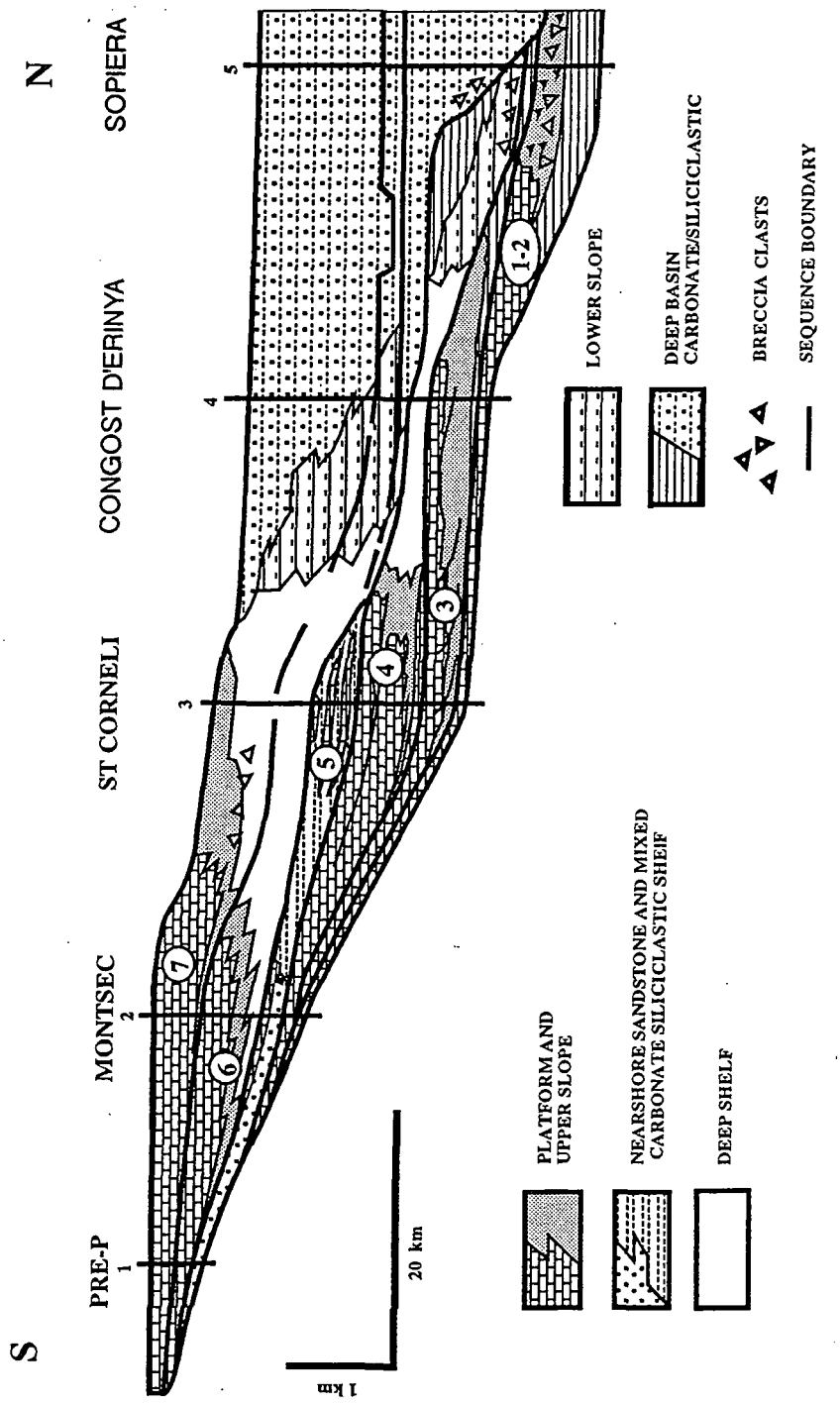
S
N
PRE-P
MONTSEC
ST CORNELI
CONGOST D'ERINYA
SOPIERA
1
2
3
4
5
1-2
1 km
20 km
PLATFORM AND UPPER SLOPE
NEARSHORE SANDSTONE AND MIXED CARBONATE SILICICLASTIC SHELF
DEEP SHELF
LOWER SLOPE
DEEP BASIN CARBONATE/SILICICLASTIC
BRECCIA CLASTS
SEQUENCE BOUNDARY

**Fig. 2.8b.**

**Fig. 2.8b.** Stratigraphic cross-section through the Cenomanian to Campanian-aged strata of the Tremp basin. Showing the sequence stratigraphic framework of Simo (1992). Line of section is shown in Fig. 2.5. Numbers in circles refer to depositional sequences which, within the Cenomanian to mid Santonian-aged strata, correspond to the following carbonate platform, slope and basinal packages: 1) The Santa Fe platform (Cenomanian); 2) the Pardina Limestone (late Cenomanian - mid Turonian); 3) the Congost platform (late Turonian - late Coniacian; 4) the Sant Corneli platform (late Coniacian - mid Santonian). From Simo (1992). See previous page.

Biostratigraphic studies of the Mesozoic stratigraphy in the southern Pyrenees include those of Bilotte and Souquet (1972), Liebau (1973), Fondecave (1975), Bilotte (1978) and Gomez-Garrido (1981). More useful biostratigraphic analyses which either synthesize or publish their own palaeontological data to provide regional correlateable frameworks include those of Hottinger (1966), Martinez (1982), Caus and Cornella (1983), Gomez-Garrido (1987), Caus and Gomez-Garrido (1989a; 1989b) and Gomez-Garrido (1989).

Consideration of the regional biostratigraphic information provided by Martinez (1982) and Gomez-Garrido (1987) in association with the global time scale of Haq et al. (1987), led Simo (1989) to refine further the lithostratigraphic and sequence stratigraphic framework for the Upper Cretaceous of the south central Pyrenees. More recently, detailed sedimentological, geochemical and palaeontological studies have allowed a detailed platform to basin correlation through the Cenomanian to Turonian-aged carbonates of the Tremp basin (Soriano, 1992; Caus et al, 1993). By incorporating these recent stratigraphic refinements, Simo (1992) produced a more up-to-date chronostratigraphic framework for the Cenomanian to Campanian strata of the Tremp basin and proposed the existence of seven depositional sequences, each comprising a carbonate platform, slope and basinal package with an approximate duration of 1.5 to 4.5 Ma (3rd-order cycles of Vail et al., 1977) (see Figs 2.8a & 2.8b).

The stratigraphic framework of Simo (1992), which is shown in Figs. 2.8a and 2.8b, has been adopted throughout this thesis; and, except for a minor addition to the sequence stratigraphic interpretation, as a result of a detailed study of the Congost platform (see chapter 7), evidence which is presented within this thesis supports such a framework.

Moving stratigraphically upwards through the Upper Cretaceous sediments of the Tremp basin the first 6 carbonate platforms, corresponding to the first 6 Cenomanian to Lower Campanian-aged depositional sequences of Simo (1992), progressively backstep in what is interpreted to be a response to them having developed against a tectonic background of basin widening and deepening during the

spreading apart of the Iberian and European plates (see Fig. 2.8)(see also Puigdefabregas & Souquet, 1986). Each of these carbonate platforms have been named according to the Lithostratigraphic unit which corresponds to their platform facies. In ascending order, beginning with the oldest, these carbonate platforms, as they will be referred to in this thesis are: 1) the Santa Fe platform; 2) the Pardina Limestone; 3) the Congost platform; 4) the Sant Corneli platform; 5) the Bastus platform; and 6) the Vallcarga platform. (see Figs. 2.8a + 2.8b)

The Cenomanian-aged Santa Fe platform and the early to middle Turonian-aged Pardina Limestone are the subject of chapter 3 in this thesis where their sedimentology, geometry and evolution are discussed in order to set the scene for the detailed study of the Upper-Turonian to Coniacian-aged Congost platform which is the main focus of this thesis (see chapters 4, 5 and 7).

# Chapter 3
# The Santa Fe and Pardina Limestones

## 3.1 Introduction

As discussed in chapter 2, the Upper Cretaceous sediments of the Tremp basin can be divided into a series of backstepping carbonate platforms. The first platform in this series represents a time period from the Cenomanian to mid-Turonian (Caus & Gomez-Garrido 1989a & 1989b) and is composed of the Santa Fe and Pardina Limestones (see Figs. 2.8a & 2.8b).

As can be seen in Fig. 3.1 the Santa Fe and Pardina Limestones outcrop over a wide area of the Tremp basin. Correlation between these outcrops is possible on the basis of lithological and palaeontological evidence. In this chapter the main features of the Santa Fe and Pardina Limestones are described from a selection of outcrops, which are then interpreted and used to provide a platform to basin cross-section through this mid-Cenomanian to mid-Turonian carbonate platform. The most basinal outcrop of the Santa Fe and Pardina Limestones, within which slope facies sediments containing blocks which are derived from the Santa Fe platform margin are to be found, is located in the steep mountain slopes to the south of Sopiera. Although information derived from this outcrop has been included within the interpretation and summary sections of this chapter (see sections 3.7.2.2 & 3.8), a more detailed description and discussion of the Santa Fe slope facies is to be found within chapter 6 (see sections 6.3 & 6.7).

By providing an insight into the evolution and geometry of the Cenomanian to mid-Turonian Santa Fe platform, this chapter is intended to set the scene for the overlying Upper-Turonian to Coniacian aged Congost platform which is the main focus of this thesis.

## 3.2 The Sierra del Montsec sections

### 3.2.1 Introduction

The Sierra del Montsec extends for 35km in an east-west direction forming an impressive topographic feature which marks the southern limit of the field area (see Figs. 2.4 & 3.1). The Montsec mountains are in fact the topographic expression

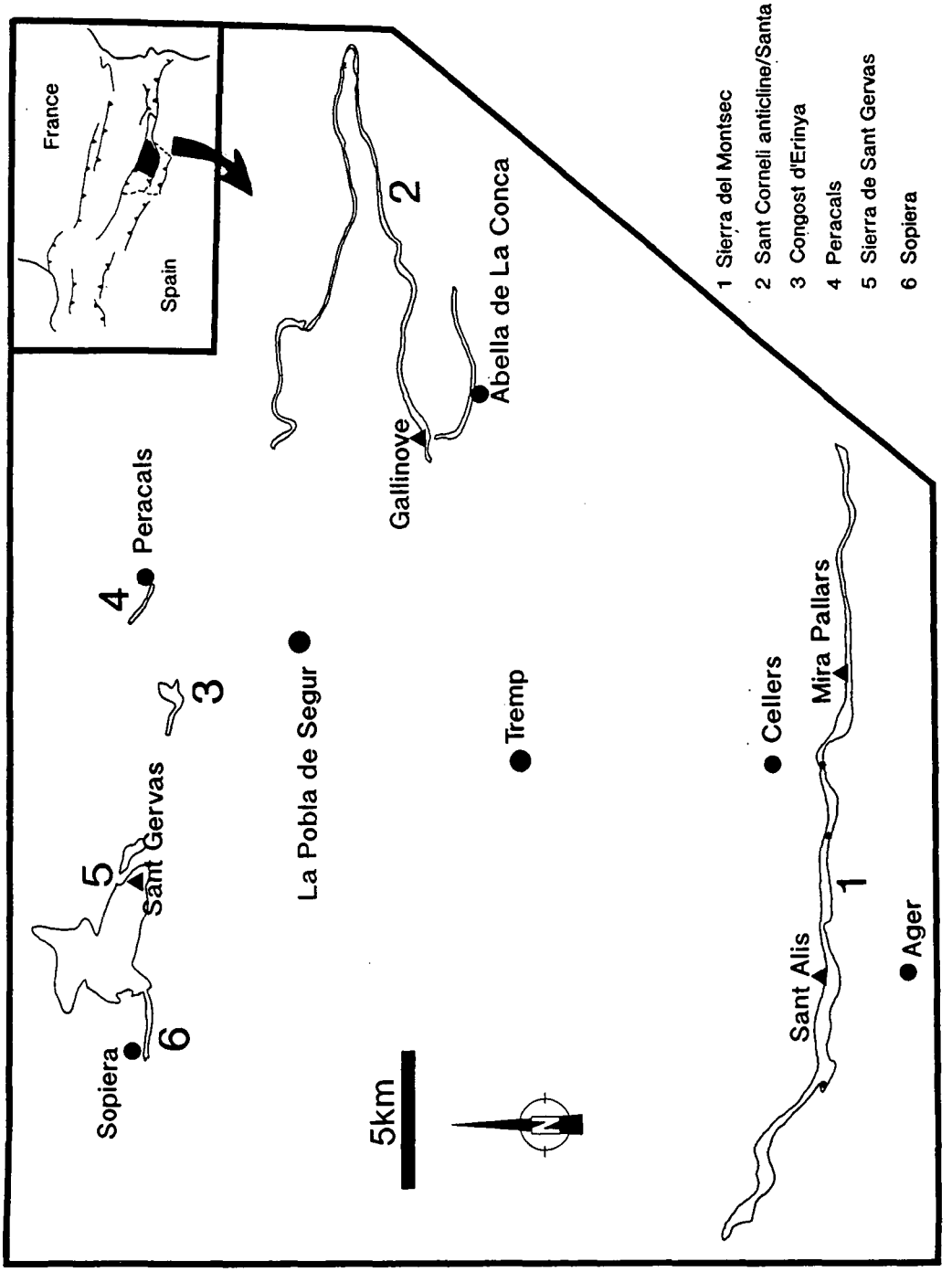


**Fig. 3.1.** Outcrop map of the Santa Fe and Pardina Limestones in the Tremp basin.

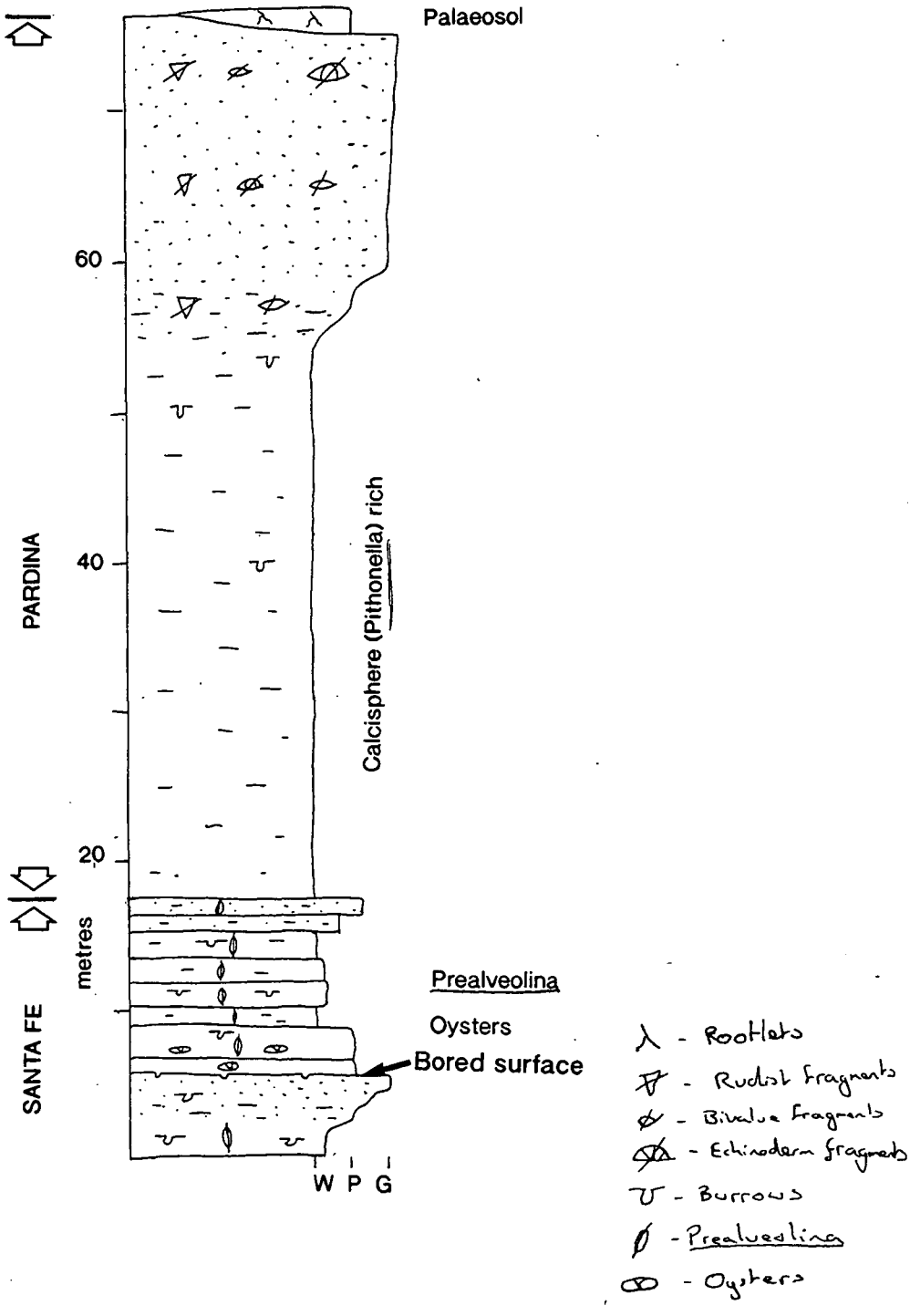


**Fig. 3.2a.** Composite stratigraphic section through the Santa Fe and Pardina Limestones in the Sierra del Montsec (outcrop 1, Fig. 3.1). Modified from Soriano (1992).

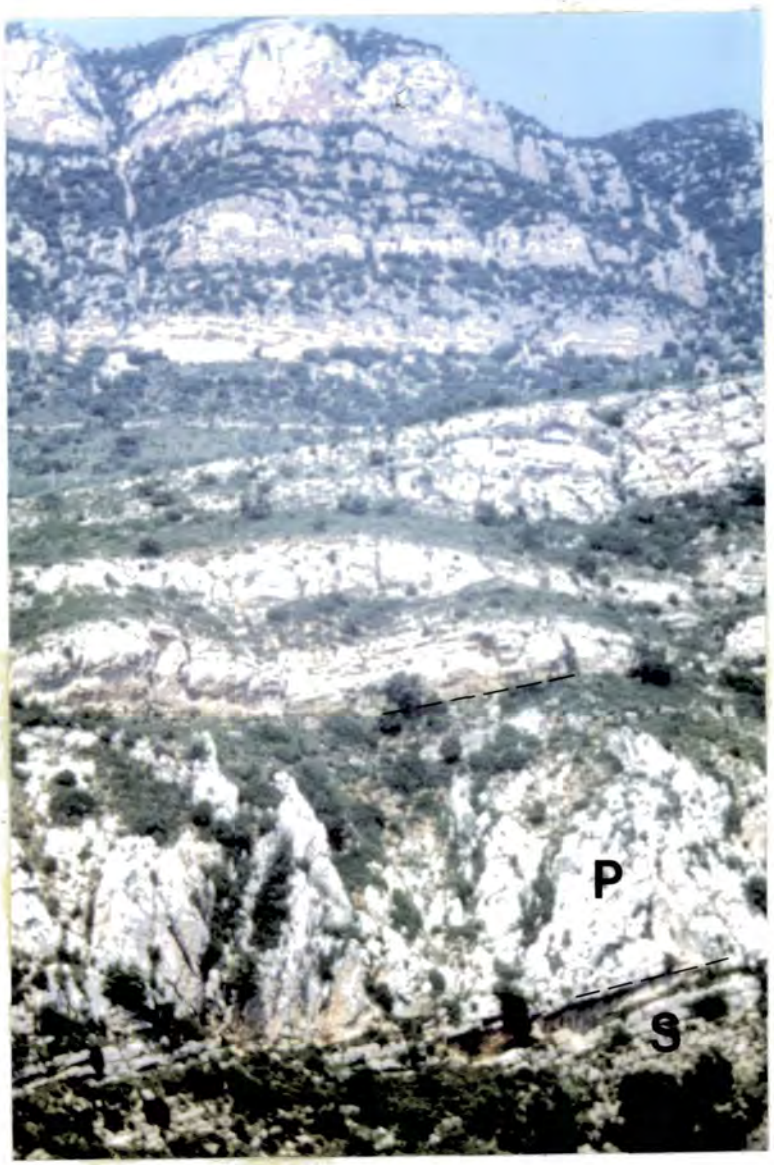


**Fig. 3.2b.** Photograph showing the typical outcrop characteristics of the Santa Fe (S) and Pardina (P) Limestones in the Sierra del Montsec. Photograph taken on the southern side of the Sierra del Montsec (outcrop 1, Fig. 3.1), to the north of Ager. Santa Fe and Pardina Limestones have a total thickness of approximately 80 metres.

of the Montsec Thrust, upon which the Mesozoic strata of the Tremp basin were moved southward and uplifted during the Eocene Pyrenean deformation. These mountains reach a maximum height of 1700m above sea-level and have southern flanks composed of steep slopes and vertical cliffs some of which are 300m high.

These steep southern slopes and cliffs provide a complete stratigraphic section through the Mesozoic strata of the Montsec thrust sheet.

The exposure of the Santa Fe and Pardina Limestones in the Sierra del Montsec is shown in Fig. 3.1 as outcrop number 1. This outcrop represents the most southern, i.e. landward, exposure of the Santa Fe and Pardina Limestones in the Tremp basin. Kate Soriano (1992) measured several metre-scale, stratigraphic sections through the Cenomanian to Santonian platform strata which are exposed along this east-west trending outcrop. Her work showed that except for slight variations in stratigraphic thickness, the general characteristics and lithofacies of the Santa Fe and Pardina Limestones are correlatable and consistent over the entire 25km east-west section provided by the Sierra del Montsec. Soriano (1992) interpreted this section to represent an east-west cross-section through the inner-platform area of the Cenomanian to mid-Turonian carbonate platform.

Figure 3.2 shows a composite stratigraphic section through the Santa Fe and Pardina Limestones (Fig. 3.2a), together with a photograph showing the typical characteristics of these two formations as they outcrop in the Sierra del Montsec (Fig. 3.2b). The descriptions of the Santa Fe and Pardina Limestones which follow is a composite one based upon the numerous sections studied in detail by Soriano (1992), together with observations made at the same localities during this study.

## 3.2.2 The Santa Fe Limestone

The Santa Fe Limestone rests unconformably on Lower Cretaceous carbonates or on Middle Jurassic dolomites. Measured sections, at numerous localities along the Sierra del Montsec, have shown the Santa Fe Limestone to be between 20 and 30 metres thick and consist of well bedded, nodular limestones, which can be divided into two units, separated by a bored, subaerial exposure surface (Soriano, 1992)(see Fig. 3.2a).

The lower unit is approximately 10 metres thick at most localities along the Sierra del Montsec and comprises a coarsening-upward interval consisting mainly of well-bedded, nodular wackestones, with peloidal packstones and grainstones within the top 2 metres. The grains within these sediments include abundant round *Prealveolina* and miliolids, together with peloids, echinoderm debris and other skeletal fragments. All of the grains have suffered intensive micritisation. The grainsize and abundance of grains increase up section. Numerous burrows are present within all these sediments. The upper surface of the peloidal grainstone which marks the top of this lower unit forms an obvious planar boundary within these otherwise

nodular sediments and is perforated by numerous borings. Isotopic studies by Soriano (1992) suggest that this surface represents a subaerial exposure surface, which has suffered later boring.

The upper unit is also approximately 10 metres thick at most localities along the Sierra del Montsec; however, unlike the lower unit it comprises a generally fining-upward series of well-bedded packstones and wackestones. The base of this upper unit is marked by a 2 to 20 cm thick packstone which contains large (up to 10 cm across) closely-packed mollusc shells, some of which appear to be unbroken. Above this mollusc-rich layer the following 1 to 2 metres consist of a packstone containing fragmented mollusc shells which decrease in abundance up section. In addition to the mollusc shells these packstones contain abundant elongate *Prealveolina,* with occasional round *Prealveolina* and miliolids, together with echinoderm and other shell debris. The remaining 8 metres or so of this upper unit consists of well bedded, bioturbated, nodular wackestones. These wackestones contain both round and elongate *Prealveolina*, together with miliolids, echinoderm debris, oyster and other shell fragments. The size and abundance of grains decreases up section.

### 3.2.3 The Pardina Limestone

The Pardina Limestone sharply overlies the well-bedded Santa Fe Limestone and is easy to recognise in the field as it lacks obvious bedding and forms massive light brown cliffs, which erode to form pillars (see Figs. 3.2a & 3.2b).

In the Sierra del Montsec the Pardina Limestone is between 26 and 60 metres thick and is very homogeneous in lithology from its base up to 75% of its total thickness. This lower part consists of fine to medium-grained wackestone/packstone containing abundant calcispheres (up to 40%), together with peloids, planktonic foraminifera, thin-shelled bivalves, echinoderm debris and a small amount of other shell fragments many of which have been completely micritised. Echinoderm fragments become less abundant up section. The uppermost 20 - 25% of the Pardina Limestone consists of a coarsening-upward package. This upper section begins with fine-grained, well-sorted peloidal packstone, with peloids, calcispheres and skeletal fragments, which coarsens quickly upwards into a medium to coarse grained grainstone (median grainsize 1mm) with abundant rudist and coral fragments together with peloids and echinoderm debris. Soriano (1992) has also described in place rudist bioherms with diameters of up to 1 metre from this upper section of the Pardina Limestone.


**Fig. 3.3a.** Photograph showing the outcrop characteristics of the palaeosol, which marks the top of the Pardina Limestone in the Sierra del Montsec (outcrop 1, Fig. 3.1). Note the red/brown colouration and the irregular dark and light coloured structures which pass through the bed. Photograph taken at top of the Pardina Limestone on the west side of Pallars river valley to the south of Cellers. Lens cap for scale.

At most of the sections in the Sierra del Montsec, the Pardina Limestone is capped by an easily weathered bed, which has a distinct red colouration (see Fig. 3.3a). In the field, irregular, vertical, cement and sediment-filled structures can be seen running through this bed (see Fig. 3.3a). When these structures are viewed in polished blocks and thin sections they have the appearance of root structures or rhizoliths (see Fig 3.3b & 3.3c). The rhizoliths range in diameter from 0.5 to 10 mm in diameter and are surrounded by thick micritic linings of up to 1mm in thickness. These micritic linings cross over the root molds in places to produce a texture which is similar in character to the alveolar texture described Esteban (1972) or the root moldic porosity of Harrison (1977) that is considered a diagnostic feature of palaeosols (Esteban & klappa, 1983).

**Fig. 3.3b.** Polished slab, cut from a sample of the palaeosol shown in Fig. 3.3a. Note the cement and sediment-filled root structures which cut vertically through the sample. Note also the red iron oxide staining around the edges of the root structures. Arrow shows way up. Ruler for scale; each fine division = 1mm.

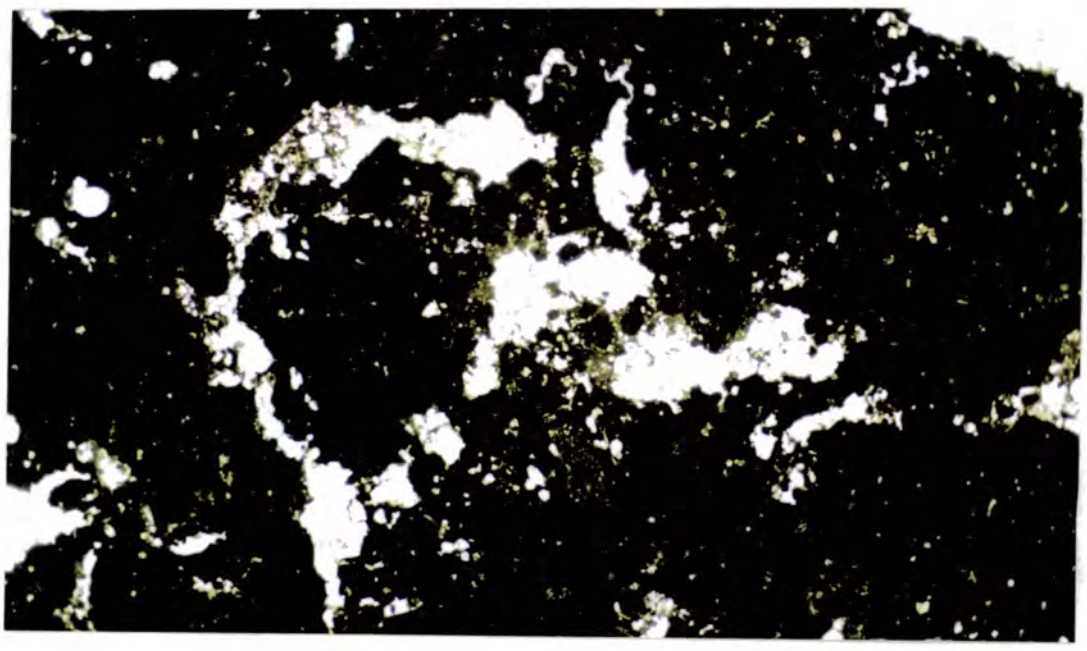

**Fig. 3.3c.** Photomicrograph, showing root structures within the palaeosol at the top of the Pardina Limestone. Note the micritic linings to the root structures and the well developed alveolar texture, where the micritic linings cross over the root structure. Field of view 12 x 7mm.

This easily-weathered bed which marks the top of the Pardina Limestone in the Sierra del Montsec is interpreted as a palaeosol, indicating that following the deposition of the upper grainstones the Pardina Limestone suffered a period of subaerial exposure. In addition to describing moldic porosity and pendant cements from within the grainstones which underlie this palaeosol, Soriano (1992) provided isotopic data which support this subaerial exposure hypothesis.

Overlying the palaeosol at the top of the Pardina Limestone, in the Sierra del Montsec there are coarse-grained bioclastic grainstones and packstones which are Santonian in age (Soriano, 1992; Caus pers. com.). The presence of these Santonian aged carbonates, resting directly upon the palaeosol at the top of the Turonian-aged Pardina Limestone, indicates a period of non-deposition which lasted for between 2 and 3 million years.

### 3.2.4 The boundary between the Santa Fe and Pardina Limestones.

Detailed palaeontological studies have shown that the surface which separates the well-bedded Santa Fe Limestone below from the massive Pardina Limestone above coincides with the Cenomanian - Turonian boundary (Caus et al., 1993). This detailed biostratigraphic work also showed the fauna of the upper part of the *R. cushmani* zone, the *W. archaeocretacea* zone and the lower part of the *H. helvetica* zone (upper Cenomanian to Lower Turonian) to be absent from these platform strata. Soriano (1992) analysed whole rock samples collected from a vertical section through the Santa Fe and Pardina Limestones. This work showed that the upper 2 metres of the bedded wackestones at the top of the Santa Fe Limestone possess a 1 $^{o}/_{oo}$ enrichment in their $^{13}C$ composition relative to that of the Pardina Limestone above and the remainder of the upper unit of the Santa Fe Limestone below.

## 3.3 The Sant Corneli anticline and Santa Fe syncline sections.

### 3.3.1 Introduction

The broad folding of the Sant Corneli anticline and Santa Fe syncline together with differential weathering has produced superb exposures of the Upper Cretaceous carbonate platforms (locality 2, Fig. 3.1). Prominent cliffs can be


**Fig. 3.4.** Photograph showing the outcrop characteristics of the Santa Fe and Pardina Limestones in the cliffs on the south side of the coll below Gallinove, which form part of the 40 km long outcrop around the Sant Corneli and Santa Fe folds (outcrop 2, Fig. 3.1). The Santa Fe Limestone (S) forms the lower, relatively thin-bedded unit while the upper, much thicker, more massive unit represents the Pardina Limestone (P). Note that bedding becomes visible again towards the top of the Pardina Limestone. The bushes on top of the Pardina Limestone mark the location of the easily-eroded Reguard formation (R), while the upper unit represents the prograding clinoforms of the overlying Congost platform (C). Total thickness of the Pardina and Santa Fe Limestones is approximately 50m.

followed for over 40km. In map view they have a roughly 'Z'-shaped outcrop as they trace out the limbs of the folds (see Figs. 3.1). The cliffs provide an impressive exposure showing a complete stratigraphic section from the unconformity on top of Lower Cretaceous sediments up through the Santa Fe and Congost platforms. When viewed from a distance the cliffs can be split into two units separated by a thin recessive package along which trees and bushes are growing (see Figs. 3.4 & 4.2). The Santa Fe and Pardina Limestones form the lower unit within these cliffs which is approximately 50m thick in most places.

As can be seen in Fig. 3.4 and 4.2, the Santa Fe and Pardina Limestones exhibit similar outcrop characteristics in these cliff exposures as they did in the Sierra del Montsec (see Fig. 3.2b), with the bedded Santa Fe Limestone forming the relatively thin lower section and the Pardina Limestone the massive, much thicker upper section.

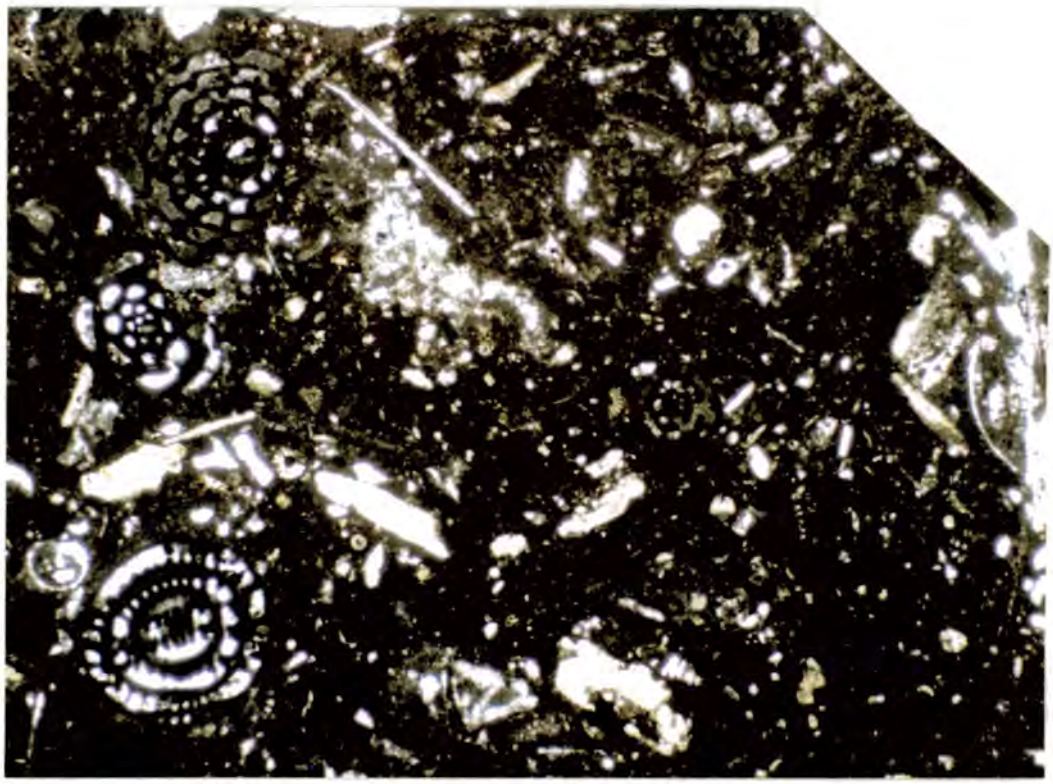

**Fig. 3.5.** Photomicrograph from the lower part of the Santa Fe Limestone. Note the abundant round *Prealveolina* and angular rudist fragments. Sample AA/2, south side of coll below Gallinove (locality 1d, Fig. 4.1). Field of view 6 x 4mm.

### 3.3.2 The Santa Fe Limestone

In these cliff sections the Santa Fe Limestone varies between 10 and 15 metres in thickness (see Figs. 3.4, 4.2 & 4.7b together with logs 1 & 2 in appendix 1). It mainly consists of bedded wackestones with some minor peloidal packstones. The wackestones are poorly sorted and heavily bioturbated, and all the shell fragments within them possess micritised margins. The main grain types present are angular mollusc and echinoderm fragments, with abundant *Prealveolina* (see Fig. 3.5). As in the Sierra del Montsec the *Prealveolina* present in the lower part of the Santa Fe are mostly of the round variety, while elongate forms are found towards the top. However, unlike the exposures in the Sierra del Montsec, there is no obvious boundary separating the Santa Fe Limestone into two intervals.

### 3.3.3 The Pardina Limestone

In these cliff sections there is no obvious bedding within the majority of the Pardina Limestone which varies between 30 and 50 metres in thickness (see Figs. 3.4, 4.2 & 4.7b together with logs 1 & 2 in appendix 1). It forms a generally coarsening-upward unit the bulk of which consists of fine grained wackestone, which is very restricted in the type of grains it contains (see Figs 3.6a & 3.6b). The most abundant grains within the wackestone which constitutes most of the Pardina Limestone are calcispheres, which sometimes account for 70% of the bioclasts. As can be seen in Fig. 3.6a, other grains within this wackestone include echinoderm debris and sponge spicules together with planktonic foraminifera. Bedding is visible within the top 5 or 6 metres of the Pardina Limestone (see Figs. 3.4 & 4.7b). Within this upper bedded section the Pardina Limestone possesses a packstone texture and contains a greater abundance of shell fragments (see Fig. 3.6b). In addition to the calcispheres, echinoderm fragments, sponge spicules and planktonic foraminifera, bivalve and brachiopod fragments are present together with some glauconite. This overall coarsening-upward succession through the Pardina Limestone is similar to that seen in the Sierra del Montsec (see Fig. 3.2a), except that the average grainsize never exceeds 0.25mm and grainstone textures are not present.

Unlike within the Sierra del Montsec, there is no obvious upper boundary to the Pardina Limestone in these cliff sections. There is a gradual transition into thinly bedded packstones which in addition to calcispheres, echinoderm fragments, sponge spicules, planktonic foraminifera and small shell fragments contain glauconite and a small amount of quartz (see Figs. 3.4 & 4.7b together with logs 1 & 2 in appendix 1).

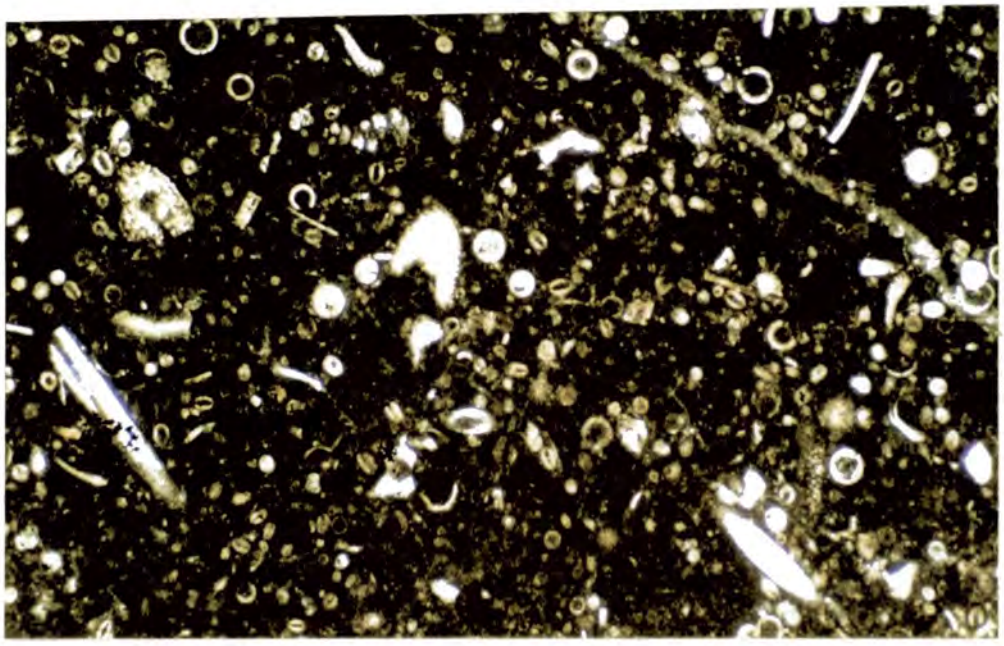

**Fig. 3.6a.** Photomicrograph showing calcisphere rich wackestone from the lower part of the Pardina Limestone. Other grains include echinoderm fragments and sponge spicules together with foraminifera. Sample AA/4, south side of coll below Gallinove (locality 1d, Fig. 4.1). Field of view 3 x 2mm.

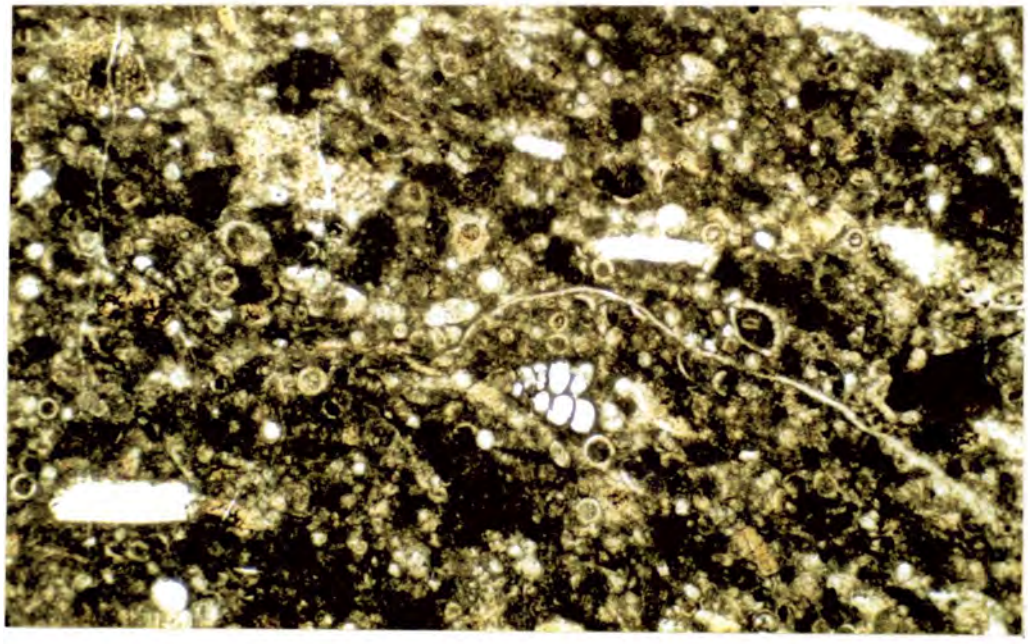

**Fig. 3.6b.** Photomicrograph showing calcisphere rich packstone from the upper part of the Pardina Limestone. Note the coarser grainsize and higher faunal diversity than within Fig. 3.6a; with additional grain types including bivalve and brachiopod fragments. Sample AA/8. Field of view 3 x 2mm.

These overlying thinly bedded packstones contain planktonic foraminifera which place them in the *Marginotruncana schneengasi* zone of Upper Turonian - Early Coniacian age (Caus & Gomez-Garrido, 1989; Caus, pers. com.) and are interpreted to represent the deep-water equivalent of the overlying progradational Congost platform (see chapter 4 & section 4.22).

## 3.4 The outcrop at Congost d'Erinya

### 3.4.1 Introduction

Congost d'Erinya (marked as locality 3 on Fig. 3.1) is a deep gorge cut by the Flamicell River, creating a superb exposure showing a complete stratigraphic section from the unconformity on top of the Lower Albian sediments, through to the St Corneli slope facies (see Figs 4.22a, 4.22b and 4.22c).

### 3.4.2 The Santa Fe and Pardina Limestones

The section begins at the north-western end of the gorge, where, looking in a north-easterly direction from the road (C 144) down to the banks of the Flamicell River, a marked angular unconformity can be seen. The sediments below this unconformity are Lower Albian in age (Simo pers. com.). Above this unconformity is a small cliff, which was originally defined as the Santa Fe Limestone Formation by Mey et al (1968). This cliff, however, can be divided into two units (see Fig. 3.7 together with log 12 in appendix 1).

The lower unit consists of bedded, bioturbated mudstones, wackestones and packstones containing abundant *Prealveolina,* miliolids, echinoderm fragments and bivalve debris. Half way up this lower unit there is an horizon rich in oysters. This lower unit is the Santa Fe Limestone *sensu stricto* after Soriano (1992) and Caus et al. (1993) which is interpreted to represent the lagoonal facies of the Santa Fe platform interior.

The upper unit is fairly homogeneous with no discernible bedding and consists of mainly wackestones with local fine-grained packstones towards its top (see Fig. 4.20b together with log 12 in appendix 1). The wackestones contain abundant (up to 80%) calcispheres, most of the rest of the grains being fine-grained echinoderm fragments, with some other shell debris. This upper unit is remarkably similar in

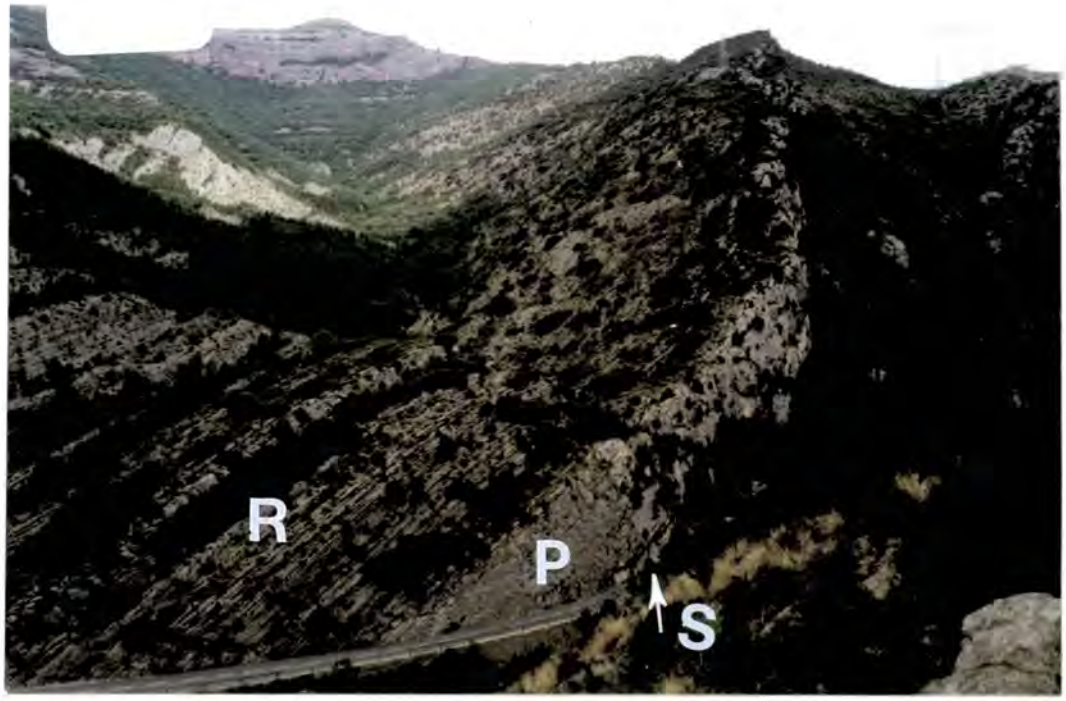


**Fig. 3.7.** Photograph taken at the northwest end of Congost d'Erinya, showing the southwest side of the gorge. The Santa Fe Limestone (S) forms the lower bedded part of the small cliff, while the Pardina Limestone (P) forms the upper more massive part to the cliff. The well-bedded more shaley sediments above represent the base of the 240 metre thick Reguard Formation (R). Crash barrier 1 metre high.

lithology and characteristics to the Pardina Limestone, which has been described from the Sierra del Montsec and Sant Corneli anticline/Santa Fe syncline outcrops (see sections 3.2.3 & 3.3.3 together with Figs 3.6a & 3.6b), and as such is interpreted to be the Pardina Limestone.

The boundary between the Santa Fe and Pardina Limestones, is unmarked at outcrop. However, whole rock stable isotope analyses performed on samples collected on a cm scale through a vertical section of this small cliff have revealed an isotopic anomaly towards the base of the massive unbedded unit which displays a marked 1 $^{o}/_{oo}$ enrichment in $^{13}C$ (Simo, pers. com). The position of this isotope anomaly is in fact marked on the outcrop with purple paint. Palaeontological studies have shown that, as in the Sierra del Montsec, this isotope anomaly coincides with the Cenomanian - Turonian boundary and the missing upper *R. cushmani*, *W. archaeocretacea* and the lower part of the *H. helvetica* biozones (upper Cenomanian to Lower Turonian)(Caus et al., 1993). Hence, by comparison with the sections in the

Sierra del Montsec this isotope anomaly can be taken to represent the boundary between the Santa Fe and Pardina Limestones (Caus et al., 1993).

The top of the Pardina Limestone in Congost d'Erinya is marked by an irregular mineralised surface which is associated with glauconite (see Figs 4.20a, 4.20b & 4.20c). This upper boundary to the Pardina Limestone is described and discussed in some detail in section 4.4.3. This surface is interpreted as a hardground which developed as a result of sediment starvation and major transgressive event which occurred at the base of the Reguard Formation and marks the beginning of the Congost sequence.

## 3.5 The outcrop at Peracals

### 3.5.1 Introduction

Peracals is a small village situated in the mountains approximately 7km to the north of La Pobla de Segur (see Figs 3.1 & 4.1). The outcrop (locality 4 on Fig. 3.1), lies a little way along a goat track to the west of the village. It is bounded above and below by thrust faults and shows a section from the upper part of the Santa Fe Limestone through the Pardina Limestone and into the lower part of the Reguard Formation (see log 13 in appendix 1). Detailed mapping and reconstruction by the Catalunya Geological Survey have shown these sediments to have occupied a palaeogeographic location basinward of the outcrop at Congost d'Erinya (see section 4.4) but landward of the outcrops around Sant Gervas and Sopiera (Simo pers. com.).

### 3.5.2 The Santa Fe and Pardina Limestones

The section begins with fine-grained, bedded wackestones and packstones containing abundant foraminifera, including miliolids and *Prealveolina*. Fragments of caprinid rudists and oysters, as well as other shell debris are common. Burrows which have been infilled with iron oxide stained packstone are present throughout these sediments.

Nine metres from the base of the outcrop there is an horizon along which nodules of iron oxide are concentrated (see log 13 in appendix 1). Above this horizon the section continues with a 9 metre thick unit which does not display any visible bedding and is composed of mainly fine-grained wackestones, which are extremely rich in calcispheres, are heavily burrowed and contain trace amounts of glauconite.

The caprinid rudists seen in the packstones and wackestones below the nodular horizon do not occur in this unit. Grainsize increases slightly upwards through this unit, as does the abundance of shell fragments and larger foraminifera. The top of this unit is marked by a bed which has a distinctive red colour (see Figs. 4.28a, 4.30a and 4.30b). This red bed is approximately 40cm thick and contains abundant burrows and nodules of iron oxide (see Fig 4.28b).

The characteristics of this outcrop are similar to those of the Santa Fe and Pardina Limestone outcrops in the Sierra del Montsec, Sant Corneli anticline/Santa Fe anticline region and at Congost d'Erinya (see sections 3.2, 3.3 & 3.4 together with Fig. 3.2a and logs 1 & 12 in appendix 1), with the lower bedded unit representing the Santa Fe Limestone and the upper more massive unit the Pardina Limestone. The development of iron oxide nodules at what would appear to be the boundary between the Pardina and Santa Fe limestones may be suggesting there was a sedimentary hiatus between the deposition of the two formations.

The red bed which marks the top of the Pardina Limestone at this locality (see Figs. 4.28a, 4.28b, 4.28c, 4.30a, 4.30b & 4.30c ) is discussed in detail in section 4.5.3, where it is interpreted to represent a hardground which developed during a hiatus in sedimentation, caused by a major transgressive event that marks the base of the Congost sequence.

## 3.6 The outcrop along the Sierra de Sant Gervas

### 3.6.1 Introduction

The Sierra de Sant Gervas is located in the far northwest of the study area (locality 5, Fig. 3.1). The resistant cliffs which form the steep slopes around this mountain, are composed of Cenomanian to mid-Turonian aged platform carbonates, which are overturned and rest upon a thrust fault which marks the southern margin of the Sierra (Simo, pers. com.)(see Fig. 6.2). The overturned nature of these carbonates is easily confirmed as geopetally-infilled bioclasts are common. Some late-Turonian to early Coniacian deep water sediments are present towards the base of the cliffs.

### 3.6.2 The Santa Fe and Pardina Limestones

The Cenomanian-aged carbonates of the Santa Fe Limestone are easily identifiable because, as is the case at the outcrops described previously, they contain

**Fig. 3.8a.** Photograph showing a large sediment-filled dissolution cavity within a coarse, skeletal debris rich packstone from the Santa Fe platform margin. Note the abundant *Pithonella*, which show up as white dots (arrowed) within the host packstone. Photograph taken on the east side of Sant Gervas (outcrop 5, Fig. 3.1). Lens cap for scale.

**Fig. 3.8b.** Photograph of a polished slab from a sample which was collected from the locality shown in Fig. 3.8a. Note the laminated sediment which is infilling the dissolution cavities. Note also the red colouration around the margins of the cavities, suggesting iron oxide mineralisation. The laminated sediment which infills these cavities is a fine-grained wackestone rich in calcispheres, similar to the basal part of the Pardina Limestone. Ruler marked in mm for scale.

the large benthic foraminifera *Prealveolina*. The Santa Fe Limestone at this outcrop has a vertical thickness of over 150m. The basal part (upper section of the outcrop) of this thick unit consists of a series of coarsening-upward cycles from wackestones to skeletal debris packstones and grainstones. The main grain types being rudist and echinoderm fragments together with *Prealveolina*. The upper section of the Santa Fe Limestone consists of bedded packstones and wackestones/floatstones, which contain very coarse angular rudist and other shell fragments (see Figs. 3.8a & 3.8b). Within these coarse-grained bedded carbonates there occur patches of closely packed caprinid rudists, forming reefal structures, some of which cover several metres in area. In addition to these rudist patches, coral boundstones occur (Simo, pers. com. & Caus et al., 1993). This upper section also contains abundant karst features in the form of cement and sediment-filled pipes and cavities (see Figs. 3.8a & 3.8b), some of which are up to a metre in diameter (Simo, pers. com.). The sediment within some of these karst cavities is a calcisphere rich, pelagic wackestone similar to that of the overlying Pardina Limestone (Dating of the infill within samples collected by Simo is being carried out at present by Esmeralda Caus at the Universitat Autonoma de Barcelona).

The Pardina Limestone is approximately 20 metres thick at the eastern edge of the Sierra de Sant Gervas, and consists entirely of fine-grained wackestones with abundant calcispheres together with echinoderm debris, local sponge spicules and some glauconite grains.

## 3.7 Discussion and interpretation

### 3.7.1 Palaeogeography

The outcrops of the Santa Fe and Pardina Limestones, which have been described in the previous sections, provide an intermittent view of a south to north (platform to basin) cross-section through the Cenomanian to mid-Turonian carbonate platform. The most southerly exposures in the Sierra del Montsec (see section 3.2) are interpreted to represent sections through the inner-platform area (Soriano, 1992; Caus et al., 1993).

After allowing for the curvature of the folds within the Upper Cretaceous carbonates of this area, the outcrops of the Santa Fe and Pardina Limestone in the region of the Sant Corneli anticline and Santa Fe syncline (see section 3.3) can be interpreted to represent a section through the mid-platform area, which had a palaeogeographic location that was at least 25 to 35 kilometres northward of the

sediments now exposed in the Sierra del Montsec (this is a minimum estimate of the distance because of the unknown throw on the Boixols thrust, which underlies the Sant Corneli anticline).

The outcrop at Congost d'Erinya (see section 3.4) represents a section through the mid platform which was palaeogeographically approximately 10km farther north still. Detailed mapping and reconstruction by the Catalunya Geological Survey have shown the sediments which outcrop at Peracals (see section 3.5) occupied a palaeogeographic location basinward of the outcrop at Congost d'Erinya; while, the sediments which outcrop around Sant Gervas (see section 3.6) and Sopiera (see chapter 6) were deposited in palaeogeographic locations even farther to the north (Simo, pers. com.).

## 3.7.2 The Santa Fe Limestone

### 3.7.2.1 The inner and mid-platform areas

The Santa Fe limestone possesses remarkably similar characteristics at all the outcrops to the south and east of the Sierra de Sant Gervas (see sections 3.2.2, 3.3.2, 3.4.2 & 3.5.2). The heavily bioturbated wackestones and packstones containing abundant benthic foraminifera together with generally angular echinoderm and mollusc fragments, suggest that these sediments were deposited in a low energy lagoonal environment. A restricted environment is suggested by the low faunal diversity and intensive bioturbation within these sediments. The similarity in characteristics of these sediments at all the outcrops indicates that this lagoon covered a wide area and suggests that the surface of deposition over this area was relatively horizontal.

The only exception to this similarity occurs in the Sierra del Montsec (see section 3.2.2), where the inner-platform sections through the Santa Fe Limestone are divided into an upper and lower unit by a bored surface which on the basis of both petrographic and isotopic evidence (Soriano, 1992) is interpreted to have suffered subaerial exposure. The lower unit can be interpreted as a shoaling-upwards succession, with the peloidal grainstones at the top representing deposition under agitated conditions, perhaps under the influence of wave action. The pendant cements within these grainstones (Soriano, 1992) emphasise the shallow conditions of their deposition. The bored exposure surface which marks the top of these grainstones indicates that this shoaling upwards succession finally ended in emergence.

The absence of these grainstones and the exposure surface from within the mid-platform sections (Sant Corneli/Santa Fe folds, Congost d'Erinya, Peracals)(see sections 3.3.2, 3.4.2 & 3.5.2), can be interpreted to indicate that while the inner-platform area (Sierra del Montsec) was experiencing shallow, probably wave-agitated conditions followed by exposure; the mid-platform area farther to the north was undergoing deeper-water conditions, so preventing the sediments from being affected by any wave action or exposure. The restricted nature of this platform-top environment, as evidenced by the low-faunal diversity, together with its large dimensions suggests that the wave action proposed to have been responsible for grainstone creation in the inner platform, rather than having originated in the open-sea, must have been generated within the extensive lagoon as a result of wind action. The accumulation of lagoonal derived grains within the inner platform area, but not within the mid-platform area suggests a landward sediment transport system on the platform top, and this may be indicating that the Santa Fe platform developed under leeward conditions.

The upper part of the Santa Fe Limestone at all the outcrops which represent sections through the inner and mid-platform areas display successions whereby grainsize and shallow-water skeletal debris abundance decrease upwards (see sections 3.2.2, 3.3.2, 3.4.2 & 3.5.2). These textural and skeletal debris content variations are accompanied by an up-section increase in the ratio of elongate to round varieties of *Prealveolina* which are present within these sediments.

Flattening trends in modern larger Foraminifera have been described as an ecological response to greater water depths (Hallock & Hansen, 1979; Reiss & Hottinger, 1984). Whether this is true for the *Prealveolina* in the Santa Fe Limestone is unknown; however, it is certainly a possibility as the up-section textural variation from packstone to wackestone could be interpreted as a deepening succession (after Soriano, 1992). The decreasing abundance of shallow-water skeletal debris could also be interpreted as the result of changes in the environmental conditions on the platform top which inhibited the presence of typical shallow-water carbonate producers (after Caus et al., 1993) (see section 3.7.3, for further discussion).

### 3.7.2.2 The platform-margin

The sediments exposed along the Sierra de Sant Gervas (see section 3.6.2) exhibit all the characteristics typical of platform-margin facies sediments. The abundant coarse grainstones and high content of skeletal fragments, together with coral boundstones within the sediments indicate a high energy, highly productive area. The series of coarsening-upward packages within the lower part of the platform

margin succession suggests that in its early stages the platform-margin experienced episodic progradation.

Large blocks of these platform-margin sediments are present within equivalent-aged upper-slope sediments which are exposed at the western end of the Sierra de Sant Gervas and at Sopiera (see section 6.3). The presence of these large blocks in the upper slope sediments suggests that the platform margin was steep and active. This, together with the fact that the platform-margin succession is over 6 times as thick as that of the platform-top, has led Simo & Puigdefabregas (1985) to suggest that this platform margin was fault controlled (see also Simo, 1986 & 1989). Simo, proposed that the platform margin developed upon an inherited fault-scarp topography which had resulted from extension during Albian rifting (Simo & Puigdefabregas, 1985; Simo, 1986; Simo, 1989).

Differential compaction is another process which should be considered as a possible cause of the greater thickness of the platform-margin succession compared to that of the lagoon, as well as a triggering mechanism for the shedding of blocks of platform-margin material down slope. Such a mechanism could be envisaged as the Santa Fe platform margin began to prograde out over more muddy basinal sediments which had been accumulating on the slope. When compared with the Lower Cretaceous sediments below the unconformity, upon which the Santa Fe lagoonal sediments and early part of the platform-margin succession were deposited, the Santa Fe slope sediments would be relatively less well cemented and more likely to yield to the pressures of compaction. Such differential compaction would increase the accommodation space at the platform margin and hence enable increased aggradation. However, such a process of differential compaction requires the presence of a pre-existing slope onto which the slope sediments to be compacted were able to accumulate. Such a prexisting slope could only be envisaged as a result of the presence of a fault scarp as was suggested by Simo and Puigdefabregas (1985) and Simo (1986 & 1989).

### 3.7.3 The boundary between the Santa Fe and Pardina Limestones

The boundary between the Santa Fe Limestone and Pardina Limestone has been shown to correspond to the Cenomanian - Turonian boundary (Caus et al., 1993). Detailed palaeontological work in both the inner and mid-platform areas (see sections 3.2.4 & 3.4.2) has shown the fauna of the upper part of the *R. cushmani* zone, the *W. archaeocretacea* zone and the lower part of the *H. helvetica* zone (upper Cenomanian to Lower Turonian) to be absent from these platform strata (Caus et al.,

1993). Within the equivalent basinal sediments which outcrop near Sopiera (see chapter, 6), these biozones are present.

Wholerock stable isotope analyses of samples taken from vertical sections across this boundary both in the inner and mid-platform areas (see sections 3.2.4 & 3.4.2), during work by Soriano (1992), have shown the sediment at this boundary to possess an anomalous $1^{o}/_{oo}$ enrichment in $^{13}C$ (Soriano, 1992; Simo pers. com.). This positive $\delta^{13}C$ is also observed within the basinal sediments which are exposed near Sopiera (see chapter 6), allowing correlation between the sediments of the platform-top and those in the basin (Caus et al., 1993). Importantly the positive $\delta^{13}C$ anomaly observed within the basinal succession occurs within the *W. archaeocretacea* biozone (Soriano, 1992; Caus et al, 1993). Similar $\delta^{13}C$ anomalies have been reported from the Cenomanian - Turonian boundary world-wide (Scholle and Arthur, 1980; Margaritz, 1985; Schlanger et al., 1987; Arthur et al., 1988). Although the reason for this anomaly is under debate it is generally agreed that it was a globally synchronous event which occurred within the *W. archaeocretacea* biozone (Schlanger & Jenkyns, 1976; Fischer & Arthur, 1977; Scholle and Arthur, 1980; Manebe & Bryan, 1985; Schlanger et al., 1987; Arthur et al., 1988 & Pederson & Calvert, 1990).

The presence of this positive $\delta^{13}C$ anomaly across the Cenomanian -Turonian boundary within both the platform and basinal sediments permits time correlation between platform and basin. Hence, the presence of this $\delta^{13}C$ anomaly within the platform succession demonstrates that the time associated with the *W. archaeocretacea* biozone is represented within the rock record, although the key fauna are absent. This rules out the suggestion from biostratigraphic data that this boundary corresponded to a period of non-depositon, perhaps due to emergence, which lasted for approximately 1 million years. However, as evidenced by the presence of mineralised nodules at this boundary at Peracals (see section 3.5.2 together with log 13 in appendix 1), deposition rates may have been locally depressed.

Caus et al. (1993), after noting the pronounced upwards-decreasing abundance of shallow-water skeletal grains within the wackestones of the Santa Fe Limestone just below this boundary (see sections 3.2.2, 3.3.2, 3.4.2 & 3.5.2), together with the fact that above the boundary within the basal part of the Pardina Limestone there are no fragments of major carbonate producers (see sections 3.2.3, 3.3.3, 3.4.2 & 3.5.2), suggested that this boundary corresponded to a eutrophication of the platform top. This interpretation was based on studies of recent carbonate platforms, where high nutrient levels can cause a disequilibrium in the ecosystem (Hottinger, pers. com. to Caus et al.). Such an interpretation is in agreement with the proposals of Pederson and Calvert (1990), who suggested that global positive $\delta^{13}C$ shifts in the Cretaceous

were a result of high primary productivity, facilitated by strong upwelling and an enhanced terrestrial nutrient supply (Manabe & Bryan, 1985).

The karstic pipes and cavities within the upper section of the platform-margin sediments, which have been infilled with fine-grained pelagic, calcisphere-rich wackestones similar to those typical of the Pardina Limestone (see section 3.6.2 together with Figs 3.8a & 3.8b) are an important feature. They suggest that following the deposition of the Cenomanian-aged Santa Fe Limestone sediments at the platform margin, there was a significant period of subaerial exposure before the deposition of the Turonian-aged Pardina Limestone. These karstic pipes and cavities are also present within many of the clasts of Santa Fe platform margin material that have been re-worked and deposited within the slope talus facies of the Reguard Formation and Sant Corneli Breccia which are exposed near the village of Sopiera (see sections 6.5 & 6.6)

Following the interpretations of Soriano (1992) and Caus et al (1993), it would appear that the subaerial exposure of the platform during the late Cenomanian and early Turonian was a local event, which was restricted to the platform margin, possibly as the result of tectonic activity (fault movement). The missing upper *R. cushmani, W. archaeocretacea* and the lower part of the *H. helvetica* biozones (upper Cenomanian to Lower Turonian), observed on the platform-top is interpreted to have been caused by a eutrophication of shallow waters which hampered the growth of carbonate producers.

### 3.7.4 The Pardina Limestone

As with the Santa Fe Limestone the Pardina Limestone displays remarkably similar characteristics at all the outcrops which represent the platform top, suggesting that the surface of deposition over this wide area was relatively horizontal. The majority of the Pardina Limestone at all these localities comprises a homogeneous wackestone which has a very restricted grain content, being very rich in calcispheres, together with planktonic foraminifera and echinoderm debris (see sections 3.2.3, 3.3.3, 3.4.2, 3.5.2 & 3.6.2).

As mentioned in the previous section (section 3.7.3) the lack of shallow-water skeletal grains within this unit can be interpreted to be partly the result of a eutrophication event on the platform-top, which caused the disappearance of carbonate-producing shallow-water fauna. The lack of shallow-water fauna within the lower part of the Pardina, together with the presence of planktonic foraminifera, also suggests that the Pardina Limestone represents a deeper water facies than the

underlying Santa Fe Limestone. Other evidence of a transgressive event at the base of the Pardina Limestone is provided by the occurrence of the Pardina Limestone above, and within the cavities of, the previously karsted Santa Fe Limestone at the platform margin (see section 3.6.2 together with Figs. 3.8a & 3.8b).

The transition from wackestone to packstone (grainstone in the inner platform) toward the top of the upper Pardina Limestone with an associated increase in skeletal debris abundance and grainsize (see sections 3.2.3, 3.3.3, 3.4.2 & 3.5.2) can be interpreted as a result of a post-eutrophication reduction in nutrient levels having allowed recolonisation of the platform by benthic fauna, together with a shoaling event brought about by renewed platform progradation. As the coarsest skeletal debris and most shallow facies sediments (grainstones) are to be found in the Sierra del Montsec sections (see section 3.2.3), it would appear that platform progradation was from south to north. This is supported by the fact that at each of the more northerly outcrops the upper part of the Pardina Limestone becomes increasingly finer grained and can be interpreted as representing a progressively more distal facies (see sections 3.2.3, 3.3.3, 3.4.2, 3.5.2 & 3.6.2). From her work in the Sierra del Montsec, Soriano (1992) also concluded that the upper part of the Pardina Limestone represented a period of platform progradation. Thickness variations in this upper part of the Pardina Limestone between various sections measured in different locations along the Sierra del Montsec led Soriano (1992) to suggest that the source of the grains was landward (to the south) of the succession which is now exposed in the Sierra del Montsec.

As mentioned by Soriano (1992), whether the grainstones, present at the top of the Pardina Limestone in the Sierra del Montsec sections, actually shoaled above sea-level or were subjected to a fall in relative sea-level, is not apparent; however, the grainstone became subaerially exposed and were reworked into a palaeosol (see section 3.2.3 together with Figs. 3.3a, 3.3b & 3.3c).

The localised hardgrounds which mark the top of the Pardina Limestone at Congost d'Erinya and Peracals (see sections 3.4.2, 3.5.2, 4.4.3 & 4.5.3 together with Figs. 4.20a, 4.20b, 4.20c, 4.28a, 4.28b & 4.28c, 4.30a & 4.30b) could be interpreted to have formed as a result of sediment starvation in the basin following this exposure on the platform. Sediment starvation would also have resulted from the transgressive event which is interpreted to have been responsible for the deposition of the deep-water glauconite-rich sediments which overlie the upper boundary to the Pardina Limestone at all localities north of the Sierra del Montsec (see sections 4.4.3, 4.5.3, 4.5.4, 4.6.2 and chapter 7 for further discussion).

## 3.8 Summary

Figure 3.9 shows a generalised platform to basin cross section through these Cenomanian and Turonian carbonates. Lines of correlation, based upon field, geochemical and palaeontological data, which have been used during this interpretation are also shown on this Figure which has been modified from Caus et al. (1993).

The Santa Fe Limestone is interpreted to represent a Cenomanian carbonate platform consisting of a wide low energy lagoon, which was protected from the open sea by a relatively narrow belt of skeletal shoals, together with coral boundstones and rudist clusters at the platform margin. This platform is interpreted to have been effected by fluctuations in relative sea-level together with global oceanic productivity variations. Following a transgressive event these Cenomanian carbonates were overlain by the Turonian Pardina Limestone which records a process of platform recovery and renewed progradation.

The low energy lagoonal facies sediments, comprising bioturbated wackestones with angular shell debris and large benthic foraminifera, display similar characteristics and possess an almost constant thickness over a wide area which was in excess of 50km across in a north-south (platform-basin) direction, suggesting that they were deposited onto a fairly horizontal surface (see section 3.7.2.1 together with Fig. 3.9). The much greater thickness of the platform margin succession when compared to that of the platform interior together with its active nature have led to the interpretation that the platform margin developed at the site of a former fault scarp, which may have suffered periodic reactivation (see section 3.7.2.2 together with Fig. 3.9). Differential compaction, as a result of platform margin progradation over deeper water sediments, may also have had a role to play in the pronounced thickness variation between the interior and margin of the platform as it could have led to increased accomodation space creation at the platform margin.

Upon the platform-top the Santa Fe Limestone can be divided into two depositional cycles (see section 3.7.2.1 together with Fig. 3.9). The lower cycle represents a shoaling-upward succession which culminated in emergence within the inner platform, while the upper cycle is interpreted to represent a deepening-upward succession.

The lower platform margin succession is interpreted to have recorded periods of episodic progradation, while within the upper section aggradation appears to have been dominant (see section 3.7.2.2). The presence of well-developed karst within the upper section of the platform margin succession indicates that the platform margin experienced a prolonged period of subaerial exposure (see section 3.7.3 together with

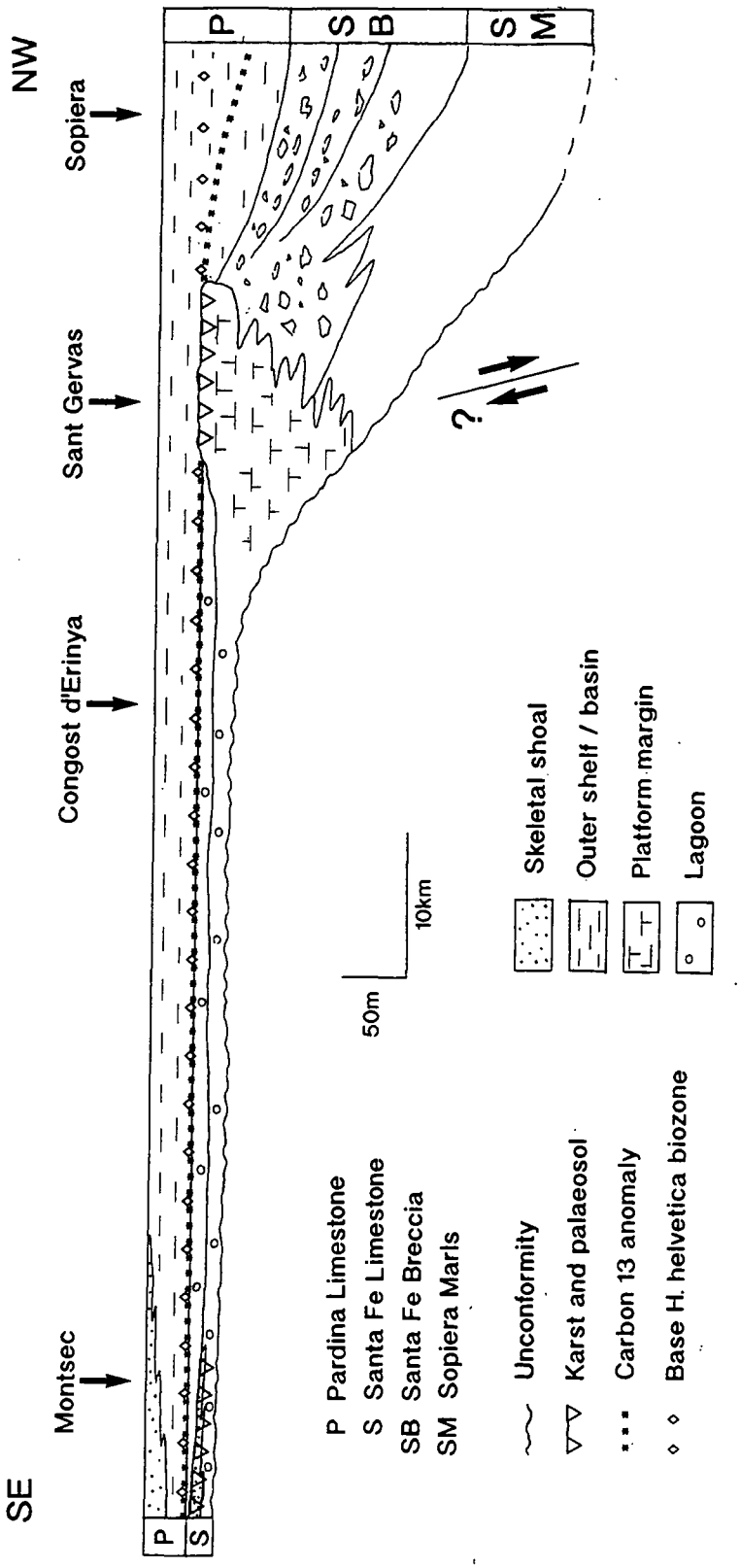


**Fig. 3.9.** Generalised platform to basin cross section through the Cenomanian to mid Turonian carbonate platform which is represented by the Santa Fe and Pardina Limestones. Lines of correlation have been based upon field, geochemical and palaeontological data. Modified from Caus et al (1993).

Figs. 3.8a & 3.8b). The interpretation that the upper part of the Santa Fe Limestone within the inner platform represents a deepening-upward succession suggests that initial exposure of the platform margin may be correlatable with that which affected the inner platform (see Fig. 3.9).

The deepening of the environment upon the platform top which is evidenced by textural changes within the upper unit of the Santa Fe Limestone is interpreted to have been accompanied by a eutrophication event, which produced a disequilibrium in the ecosystem and inhibited the growth of benthic fauna such as large foraminifera and molluscs (see section 3.7.3). The fact that the sediments at the upper boundary of the Santa Fe Limestone show anomalous positive $\delta^{13}C$ compositions which can be correlated with similar world-wide anomalies suggests that this eutrophication may have been controlled by global oceanic events (see section 3.7.3).

The Pardina Limestone, with its dominantly wackestone texture and low faunal diversity with abundant calcispheres and planktonic foraminifera which overlies the Santa Fe Limestone both in the inner platform and at the platform margin, is interpreted to represent a deeper-water facies which was deposited over the whole of the Santa Fe platform area as a result of a rise in relative sea-level (see section 3.7.4 together with Fig. 3.9). The deposition of the Pardina Limestone may in fact be a result of a continuation of the deepening event which is recorded by the upper Santa Fe Limestone. The upper section of the Pardina Limestone, with its increasing shell fragment and benthic faunal assemblage is interpreted as a shoaling-upward succession representing platform recovery and progradation (see section 3.7.4). Within the succession which is exposed in the most southerly outcrop this shoaling-upward succession culminated in subaerial exposure, while farther to the north localised hardgrounds developed as a result of sediment starvation (see sections 3.7.4, 4.4.3, 4.5.3, 4.5.4 & 4.6.1). It was upon this foundation that the Congost platform developed.

# Chapter 4
# The Congost platform

## 4.1 Introduction

As discussed in chapter 2, the Upper Cretaceous sediments of the Tremp basin can be divided into a series of backstepping carbonate platforms. The Congost platform is the second platform in this series (see Figs 2.8a & 2.8b) and comprises a platform, slope and basinal package which represents a time period that began in the Upper Turonian and continued through to the Middle Coniacian.

The sediments which make up the Congost package are well exposed in the northwest of the Tremp basin. The outcrops which have been studied provide an almost continuous platform to basin cross-section and are shown in Figure 4.1. These outcrops are described in the following sections.

## 4.2 The Sant Corneli Anticline and Santa Fe Syncline Outcrop

### 4.2.1 Introduction

The broad folding of the Sant Corneli anticline and Santa Fe syncline together with differential weathering has produced superb exposures of the Upper Cretaceous carbonate platforms. Prominent cliffs can be followed for over 40km. In map view they have a roughly 'Z' shaped outcrop as they trace out the limbs of the folds (see Fig. 4.1). The cliffs provide an impressive exposure showing a complete stratigraphic section from the unconformity on top of Lower Cretaceous sediments up through the Santa Fe and Congost platforms and by walking over the top of the cliffs the section can be followed up into St Corneli slope sediments. When viewed from a distance the cliffs can be split into two units separated by a thin recessive package along which trees and bushes are growing (see Fig. 4.2). The lower unit is much thinner than the upper one and although it varies slightly in thickness along the cliff it is approximately 50m thick in most places. This lower unit is composed of the lagoonal carbonates of the 'Santa Fe' platform and overlying Pardina Limestone (see chapter 3). The much thicker upper unit, which is up to 120m thick, is made up of carbonates of the Congost platform.

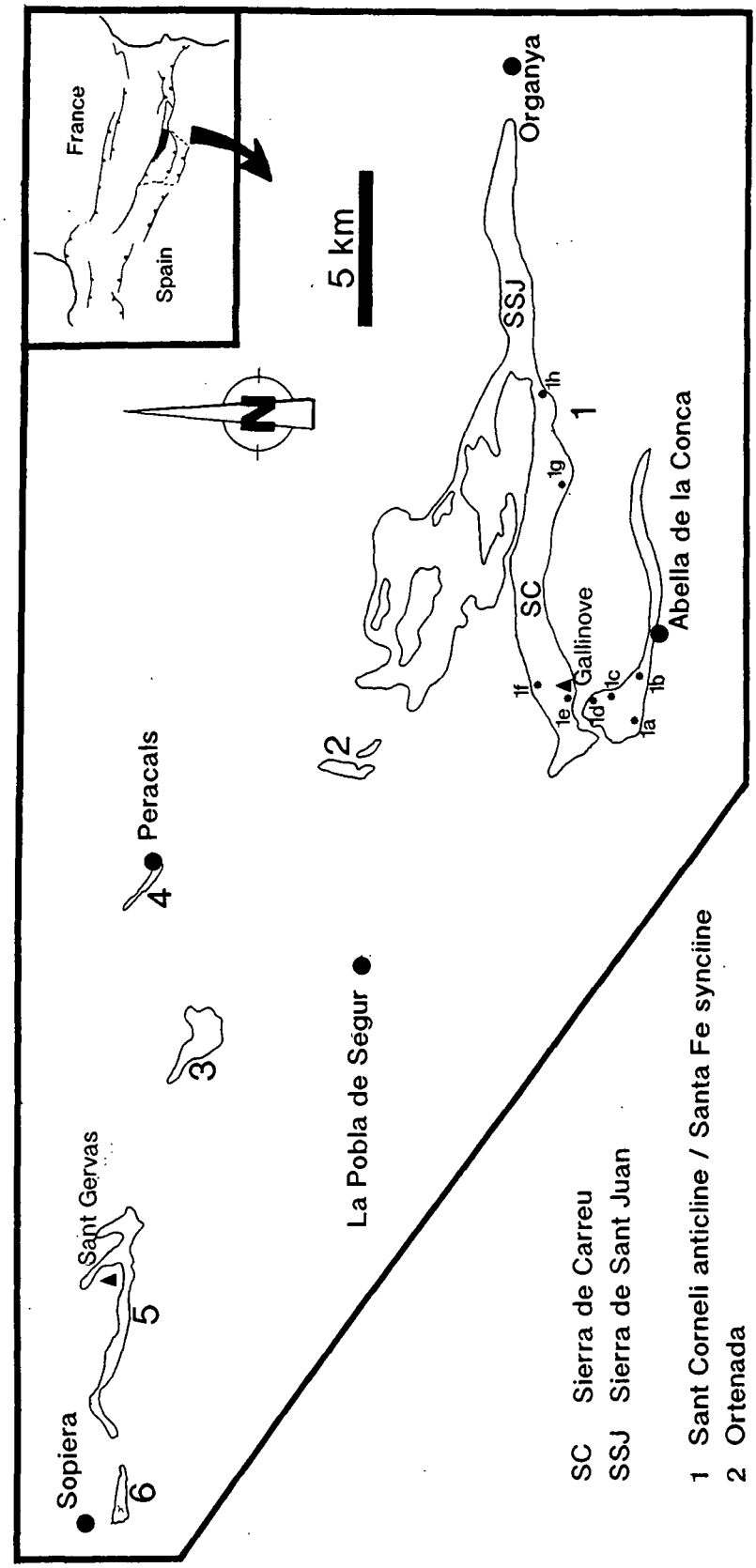


**Fig. 4.1.** Outcrop map of the Congost platform, slope and basinal sediments in the Tremp basin. Localities which are described in this chapter have been labelled.


**Fig. 4.2.** Northeastward view of a section of the Sierra de Carreu. The line of bushes (arrowed) towards the base of the cliff marks the position of the recessive Reguard Formation, which separates the Santa Fe and Pardina Limestones (SP) + sp below from the Congost platform unit (C) above. Note clinoforms, which are dipping to the northwest, within the Congost platform unit. Cliff is 170 metres high.

## 4.2.2 The Reguard Formation

### 4.2.2.1 Description

The recessive unit resting on top of the Pardina Limestone is the Reguard Formation. It is approximately 6 metres thick and can be traced along the whole length of the cliffs around the Sant Corneli and Santa Fe folds (see Figs. 4.2, 4.4, 4.6 & 4.7b together with log 1 in appendix 1)). At its base this recessive unit consists of a very fine grained wackestone which has a grainsize of approximately 0.025mm (see Fig. 4.3b(i)). Moving upwards the texture of the unit changes to that of a packstone and the grainsize increases gradually to approximately 0.1mm at the top of the unit (see Fig. 4.3b(ii)). The packstone contains calcispheres, sponge spicules, planktonic foraminifera, quartz grains (1 - 3%) and many small shell fragments including echinoderm and bivalve debris. The increase in grainsize upward through this unit is accompanied by an increase in the abundance of shell debris and multi-chambered foraminifera, as well as the appearance of glauconite grains in some places. The boundary between this recessive unit and the overlying clinoforms of the Congost

platform is a gradual one, which is difficult to pin-point at close quarters in the field (see Fig. 4.3a).

### 4.2.2.2 Interpretation

The Reguard Formation is interpreted to represent a starved deeper-water facies which was being deposited basin-ward of the advancing Congost platform. The gradual increase in grainsize and platform derived material upwards through this unit (see Figs. 4.3b(i) and 4.3b(ii)) is a result of the prograding platform. As the platform advanced then at any one point in the basin there would be a gradual increase in the supply of fine grained skeletal debris from the platform top. The transitional nature of the upper boundary of this formation (see Fig 4.3b) is a result of the gradual facies change from deep-water pelagic sediments to the slope facies of the advancing Congost platform.

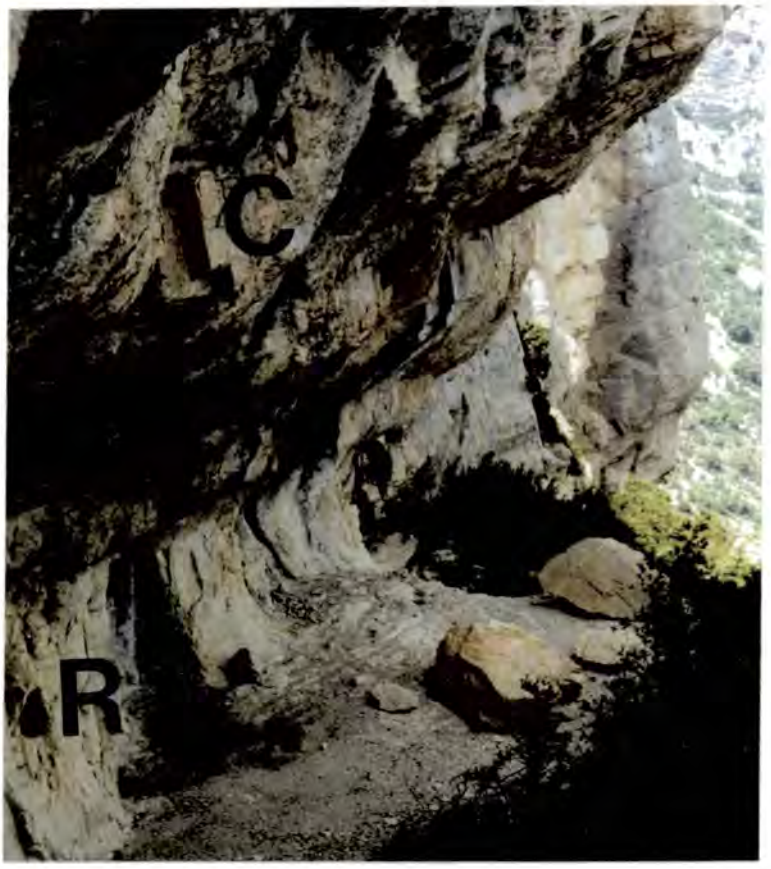


**Fig. 4.3a.** The recessive Reguard Formation (R) outcropping at the base of the Congost clinoform unit (C). Note, there is no distinct boundary between the two units, only a gradual increase in grainsize and resistance to weathering. Cliffs to the north of Abella de la Conca (locality 1c, Fig. 4.1). Rucksack 0.5 metres in height for scale.

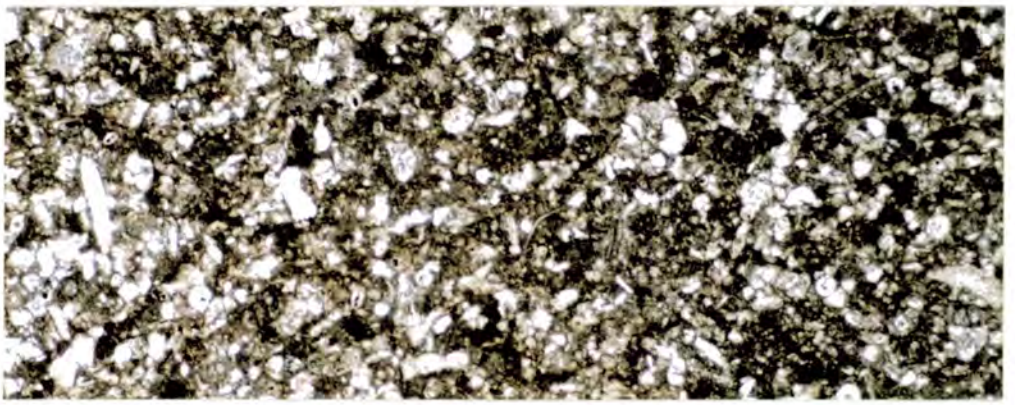

**(i)**

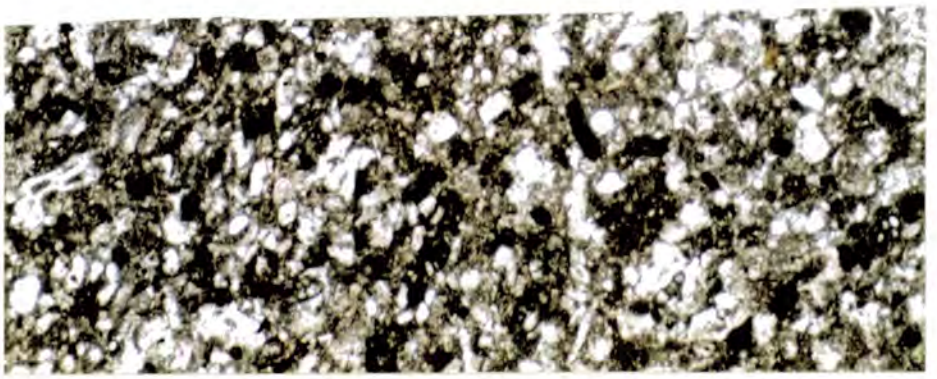

**(ii)**

**Fig. 4.3b.** Photomicrographs taken under crossed polarised light from (i) towards the base and (ii) towards the top of the Reguard Formation. Both consist of fine grained packstones containing calcispheres, fine grained shell debris, sponge spicules, silt grade quartz, foraminifera and some glauconite. Note, the larger grainsize and greater amount of shell debris within sample (ii). Samples (i) AZ/1 and (ii) AZ/9. Cliffs to the north of Abella de la Conca ( locality 1c, Fig. 4.1). Field of view 3 x 1mm for both.

## 4.2.3 The Congost platform clinoform unit

### 4.2.3.1 Introduction

The cliffs around and to the north of Abella de la Conca and their continuation along the Sierra de Carreu and Sierra de Sant Juan are the best exposed and most easily accessible parts of the outcrop (see Figs. 4.1, 4.2, 4.4 & 4.6). These cliffs, which are 22km in length and have an overall east-north-east to west-south-west orientation, represent the southern flank of the Santa Fe syncline and provide a continuous section through the Congost platform.

When viewed from a distance the cliffs appear for the most part to be horizontally bedded. However, in the places where the orientation of the cliffs is offset from the general east-north-east to west-south-west direction, the Congost limestone can be seen to consist of gently dipping clinoforms (see Figs. 4.2 and 4.5).

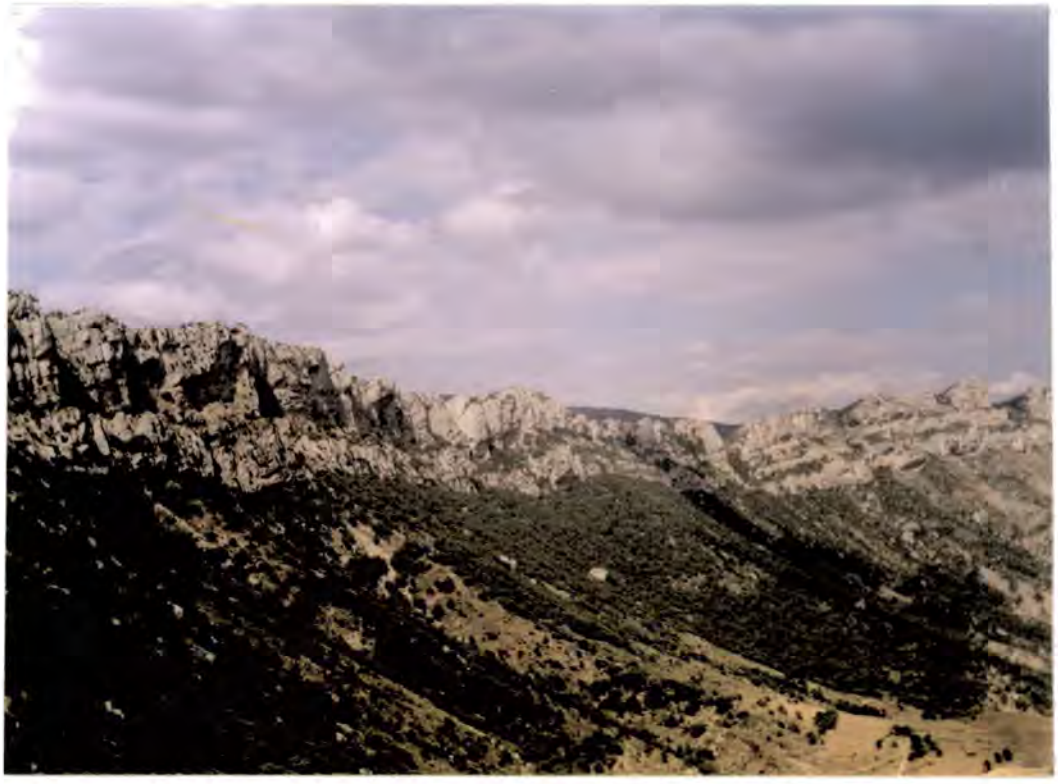

**Fig. 4.4.** Northeastward view of the eastern end of the Sierra de Carreu. The Congost platform sediments form the upper part of the cliffs, above the line of bushes which mark the location of the Reguard Formation. The cliff is 160 metres high.

**Fig. 4.5.** Sigmoidal clinoforms of the Congost platform, dipping towards the north-northwest. West side of coll below Gallinove (locality 1d, Fig. 4.1). 4 metre high wall (circled) for scale.

### 4.2.3.2 Geometrical overview

The clinoforms are best seen, and are most steeply dipping, in parts of the cliffs that have a northwest-southeast orientation. One such location is on the west side of the coll below Gallinove (locality 1d on Fig. 4.1), where the clinoforms can be seen to possess a sigmoidal geometry and are dipping to the northwest (see Fig. 4.5). Measurements of the present angle of dip of the clinoforms, relative to the beds of the underlying Pardina Limestone show that when they were deposited they had an original dip to the north-northwest with a greatest angle of 16$^{o}$.

The thickness of the Congost Limestone clinoform unit can be seen to vary gradually along the length of these cliffs from approximately 80 metres at the coll below Gallinove to around 120 metres along the east-north-eastern end of the Sierra de Sant Juan. This variation in thickness is best seen in the cliffs just to the north of Abella de la Conca (localities 1b through to 1d on Fig 4.1), where a north-south cross-section through the Sant Corneli anticline can be seen (see Fig 4.6). The village of Abella de la Conca is actually built into the cliffs which form the southern limb of this fold. Here the Congost clinoform unit is only 35-40 metres thick, however; as it

**Fig. 4.6.** Northwestward view of the Sant Corneli anticline. The coll below Gallinove can be clearly seen just to the right of centre. Note that the Congost platform clinoform unit (arrowed) is much thinner (35 metres) on the southern limb, than it is on the northern one (80 metres).

is traced northwards around the fold, its thickness gradually increases until the 80 metre thick section at Gallinove is reached.

At the localities where the clinoforms can be clearly seen their lower boundaries display a parallel relationship with the top of the Pardina Limestone Formation (see Figs 4.2 and 4.5). These small scale observations are supported by the uniformity in thickness of the deep water facies (Reguard Formation) around the whole of the Sant Corneli and Santa Fe fold outcrop. From a distance the lower boundary of the clinoform unit appears to show a down-lap relationship; however, when examined more closely the boundary can be seen to be one of gradual facies change and thinning of the clinoform strata into the horizontally-bedded pelagic sediments of the Reguard Formation (see Fig. 4.3b).

The upper boundary of the clinoform unit, when viewed from a distance, can be seen to exhibit top-lap whereby the inclined strata forming the clinoforms terminate against the horizontally-bedded carbonates of the platform top (see Fig. 4.2). The latter, where they are accessible, are of a uniformly small thickness (10 -15 metres) over the entire outcrop around the Sant Corneli and Santa Fe folds.

### 4.2.3.3 Sedimentological overview

Moving east-north-eastwards along the cliffs which mark the southern flank of the Santa Fe syncline there is a slight increase in the grainsize of sediments forming these clinoforms. In the cliffs around Abella de la Conca there is a prevalence of fine-grained packstone (< 0.25mm grainsize), whereas in the cliffs at locality 1g (see Fig. 4.1) and farther to the east near Boixols, the clinoforms are composed, for the most part, of medium to coarse grained packstone and grainstone ( 0.25 - 3mm grainsize).

All along the outcrop of the Congost Limestone clinoforms there is a vertical variation in grainsize (see Fig. 4.7b together with log 3 in appendix 1). On a large scale there is an overall coarsening upwards through the cliff sections from a fine-grained (0.1mm) packstone containing small shell fragments, calcispheres and quartz (<3%) resting on top of the Reguard Formation up to a coarse-grained (>1mm), well-rounded grainstone containing abundant shell fragments, peloids, miliolids and other large benthic foraminifera, at the top of the clinoform cliff sections. Detailed logging and sampling revealed that these cliff sections can be divided up into several 10 to 20 metre thick, coarsening-upward units. Each unit includes several clinoforms and has boundaries which are marked by sharp grainsize variations.

### 4.2.3.4 Measured section along the west side of Gallinove

The measured section from the west side of Gallinove (locality 1e on Fig.4.1) shows the cyclic nature of the Congost Limestone clinoforms well (see Figs. 4.7a & 4.7b). Forty metres from the base of the cliff the very fine-grained, easily-weathered Reguard Formation is reached. The fine-grained packstone of the Reguard contains small shell fragments, calcispheres, sponge spicules and quartz grains. The Reguard shows a gradual increase in grainsize and in the relative abundance of shell debris and benthic foraminifera upwards.

The gradual changes in grainsize and relative abundance of bioclasts continue upwards into the base of the Congost clinoform unit and form the first coarsening-upward cycle which ends 51 metres from the base of the section. Towards the top of this first cycle the relative abundance of quartz grains increases to almost 10% . The upper surface of this first cycle has a distinct red colour and an irregular topography with a relief reaching 40cm (see Fig. 4.8a). In thin section this surface can be seen to be perforated by numerous borings, some of which are infilled by the overlying sediment (see Figs. 4.8b & 4.8c).

The overlying sediment has a packstone texture and contains the same grain types as that below, but has a slightly smaller grainsize and lower relative abundance of shell debris. The most striking feature of this packstone though is that it contains abundant glauconite grains which are relatively large (up to 0.3mm), when compared to the very fine-grained nature of this packstone (see Fig. 4.8b). Continuing up section through this second cycle the abundance of glauconite decreases rapidly within metres until it is only present in trace amounts. Similar variations in grainsize and relative abundance of grains to those in the cycle below are observed in the packstones of this cycle. This second cycle is approximately 10 metres thick and contains 9 visible beds which when seen from a distance represent clinoforms. Grainsize increases gradually through the cycle until the top bed is reached which shows a marked increase in grainsize from that below and consists of a medium to coarse grained (approximately 0.5mm) very closely packed grainstone containing abundant rectangular mollusc fragments, some echinoderm debris and peloids.

The third cycle covers 20 metres of the section and begins with a sharp boundary on top of the grainstone of the second cycle. It consists of a fine-grained (<0.1mm) packstone containing small shell fragments, calcispheres, quartz grains and foraminifera. The cycle shows the familiar increases in grainsize and relative abundance of shell debris and foraminifera towards its top and includes several distinct beds.


**Fig. 4.7a.** West side of Gallinove (locality 1e, Fig. 4.1), showing the Santa Fe Limestone (S), the Pardina Lmst. (P), the Reguard Formation (R), and the Congost platform slope sediments (C). Path of measured section M2 is marked by the black line.

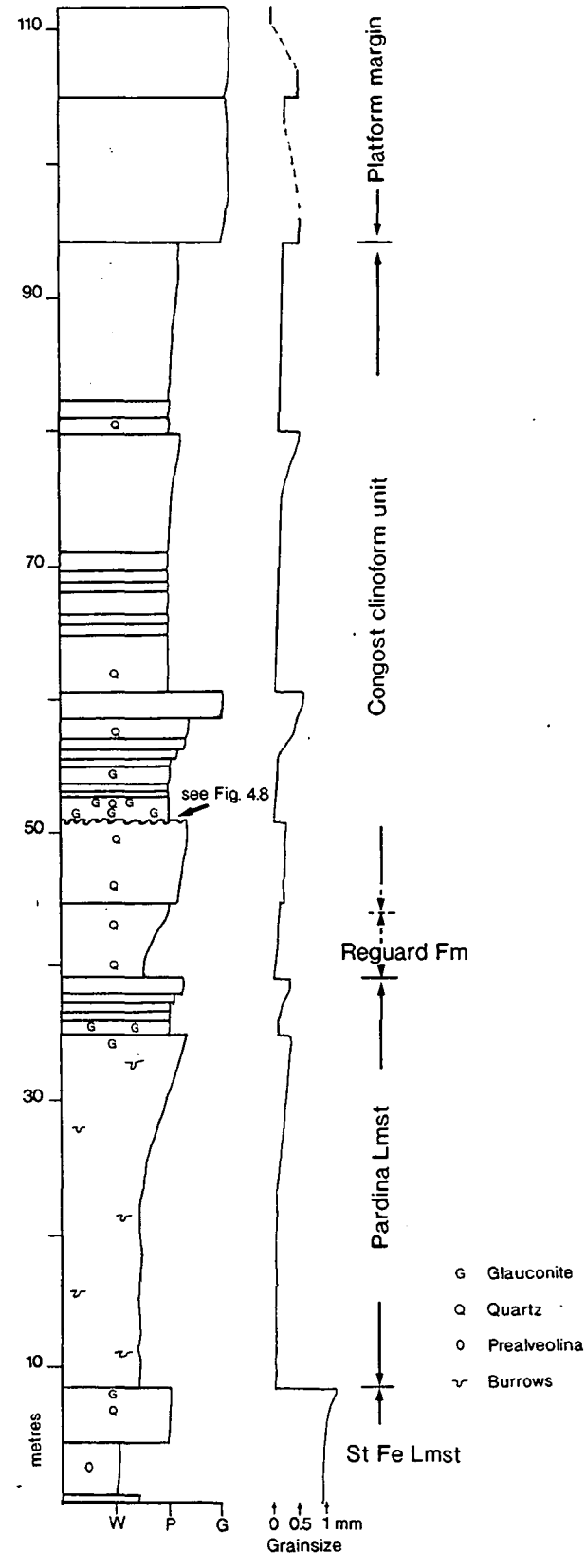


**Fig. 4.7b.** Measured section M2. Note the four coarsening upward cycles within the Congost clinoform unit.

Above this third cycle grainsize fines once again; however, 14 metres farther up the section there is an abrupt facies change where the fine-grained packstones give way to medium and coarse-grained grainstones. These grainstones contain abundant rectangular bivalve fragments with micrite rims, echinoderm debris, peloids and miliolids. In fact these grainstones are very similar in character to the grainstone seen at the top of the second cycle. The remaining 18 metres of section before the top of the cliff consist of medium and coarse grainstones. At the very top of the cliff the grainstones are very well rounded and contain a greater relative abundance of peloids, miliolids and other benthic foraminifera than the grainstones lower down.

Following the section over the top of the cliff and down the dip slope behind reveals easily eroded beds containing large hippuritid rudists and small isolated coral colonies in life position (see logs 6 & 7 in appendix 1). These rudists and corals are set in a micritic matrix, which contains miliolids and other benthic foraminifera, as well as some angular shell debris. These beds mark the beginning of the platform top sediments.

---

**Fig. 4.8.** Red horizon with irregular relief, from the top of the first coarsening upward cycle within the Congost clinoform unit, on the west side of Gallinove (see Fig. 4.7b)(locality 1e, Fig. 4.1).

**a)** Field photograph. Note the borings within the red horizon (light coloured patches) and the abundant glauconite (green specks) in the overlying sediment. Lens cap for scale.

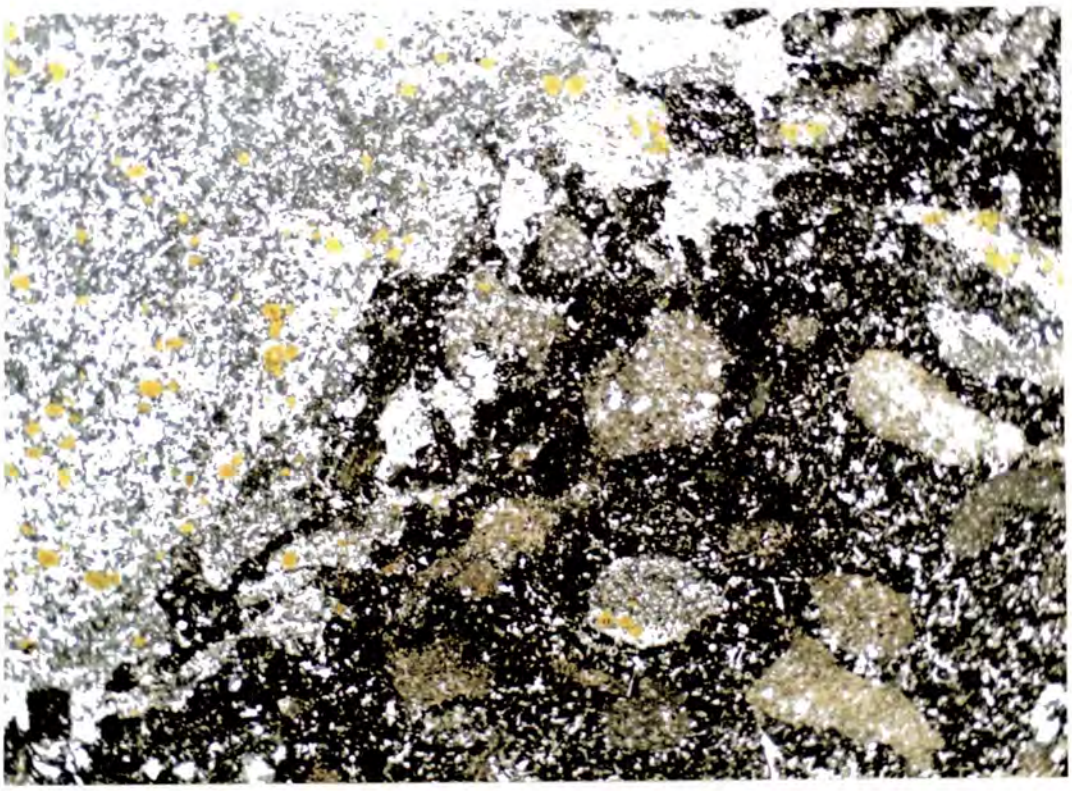

**b)** Photomicrograph. Note the abundant glauconite in the overlying fine grained packstone (top left). Note also the abundant borings within the red horizon (bottom right), some of which contain the distinctive overlying packstone. Sample M2/17. Field of view 12 x 7mm.

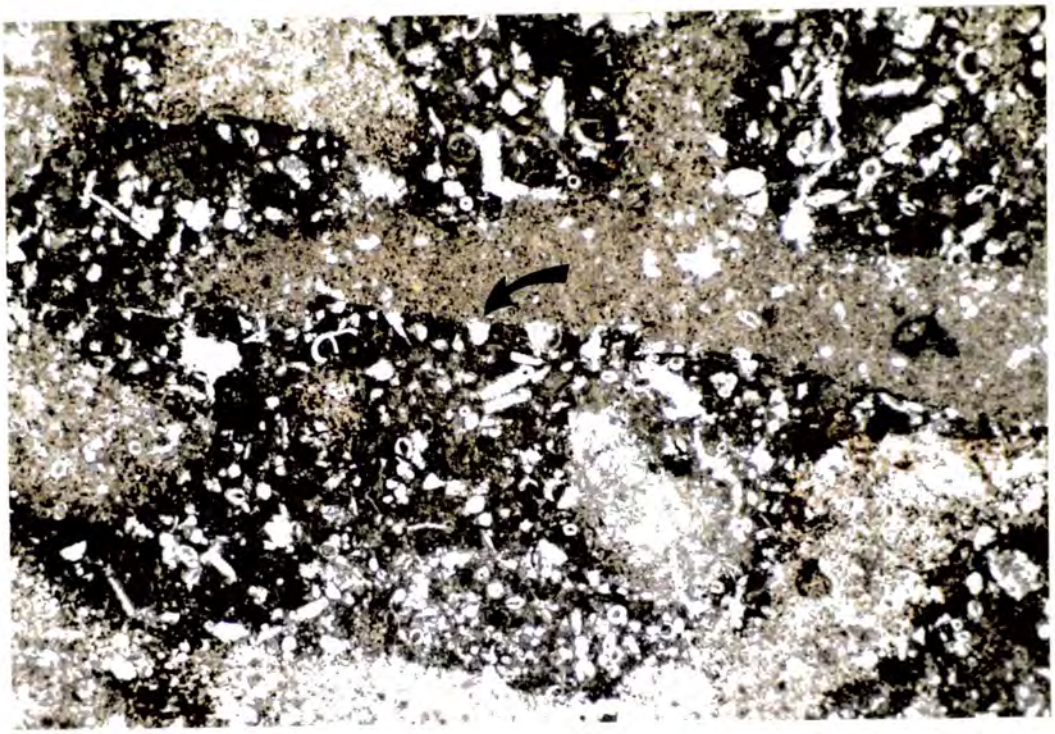

**c)** Photomicrograph, showing close up of the borings within the red horizon. Note the truncation of grains at the edge of the borings (arrowed). Sample M2/17. Field of view 3 x 2mm.

### 4.2.3.5 Discussion and interpretation

The large-scale geometry of the Congost platform in the region of the Santa Fe and Sant Corneli folds is that of a wide tabular progradational body which thickens slightly in a basinward direction (see Fig. 4.6). The progradational nature of the platform is shown by the presence of clinoforms (see Figs. 4.2 and 4.5) and the overall coarsening upward nature of the carbonates through the various vertical sections studied (see Fig. 4.7 together with log 3 in appendix 1). The general direction of progradation can be inferred to have been towards the north-northwest as this is the direction in which the clinoforms are seen to possess their greatest angle of dip.

Work by Bosellini in the Italian Dolomites (Bosellini, 1984) has suggested that the nature of a platform's progradation is controlled by a number of factors which interact with each other (see Fig. 4.9). These factors include: (1) The rate of basinal sedimentation, which will control the basal relationships of the prograding clinoforms. (2) The rate of subsidence of the platform, which will mainly control the top relationships of the prograding platform and its rate of lateral progradation, but will also effect the basal relationships and angle of slope of the clinoforms. (3) The width of the platform, which will control the slope declivity and can have some influence on the rate of progradation. (4) The depth of the surrounding basin, which will mainly influence the slope declivity and the rate of progradation. (5) Variations in sea-level, which will mainly influence the top relationships. Also important is the nature of the sediment, a reflection of the energy level of the platform and the organisms producing carbonate, which will have an effect on the angle of the platform's slope (Kenter, 1990).

The progradational nature and the vast volume of sediment contained in the Congost clinoforms suggest that the Congost platform top was a highly productive area. The top-lap of the upper boundary of the clinoforms together with the small and uniform thickness of the platform top sediments (see Fig. 4.2) suggests that during their deposition accommodation space on the platform top was not increasing. Once the platform top carbonates had built up to or very near to base level then carbonate production continued but virtually all the sediment produced was transported off the platform to be incorporated into the advancing clinoform strata. The platform top system would have been advancing over the top of the clinoforms as they prograded. The fact that the platform top system was able to move basinward in order to fill the available accommodation space suggests that any protective barrier would have been mobile in nature.

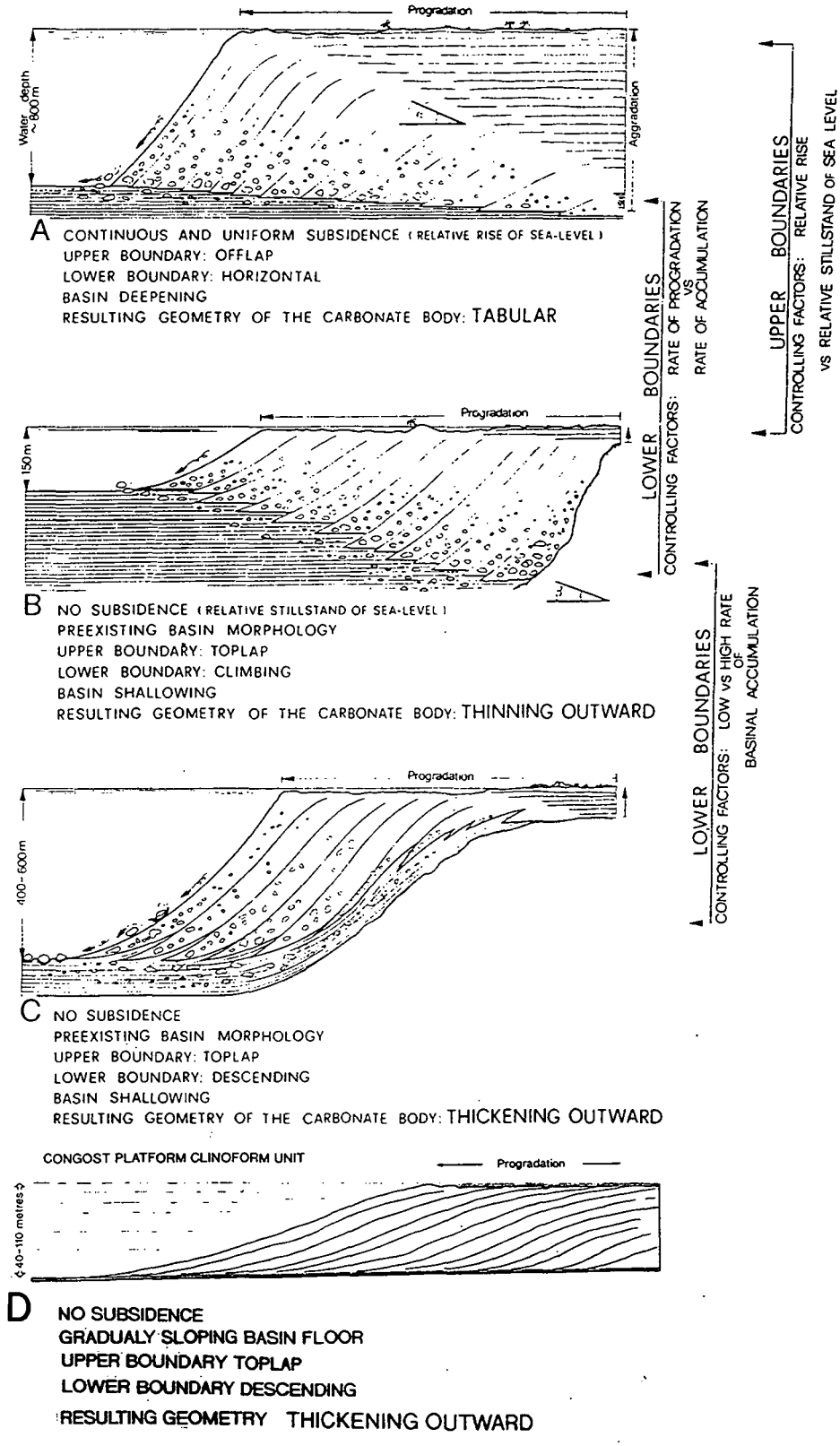


**Fig. 4.9.** The basal and top relations of prograding clinoform packages, from the Triassic of the Dolomites (A, B and C) (Bosselini 1984), compared to those of the Congost platform clinoform unit (D).

The gradual basinward increase in thickness of the platform indicates that it was prograding onto a sea floor which was sloping in a basinward direction. Although in reality this slope would have been variable in nature, an estimate of the gradient of the slope can be made by applying simple trigonometry to information derived from the north-south cliff section through the Sant Corneli anticline (see Fig. 4.6). This cliff section shows the prograding Congost platform to increase in thickness from 35 to 80 metres over a horizontal distance of approximately 4 kilometres (after allowing for the curvature of the fold), which after calculation, indicates that this part of the sea floor had an overall inclination of approximately $0.6^0$ below horizontal in a northerly direction.

The nature of the basal part of the platform, whereby the lower boundary of the clinoforms rests on top of a very thin package of deep-water sediments (the Reguard Formation), which have a fairly constant thickness over the entire length of the 40km long outcrop, can be interpreted to suggest that either the rate of sedimentation in the basin was very slow or that the rate of platform progradation was rapid. The most likely explanation would be a combination of both these situations.

The $16^0$ maximum slope of the Congost platform clinoforms (see Figs. 4.2 and 4.5) seems to agree with data collected by Kenter (1990) which suggests that slope declivity is a factor, amongst other things, of the dominant sediment fabric and the height of the slope. The maximum clinoform slope angle of $16^0$ is similar to that measured on the slopes of other fossil carbonate platforms which have a dominant packstone fabric and are of a comparable height to the Congost platform (see Fig. 4.10B). When this $16^0$ slope angle for the Congost platform is plotted on a graph showing height versus slope angle together with data taken from the flanks of Triassic carbonate platforms in the Italian Dolomites, it can be seen that the slope of the Congost clinoforms plots on the trend suggesting that slope declivity is related to slope height (see Fig. 4.10A).

From his work in the Dolomites Bosellini (1984) noted that there was a tendency for slope sediments composed of mud, sand and gravel to flatten out in their lower parts and produce oblique-tangential or sigmoid-oblique progradation patterns, whereas oblique - parallel patterns are more common where the sloping strata are composed of coarser talus debris (mega-breccias). The sigmoidal nature of the Congost clinoforms (see Figs 4.2 and 4.5) is probably a function of their fine-grained and mud-rich sediment. The nature of the sediment would mean that, after moving down the slope under the influence of gravity, fine sediment continued travelling in suspension so that the lower parts of the slope become flattened.

The deposition of sediment away from the foot of the slope may also suggest that sediment transport was enhanced by currents which may have been brought about

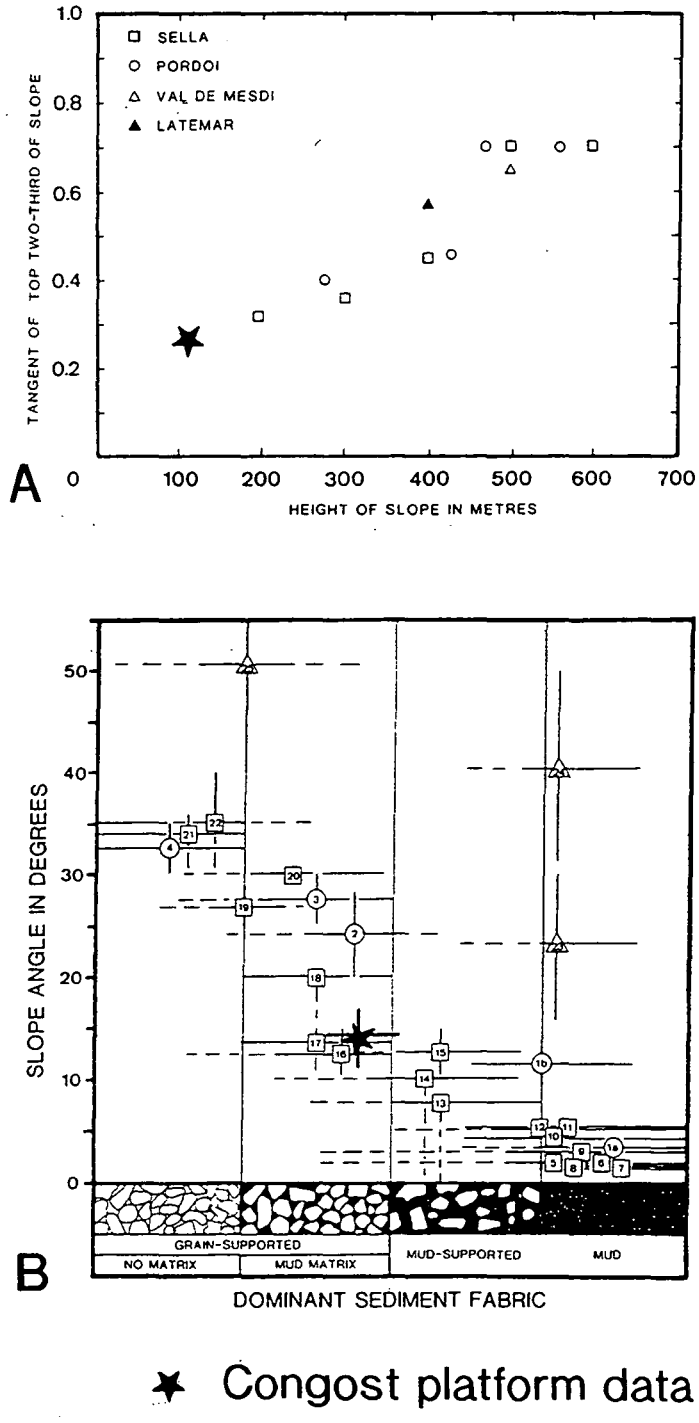


**Fig. 4.10.**

**A)** Plot of slope height vs. overall dip from Triassic carbonate platforms of the Dolomites (Kenter 1990). Congost platform data have been added.

**B)** Plot of slope angle vs. dominant sediment fabric for carbonate platform flanks, both recent and ancient, from around the world (Kenter 1990). Data from the Congost platform have been added.

by the action of offshore winds. Transport of sediments in this way would suggest that these sigmoidal clinoforms were in fact analogous to the concave upwards fore sets seen in the cross bedding of fluvial sandstones. The presence of a strong offshore wind is also suggested by the presence of silt-grade quartz grains, which are particularly evident in horizons that are relatively starved of platform-derived material. If it is assumed that this silt-grade quartz was blown in at a fairly constant rate then the variation in its concentration indicates that there was a slower rate of carbonate sediment supply during the deposition of finer grained slope sediments.

Several measured sections in this study have shown the inclined slope sediments to be cyclic (see Fig. 4.7 together with log 3 in appendix 1). These 10 to 20 metre thick cycles record a gradual change in sedimentation at any one point on the slope from finer grained material with a lower relative abundance of platform-derived grains (relatively more distal facies) to coarser usually less mud rich sediments which contain a greater abundance of platform-derived material (relatively more proximal facies). The cycle boundaries are marked by abrupt changes from the more proximal facies below to the more distal facies above.

In the measured section at Gallinove (see Fig. 4.7), the top of the lowest coarsening upwards cycle is marked by an irregular surface which has a distinctive red colour and has been attacked by boring organisms (see Figs. 4.8a, 4.8b & 4.8c). This bored surface is overlain and infilled by sediment which contains abundant glauconite grains. This surface is interpreted to represent a localised hardground which developed during a period marking the end of the depositional cycle, when the lower part of the platform slope was starved of sediment. The glauconite which overlies and infills the borings into this surface suggests that sedimentation rates following the development of the hardground were sufficiently slow and that there was sufficient metabolizable organic matter present for a postoxic-nonsulphidic environment to develop (Berner, 1981; Odin and Matter, 1981).

The cycles within the clinoforms could be the result of variations in platform productivity due to environmental factors or they may be related to small-scale relative sea-level fluctuations. As the source for these clinoform sediments would ultimately have been on the platform top then it is important to study the platform top sediments before reaching any conclusions regarding the cause of these cycles.

## 4.2.4 Platform-top sediments

### 4.2.4.1 Introduction

In a few places where the cliffs are high enough the inclined strata of the Congost Limestone clinoforms can be seen to have an upper boundary where they terminate against a relatively thin unit of horizontally-bedded strata (see Fig. 4.2). Elsewhere these horizontally-bedded carbonates can be found by searching on the dip slopes behind the cliffs (see logs 6 & 7 in appendix 1). At all the localities where the platform-top carbonates occur the nature and thicknesses of the sediments are remarkably similar (see Fig. 4.11c together with logs 4, 6 & 7 in appendix 1).

### 4.2.4.2 Sedimentological features

The lowest beds consist of medium to coarse grained grainstones containing a variety of sub-rounded grains with micritic rims including fragments of echinoderms, bivalves, brachiopods, bryozoans, coralline algae as well as miliolids and other benthic foraminifera.

Above the grainstones, several beds of fine to medium grained packstones usually occur. These packstones contain a large number of micritised miliolids and other large benthic foraminifera together with peloids, some of which appear to be the result of the total micritisation of shell fragments. Also present are some fairly angular fragments of echinoderms, rudists and other shells.

Above these packstones there is an easily eroded unit which varies from 5 to 10 metres in thickness depending on the locality. Where well exposed and of sufficient thickness, such as on the slopes above Casa Borrell (locality 1b, Fig. 4.1), this unit can be seen to consist of a series of beds (see Figs. 4.11a, 4.11b and 4.11c together with log 4 in appendix 1)) approximately 2 metres thick, with a weathering profile whereby the base and central part have been eroded back relative to the more resistant upper 20 to 40cm. The beds contain rudists and small coral colonies together with other small organic frameworks, in life position, surrounded by a wackestone matrix. The corals and rudists are usually in fairly equal abundances, however sometimes beds occur which contain many more coral colonies than they do rudists, and visa versa (eg Fig. 4.11c). The wackestone matrix contains mainly large angular fragments of rudists and corals with some echinoderm and other shell debris as well as miliolids and other large benthic foraminifera (see Fig. 4.11c(ii)). The large fragments of coral and rudist in this wackestone are commonly enveloped by coralline algae. These fragments also contain many borings, some of which are quite

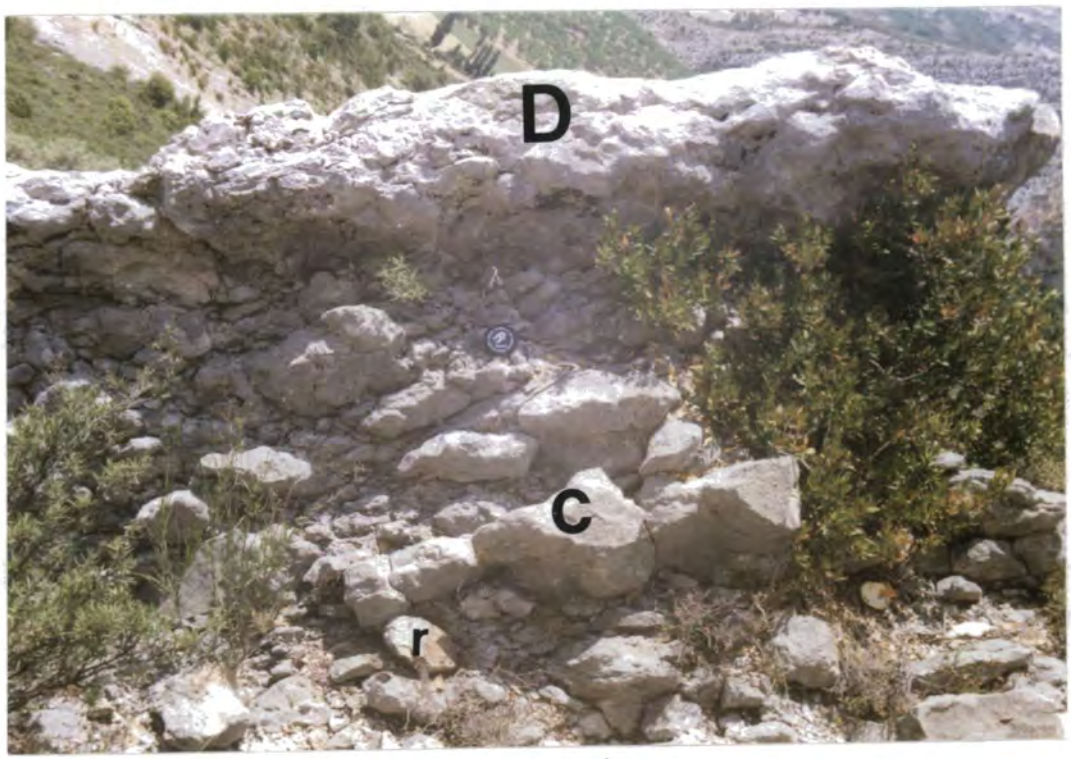


**Fig. 4.11a.** Typical bed of Congost platform top sediments exposed above Casa Borrell (locality 1a, Fig. 4.1). Note the rudists(r) and coral colonies (c), which are surrounded by an easily eroded wackestone matrix. The upper part of this bed (D) has a packstone texture and contains abundant skeletal debris. Lens cap for scale.

**Fig. 4.11b.** Close up of large hippuritid rudist. Above Casa Borrell (locality 1a, Fig. 4.1). Lens cap for scale.

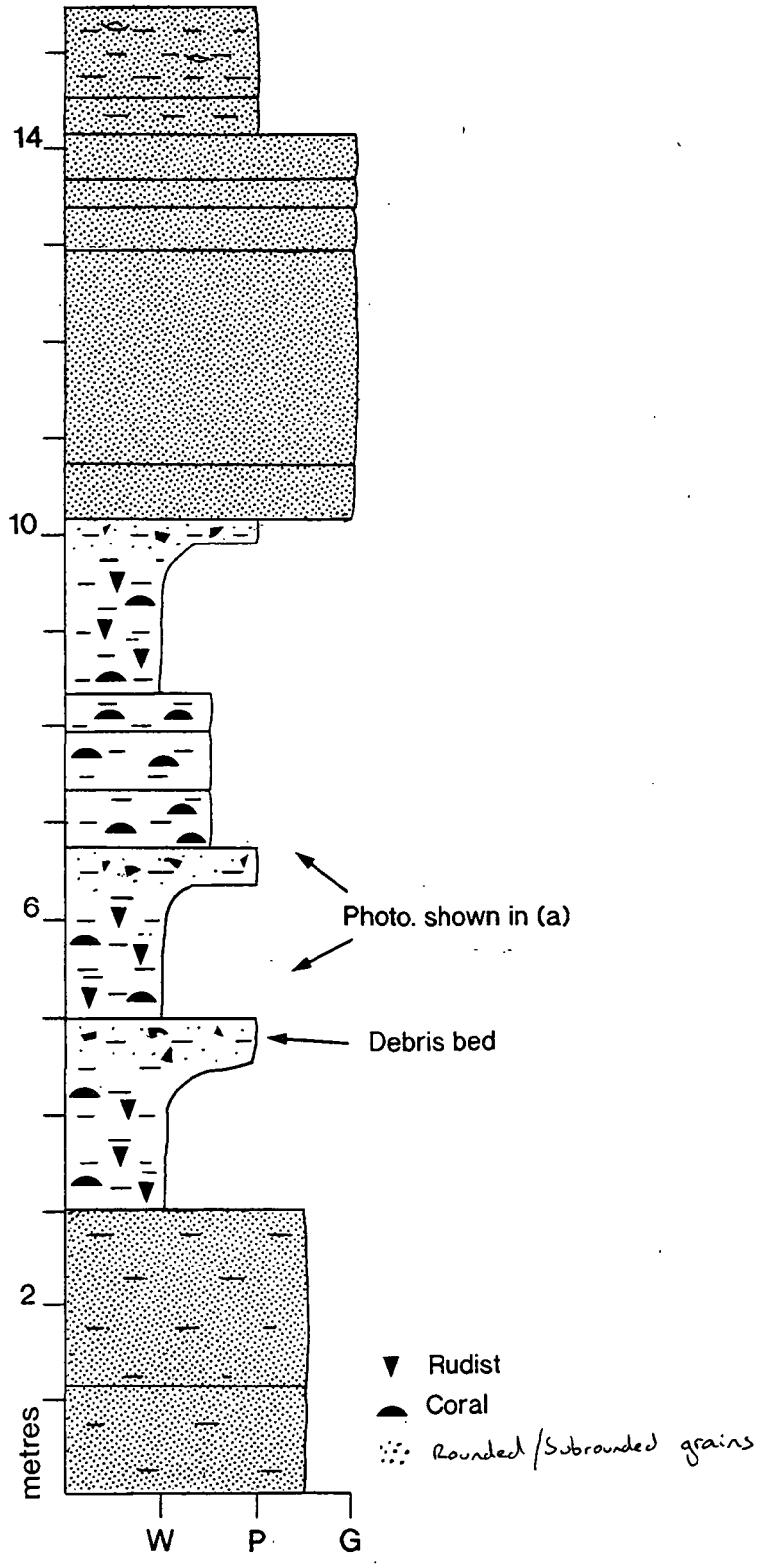


**Fig. 4.11c.** Sedimentary log through the platform top sediments, exposed above Casa Borrell (locality 1a, Fig. 4.1). Note, the 4 metre thick grainstone bed at the top of these sediments. Position of photograph Fig.4.11a is marked.

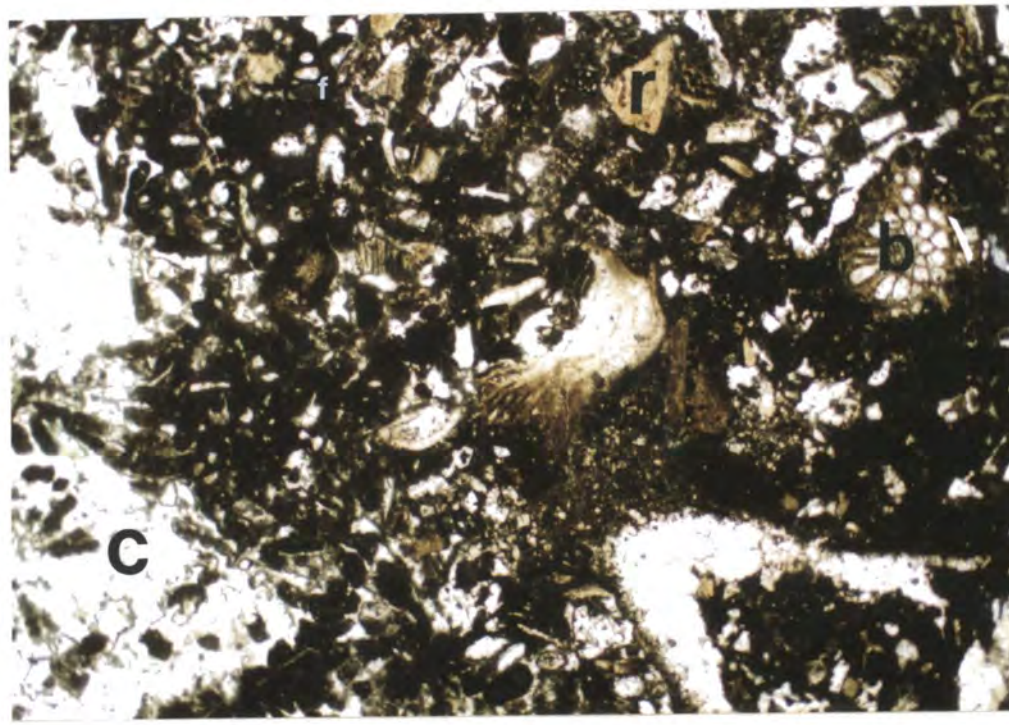


**Fig. 4.11c(i).** Photomicrograph of a packstone debris bed. Note the pervasive dissolution which has effected the originally aragonitic shell fragments. Fragments of coral (c), rudist (r), bryozoan (b) and foraminifera (f) can be seen. Sample AX/9, Casa Borrell (locality 1a, Fig. 4.1). Field of view 12 x 7mm.

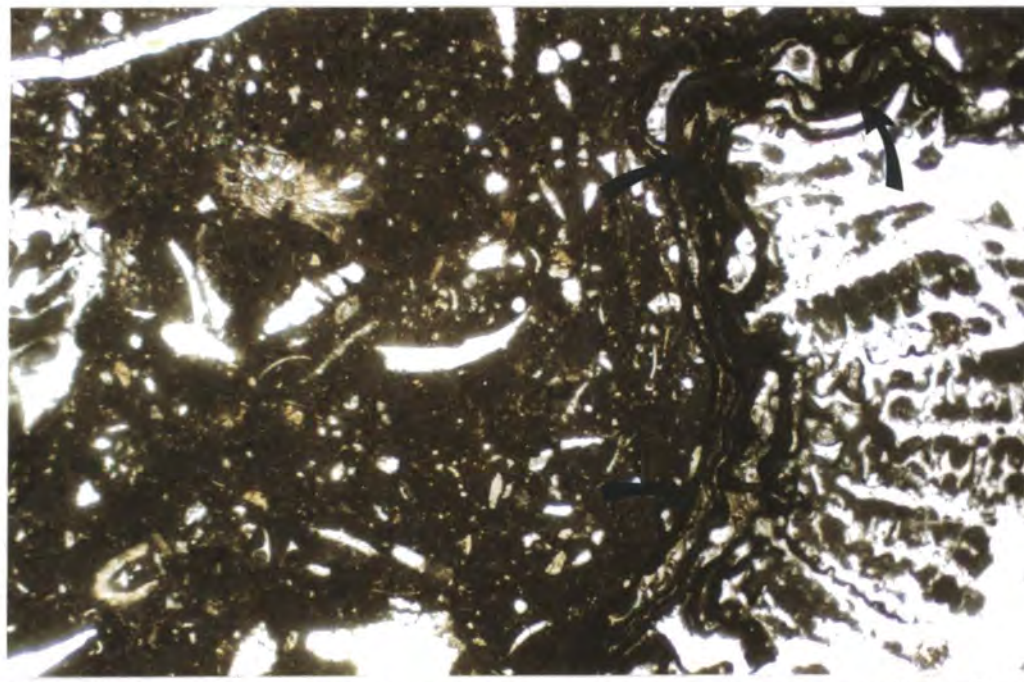

**Fig. 4.11c(ii).** Photomicrograph of the wackestone matrix which surrounds the rudists and corals. Note that almost all the shell fragments have been replaced by calcite spar. Note also the algal colony (arrowed), which has grown around the edge of a coral fragment. Sample AH/5, Casa Borrell (locality 1a, Fig. 4.1). Field of view 12 x 7mm.

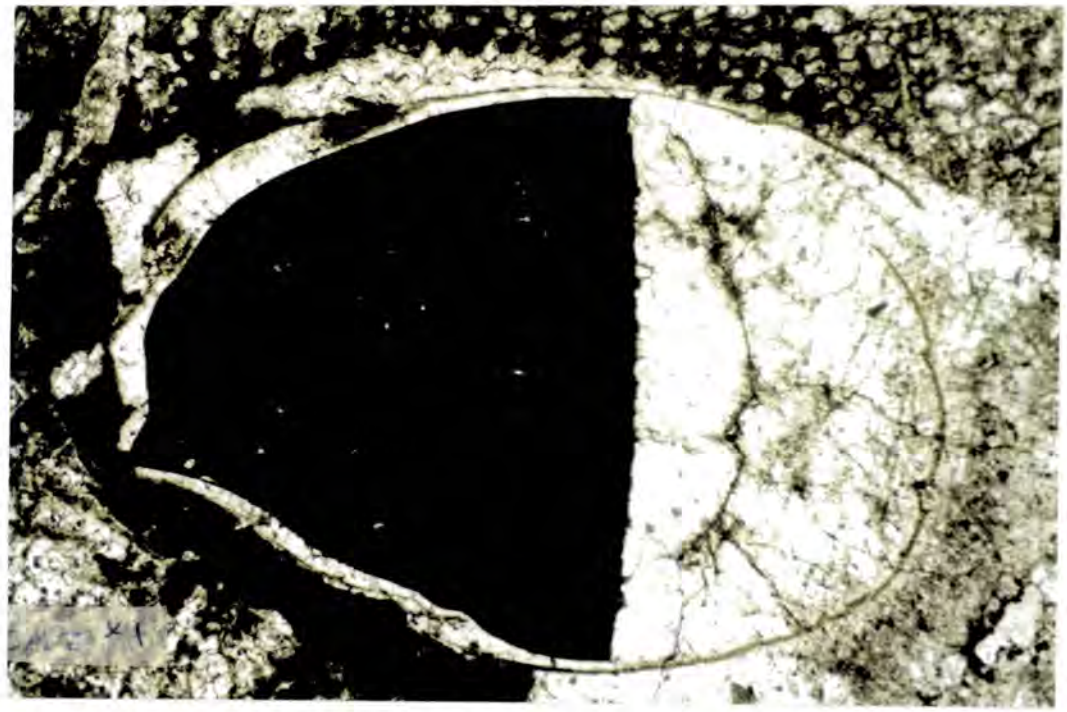

**Fig. 4.11c(iii).** Photomicrograph showing a typical boring within a coral, from the Congost platform top sediments. Note the Lithophagid bivalve shell which is still present. Sample CA/2, north side of Gallinove (locality 1f, Fig4.1). Field of view 12 x 7mm.

large and contain the shells of lithophagid bivalves (see Fig. 4.11c(iii)). The upper, less easily eroded top layers to the beds have more of a packstone texture and contain fragments of rudists, corals, bryozoans, bivalves, brachiopods, echinoderms and other organisms as well as miliolids and other foraminifera (see Fig. 4.11c(i)). When the skeletal fragments in the packstones layers at the top of these beds are compared to those in the wackestone matrix surrounding the rudists and corals it is noticeable that on average their size is slightly smaller and also that they do not possess any coatings of coralline algae.

Everywhere along the cliff exposures where these platform top sediments can be found, there is a prominent resistant bed 3 to 4 metres thick which rests with a sharp base on top of the rudist and coral unit (see Figs. 4.11c & 4.12a together with logs 4, 5, 6 & 7 in appendix 1). At most localities this resistant bed is composed of sub-rounded, poorly sorted grainstone (see Fig. 4.12b) which is fine/medium grained at the base of the bed and coarsens upwards towards the top. The grainstone contains abundant miliolids and benthic foraminifera, particularly at the base of the bed. Upwards as the grainsize increases then so does the abundance of skeletal fragments, including fragments of rudist, coral, bryozoan, echinoderm, algae, brachiopod and bivalve. At some localities this resistant bed has a packstone texture; however, the grain content and coarsening-upward nature of the bed are still the same.

The upper surface of this prominent and extensive bed is fairly planar and is overlain by quartz-rich packstones, which contain abundant oysters and have a distinctive brown colour.


**Fig. 4.12a.** Eastward view of the slopes above Casa Borrell (locality 1a, Fig.4.1). Bedding dips to the south as part of the southern limb to the Sant Corneli anticline. Here a section through the upper part of the Congost clinoform unit (C), Congost lagoonal sediments (L), and the deep shelf sediments of the overlying Sant Corneli platform (S) can be seen. Note the prominent bed marking the top of the Congost lagoonal sediments (arrowed). Track 2 metres wide for scale.


**Fig. 4.12b.** Photomicrograph showing the poorly sorted grainstone of which the prominent bed in (**a**) is composed. Note the large number of milliolids (M) and other multichambered foraminifera (F), together with various types of shell debris. Note also the well developed micritic margins around all grains. Sample AX/18 from above Casa Borrell (locality 1a, Fig 4.1). Field of view 3 x 2mm. (Note that photograph is upside down)

### 4.2.4.3 Interpretation of these sedimentological features

The sub-rounded and mud-free nature of the grainstones which are found in the lower parts of these exposures suggests that they were deposited in a relatively high energy environment. Such an environment would have been present above wave base on the upper part of the platform slope. As such, these beds are interpreted to represent the upper parts of the clinoform strata.

The mud-rich packstones found above the grainstone beds suggest that the high energy environment of grainstone deposition was superseded by one of lower energy. The large amount of micritisation which has effected the grains suggests that they have been subjected to a large amount of biological activity. The high content of miliolids and other large benthic foraminifera would suggest that these sediments have been derived from a lagoonal environment. These packstones may represent muddy lagoonal debris that accumulated in semi-protected areas, perhaps located just lagoonward of the advancing platform margin. Their presence above the high energy grainstones indicates that with time the lower energy lagoonal sediments were prograding out over the upper parts of the clinoform strata.

The coral and rudist beds (see Figs. 4.11a, 4.11b & 4.11c together with logs 4, 5, 6 & 7 in appendix 1) which form the recessive units found above the grainstone and packstone beds can be interpreted to have been deposited in a lagoonal environment. The lower more easily eroded parts of these beds represent low energy environments, where the large hippuritid rudists and small coral colonies were able to grow along with the many benthic foraminifera which are present. The large benthic foraminifera include types that only thrived under restricted conditions in very shallow water, possibly only centimetres deep (Caus pers. com.). The large and irregular nature of the skeletal fragments and the algal colonies which have grown around their edges (see Fig. 4.11c(ii)) is more evidence for the low energy nature of the environment. The large amount of micrite which surrounds these lagoonal organisms and their debris would have been produced by the action of boring organisms such as the lithophagid bivalves whose shells are still present in some of the borings (see Fig 4.11c(iii)). The large numbers of miliolids present indicate that this lagoon was probably fairly restricted, suggesting that it was separated from the open sea by some kind of barrier; however, the upper skeletal debris rich parts of the beds may suggest that this barrier was breached periodically, as the packstones, which form these more resistant layers (see Fig. 4.11c(i)), probably record the result of wave action agitating and breaking down the lagoonal sediments.

The prominent bed which marks the top of the platform-top sediments, at all localities where they are exposed (see Figs. 4.11 & 4.12a together with logs 4, 5, 6 &

7 in appendix 1), is composed of grains which could have been produced by the reworking and winnowing of the skeletal organisms present within the low energy lagoonal sediments (see Fig. 4.12b). Its sharp horizontal base indicates that it may have been erosive in nature and suggests that during the deposition of this grainstone/packstone the upper parts of the lagoonal sediments were planed off. It is postulated that this extensive grainstone/packstone unit may in fact represent skeletal sands that once formed protective banks on the seaward side of the lagoon which have migrated back rapidly over the top of the lagoonal sediments. This rapid lagoonward migration of skeletal sands which eventually covered the entire platform interior suggests that there has been a marked increase in the energy of this platform top environment. At the present day large areas of the Bahama-Florida platforms are dominated by skeletal sands which are being transported in an overall landward direction by intensive tidal currents which have breached the barriers at the platform rim (Schlager, 1994). This situation results when the rate of carbonate sediment production is exceeded by the rate of increase in accommodation space.

The brown oyster-rich packstones containing abundant silt-grade quartz overlying the prominent skeletal debris bed, are typical of the Anserola Formation sediments which are found on top of the Congost platform carbonates throughout the study area (see sections 4.3.2.2 and 4.4.5.3 together with Figs. 4.17c, 4.26 & 6.11). They are interpreted to represent the deep shelf facies of the overlying Sant Corneli platform.

### 4.2.4.4 Dissolution features and their significance

One of the most striking features of the platform-top lagoonal sediments is that all the originally aragonitic shell fragments within the wackestones and packstones have been dissolved out and replaced by calcite spar (see section 5.5.4 together with Figs. 4.11c(i) & 4.11c(ii)). It is only the originally calcitic or heavily micritised fragments and foraminifera which have survived.

At many of the outcrops where these platform top sediments can be found, an interconnecting network of small calcite spar filled pipes and cavities can be seen running through both the prominent grainstone/packstone bed and the muddy lagoonal sediments (see Fig. 4.13). These pipes and cavities are very irregular in size and shape but are never wider than a few centimetres. They can also be found in the underlying grainstones/packstones of the clinoform strata, although they are much less common and only appear to effect the upper few metres. Most of these structures have been filled by large calcite spar crystals which in the larger cavities reach 5mm

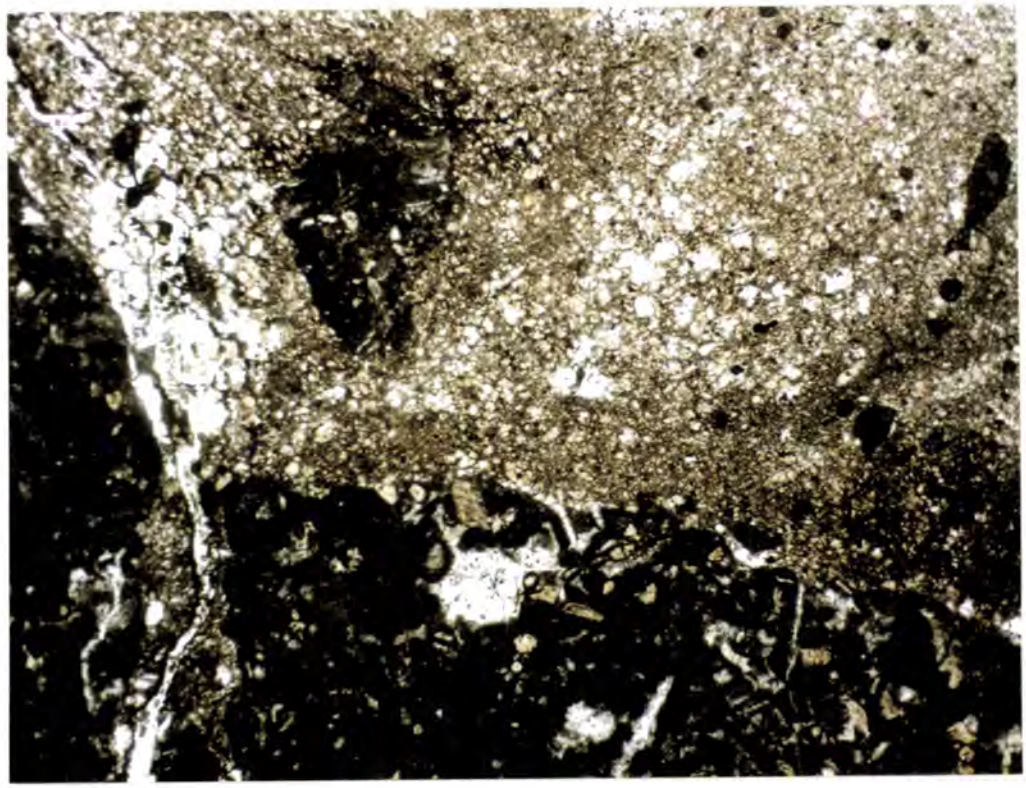

**Fig. 4.13.** Photomicrograph showing a large crystal silt filled cavity within a poorly sorted wackestone from the Congost platform top sediments. Sample AH/11 from above Casa Borrell (locality 1a, Fig 4.1). Field of view 12 x 7mm.

in diameter; however, some of the cavities also contain micritic sediment which is associated with large patches of crystal silt.

These features together with isotopic studies and cathodoluminescence work, which will be discussed further in the chapter 5 (see section 5.5.4), suggest that these platform-top sediments were effected by meteoric waters that caused dissolution as well as some cement precipitation and resedimentation.

The interpretation that these lagoonal sediments were deposited in a very shallow environment (see section 4.2.4.3) would mean that any slight fall in relative sea-level would have caused them to become exposed. Thus it is probable that the pervasive dissolution which has effected these sediments may be the result of several exposure events. The network of spar and crystal silt filled pipes and cavities that can be traced throughout these sediments (see Fig. 4.13) would appear to represent a well developed karst system and suggests that following deposition of the grainstone/packstone bed over the top of the lagoonal sediments, the Congost platform was subjected to a major period of subaerial exposure.

## 4.2.5 Explanation for the cycles within the clinoform unit

### 4.2.5.1 Introduction

By combining information derived from both the clinoform strata (see section 4.2.3) and the overlying unit of platform-top sediments (see section 4.2.4) it is possible to build up a picture of the processes which may have been responsible for the development of cycles within the clinoform strata.

### 4.2.5.2 The nature of the platform margin

As postulated in section 4.2.4.3 the protective barrier to the lagoon may have been a series of low amplitude skeletal sand banks, which would have been quite mobile and easily reworked. These skeletal sand bars could have provided the source for some of the coarsest material which was washed off the front of the platform onto the slope to form the coarsest layers in the prograding clinoforms. As the platform prograded then the skeletal sand bars would have advanced with it, so allowing the protected lagoon behind to follow. The packstone/grainstone banks seen in the outcrop near Ortenada may in fact be remnants of the skeletal sand bars which were a feature of the platform margin (see section 4.3.2.2 together with Figs. 4.15a & 4.15b).

### 4.2.5.3 Important features shown by the platform-top sediments

The skeletal debris rich packstone horizons in the lagoonal sediments (see section 4.2.4.2 together with Figs. 4.11a and 4.11c) indicate that periodically the banks at the platform margins were breached and high energy conditions effected the lagoons, while the pervasive dissolution which effected the lagoonal sediments (see sections 4.2.4.3 & 5.5.4 together with Figs. 4.11c(i) and 4.11c(ii)) may have been the result of several periods of exposure.

These features could be the result of small-scale relative sea-level fluctuations affecting the platform. During periods of rising relative sea-level the net sediment transport direction at the platform margin would have been lagoon-ward and tidal channels could have broken through the skeletal sand banks of the platform margin. An ensuing period of falling relative sea-level would have resulted in the net sediment transport direction at the platform margin being basin-ward again, which would cause the tidal channels to become infilled and some parts of the shallow lagoons to become exposed. It should be noted that a fall in relative sea-level is the only process which could be responsible for exposure of the lagoonal sediments.

#### 4.2.5.4 Conclusions

The fluctuations of the net sediment transport direction, proposed to have been operating at the platform margin as a result of changes in relative sea-level (see section 4.2.5.3) could also have produced the cycles observed in the slope sediments.

During periods when the net transport direction was lagoon-ward, only a relatively small amount of platform-derived material would be deposited down the slope, whereas, during the periods of net basin-ward sediment transport, deposition on the slopes would be dominated by platform-derived material.

Following the blockage of tidal channels, sedimentation on the platform slope would have only involved the finest wind blown material from the platform top, together with pelagic fall-out. As discused previously (see section 4.2.3.5) the basal characteristics of the platform together with the uniformly thin nature of the Reguard formation suggest that pelagic fall-out was a slow process at this time. During these periods the lower slopes of the platform would have been starved of sediment, creating conditions whereby hardgrounds and/or glauconite could develop, such as is seen in the measured section at Gallinove (see section 4.2.3.4 together with Figs. 4.7b, 4.8a, 4.8b & 4.8c).

## 4.3 The Outcrop at Ortenada

### 4.3.1 Introduction

Ortenada is a small village situated in the mountains approximately 6km east of La Pobla de Segur and can be reached by taking the narrow road which passes through the village of Claverol. The outcrop of Congost platform sediments is situated in a small river valley (dry in summer) on the north-west side of the village (locality 2 on Fig. 4.1). This outcrop represents an extension of the Santa Fe syncline's northern limb and is in such a position that it can be interpreted to represent a part of the Congost platform which lies basinward of the outcrops around the St Corneli anticline, but landward of the outcrop at Congost d'Erinya.

## 4.3.2 Sedimentological and geometric features

### 4.3.2.1 Inverted stratigraphy

The first thing to note about this outcrop is that it is stratigraphically inverted. The inverted nature of this outcrop can be inferred from the following features: (1) The lowest part of the outcrop is dominated by the distinctive brown coloured, quartz-rich sediments containing oysters which are typical of the basal part of the Sant Corneli Formation; (2) Some of the oysters in these Sant Corneli sediments can be seen to contain geopetal infills which also suggest the beds are inverted; (3) These brown calcarenites pass upwards into Congost platform top sediments which include numerous inverted Hippuritid rudists and coral colonies (see Fig. 4.14a); (4) Many of these corals and rudists contain borings with geopetal sediment fills that indicate the overturned nature of these sediments (see Fig. 4.14b); (5) The top of the outcrop consists of parallel-bedded, skeletal debris rich packstones and grainstones which are interpreted to represent sediments from the upper-most part of the Congost platform slope.

### 4.3.2.2 Description

The platform-top sediments at this locality, being a little over 30 metres thick, are much thicker than any of those exposed in the outcrops around the Sant Corneli and Santa Fe Folds. Figure 4.15 shows a photograph and line drawing which indicate the main features of the outcrop (see also logs 8 & 9 in appendix 1). To avoid confusion the following description of this stratigraphicaly inverted outcrop will begin with the oldest strata and work down the outcrop to the youngest strata; however, it will be worded as if the outcrop were in fact in its original orientation with the youngest strata at the top.

The section begins with well-bedded (1 to 2 metres thick) grainstones (see Fig. 4.15). These grainstones consist of well-rounded 1 to 2mm sized skeletal fragments and lithoclasts of reworked sediment (see Fig. 4.16a). The skeletal fragments all have well developed micrite rims, with some containing abundant borings around their edges. Skeletal grains include fragments of rudist, coral, bryozoan, brachiopod, echinoderm, coralline algae as well as miliolids and other benthic foraminifera. Some of the grains have been completely micritised to form peloids. Rounded lithoclasts of packstone containing sub-angular fragments of rudists and bryozoans are common. Silt-grade quartz is also present in small amounts.

**Fig. 4.14a.** Conical hippuritid rudist, within the lagoonal sediments at Ortenada (locality 2, Fig 4.1). The photograph is orientated with its top towards the top of the outcrop. Note the inverted nature of the rudist. Pen for scale.

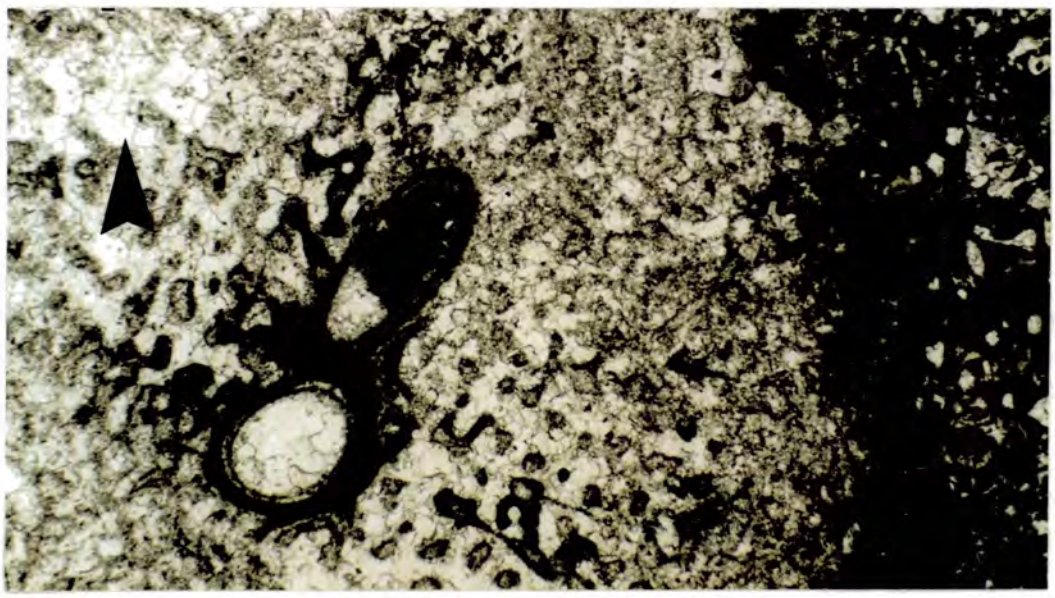

**Fig. 4.14b.** Photomicrograph, showing a boring within a coral from the lagoonal sediments at Ortenada (locality 2, Fig 4.1). The arrow shows the way up of the sample, as it was collected at outcrop. The geopetal infill indicates that the coral has been inverted since cementation. Sample OZ/17, Ortenada. Field of view 6 x 4mm.

A

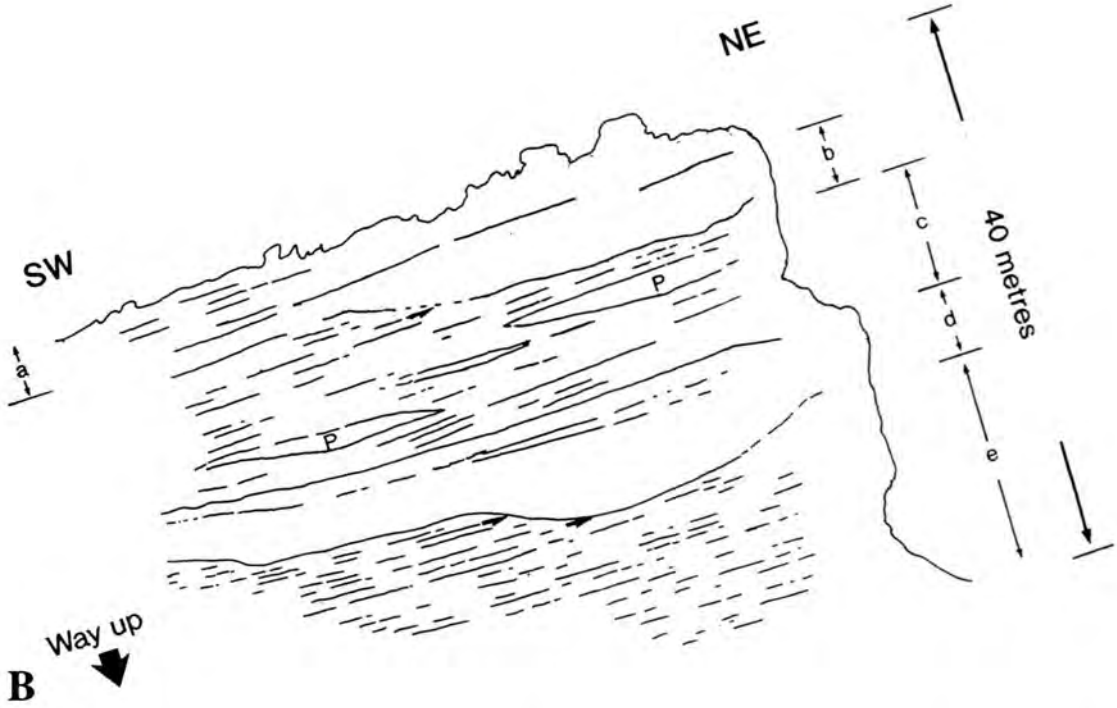


B

**Fig. 4.15.** Photograph (A) and line drawing (B) showing a northwestward view of the outcrop in the river valley at Ortenada (locality 2, Fig. 4.1). Note that the outcrop is stratigraphicaly inverted. The line drawing has been labelled to aid the description in the text; a) well bedded grainstones, b + d) grainstone/packstone bodies with a bank like geometry, c + e) nodular mud-rich sediments with corals and rudists in life position, P) Lens shaped bodies of skeletal debris rich packstone. Note the onlap of the coral and rudist beds onto the upper surface of the bank shaped features (arrowed).

**Fig. 4.16.** Photomicrographs from the outcrop at Ortenada (locality 2, Fig. 4.1)

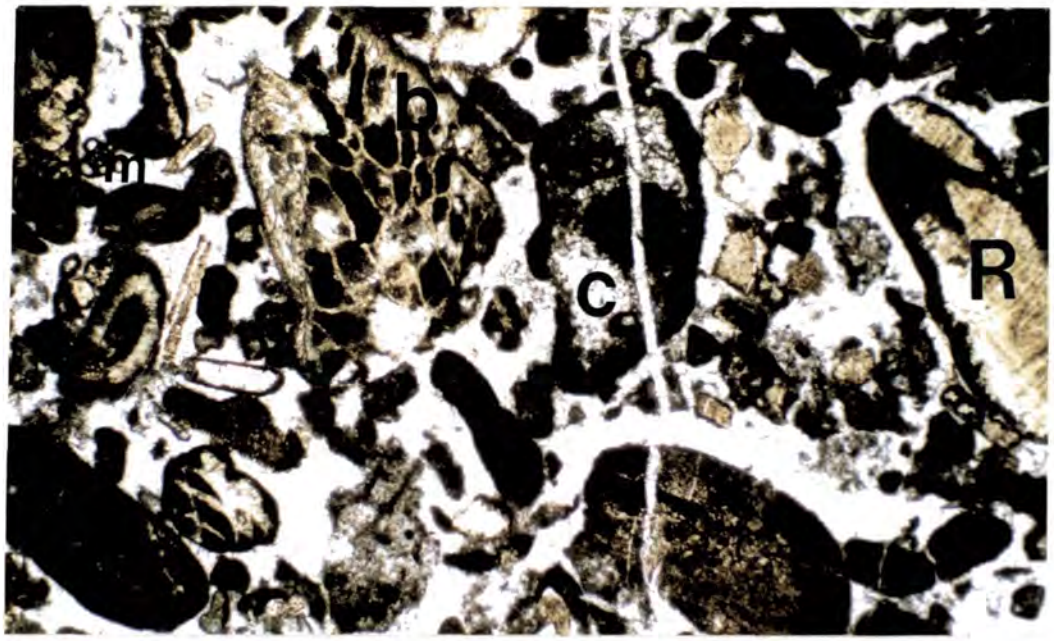


**a)** Grainstone from the base (stratigraphic) of the well bedded strata at the top of the outcrop (unit a, Fig. 4.15). Note the subrounded nature of the grains and their well developed micritic margins. Skeletal grains include fragments of rudist (R), coral (c), bryozoan (b) and miliolids (m). Sample OZ/30. Field of view 6 x 4mm.

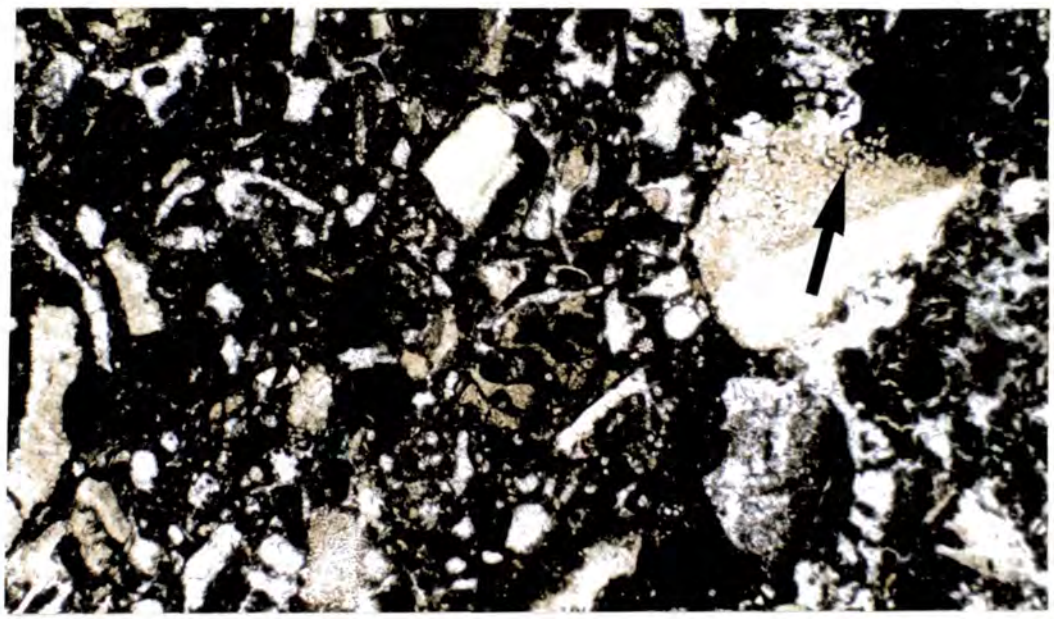

**b)** Packstone from the top (stratigraphic) of the well bedded strata at the top of the outcrop (unit a/b, Fig. 4.15). Note the angular nature of the skeletal fragments. Note also the fragmentation which has occurred around the edge of the large piece of rudist shell (arrowed). Sample OZ/28. Field of view 6 x 4mm.

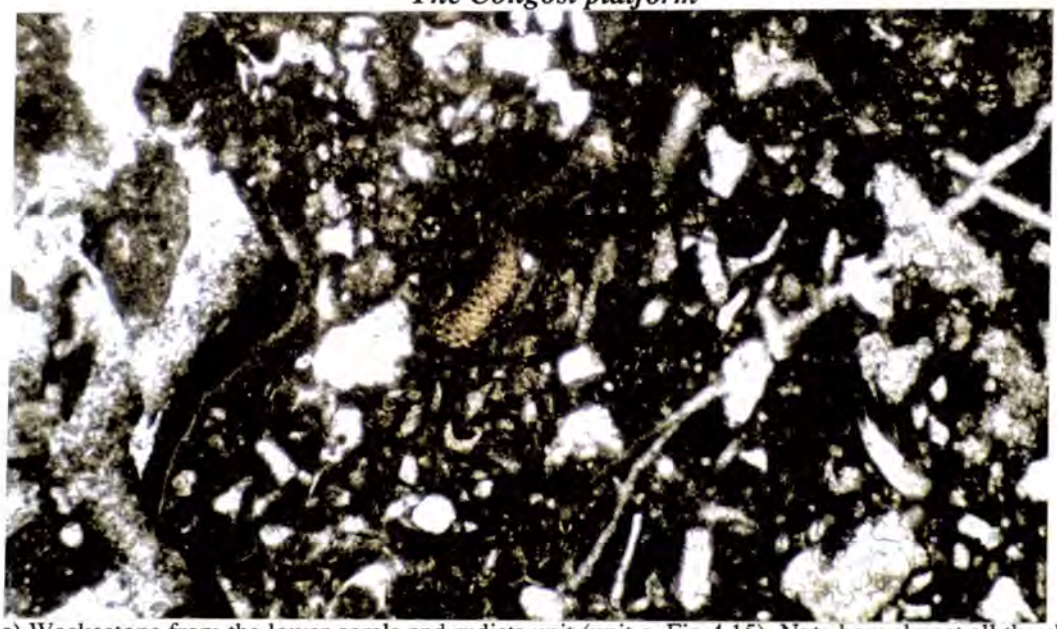

c) Wackestone from the lower corals and rudists unit (unit c, Fig 4.15). Note how almost all the shell fragments have suffered dissolution. Sample OZ/23. Field of view 3 x2mm.

Moving up section the texture of these well-bedded carbonates changes to that of a packstone with a slightly coarser less well sorted grainsize (0.5 to 4mm)(see Fig. 4.16b). As well as being larger the skeletal fragments of this packstone are less well rounded than those of the grainstones below, in fact some could be described as being sub-angular. Skeletal debris includes that of rudist, bryozoan, echinoderm, coral, brachiopod, coralline algae, miliolids and other benthic foraminifera. The edges of most grains are micritised and contain borings. Some of the skeletal fragments are also slightly fragmented at their margins. A number of the larger fragments of rudist and coral are enveloped by colonies of coralline algae which have grown around their edges.

The upper part of these well-bedded skeletal debris rich packstones and grainstones has a bank like geometry (see Figs. 4.15a & 4.15b). This bank shaped feature has approximately 3 metres of relief and creates a surface which has been onlaped by the overlying less well-bedded, nodular strata containing abundant hippuritid rudists, small colonies of coral and other colonial organisms. The sediment of which the bank is composed mostly has a packstone texture although there are small patches of grainstone. The grains are sub-rounded and include fragments of rudists, echinoderms, bryozoans, coral, coralline algae as well as miliolids and other benthic foraminifera. The skeletal fragments all possess micritised and bored rims with some of the rudist and echinoderm fragments having very sutured margins. Peloids, completely micritised grains and lithoclasts of reworked wackestone are also common.

The unit which onlaps the upper surface of the packstone bank is approximately 12 metres thick (see Figs. 4.15a & 4.15b) and is dominantly composed

of nodular, mud-rich sediments containing large hippuritid rudists (see Fig. 4.14a), corals (see Fig. 4.14b) and other colonial organisms, many of which are in life position. These nodular rudist and coral beds are interbedded with lens-shaped, skeletal debris rich packstones which are more resistant to weathering than the surrounding nodular sediments.

The nodular matrix around the rudists and corals generally has a wackestone texture (see Fig. 4.16c) and contains abundant angular shell fragments most of which have suffered the effects of dissolution and are now only present as drusy calcite spar with micrite rims marking the original position of the grain margins. The few skeletal grains which have survived this pervasive dissolution and replacement are some fragments of rudists, echinoderms and brachiopods as well as numerous miliolids and other lagoonal foraminifera. Fragments of coral can also be identified from the internal sediment and micritic linings of the skeletal walls. The skeletal fragments all possess micritised and fragmented margins. Some of the larger fragments of rudist and coral have envelopes of encrusting coralline algae. Numerous borings are present in the coral colonies and outer calcite walls of the rudists.

The lens-shaped beds of this unit (see Figs. 4.15a & 4.15b) mainly possess a packstone texture, although pockets of grainstone do occur. These packstones consist of sub-rounded skeletal fragments, almost all of which have been effected by dissolution and have been replaced by calcite spar. Grains present include fragments of rudist, coral, bryozoan, echinoderm, brachiopod, as well as whole miliolids and other benthic foraminifera, which have been preserved by being completely micritised. The skeletal grains all have micritised and bored margins, with some of them having been completely micritised to form peloids. In addition to peloids, reworked wackestone lithoclasts are common.

Resting on top of these nodular rudist and coral beds, there is a prominent unit with a planar lower boundary and a bank-shaped upper surface with a relief of approximately 2 metres (see Figs. 4.15a & 4.15b). This bank-like unit is composed of sub-rounded packstone containing skeletal debris, peloids, lithoclasts as well as a few foraminifera and is petrographically very similar to the bank-like feature described earlier.

The upper surface of the skeletal debris bank creates a topography which has been onlapped by the overlying sediments (see Figs. 4.15a 7 4.15b). These overlying sediments contain numerous rudists, corals, and other colonial organisms in life position which are surrounded by a nodular wackestone containing some lagoonal foraminifera and angular skeletal fragments of various sizes. Most of these skeletal fragments have been dissolved and replaced by calcite spar. The edges of the skeletal shell fragments have been fragmented, bored, micritised and sometimes encrusted by

colonial organisms such as serpulids or coralline algae. These sediments mark the base of a 10 metre thick unit of nodular sediments which, unlike the coral/rudist unit below, does not contain any lens-shaped beds of sub-rounded skeletal debris (see Figs. 4.15a & 4.15b).

The top of this unit is marked by a 0.5 metre thick bed, consisting of a medium/coarse (<0.5-1mm) grained packstone which has a large variation in grainsize and a mixture of sub-rounded to angular skeletal fragments (see Figs. 4.17a and 4.17b together with logs 8 & 9 in appendix 1). Almost all the skeletal fragments have been dissolved out and replaced by drusy calcite spar, leaving only some echinoderm, bivalve (possibly oyster), brachiopod and bryozoan fragments with their original structure still showing. These originally calcitic grains commonly show patchy silicification. Thick micrite rims and completely micritised grains are the only

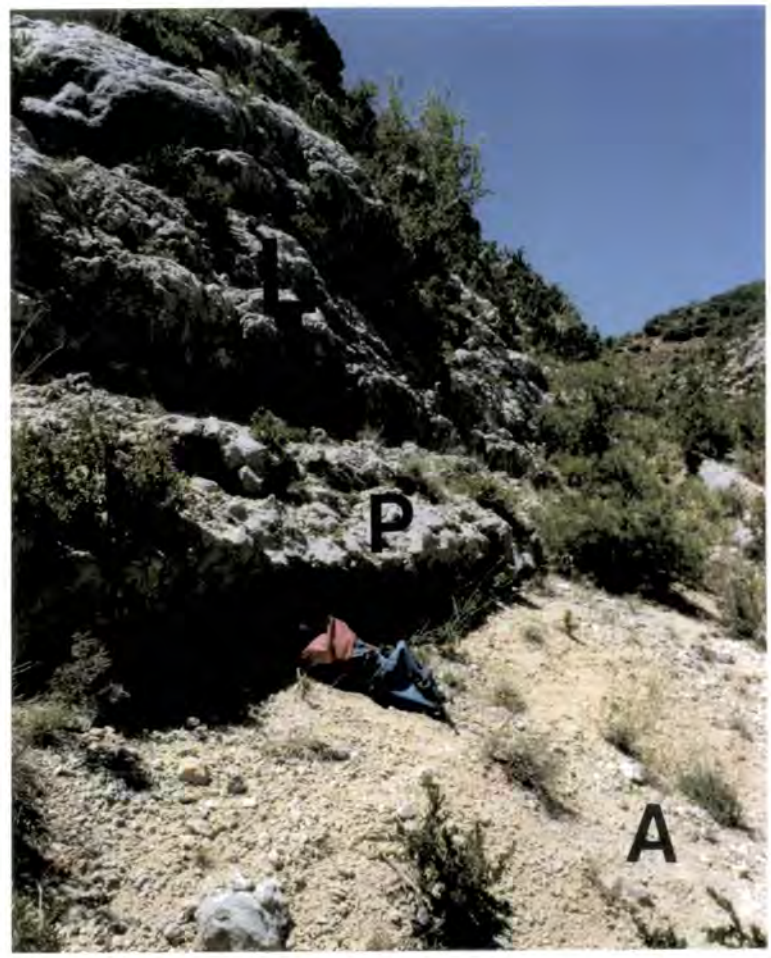


**Fig. 4.17a.** Photograph showing the base of the cliff at Ortenada (locality 2, Fig 4.1). Note that the stratigraphy is inverted. The youngest coral and rudist unit (L)(unit e, Fig. 4.15) is capped by a prominent bed of packstone (P), which in turn is overlain by easily weathered, nodular, fine grained sediment with a distinctive brown colour (A). Red rucksack is 0.5 metres long.

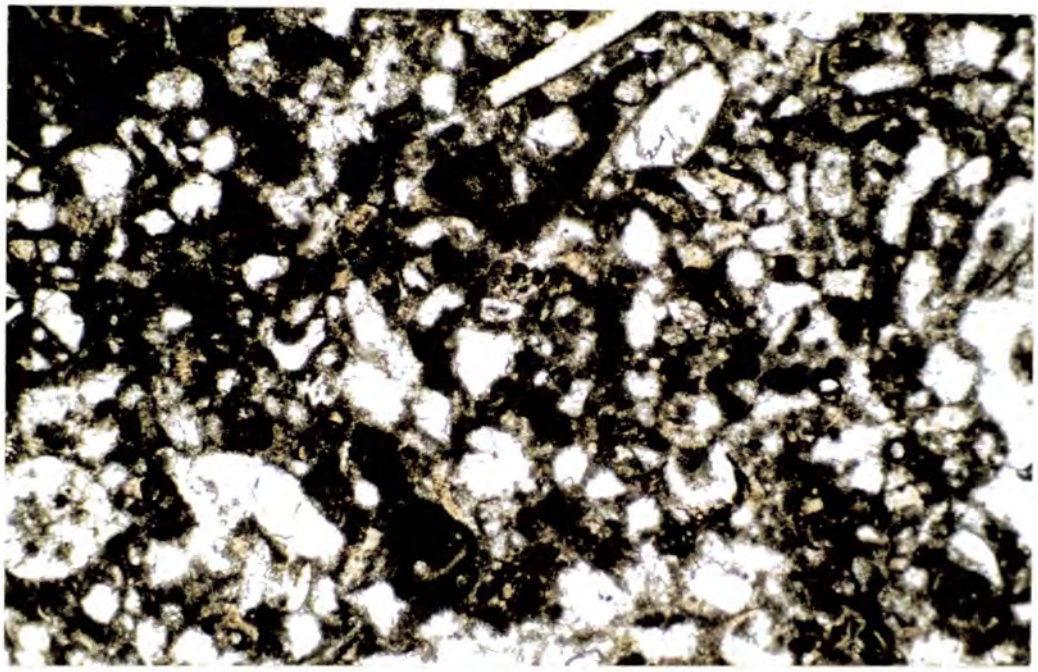

**Fig. 4.17b.** Photomicrograph showing the packstone of which the prominent bed (marked P in Fig 4.17a) is composed. Note that almost all the skeletal fragments have suffered dissolution. Well developed micritic margins now mark the former positions of bioclasts. Ortenada sample OY/4. Field of view 3 x 2mm.

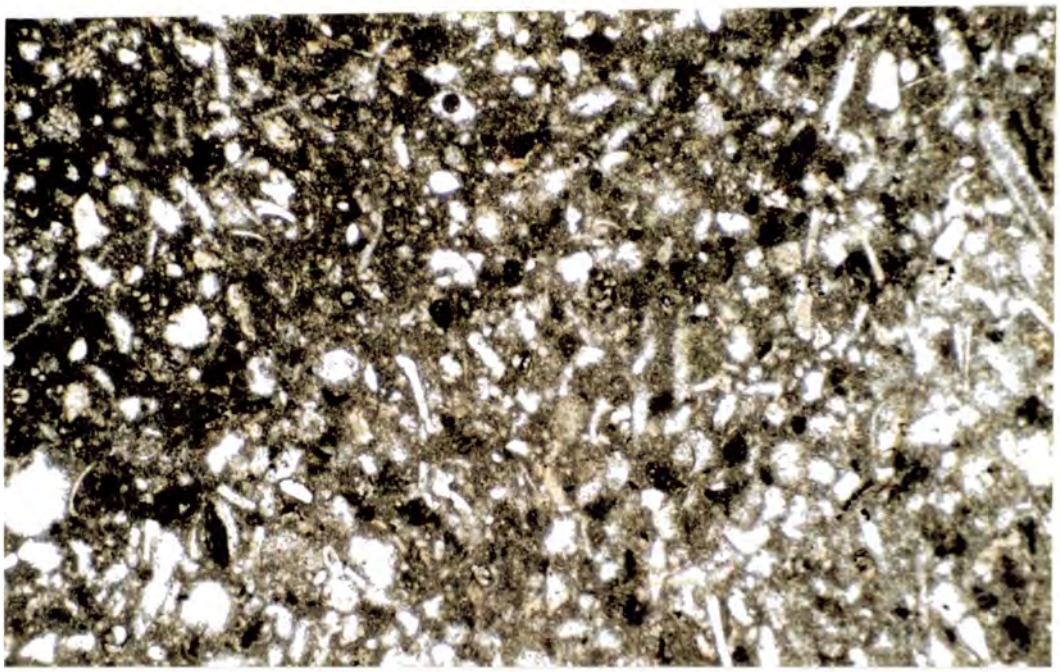

**Fig. 4.17c.** Photomicrograph of the nodular brown packstone (marked A in Fig. 4.17a) which overlies the prominent packstone bed. Note the foraminifera, sponge spicules and quartz grains. Ortenada sample OY/2. Field of view 3 x2mm.

remnants of the other skeletal fragments. Also present are calcispheres, sponge spicules, a trace of silt grade quartz and many multi-chambered foraminifera.

The top of this thin bed of medium/coarse grained packstone forms a prominent feature which stands proud of the outcrop (see Fig. 4.17a), because the sediment which stratigraphicaly overlies this bed has been weathered back into the slope. The overlying easily weathered sediment is fine grained, very nodular and has a noticeable brown colour. Thin sections of this sediment (see Fig. 4.17c) have shown it to consist of a fine grained packstone (<0.2mm) which contains abundant foraminifera (benthic and planktonic), bivalve fragments, echinoderm fragments, bryozoan fragments, sponge spicules, thin-shelled bivalves, calcispheres and a trace amount of silt grade quartz. There are also local larger fragments of bryozoans and oysters which show patches of silicification.

Moving up section it is noticeable that within a few metres the abundance of both benthic foraminifera and bryozoan fragments has decreased. The easily weathered nodular nature of this unit produces poor exposure, however; 20 metres further up the section a very similar fine-grained packstone containing planktonic foraminifera, calcispheres, sponge spicules, thin-shelled bivalves together with small fragments of bivalves and echinoderms, a trace of quartz and the occasional large partly silicified oyster can be found.

#### 4.3.2.3 Summary and interpretation

This outcrop is interpreted to represent a section through the platform margin and lagoonal sediments of the Congost platform, together with a small amount of the overlying deep slope sediments of the Sant Corneli platform.

The well-rounded and mud-free nature of the grainstones at the base of the section (see Fig. 4.16a), suggests that they were deposited in a relatively high energy environment. Such an environment would have been present above wave base on the upper part of the platform slope and at the platform margin. In fact these grainstones are interpreted to represent skeletal sands that were accumulating at the platform margin in the form of shallow sand banks and bars which protected the platform top from the open sea. The skeletal grains and lithoclasts would have been derived during periods when high tides and storms were able to disrupt and rework material from the lagoons and shoals of the platform top. During the process of platform progradation these platform margin sands would be moved down slope to form the upper parts of the prograding clinoforms, which would eventually be preserved as the platform top system moved over them.

The well rounded grainstones are overlain by slightly coarser, poorly-sorted and less well-rounded packstones (see Fig 4.16b), suggesting that the high energy environment of grainstone deposition was superseded by one of lower energy. This would be the result of progradation of the platform top over the higher energy of the platform margin. The micritised and bored margins to most of the skeletal fragments suggests that they have been subjected to bio-erosive activity, while the fragmented edges around a few of the grains imply that some of this bio-erosion took place in situ and was followed by very little movement of the grains. This again suggests a low energy environment for deposition, as does the colonisation of some of the larger fragments by coralline algae. These sediments may represent muddy lagoonal debris that has been washed off the lagoon by low energy tidal currents and has accumulated in protected areas lagoonward of the skeletal sand banks.

The bank shaped units of skeletal debris present in this section (see Figs. 4.15a & 4.15b) may in fact be representative of the skeletal sand banks that are interpreted to be a feature of the Congost platform margin (see sections 4.2.4.3, 4.2.5.2 and 4.4.5.1). The packstone texture observed within these units may reflect the fact that these banks were located on the platform top, themselves being protected from the full force of the open ocean by larger and less muddy banks at the platform margin.

The thick nodular units which onlap the upper surfaces of the carbonate sand banks (see Figs. 4.14a, 4.14b, 4.15a & 4.15b) are, except for their greater thickness, identical in nature to the platform top sediments seen elsewhere on the Congost platform (see sections 4.2.4.2, 4.4.5.2 and 4.4.5.3 together with Figs. 4.11, 4.23 and 4.24), and are interpreted to have been deposited in a semi-protected shallow lagoonal environment.

One interesting difference between the two lagoonal units seen at this locality is that the lower lagoonal unit includes several lens-shaped packstone beds, whereas the upper unit does not (see Figs. 4.15a & 4.15b). These packstone lenses, which contain sub-rounded skeletal debris, peloids, foraminifera and lithoclasts, can be interpreted to represent small shoals of lagoonal debris that were migrating across the shallow lagoon floor, possibly under the influence of tidal currents. It is postulated that these tidal currents would have been able to access the shallow lagoons through channels that were present between the carbonate sand banks around the platform margin. This difference between the two units may be indicating that the upper unit experienced less tidal and/or storm action. This would suggest that during deposition of the upper unit of lagoonal sediments the lagoon was better protected than it had been during the deposition of the lower unit.

The thin bed of packstone which marks the top of the coral/rudist lagoonal unit (see Figs. 4.17a and 4.17b) could be interpreted to be equivalent to the prominent grainstone/packstone bed present on top of the Congost lagoonal sediments in the outcrops around the Sant Corneli and Santa Fe folds (see section 4.2.4.2 together with Figs. 4.11b, 4.12a & 4.12b). However, skeletal fragments showing patchy silicification have not been seen in the grainstone/packstone beds at these other outcrops; instead, they do appear to be a feature of the overlying deep shelf sediments of the Sant Corneli platform.

The presence of planktonic foraminifera, thin-shelled bivalves and the very fine nature of the shell fragments within the overlying brown-coloured packstone (see Fig. 4.17c) would suggest a deep slope or basinal environment of deposition where only the finest of material from the platform top was deposited. The brown colour and the presence of the occasional larger fragments of oyster or bryozoan which have been partly silicified are typical of sediments from the Sant Corneli sequence (see sections 4.2.4.2 and 4.4.5.3 together with Figs. 4.26 & 6.11). This unit is therefore interpreted to represent the deep slope sediments of the Sant Corneli platform. The large number of sponge spicules (now replaced by calcite spar) contained within this sediment would probably have provided the source of the silica for the silicification that has effected some of the calcite shell fragments in these Sant Corneli slope sediments.

## 4.3.3 Dissolution pipes and cavities

### 4.3.3.1 Irregular shaped cavities and their significance

Samples of the wackestone matrix from towards the top of the lowest coral/rudist unit and samples from throughout the upper coral/rudist unit have revealed interesting irregular shaped cavities which vary in size from very small to a maximum of 2cm in diameter. Some of these cavities contain patches of crystal silt and small amounts of micrite, with the remaining space having been occluded by very coarse calcite spar (see Fig. 4.18). When studied using cathodoluminescence, this calcite spar was found to be non-luminescent and displayed the same black colour typical of the cements found in the dissolution cavities within the lagoonal sediments from the outcrops of the Congost platform around the Sant Corneli and Santa Fe folds (see sections 5.5.4.7 & 5.5.4.8).

The remarkable similarity between these cavities and those that are seen in the Congost lagoonal sediments from the outcrops around the Sant Corneli and Santa

Fe folds (see section 4.2.4.4 and Fig. 4.13) would suggest that they were formed by similar processes. As discussed in the chapter on diagenesis (see sections 5.5.4.7 & 5.5.4.8) the general character of such cavities, along with stable isotopic and cathodoluminescence studies, suggests that they are the result of karst processes. These processes are interpreted to have involved dissolution by meteoric waters followed by the reworking and precipitation of meteoric cements.

The presence of these cement-filled, dissolution cavities throughout the upper lagoonal unit and top part of the lower one can be interpreted in different ways. One interpretation would be that following the deposition of the upper lagoonal unit there was a major period of subaerial exposure, the effects of which penetrated down into the top part of the lower unit. Another interpretation would be that these cavities could be the result of more than one period of exposure which effected the lagoonal sediments at various times during their deposition. The benthic foraminifera present suggest that these lagoonal sediments were deposited in a very shallow environment (< 50cm)(Caus pers. com.), so it is quite likely that any small-scale fluctuations in relative sea-level would have caused them to become exposed.

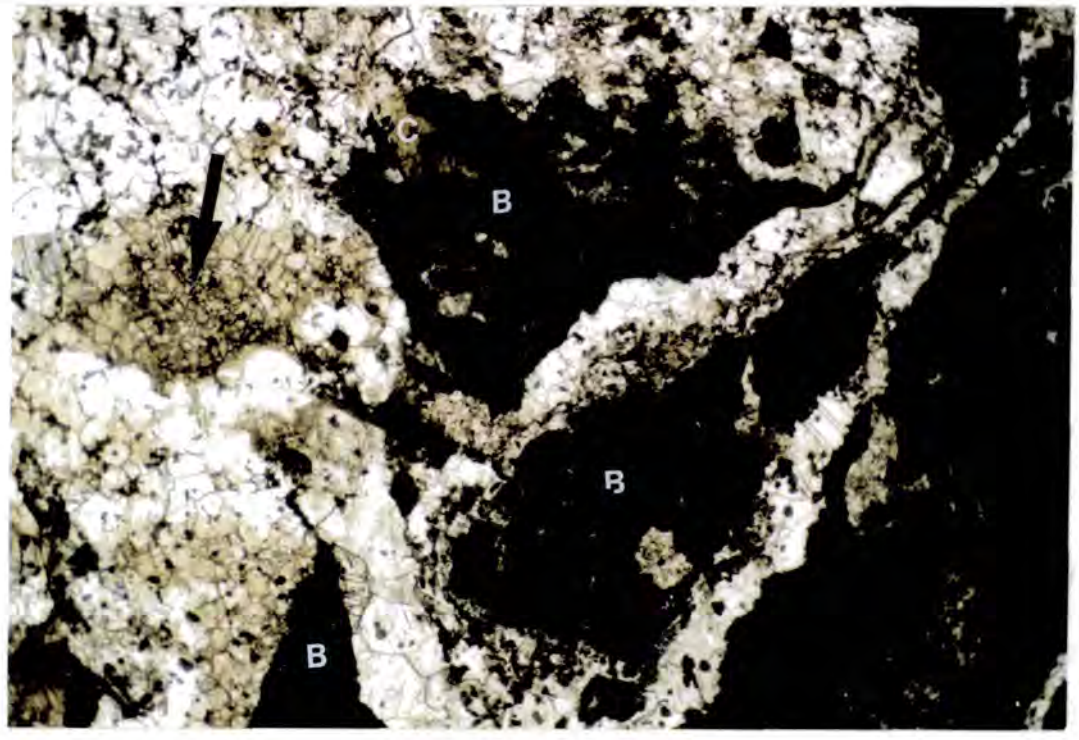


**Fig. 4.18.** Photomicrograph, showing a calcite spar filled dissolution cavity from within the lagoonal wackestone at Ortenada (unit e, Fig 4.15). Note the irregular shaped blocks of host wackestone (marked B) and the patch of crystal silt (arrowed). Note also how originaly calcitic shell fragments (marked C), protrude futher into the cavity than the surrounding matrix. Ortenada sample OY/11. Field of view 12 x 7mm.

### 4.3.3.2 Vertical sediment filled pipes and their significance

In several places throughout the outcrop irregular shaped pipes (1 to 5cm diameter) which are filled with a brown coloured sediment can be seen (see Fig. 4.19a together with log 9 in appendix 1). These pipes are difficult to trace through the nodular sediments but can be seen in several of the lens shaped skeletal debris beds of the lowest rudist/coral unit (see Fig. 4.15). They can also be found cutting through the well bedded packstones and grainstones towards the top of the outcrop, some 34 metres stratigraphicaly below the top of the Congost lagoonal sediments. Where they can be seen these pipes have a general vertical orientation and can usually be traced through several beds before becoming too difficult to see. The walls of these pipes are very irregular and in places smaller pipes can be seen branching off the larger ones.

When these pipes are studied in thin section (see Fig. 4.19b) it can be seen that as well as being very irregular the walls of these pipes truncate some of the shell fragments in the host rock. Traces of calcite cement as well as small accumulations of iron oxide are present in patches along the edge of the pipes. In places thin, irregular, branch-like features which have been impregnated with iron oxide can be seen to come off the pipes and penetrate the surrounding host rock. The sediment infilling the pipes is a medium/coarse grained, skeletal debris rich packstone and has a distinctive brown colour which is due to the fact that the micritic matrix and some of the grains have been impregnated with iron oxide.

The skeletal debris constituents of this packstone infill are predominantly fragments of calcitic skeletons (<0.5 -1mm), in particular those of rudists and other bivalves (possibly oysters), with fragments of bryozoan and echinoderms also being common (see Fig. 4.19b). Some of the fragments contain small patches of chert. These calcitic skeletal fragments do not have well-developed micrite rims but instead they all possess crenulated margins. These fragments are sub-angular and there is a tendency for their long axes to be aligned parallel with the pipe walls.

Other skeletal grains include fragments of coralline algae, a few miliolids and other multi-chambered foraminifera as well as some recrystalised fragments of coral and other shell debris. These fragments of coral and other originally aragonitic shells which have been replaced by a fine-grained calcite spar are in most cases poorly preserved but it can be seen that they are all fairly well rounded and possess micritised margins (see Fig. 4.19b). Commonly the micrite envelopes have been impregnated with iron oxide. In fact several of these recrystallised grains have been almost totally replaced by iron oxide. Also present in the packstone pipe infills are irregularly shaped lithoclasts of wackestone which, except for the fact that they have

**Fig. 4.19a.** Narrow dissolution pipe cutting through the lagoonal sediments (unit c, Fig. 4.15) at Ortenada. Note the irregular outline and the brown colouration of the packstone infill. Pencil for scale.

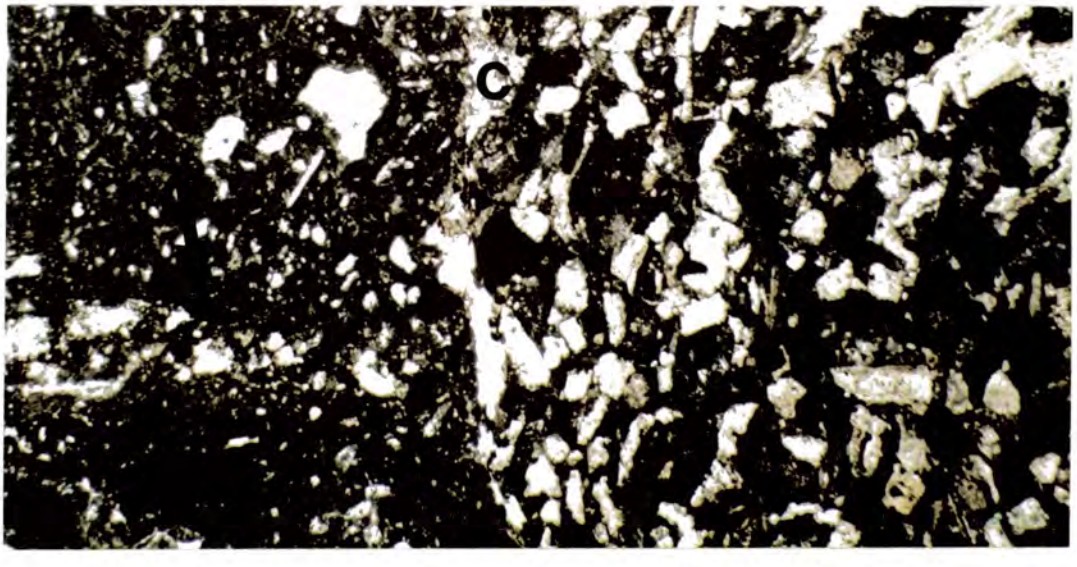


**Fig. 4.19b.** Photomicrograph, showing the host lagoonal wackestone on the left and a dissolution pipe with its packstone infill on the right. Note, the patches of calcite cement present along the pipe margin (C), the pervasive dissolution of shell fragments within the host wackestone, the predominance of calcite shell fragments within the pipe infill (internal structure visible), the crenulated margins of grains within the infill and the irregular iron oxide impregnated branch like feature which is penetrating the host wackestone (arrowed). Ortenada sample OZ/15. Field of view 6 x 4mm.

been heavily impregnated with iron oxide, are very similar in character to the wackestone through which the pipes pass.

The general nature and irregular outline of these pipes would suggest that they are a product of dissolution. Stable isotope analysis of the surrounding host rock for these pipes suggests that they have been effected by meteoric waters (see Section 5.5.4.10). These pipes are probably a result of fracturing followed by dissolution enlargement, which are common processes associated with subaerial exposure of carbonates. There have been many similar examples described from the geological record by various workers (e.g. Desrochers & James., 1988; Meyers, 1988, Vera et al., 1988 & Wright, 1988). Modern examples of fissures and neptunian dykes can be found on the Bahama Banks today (Smart et al., 1988).

The predominance of calcitic fragments within the packstone infill of these pipes (see Fig. 4.19b) is unusual, as most of the Upper Cretaceous sediments from this area contain an abundance of what was originally aragonitic debris (see Figs. 4.11c(i), 4.11c(ii), 4.11c(iii), 4.12b, 4.13, 4.16a, 4.16b, 4.16c, 4.17b, 4.23a, 4.23b & 4.24d). This may be indicating that originally aragonitic shell fragments were preferentially removed during the reworking of the source material for this pipe infill. The highly crenulated margins of the calcitic shell fragments (see Fig. 4.19b) may be suggesting that they have been subjected to chemical etching. Similar features to these have been described by Meyers (1988) from fissure infills in Mississippian Limestones of New Mexico. One possible interpretation of these two features is that the major constituent of this pipe infill is the product of weathering and dissolution of a skeletal debris rich bedrock in the upper vadose zone, possibly in a subsoil setting.

The well rounded and poorly preserved, originally aragonitic grains contrast with the more abundant, calcitic shell fragments of this infill which are fairly angular and do not possess micritic margins (see Fig. 4.19b). However, they are very similar to those seen in the lagoonal sediments forming the pipe walls. These coral and other shell fragments have been impregnated with iron oxide as have the irregular-shaped lithoclasts of wackestone. These constituents of the pipe infills are interpreted to be derived from the disintegration of the surrounding wall rock. The irregular, iron oxide rich, branch-like features seen to be coming out of the pipes and penetrating the wall-rock (see Fig. 4.19b), are interpreted to represent the early stages of this wall-rock reworking.

Although these pipes could not be traced to an exposure surface, the fact that some of the shell fragments of the infill show patches of silicification may be an important clue as to the timing of their formation. Moving up the section, the first appearance of partly silicified shell fragments is in the thin packstone bed which marks the top of the lagoonal sediments of the Congost platform (see section 4.3.2.2

together with Fig. 4.17c). This would suggest that the maximum age of the pipe infill would be the time of deposition of this packstone bed.

Another important feature is that these pipes and dissolution cavities which are seen throughout the Congost lagoonal sediments do not occur in the overlying Sant Corneli sediments, suggesting that the subaerial exposure event which produced these features occurred before the deposition of the Sant Corneli deep slope sediments. The interpretation that these Sant Corneli sediments were deposited in a deep slope environment (see section 4.3.2.3) would also make them less susceptible to exposure than the underlying shallow lagoonal sediments of the Congost platform top.

The coarse grained nature of the pipe infill indicates that it could not have its origins in the very fine grained Sant Corneli sediments seen at this outcrop (see section 4.3.2.2 & Fig.4.17c); however, coarser grained Sant Corneli packstones can be seen directly overlying Congost platform-top sediments elsewhere (see sections 4.2.4.2 & 4.4.5.3 together with Fig. 4.26).

From the evidence available, it would appear that the most likely location for the surface exposed during the formation of these dissolution-enhanced fissures, would be the top of the packstone bed marking the boundary between the Congost lagoonal sediments below and the deeper shelf sediments of the Anserola Formation above (see Fig. 4.17a). The fact that this bed is heavily leached, having had almost all its constituent shell fragments dissolved away to be replaced by calcite spar (see Fig. 4.17b), is probably a result of this bed having been subjected to the effects of meteoric waters during the time it was exposed. As suggested earlier the etched calcite shell fragments present within the pipe infill may be remnants of the weathering products of this bed that were washed down the fissures which would have been open at the surface.

The fact that these solution-enhanced fissures can be seen cutting through the grainstone beds which occupy a stratigraphic position some 34 metres below the proposed exposure surface, would suggest they were produced by a major exposure event involving a relative sea-level fall of a least 40 metres.

## 4.4 The Congost d'Erinya outcrop

### 4.4.1 Introduction

Congost d'Erinya (marked as locality 3 on Fig 4.1) is a deep gorge cut by the Flamicell River, creating a superb exposure showing a complete stratigraphic section

from the unconformity on top of the Lower Albian sediments, through to the St Corneli slope facies (see Figs 4.22a, 4.22b & 4.22c). Exposed in this gorge, there is a shelf-margin section through the whole Congost sequence. This shelf margin section is the most basinward outcrop of the Congost platform and therefore represents the final stages in the development of the Congost platform. The section through the Congost platform sediments begins with the basal sequence boundary represented by a flooding of the underlying Santa Fe platform, then continues up through 240m of marl, on top of which is the platform margin, where there is a set of prograding parasequences composed of coral reefs and associated debris overlain by lagoonal sediments. The top of the lagoonal sediments shows evidence of subaerial exposure and they are overlain by the deeper shelf sediments of the overlying St Corneli sequence.

## 4.4.2 The Santa Fe and Pardina Limestones

The Santa Fe and Pardina Limestones, which are exposed at the north-western end of the gorge have been described and discussed previously in chapter 3.

## 4.4.3 The upper boundary of the Pardina Limestone

### 4.4.3.1 Description

The top of the Pardina Limestone is marked by a slight grainsize increase and the appearance of glauconite (see log 12 in appendix 1). Moving up the section the glauconite first appears in a massive bed, approximately 50cm thick, where it has grown inside the voids created by the dissolution of shell fragments (probably originally aragonitic) (see Fig. 4.20b). The glauconite has grown after the precipitation of a calcite spar cement around the edges of these dissolution voids. The upper surface of this bed is very irregular and contains cavities, which have been infilled by the overlying sediment (see Fig. 4.20a). The edges of these cavities are marked by the discolouration (light brown) of the surrounding host rock. The sediment which overlies this surface and infills the cavities is a fine-grained wackestone containing abundant calcispheres and glauconite (Basal Reguard Formation)(see Fig. 4.20c). The glauconite in this overlying wackestone occurs as either discrete grains or as infills to foraminifera tests and is so abundant that it gives the wackestone a green colour. With the exception of a couple of beds the abundance

of glauconite decreases rapidly up section, being only present in trace amounts just 70cm above the irregular surface

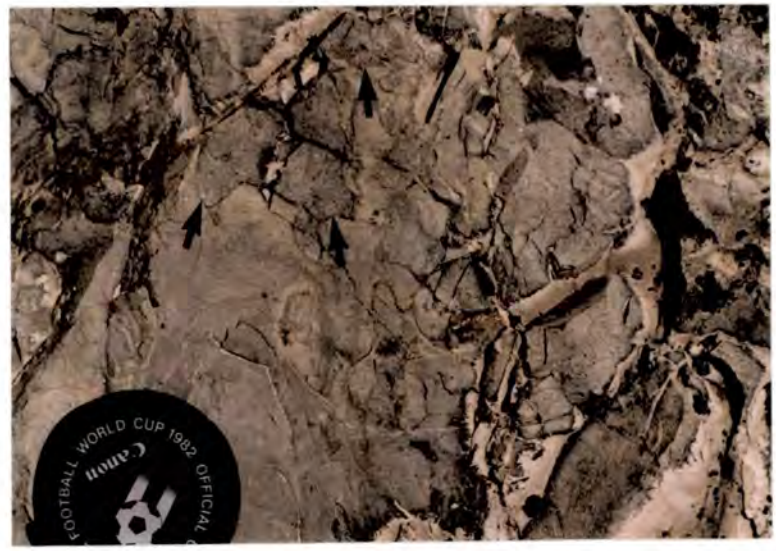


**Fig. 4.20a.** The irregular upper surface of the Pardina Limestone (arrowed). Note the large amount of glauconite (green specks) within the sediment which overlies this surface and infills the irregularities. Congost d'Erinya. Lens cap for scale.

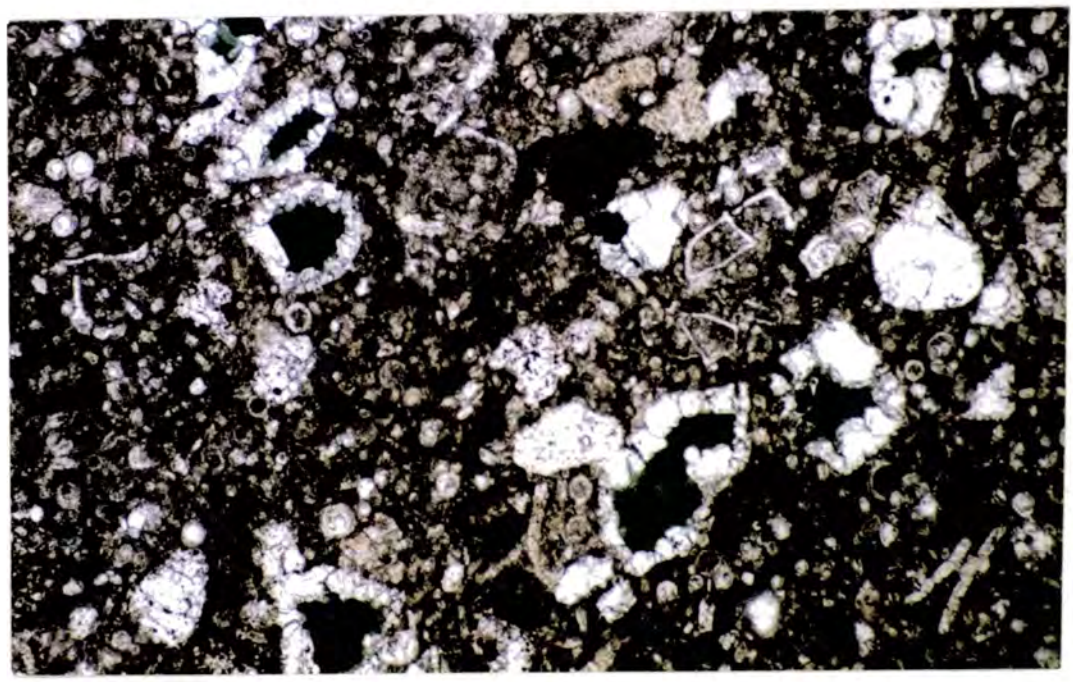

**Fig. 4.20b.** Photomicrograph showing calcisphere rich packstone from the top bed of the Pardina Limestone. Note the specific occurrence of glauconite, which has grown after calcite spar, inside the voids created by dissolution of shell fragments. Congost d' Erinya sample 1100. Field of view 3 x 2mm.

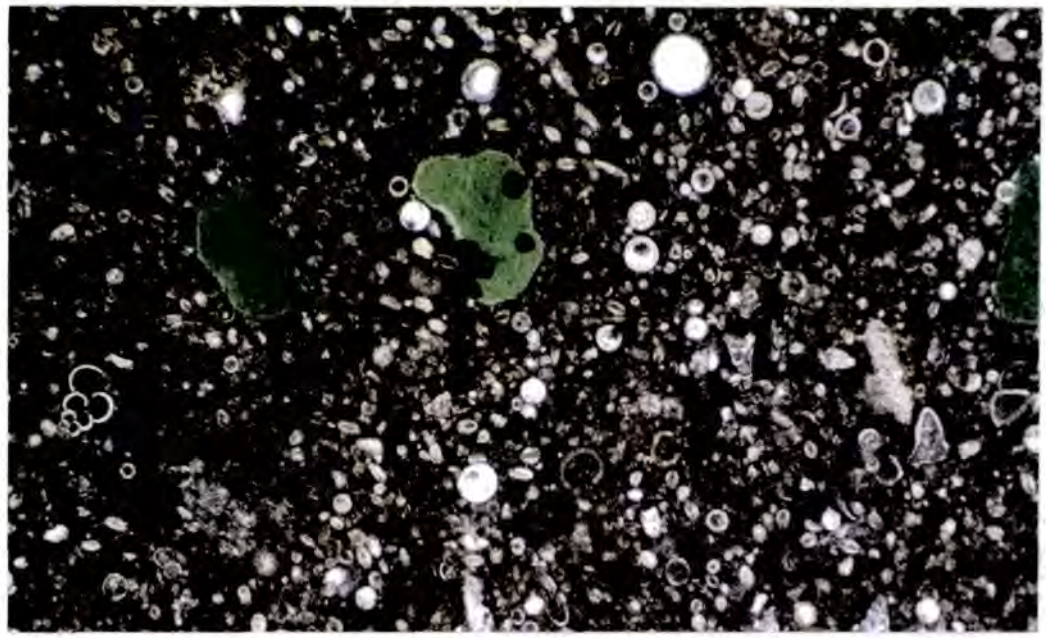

**Fig. 4.20c.** Photomicrograph showing the calcisphere, and planktonic foraminifera rich wackestone, which overlies and infills the irregular surface at the top of the Pardina Limestone Note the glauconite occurs either as discrete grains or as infills to foraminifera tests (arrowed). Congost d'Erinya sample 1150. Field of view 3 x 2mm.

### 4.4.3.2 Discussion

The glauconite seen in the bed which marks the top of the Pardina Limestone is unusual as it occurs as the final precipitate within dissolution voids (see Fig 4.20b). This may be the result of early dissolution and cementation taking place at or just below the sea-bed during a time of reduced sedimentation. The chemistry of Cretaceous ocean water was such that the stable precipitate was low Mg calcite (Sandberg, 1983 & 1985), so that sea-water may well have been undersaturated with respect to aragonite. Dissolution of aragonite on the seafloor, or just below could have occurred, especially at times of slow sedimentation. Dissolution of aragonite at Jurassic hardgrounds has been documented (Palmer et al., 1988). The occurrence of glauconite as discrete grains and as an infill of foraminifera tests in the bedded wackestones immediately overlying this bed suggests that conditions on the sea-floor above the bed were favourable for glauconite growth. This would have been a period of slow sedimentation, when there was sufficient metabolizable organic matter to produce a postoxic-nonsulphidic environment due to decomposition by oxygen-consuming bacteria (Berner, 1981; Odin & Matter, 1981). The irregular and discoloured nature of the upper surface to the bed may be due to the action of boring organisms and slight chemical alteration during this period of reduced sedimentation.

#### 4.4.3.3 Summary and interpretation

It is interpreted that the presence of this glauconite at the top of the Pardina Limestone represents a major transgressive event which occurred at the base of the Reguard Formation and marks the beginning of the Congost-A sequence (see chapter 7). Outcrops in the Sierra del Montsec show evidence of subaerial exposure marking the top of the Pardina Limestone (see sections 3.2.3). The fact that no evidence is seen in Congost d'Erinya to suggest that there was a relative low stand in sea-level prior to this transgressive event, could be the result of tectonically induced basinward tilting that was effecting Upper Cretaceous deposition in the Tremp basin (see sections 2.3, 2.4, 4.5.4.2, 4.6.2 & 7.2.1). This tilting had the effect of enhancing exposure on the inner shelf, while keeping the outer platform submerged. The rise in relative sea-level would have decreased the sedimentation rate and changed the circulation patterns on the sea-bed, whilst also possibly being responsible for an increase in organic matter production due to the associated increase in area of shallow seas (Jenkyns, 1980). The slow down in sedimentation, perhaps coupled with organic matter degredation may have led to the dissolution of aragonitic shell fragments from the deep lagoonal sediments at the top of the Pardina Limestone. The slow sedimentation rates and probable low circulation rates coupled with the decomposition of organic matter created the postoxic-nonsulphidic sea floor environment in which glauconite grows. While glauconite was growing in the sediments which where slowly accumulating above the transgressive surface, pore waters could have filtered down into the top part of the Pardina Limestone, so that glauconite was precipitated in the micro-environments within the voids created by the earlier dissolution of shell fragments.

### 4.4.4 Deep shelf to platform margin transition of the Congost platform

#### 4.4.4.1 Deep shelf facies (The Reguard Formation)

Above the Pardina Limestone, glauconite occurs as discrete grains and as an infill of foraminifera tests set in well-bedded, bioturbated, wackestone rich in calcispheres (see Fig. 4.20c). With the exception of several horizons, the abundance of glauconite decreases rapidly up section. These bedded wackestones are the start of 240m of bioturbated nodular lime-mudstones and wackestones, with shaley horizons,

**Fig. 4.21.** Photograph taken at the northwest end of Congost d'Erinya, showing the southwest side of the gorge. Above the Pardina Limestone (P), the 240 metre thick Reguard Formation can be seen. Landrover for scale.

containing abundant planktonic foraminifera (see Figs. 4.21 & 4.22c). These planktonic foraminifera belong to the *Marginotruncana schneengasi* zone, which forms part of the Late Turonian to the Early Coniacian ( Gomez-Garrido, 1981, 1987, 1989; Caus & Gomez-Garrido, 1989a; 1989b). Also present are numerous calcispheres, small fragments of echinoderms and traces of other fine shell debris.

These bioturbated wackestones have been interpreted as representing a deep shelf facies, where most of the sedimentation was due to pelagic fall-out, with only the smallest shell fragments being brought in by current activity. These sediments are known as the Reguard Formation (Souquet, 1967).

### 4.4.4.2 Transition to platform margin facies

The deep-water wackestones of the Reguard Formation form the lower part of a prominent cliff on the west side of the gorge. Moving up through the section, the deep-water wackestones begin to coarsen up slightly until well-rounded fine-grained packstones are reached (see Figs. 4.22a & 4.22c together with log 10 in appendix 1). These well-rounded packstones mark the base of the platform margin succession.

## 4.4.5 The three platform margin units and their significance

### 4.4.5.1 Introduction

The prominant cliff on the west side of the gorge provides excelent exposure of the platform margin sediments. The platform margin succession can be divided into 3 units on the basis of sedimentology, internal geometry and the presence of on-lap surfaces (see Figs. 4.22a, 4.22b & 4.22c).

### 4.4.5.2 Unit 1

Bedding in unit 1 is not as well defined as that of the underlying deep-water wackestones. When viewed from a distance, unit 1 can be seen to thicken towards the south and to possess a slightly mounded internal geometry (see Figs. 4.22a & 4.22b).

At the southern edge of the cliff, unit 1 is approximately 55m thick, and consists of three coarsening-upward packages (a, b and c)(see Fig. 4.22c). The lowest (a) grades upwards from a medium-grained, bioturbated wackestone with planktonic foraminifera, through to a medium-grained well-rounded packstone with shell debris and abundant benthic foraminifera. The middle package (b) grades upwards from wackestone with planktonic foraminifera, through to a very coarse, sub-rounded grainstone with shell debris and benthic foraminifera. The upper package (c) is much coarser and begins with a medium grained, well-rounded packstone, then it grades upwards through very coarse grainstones, and is capped by a slightly recessive bed. The latter has a coarse wackestone texture consisting of large fragments of rudists, corals and other shell debris, with miliolids and other benthic foraminifera set in a micritic matrix. This coarse wackestone, when traced across the outcrop appears to pinch out basinward as it meets the mound-like topography of the underlying coarse skeletal grainstone (see Figs. 4.22a & 4.22b).

The three coarsening-upward packages can be interpreted as representing periods of progradation of the platform margin. The slightly recessive bed with a wackestone texture at the top of the unit, may represent a shallow lagoonal environment. The coarse well-rounded nature of the grainstones and their mounded geometries suggest that they may have formed banks at the platform margin, so protecting the lagoonal environments behind them. In fact, as mentioned above, at the southern edge of the cliff lagoonal sediments can be seen to onlap the southern flank of one of these grainstone banks (see Figs. 4.22a & 4.22b). When the three coarsening-upwards packages are taken together as a unit, they can be interpreted as

**Fig. 4.22a.** Photograph, looking southwestward at the impressive cliff face which forms the southwest side of Congost d'Erinya. Truck at bottom left for scale.

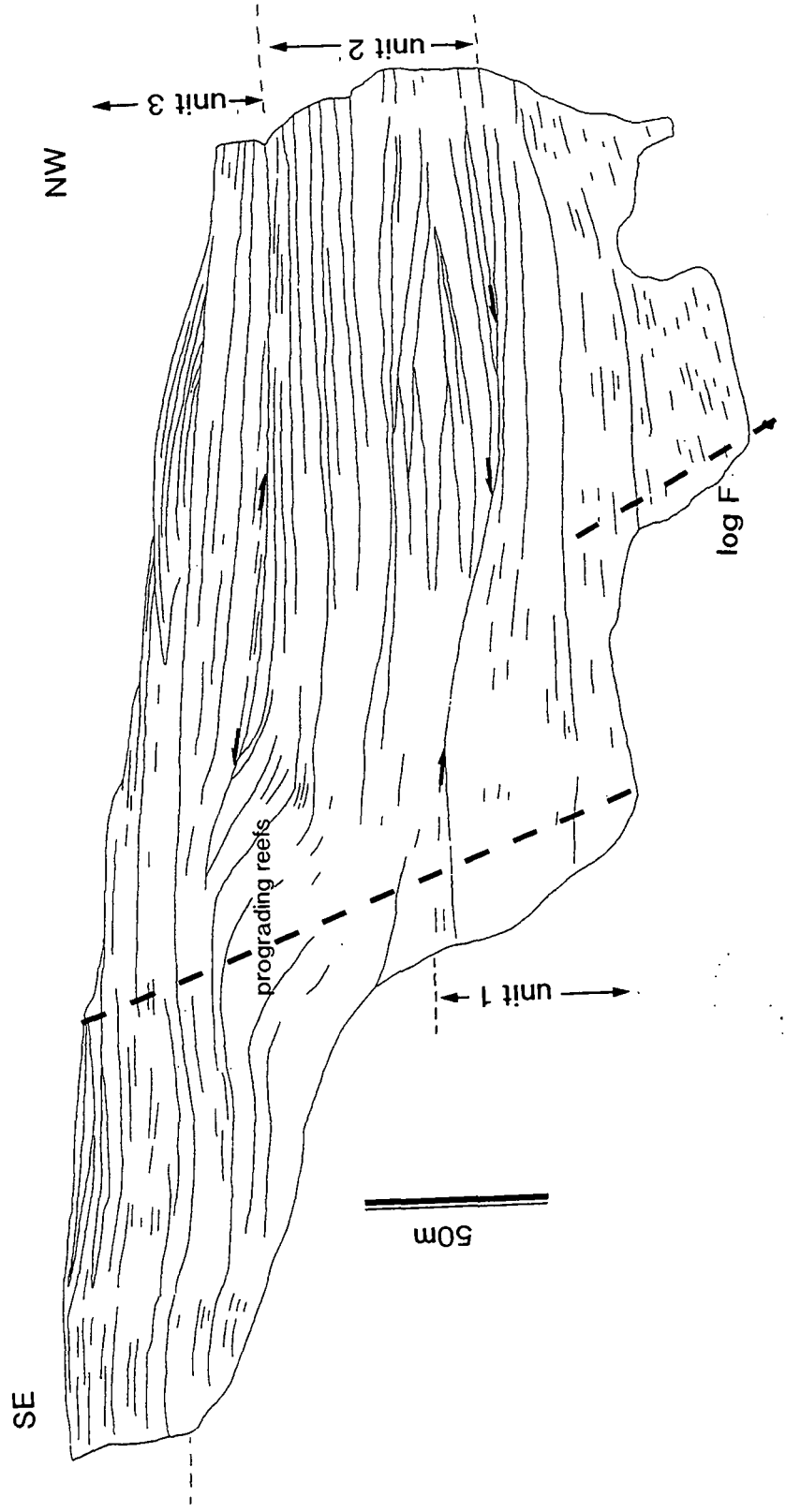


**Fig. 4.22b.** Line drawing of the cliff face which forms the southwest side of Congost d'Erinya (see also Fig. 4.23a). This drawing emphasises the main geometrical features. The outcrop can be divided into 3 units on the basis of sedimentology, internal geometry and on-lap surfaces (arrowed). The units are labelled as described in the text. The path of stratigraphic log F (see Fig. 4.23c) is shown.

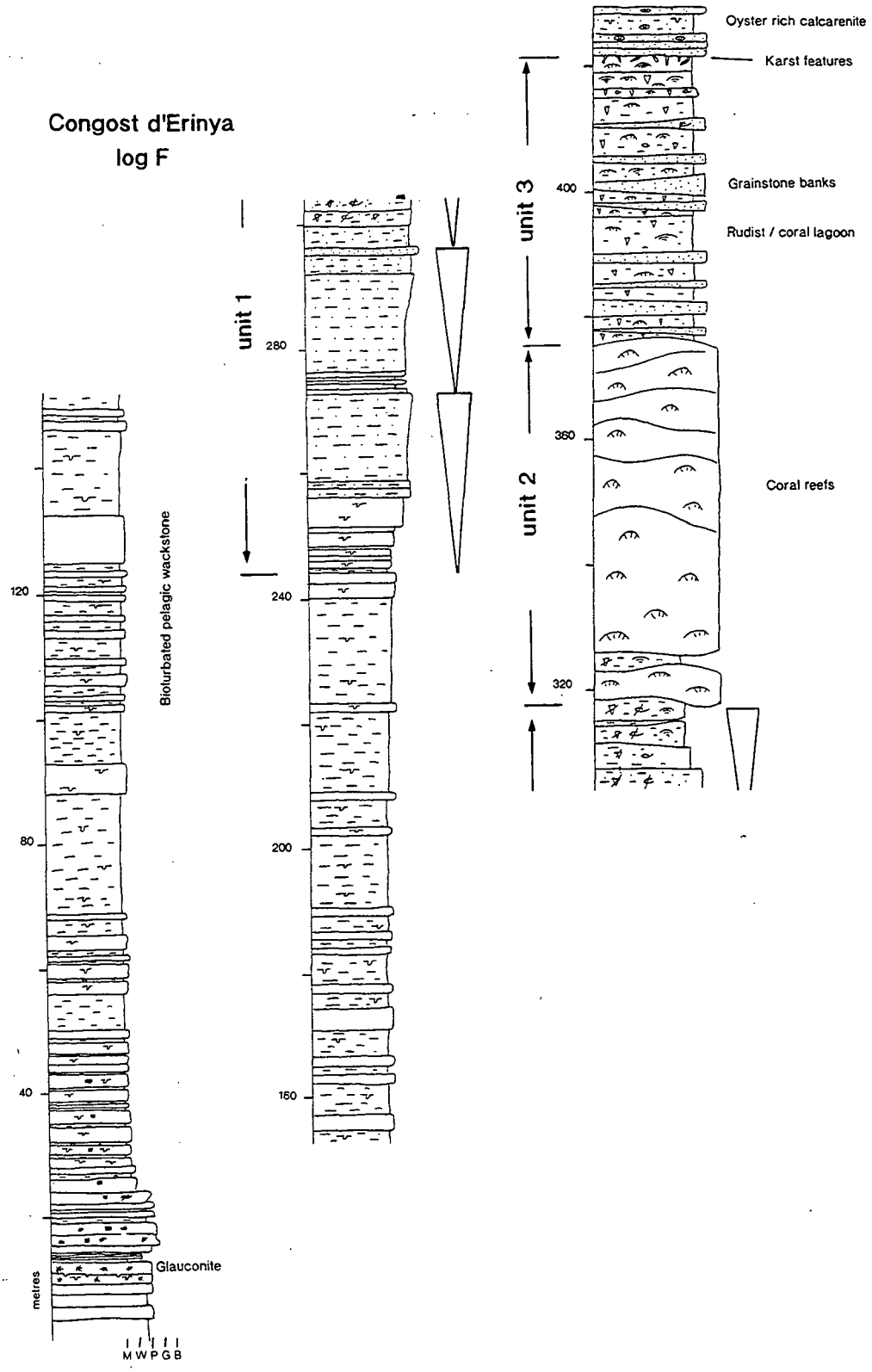


**Fig. 4.22c.** Stratigraphic log (log F) through the outcrop on the southwest side of Congost d'Erinya. The section begins at the northwest end of the gorge with the upper part of the Pardina Limestone (see Figs 4.20 and 4.22) and continues up through the stratigraphy until the top of the Congost platform sediments are reached at the southeast end of the gorge (see Figs 4.23a and 4.23b).

representing progressively more shallow-water facies, and this indicates that unit 1 as a whole represents a period of platform progradation.

### 4.4.5.3 Unit 2

Unit 2 is approximately 60m thick and consists of a series of buildups which can be clearly seen towards the western end of the cliff (see Figs. 4.22a, 4.22b & 4.22c). These buildups are composed entirely of coral. Moving up section, the buildups become progressively smaller in overall size and each successive buildup occupies a more basinward position than the last. This basinward stepping is much more pronounced in the younger, much smaller buildups. When the cliff is viewed from a distance, bedding planes can be traced from the well-bedded strata behind the buildups, around the buildups themselves, on down the foreslopes and into the thinner-bedded sediments on the basinward side of the buildups.

The lower portion of the well-bedded strata on the landward (southern) side of the buildups consists, for the most part, of coarse packstones and wackestones (see Fig. 4.23a). These mud-rich beds contain a wide variety of sub-angular shell fragments, including debris from hippuritid rudists and corals as well as a large number of miliolids and other benthic foraminifera. Moving up section these debris-rich beds are interbedded with coarse wackestones, generally less rich in shell debris, but containing miliolids, large hippuritid rudists and small coral colonies, apparently in life position (see Figs. 4.23b & 4.23c). These rudist and coral beds become more common vertically up section.

The sediments on the basinward side of the prograding coral reefs cannot be studied directly, as they are inaccessible. From a distance these beds can be seen to consist, for the most part, of easily weathered material, with occasional thin, more prominent layers (see Figs. 4.22a & 4.22b). The latter can be used to pick out the bedding, which in the lower half of unit 2 is chaotic, with beds dipping in opposite directions and being truncated, both in an up-dip and a down-dip direction. This truncation shows up as onlap onto the upper surface of unit 1 (see Figs. 4.22a & 4.22b). The bedding in the upper half of unit 2 is fairly planar, and can be traced back as time lines up the slope of the reef front (see Figs. 4.22a & 4.22b).

The coral buildups with their aggradational/progradational geometry, with probable lagoonal facies sediments on their landward side (see Figs. 4.22a, 4.22b & 4.22c), suggest that unit 2 may represent a period during which the platform margin was aggrading as well as prograding. The coral reefs would have represented the high-energy facies, while the hippuritid rudists and small isolated coral colonies (see Fig. 4.23c) were restricted to the low-energy environment provided by the back-reef

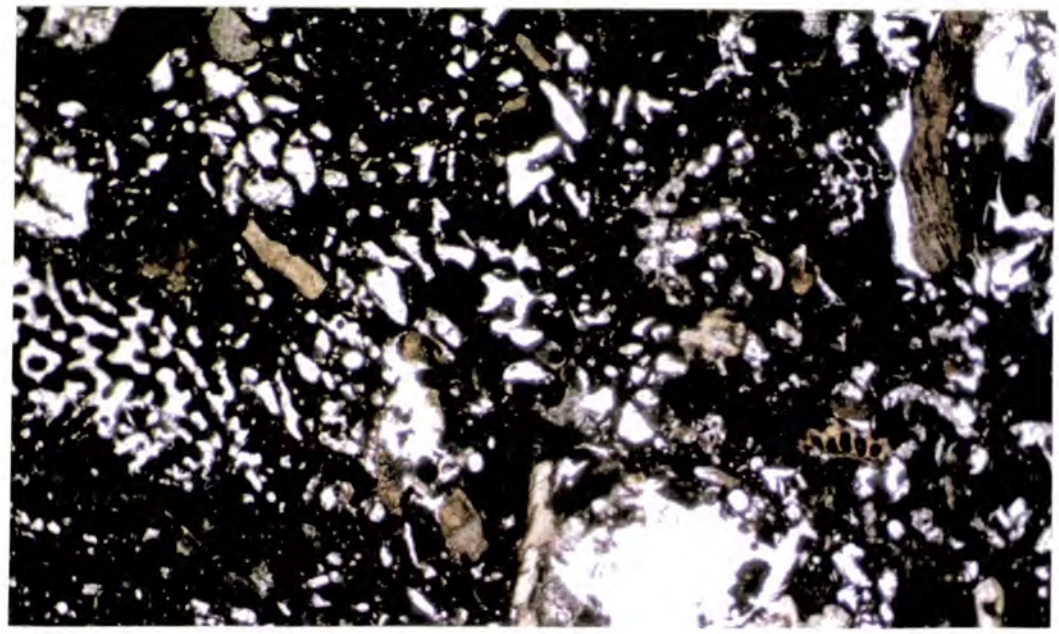

**Fig. 4.23a.** Photomicrograph showing a sample of the packstone, which occurs in the bedded strata landward of the reefs in unit 2 of the cliff section at Congost d'Erinya (see Figs. 4.23a, 4.23b and 4.23c). Note the variety of subangular shell fragments, together with the dissolution that has occurred. Congost d'Erinya sample F4/1. Field of view 12 x 7mm.

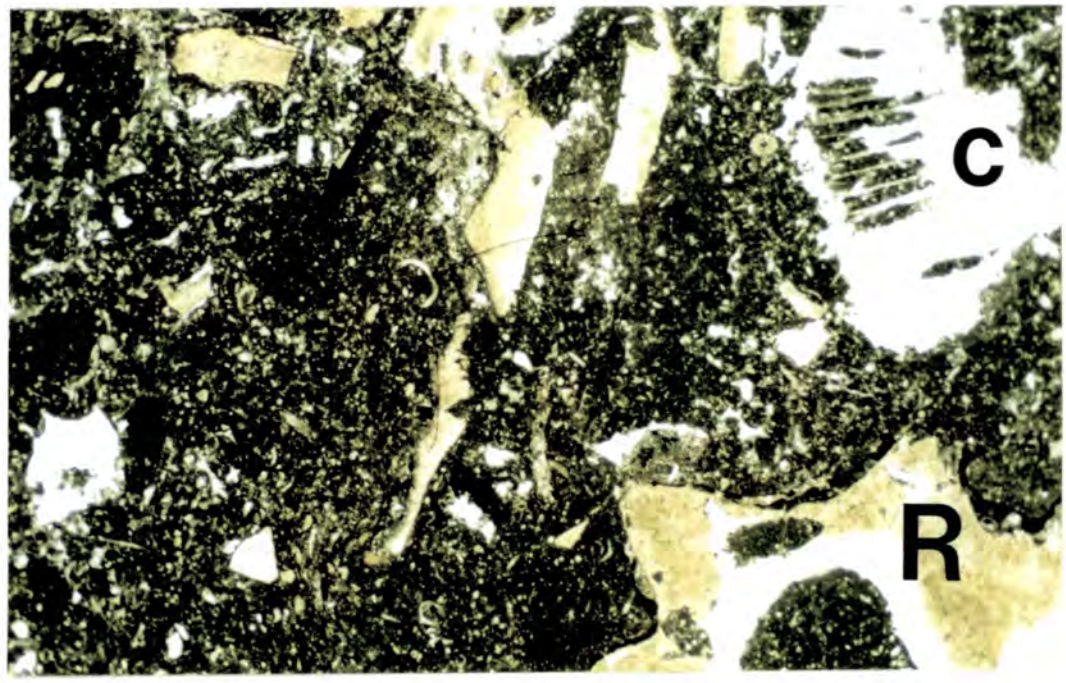


**Fig. 4.23b.** Photomicrograph showing lagoonal wackestone from landward of the reefs in unit 2 of the cliff section at Congost d'Erinya (see Figs. 4.23a, 4.23b and 4.23c). Note the angular nature of the rudist (R) and coral (C) debris as well as the evidence of bioturbation (arrowed). Congost d'Erinya sample FC/3. Field of view 12 x 7mm.

**Fig. 4.23c.** Photograph showing rudists (arrowed), surrounded by nodular wackestone within the bedded strata landward of the reefs in unit 2 of the cliff section at Congost d'Erinya (see Figs. 4.23a, 4.23b and 4.23c). Chisel 25cm long for scale.

lagoons, in which miliolids also flourished. These low-energy lagoonal sediments are interbedded with poorly sorted sub-angular packstones (see Fig 4.23a), containing coral debris and a wide variety of shell fragments, which can be interpreted as possible storm deposits, with debris derived from the reefs. These storm deposits are more common in the lower part of the unit.

The weathering characteristics of the sediments on the basinward side of the reefs (see Fig 4.22a), suggest that they are fine-grained in nature, with the more prominent beds representing better cemented layers or possibly coarser material, which was derived from the reef. The chaotic nature and up-dip/down-dip truncation of these sediments (see Figs. 4.22a & 4.22b) suggest that they may have been effected by slumping. Evidence of slumping in the Congost slope sediments is also seen in the outcrop at Peracals (see section 4.5.4.2 together with Figs 4.30a, 4.30b, 4.30c, 4.31a & 4.31b).

The changing character of unit 2 with height (see Figs. 4.22a, 4.22b & 4.22c) may be giving an indication as to the nature of relative sea-level fluctuations through time. The fact that the rudist and coral lagoonal beds become more common vertically, at the expense of the associated storm deposits, suggests that breaching of the reefs was much more infrequent during the later stages of unit 2 than it was at the beginning. The fact that the older reefs are larger in size and that they do not step

progressively basinward as much as the younger ones, should also be noted. Taken together these observations suggest that accommodation space was increasing much more rapidly during the early stages of unit 2 than it was towards the end.

#### 4.4.5.4 Unit 3

The upper surface of unit 2 is erosional and truncates the top of the last three reefs (see Figs. 4.22a & 4.22b together with log 11 in appendix 1). The overlying sediments of unit 3 on-lap onto the topography created by the reefs at the platform margin, and appear to downlap onto the equivalent surface as it is traced basinward (see Figs. 4.22a & 4.22b). Unfortunately these sediments are inaccessible; however, their weathering profile suggests that they coarsen upwards until they have infilled the topography due to the underlying reefs.

The upper part of unit 3 consists of a series of interfingering recessive and more prominent beds (see Figs. 4.22a, 4.22b & 4.22c). The recessive beds range in thickness from 1 to 4 metres. The majority of the recessive beds contain large hippuritid rudists and small isolated coral colonies in life position (see Figs. 4.24a, 4.24b & 4.24c). These rudists and corals are set in a micritic matrix, which contains miliolids and other benthic foraminifera, as well as some angular shell debris (see Fig. 4.24d). The prominent beds are typically lenticular (see Fig 4.25a) and range in thickness from 0.5 to 3 metres. They are composed mainly of grainstone, although some have a packstone texture. The grainstones contain of a variety of well-rounded skeletal debris, as well as abundant miliolids and other large benthic foraminifera. The grains all possess micritic rims, with the usual early cement being a rim of stubby calcite crystals, although locally pendant cements are present, particularly on the underside of brachiopod fragments (see Fig 4.25b).

The sediments of the upper part of unit 3 can be interpreted as having been deposited in a lagoonal environment. The majority of the recessive beds represent low-energy environments, where large hippuritid rudists and small coral colonies were able to grow. The large amount of micrite which surrounds these rudists and corals (see Fig. 4.24d), would in part have been produced by the action of boring organisms, such as Lithophagid bivalves and clionid sponges, whose bores are abundant in the outer walls of the rudists and corals (see Fig. 4.24d). Occasional storm events could have disrupted these lagoons, causing the rudists and corals to be uprooted from their muddy substrate and fragmented to produce skeletal debris. The lenses of grainstone and packstone which interfinger with these lagoonal sediments (see Figs. 4.25a & 4.25b) can be interpreted as banks of skeletal debris, derived from the reefs and lagoons during storms. These banks would probably have been

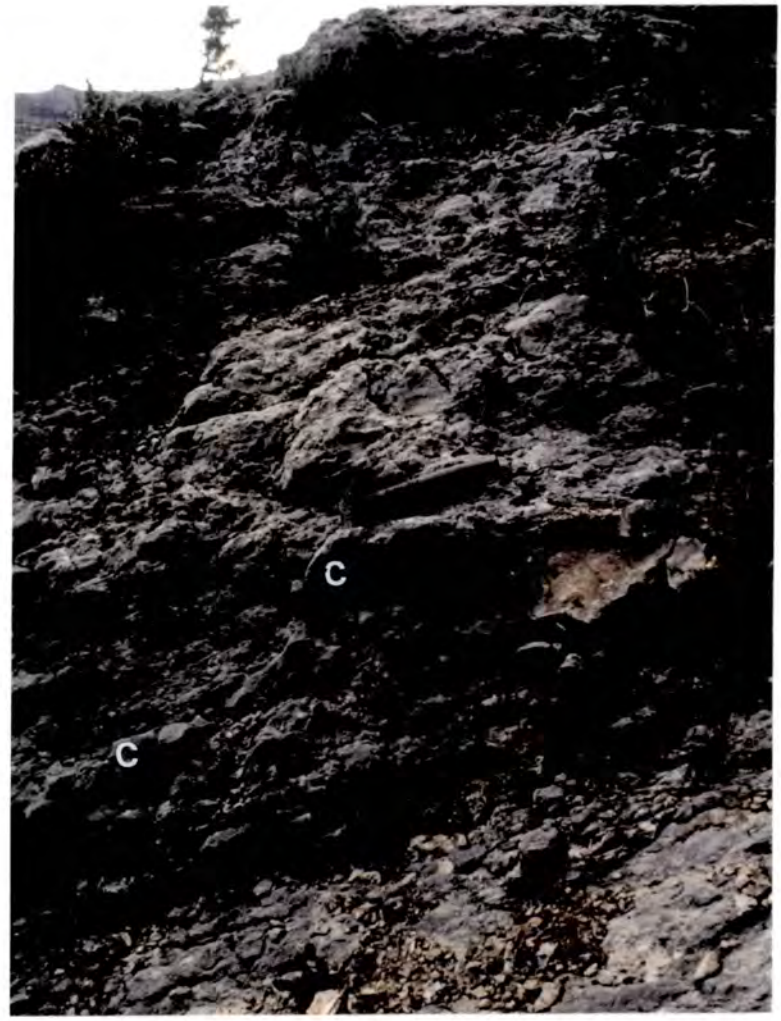


**Fig. 4.24a.** Photograph showing some of the sediments within unit 3 of the cliff section at Congost d'Erinya (see Figs. 4.23a, 4.23b and 4.23c). Note, the coral colonies (C), surrounded by nodular mud rich sediment. Hammer is 35cm long.


**Fig. 4.24b.** Close up of a coral colony from within unit 3 of the cliff section at Congost d'Erinya (see Figs. 4.23a, 4.23b and 4.23c). Pen for scale.

**Fig. 4.24c.** Close up of a hippuritid rudist from within unit 3 of the cliff section at Congost d'Erinya (see Figs. 4.23a, 4.23b and4.23c). Lens cap for scale.

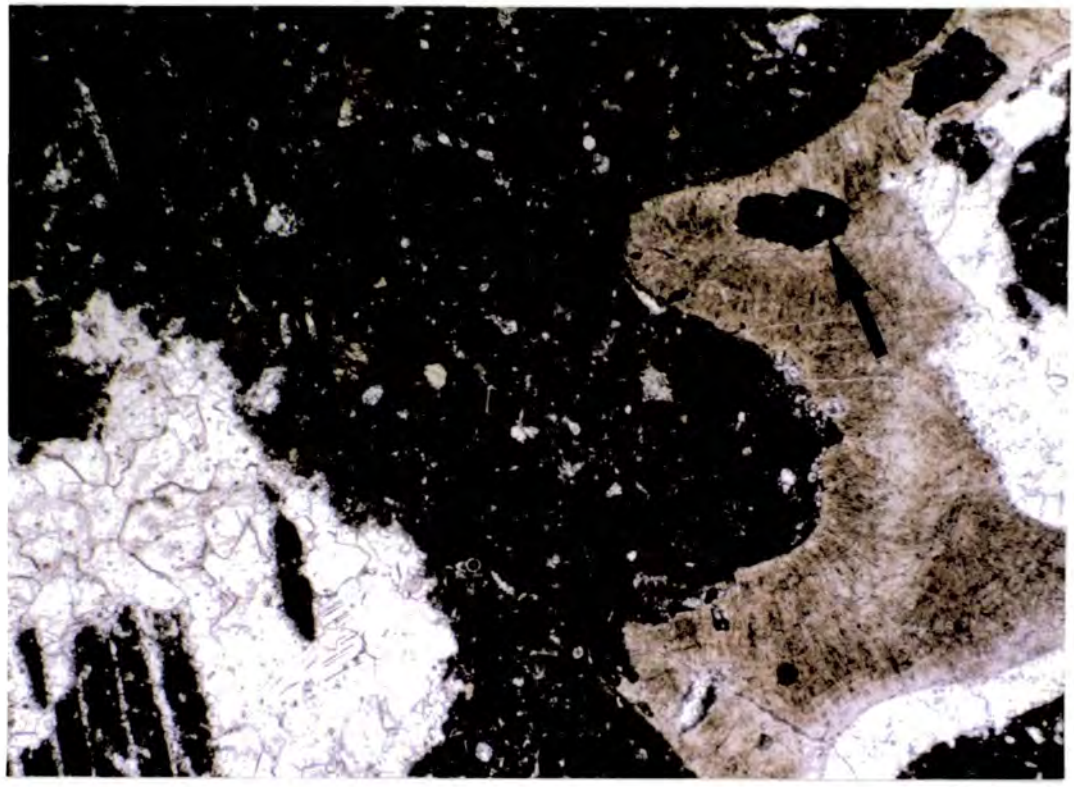

**Fig. 4.24d.** *Photomicrograph* showing wackestone which surrounds the corals and rudists within the lagoonal sediments, from unit 3 of the cliff section at Congost d'Erinya (see Figs. 4.23a, 4.23b and 4.23c). Note the dissolution of the originally aragonitic coral fragment and the boring (arrowed) within the piece of rudist shell. Sample FB/1, Congost d'Erinya. Field of view 6 x 4mm.


**Fig. 4.25a.** Prominent grainstone bed (G) from within unit 3 of the cliff section at Congost d'Erinya (see Figs. 4.23a, 4.23b and 4.23c). Note the lenticular shape of this bed and the more easily weathered nodular beds above and below. The nodular beds contain rudists and corals. Person for scale.

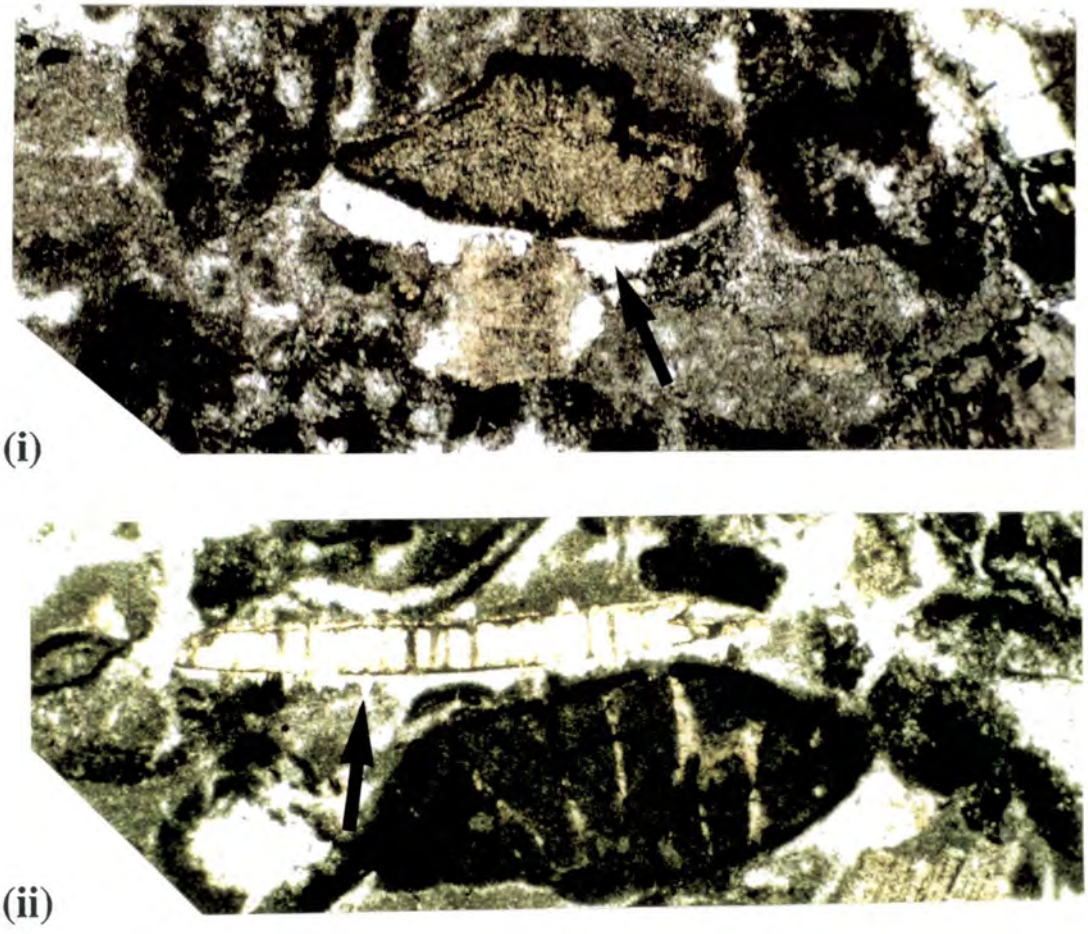


**Fig. 4.25b.**

**Fig. 4.25b.** Photomicrographs showing packstones from one of the lenticular beds within unit 3 of the cliff section at Congost d'Erinya (see Figs. 4.23a, 4.23b and 4.23c). Note the pendant cements (arrowed) below the echinoderm fragment in (i), and the brachiopod fragment in (ii). Both from Congost d'Erinya sample F4/2. Fields of view 6 x 4mm. See previous page.

migrating near the margins of the lagoon. The well-rounded nature of the grains indicates the probable high-energy environment and mobile nature of the substrate during these storms. The local occurrence of pendant cements in these grainstones (see Fig. 4.25b) may indicate that periodicaly these carbonate 'sand banks' became emergent. This emphasises the shallow nature of this back-reef environment.

The top of these lagoonal sediments is marked by a sharp boundary with overlying sediments which consist of distinctive brown-coloured, quartz-rich packstones and wackestones with abundant oysters (see Fig. 4.26). These sediments are similar to those seen above the Congost platform-top sediments elsewhere (see sections 4.2.4.2, & 4.3.2.2 together with Fig. 4.17c) and mark the base of the Anserola Formation, which is interpreted to represent the deep shelf facies of the overlying Sant Corneli platform.

**Fig. 4.26.** Photograph showing oysters within the brown coloured quartz rich packstones of the Anserola Formation, which overlie the Congost platform lagoonal sediments in Congost d'Erinya. Pen for scale.

## 4.4.6 The upper boundary of the Congost platform

### 4.4.6.1 Cement-filled pipes

When the top few metres of the lagoonal sediments in unit 3 are studied closely an interconnecting network of cement-filled pipes can be seen. These pipes criss-cross the lagoonal sediments creating a pseudo-breccia in places (see Fig. 4.27). They only appear to have penetrated the top 3 metres, and are small in size, ranging from small cracks less than 5mm across to a maximum size of 5cm across. When studied in thin section the pipes can be seen to truncate grains at their margins and are infilled by interesting cements (see Figs. 5.40, 5.41a & 5.41b).

The interesting infill to these pipes is described and interpreted in some detail in section 5.6.5.2.

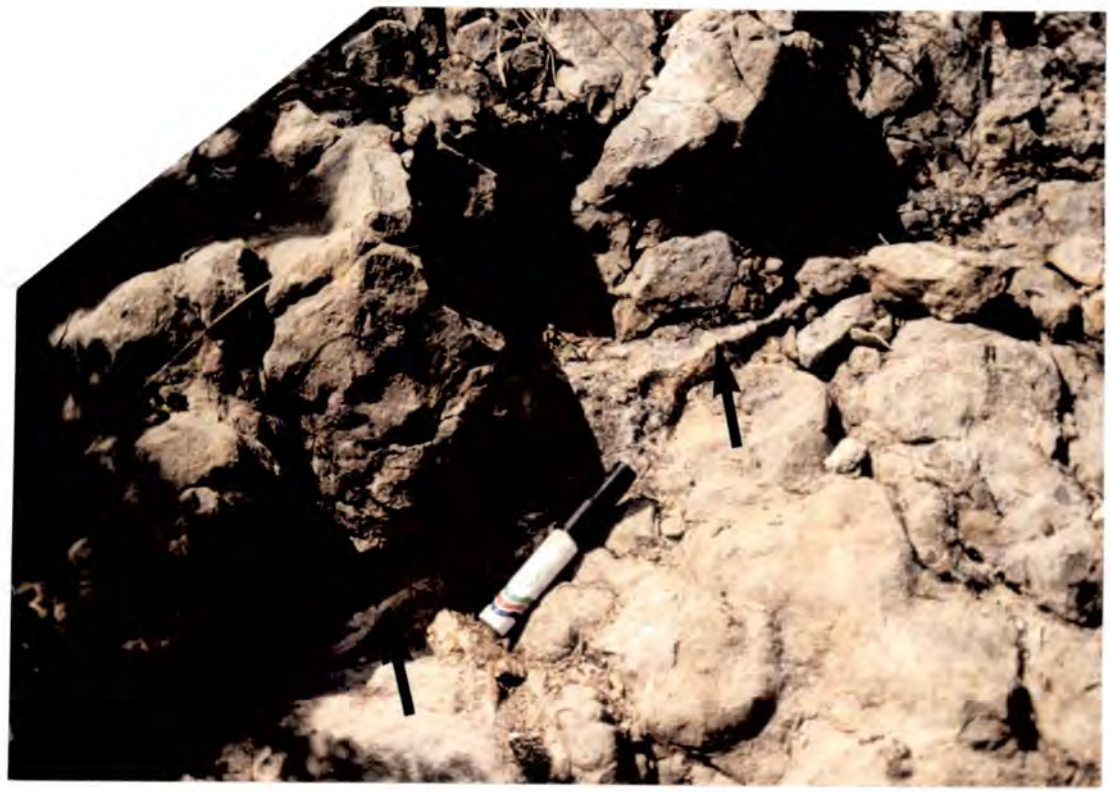

**Fig. 4.27.** Photograph showing the very top of the lagoonal sediments (unit 3) in the cliff section at Congost d'Erinya (see Figs. 4.23a, 4.23b and 4.23c). Note the interconnecting network of cement filled pipes (arrowed), creating a pseudo-breccia. Pen for scale.

#### 4.4.6.2 Interpretation

The nature of the cements within this network of pipes (see section 5.6.5.2 along with Figs. 5.40, 5.41a & 5.41b), together with isotopic analyses and cathodoluminescence studies (see sections 5.6.5.2 and 5.6.7), suggest that these features may be the result of karstic processes.

The pipes (see Figs. 4.27, 5.40, 5.41a & 5.41b) are interpreted to have formed as a result of dissolution by meteoric waters, and near-surface fracturing, with the interesting infills being a result of the reworking of an early speleo-cement lining to the walls of the pipes (see section 5.6.5.2).

The presence of these karst features in the upper few metres of the lagoonal sediments, but not in the deep shelf sediments of the Anserola Formation above, would suggest that prior to the deposition of the Anserola Formation, the Congost platform top underwent a period of exposure. This would indicate that the development of this part of the Congost platform was halted by a significant fall in relative sea-level.

## 4.5 The outcrop at Peracals

### 4.5.1 Introduction

Peracals is a small village situated in the mountains approximately 7km to the north of La Pobla de Segur (see Fig. 4.1). The outcrop (locality 4 on Fig. 4.1), lies a little way along a goat track to the west of the village. It is bounded above and below by thrust faults and shows a section from the upper part of the Santa Fe Limestone through the Pardina Limestone and into the lower part of the Reguard Formation. Detailed mapping and reconstruction by the Catalunya Geological Survey have shown these sediments to have occupied a palaogeographic location basinward of the outcrop at Congost d'Erinya (see section 4.4) but landward of the outcrops around Sant Gervas and Sopiera (Simo pers. com.).

### 4.5.2 The Santa Fe and Pardina Limestones

The Santa Fe and Pardina Limestones which form the lower part of this outcrop have already been described and discussed in chapter 3 (see section 3.5).

## 4.5.3 The upper boundary of the Pardina Limestone

### 4.5.3.1 Red bed

As mentioned in section 3.5.2 the top of the Pardina Limestone at this locality is marked by a distinctive red bed which is approximately 40cm thick (see Figs. 4.28a, 4.28b, 4.30a & 4.30b). This red bed is composed of a packstone rich in calcispheres. The upper part of this bed contains abundant glauconite as well as numerous small nodules of iron oxide, some of which are in the shape of burrows or possibly borings (see Fig. 4.28b). When viewed under the microscope (see Fig. 4.28c) the glauconite can be seen to have the same unusual mode of occurrence as that found in the top bed of the Pardina Limestone Formation in Congost d'Erinya (see section 4.4.3 & Fig. 4.20b). This glauconite has grown inside cavities which in most cases have already been partly infilled by a calcite spar cement. The appearance of most of the cavities suggests that they were created by the dissolution of shell fragments (probably originally aragonitic), although some of them can be seen to possess crystalline walls, suggesting that they may have been the tests of large single chambered foraminifera.

**Fig. 4.28a.** Red bed, which marks the top of the Pardina Limestone at Peracals. Hammer 40cm long.

**Fig. 4.28b.** Close up, showing the upper surface of the red bed which marks the top of the Pardina Limestone at Peracals (see Fig. 4.28a). Note the nodules of iron oxide along the margins of borings (arrowed). Lens cap for scale.

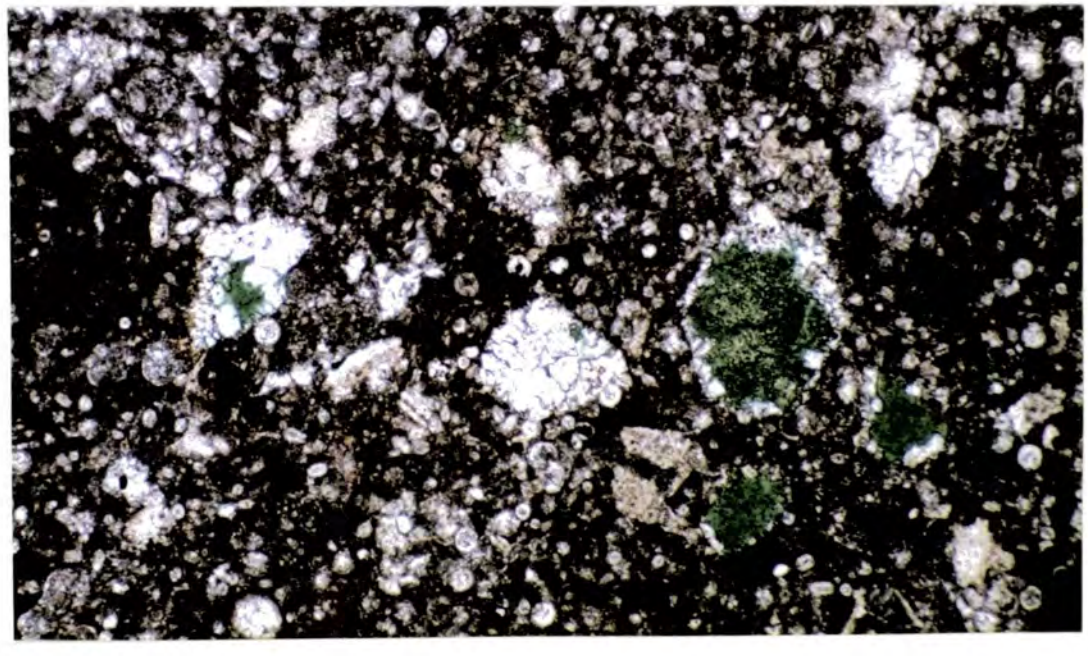

**Fig. 4.28c.** Photomicrograph, showing the calcisphere rich packstone from the red bed, which marks the top of the Pardina Limestone at Peracals (see Fig. 4.28a). Note the occurrence of glauconite which has grown after calcite spar, inside the voids created by the dissolution of shell fragments. Peracals sample PA/13. Field of view 3 x 2mm.

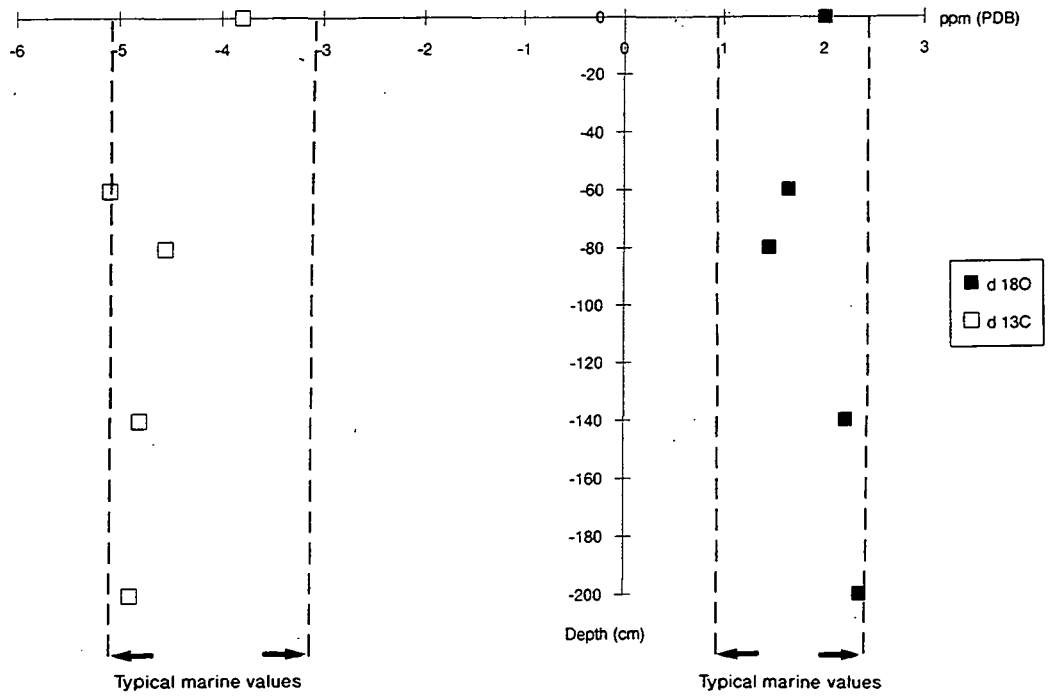


**Fig 4.29.** Plot, showing the stable isotopic (carbon and oxygen) composition of samples vs. the depth below the top of the red bed at Peracals from where the samples were collected.

### 4.5.3.2 Discussion and interpretation

The remarkable similarity in mode of occurrence between the abundant glauconite towards the top of this red bed and that found in the bed interpreted to represent he top of the Pardina Limestone Formation in Congost d'Erinya (see section 4.4.3 together with Figs. 4.20b & 4.28c), suggests that they were formed by the same processes and were probably synchronous.

Whole rock samples from the red bed and the underlying wackestone were analysed for the stable isotopes of oxygen and carbon. This analysis was carried out in order to check for any evidence of a meteoric influence during the development of the red bed. The results did not suggest that there had been any meteoric influence, as all the samples possessed isotopic characteristics similar to those of other unaltered marine sediments from this area (see Fig. 4.29 together with sections 5.2 & 5.4).

As discussed previously (see section 4.4.3.2), the occurrence of glauconite as the last infill to dissolution voids suggests an environment of formation below the seabed during a period of reduced sedimentation. In the same way that the glauconite bed at the top of the Pardina Limestone in Congost d'Erinya was interpreted (see section 4.4.3.3); it is postulated that the red bed seen here (see Figs. 4.28a, 4.30a and

4.30b) represents a hardground which developed during a hiatus in sedimentation, caused by a major transgressive event that marks the base of the Congost sequence.

## 4.5.4 The base of the Reguard Formation

### 4.5.4.1 Chaotic unit

Above the red bed, marking the top of the Pardina Limestone, there is a five metre thick unit which contains a number of large (e.g. 4m by 0.4m) elongate blocks that dip with different angles towards the east (see Figs. 4.30a & 4.30b together with log 13 in appendix 1). When viewed in thin section some of these blocks consist of packstone containing abundant calcispheres (80% of grains), together with some fine-grained echinoderm debris and the occasional planktonic foraminifera. Other blocks consist of packstone with abundant calcispheres, echinoderm debris, other small shell fragments and larger foraminifera, as well as some glauconite which has grown as the last infill to otherwise calcite spar filled voids.

Although it has not yet been possible to date these blocks biostratigraphically, comparisons with thin sections of samples collected from the Pardina Limestone and Reguard Formations at Congost d'Erinya and the outcrops in the region of the Sant Corneli and Santa Fe folds (see sections 3.3.3, 3.4.2, 4.2.2.1, 4.4.3.1 & 4.4.4.1 together with Figs. 3.4, 4.3b(i), 4.3b(ii), 4.20b, 4.20c & 4.28c) suggest that some of these blocks are from the Pardina Limestone and some from the lowest part of the Reguard Formation.

Surrounding these large blocks there is a chaotic conglomerate containing various sizes of sub-rounded, fine-grained, packstone clasts (see Fig. 4.30c). Although again limited by lack of biostratigraphic information, petrographic study has revealed that these clasts may also have been derived from both the uppermost Pardina Limestone as well as the lowermost Reguard Formation.

At the top of this chaotic unit there are several channel-shaped features (see Figs. 4.30a, 4.30b & 4.31a together with log 13 in appendix 1) containing a mixture of small sub-rounded clasts (1-10cm diameter), some of which are red in colour. These channel-shaped features are between 2 and 4 metres wide and approximately 1 to 1.5 metres deep. They are capped by well-cemented limestones. The top surface of which contains abundant nodules of iron oxide (see Fig 4.31a). Some of the iron oxide nodules appear to have the shape of small burrows or borings.

When the infills of these channel shaped features are studied in thin section the clasts can be seen to be of a variety of different types (see Fig. 4.31b). Many


**Fig. 4.30a.** Photograph taken at an oblique angle to the outcrop at Peracals. Note the blocks (B) and channels (C) within the chaotic unit above the red bed. Measuring staff is 110cm long.

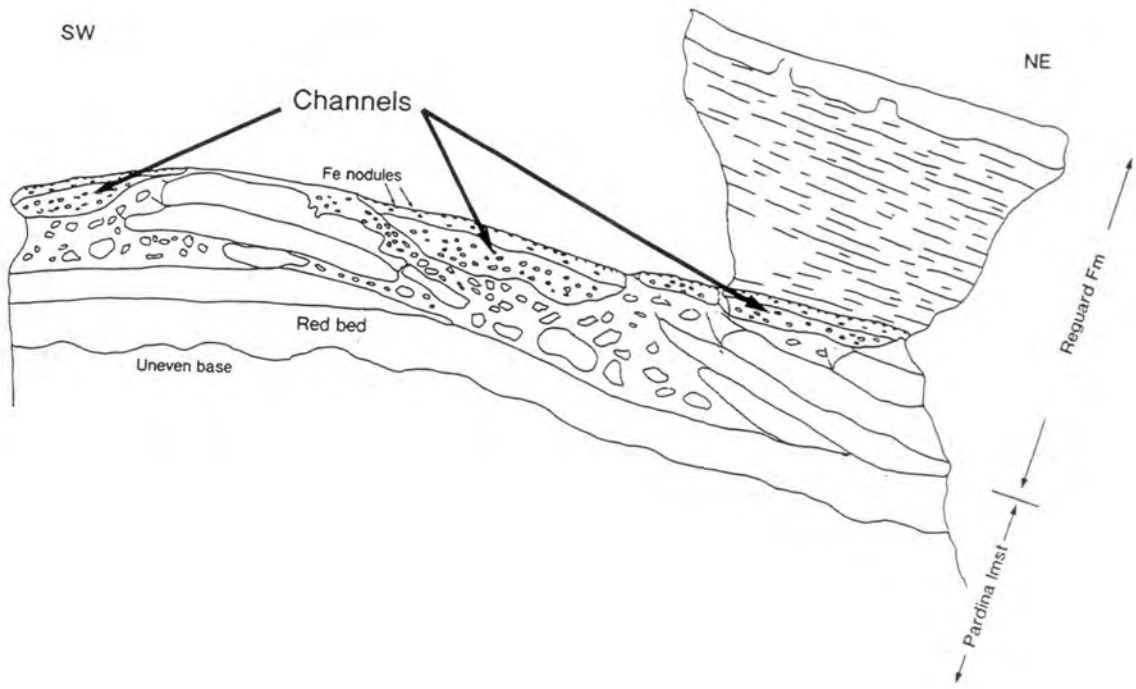


**Fig. 4.30b.** Field sketch showing the chaotic unit above the red bed at Peracals (see also Fig. 4.31a). Note that perspective means the red bed appears relatively thicker than it actually is.

**Fig. 4.30c.** Close up photograph showing the subrounded clasts within the matrix that surrounds the large elongate blocks in the chaotic unit at Peracals (see Figs. 4.31a and 4.31b). Pen cap for scale.

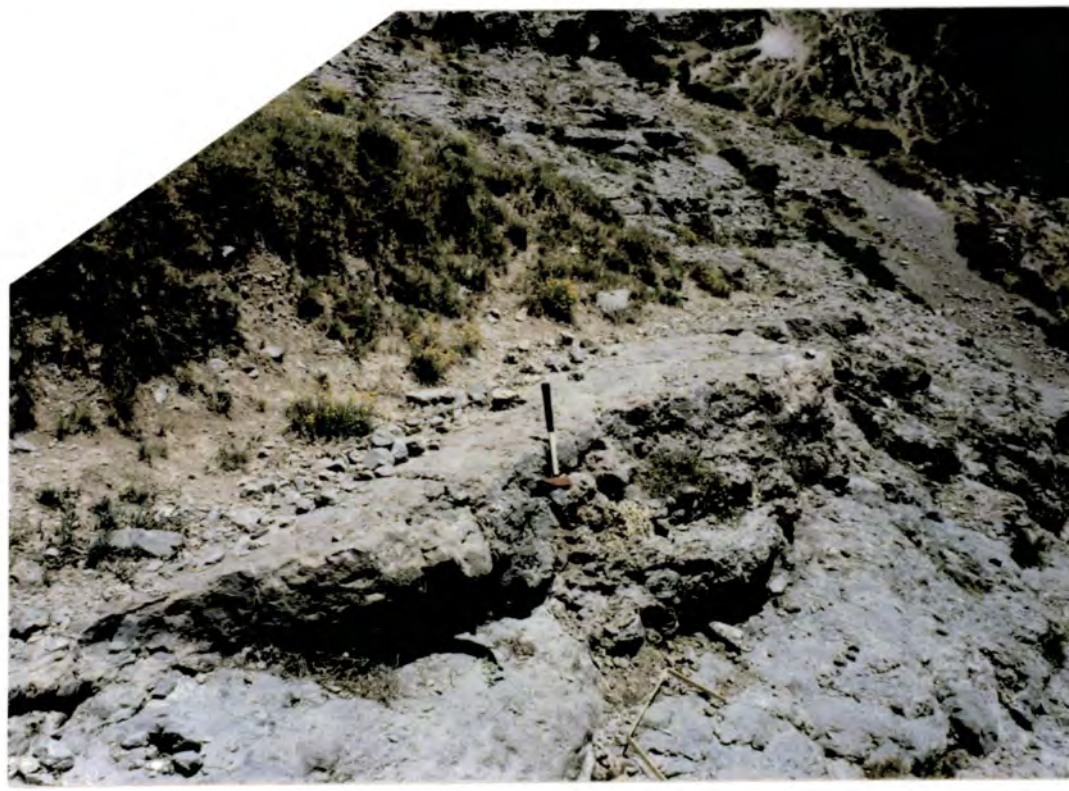

**Fig. 4.31a.** One of the channels within the upper part of the chaotic unit at Peracals. Note the nodules of iron oxide on the upper surface of the channel. Hammer 40cm long.

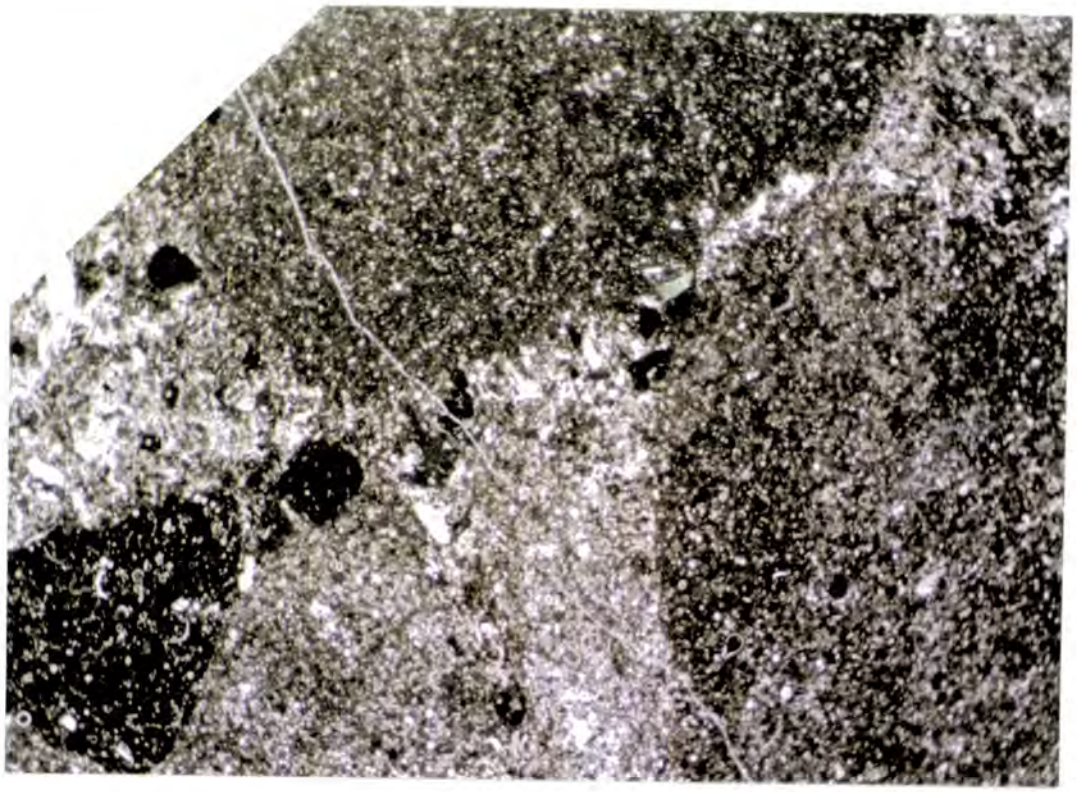

**Fig. 4.31b.** Photomicrograph, showing some of the sediment from within the channel shown in Fig. 4.32a. Note the rounded clasts of calcisphere-rich wackestone and the glauconite grain which occurs in the matrix. Peracals sample PA/17. Field of view 12 x 7mm.

consist of a fine-grained calcisphere-rich wackestone with planktonic and agglutinated benthic foraminifera, together with echinoderm and occasional bivalve fragments. Also common are clasts composed of very fine grained packstone containing mainly closely-packed calcispheres with some small echinoderm fragments and planktonic foraminifera, together with trace amounts of quartz and some small glauconite grains. Others are slightly coarser grained packstones which together with a large number of calcispheres and echinoderm fragments contain numerous benthic foraminifera as well as other shell debris.

When the clasts in the channel-shaped features are compared petrographically with samples of the Pardina Limestone and Reguard Formation from elsewhere (see sections 3.3.3, 3.4.2, 4.2.2.1, 4.4.3.1 & 4.4.4.1 together with Figs. 3.4, 4.3b(i), 4.3b(ii), 4.20b, 4.20c & 4.28c), it can be concluded that these too represent a mixture of debris which may be derived from both the very top of the Pardina Limestone as well as the lowest beds of the Reguard Formation. The red coloured clasts may have originated from a red bed, similar and possibly synchronous with the one seen here which is interpreted to represent a hardground marking the top of the Pardina Limestone Formation.

The top of the channel-shaped features all lie in approximately the same horizontal plane (see Figs. 4.30a, 4.30b & 4.31), above which bedding is conformable again. The sediments which overlie these channels make up the remainder of the outcrop and consist of shaley, bioturbated, fine grained packstones with local, better cemented, slightly coarser grained beds. These packstones contain closely-packed calcispheres (70 - 80% of grains) together with small echinoderm fragments, planktonic foraminifera, a small amount of other shell debris and trace amounts of silt sized quartz and glauconite.

### 4.5.4.2 The significance of the chaotic unit

The general nature of this chaotic unit (see Figs. 4.30a & 4.30b) and the fact that it contains a mixture of blocks and clasts of sediment which appear to have been derived from both the very top of the Pardina Limestone and the lower part of the overlying Reguard Formation, suggest it may be the result of a major slide event due to slope failure. This slide would appear to have started with the movement of large blocks which have become surrounded by smaller clasts of sediment. The rounded nature of the smaller clasts (see Fig. 4.30c) is probably the result of the mechanical action of surrounding debris during the slide process. The final episode of this major event would appear to have been the development of small channels which carried some of the finer grained debris.

The presence of iron nodules, some of which are in the shape of borings, along the top surface of these channels (see Fig. 4.31a together with log 13 in appendix 1) would suggest that there was a period of very low sedimentation rates following the slide event, during which time the upper surface of the channels were cemented sufficiently for boring organisms to colonize them. This low sedimentation rate and associated hardground development may be related to the major trangressive event postulated to have occurred at the base of the Reguard Formation (see sections 4.4.3.3, 4.5.3.2 & 7.3).

This major slide event must have occurred soon after the development of the proposed hardground, at the top of the Pardina Limestone (see sections 4.4.3.3 & 4.5.3.2), and would need to have been of fairly high energy for it to be capable of ripping up clasts and blocks from below this well-cemented surface.

The Pardina Limestone is interpreted to have been deposited on a fairly deep, wide open shelf with an approximately horizontal surface of deposition (see section 3.7.4). The presence of this major slide unit indicates that either during, or soon after the development of the hard-ground marking the top of the Pardina Limestone a slope must have developed. This would indicate that tectonic activity

was effecting the basin at this time. This tectonic activity may in fact have been the driving force behind the sliding that produced the chaotic unit described above. It should also be considered that this tectonic activity may have played a role in the trangressive event postulated to have been responsible for the reduced sedimentation and hence hardground development at the top of the Pardina limestone (see section 7.3.6.1 for further discussion).

## 4.6 Summary of Congost platform geometry and evolution

### 4.6.1 Introduction

As mentioned in section 4.1, the outcrops described in this chapter provide an intermittent view of a platform to basin cross-section through the Congost platform (Fig 4.1). Using information from these outcrops it is possible to build up an hypothesis as to how this platform evolved through time.

### 4.6.2 Hypothesis

It is proposed that the development of the Congost platform followed a period of major transgression (see sections 3.7.4, 4.4.3.3 & 4.5.3.2). This transgressive event is inferred from the following features: (1) The development of a hardground and associated glauconite indicating a period of reduced sedimentation at the boundary between the Pardina Limestone and Reguard Formations (see sections 3.4.2, 3.5.2, 4.4.3.2 and 4.5.3.2 together with Figs. 4.20a, 4.20b, 4.20c, 4.28a, 4.28b & 4.28c); (2) The presence of the deeper water, calcisphere and planktonic foraminifera rich Reguard Formation immediately above this horizon (see sections 3.3.3, 4.2.2, 4.4.4.1 & 4.5.4.1 together with Figs. 4.2, 4.4, 4.6, 4.21 & 4.22c) ; (3) The more landward final position of the Congost Platform margin relative to that of the underlying Santa Fe Platform (see sections 2.3 & 2.5 together with Fig. 2.8b).

It should also be noted that in order to create the sloping shelf, onto which it is postulated that the Congost platform prograded (see section 4.2.3.5), basinward tilting must have occurred either during, or soon after this transgressive event and this may have been responsible for some sliding and resedimentation on the sea-floor (see sections 4.4.3.3 & 4.5.4.2 together with Figs. 4.30a, 4.30b & 4.30c). This basinward tilting would have created a gently sloping depositional surface onto which the calcisphere and planktonic foraminifera rich Reguard Formation slowly accumulated.

The Congost platform appears to have begun life as a shallow lagoon which developed at the edge of this gently sloping shelf and was semi-protected from the open sea by mobile skeletal sand shoals (see sections 4.2.3.5, 4.2.4.3, 4.2.5.2 & 4.3.2.2 together with Figs. 4.11a, 4.11b, 4.15a & 4.15b). It is postulated that skeletal debris derived from this shallow lagoon via tidal channels and wind action began to prograde out onto the gently sloping shelf to form clinoforms (see sections 4.2.3.5, 4.2.4.3, 4.2.5.2, 4.2.5.3 & 4.2.5.4 together with Figs. 4.2 & 4.5). As this debris prograded it would have filled the available accommodation space and enabled the shallow lagoon and shoal system to move basinward (see section 4.2.3.5). The platform continued to prograde basinward and gradually gained in height (see sections 4.2.3.2 & 4.2.3.5 together with Fig. 4.6), as it filled the space provided by the increasing water depth above the sloping basin floor.

The rate of clinoform progradation would have been very rapid compared to the accumulation rate of the pelagic Reguard Formation sediments (see section 4.2.3.5) which were being deposited away from the reaches of all but the finest wind blown platform material. This had the effect of causing the base of the advancing clinoforms to remain almost parallel with the top of the Pardina Limestone Formation (see section 4.2.3.2 together with Figs. 4.2 & 4.5) and ensured that the Reguard Formation has an almost uniform thickness of only a few metres over the whole area displayed by the outcrop around the Sant Corneli and Santa Fe folds (see section 4.2.2.1 together with Figs. 4.2, 4.4 & 4.6).

This phase of rapid progradation appears to have been a cyclic process, based on the grainsize variations in the clinoform sediments (see sections 4.2.3.3 & 4.2.3.4 together with Fig. 4.7b & logs in appendix I),which are interpreted to indicate that the net sediment transport direction at the platform margin varied with time (see sections 4.2.5.3 and 4.2.5.4). This may be suggesting that the platform was effected by small scale fluctuations in relative sea-level. These relative sea-level fluctuations also effected the shallow lagoons of the platform top (see section 4.2.5.3); debris beds (see sections 4.2.4.2 & 4.2.4.3 together with Figs. 4.11a & 4.11c) were deposited during times when relative sea-level was rising and the protective banks at the platform margin were breached, while during periods of sea-level fall the shallow lagoons became exposed (see section 4.2.4.4). However; during the entire period of this rapid progradation there was very little increase in overall accommodation space (see section 4.2.3.5), with the result that the lagoonal sediments were deposited with a uniform thickness over the whole of the platform top (see section 4.2.3.2). This phase of rapid progradation covered a distance of at least 15km and created a platform which was probably over 30km wide.

This first phase of platform progradation appears to have been brought to an end by the rapid migration of skeletal sands over the entire platform interior (see sections 4.2.4.2, 4.2.4.3 4.3.2.2 & 4.3.2.3 together with Figs. 4.11c, 4.12a, 4.12b, 4.17a & 4.17b), indicating an increase in energy on the platform top. This would suggest that the rate of carbonate production had been exceeded by the rate of increase in accommodation space.

The final chapter in this phase of platform development, however, appears to have been a period of subaerial exposure which caused the development of karst features (see sections 4.2.4.4 & 4.3.3 together with Figs. 4.13, 4.18, 4.19a, 4.19b & 4.19c). In addition to affecting the extensive unit of skeletal sand, the karst penetrated down through the lagoonal sediments. The depth of penetration of these karst features would suggest that they were related to a major fall in relative sea-level which had a magnitude of at least 40 metres (see section 4.3.3.2).

During this major fall in relative sea-level if the platform were to continue growing it would have been forced basinward. It is proposed that the results of this forced regression can be seen in the platforms most basinward outcrop at Congost d'Erinya (see sections 4.4.4, 4.4.5 & 5.7.3 together with Fig. 5.45). During this last stage of its development the characteristics of the platform had changed.

This final phase of platform evolution involved the growth of coral reefs at the platform margin and the development of a geometry which shows aggradation as well as progradation (see section 4.4.5.2 together with Figs. 4.22a and 4.22b). The geometry and stacking pattern of the reefs and associated lagoonal sediments indicate that aggradation decreased with time. This suggests that although this phase of platform evolution occurred during a time of increasing accommodation space, the rate of increase in accommodation space was decreasing with time. In fact the erosional surface marking the top of the stacked reefs could be indicating that this decrease in the rate of accommodation space creation may have culminated in a period of platform exposure.

The platform recovered again with the deposition of more shallow lagoonal sediments (see section 4.4.5.3 together with Figs. 4.24a, 4.24b, 4.24c, 4.24d, 4.24e, 4.25a & 4.25b). However; the development of the Congost platform finally came to an end during a period of subaerial exposure which produced an intersecting network of speleo-cement filled dissolution pipes and cavities marking the top of the lagoonal sediments at Congost d'Erinya (see section 4.4.6 together with Figs. 4.27a 4.27b).

# 4.7 Rudist and coral distribution and its significance

## 4.7.1 Introduction to previous research

Rudists were sessile epifaunal suspension-feeding bivalves, which were abundant in low latitude, carbonate dominated, shallow marine environments, from the late Jurassic to the late Cretaceous. Several authors have portrayed rudists as 'reef-builders' (eg. James, 1984; Fagerstrom, 1987) and some have suggested that rudists dominated 'reefs' during the Upper Cretaceous. It has been suggested that rudists achieved their dominance through direct competitive displacement of the corals from the reef communities, after evolving new morphological and ecological features which allowed them to compete successfully (eg. Kauffman & Johnson, 1988).

Scott et al. (1990) criticized the competitive displacement model and showed that corals and rudists continued to thrive together on some Upper Cretaceous shelf and platform margins. They suggested that although some rudists lived side-by-side with corals they in fact thrived in different habitats, with the corals flourishing on the seaward flanks of platform margins and the rudists in the inner-shelf and platform areas. The dominance of rudists during the Upper Cretaceous is attributed to the coral reefs of the early Cretaceous having been unable to cope with mid-Cretaceous fluctuations in productivity (Scott, 1988) coupled with rises in sea-level, while the rudists of the platform interiors remained relatively unaffected by these environmental variations.

This criticism of the competitive displacement model was continued by Ross & Skelton (1993). In addition to the environmental restriction of corals and independent diversification of rudists into a range of platform and shelf facies, they added that patterns of carbonate sediment production and transport during the Cretaceous may have led to a predominance of mobile sand facies, particularly at shelf margins, which would have been inhibiting for coral growth, but favourable for the spread of the various sediment-adapted rudist assembledges which they discuss.

## 4.7.2 Rudists and coral colonies of the Congost platform

### 4.7.2.1 The platform top

As described in the earlier parts of this chapter (see sections 4.2.4.2 & 4.3.2.2 together with Figs 4.11a, 4.11b, 4.11c, 4.14a & 4.14b together with logs 4, 5, 6, 7, 8 & 9 in appendix 1) the lime-mud rich, platform top sediments, which can be

seen at various localities in the region around the Sant Corneli and Santa Fe folds contain both rudists and small coral corals in life position. The corals and rudists are usually in fairly equal abundances, however sometimes beds occur which contain many more coral colonies than they do rudists, and visa versa (eg Fig. 4.11c). These sediments are interpreted to have been deposited in a semi-protected, low energy, shallow lagoonal environment (see sections 4.2.4.3 & 4.3.2.3) within the platform interior.

### 4.7.2.2 Congost d'Erinya

Also described earlier was the outcrop in Congost d'Erinya, where a section through the platform margin is exposed (see sections 4.4.4 & 4.4.5 together with Figs. 4.22a, 4.22b & 4.22c and logs 10 & 11 in appendix 1). As already mentioned, this outcrop represents the later stages in the development of the Congost platform. Here, reefs which are composed entirely of coral can be seen to occupy the platform margin, while rudists together with small coral colonies are found in life positions within the mud rich sediments of the back-reef lagoons (see Figs. 4.23c, 4.24a & 4.24b).

### 4.7.2.3 Conclusions

The evidence presented by the Congost platform would appear to support the view that corals and rudists were able to live together when the environmental conditions allowed, but actually thrived under different conditions from one another.

The occurrence of coral colonies and rudists together within the same lagoonal communities, would suggest that they were not in direct ecological competition with each other.

The coral dominance at the platform margin in the form of reefs while rudists were restricted to the back-reef lagoons, as seen in Congost d'Erinya, would suggest, perhaps, that corals thrived in slightly deeper, higher energy environments than rudists. Another factor in this apparent dominance of corals at the platform margin, during the final stages of platform development maybe that, unlike colonial corals, rudists grew as discrete individuals. Thus rudists would have been unlikely to form rigid organic frameworks in a high energy environment.

This view that corals thrived in slightly deeper, higher energy conditions than rudists offers an explanation for the occurrence of beds, within the platform top strata, which contain either mainly corals or mainly rudists. That is, that these beds represent periods of differing environmental conditions on the platform top, with the

coral dominated beds perhaps representing periods when slightly deeper, higher energy conditions prevailed, and the rudist dominated ones perhaps representing times of very shallow, lower energy conditions.

# Chapter 5
# Diagenesis of the Congost platform-top sediments

## 5.1 A brief introduction to carbonate diagenesis.

### 5.1.1 Introduction

There is an extensive literature on carbonate diagenesis, which has been reviewed recently in James & Choquette (1983, 1984 and 1986), Moore (1989), McIlreath & Morrow (1990), Tucker & Bathurst (1990), Tucker & Wright (1990) and Tucker (1991; 1993). Carbonate diagenesis operates in three principal environments: the marine, meteoric and burial environments (Fig. 5.1). Recognition of the products of a particular diagenetic environment depends upon a combination of field studies, petrographic examination and geochemical techniques, and even then a particular diagenetic environment is easily inferred but proven with difficulty. The three principle diagenetic environments are briefly discussed in the following sections, with regard to major controls and processes.

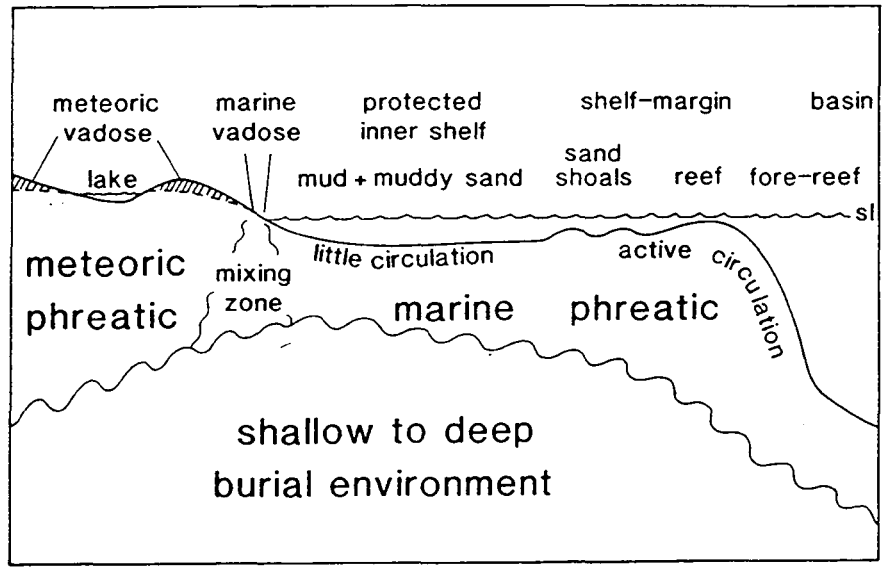


**Fig. 5.1** Carbonate diagenetic environments, schematically drawn for a rimmed shelf with unconfined aquifers. From Tucker & Wright (1990).

## 5.1.2 The marine environment

### 5.1.2.1 Dominant controls on marine diagenesis

The dominant controls on diagenesis in the marine environment are seawater chemistry, the degree of seawater circulation through the sediments, climate and the rate of sedimentation.

### 5.1.2.2 The Recent

In modern, low-latitude, shallow-marine environments, sea-floor diagenesis mainly involves the precipitation of cements and the micritization and destruction of grains due to the action of microbes and other organisms. Typical cements are composed of aragonite and high-Mg calcite, usually with acicular and botryoidal, and bladed and peloidal morphologies respectively (Fig. 5.2). Cementation is most common in areas where seawater is pumped through the sediments, such as within reefs and sand shoals along shelf margins, but it also occurs in areas of evaporation, as on tidal flats and beaches. Micritisation of grains occurs almost everywhere, but is most prevalent in quieter-water locations, where cementation is limited and there is little sediment movement, such as within platform top lagoons.

In modern, mid to high-latitude, shallow marine environments, seawater is undersaturated with respect to aragonite and calcite. In these environments carbonates are rarely cemented and it is common for both calcite and aragonite grains to be effected by dissolution (Alexandersson, 1978). Dissolution also occurs in modern, relatively deep water environments, where increasing pressure and decreasing temperature result in the undersaturation of seawater (Bramlette, 1961; Berger, 1968 & 1978; Takahashi, 1975).

### 5.1.2.3 The ancient

Ancient marine cements are most commonly documented from fossil reefs, where they usually display fibrous morphologies (eg. James, 1983). However, most limestones have a first generation of cement which can be interpreted as marine. Ancient marine cements show a variety of morphologies which range from acicular, columnar to equant crystals that are typically arranged as isopachous rims around grains, to micrite sized crystals which cannot be resolved microscopically. Many of these cements do not have exact modern equivalents, and if they were originally composed of aragonite or high-Mg calcite they will normally have been altered, to be

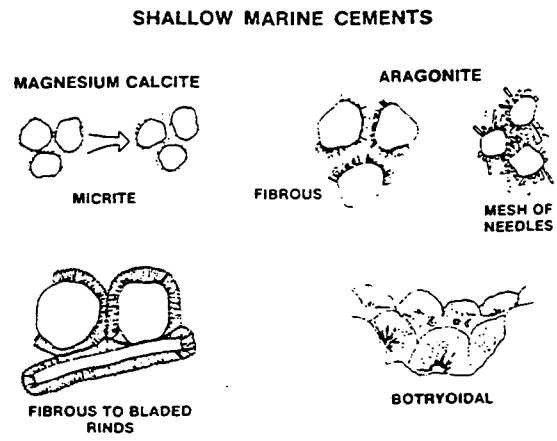


**Fig. 5.2** Typical morphologies of modern marine cements. From James & Choquette (1983).

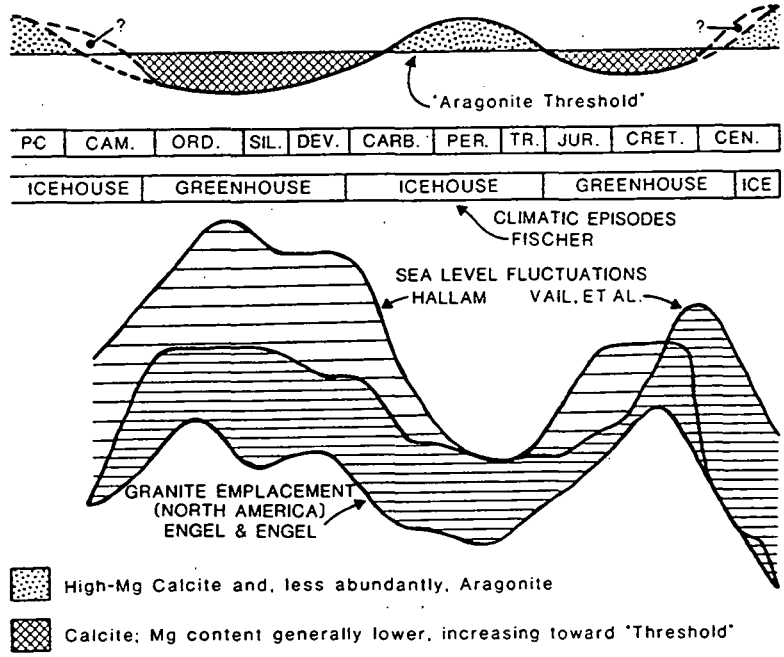


**Fig. 5.3** Cyclic variation in marine carbonate precipitates compared with the first order sea level curves of Vail et al. (1977) and Hallam (1977), together with the global greenhouse/icehouse climatic cycles of Fischer (1981, 1982, 1984a, b). From Sandberg (1983).

present as low-Mg calcite in limestones today. However, careful petrographic and geochemical study can reveal their original mineralogies.

Common features of ancient marine cements are: (1) they are usually the first cement generation; (2) they usually form isopachous rims around grains; (3) they may be cut by borings; (4) they may be associated with internal sediments; (5) the crystals are non-ferroan and non-luminescent; and (6) they may occur within intraclasts (Bathurst, 1975; James & Choquette, 1983).

It is now known, particularly from studies of ooids (Sandberg, 1983; Wilkinson et al., 1985), that the composition of marine calcium carbonate precipitates has varied through the Phanerozoic. This variation in mineralogy of marine calcium carbonate precipitates appears to have been cyclic, with periods when aragonite and high-Mg calcite were dominant (Cambrian, Pennsylvanian-Triassic, Cenozoic) and periods when low-Mg calcite was dominant (mid-Palaeozoic, Jurassic/Cretaceous)(see Fig. 5.3).

The cyclic variation in marine calcium carbonate precipitates shows some correlation with both the global greenhouse to icehouse climatic cycles of Fischer (1981, 1982, 1984a, b) and the first order (i.e. on the scale of hundreds of millions of years) sea-level curves of Vail et al. (1977) and Hallam (1977)(see Fig. 5.3). The underlying control behind both the first order eustatic sea-level variations and the global climatic cycles is thought to be the Earth's heat flow, through its effects on rates of sea-floor spreading and subduction, which in turn will effect the concentration of mantle-derived atmospheric $CO_2$ (Fischer, 1981, 1982, 1984a, b; Veevers, 1990). These same controls can be inferred for the variations in mineralogy of marine precipitates through time, with changes in seawater chemistry, principally in $PCO_2$ and Mg : Ca ratio, being brought about by changes in sea-floor spreading and subduction rates (Wilkinson et al., 1985).

The cyclic variation in marine calcium carbonate precipitates through the Phanerozoic is an important consideration in any diagenetic study of Cretaceous carbonates. This is because the Cretaceous was a period during which the precipitation of low-Mg calcite was preferred. Thus, in contrast with today, it is possible that Cretaceous shallow tropical seas were undersaturated with respect to aragonite, and that the dissolution or neomorphic replacement of aragonite allochems could have taken place in marine waters, even on the sea-floor (as described from certain Ordovician and Jurassic hardgrounds, Palmer et al., 1988).

## 5.1.3 The meteoric environment

### 5.1.3.1 Introduction

Meteoric exposure of carbonate sediments or limestones creates a complex diagenetic environment where the processes of dissolution, cement precipitation and mineralogical transformation (neomorphism) occur contemporaneously. The meteoric diagenetic environment can be divided into several zones (see Fig. 5.4), with each zone having distinctive suites of processes and products. The water table represents an important interface in meteoric diagenesis as it separates the vadose zone (only intermittent saturation) from the phreatic zone (permanently saturated).

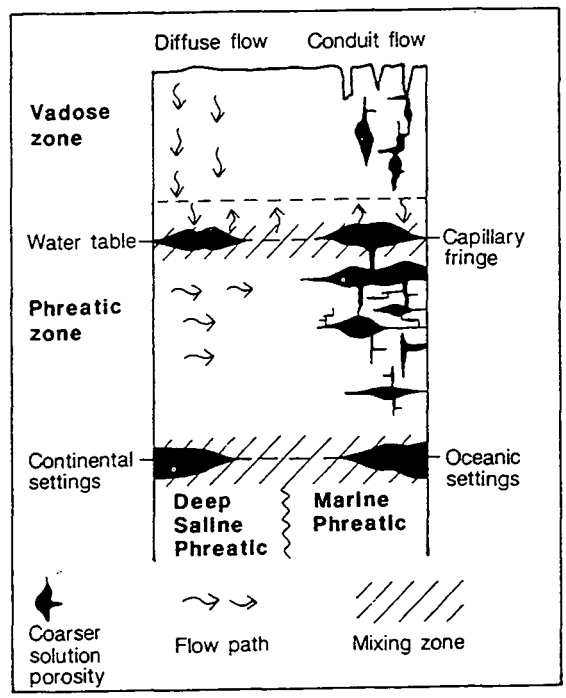


**Fig. 5.4** Groundwater zones. Scales are highly variable. From Tucker & Wright (1990).

### 5.1.3.2 Dissolution and cement precipitation

Dissolution occurs as a result of carbonate undersaturated meteoric waters, which are acidified by atmospheric and soil $CO_2$ , as well as by soil acids. Any form of calcium carbonate can dissolve, although aragonitic grains are particularly susceptible and will tend to be removed preferentially if present with calcite grains or cement. Dissolution of limestone may also occur, which particularly in humid climates can lead to the development of spectacular karst formations. Aragonite and

high-Mg calcite are more soluble than low-Mg calcite in meteoric waters and their dissolution can lead to supersaturation with respect to calcium carbonate.

Dissolution of carbonate can eventualy lead to supersaturation of meteoric waters which typically possess a low Mg/Ca ratio. This can result in precipitation of low-Mg calcite cements. Cementation varies considerably in extent and morphology, with particular differences being apparent between those from the vadose as opposed to those from phreatic environments. Some typical vadose and phreatic cement morphologies are shown in Fig. 5.5.

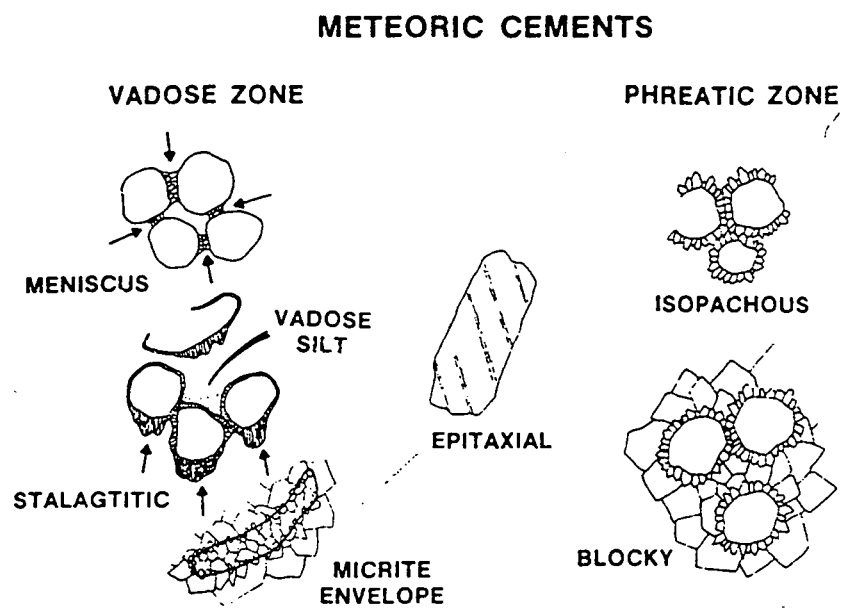


**Fig. 5.5** Typical vadose and phreatic cement morphologies. From James & Choquette (1984).

### 5.1.3.3 Mineralogical transformations

In some instances rather than suffering total destruction through the process of dissolution, originally high-Mg calcite and aragonite components are observed to have been replaced by low-Mg calcite, while still retaining much of their original fabrics or microstructures.

In the case of original high-Mg calcite the textural effects of transformation can only usually be seen with the aid of an SEM (Towe & Hembleben, 1976; James & Choquette, 1984). The process is thought to operate through microscale dissolution and precipitation (Manze & Richter, 1979).

The retention of relict microstructures often observed within originaly aragonitic bioclasts, could also only have been achieved if the replacement of aragonite by low-Mg calcite had occurred, without a cavity stage. It has been

proposed that such neomorphism (Folk, 1965) is an in-situ process of dissolution-reprecipitation across a thin (1μm or less) film of water (Kinsman, 1969; Sandberg et al., 1973; Pingitore, 1976; Al-Aasm & Veizer, 1986a). Such a micron sized boundary has been photographed with the aid of an SEM by Winland (1971)(Pingitore, 1976, his fig. 6).

Differences in the products of neomorphism between the vadose and phreatic environments have been observed by Pingitore (1976), during his study of Pleistocene corals. Pingitore noted that many of the corals which had undergone meteoric-phreatic-alteration had developed coarsely crystalline 'cross-cutting mosaics', in which individual calcite crystals extended out from within the original coral skeleton into the void filling cement; all vadose-altered corals on the other hand displayed much finer crystalline 'fabric selective mosaics', whereby the replacement calcite crystals rarely extended beyond the original skeletal boundaries. In addition to these obvious textural differences, Pingitore noticed that, unlike the vadose altered corals, the meteoric-phreatic-altered corals had not retained much organic tissue and preservation of the microstructure was poor. He interpreted this to be a result of meteoric-phreatic-alteration having involved the development of a zone of temporary, but extensive secondary porosity (chalk zone), several mm thick, which separated the unaltered aragonite from the replacement calcite. Such a 'chalky' zone was in fact observed by Pingitore within samples for which phreatic transformation was incomplete (fig. 8 in Pingitore, 1976).

#### 5.1.3.4 Dominant controls on meteoric diagenesis

Important controls on the style and degree of meteoric diagenesis include climate, the amplitude and duration of relative sea-level fluctuations causing subaerial exposure, the original sediment mineralogy and whether or not the sediment is lithified at the time of exposure.

## 5.1.4 The burial environment

### 5.1.4.1 Introduction

Burial diagenesis begins as soon as sediment becomes buried below the reach of near-surface marine and/or meteoric diagenetic processes, and operates over a considerable range of depth, pressure and temperature under the influence of pore-fluids with varied salinity, chemistry and origin. The most common result of burial

diagenesis is the destruction of porosity, through the processes of cementation, compaction and pressure dissolution. However, porosity can also be gained, through either compactional/tectonic fracture or the dissolution of metastable grains.

### 5.1.4.2 Compaction and cementation

Overburden pressure during burial results in both mechanical and chemical compaction, which can cause large thickness reductions in carbonate sequences. The onset of compaction will cause the migration of pore-fluids, which in turn will allow cementation to take place.

Mechanical compaction, in the form of dewatering and the rearrangement of particles, begins as soon as there is overlying sediment. As the sediment undergoes progressively deeper burial, closer grain packing can occur and a preferred orientation of elongate clasts may develop. Ultimately, mechanical compaction can result in the fracture of grains and cement fringes and lead to the ductile deformation of both grains and sediment.

Chemical compaction and pressure dissolution result in the dissolution of grains and sediment, which is thought to provide an important source of calcium carbonate for burial cementation. Fabrics and structures which evolve as a result of pressure dissolution include: fitted fabrics, dissolution seams, and stylolites (For descriptions of these features see Buxton & Sibley, 1981; Bathurst, 1987).

Cementation in the burial environment generally involves some form of coarse calcite spar, and usually results in the complete occlusion of porosity. Burial spars are typically ferroan, with depleted $^{18}O$ contents when compared to marine or earlier meteoric cements. The burial origin of a cement can only be confirmed through petrographic study if there is textural evidence for its precipitation having followed mechanical or chemical compaction.

### 5.1.4.3 Dominant controls on burial diagenesis

The main controls on the burial diagenesis of carbonate sediments are the burial history and overburden pressure, pore-fluid composition and pressure, and organic maturation. The original composition of the sediment, particularly the lime mud and clay content, together with its early diagenetic history, especially the degree of cementation, will also effect burial diagenesis.

## 5.2 An introduction to stable isotope analysis

### 5.2.1 Introduction

The carbon and oxygen stable isotope compositions of calcite cements provide a useful tool for interpreting the diagenetic environment of their precipitation. Comprehensive reviews of the use of carbon and oxygen isotopes in this way are provided by Hudson (1977) and Anderson & Arthur (1983). The method employed for stable isotope study during this study is set out in appendix 2.

### 5.2.2 Isotopic signatures of marine precipitates

During any study of carbonate diagenesis involving stable isotope analysis, it is important to establish the starting composition of carbonate assemblages in order to provide a baseline for comparison with diagenetic phases. For the majority of carbonates, precipitation and deposition began in marine waters, the isotopic composition of which has varied with geological time (see Fig. 5.6) (Wilson et al.,

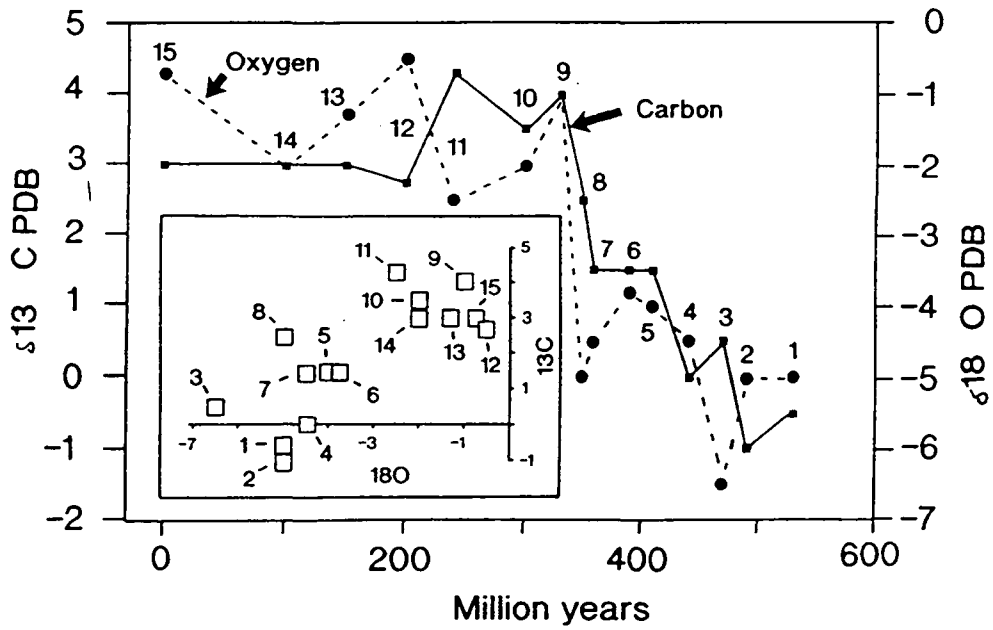


**Fig. 5.6** Secular variation of carbon and oxygen isotopic composition of marine cements during the Phanerozoic. Numbered time intervals are: 15 = Holocene; 14 = Cretaceous (Aptian-Albian); 13 = Jurassic (Kimmeridgian); 12 = Triassic (Norian); 11 = Permian (Kasanian); 10 = Pennsylvanian (Moscovian); 9 = Mississippian; 8 = Late Devonian; 7 = Mid Devonian 6 = Late Silurian; 5 = Mid Silurian; 4 = Late Ordovician; 3 = Mid Ordovician; 2 = Early Ordovician; 1 = Early Cambrian. From Lohmann (1988).

1983; James & Choquette, 1983; 1984; Given & Lohmann, 1985; Popp et al., 1986; Longstaffe, 1987; Lohmann, 1988). The oxygen isotopic signatures of shallow-marine precipitates depend largely upon the $\delta^{18}O$ of sea-water and its temperature. Carbon isotopic signatures of marine precipitates depend upon the $\delta^{13}C$ of sea-water but are also effected by the involvement of organics. An estimate of the isotopic composition of palaeomarine-waters can be derived through the analysis of unaltered primary marine components, such as marine cements (e.g. Prezbindowski, 1985; Given & Lohmann, 1985) or the tests of calcite secreting organisms. Care must be taken when choosing shell material for this purpose, as fractionation occurs within the tests of some organisms during growth. The shells of molluscs, brachiopods (e.g. Popp et al., 1986) and planktonic foraminifera are the most reliable sources of marine isotopic signatures (Anderson & Arthur, 1983).

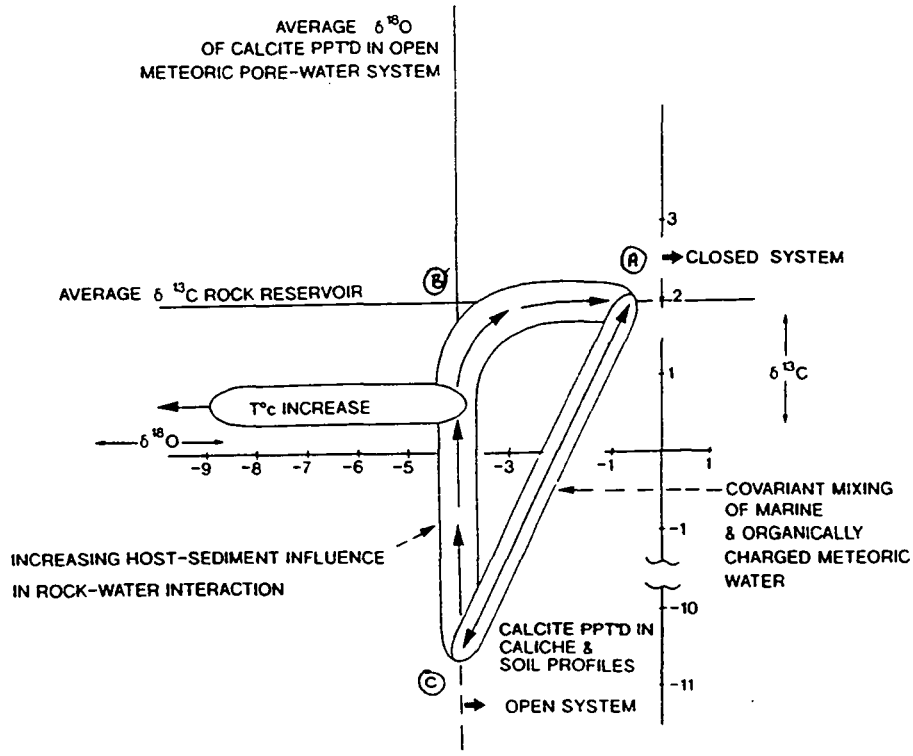


**Fig. 5.7** Likely oxygen and carbon isotope compositions and trends for carbonates undergoing meteoric diagenesis. Point A represents marine sediments; point B represents situations where light meteoric oxygen has entered the system but no soil profile exists to provide light carbon and point C is typical for vadose zones where light carbon is provided from an overlying soil profile. Diagenetic calcites precipitated within a marine-meteoric mixing zone have a tendency to plot along the co-variant trend between A and B. From Moss (1992). Adapted from Allan & Mathews (1977), (1982), Hudson (1977), Wilson et al. (1983) and Lohmann (1988).

## 5.2.3 Typical isotopic signatures of meteoric cements

### 5.2.3.1 General summary

Cements which have been precipitated from meteoric waters tend to be depleted in both $^{13}C$ and $^{18}O$ relative to marine isotopic compositions (see Fig. 5.7) (Gross, 1964; Allan & Mathews, 1977; Hudson, 1977; Allan & Mathews, 1982; Lohmann, 1988). The depletion in $^{18}O$ is due to the fact that rain-water is depleted in $^{18}O$ relative to oceanic water as a result of fractionation during evaporation. This depletion in $^{18}O$ becomes more pronounced with increasing geographic latitude (Dansgaard, 1964; Yurtsever & Gat, 1981; Hays & Grossman, 1991). The depletion in $^{13}C$ is mostly a result of the incorporation of depleted $CO_2$ derived from organics during the passage of meteoric waters through the soil zone.

### 5.2.3.2 Expected $\delta^{18}O$ signature of meteoric water for this study

Latitude and temperature are the primary factors controlling the isotopic compositon of meteoric cements (Dansgaard, 1964; Yurtsever & Gat, 1981; Hays & Grossman, 1991). Hays & Grossman (1991) compiled isotope and palaeolatitude data for meteoric cements ranging in age from Devonian to Recent and in palaeolatitude from 3.5° to 83° (see Fig. 5.8c). These data from ancient meteoric cements showed a marked similarity to theoretical $\delta^{18}O$ values for calcite precipitated in equilibrium with modern meteoric waters at various latitudes. This suggests that any variations in palaeotemperatures with latitude over geological time (eg. Barron, 1986) have had only minor effects on the $\delta^{18}O$ composition of cements precipitated from meteoric waters at particular palaeolatitudes, at least within the accuracy of isotopic analysis.

The palaeolatitude of the Tremp basin during the Upper Cretaceous is thought to have been between 30° and 40° north (Owen, 1983). Comparison of theoretical $\delta^{18}O$ compositions of meteoric cements precipitated from meteoric waters at particular palaeolatitudes for the present day (Fig. 5.8B), with empirical data from meteoric cements of the geological past (Fig. 5.8C), suggests that meteoric cements precipitated at such latitudes would have $\delta^{18}O$ compositions between -4 and -8 ‰ (PDB).

Although latitude and temperature are the primary controlling factors of the $\delta^{18}O$ compositions of meteoric cements, the effects of evaporation, orography, diagenesis and seawater $\delta^{18}O$ can also have an effect. Evaporation of meteoric water prior to cement precipitation can cause significant increases in the $\delta^{18}O$ composition of meteoric cements, while proximity to mountains can produce $^{18}O$ depletions in

excess of the latitudinal effect. These factors should be born in mind during any interpretation of isotope analyses.

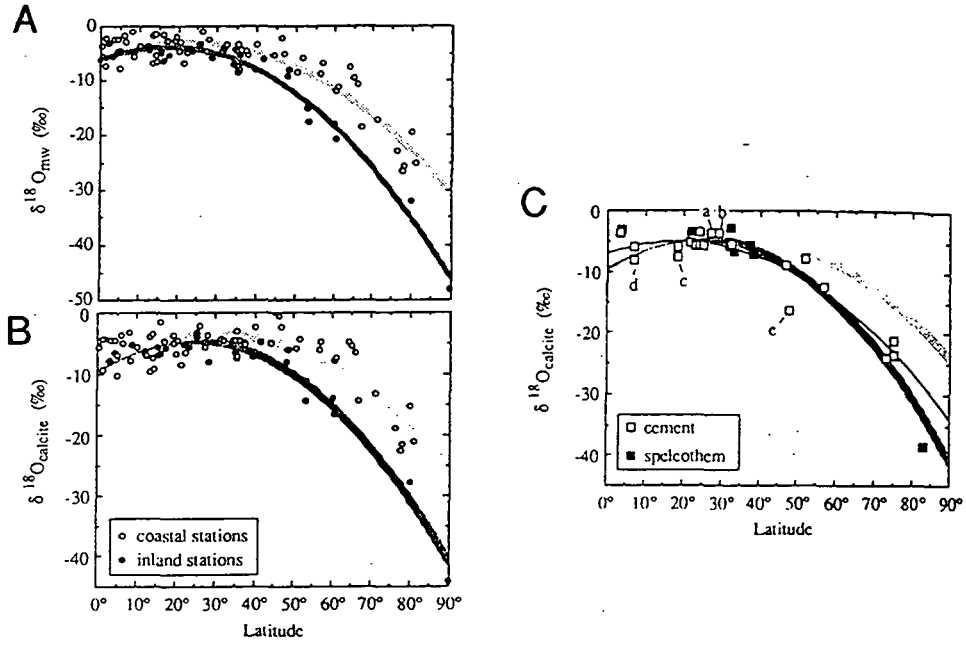


**Fig. 5.8** Chart A shows the empirical $\delta^{18}O$ values for modern meteoric precipitation at various latitudes. From which the theoretical $\delta^{18}O$ values for meteoric calcites at various latitudes shown in chart B, have been derived. Chart C shows empirical $\delta^{18}O$ values for meteoric cements of various ages plotted against paleolatitude. Note the similarity between B and C. From Hays & Grossman (1991).

## 5.2.4 Isotopic signatures of burial cements

Cements precipitated from fluids during burial can show a wide range of isotopic compositions, which are related both to the isotopic composition of the porefluid and the temperature of precipitation. Depleted burial cements can be a result of aquifer recharge by isotopicaly light meteoric fluids or precipitation at high temperature (Prezbindowski, 1985; Woronick & Land, 1985). Another important consideration during studies of burial cements is that organic maturation in the burial environment produces fluids which are depleted in $^{13}C$. However, because the carbon reservoir within carbonate systems is so large, unless recharge occurs, the original $\delta^{13}C$ signature of fluid which enters the burial realm tends to become overprinted by $CO_3^{2-}$ derived from interaction with the host rock (usually with average marine values). The oxygen isotopic composition of cements precipitated during burial is not

effected by such wall rock interaction, but is effected by the temperature of precipitation. Increasing fractionation of $^{18}O/^{16}O$ with increasing temperature results in cements which are increasingly depleted in $^{18}O$.

## 5.3 The importance of rudists and corals

### 5.3.1 Introduction

As described in chapter 4 (sections 4.2.4.2, 4.3.2.2 & 4.4.5), the sediments of the Congost platform-top are typically very mud rich. They consist, in the most part, of easily weathered units which contain abundant rudists and small coral colonies set in a wackestone matrix, and are commonly interbedded with poorly sorted, skeletal debris rich packstones. The mud-rich nature of these Congost platform-top sediments, means that primary interskeletal pore-space is limited. Detailed diagenetic studies would be difficult if it were not for the presence of rudists and corals, whose intraskeletal cavities provided primary pore space, which along with the secondary porosity created by the dissolution of their skeletons provided voids into which cements could be precipitated. The outer originally calcitic layers of rudists also provide an opportunity to investigate the isotopic composition of primary marine calcite.

### 5.3.2 Rudists and their diagenetic implications

#### 5.3.2.1 Introduction

The evolutionary history of rudists was summarized by Skelton (1978; 1985) and their classification has been discussed by Skelton & Gili (1991), who identified several different families. Large, solitary hippuritids are the most common rudists to be found within the Congost lagoonal sediments, although radiolitids and caprinids are also present.

#### 5.3.2.2 Implications of rudist mineralogy and morphology

The original mineralogy and nature of rudist shells was first described by Kennedy & Taylor (1968). They showed that hippuritid rudists possessed bi-mineralic shells, consisting of an inner aragonitic layer with a crossed-lamellar or

complex crossed-lamellar structure and an outer low-Mg calcite layer, built up of blocks of radiating calcite needles. The intraskeletal cavities within hippuritid rudists and the bi-mineralic nature of their shells have important implications for this diagenetic study.

The intraskeletal cavities provided ideal locations for the development and preservation of protracted cementation sequences. Thus, these rudists can provide information about the diagenetic history of the Congost lagoonal sediments which, due to their fine grained nature, would otherwise have failed to provide full cementation sequences.

The originally bi-mineralic shell of the rudists provides the opportunity for a comparative diagenetic study, with the originally aragonitic layers of the shell being much more sensitive to diagenesis than the originally low-Mg calcite layers. The originally aragonitic shell layers have been effected by dissolution and/or neomorphism during diagenesis. Where dissolution of the originally aragonitic shell layers occurred it produced a secondary, moldic porosity which has now been occluded by later calcite spar cements. The outer originally low-Mg calcite shell layers, being more diagenetically stable than the aragonitic layers, have not been affected by dissolution, so that, where strong enough, they have acted as rigid casings to prevent collapse and preserve the sometimes fragile dissolution relationships of the internal originally aragonite shell layers.

#### 5.3.2.3 Other studies of rudist diagenesis

Ross (1989) studied the skeletal diagenesis of rudists from several Tethyan rudist complexes. He showed many of the neomorphic fabrics and dissolution relationships which can be produced and preserved within rudist skeletons, with particular attention to their use as an indicator of diagenetic environment. He also suggested that isotopic signatures together with the fabrics shown by the neomorphosed part of rudist shells reflected different environments of aragonite neomorphism. Other useful studies concerning rudist diagenesis include those of Al-Aasm & Veizer (1986a & 1986b), who examined elemental and isotopic trends within both the originally aragonitic and originally low-Mg calcite shell layers of several different rudist families during diagenetic stabilization. However, they only considered that neomorphism and dissolution could have taken place during meteoric diagenesis.

### 5.3.3 Corals and their diagenetic implications

As would be expected for an Upper Cretaceous carbonate platform, the corals which grew in the lagoons and, at times, along the margin of the Congost platform were aragonite secreting Scleractinia.

The originally aragonitic exoskeletons of these corals, being diagenetically unstable like those of the rudists, have been affected by neomorphism and/or dissolution during diagenesis. In some cases dissolution has led to the creation of secondary porosity. However, unlike rudists, corals do not possess an outer, relatively diagenetically stable, calcite shell, and so are liable to undergo collapse during dissolution.

It should also be noted that although these corals possessed primary intraskeletal cavities, the cavities were small and poorly connected, so that contrasting with the primary cavities of rudists, protracted cementation sequences are uncommon.

A useful study concerning the effects of meteoric diagenesis on corals is that of Pingitore (1976), who compared the results of alteration in the vadose zone to those of alteration in the phreatic zone (see section 5.1.3.3).

## 5.4 Isotopic analysis of rudist shells from the Congost platform

### 5.4.1 Introduction

As mentioned in section 5.2, in any study of carbonate diagenesis which involves isotopic analysis, it is imperative to estimate the initial composition of marine carbonate. The low-Mg calcite mineralogy of the outer part of rudist skeletons means that they are relatively stable diagenetically. Such diagenetically stable shell material can be a useful indicator of the original isotopic composition of marine carbonate.

### 5.4.2 Estimating Cretaceous marine carbonate compositions

Several authors have estimated the initial isotopic compositon of Cretaceous marine carbonate (Scholle & Arthur, 1980; Wilson et al., 1983; Czerniakowski et al., 1984; Moldovanyi & Lohmann, 1984; Woo, 1986; Al-Aasm & Veizer, 1986b; Enos, 1988). Three of these studies involved the use of rudist skeletons (Moldovanyi &

Lohmann, 1984; Al-Aasm & Veizer, 1986b; Enos, 1988). The data gathered by Al-Aasm & Veizer (1986b) and Enos (1988) fell well within the compositional field of the samples analysed by Moldovanyi & Lohmann (1984), which ranges from -2.0‰ to -5.0‰ $\delta^{18}O$ (PDB) and +1.8‰ to +4.0 ‰ $\delta^{13}C$ (PDB). Moldovanyi & Lohmann suggested that the isotopically heaviest values gained during their study of approximately -2.0‰ $\delta^{18}O$ and +4.0 ‰ $\delta^{13}C$ represented a good estimate of the original marine carbonate composition for the Cretaceous. This estimate is compatible to those made by other authors.

### 5.4.3 Petrography of the outer calcite layer of rudist shells

As discused in section 5.3.2.2, rudists possessed bimineralic shells, which, in the case of those found within the Congost platform-top sediments, has resulted in fabric selective dissolution and neomorphism (see sections 5.5.4 & 5.6.4). All originally aragonitic shell layers have suffered either dissolution or neomorphic replacement during diagenesis, whereas the outer low-Mg calcite shell layers have been relatively well preserved.

**Fig. 5.9** Photomicrograph taken under crossed polarised light, showing the prismatic structure within the outer shell layer of a hipuritid rudist from the lagoonal sediments of the Congost platform. Note the sweeping extinction within each of the prisms which is due to the fact that they are each composed of a divergent array of fibrous crystalites. Note also the sediment filled boring which are common features within these rudist shells. Sample FB/2, Congost d'Erinya. Field of view 3 x 2mm.

The outer shell layers of these Congost rudists display microstructures which are built up of a series of elongate prisms, arranged perpendicularly to distinctive growth lines (see Fig. 5.9). Each of the prisms contains a divergent array of fibrous crystallites, which produce sweeping extinction patterns. These prisms vary in size both within individual shells and between different rudists, but usually they have widths between 0.5 and 1mm. Staining with Alizarin red S and potassium ferricyanide solutions (Dickson, 1965; 1966), has shown these outer shell layers to be non-ferroan, and under cathodoluminescence they are completely non-luminescent. The only interruptions to these well preserved microstructures are numerous sediment filled borings (sponges, algae and bivalve), and patches of silicification (see sections 5.5.6 and 5.6.6)

These features displayed by the outer shell layers of Congost rudists are similar to previous descriptions of unaltered low-Mg calcite rudist shell material (Kennedy & Taylor, 1968; Skelton, 1976; Al-Aasm & Veizer, 1986a) and suggest that they have suffered very little, if any, diagenetic alteration. Such shell material can be useful during isotopic analysis as an indicator of initial isotopic compositions.

## 5.4.4 The isotopic composition of Congost rudist shells

Fig. 5.10 shows the isotopic composition of originally calcitic rudist shells from the Congost platform-top, together with the data from previous isotopic studies of unaltered rudist skeletons. As can be seen in Fig. 5.10, only two of the Congost platform samples show a similarity to data from previous studies, while compared to the best estimate of the original composition of Cretaceous marine carbonate, all the samples from the Congost platform are depleted in both $^{13}C$ and $^{18}O$. Calcite rudist shells from the lagoonal sediments of the Congost d'Erinya outcrop show depletions of up to -2 ‰ $^{18}O$ and -2.7 ‰ $^{13}C$ (PDB), relative to the estimate of Cretaceous marine precipitates of Moldovanyi & Lohmann (1984). Rudist shells from the Congost lagoonal sediments exposed in the outcrops in the region of the Sant Corneli anticline and Santa Fe syncline show even greater depletions of up to -3 ‰ $^{18}O$ and -4.3 ‰ $^{13}C$ (PDB) relative to this estimate of Cretaceous marine precipitates.

## 5.4.5 Discussion and interpretation

The significant depletions in both $^{18}O$ and $^{13}C$ shown by originally low-Mg calcite rudist shell layers from the Congost platform, relative to accepted estimates of

Cretaceous marine precipitate compositions from the literature, suggest that either they were precipitated in an isotopicaly distinctive environment, or that some replacement, in the presence of isotopicaly depleted pore-fluids, has taken place. As will be discused below it is probable that the composition trend displayed by these shell samples results from a combination of these factors.

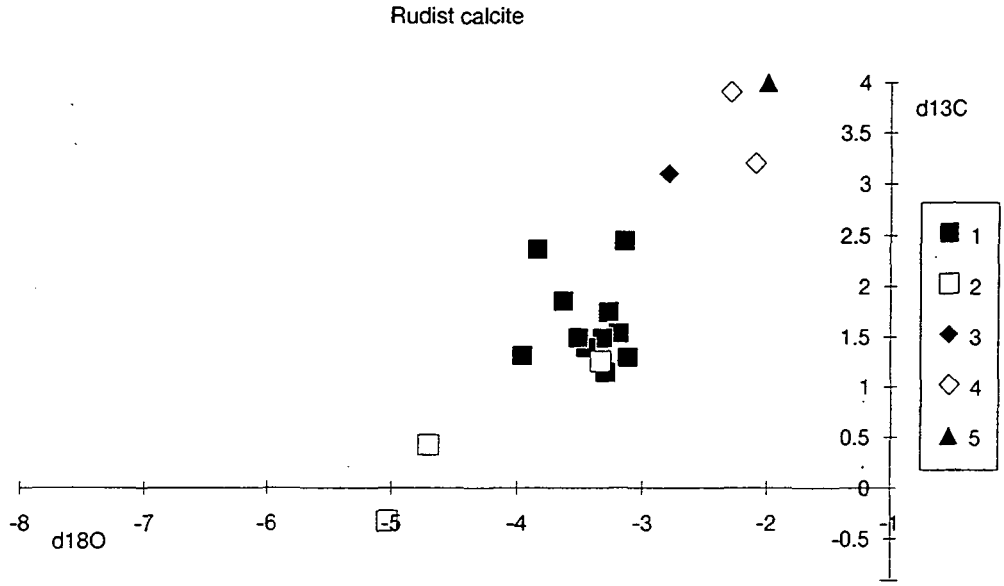


**Fig. 5.10** Oxygen and carbon isotope cross-plot for a number of originally calcitic rudist shells from the Congost platform-top, together with best estimates of Cretaceous marine calcite compositions from previous isotope studies of unaltered rudist skeletons. 1 = shells from the Congost d'Erinya outcrop; 2 = shells from outcrops in the region of the Sant Corneli anticline; 3 = Enos (1988); 4 = Al-Aasm & Veizer (1986b) and 5 = Moldovanyi & Lohmann (1984). See text for detailed discussion.

The lack of any petrographic evidence for these shells having suffered replacement (see section 5.4.3), suggests that at least some of these depleted values may in fact represent the original composition of these shells. In a similar way to the approach of Moldovanyi & Lohmann (1984) and Given & Lohmann (1986), the samples with the heaviest isotopic values (-3.1 ‰ $\delta^{18}O$ and 2.4 ‰ $\delta^{13}C$, PDB) can be used to give an estimate of the original carbonate composition. In order to explain how these shells could have been precipitated with such depleted values, relative to accepted estimates of Cretaceous marine precipitates, it is necessary to consider the environment in which these rudists grew.

In sections 4.2.4.3 and 4.4.5.3 the lagoonal sediments of the Congost platform were interpreted to have been deposited under very shallow, restricted conditions, which during the first phase of platform development, were protected from the open sea by skeletal sand banks, and later in the second phase of development, by coral reefs (see section 4.6). The benthic foraminifera which are abundant within the mud rich sediments that surround the rudists and corals are of distinctive types which only thrived in shallow restricted environments (Caus pers. com.). Following a study of clay mineral assemblages, Nagtegaal (1972) suggested that the palaeoclimate during the deposition of the Upper Cretaceous in the Tremp basin was sub-tropical to tropical but could have been either arid or humid. In later sections (5.5.4, 5.5.5, 5.6.4 & 5.6.5), diagenetic features have been interpreted to suggest that the Congost platform developed under humid climatic conditions. Under such sub-tropical, humid climatic conditions, where rain fell in abundance, the water within the shallow lagoons of the Congost platform, which were protected from the open sea, would be likely to have had a fairly high temperature and have been of mixed meteoric and marine composition. Under such conditions, the isotopic composition of lagoonal waters would not only be depleted (relative to open marine waters) in $^{18}O$ as a result of rain-water falling within the lagoons, but if rain-fall was high, as is suggested by some diagenetic features, then run-off from adjacent land surfaces and the associated incorporation of soil derived $CO_2$ could have produced a significant depletion in $^{13}C$.

The isotopically heaviest values shown by these calcite rudist shell samples, of approximately -3.1 ‰ $\delta^{18}O$ and 2.4 ‰ $\delta^{13}C$ (PDB), are interpreted to represent a best estimate of their original composition and are considered to be a result of the distinctive isotopic environment of a restricted lagoon under humid, tropical, climatic conditions. The more depleted values, on the other hand, contrary to the evidence provided by petrographic study, are interpreted to suggest that some recrystallisation of rudist shells may have taken place. → ? micro-scale recrystallisation?

The more depleted values display a trend which suggests varying amounts of recrystallisation. The significant depletion in $^{13}C$ of up to 2.8 ‰ (PDB) with respect to the least depleted values (interpreted as a best estimate of the original composition), suggests that recrystallisation must have occured in an open system under the influence of fluids with light $\delta^{13}C$ composition. The light $\delta^{13}C$ compositions could have resulted from either organically-charged meteoric waters or from organic maturation in the burial realm. The interpretation that the majority of the cementation of these sediments occurred either at the surface or in the shallow phreatic environment (see section 5.7), together with the fact that they have only been

subjected to shallow burial (see chapter 2), suggests that organically charged meteoric fluids are the most likely source of the light $\delta^{13}C$ values.

The fact that the shells of rudists which were found at the outcrops in the region of the Sant Corneli anticline and Santa Fe syncline show greater depletion in both $^{18}O$ and $^{13}C$ than the rudist shells from Congost d'Erinya, (see Fig. 5.10) suggests that they have undergone a greater degree of recrystallisation under the influence of depleted meteoric waters. This is perhaps more evidence for the separation of Congost platform development into two distinct phases (see section 4.6) and could suggest that the platform-top sediments of the first phase of platform development (those outcroping in the region of the Sant Corneli anticline and Santa Fe syncline) were subjected to a greater degree of diagenetic alteration in the presence of meteoric waters than those of the second phase of platform development (those outcropping in Congost d'Erinya).

## 5.5 Sant Corneli anticline, Santa Fe syncline and Ortenada outcrops

### 5.5.1 Introduction

The sedimentology, geometry and general nature of the platform top sediments seen at these outcrops have been described in chapter 4 (see sections 4.2.4, & 4.3.2). During the discussion in chapter 4 (see section 4.6 for summary), it was suggested that these outcrops can be grouped together as representing the first phase of Congost platform development, during which time the platform top was dominated by shallow, muddy lagoons, that were protected from the open sea by mobile sand bars and provided an environment within which rudists, large benthic foraminifera, echinoids and small coral colonies flourished. The discussion in chapter 4 also suggests that this first phase of platform development was one of rapid progradation which, although effected by small scale fluctuations in relative sea-level, occured over a period of time when there was very little overall increase in accommodation space. Also proposed in chapter 4 was that this first phase in the development of the Congost platform was brought to an end by a major fall in relative sea-level, which caused karstification.

Through the study of thin-sections (particularly those taken from rudists), using both standard petrography and cathodoluminescence, it has been possible to place phases of cementation, dissolution and neomorphism into a relative time order, and thereby suggest a succession of diagenetic events which may have affected these

platform top sediments. In some cases stable isotope analyses have aided the interpretation of some of these diagenetic features. Comparison of samples from the platform top sediments found at the various outcrops around the Sant Corneli and Santa Fe folds with those from Ortenada suggests that they have all undergone very similar diagenetic histories and this therefore supports the hypothesis that these outcrops can be grouped together as representing one phase of platform development.

In the following sections these diagenetic features are described and interpreted in their approximate order of formation.

## 5.5.2 Micritisation

Micritisation has effected almost all the carbonate allochems within these platform top sediments. The micritisation has produced thick micritic envelopes around most of the shell fragments, while some grains, particularly the shells of foraminifera, have been completely micritised (see Figs. 4.12b, 4.16a, 4.16b & 4.17b). In many cases the micritisation has been so intense that identification of the origin of the grains is impossible.

Micritic envelopes which formed upon originally aragonitic bioclasts were resistant to subsequent dissolution and neomorphism which removed or replaced unmicritised aragonite skeletons (see Fig. 5.19). As will be seen in later sections these micritic envelopes provide a useful tool during diagenetic studies involving rudists, as they can indicate the original positions of aragonitic shell layers (see sections 5.5.4.3, 5.5.4.4, 5.5.4.5 & 5.5.4.6, together with Figs. 5.21, 5.22, 5.23, 5.24, 5.27 & 5.29).

The micritised margins around larger bioclasts, such as brachiopods or rudist bivalves, are often associated with borings into the shell wall.

Micritisation is a common phenomenon typical of platform-top/lagoonal environments and has been described by many authors. Most micritisation occurs near the sediment/water interface (Kobluk & Risk, 1977), but may also occur more than a metre below (May & Perkins, 1979). Micritisation results from the action of endolithic algae, fungi and bacteria, whose borings penetrate the margins of skeletal grains, to be subsequently filled by fine grained sediment or cement. In these lagoonal sediments micritisation would have been promoted by the protected nature of the environment and the relatively slow rate of sedimentation. Longman (1980) referred to such environments as 'stagnant marine phreatic', where, because of the slow rate of water movement through the sediment and/or unfavourable fluid chemistry, cementation is limited and micritisation becomes the dominant early diagenetic process.

## 5.5.3 Marine cementation

### 5.5.3.1 Introduction

The most obvious early cement generations within the lagoonal facies sediments are to be found lining some of the intraskeletal cavities of rudists and corals. However, the presence of other early cement generations within the wackestones and packstones of the lagoons can be inferred from such features as the preservation of uncrushed moulds of originaly aragonitic shell debris, which indicate that matrix lithification was advanced prior to dissolution (see Figs. 4.11c(i), 4.11c(ii), 4.16a, 4.16b, 4.16c, 4.17b, 5.18, 5.19, 5.20, 5.26, 5.37 & 5.38). This lithification probably involved the precipitation of micrite sized crystalites which are indistinguishable from the micrite within these mud rich sediments.

There are two very different morphologies of the early cement generations present within the intraskeletal cavities of rudists. These are bladed to stubby calcite crystals and fan shaped splays (botryoids) of elongate calcite crystallites. Out of the 15 rudist samples which were collected from these outcrops and thin sectioned; 9 contained botryoidal type cements and 6 contained the bladed to stubby isopachous cements, within their primary intraskeletal cavities.

Early cements, in the form of isopachous fringes of fibrous calcite, can also be found lining the interskeletal cavities within the high energy facies grainstones which mark the top of the Congost platform-top sediments.

### 5.5.3.2 Bladed to stubby, isopachous cements

Figure 5.11, shows isopachous, bladed to stubby calcite cements lining the primary pore space within a rudist from lagoonal sediments which outcrop on the slopes above Casa Borrell (locality 1a, Fig 4.1). These bladed/stubby calcite crystals are slightly elongate in character, inclusion rich, non-luminescent (see Fig. 5.22) and range in length from 25μm to 100μm. Where present, these crystals form isopachous fringes which create the second lining, after micrite, to what were primary intraskeletal cavity walls and completely encircle the primary pore space (see also Figs. 5.24, 5.27 & 5.29). In some cases these fringes are composed of a series of small splays, each consisting of a number of bladed crystals which have grown in a slightly irregular but radiating pattern.

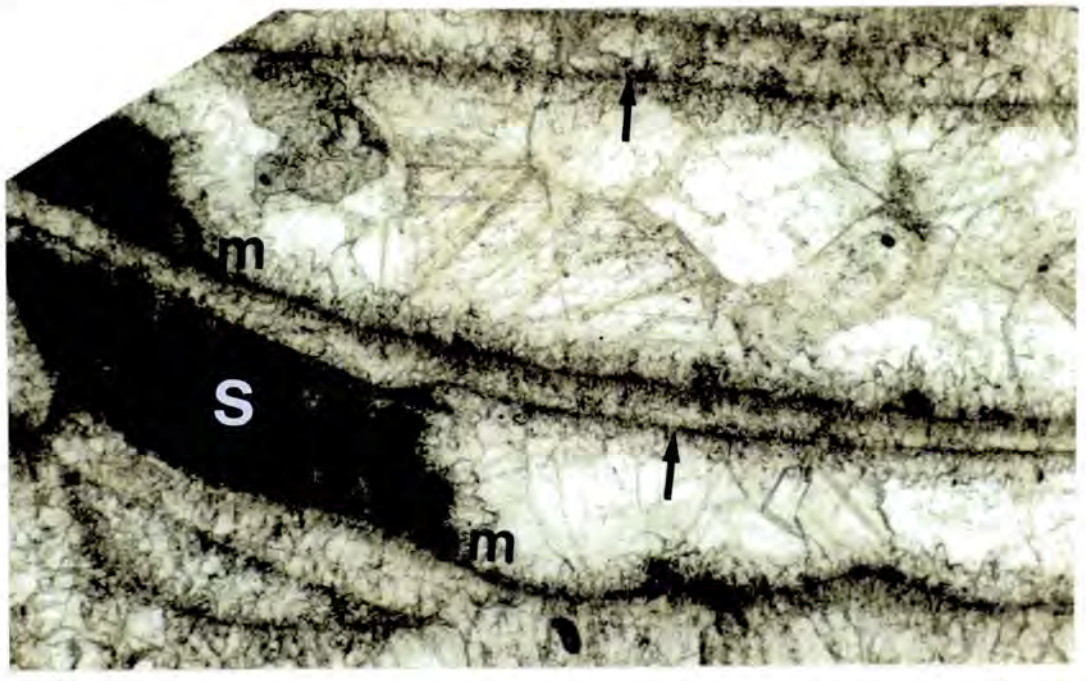


**Fig. 5.11.** Photomicrograph, showing bladed/stubby, isopachous marine cements (m), which completely encircle the primary pore space within this rudist. The intraskeletal cavities have been partly filled by sediment (s). Note also the well developed micritic margins (arrowed), marking the edges of the former aragonitic tabulae (now calcite). The slightly brown colouration (displays pseudopleochroism when rotated) and abundant inclusions towards the edges of the tabulae suggest that the tabulae have been neomorphically replaced (at least at their margins). Sample AX/7, Casa Borrell (locality 1a, Fig. 4.1). Field of view 3 x 2mm.

These cements only occur within intraskeletal cavities which have micritised internal margins and are sometimes present within intraskeletal cavities which have been partly filled by marine sediment. Where sediment is present the bladed/stubby cement fringes have grown around the edges of the remaining pore space. These cements are never present within areas of skeletal dissolution, although this has clearly occurred within some samples where this type of cement is present.

From this petrographic information, the bladed to stubby calcite is interpreted to have been an early precipitate which formed either at the surface or during very shallow burial, probably while these lagoonal sediments were saturated with marine fluids. This conclusion was reached for the following reasons: The close association of this cement generation to micrite linings and sediment infills suggests that it was an early precipitate; the fact that its occurrence is restricted to primary pore spaces indicates that it was precipitated before any undersaturated pore fluids caused dissolution; A pre-dissolution timing is also indicated by the presence of this cement generation along the edges of collapsed micritic margins (see section 5.5.4.3); the

isopachous nature of this cement generation and the fact that it has completely encircled the available pore space are typical features of many ancient and recent marine cements.

Mg-calcite marine cements with a comparable morphology to these have been described by James and Ginsburg (1979) from modern limestones along the seaward margin of Belize Barrier.

### 5.5.3.3 Botryoidal cements

These botryoidal cements are easily identified in thin section as they are rich in inclusions which are typically arranged in a radiating pattern (see Figs. 5.12a, 5.12b, 5.13, 5.14, 5.15a & 5.15b). Occasionally within a thin section a single isolated crystal can be found and the radiating fans of inclusions can be seen to create a semicircular to circular shape, suggesting that these cements are hemispherical in three dimensions (see Figs. 5.12a, 5.12b, 5.13, 5.15a & 5.15b). All the botryoids observed have generally been of similar sizes with diameters in the region of 1mm. Under crossed polars some of the botryoids display radial fabrics of elongate calcite crystallites (see Figs. 5.12b & 5.13). When viewed under high power the inclusions at the edges of some botryoids can be seen to form angular protrusions, with a median width of 50μm, which may represent the terminations of these crystalites (see Figs. 5.13 & 5.14). Under cathodoluminescence, the botryoids are generally non-luminescent; however, brightly luminescent specks are sometimes observed (see Fig. 5.15).

The botryoidal inclusion arrays are usually enclosed by large calcite crystals. In some instances these large calcite crystals not only enclose the botryoid but cross into the originally aragonitic tabulae which form the intraskeletal cavity walls (see sections 5.5.4.4, 5.5.4.5 & 5.5.4.6 for further discussion) (see Figs. 5.12a, 5.12b & 5.15a).

The botryoids may occur isolated, but are more commonly arranged with others to form a cement fringe, with each adjacent botryoid having grown into the other, preventing complete hemispherical shapes from forming (see Figs. 5.12a & 5.12b). These botryoidal cements occur with equal frequency on lower, upper and side walls of the intra-skeletal cavities (see Figs. 5.12a & 5.12b). In fact it is usual for cavities to have been completely occluded by botryoidal cements, which have grown inwards from all sides of the pore space and they can be several layers thick (see Figs. 5.12a & 5.12b). The compromise boundaries which result from total occlusion of primary cavities by these cements, together with the fact that the crystals which enclose the botryoidal inclusion arrays cross over skeletal boundaries, results in the

**a)**

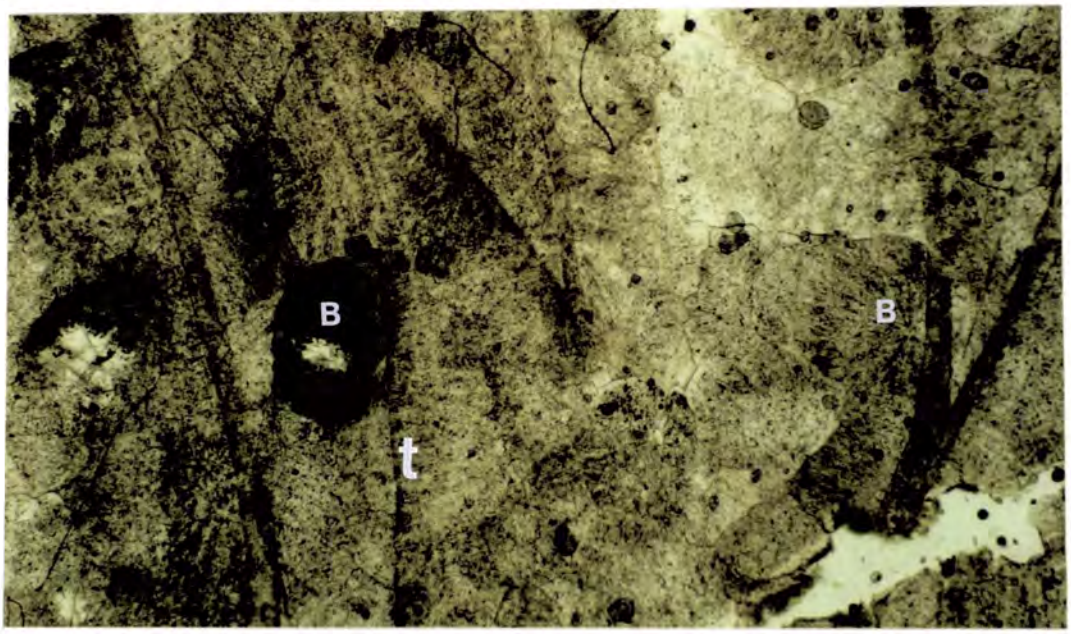


**b)**

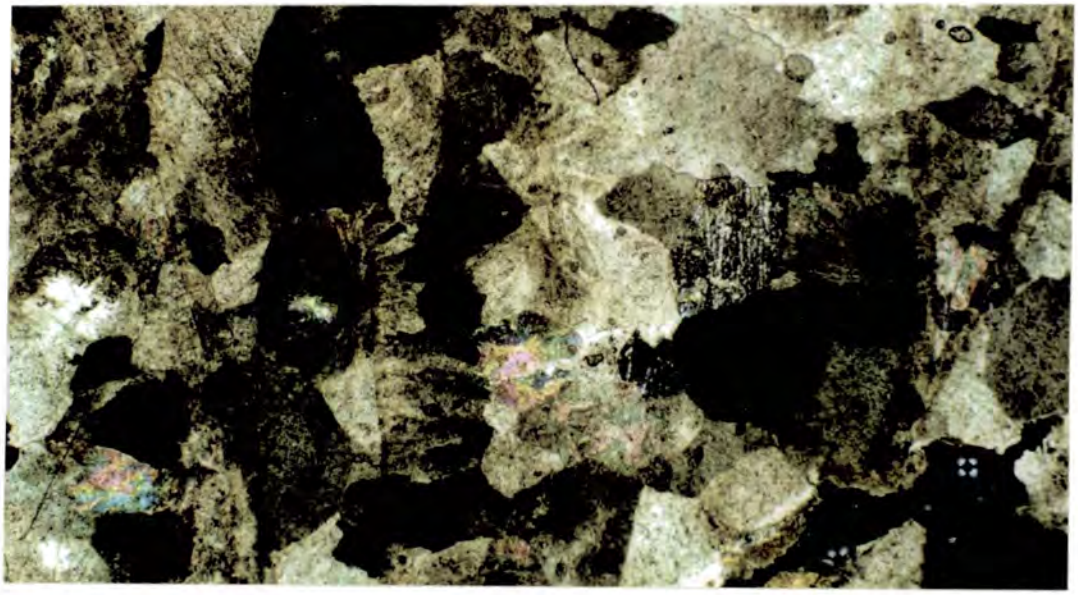

**Fig. 5.12.** Paired photomicrographs under plane polarised (a) and cross polarised light (b), showing inclusion rich, botryoidal marine cements occluding the intraskeletal cavities of a rudist. Note the hemispherical shape of the individual botryoids (2 good examples marked B). The radiating patterns of inclusions which form the botryoids appear enclosed within large crystals, which under crossed polars (b), can be seen to cross over the former aragonitic tabulae (t) which surround the intraskeletal cavities. Note also the brown colouration (organics) of the tabulae and their preserved relict microstructure, indicating neomorphic replacement. Sample AX/12, Casa Borrell (locality 1a, Fig. 4.1). Field of view 6 x 4mm.

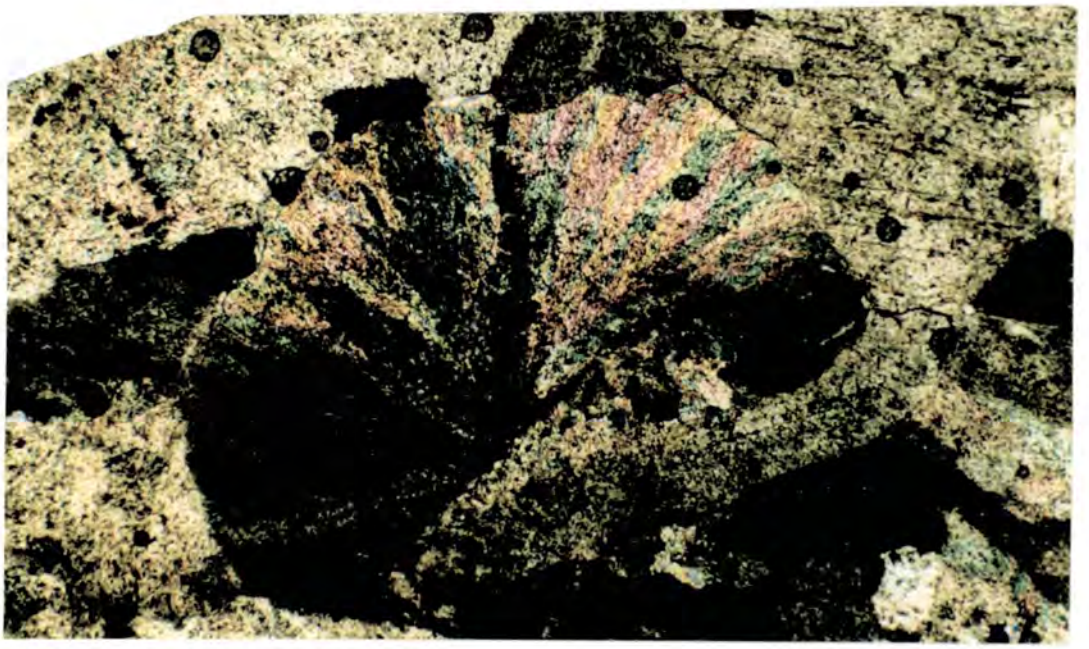

**Fig. 5.13.** Photomicrograph taken under crossed polarised light, showing the radial fabric of elongate calcite crystallites, displayed by many botryoidal cement crystals. Sample AX/12, Casa Borrell (locality 1a, Fig. 4.1). Field of view 3 x 2mm.

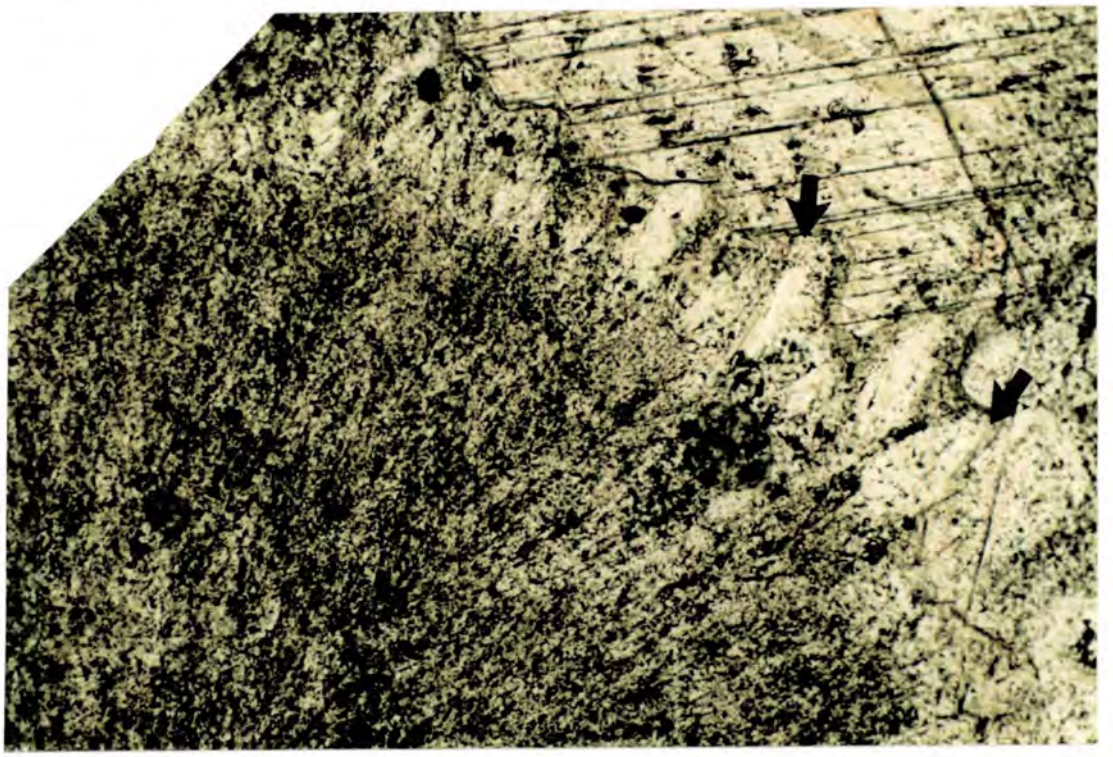

**Fig. 5.14.** Photomicrograph, showing the edge of a botryoidal cement crystal. Note the angular protrusions which mark the edge of the botryoid (arrowed). Sample AX/2B, Casa Borrell (locality 1a, Fig. 4.1). Field of view 1.3 x 0.8mm.

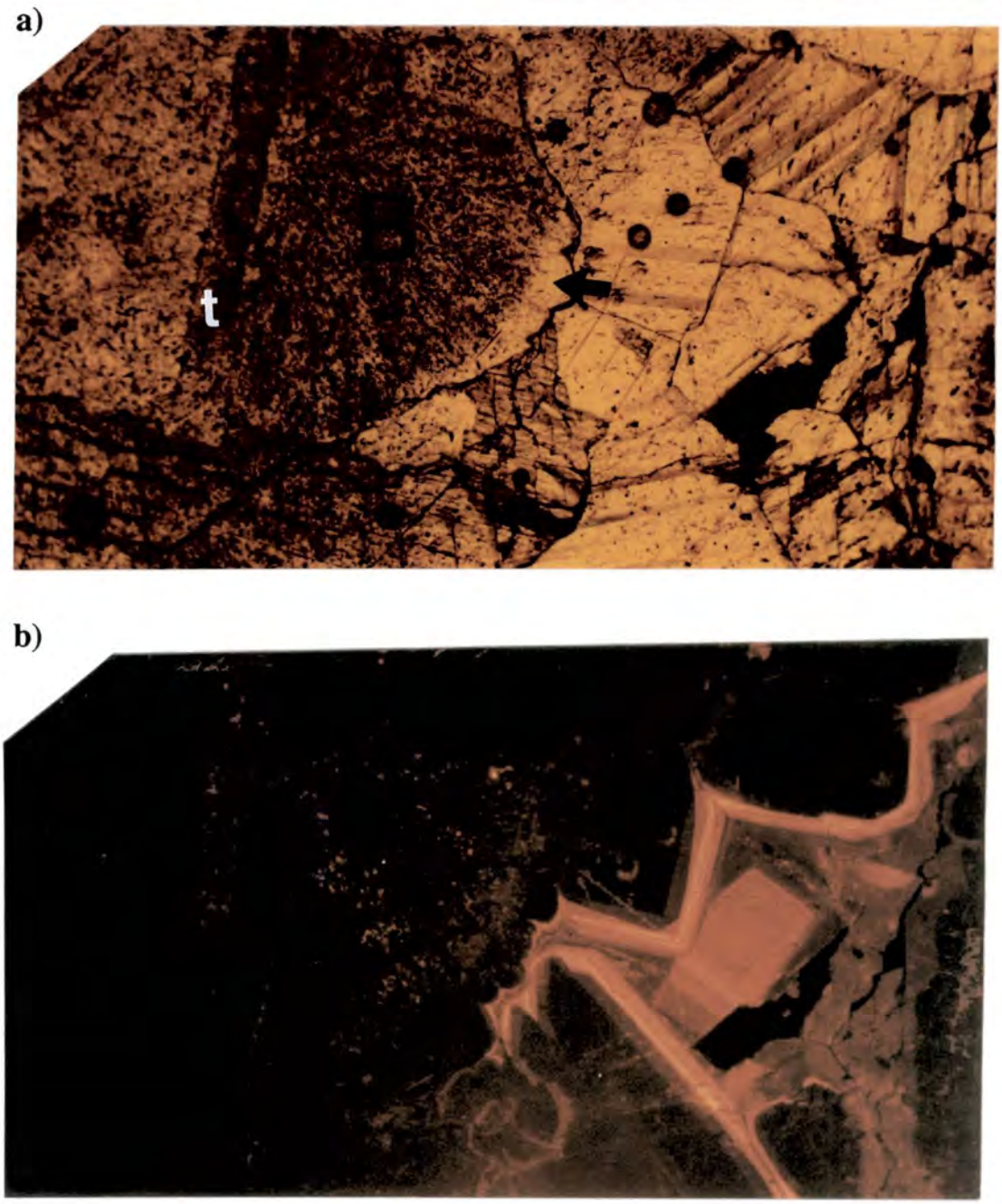


**Fig. 5.15.** Paired photomicrographs under normal light (a) and CL (b), showing a well developed botryoidal cement crystal (B), seeded upon an originally aragonitic rudist tabulae (t) at the edge of an intraskeletal cavity. The calcite crystal which encloses the botryoidal inclusion array can be seen clearly (arrowed). Note the brightly luminescent specks within the otherwise non-luminescent botryoid, possibly indicating the presence of microdolomite inclusions or some minor, later dissolution and precipitation of bright luminescent calcite. Later zoned non-luminescent- brightly luminescent equant, relatively inclusion free calcite spar cements can be seen occluding the remaining pore space towards the centre of the cavity. Sample AX/12, Casa Borrell (locality 1a, Fig. 4.1). Field of view 2mm across.

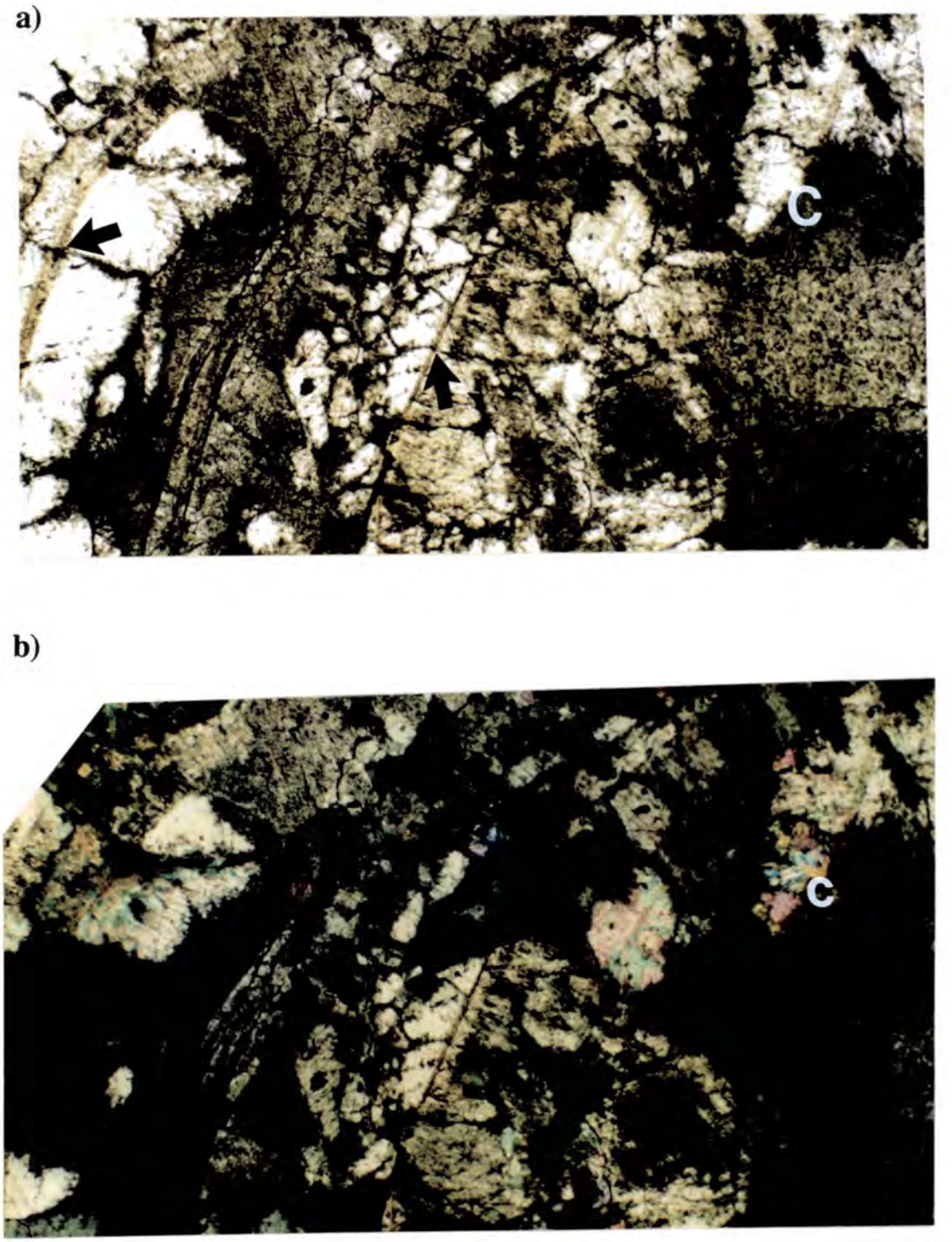


**Fig. 5.16.** Paired photomicrographs under plane polarised (a), and cross polarised light (b), showing mosaic of both inclusion rich botryoidal type crystals and relatively inclusion free equant calcite crystals. Both crystal types cut across former aragonitic tabulae and shell layers, now present as brown ghost like features displaying relict microstructures (some of these cross cutting features are arrowed). Under crossed polars (b), some of the inclusion free crystals display similar radial patterns of crystalites as do the inclusion rich botryoidal crystals. There are also composite crystals (part inclusion rich botryoid and part inclusion free)(marked C). These features are discussed within the text. Sample CA/5, north side of Gallinove (locality 1f, Fig. 4.1). Field of view 6 x 4mm.

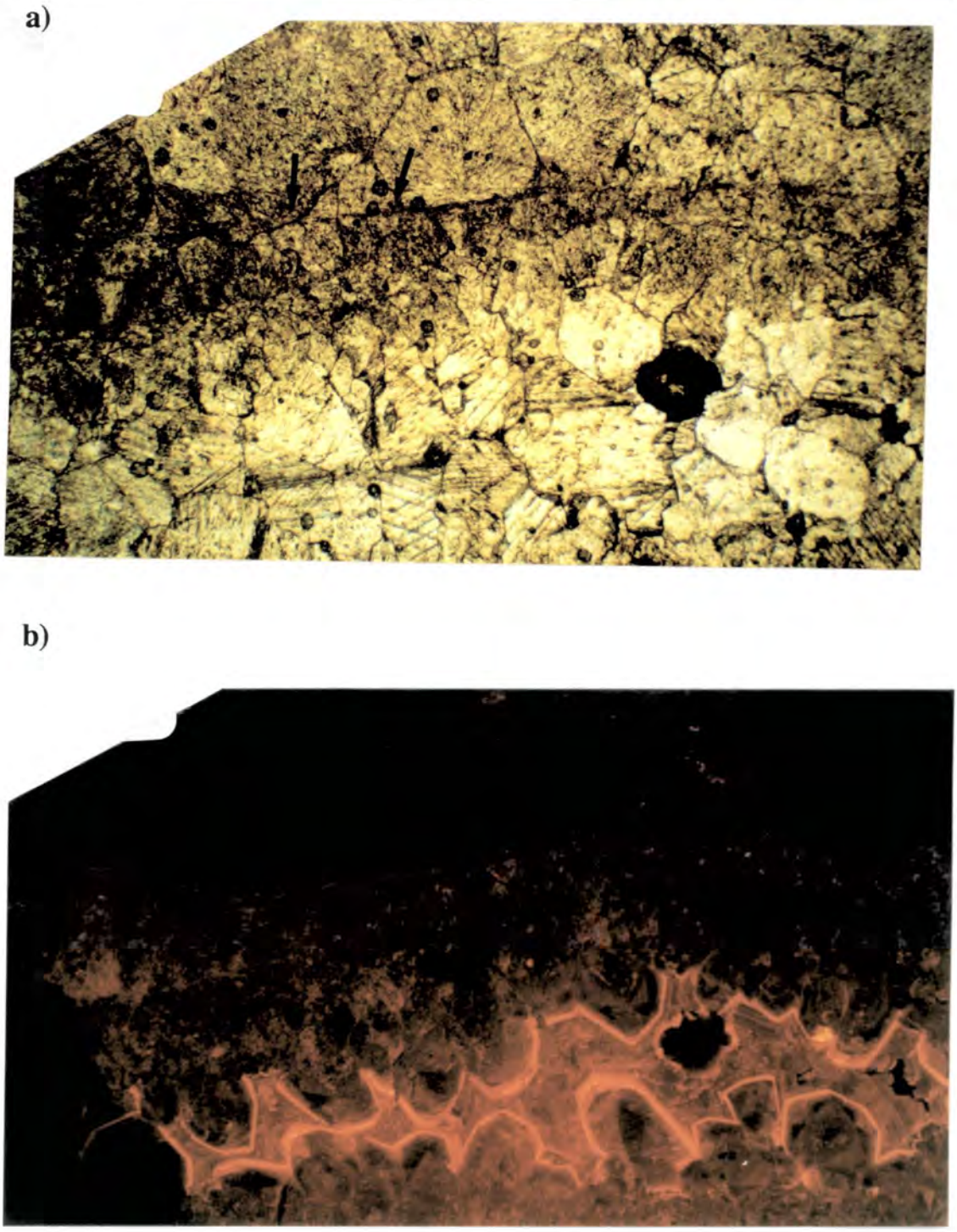


**Fig. 5.17.** Paired photomicrographs under normal light (a) and CL (b), showing the heterogeneity in marine cement distribution between adjacent intraskeletal cavities. One cavity is totally occluded by well developed botryoidal marine cements, whereas the other contains only a thin lining of inclusion rich cements, with the remaining pore space having been occluded by zoned-luminescent calcite spar, typical of precipitation from burial fluids. Note the ghosted relict microstructure of the former aragonitic tabulae within some of the botryoidal crystals, displaying a cross-cutting replacement fabric (arrowed). Sample AX/2, Casa Borrell (locality 1a, Fig. 4.1). Field of view 4.5mm across.

development of an equant mosaic fabric which can cover a large area of the rudists interior. In many cases the botryoidal cements are associated with coarse, equant, inclusion-free spar, which can cover quite large areas of a rudist's interior and exhibit a similar mosaic fabric (see Figs. 5.16a & 5.16b). Some of the inclusion free calcite crystals also exhibit similar radiaxial extinction patterns to those displayed by the botryoidal cements (see Fig. 5.16b).

Unlike the bladed/stubby cements described above, these botryoidal cements are found within intra-skeletal cavities which do not have well developed micritised internal margins. It should also be noted that no botryoidal cements have been observed within cavities that contain any internal sediment. The distribution of botryoids is extremely varied within individual rudists; in some cases adjacent, seemingly identical cavities can either lack or be completely occluded by them (see Figs. 5.17a & 5.17b).

Like the bladed/stuby cements, these botryoidal cements are never present within areas of skeletal dissolution, although this has clearly occurred within some of samples where this type of cement is present.

These botryoidal cements are interpreted as marine, for the following reasons: where present, they represent the first cement generation within the pore space (see Figs. 5.12, 5.15 & 5.17); they commonly completely encircle the available pore-space (see Figs. 5.12 & 5.17), which is a typical feature of many ancient and modern marine phreatic cements; the irregularity in distribution (often between adjacent pore space)(see Fig. 5.17) is a characteristic feature of marine cementation (Schroeder, 1972; James et al., 1976; Goldsmith & King, 1987); petrographic features, such as the absence of these cements from secondary pore space, indicate that they were precipitated before any dissolution took place.

By analogy with the acicular aragonite botryoids seen in modern carbonates (eg. Ginsburg & James, 1976), marine cements with a botryoidal morphology from both Recent and ancient limestones, were generally thought to have been precipitated as aragonite. However, originally aragonitic botryoids can be up to 10cm in diameter and are composed of acicular crystallites averaging 2 μm in width which have square terminations (Ginsburg & James, 1976, Loucks & Folk 1976); these botryoids on the other hand, have diameters in the region of 1mm and appear to have been formed of crystallites which are approximately 50μm wide and have angular terminations (see Figs. 5.13 & 5.14). These botryoids also differ from former aragonitic botryoids, in that they appear to display a replacement fabric which involves large enclosing calcite crystals, that commonly possess a radial subcrystal fabric (see Figs. 5.12, 5.13, 5.15 & 5.16); By way of comparison, the typical replacement fabric exhibited by calcitised former aragonitic botryoids is characterised by a mosaic of small replacement crystals

with a random optical orientation (Davies, 1977; Mazzullo, 1980; Heckel, 1983; Aissaoui, 1985).

Botryoidal cements, with almost identical petrographic characteristics to these have been described from the inter-tabular pores of Cretaceous rudists by Ross (1989 & 1991). During his study, he found the botryoids to be depleted in strontium compared to the calcitised skeletal aragonite from the host rudists; XRD analyses showed minor aragonite peaks for the calcitized aragonite skeleton but not for the botryoids; SEM microscopy showed aragonite relicts within the calcitised skeleton but not the botryoids which, significantly, contained microdolomite inclusions. These features together with their petrographic characteristics led Ross to suggest that the botryoidal cements were originaly precipitated as high-Mg calcite.

Other similar cements [cements], from the Devonian of Western Australia were described as radiaxial fibrous calcites by Kendall (1985). Kendall concluded that these cements were precipitated as calcite in the marine phreatic realm and that their radiaxial subcrystal fabric, rather than being a result of neomorphic replacement, was in fact a primary feature which resulted from a process of split crystal growth.

The petrographic characteristics of these botryoidal cements, together with their similarity to those described by Kendall and Ross, suggest that rather than representing former aragonitic cements they were in fact calcite precipitates. The brightly luminescent specks which can be seen when these cements are viewed under cathodoluminescence may represent microdolomite inclusions (see Fig. 5.15). If these bright specks are microdolomite inclusions then a high-Mg calcite precursor is strongly suggested (Lohmann & Meyers, 1977; Davies, 1977; James & Klappa, 1983; Enos, 1986; Tucker & Hollingworth, 1986). Whether the coarse calcite crystals which enclose the botryoidal inclusion arrays or their radiaxial subcrystal fabrics are primary or secondary replacement features is discused further in sections 5.5.4.4, 5.5.4.5 and 5.5.4.6.

The mosaics of equant, inclusion-free calcite spar which occur in association with these botryoidal cements (see Fig. 5.16) are also discussed further in sections 5.5.4.4, 5.5.4.5 & 5.5.4.6, where after consideration of both petrographic features and the results of isotopic analysis it appears probable that these equant cements may in fact have similar origins to the botryoidal cements.

### 5.5.3.4 Fibrous calcite cements

These occur within the grainstones which lie stratigraphicaly on top of the lagoonal facies rudist and coral units (see sections 4.2.4.2, 4.2.4.3 & 4.3.2.2). Typical fibrous cements from these grainstones are shown in Fig. 5.18. They consist of bladed

to columnar shaped crystals which have a length of approximately 50μm and are much longer than they are broad (a length to width ratio of approx. 6:1). They are rich in inclusions and are non-luminescent. They are never present within areas of skeletal dissolution, although this has clearly occurred within some of the samples where this cement is present (see Fig. 5.18).

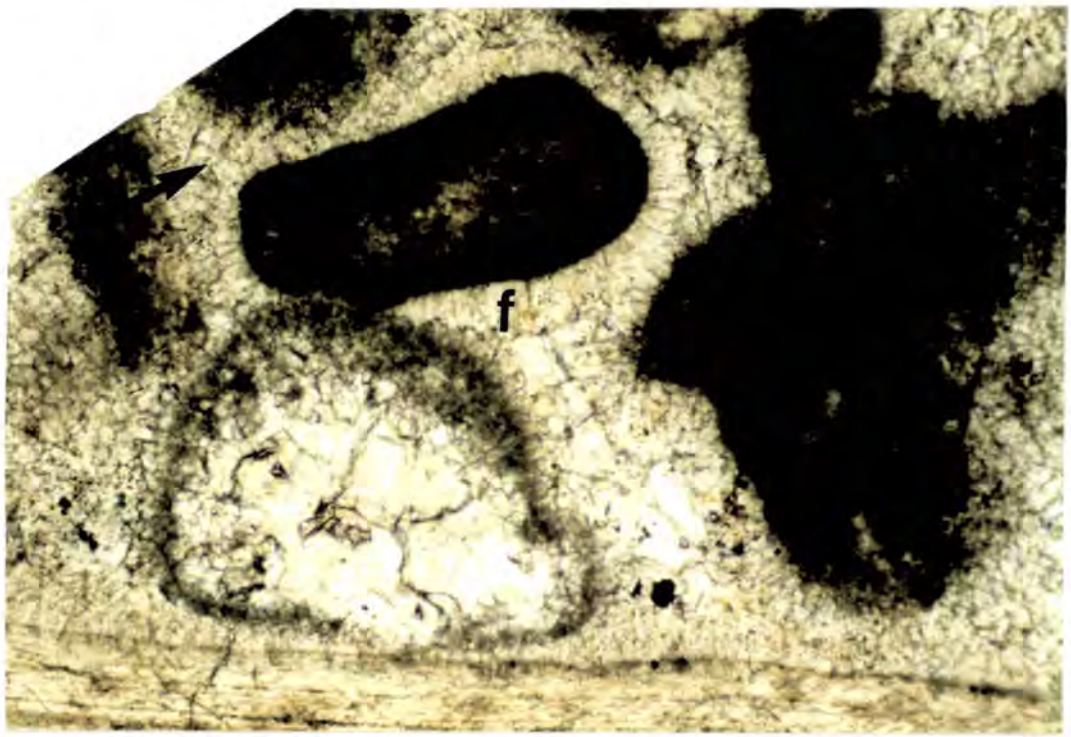


**Fig. 5.18.** Photomicrograph, showing isopachous, fibrous calcite cements (f), fringing skeletal fragments and peloids within the grainstone which lies stratigraphically on top of the lagoonal facies sediments at most localities in the Sant Corneli anticline region. Note the spar filled cavity, with a well developed micrite margin, representing the former position of an aragonitic skeletal fragment which has suffered dissolution. The fibrous cements are absent from within this cavity, indicating that their precipitation preceded dissolution of aragonitic allochems. Note also the polygonal compromise boundaries produced through the growth of these isopachous cements into small areas of primary intragranular pore space (arrowed). Sample CB/10, north side of Gallinove (locality 1f, Fig. 4.1). Field of view 1.3 x 0.8mm.

The columnar to bladed crystals have grown perpendicular to their substrates and form isopachous rims around grains which, after micritised margins, provide the second lining to the primary intragranular pore-space (see Fig. 5.18). There is a tendency for this cement to be better developed on grains which were originally composed of calcite. In places where the primary intragranular pore space was small these fringes of cement have grown inwards with equal thickness from all sides to

completely occlude the pore space, and form polygonal compromise boundaries (see Fig. 5.18).

High-Mg calcite cements with comparable morphologies to these have been recorded from most modern marine cemented limestones (eg. Macintyre et al., 1968; Land & Goreau, 1970; Marlowe, 1971; Schroeder, 1972; James et al., 1976). The growth of bladed spar, as fibrous, isopachous fringes is particularly common in high energy reefal environments although, as in this case, they are also known to occur within grainstones (eg. Shinn, 1969; James et al, 1976). Fibrous, isopachous cements composed of aragonite are also common in modern marine cemented limestones (eg. Ginsburg & Schroeder, 1973); however, the individual crystals of aragonite tend to have an acicular rather than bladed or columnar habit.

The absence of dissolution effects or replacement textures and hence good preservation of these cements suggests an original calcite mineralogy. Whether these cements were originally low-Mg or high-Mg calcite is a matter for speculation. However, unlike the botryoidal cements, no bright specks can be seen when these cements are viewed under cathodoluminescence, which may be indicating that no crystals of microdolomite are present and hence the possibility that these cements were originally low-Mg calcite.

The isopachous pore-lining nature of these cements is indicative of precipitation under phreatic conditions. These cements are interpreted as having been precipitated on the sea-floor or just below in the presence of marine pore-waters.

#### 5.5.3.5 Factors controlling marine cement distribution

The best developed marine cement generations are to be found within the intraskeletal cavities of rudists (see Figs. 5.11, 5.12, 5.13, 5.14, 5.15, 5.16 & 5.18). The lack of abrasion and substrate stability inside these cavities would probably have been important factors in encouraging marine cement growth. One of the most striking features of the early cement generations which have been observed within these intraskeletal cavities is their heterogeneity.

Early cementation in the cavities of some rudists has been dominated by botryoidal cements while in others stubby or bladed isopachous cements dominate. These variations in cement type occur between rudists within the same stratigraphic horizons and even between rudists which are separated by only a few centimetres. Smaller scale heterogeneities in marine cementation can be observed within individual rudists, particularly those in which botryoidal cements dominate. In some cases adjacent, seemingly identical cavities can either lack or be completely occluded by these early marine cements (see Fig. 5.17).

Important features of this heterogeneity in cement distribution is that stubby to bladed isopachous cements are found within intraskeletal cavities containing internal sediments and that micritisation has always preceded the growth of these cements (see Fig. 5.11); botryoidal cements on the other hand, have not been found within cavities containing internal sediment, nor are they always preceded by such intense micritisation of the cavity walls (see Fig. 5.12). These features would suggest that botryoidal cements developed preferentially within rudists with pore spaces which were completely enclosed, even to the microbes which would have caused micritisation, while the growth of stubby to bladed cements was restricted to rudists with more open intraskeletal cavities. Perhaps these features are indicating a variation in shell porosity and/or susceptibility to the effects of boring organisms between different rudist genera.

The occurrence of botryoidal cements within completely enclosed pores is initially surprising; however, this is a common feature of marine cements and can be explained by ion diffusion through porous chamber walls (Alexanderson 1972). The fact that these cements show variations between adjacent, seemingly identical chambers, suggests a microenvironmental control on their distribution. Computer modelling by Goldsmith and King (1987) has suggested that local permeability variations could be the cause of such small scale variations in marine cements.

Well developed marine cements also occur within the grainstones which lie stratigraphicaly on top of the lagoonal facies rudist and coral units (see sections 4.2.4.2, 4.2.4.3 & 4.3.2.2)(see Fig. 5.18). In section 4.2.4.3 it was postulated that these grainstones represented a period of increased energy on the platform top which caused the rapid lagoonward migration of skeletal sands that once formed banks and bars on the seaward margin of the lagoon. During such transgressive events, sea-level rises, energy on the platform top increases, waves and currents pump seawater through the sediments and there is often a decrease in carbonate production. Such an environment would correspond to the 'active marine phreatic' environment of Longman (1980) and it is under such conditions that marine cementation would have been promoted.

Observations made by Shinn (1969) in the Arabian Gulf have shown contemporary seafloor cementation of open shelf sand sheets. His observations suggest that cementation is dependant on water flow through the sediment. However, he also noted that under highly agitated conditions, cementation is inhibited by grain movement and conversely if sedimentation rates are too low, cementation at the sediment-water interface will plug pore space and inhibit the process. Hence, for marine cementation to effect any reasonable thickness of sediment, an optimum

relationship between sedimentation rate, seawater circulation and grainsize (permeability) must exist.

## 5.5.4 Dissolution and neomorphism

### 5.5.4.1 Introduction

As already noted in previous sections (see sections 4.2.4.4 & 4.3.2.2), these platform-top sediments have suffered extensive dissolution. All aragonitic skeletal fragments within these sediments have been dissolved, and the resultant voids occluded by calcite spar. As would be expected the originally aragonitic shell layers and tabulae within rudists have also suffered some dissolution. However, unlike the originally aragonitic shell fragments present within the muddy lagoonal sediments, which have suffered wholesale dissolution, the originally aragonitic shell layers and internal tabulae of rudists display the effects of both dissolution and neomorphism. At many localities, in addition to the wholesale dissolution of aragonitic grains, networks of dissolution pipes and cavities which cut through these platform-top sediments have been observed (see sections 4.2.4.4, 4.3.3 7 4.4.6).

### 5.5.4.2 Wholesale dissolution of aragonitic grains

All of the originally aragonitic grains from throughout these platform-top sediments are now represented by equant or drusy calcite spar filled moulds (see Figs. 4.11c, 4.16, 4.17b, 5.18, 5.19, 5.20, 5.26, 5.37 & 5.38). The vast majority of these calcite filled moulds are either surrounded by or contain the collapsed remnants of micritic margins which once enveloped the now missing aragonitic grains (see Fig. 5.19). In some cases, particularly for coral fragments, micritisation has preserved the general morphology of aragonitic skeletal fragments. Where internal sediment was present within aragonitic skeletal fragments, unless held in place by micritic pore linings, it has usually collapsed to the base of the spar filled cavity but has almost always retained its mouldic shape (see Fig. 5.20).

Evidence for these originally aragonitic grains having been replaced through neomorphic processes would include such features as inclusion ghosting of relict microstructure, pseudopleochroism or anisotropy of replacement crystals. The lack of any such features suggests that these grains have suffered dissolution. This interpretation is also suggested by the presence of collapsed micritic margins and/or

internal sediment which indicate that at some stage the now spar filled moulds were devoid of solid material (see Fig. 5.20).

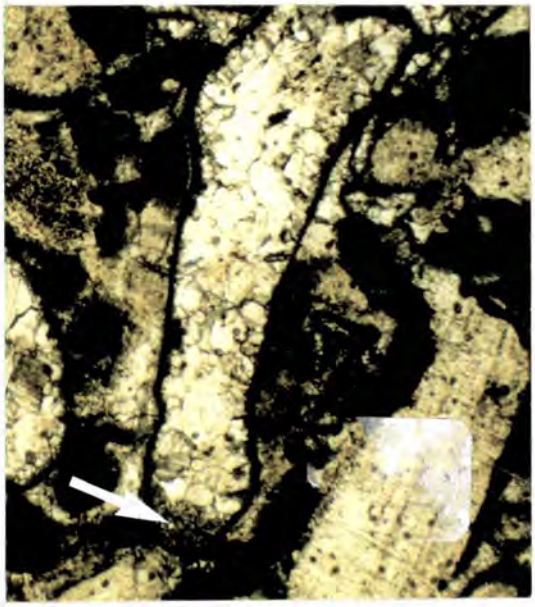

**Fig. 5.19.** Photomicrograph, showing calcite spar filled mould, surrounded by a well developed micritic margin, representing the former position of an aragonitic skeletal fragment which has suffered dissolution. The fine sediment, which has accumulated at the bottom of the mould (arrowed), probably represents micritic material derived from borings into the sides of the fragment which was not completely cemented prior to dissolution. Its presence indicates that the now spar filled mould was at some stage devoid of solid material. Sample AD/4, Gallinove (locality 1e, Fig. 4.1). Field of view 3 x 4mm.

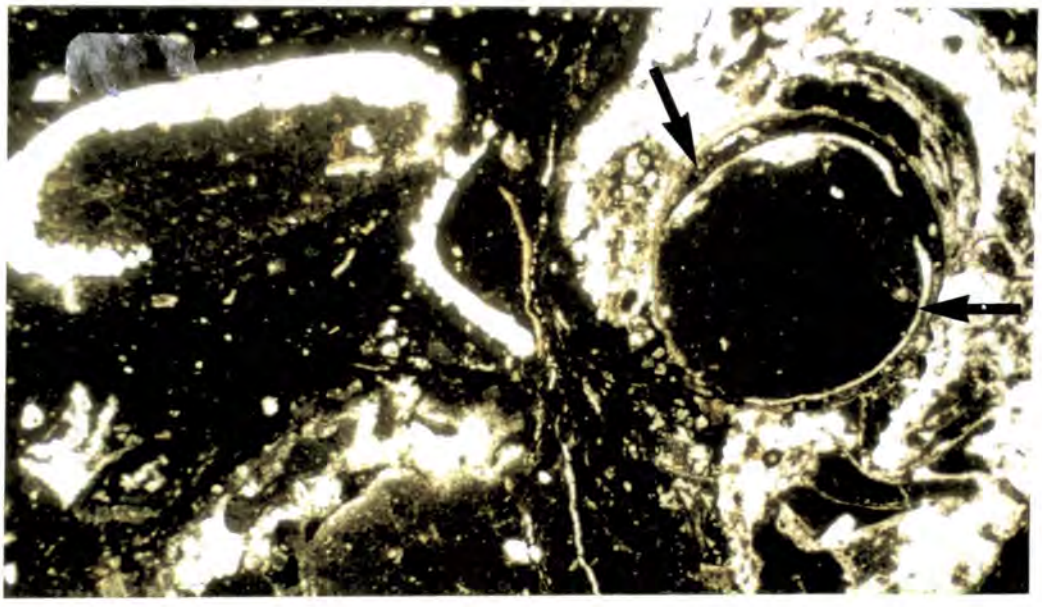

**Fig. 5.20.** Photomicrograph, showing calcite spar filled moulds, representing the former position of aragonitic skeletal fragments within this lagoonal wackestone. Note the internal sediment from within these moulds has suffered collapse, but in most cases has retained its original shape, which together with the fact that these moulds have remained intact indicates that matrix lithification preceded dissolution. This collapsed internal sediment includes the contents of a lithophagid bivalve boring, included in which is the mould of the bivalve shell itself (arrowed). Sample CA/3, north side of Gallinove (locality 1f, Fig 4.1). Field of view 11 x 5mm.

The presence of micritic margins indicates that dissolution did not occur until after micritisation of the grain margins had taken place. As the spar filled moulds did not collapse during their void stage and, if present, internal sediments have retained the shapes of the pore spaces which they infilled, lithification of the sediment must have been advance prior to dissolution. The lack of any marine cements within the moulds would suggest that all marine cementation had occurred before this dissolution took place.

### 5.5.4.3 Dissolution of rudist aragonite

#### i) Collapse of micritised margins

The effects of dissolution can be observed within most of the rudists studied. One of the most obvious features, which indicates that dissolution has occurred, is the presence of collapsed micritised margins to originally aragonitic tabulae (see Fig. 5.21). The collapse of micritised margins is often only seen in a few places within a particular rudist, and in some it has not occurred at all.

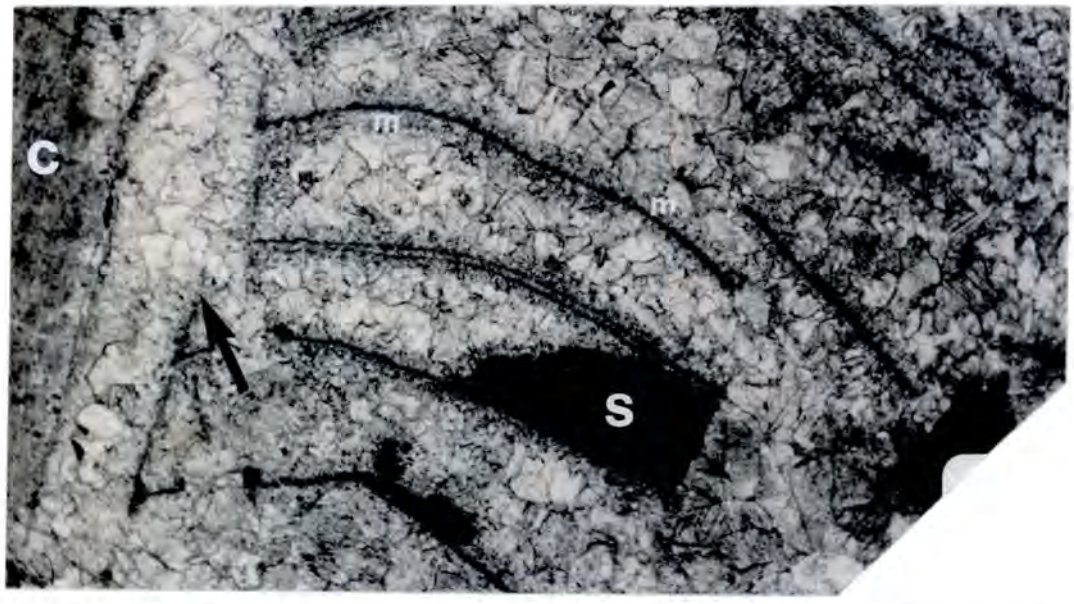


**Fig. 5.21.** Photomicrograph, showing the effects of dissolution in the form of collapsed micritised margins to originally aragonitic tabulae within a rudist. Note also the isopachous bladed/stubby marine cements (m) which can be seen lining the former primary intraskeletal cavities and have grown upon the geopetal internal sediments (s) within these cavities. The former margin to the aragonitic shell layer which ran along the inside of the calcite shell (c) is shown by the partially collapsed micritic margin (arrowed). Note that no isopachous, inclusion rich marine cements are present within the secondary pore space representing the former location of this aragonitic shell layer. Sample OZ/18, Ortenada (locality 2, Fig. 4.1). Field of view 11 x 5mm.

In many of the rudist samples where dissolution has taken place, only limited internal collapse has occurred. This lack of internal collapse, even after dissolution of all aragonite, is probably in part due to the presence of the well developed early marine cements which can be seen lining the primary intraskeletal cavities of these rudists (see section 5.5.3)(see Fig. 5.21). The heterogeneity in distribution of these early marine cements (see section 5.5.3.5 together with Fig. 5.17) may have been a contributing factor in allowing internal collapse to occur within some areas of a particular rudist, while the remainder was preserved intact.

The marine cement generations are also relevant during this diagenetic study as their presence within the primary intraskeletal cavities but not the secondary voids, allows the conclusion that dissolution post-dated marine cementation (see Fig. 5.21).

### ii) Cement-filled dissolution voids

When some samples are viewed under cathodoluminescence, zoned cements can be seen within areas which were originally occupied by aragonitic shell layers (see Fig. 5.22). The fact that these cements have been precipitated indicates that dissolution cavities must have existed in place of the skeletal aragonite. Dissolution is also suggested when calcite spar, which now occupies the former positions of aragonitic shell layers, does not exhibit any of the characteristics associated with neomorphic replacement.

---

**Fig. 5.22.** Paired photomicrographs under normal light (a) and CL (b), showing zoned calcite spar cements both within primary intraskeletal cavities and areas which were originally occupied by aragonitic rudist tabulae (T). The position of the former aragonitic tabulae is shown by the presence of a micritic margin (arrowed) and inclusion rich early marine cements along its outside edge (m). The presence of zoned cements within the area formerly occupied by the aragonitic tabulae indicates that dissolution has occurred. However, note that the outer parts of this area have a slight brown colouration in normal light and that the zoned-luminescent cements only occur in the centre of the former tabulae. This outer brown coloured zone shows a slight pseudopleochroism and is interpreted to indicate that the margins of the tabulae suffered neomorphic replacement, with the later dissolution being restricted to the interior of the tabulae. Sample AX/3, Casa Borrell (locality, 1a Fig. 4.1). Field of view 2mm across. See following page.

---

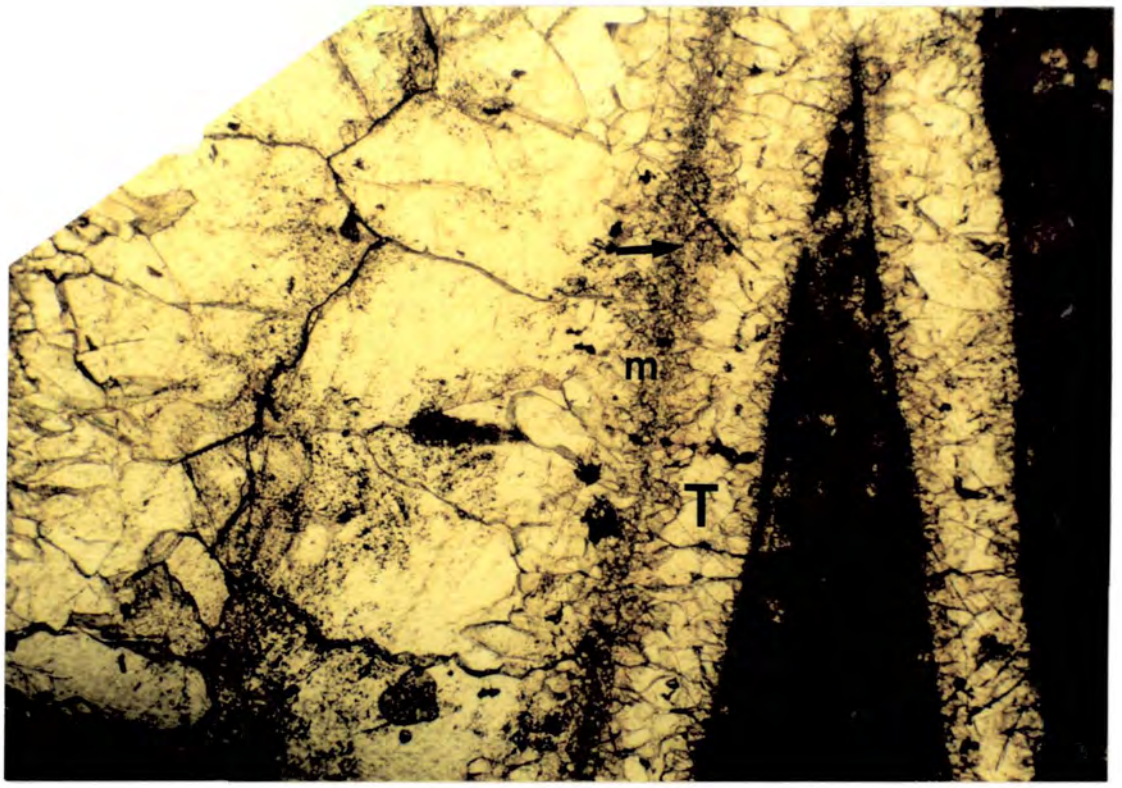


**Fig. 5.22a.** (see previous page for caption)

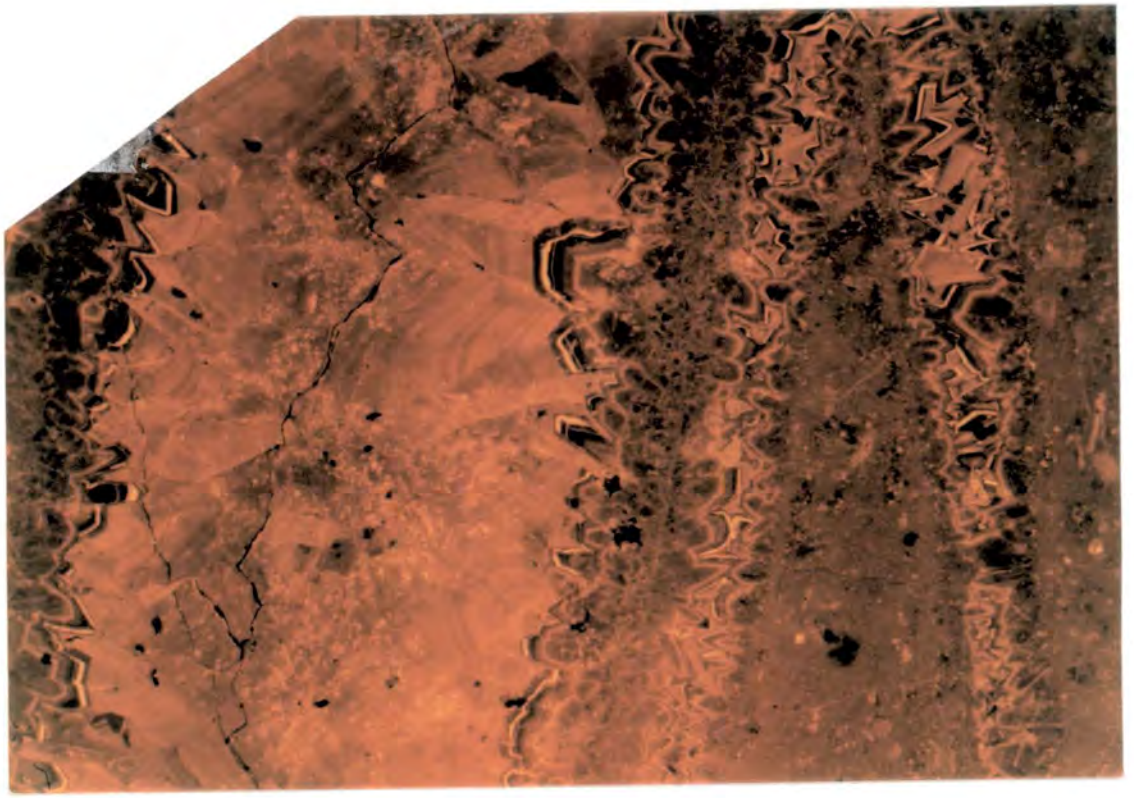

**Fig. 5.22b.** (see previous page for caption)

### iii) The occurrence of crystal silt and its implications

The secondary porosity within some rudist samples has in part been filled with crystal silt (see Figs. 5.23, 5.24 & 5.29). This crystal silt consists of irregularly shaped, silt sized (<20μm diameter) fragments of crystalline calcite, together with some micritic material and lacks any recognisable skeletal debris. In some cases, especially in the larger cavities these accumulations of crystal silt possess a laminated structure (see Fig. 5.23). The texture and character of this crystal silt is distinct from that of the pre-marine-cementation internal sediments and it can be found within both primary and secondary pore space (see Figs. 5.24 & 5.29).

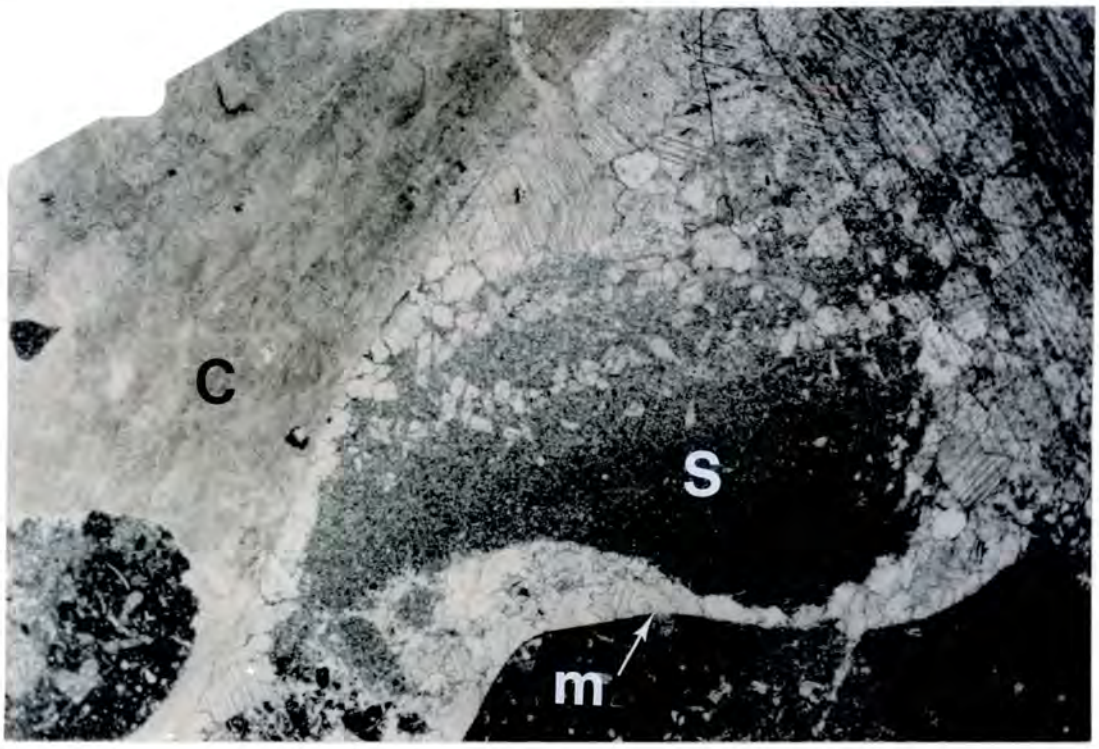


**Fig. 5.23.** Photomicrograph, showing an accumulation of crystal silt within the secondary porosity after an aragonitic rudist shell layer. C = outer calcite shell layer; m = micritic margin marking the outer edge of the former aragonitic internal shell layer; S = crystal silt. The coarse calcite spar which surrounds the crystal silt is non-ferroan and non-luminescent. Note the laminated and slightly graded nature of this geopetal crystal silt accumulation. The presence of the crystal silt indicates that the aragonitic shell layer suffered dissolution. This crystal silt is interpreted to have been deposited from flowing meteoric waters in a vadose environment (Dunham, 1969). Sample OZ/18, Ortenada (locality 2, Fig 4.1). Field of view 12 x 7mm.

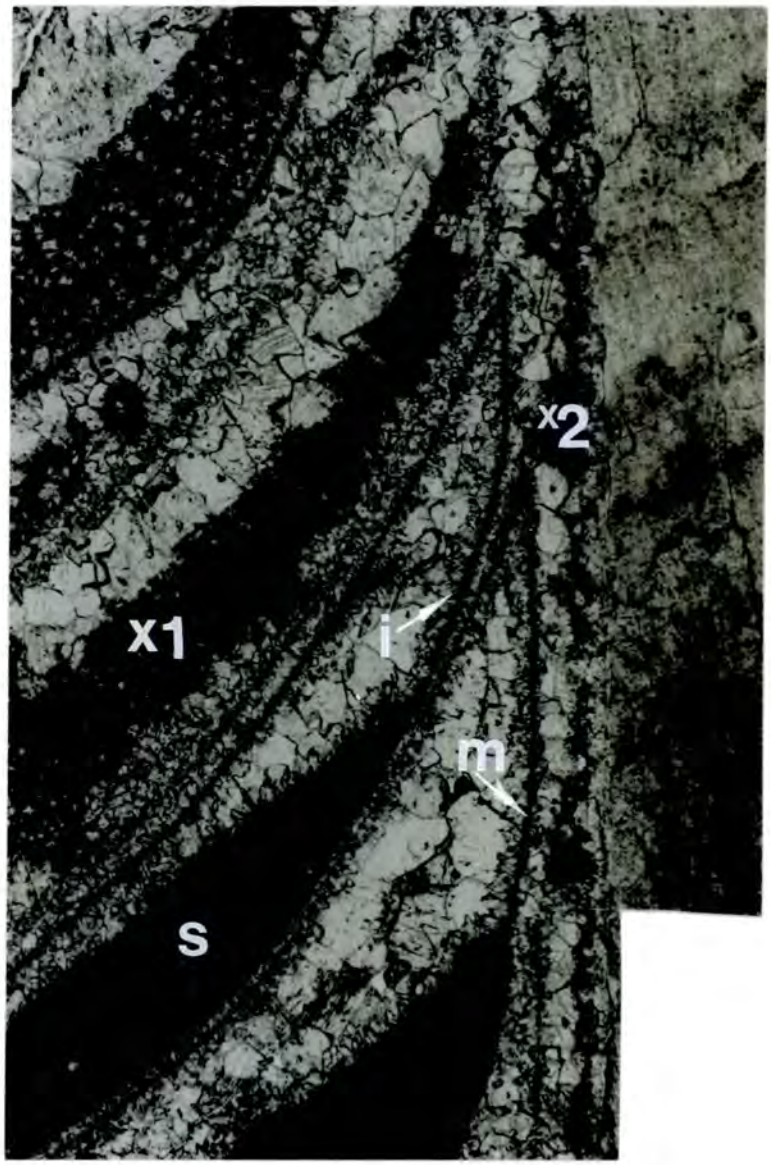


**Fig. 5.24.** Photomicrograph, showing accumulations of crystal silt within both primary and secondary cavities. C = outer calcite shell layer; m = micritic margins marking the outer edge of the former aragonitic internal shell layers and tabulae. i = isopachous marine cements lining primary intraskeletal cavities; S = marine sediment partly infilling intraskeletal cavities; X1 = crystal silt within primary intraskeletal cavity; X2 = crystal silt within secondary cavity after former aragonitic shell layer. X1 can be seen to be surrounded by both isopachous marine cements and a coarser calcite spar. X2 occurs towards the centre of the area once occupied by aragonite (former margins to aragonite shown by micritisation), and is surrounded by only equant calcite spar as isopachous marine cements are absent from this secondary cavity. Hence, dissolution and crystal silt deposition can be clearly seen to have postdated isopachous marine cement precipitation, while marine sediments infilled the primary cavities prior to this marine cementation. Sample OZ/X, Ortenada (locality 2, Fig. 4.1). Field of view 6 x 4mm.

When present within primary intraskeletal cavities, unlike any pre-marine-cementation internal sediments, the crystal silt always rests upon earlier cement generations (see Figs. 5.24 & 5.29). In fact in most cases the earlier cement generations, not only include isopachous marine cements, but also a second relatively inclusion free, coarser, more equant, non-ferroan calcite cement generation. Significantly, this second cement generation usually forms a much thicker layer on the roof of the cavity than it does below the crystal silt. Where present within secondary cavities the crystal silt is also surrounded by earlier cement; however, as marine cements are absent from these dissolution voids only the coarse spar is present (see Figs. 5.23, 5.24 & 5.29). When viewed under cathodoluminescence the crystal silt and the equant, relatively inclusion free spar which surrounds it are non-luminescent. Staining with Dickson's solution (Dickson, 1965, 1966) has revealed that non-luminescent spar which is associated with this crystal silt is non- ferroan.

Crystal silt was first described by Dunham (1969), who suggested that its formation was a result of percolating meteoric waters mechanically depositing the silt sized particles, which had been derived from the internal erosion of host sediment and cement crystals in the vadose zone. Since this first interpretation, the presence of crystal silt within the pores of carbonates, which have undergone meteoric diagenesis, has been noted by several authors who have interpreted its origins in similar ways (eg. Walls et al., 1979; Grover & Read, 1983; Kahle, 1988; Meyers, 1988; Mussman et al., 1988).

The general characteristics of the crystal silt which occurs within these rudists, are extremely similar to that of the 'vadose silt' described by these authors and thus it is interpreted to have had a similar origin.

The occurrence of this 'vadose silt' within primary cavities where it is surrounded by isopachous marine cements and a second non-luminescent, more equant spar (see Figs. 5.24 & 5.29), indicates that the deposition of 'vadose silt' not only postdated marine cementation but also a second phase of cementation. The non-luminescence of this second, non-ferroan cement generation suggests that it was precipitated from oxidising pore fluids (positive Eh), in which $Mn^{2+}$ and $Fe^{2+}$ would not be available for incorporation into any precipitates (Frank et al., 1982; Grover & Read, 1983; Dorobek, 1987; Mussman et al., 1988; Niemann & Read, 1988). The fact that it is usually better developed as a lining to the roof of the cavity than below the crystal silt suggests a pendant habit, although this may in fact be a result of contemporaneous deposition of the 'vadose silt' upon the cavity floor, which would have restricted cementation to the roof. These characteristics of the second cement generation and its association with the 'vadose silt' suggest that it was precipitated within a vadose environment. Similar non-luminescent cements are the major cement

in the Pleistocene-Holocene carbonates cemented in near surface, meteoric environments in Shark Bay, Yucatan and Barbados (Meyers, 1974; Grover & Read, 1983).

The presence of 'vadose silt' together with what are probably meteoric cements within some of these secondary pore spaces strongly suggest that the dissolution of rudist aragonite took place as a result of exposure to meteoric waters in a vadose environment.

### 5.5.4.4 Neomorphic replacement of rudist aragonite

Within most of the rudist samples studied, in addition to the features which indicate that some dissolution has occurred, there are areas of the originally aragonitic skeleton within which the internal microstructure has been preserved (see Figs. 5.11, 5.12, 5.16, 5.22, 5.25, 5.26, 5.27 & 5.29). The retention of such relict structures can only be achieved if the replacement of aragonite by low-Mg calcite occurs without a cavity stage. Another common feature indicating that neomorphic replacement, rather than dissolution, has taken place, is the preservation of in-situ boring infills within originally aragonitic shell layers (see Fig. 5.25). These boring infills, although they were probably lithified along with other matrix material during early marine diagenesis, would not have remained in situ if the aragonitic shell which supported them had suffered dissolution.

**Fig. 5.25.** Photomicrograph showing neomorphicaly replaced aragonitic shell layers within a rudist. Note the ghost like relict crossed lamellar microstructure (arrowed), and the in situ preservation of sediment filled borings, indicating that the aragonite was replaced without a cavity stage. The small size of the calcite crystals and only ghost like relict microstructure are typical of 'fabric selective' type replacement. Sample CA/1, north side of Gallinove (locality 1f, Fig. 4.1). Field of view 6 x 3mm.

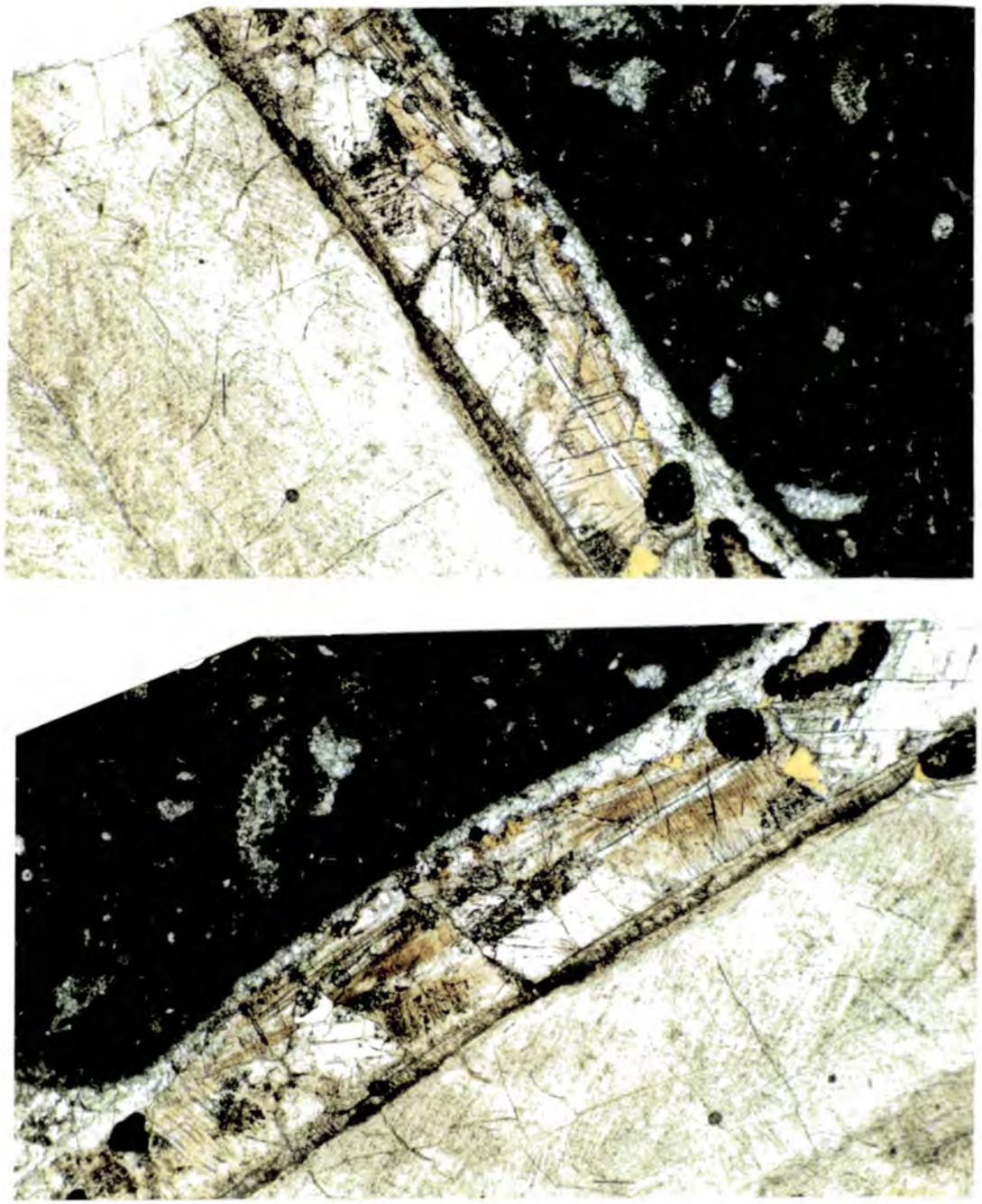

**Fig. 5.26.** Paired photomicrographs taken at 90$^{O}$ of stage rotation from each other, showing a former aragonitic internal rudist shell layer displaying strong pseudopleochroism from light to dark brown. Note also the well preserved relict microstructure. This pseudopleochroism is thought to be the result of orientated organic inclusions and together with the relict microstructure indicates that the aragonitic shell layer has been replaced neomorphically without a cavity stage. Note the coarse nature of the replacement calcite crystals, which is a typical feature of 'cross cutting' type neomorphic replacement. The clear, calcite spar filled cavity towards the margin of this former aragonitic shell layer suggests that marginal dissolution has occurred. Sample CA/5, north side of Gallinove (locality 1f, Fig. 4.1). Field of view 3 x 2mm.

In addition to the preservation of relict microstructure, it is also common for the calcite spar which now occupies the areas of originally aragonitic skeleton to display a variation in colour from light to dark brown when they are rotated in plane polarised light (see Fig. 5.26). This pseudopleochroism is identical to that described by Hudson (1962), from neomorphically replaced bivalve shells, which he proposed was the result of orientated organic inclusions within the neomorphic spar.

The areas of originaly aragonitic skeleton within these rudists which display features suggesting that they have been neomorphically replaced show a variety of replacement fabrics. However, the replacement fabrics can generally be divided into either 'fabric selective' or 'cross-cutting' types.

**(i) 'Fabric selective' replacement fabrics**

The 'fabric selective' replacement fabrics consist of relatively small replacement calcite crystals (median diameter of 100μm) which do not extend beyond the original boundaries of the replaced skeleton. Within originally aragonitic tabulae or shell layers which show 'fabric selective' replacement (see Figs. 5.25 & 5.27), it is common for the margins to be coloured brown, display strong pseudopleochroism and have well preserved relict microstructure, whereas the remaining area is filled by inclusion-rich spar, displaying only some slight traces of pseudopleochroism (see Fig 5.27).

After comparison with Pingitore's observations (1976) (see section 5.1.3.3). it would seem a correct interpretation that the rudist samples displaying 'fabric selective' replacement fabrics exhibit all the features consistent with them having undergone neomorphic replacement within a vadose environment. The well preserved relict microstructure, and high content of organic material (evidenced by the brown colouration/pseudopleochroism), occurring preferentially at the margins to originaly aragonitic shell layers suggests that preservation may have been aided by the action of microbes at these margins. Within the remainder of these areas preservation of microstructure or organic material is only patchy. This poor preservation perhaps suggests that rather than replacement having occurred entirely as a result of an in-situ process of dissolution-reprecipitation across a thin (1μm or less) film of water (Kinsman, 1969; Sandberg et al., 1973; Pingitore, 1976; Al-Aasm & Veizer, 1986a), some temporary chalkification occurred (Pingitore, 1976). Such a scenario could be envisaged within a humid climatic setting, where large amounts of rainfall could saturate the sediments to produce temporary phreatic conditions within an otherwise vadose environment.

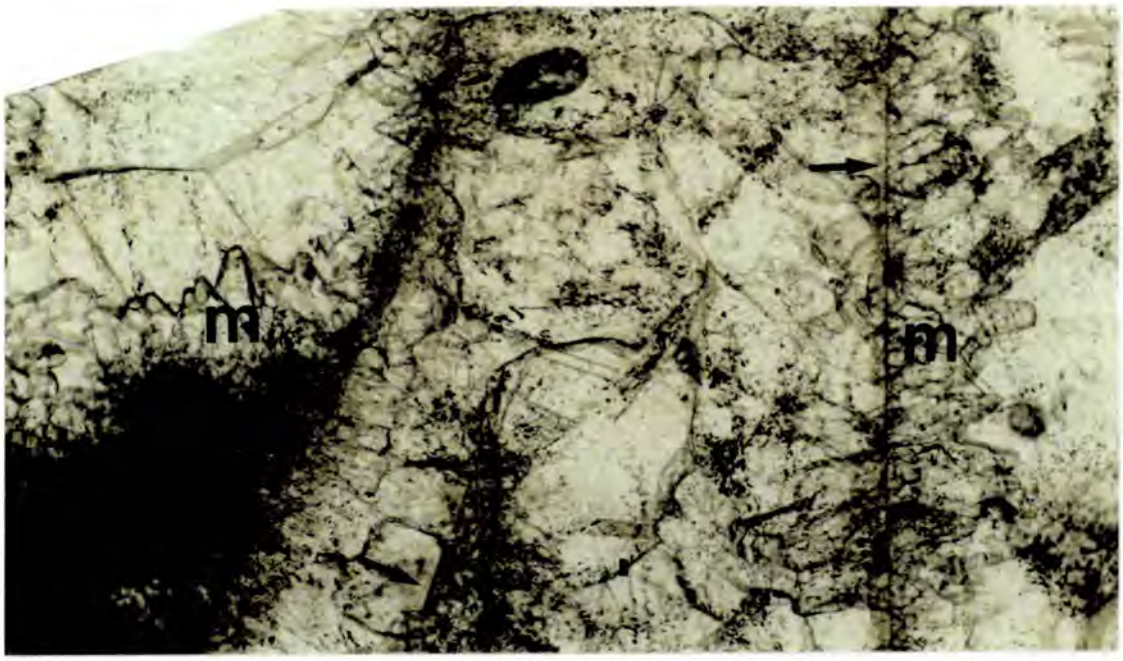


**Fig. 5.27.** Photomicrograph, illustrating 'fabric selective' type neomorphic replacement of a former aragonitic tabula. Note the brown colouration and relict microstructure at the margins of the tabula (arrowed), as well as the inclusion ghosted fabric within its interior, indicating neomorphic replacement, rather than dissolution, has occurred. Well developed isopachous bladed/stubby marine cements (m) can be seen growing out from the micritised margins of the tabula into primary intraskeletal cavities. Sample AX/7, Casa Borrell (locality 1a, Fig. 4.1). Field of view 1.3 x 0.7mm.

### (ii) 'Cross-cutting' replacement fabrics

The 'cross-cutting' replacement fabrics consist of replacement calcite crystals which are relatively large (median diameter of 400μm), usually equant and extend out from within the original aragonitic skeleton into the void-filling cement. In rudists where this 'cross-cutting' replacement fabric is observed, the originally aragonitic shell areas are usually a distinct brown colour, are often pseudopleochroic and tend to show well preserved relict microstructures (see Figs. 5.12, 5.16 & 5.26).

Interpretation of the 'cross-cutting' replacement fabrics, observed within these rudists is slightly problematical. The meteoric-phreatic-altered corals ('cross-cutting mosaics') described by Pingitore (1976) had not retained much organic tissue and preservation of the microstructure was poor. He interpreted this to be a result of meteoric-phreatic-alteration having involved the development of a zone of temporary, but extensive secondary porosity (chalk zone), several mm thick, which separated the unaltered aragonite from the replacement calcite.

However, within the rudists from the Congost platform, which display 'cross-cutting' replacement fabrics, the originally aragonitic areas possess well preserved

relict microstructures, are usually a distinct brown colour and often display pseudopleochroism. These features would indicate that much of the original organic tissue has been preserved, suggesting that neomorphism had not involved an intermediate stage of chalkification.

It is possible that the differences between the 'cross-cutting' replacement fabrics observed within the Congost rudists and those from the meteoric-phreatic altered corals of Pingitore (1976) are something to do with the contrasting microstructures of corals and rudists. However, as is discussed below, it seems probable that these differences may have resulted from different environments of neomorphism.

Another interesting feature of the 'cross cutting' replacement fabrics is that they are only ever found within rudists which contain botryoidal marine cements (see section 5.5.3.3) within some of their intraskeletal cavities (see Figs. 5.12 & 5.16). As has already been mentioned (section 5.5.3.3) the botryoidal cements consist of botryoidal inclusion arrays, contained within large calcite crystals which, when seeded upon a cavity wall, not only enclose the inclusion arrays but cross into the originally aragonitic intraskeletal cavity walls. The compromise boundaries which result from total occlusion of primary cavities by the botryoidal cements, together with the cross-cutting relationship they display with the originally aragonitic cavity walls, results in the development of an equant mosaic fabric, which can cover a large area of the rudists interior.

Within such rudists there are also areas which have been occluded and replaced by coarse, equant, inclusion-free spar, exhibiting a similar 'cross-cutting' replacement fabric (see Fig. 5.16). Some of these inclusion-free calcite crystals possess similar radiaxial extinction patterns to those displayed by the botryoidal cements. There are also cases where seemingly single crystals are composed in one part of inclusion-rich calcite, displaying the features associated with the botryoidal marine cements, and in the other part of the inclusion-free calcite.

The 'cross-cutting mosaics' displayed by botryoidal marine cements are discussed below (section 5.5.4.6), where the possibility that the neomorphic replacement of rudist tabulae occurred during the growth of these marine cements, is considered. The close association between the 'cross-cutting mosaic' inclusion-free spar and the botryoidal cements, together with the similarity in the fabrics and gross morphology that they display, strongly suggests that either the inclusion free spar represents a neomorphic replacement of the botryoidal cements or that they in fact represent the same cement generation (see Fig. 5.16). The only obvious difference between the two would appear to be the presence or absence of inclusions.

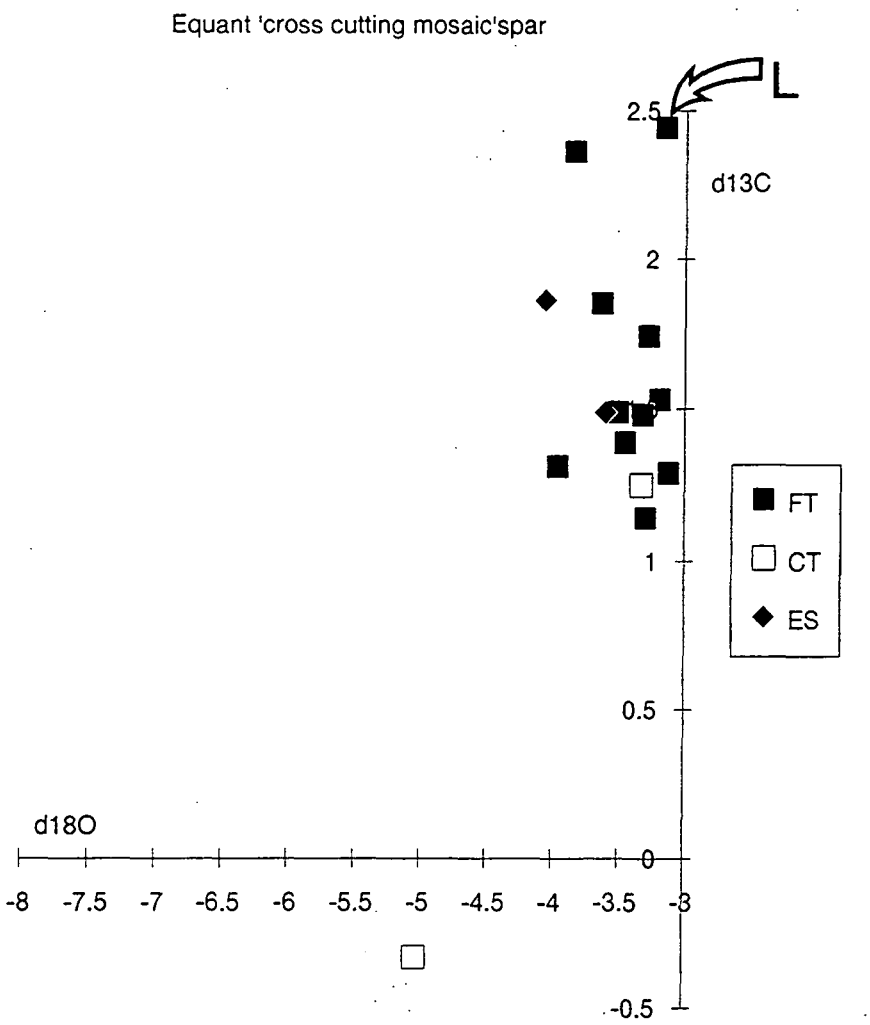


**Fig. 5.28.** Carbon and oxygen isotope cross-plot, showing the compositions of inclusion-free spar, which replaces originally aragonitic shell layers within rudist samples collected from lagoonal sediments which outcrop on the north side of Gallinove (locality 1f, Fig. 4.1), together with the compositions of calcite rudist shells. L = Best estimate of lagoonal carbonate composition (see section 5.4.5);FT = calcite rudist shell from Congost d'Erinya; CT = calcite rudist shells from this locality; ES = inclusion free neomorphic spar.

The isotopic composition of such 'cross-cutting mosaic' inclusion-free spar is shown in Fig. 5.28, together with analyses of rudist calcite tests and a best estimate for the original composition of precipitates within the lagoonal environment of the Congost platform (see section 5.4.5). The similar isotopic composition of the inclusion free spar to that of the isotopically heaviest compositions for rudist calcite, suggests that the inclusion-free spar was probably precipitated from lagoonal waters.

Inclusion-free calcite, within otherwise inclusion-rich growth layers of radiaxial-fibrous calcite, precipitated from marine waters, has been documented by Kendall (1985). He described the feature as giving 'a false impression that the radiaxial calcite had suffered neomorphism', which is precisely the first impression given by the fabrics observed in this study. Kendal (1985) suggested that most inclusions within such marine cements are in fact fluid-filled microcavities. He went on to interpret the occurrence of inclusion-free areas within such cement generations, to be a result of the elimination of former fluid-filled inclusions through the later growth of calcite within them. Why this should have occurred in some areas and not others is unknown.

The 'cross cutting' replacement fabrics (see Figs. 5.12 & 5.16) which occur in association with botryoidal marine cements are interpreted to be a result of neomorphic replacement which occurred while the botryoidal marine cements were developing in a marine-phreatic environment. This interpretation is discused further in section 5.5.4.6.

### 5.5.4.5 Partial dissolution/neomorphism of rudist aragonite

The originally aragonitic shell layers and tabulae within many of the rudists studied display a combination of dissolution and neomorphic fabrics. Commonly, the margins of originally aragonitic shell layers have been replaced by inclusion-rich, often pseudopleochroic, neomorphic spar, while the interiors display features suggesting that they have suffered dissolution (see Figs. 5.11, 5.22 & 5.29). Occasionally the converse relationship is observed, whereby the margins of originally aragonitic layers appear to have suffered dissolution, while the interiors display well developed neomorphic fabrics (see Fig. 5.26).

Marginal neomorphism/internal dissolution appears to be particularly common where the tabulae and shell layers concerned form the walls to cavities which contain well-developed marine cement generations (eg. Figs. 5.11, 5.22 & 5.29). Marginal dissolution/internal neomorphism on the other hand has usually occurred along the margins of aragonitic shell layers which form the walls to open cavities (due to breakdown of the external shell as a result of either fracture or borings) which have been filled with sediment (eg. Fig. 5.26). Where botryoidal marine cements occur (see sections 5.5.3.3, 5.5.3.4, 5.5.4.6), it is usual for the internal tabulae which surround the internal cavities to be entirely neomorphosed (see Figs. 5.12, 5.15, 5.16 & 5.17).

Partial dissolution has been described by James (1974) from Holocene corals which were undergoing meteoric diagenesis. The partial dissolution was in this case


**Fig. 5.29.** Photomicrograph, showing partial neomorphism of an originally aragonitic shell layer within a rudist. The central area of the originally aragonitic shell layer is now occupied by equant inclusion free calcite spar cement (c), while the margins are now composed of inclusion rich microcrystalline neomorphic calcite crystals which display some relict microstructure (arrowed). The dissolution of the interior of this shell layer appears to have enabled the neomorphicaly replaced margin to have fallen away from the calcite outer shell layer to create an enlarged secondary cavity for occlusion by calcite spar cement. Sample OZ/18, Ortenada (locality 2, Fig. 4.1). Field of view 7 x 7mm.

due to microstructural differences between the centre and margins of trabeculae. Marginal neomorphism/internal dissolution relationships have also been described from within Cretaceous rudists by Ross (1989). He noted that, unlike the corals studied by James (1974), microstructural differences were unlikely to have been the cause, and attributed the phenomena to early marine neomorphism of tabulae margins, followed by later dissolution of the internal areas.

Within this study, although cases of marginal neomorphism are much more common than those showing marginal dissolution, the occurrence of both relationships within otherwise seemingly identical shell layers or tabulae suggests that they are not the result of microstructural differences between inner and outer parts of aragonitic shell layers. The observed restriction of marginal dissolution/internal neomorphism to the walls of open cavities which have been filled with lagoonal sediment, while marginal neomorphism has preferentially effected the walls of mainly enclosed cavities within which marine cements are well developed, suggests

environmental controls on the occurrence of these partial dissolution features. Likely controlling factors may have been similar to those suggested to have effected the distribution of marine cements, such as shell porosity-permiability and/or the presence and type of any surrounding matrix, which would both have effected any pore-fluid flow.

### 5.5.4.6 Possible marine neomorphism

Where marginal neomorphism/internal dissolution is observed, it is possible that some of the marginal neomorphism occurred prior to dissolution (such as was proposed by Ross, 1989). Such early neomorphism would have rendered the margins of the originally aragonitic shell layers resistant to subsequent dissolution. The close association of marginal neomorphism with marine cements (eg. Figs. 5.11, 5.22 & 5.29) suggests that the proposed early neomorphism may in fact have taken place under the influence of marine fluids (the possibility of neomorphism occurring within Cretaceous marine environments has been discussed in section 5.1.2.3). This possibility of some neomorphism having occurred within the marine realm can be investigated further by considering the neomorphic fabrics which are observed in association with botryoidal marine cements (see also section 5.5.4.4).

Where botryoidal marine cements (see section 5.5.3.4) are present within intraskeletal cavities, the boundaries to the large calcite crystals that enclose the botryoidal patterns of inclusions are observed to cross over into the now neomorphosed, originally aragonitic tabulae, forming the cavity walls (see Figs. 5.12, 5.15, 5.16 & 5.17). Similar replacement fabrics are also displayed by the inclusion-free calcite spar which commonly occurs in association with botryoidal-type cements (see Fig. 5.16). As discused in section 5.5.4.4, these inclusion-free calcite crystal mosaics have isotopic compositions compatible with precipitation within a lagoonal environment (see Fig. 5.28) and are interpreted to have a similar origin to the botryoidal cements.

Similar crystal boundaries, observed to surround and enclose botryoidal patterns of inclusions which display radiaxial patterns of extinction have been described by Kendall & Tucker (1973) and Ross (1989 & 1991). They interpreted them to have resulted from a complex replacement of an earlier acicular (botryoidal) calcite cement. Such coarse, equant, replacement fabrics, which cross over skeletal boundaries, are typical of neomorphism which occurs within a meteoric-phreatic environment (Pingitore, 1976). However, if the fabrics observed in this study had resulted from such a replacement process, then why would the coarse neomorphic

spar have cross-cut skeletal boundaries but not the boundaries between the proposed fan shaped bundles of acicular calcite crystals?

In a follow-up to Kendall & Tucker (1973), Kendall (1985) proposed that, rather than representing replacement fabrics the enclosing crystal boundaries are in fact a primary feature. He suggested that they represent the crystal margins of coarsely-crystalline marine calcite cements, which split into a series of subcrystallites as they grew. Such an interpretation of the enclosing crystal boundaries to these pseudobotryoidal cements would suggest that neomorphism of the surrounding, originally aragonitic rudist skeleton took place during the growth of these distinctive marine cements.

### 5.5.4.7 Cement and crystal silt filled dissolution pipes and cavities

As already described in sections 4.2.4.4 & 4.3.3, interconnecting networks of cement and crystal silt filled pipes and cavities have been observed cutting through the platform top sediments (see Figs. 4.13 & 4.18). These pipes occur within the grainstones/packstones which mark the top of these platform-top sediments as well as the muddy lagoonal facies and the upper few metres of the underlying upper slope facies grainstones and packstones.

These pipes and cavities are very irregular in shape and range in size from 10's of microns up to a few centimetres in width. At the edges of these cavities both skeletal fragments and their enclosing matrix have been truncated. However, originally calcitic fragments (internal microstructure preserved), although truncated, often protrude further into the cavities than the micritic matrix which surrounds them. At the edges of some of the larger cavities narrow 'branches' can be seen to penetrate the host sediment and sometimes irregularly shaped blocks of the host sediment have become detached from the cavity walls. What would appear to be fragmented and heavily leached remnants of such blocks can be seen amongst the cement and crystal silt (see below) which fills the cavities (see Fig. 4.18).

The irregular shape of these cavities suggests that they were formed by dissolution and fracture, with the removal of blocks from the cavity walls suggesting a process of stoping during propagation of the cavities and cracks. The protrusion of originally calcitic shell fragments into the cavities also suggests a dissolution origin, as their relatively coarse crystalline nature would have rendered them more resistant to dissolution than the surrounding fine grained matrix.

These cavities are infilled by coarse equant calcite spar, irregularly shaped 'clasts' of the host rock and accumulations of crystal silt (see Figs. 4.13, 4.18, 5.30 & 5.31). The crystal silt consists of irregularly shaped fragments of crystalline calcite

**Fig. 5.30 and 5.31.** Paired photomicrographs under normal light (a) and CL (b), showing the coarse calcite spar cement and crystal silt from toward the centre of a dissolution cavity(5.30a & b show a different field of view to that in 5.31a & b). The coarse calcite has grown in from the edges, while the crystal silt infills the centre of the dissolution cavity. Note the fragmentation of the coarse calcite crystals at their margins. Under CL (b), the coarse spar is generally non-luminescent, with a bright orange late zone. However, well within the outer margins of the crystals which are visible under normal light (a), its luminescence appears to have been overprinted by the bright orange luminescence associated with the crystal silt. Sample AH/11, Casa Borrell (locality 1a, Fig. 4.1). Field of view 4.5mm across.

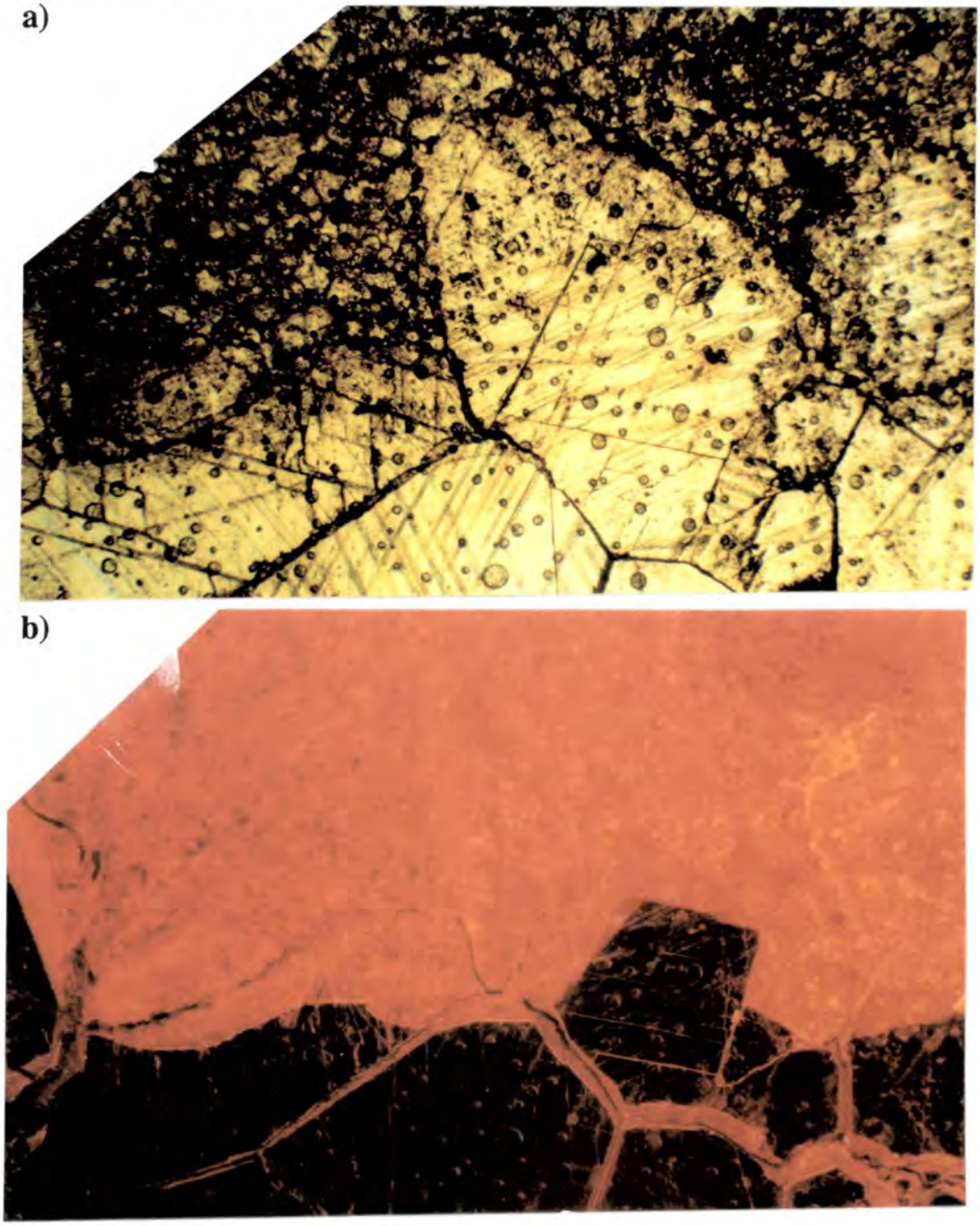


**Fig. 5.30.**

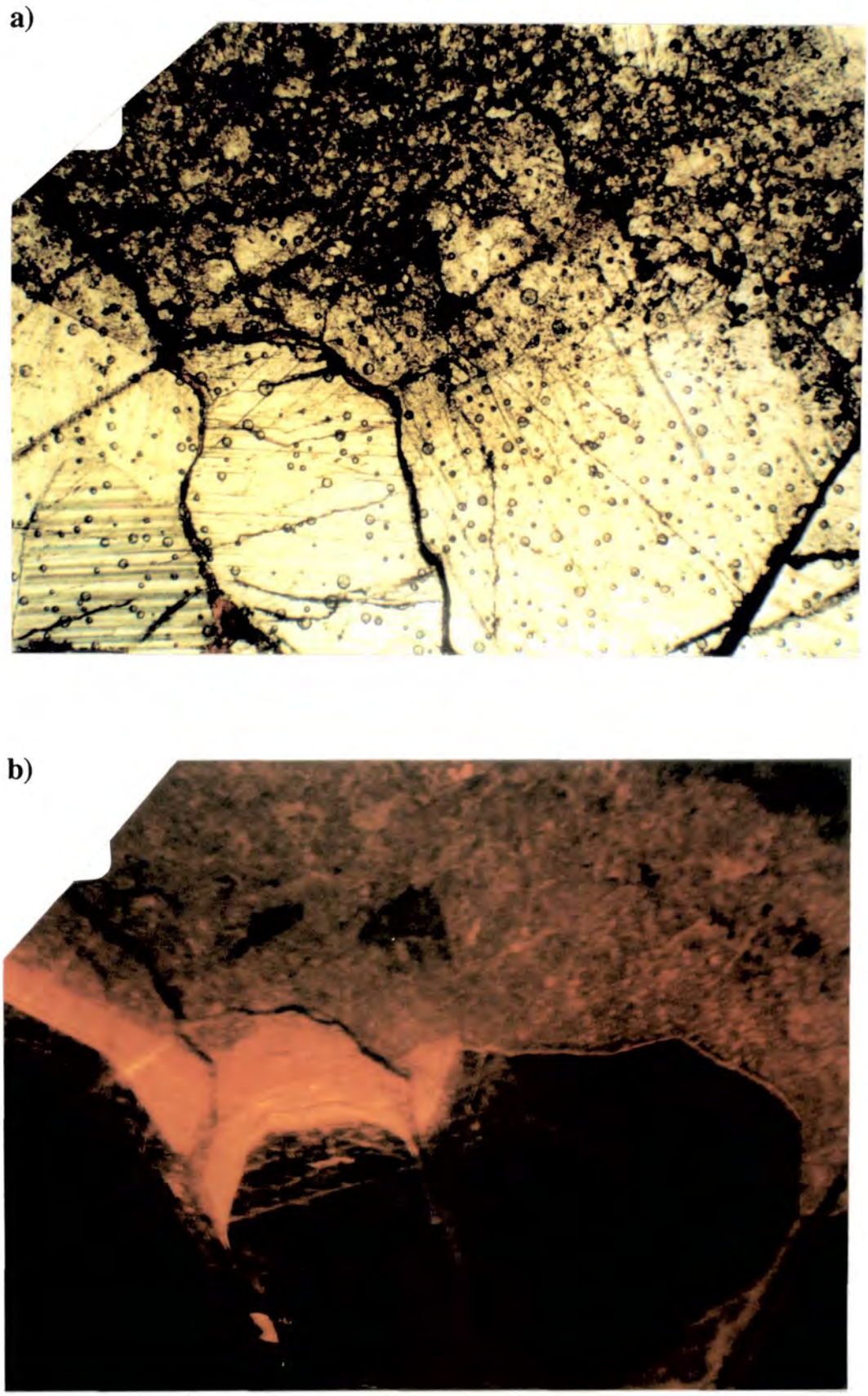


**Fig. 5.31.** (see previous page for caption)

together with some micritic material and lacks any recognisable skeletal debris; it is much coarser (20 - 150μm) than that which occurs within the dissolution voids of rudists. The crystal silt usually occurs towards the centre of the cavities but can also be seen to completely fill them in some places. Staining with Dickson's solution (Dickson, 1965, 1966) has revealed the coarse, equant spar to be non-ferroan. Under cathodoluminescence this non-ferroan, coarse, calcite spar is mostly non-luminescent; however, in places it displays a late zone with a bright orange luminescence. The crystal silt shows a dull-bright orange luminescence.

Comparison of the same view under normal light and cathodoluminescence reveals several features to suggest that the crystal silt postdates the equant spar and may in fact have its source in the alteration and disintegration of the coarse calcite crystals. Some of these features can be seen in Figs. 5.30 & 5.31; which show CL and normal light views, from towards the centre of a dissolution cavity, where the coarse non-luminescent calcite crystals have been fragmented at their margins and overprinted by the bright orange luminescence, associated with the crystal silt. In some samples the coarse calcite spar is separated from the sides of the cavity and occurs as 'rafts' with highly fragmented margins within the crystal silt. It is very common for the late bright zone at the margins of spar crystals to have been truncated by the crystal silt (see Fig. 5.31).

The early, wide, non-luminescent zone of non-ferroan, calcite spar, forming the first cement within the dissolution cavities, followed by the later, thinner, bright-orange luminescent zone within some cavities (see Fig. 5.31), suggests that precipitation began from oxidising pore fluids which later evolved to become reducing. This is a common feature of many meteoric cements (Frank et al., 1982; Grover & Read, 1983; Dorobek, 1987; Mussman et al., 1988; Niemann & Read, 1988). The reducing conditions could have been brought about by stagnation of the porefluids, and would have been promoted by the large amount of organic material present within these lagoonal sediments. Grover and Read (1983) noted, after Turner & Patrick's (1968) study of waterlogged soils, that such reducing conditions could be produced by water saturation, and then stagnation, during periods of excessive rainfall (perhaps suggesting a humid climate).

The bright orange luminescence of the crystal silt, together with that of the margins to the earlier calcite spar, whose alteration appears to be associated with the crystal silt (see Figs. 5.30 & 5.31), poses a problem. This is because the bright luminescence suggests that this accumulation of crystal silt formed under reducing pore fluid conditions, which undermines the, seemingly correct, interpretation that crystal silt is deposited from quickly flowing vadose waters (Dunham, 1969).

Closer examination of the margins of the coarse calcite spar adjacent to the crystal silt, under cathodoluminescence, reveals distinct planar boundaries between the parts of the coarse calcite crystals which have remained unaffected by the crystal silt deposition and those that have been altered (see Figs. 5.30 & 5.31). These planar boundaries truncate both the early non-luminescent zone and, where present, the later bright zone of the coarse calcite spar. When viewed under both cathodoluminescence and normal light, comparison reveals that these planar boundaries occur up to 1mm inside the obviously fragmented margins of the large calcite crystals (see Figs. 5.30 & 5.31).

These features observed at the margins to the calcite cement would suggest that, in addition to physical erosion at the edges during crystal silt formation, the calcite spar also underwent some chemical alteration which penetrated deep within the crystals and may in fact have been a factor in rendering the spar susceptible to physical erosion. Such chemical alteration of the coarse calcite spar, suggests that either during or just before crystal silt formation, the pore fluid chemistry had evolved to such an extent that the earlier coarse calcite spar precipitate was no longer stable. Perhaps it should also be noted at this point that as well as being much coarser than the crystal silt within the secondary porosity of rudists (see section 5.5.4.3), it is in fact much coarser than the 'vadose silt' (median diameters 10 to 25μm) described by other workers (Dunham, 1969; Walls et al., 1979; Grover & Read, 1983; Kahle, 1988; Meyers, 1988; Mussman et al., 1988).

Could these features be suggesting that, rather than having been deposited from meteoric waters in the vadose environment, the formation of this crystal silt, together with the associated alteration and dissolution of the coarse calcite spar, was in fact the result of aggressive pore fluid migration in the burial realm?

There is much documented evidence to suggest that aggressive pore fluids exist in the burial environment and that they can be responsible for the dissolution of carbonates. Reviews of such mesogenetic dissolution by Moore (1989) and Mazzullo & Harris (1992) suggest that organic matter degradation can produce suitably aggressive fluids and that these fluids are particularly effective where there are pre-existing conduits. Such conduits could include partly occluded dissolution pipes and cavities.

In the next section (5.5.4.8) isotopic evidence is presented, which supports the interpretation that these cavities resulted from near-surface dissolution through the action of meteoric waters and that the non-luminescent, equant cements within them precipitated from meteoric pore fluids. The isotope data also suggest that burial fluids may have been responsible for the alteration and dissolution of the coarse calcite spar and creation of the associated crystal silt within these dissolution cavities

### 5.5.4.8 Stable isotopes from cement and crystal silt-filled cavities

Samples drilled out from the wall rock adjacent to these pipes and cavities, together with samples of the non-luminescent, equant spar and samples of the crystal silt were analysed for their stable isotope compositions. The results of these analyses are shown in Fig. 5.32, together with the compositions of calcite rudist shells collected from Congost d'Erinya. The isotopically heaviest of the rudist shell samples are interpreted to represent a best estimate of the original composition of these lagoonal carbonates (see section 5.4).

The wall rock samples are depleted in both $^{18}O$ and $^{13}C$ with respect to the best estimate of lagoonal carbonate composition, suggesting that they have suffered some alteration. The significant depletion in $^{13}C$ of between approximately -2 to -4 ‰ suggests that alteration occurred in an open system, with light $\delta^{13}C$ values coming from $CO_2$ introduced into the pore fluids from either soil gas or organic maturation. The $\delta^{18}O$ values of between -4.7 and -6.9 ‰ (PDB) obtained for these samples are compatible with the isotopic signatures which would be expected for precipitates from meteoric waters at sedimentary temperatures in the Tremp basin during the Upper Cretaceous (see section 5.2.3.2). In section 5.5.4.7 petrographic evidence suggesting that these dissolution cavities were created through the action of meteoric water was presented. In the light of this, the isotopic compositions of the wall rock are interpreted as a result of alteration in the presence of organically charged meteoric waters and hence provide further evidence for the meteoric dissolution hypothesis.

The overall trend shown by these wall rock samples is interpreted to be a co-variant trend (after Wilson et al., 1983; James & Choquette, 1984; Lohmann, 1988) produced by the mixing of marine carbonate and organically-charged meteoric water. This sort of trend is produced by variable degrees of fluid-rock interaction.

The equant spar cements show even lighter isotopic compositions than the wall rock samples, especially in $\delta^{13}C$. The significant depletion in $^{13}C$ of -7.8 ‰, together with the -2.2 ‰ $^{18}O$ depletion with respect to the best estimate of original lagoonal carbonate composition, taken together with the petrographic evidence presented in section 5.5.4.7, is interpreted to suggest that these cements were precipitated from organically charged meteoric fluids in an open system. Although the isotopic compositions of these non-luminescent calcite spar samples are significantly lighter than those of the wall rock samples they plot on the same co-variant trend. The isotopic composition of these cements may well represent a good approximation of the isotopic signature of the meteoric waters deemed to have been

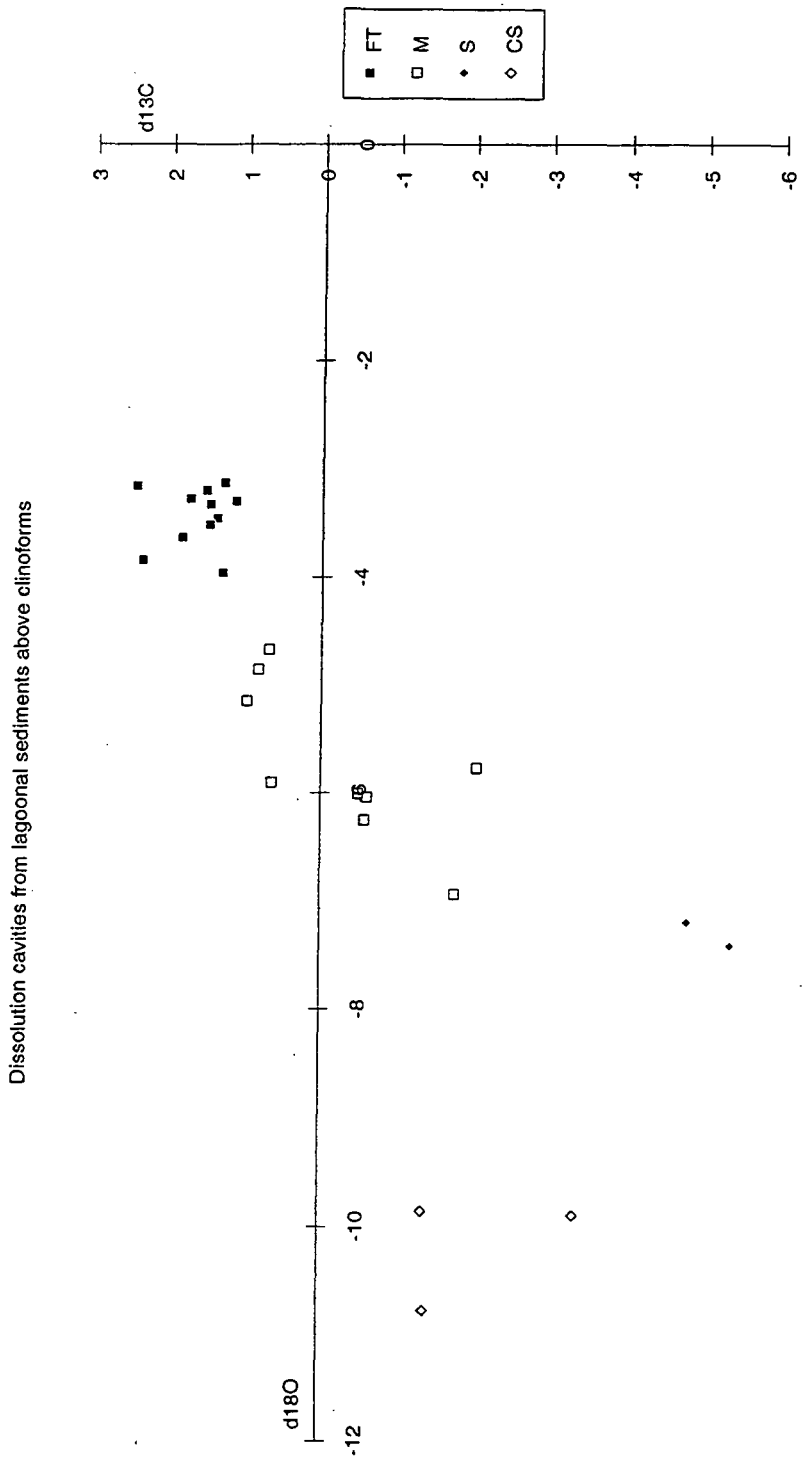


**Fig. 5.32.** Carbon and oxygen isotope cross-plot showing the composition of samples drilled out from the wall rock (M) adjacent to dissolution pipes, together with samples of the non-luminescent calcite spar (S) and crystal silt (CS) which infill the pipes. To aid interpretation the compositions of these samples have been plotted together with those of calcite rudist shells (FT) from the Congost d'Erinya outcrop. The dissolution pipe samples were drilled from specimens which were collected from the outcrops above Casa Borrell and on the north side of Gallinove (localities 1a & 1f, Fig. 4.1).

responsible for the alteration of the wall rock and precipitation of the equant, non-luminescent cements.

The samples of crystal silt do not plot within the co-variant trend shown by the cement and wall rock samples. They are significantly depleted in $^{18}O$ relative to both the wall rock samples and the calcite spar, suggesting that the fluids from which they gained their isotopic signatures were not only isotopically light but were also probably at a much higher temperature than those responsible for the signatures of the other samples. This significant depletion in $^{18}O$ of approximately -7 ‰ (PDB) and in $\delta^{13}C$ of between -3.9 and -5.8 ‰ (PDB), with respect to the best estimate of the composition of lagoonal carbonate, of the samples of crystal silt suggests that burial fluids may have been responsible for the alteration and dissolution of the coarse calcite spar and creation of the associated crystal silt.

### 5.5.4.9 Sediment filled, vertical dissolution pipes

A detailed description of these features can be found in section 4.3.3.2 (see Figs. 4.19a & 4.19b). However, it should be noted again that these features are interpreted to have formed as a result of subaerial exposure which was brought about by a fall in relative sea-level of at least 40 metres.

### 5.5.4.10 Stable isotope study of a sediment filled dissolution pipe

A whole rock sample from the sediment infill of a pipe together with a whole rock sample of the wall rock directly adjacent to the pipe were analysed for their stable isotope compositions. The results of these analyses are plotted on Fig. 5.33, together with the compositions of calcite rudist shells from Congost d'Erinya. As discussed in section 5.4 the isotopically heaviest compositions of calcite rudist shells are interpreted to represent a best estimate of the original composition of Congost lagoonal carbonate. Both the sediment infill and the wall rock are depleted in both $^{18}O$ and $^{13}C$ with respect to the compositions of calcite rudist shells. They in fact possess similar isotopic compositions to the wall rock samples from adjacent to the cement and crystal silt filled cavities (see section 5.5.4.8 together with Fig. 5.33) and are similarly interpreted to have been altered in the presence of organicaly charged meteoric waters.

Hence, the stable isotopic compositions of these samples provide more evidence for the interpretation that these vertical sediment-filled dissolution pipes resulted from the action of meteoric fluids during a period of subaerial exposure.

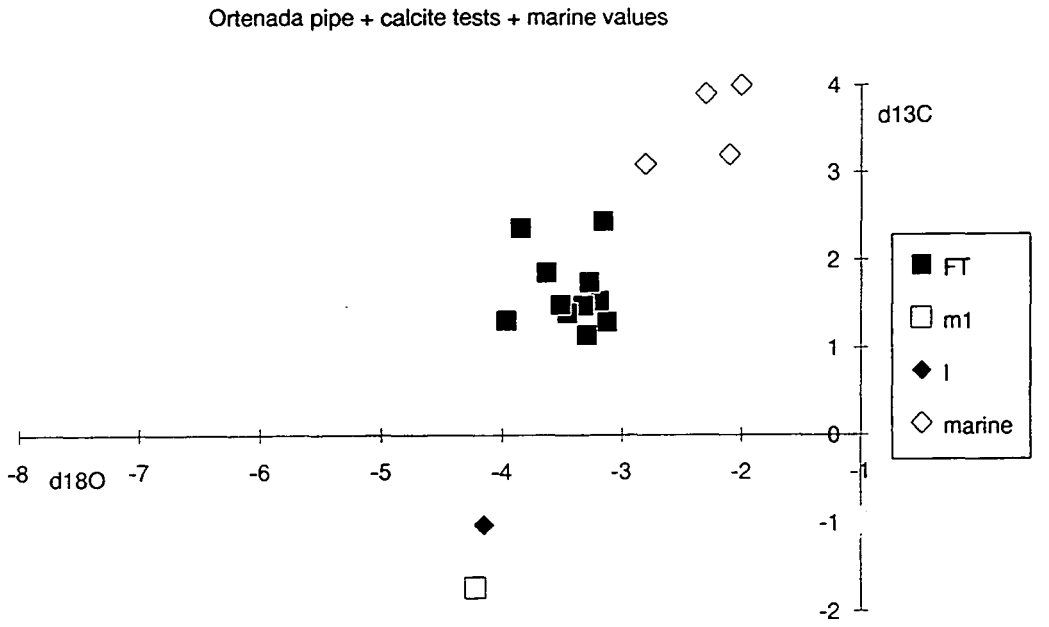


**Fig. 5.33.** Carbon and oxygen isotope cross plot showing the composition of a whole rock sample from the wall rock (m1)., directly adjacent to a sediment filled dissolution pipe in the lagoonal sediments which outcrop at Ortenada (locality 2, Fig. 4.1), together with a whole rock sample of the sediment which infills the pipe (I). These samples have been plotted together with the compositions of calcite rudist shells from Congost d'Erinya (FT) and estimates of the composition of Cretaceous marine carbonate precipitates from the literature (marine) (Moldovanyi & Lohmann, 1984; Al-Aasm & Veizer, 1986b; Enos, 1988).

## 5.5.5 Calcite spar cementation

### 5.5.5.1 Early, generally non-luminescent calcite spar

Coarse equant, calcite spar cements which occur as the earliest infills to dissolution pipes and cavities within these platform-top sediments, have been described and interpreted on the basis of petrographic, cathodoluminescence and isotopic information in sections 5.5.4.7 and 5.5.4.8 (see Figs. 4.13, 4.18, 5.30 & 5.31). These cements are interpreted as having precipitated from organically charged meteoric waters in a shallow vadose/phreatic environment.

Non-luminescent calcite spar cements, which occur in association with 'vadose silt', within both primary and secondary cavities of rudists have also been

described and interpreted in an earlier section (section 5.5.4.3)(see Figs. 5.23, 5.24 & 5.29). The early timing of these cements is demonstrated by the fact that they predate the deposition of vadose silt. These cements are also interpreted to have precipitated from meteoric waters in a shallow vadose/phreatic environment.

All of the originally aragonitic grains from throughout these platform-top sediments are now represented by equant or drusy calcite spar-filled moulds (see Figs. 4.11c, 4.16 & 4.17b). The calcite spar which fills these moulds is generally non-luminescent and non-ferroan (revealed by staining) which suggests that it too, was precipitated from oxidising pore-fluids.

Throughout the majority of these platform-top sediments, with the exceptance of early marine pore-lining cement generations (see section 5.5.3), much of the primary and secondary porosity has been occluded by non-luminescent calcite spar, which in many cases appears to have been meteoric in origin. This would suggest that much of the cementation of these carbonates occurred early on in their history, prior to any significant burial.

### 5.5.5.2 Later zoned-luminescent calcite spar

Within these platform-top carbonates, zoned-luminescent cements do occur, but are restricted to the primary and secondary cavities of only a few rudists (see Figs. 5.17 & 5.22), with small amounts being present towards the centre of some primary pores within corals.

When present within the primary intraskeletal cavities of a rudist or coral, these zoned cements always post-date the generally non-luminescent, marine cements and have usually occluded all the remaining pore-space (see Figs. 5.17 & 5.22). As the marine cements display a marked heterogeneity in distribution (see section 5.5.3), then so too, do these zoned-luminescent cements. As would be expected these cements are best developed within relatively large intraskeletal cavities, which only possess a thin lining of earlier, marine cements.

Within rudists whose primary intraskeletal cavities have been occluded by these zoned cements, it is also common for areas once occupied by originally aragonitic skeleton, to contain such cements (see Figs. 5.22). In most of these cases, as marine cements do not occur in such secondary dissolution cavities, zoned cements have filled the entire area once occupied by aragonite. However, some of the originally aragonitic tabulae and shell layers, display evidence of marginal neomorphism (see sections 5.5.4.5 & 5.5.4.6) which has restricted the development of secondary pore-space, and hence the precipitation of zoned cements, to their central areas (see Fig. 5.22).

Within most cavities where these cements occur they display broadly-similar patterns of zonation under cathodoluminescence, although, as would be expected, within the smaller cavities only the earliest zones are present. Fig 5.22b shows a typical zonation pattern of these cements. The oldest part of the cement is non-luminescent with a slight dull-orange tinge, followed by a bright orange band defining a scalenohedral shape. This is succeeded by subsequent very fine, less bright bands of orange which parallel the outline of the first. A completely non-luminescent zone follows before a very bright orange band, still defining the original scalenohedral shape. The very bright orange band is followed by another completely non-luminescent zone. This final non-luminescent zone is followed by a wide zone, showing orange luminescenece with faint banding, that usually occludes the remaining pore-space. This wide, final orange zone is brightest in its earlier parts and becomes increasingly dull towards the centre of the pore-spaces. Figure 5.22 shows a number of early non-luminescent - bright orange zone pairs defining scalenohedral shapes; although this is a typical pattern, the number and exact characteristics of these early zones vary from sample to sample (compare with Fig. 5.17).

Staining with a mixture of potassium ferricyanide and Alizarin red S acidic solutions (after Dickson, 1965, 1966) revealed that the vast majority of these cements are non-ferroan, with ferroan zones being present only in some of the youngest cement, towards the centre of the largest cavities (see Fig. 5.34).

The oldest parts of these cements display the non-luminescent - bright orange luminescent pattern common in many limestones (Frank et al., 1982; Grover & Read, 1983; Choquette & James, 1987; Tucker & Wright, 1990). The non-luminescence of the first zone suggests that precipitation began from oxidising pore-fluids and the following bright zone indicates that porefluids had become reducing. This is a common feature of many cements which are thought to have been precipitated from meteoric waters (Grover & Read, 1983; Dorobek, 1987; Mussman et al., 1988; Niemann & Read, 1988). The reducing conditions could have been brought about by the stagnation of pore-fluids, and would have been promoted by the large amount of organic material present within these lagoonal sediments (Champ et al., 1979). The repeated non-luminescent calcite zones, observed within some samples, could then indicate that these samples had suffered repeated periods during which there was a renewed influx of fresh meteoric waters. These sort of conditions are typical of shallow burial phreatic environments, particularly in humid climates, where repeated freshwater recharge to the aquifer as a result of rainstorms, could occur.

The final wide zone of orange luminescence suggests the permanent onset of reducing pore-fluid conditions, which would have permitted the incorporation of

Mn2+ and Fe2+ ions (if available) into precipitates. The decreasing brightness in luminescence of this final orange luminescent zone towards the centre of cavities is also a common feature of many limestones, and has been interpreted by many to be a result of an increasing iron:manganese ratio in the cement (Frank et al., 1982; Grover & Read, 1983; Dorobek, 1987; Mussman et al., 1988; Niemann & Read, 1988). This increasing iron content within such cements is thought to be a result of precipitation from progressively more reducing pore-waters. The fact that staining has revealed ferroan calcites towards the centre of some of the larger rudist cavities in this study, would appear to be in agreement with this interpretation of such luminescence patterns (see Fig. 5.34).

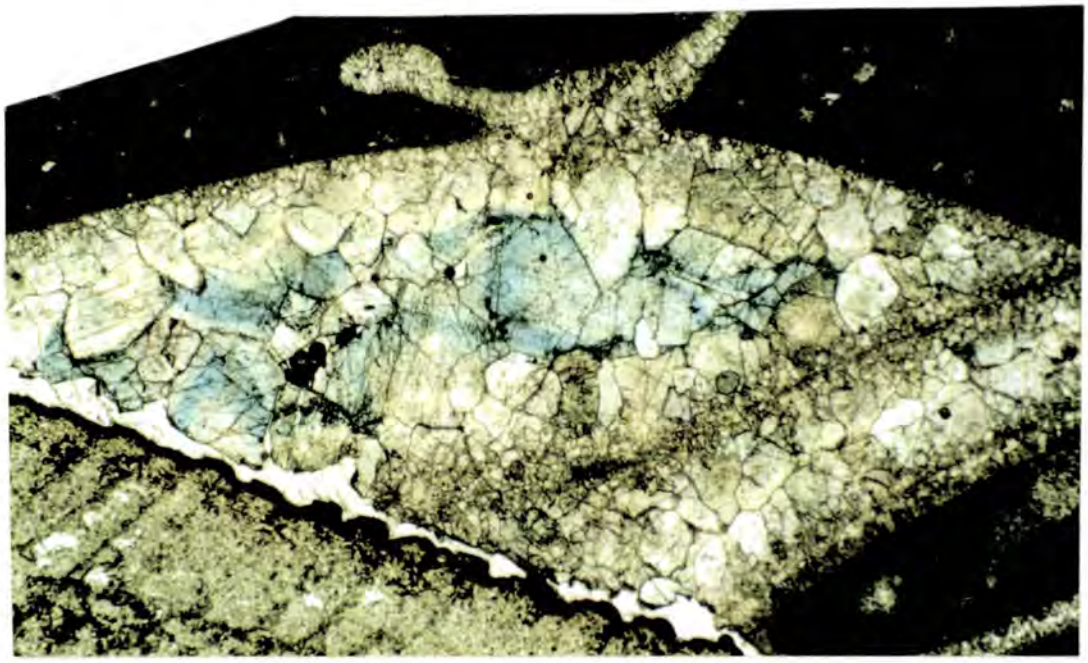

**Fig. 5.34.** Photomicrograph, showing the equant calcite spar within a primary intraskeletal rudist cavity, after staining with an acidic solution of Alizarin red S and Potassium Ferricyanide. Note the blue staining towards the centre of the cavity, indicating the presence of ferroan zones. The earlier zones are stained a light pink colour, indicating a non-ferroan composition, as are the isopachous, inclusion rich, marine cements which can be seen lining the margins of the cavity. Sample AX/9X, Casa Borrell (locality 1a, Fig. 4.1). Field of view 6 x 4mm.

### 5.5.5.3 Summary of calcite spar cementation

Much of the remaining primary and secondary pore-space within the platform-top sediments (after marine cementation) has been occluded by non-luminescent, non-ferroan equant or drusy calcite spar cements (see Figs 5.11, 5.19, 5.20, 5.21, 5.23, 5.24, 5.27, 5.29, 5.30 & 5.31). The non-luminescence of these non-ferroan cements is interpreted to indicate that they were precipitated from oxidising pore-fluids (Frank et al., 1982; Grover & Read, 1983; Dorobek, 1987; Mussman et al., 1988; Niemann & Read, 1988). The isotopic signatures of some of these cements strongly suggest that they were precipitated from organically charged meteoric waters (see section 5.5.4.8, together with Fig. 5.32). The association of these cements with secondary porosity, some of which also contain vadose silt, strongly suggests that some of these cements were in fact precipitated from meteoric fluids in a vadose environment.

The primary and secondary pore-spaces within some rudists escaped total occlusion by these non-luminescent, non-ferroan cements (see Figs. 5.15, 5.17 & 5.22). Within these cavities non-luminescent, non-ferroan cements are only found forming the earliest cement generations around the edges. The earliest non-luminescent/bright luminescent zones within these cavities are interpreted to suggest that precipitation occurred within a shallow burial phreatic environment which was subjected to sporadic recharge by fresh oxidising (probably meteoric) waters. The variability in these early zones between samples, collected from within close proximity (<10 metres in some cases) to each other, suggests local variations in porewater chemistries, perhaps, brought about by local permeability variations. These early zones are followed by a broad bright orange to dull orange zone which occludes the main part of these cavities and becomes ferroan in its later stages, suggesting increasingly reducing porewater conditions. This may indicate precipitation within deeper burial environments (see Figs. 5.15, 5.17, 5.22 & 5.34).

The fact that cavities within some rudists escaped total occlusion by non-luminescent cements, suggests a marked local variability in pore-water flow and chemistry. However, the presence of secondary cavities (now occluded by zoned cements) within these rudists (see Fig. 5.22), indicates that the fluids responsible for dissolution were able to reach them before this apparent restriction of fluids occurred. The reasons for these marked local variations in cementation histories remain unresolved. However, at least they demonstrate the complexity of studying diagenetic histories and the importance of studying several samples from a locality, before coming to any overall conclusion.

## 5.5.6 Silicification

Silicification has effected most of the rudists examined. Microquartz networks, which have often become amalgamated to form equant quartz crystals, replace both skeletal carbonate and cements.

This replacement silica is most common within the originally calcitic, outer shell layers. When present within a rudist's interior, the silica not only replaces isolated areas of originally aragonitic tabulae but also areas of any adjacent marine cements as well (see Fig. 5.35). The silica commonly mimics the microstructure of neomorphic calcite as well as the inclusion patterns within the marine cements.

This silicification would appear to have occurred after marine cementation and neomorphic replacement of aragonite. However, it is not known whether it post-dated precipitation of the zoned calcite spar cements or not.

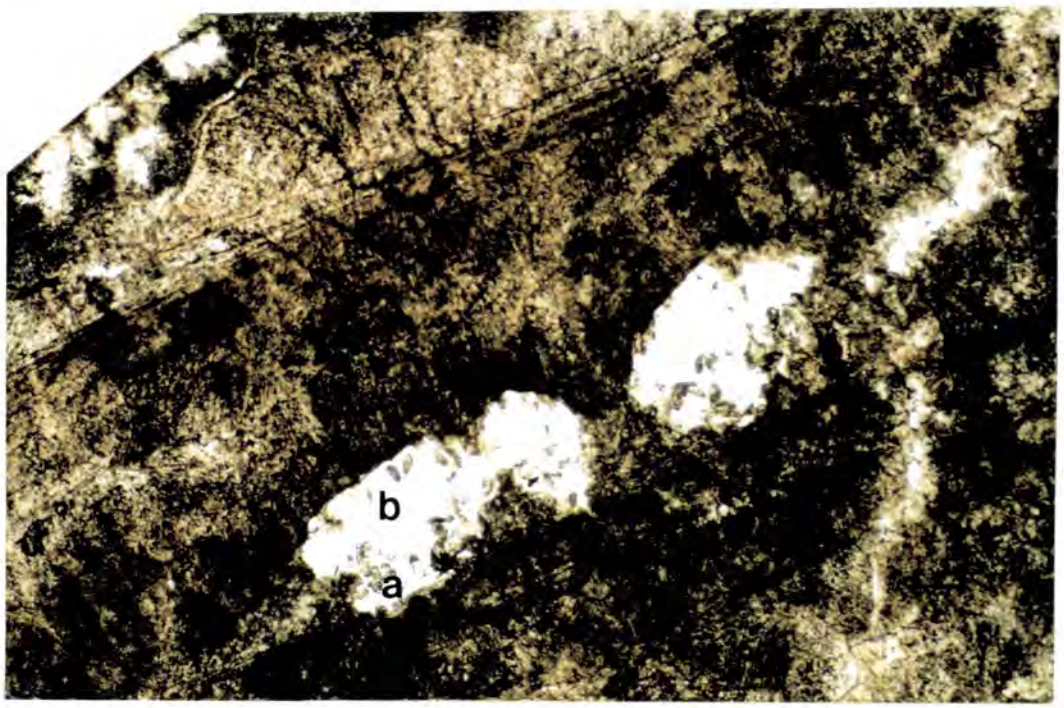


**Fig. 5.35.** Photomicrograph, showing the silicification which has effected the rudists within the platform-top sediments. Note that the silica networks have replaced both the originally aragonitic shell layers (a) and the inclusion rich botryoidal marine cements (b). Inclusions within the silica mimic the relict microstructure of the former aragonitic tabulae and the botryoidal arrays within the marine cements. Note also that the networks have become amalgamated to form equant quartz crystals. Sample AX/12, Casa Borrell (locality 1a, FIg. 4.1). Field of view 6 x 4mm.

### 5.5.7 Late stage mineralisation

Towards the centre of the largest cavities within some rudists, coarse mosaics of baroque dolomite occur (see Fig. 5.36). Locally the baroque dolomite is accompanied by crystals of flourite and/or drusy megaquartz

The baroque dolomite is brown in colour and forms very large, inclusion rich, crystals (up to 8mm across), with characteristic curved edges and twin planes. Staining with Dickson's solution (Dickson 1965, 1966) reveals this baroque dolomite to have a high but variable iron content. In some cases the baroque dolomite occurs in association with flourite and/or large crystals of megaquartz, which have grown from the same surface of earlier zoned calcite cement as each other. When they occur together all three minerals display equant habits. An interesting feature of the flourite, and one that aids in its identification, is that it develops a permanent, purple colouration after bombardment with electrons under the luminoscope.

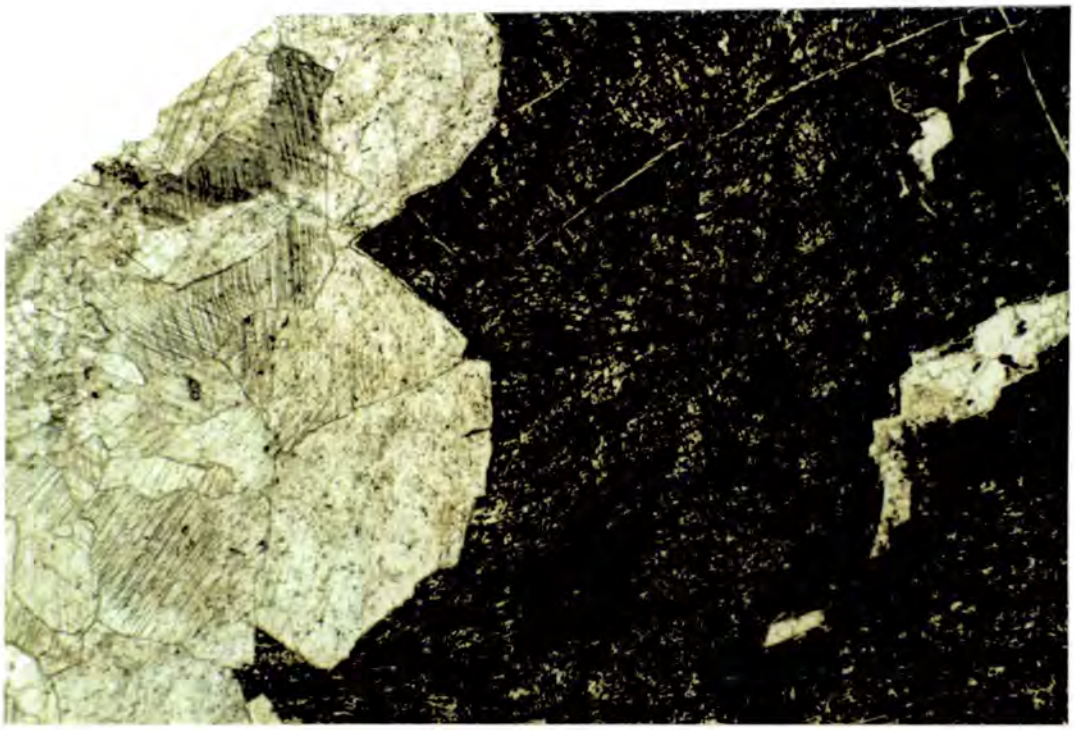

**Fig. 5.36.** Photomicrograph showing coarse mosaic of baroque dolomite which has grown as the final infill, after calcite, to the central cavity of a rudist from the lagoonal sediments of the Congost platform. Note the curved cleavage planes which are a distinctive feature of baroque dolomite. The dark brown colouration of this baroque dolomite suggests a high iron content. Sample OZ/13, Ortenada (locality 2, Fig. 4.1). Field of view 6 x 4mm.

Baroque dolomite occurring in association with flourite has been described as a late stage hydrothermal cement in many limestones (Choquette, 1971; Radke & Mathis, 1980; Mathis, 1978; Ross, 1989). Radke and Mathis (1980) suggested that baroque dolomite forms at temperatures in excess of 60°C.

The baroque dolomite and occasional flourite and/or megaquartz, observed within some of the Congost rudists, are interpreted as late stage hydrothermal precipitates, whose distribution was controlled by the availability of any remaining pore-space. The fact that in some cases all three minerals have grown from the same surface of earlier zoned calcite spar and that they all display equant habits, means that they cannot be separated in terms of relative time of precipitation.

## 5.6 The Congost d'Erinya outcrop

### 5.6.1 Introduction

The sedimentology, geometry and general nature of the platform-top sediments seen in the outcrop on the west side of Congost d'Erinya have been described and interpreted in detail in section 4.4.4. During the discussion in chapter 4 (see section 4.6 for summary), it was suggested that the outcrop in Congost d'Erinya represented a second and final phase of Congost platform development, which resulted from a period of forced regression. During this final phase of development coral reefs formed barriers at the platform margin, while rudists, small coral colonies, echinoids and foraminifera flourished in shallow, protected lagoons. The geometry and stacking patterns of the outcrop suggest that this part of the platform developed during a period of increasing accommodation space, however, the rate of increase in accommodation space was decreasing with time. This phase of platform development finally came to an end during a period of subaerial exposure and karstification.

Through the study of thin-sections, using both standard petrographic techniques and cathodoluminescence, it has been possible to place phases of cementation, dissolution and neomorphism into a relative time frame, and thereby suggest a succesion of diagenetic events which may have affected these platform top sediments. As in section 5.5, stable isotope analyses have aided the interpretation of some of these diagenetic features. Comparison of the Congost d'Erinya platform-top sediments to those from the group of outcrops in the region of the Santa Fe and Sant Corneli folds, suggests that they have undergone very similar diagenetic histories. There are, however, some important differences.

In the following sections, diagenetic features, observed within the samples from the Congost d'Erinya platform-top sediments, are described and interpreted in their approximate order of formation. However, to avoid repetition, where these features are the same as those which have already described, from the Congost platform-top sediments which outcrop in the region of the Santa Fe and Sant Corneli folds (those interpreted to represent the first phase of platform development), the reader is referred to section 5.5. Also, where appropriate, descriptions take the form of a comparison with particular diagenetic features which were observed to occur within the platform-top sediments which outcrop elsewhere (section 5.5). The group of outcrops which includes all those from the area around the Sant Corneli anticline and Santa Fe Syncline together with the outcrop at Ortenada, shall be referred to as the Sant Corneli group of outcrops throughout the rest of this section.

## 5.6.2 Micritisation

Micritisation has effected almost all the carbonate allochems within these platform top sediments. See section 5.5.2 for a description and interpretation of the features resulting from this micritisation. Well developed micritic margins can be seen around skeletal fragments in Fig. 4.25b, and mark the former position of the originally aragonitic tabulae within rudists and corals in Figs. 5.39 & 5.42.

## 5.6.3 Marine cementation

As with the platform-top sediments exposed in the Sant Corneli group of outcrops (see section 5.5.3), the most obvious early cement generations are to be found lining the intraskeletal cavities of rudists and corals (see Figs. 5.39, 5.42 & 5.43). There is also much evidence that matrix lithification, in the form of micrite sized crystallites, within the lagoonal wackestones and packstones was well advanced prior to dissolution (see Figs. 4.23a, 4.23b, 4.24d & 5.37),

However, unlike the platform-top sediments from the Sant Corneli group of outcrops, only one morphology of early cement generation has been observed within the intraskeletal cavities of rudists and corals from Congost d'Erinya. They are bladed to stubby isopachous calcite cements (see section 5.5.3.2)(see Figs. 5.39, 5.42 & 5.43). Botryoidal type cements (see section 5.5.3.3) have not been found within any of the rudist samples so far studied from this locality.

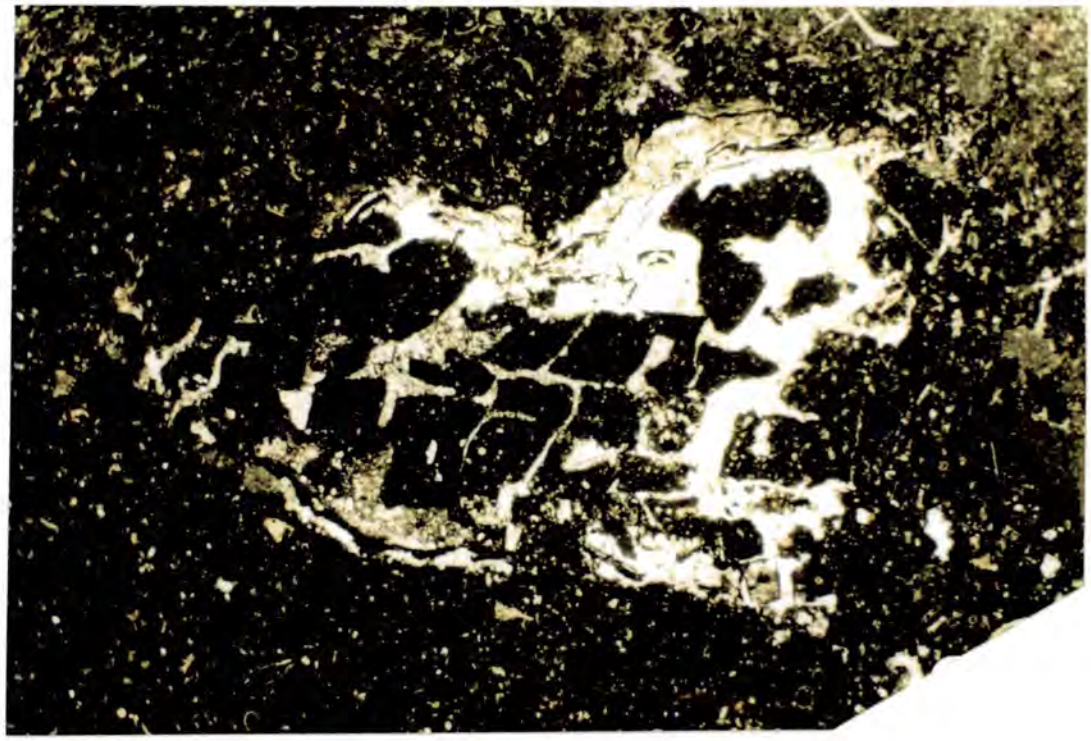

**Fig. 5.37.** Photomicrograph, showing calcite spar filled moulds, representing the former position of an aragonitic skeletal fragment within this lagoonal wakestone. The internal sediment within the former rudist fragment has suffered collapse; however it has retained its former shape, which together with the fact that the mould exists indicates that matrix lithification was advanced prior to dissolution. The collapse of the internal sediments indicates that the originally aragonitic rudist fragment suffered dissolution rather than neomorphism (which would not have involved a cavity stage). Note also the encrusting algae around the edges of this former rudist fragment. Sample F2/10, Congost d'Erinya. Field of view 12 x 7mm.

The bladed to stubby isopachous cements are most commonly found lining the primary intraskeletal cavities of corals and rudists within the lagoonal sediments, as well as the cavities within the corals which form the buildups at the platform margin (see section 4.4.5.2 together with Figs. 4.23a, 4.23b and 4.23c). These bladed to stubby cements are also found forming rims to the grains within the lenticular grainstone beds. Occasionally, as shown by Fig. 5.38, these bladed/stubby, isopachous cements can be found lining primary cavities within the lagoonal wackestones.

In Fig. 5.38, bladed to stubby isopachous cements can be seen lining the cavity within a brachiopod shell. The fact that these cements become increasingly well developed towards the top of the geopetal sediment infill, suggests a synsedimentary timing for their development.

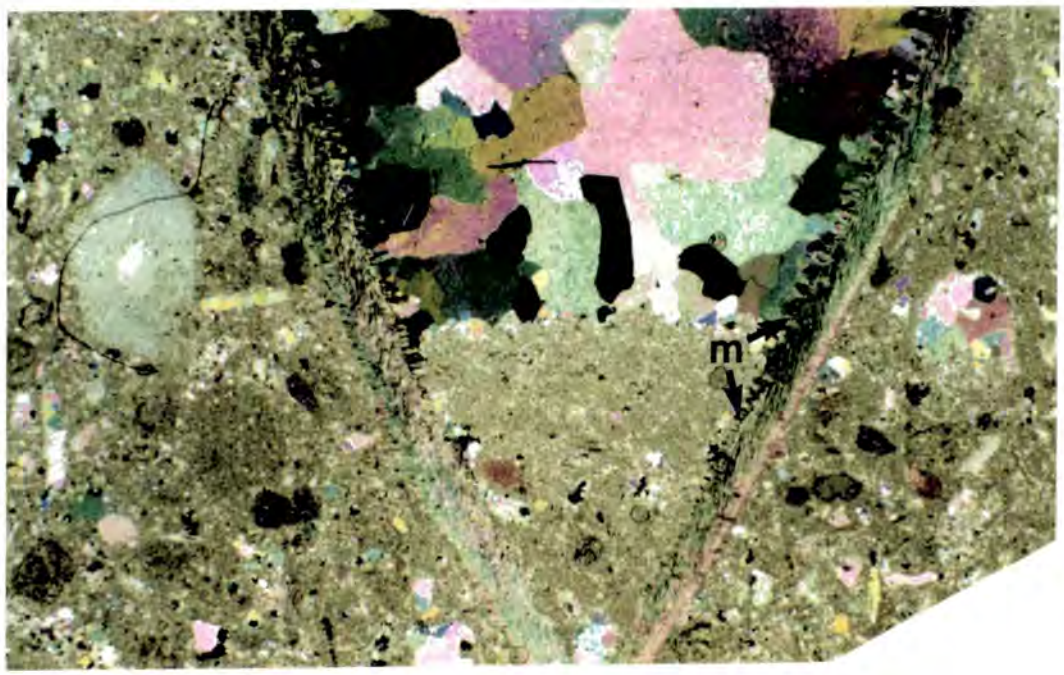


**Fig. 5.38.** Photomicrograph, showing isopachous marine cements (m) lining the primary cavity provided by a brachiopod shell within a lagoonal wackestone. The syndepositional timing of these cements is demonstrated by the fact that they become increasingly better developed towards the top of the geopetal sediment infill. Sample FB/11, Congost d'Erinya. Field of view 6 x 4mm.

The reason why no botryoidal type cements have been observed within any of the samples collected from Congost d'Erinya during this study is a matter for speculation. It is possible that they do occur, but by chance none were collected. However, bearing in mind the 60% occurrence of botryoidal cements within the rudists from the Sant Corneli group of outcrops (see section 5.5.3.2), as 12 rudist samples were collected from this locality, this would seem unlikely. Perhaps the lack of botryoidal cements within these Congost d'Erinya sediments is indicating that different pore-fluid flow regimes, from those which effected the lagoons during deposition of the platform-top sediments seen at the Sant Corneli group of outcrops, were in operation on the platform-top during deposition.

Differing fluid flow regimes on the platform-top during these two separate phases of platform development would seem likely, following the interpretation, from outcrop geometries, that they were deposited against differing backgrounds of accommodation space change (see section 4.6). In fact the presence of lenticular grainstone beds, which are interpreted to represent mobile skeletal carbonate 'sand banks', within the platform-top sediments exposed in Congost d'Erinya, suggests a

higher energy regime than that in effect during the deposition of the platform top sediments seen in the Sant Corneli group of outcrops.

## 5.6.4 Dissolution and neomorphism

### 5.6.4.1 Wholesale dissolution of aragonitic grains

As with those from the Sant Corneli group of outcrops, these platform-top sediments have suffered extensive dissolution. All aragonitic skeletal fragments have been dissolved and the resultant voids occluded by calcite spar (see Figs. 4.23a, 4.23b, 4.24d, 5.37 & 5.38). See section 5.5.4.2 for a description and interpretation of the features resulting from this dissolution.

### 5.6.4.2 Dissolution and neomorphism of rudist aragonite

Similar evidence to that described previously for rudist samples from the Sant Corneli group of outcrops, also suggests that: in addition to most areas of originally aragonitic skeleton within rudists having suffered dissolution (see section 5.5.4.3), many areas have undergone neomorphic replacement (see section 5.5.4.4). However, there is a distinct difference between the infills to secondary dissolution cavities within the samples from Congost d'Erinya and those from the Sant Corneli group of outcrops (This is discussed further in section 5.6.5). Another important feature is that all the neomorphic fabrics observed within the Congost d'Erinya rudists have been of the 'fabric selective' type (see section 5.5.4.4)(see Figs. 5.39 & 5.43).

There is some evidence of marginal neomorphism (see section 5.5.4.5) having effected some of the originally aragonitic tabulae and shell layers within rudists from Congost d'Erinya. Where this is the case, the remainder of the area originally occupied by aragonite has been occluded by zoned-luminescent calcite spar (see Fig. 5.39).

The fact that all the neomorphic fabrics observed within the Congost d'Erinya rudists have been of the 'fabric selective' type (see section 5.5.4.4), may be suggesting that, even where marginal neomorphism has taken place, the neomorphism of rudist aragonite, occurred within a vadose environment (see sections 5.5.4.4, 5.5.4.5. and 5.5.4.6). The likely composition of the fluids responsible for the neomorphic replacement of rudist aragonite is discussed with the aid of stable isotope information in section 5.6.7.

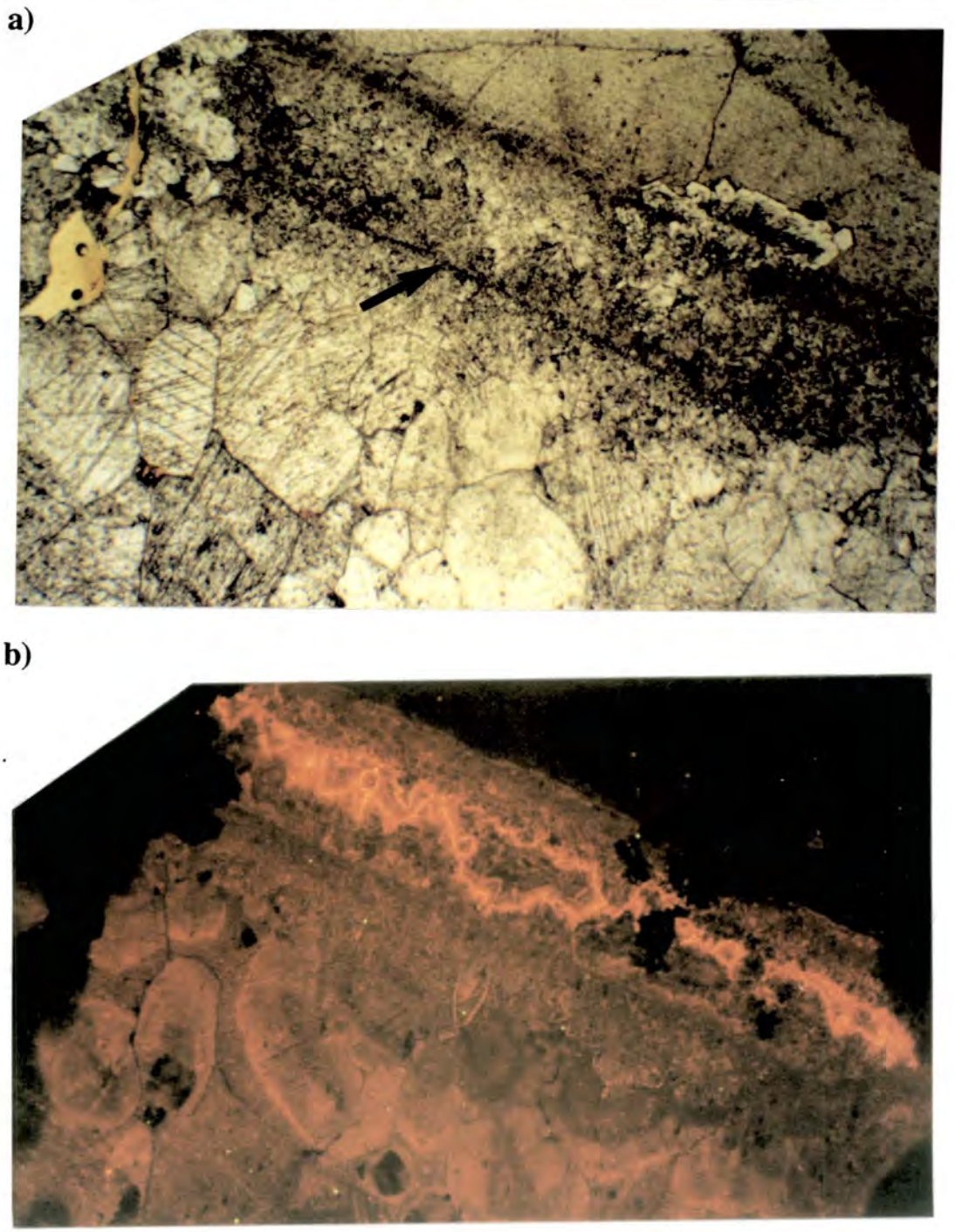


**Fig. 5.39.** Paired photomicrographs taken under normal light (a) and CL (b), showing zoned-luminescent calcite spar cements towards the centre of the area originally occupied by the inner aragonitic shell layer of this rudist. The former margin to the aragonitic shell layer is marked by a micritic margin (arrowed). Note how the zoned-luminescent cements are restricted to the centre of the originally aragonitic shell layer, whereas the margins are composed of non-luminescent, microcrystalline, inclusion rich calcite within which traces of relict microstructure can be seen. This indicates that this originally aragonitic shell layer has suffered marginal neomorphism, together with internal dissolution. Sample FB/21A, Congost d'Erinya. Field of view 4.5mm across.

#### 5.6.4.3 Network of cement filled dissolution pipes

As already described in section 4.4.6, the top few metres of the lagoonal sediments in Congost d'Erinya are cut by an interconnecting network of cement-filled pipes. These cement filled pipes have a range of sizes up to a maximum of approximately 8cm in diameter. They have smooth but irregular margins and form such closely spaced networks which criss-cross the lagoonal sediments that they create a pseudobreccia in places (see Fig. 4.27).

The smooth, but irregular outlines to these pipes suggest that they formed as a result of dissolution and fracture. The dissolution which created this pipe network could only realistically have been caused by the action of meteoric waters.

These pipes are interpreted as karstic features which formed as a result of dissolution by meteoric waters, perhaps aided by the process of near-surface fracturing. The presence of this network of dissolution pipes, marking the top of the Congost platform-top sediments, indicates that this phase of platform development was halted by a significant fall in relative sea-level. The cement which infills this network of dissolution pipes is discussed below in section 5.6.5.2 and again in section 5.6.7 where the results of stable isotopic analyses are discused.

### 5.6.5 Other cement generations

#### 5.6.5.1 Pendant cements

Samples collected from the lenticular shaped grainstone beds, interpreted to represent banks of skeletal debris which migrated around the platform-top (see section 4.4.5.3 together with Figs. 4.25a, 4.25b(i) & 4.25b(ii)), contain some grains (particularly brachiopod fragments) which possess pendant cements. The pendant cements are composed of non-ferroan, non-luminescent calcite.

These pendant cements are interpreted to represent precipitates from oxidising pore-waters which formed in a vadose environment. The local occurrence of these pendant cements is taken to indicate that periodically the carbonate 'sand banks' became emergent and this emphasises the shallow nature of these lagoons.

### 5.6.5.2 Cements which infill dissolution pipes

The dissolution pipes which form an interconnecting network within the top few metres of the Congost platform lagoonal sediments in Congost d'Erinya have been infilled with an interesting cement fabric.

From polished slabs and thin sections (see Fig. 5.40), the first component of the pipe infill is seen to be rectangular clasts of calcite cement (maximum size approx. 12mm by 5mm). These 'cement clasts' are composed of elongate, inclusion-rich crystals of non-ferroan calcite, with a brown colouration, arranged parallel to one another. The elongate crystals have all grown in the same direction, and their long axes have formed the narrow sides of these rectangular 'cement clasts'. The youngest ends of these elongate crystals are evident from their angular terminations and upon these there is commonly several millimetres of laminated sediment. This sediment contains a mixture of micrite and crystal silt. The 'cement clasts' are randomly oriented and are cemented together by a coarse, non-ferroan calcite spar cement, which is relatively inclusion-free and is in the form of elongate crystals which radiate out from the sides of the 'cement clasts'. Away from the cement 'clasts', this coarse, relatively inclusion free calcite spar has a drusy habit.

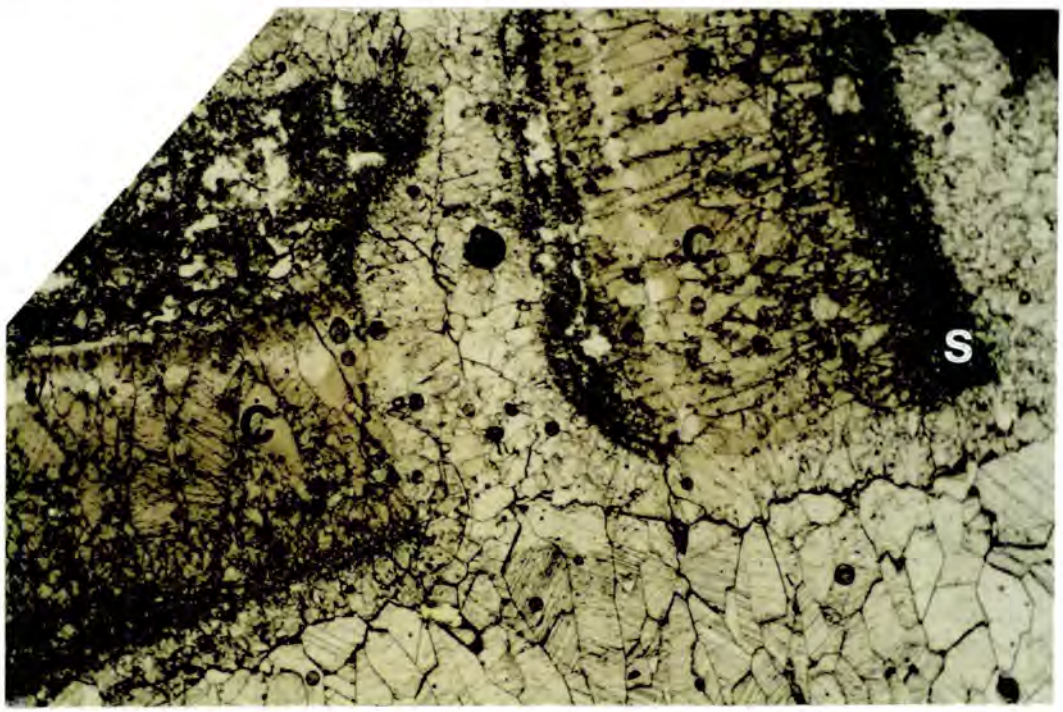


**Fig. 5.40.** Photomicrograph, showing the cement and sediment which infills the interconnecting network of dissolution pipes shown in Fig. 4.28a. Note the rectangular clasts (C) of elongate, inclusion rich calcite crystals. Note also the micrite and crystal silt (S), which lies along the edges of these clasts. Congost d'Erinya sample FB/24. Field of view 12 x 7mm.

Under cathodoluminescence (see Fig. 5.41) the 'cement clasts' are completely non-luminescent, while the sediment which rests upon their youngest sides shows a dull orange luminescence. The coarse calcite spar which surrounds the 'cement clasts' displays an early, wide zone of growth which is totally non-luminescent. This early non-luminescent zone fills much of the remaining pore space. However, within isolated pockets, towards the centre of the areas between 'cement clasts' luminescent zones of calcite spar occur. Within these pockets the non-luminescent zone is followed by a thin bright orange zone which defines a scalenohedral shape. The thin bright orange zone is in turn followed by a wide zone of relatively dull-orange luminescence, which occludes the remaining pore-space. The luminescence of this final cement zone becomes increasingly dull towards the centre of the pockets of luminescent cement.

The non-luminescence of the 'cement clasts', together with that of the earliest zone within the relatively inclusion free, non-ferroan calcite spar which surrounds them, suggests that they were precipitated from oxidising fluids (Frank et al., 1982, Grover & Read, 1983; Dorobek, 1987; Mussman et al., 1988; Niemann & Read, 1988). The thin bright orange zone which follows the non-luminescent cements and is, in turn, followed by increasingly dull, orange luminescent cements, is a zonation succession which is often observed in cathodoluminescence studies of limestones. Such a cement-zonation sequence is indicative of pore-water conditions which began as oxidising but evolved under increasingly reducing conditions (Frank et al., 1982, Grover & Read, 1983; Dorobek, 1987; Mussman et al., 1988; Niemann & Read, 1988). The bright orange band signifies the onset of reducing conditions which permit the inclusion of $Mn^{2+}$ into precipitates, while the increasingly dull, orange luminescence which follows indicates that pore-waters became increasingly reducing and allowed the precipitation of cements with an ever increasing $Fe^{2+}$:$Mn^{2+}$ ratio.

These pipes (see Fig. 4.27) are interpreted to have formed as a result of dissolution by meteoric waters, and near-surface fracturing, with the 'cement clasts' (see Figs. 5.40 & 5.41) being possible remnants of an early speleo-cement lining to the walls of the pipes. The sediment layer on the 'youngest' sides of the 'cement clasts' could be sediment that had washed into the pipes and become cemented to them while they still formed the wall lining. Later reworking of these speleo-cements has broken them off the dissolution pipe walls, to form the randomly-oriented 'cement clasts'. The rectangular nature of these 'cement clasts' is the result of the elongate fabric of the calcite crystals, which made up the original speleo-cement lining. The clasts were then cemented together by a phase of calcite spar cementation which began under the influence of oxidised porefluids; however, as the pore-space became increasingly occluded, the pore-fluids evolved to become increasingly reducing.

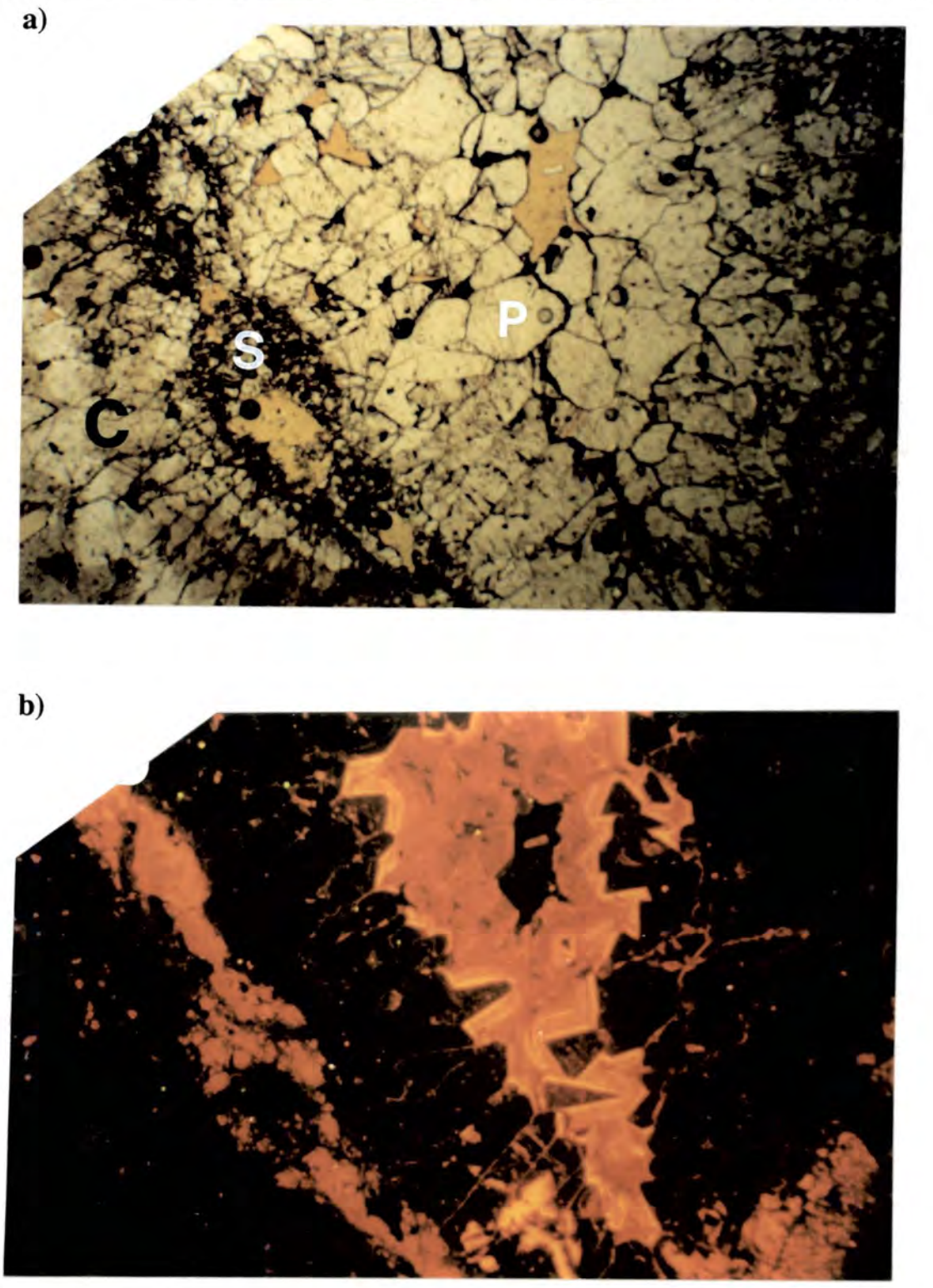


**Fig. 5.41.** Paired photomicrographs taken under normal light (a) and CL (b), showing the 'cement clasts' (C), sediment (S) and coarse calcite spar (P) seen in Fig. 5.40. The 'cement clasts' are non-luminescent, as are the earliest zones of the relatively inclusion free spar which surrounds them. Note the bright-dull orange zones of luminescence which occur towards the centre of the area of calcite spar between the 'cement clasts'. Sample FB/24, Congost d'Erinya. Field of view 4.5mm across.

The initial dissolution which created these pipes along with the precipitation of the speleo-cements (now forming the cement clasts) is interpreted to have taken place within a vadose environment. However, the development of the coarse, cavity occluding cements which followed would have required the saturated conditions of a phreatic environment. It is possible that such saturated conditions could have developed in a shallow burial setting under humid climatic conditions, during periods of excessive rainfall. The zonation sequence displayed by the coarse cavity occluding cements, when viewed under cathodoluminescence, suggests that stagnation of the porewaters took place. Such stagnation of the pore-waters within the dissolution pipes would have been aided by the impermeability of the previously-cemented carbonates which surround them.

Further evidence for these cements having precipitated from meteoric waters is presented in section 5.6.7, where the results of stable isotopic analysis are discussed.

### 5.6.5.3 Zoned-luminescent calcite spar

Unlike the samples from the Sant Corneli group of outcrops, described in sections 5.5.4.3, non-luminescent equant calcite cements are never observed to have completely occluded either the primary or the secondary cavities within rudists or corals from Congost d'Erinya. If non-luminescent cements do occur within the primary or secondary cavities of rudists from Congost d'Erinya, then they only form the first thin zone, preceeding otherwise luminescent-zoned cements (see Figs. 5.39 & 5.42). Another difference between the cavity infills observed within the rudists from Congost d'Erinya and those within the rudists from the Sant Corneli group of outcrops is that no crystal silt has been observed within any of the Congost d'Erinya rudists.

The cavities produced by dissolution within rudists from the Congost d'Erinya outcrop are always observed to have been occluded by relatively inclusion free calcite spar which, when viewed under cathodoluminescence, shows zoned-luminescence (see Fig. 5.39).

These zoned-luminescent cements possess similar zonation sequences to those which occur within some of the intraskeletal and secondary cavities of samples from other localities. See section 5.5.5.2 for a detailed description and interpretation of these cements.

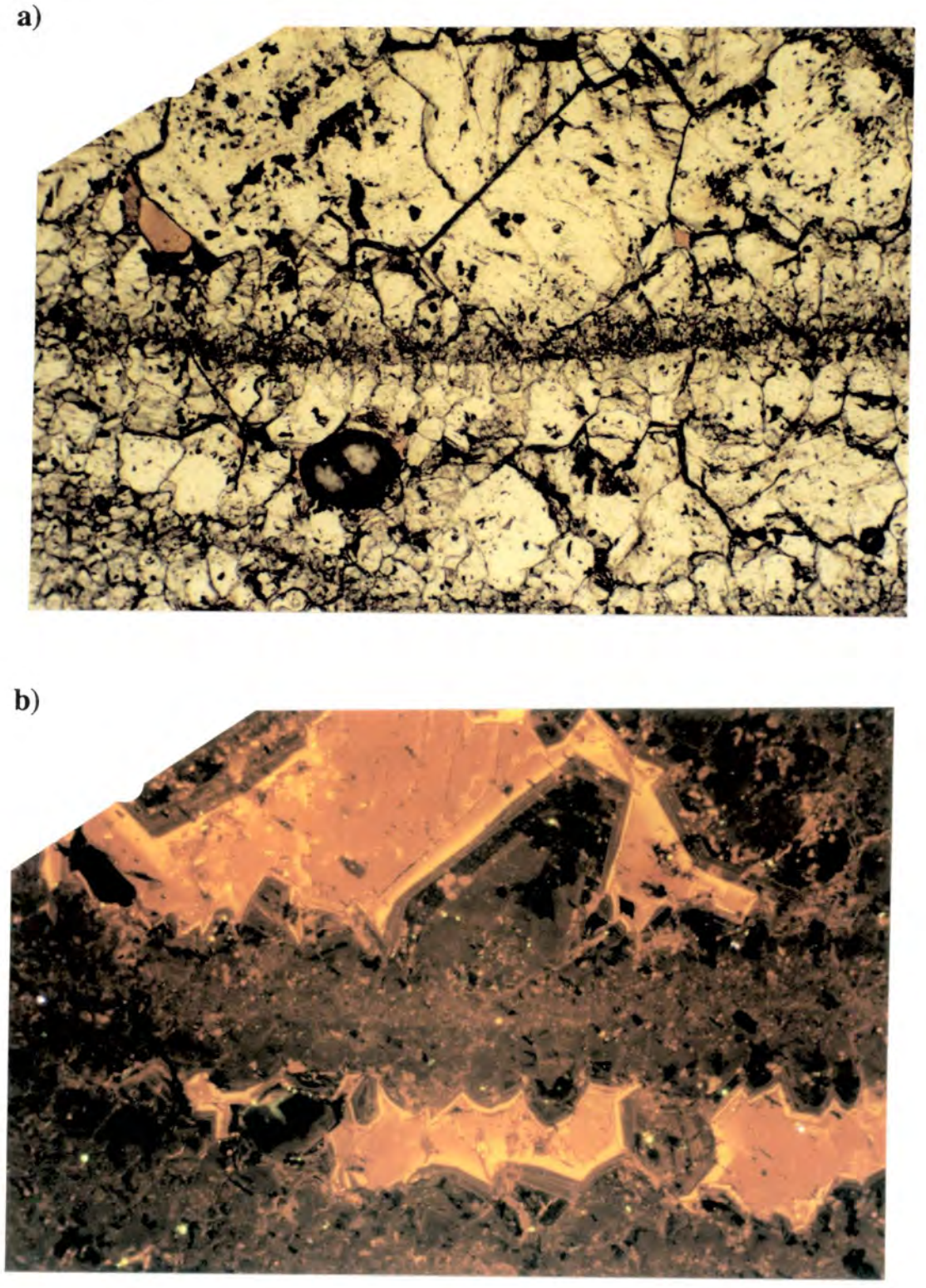


**Fig. 5.42.** Paired photomicrographs taken under normal light (a) and CL (b), showing intraskeletal cavities within a coral. Note the zoned non-luminescence to bright orange to dull orange luminescence of the majority of the pore filling cements. These zoned cements provide the second lining to the cavities after the non-luminescent stubby/bladed, isopachous marine cements. Sample FB/13B, Congost d'Erinya. Field of view 4.5mm across.

## 5.6.6 Silicification and late stage mineralisation

Similar evidence of silicification and late stage mineralisation can be found within these Congost platform-top sediments as has already been described for the Sant Corneli group of outcrops (see Figs. 5.39 & 5.43). See sections 5.5.6 & 5.5.7 for descriptions and interpretations of the evidence for these diagenetic events.

However, the late stage precipitates of baroque dolomite, quartz and flourite are much more common, and fill a much greater percentage of the pore-space, within the cavities of rudists and corals from Congost d'Erinya than within the rudist cavities from the Sant Corneli group of outcrops (see Fig. 5.43).

The distribution of these late stage precipitates appears to have been controlled by the availability of remaining pore-space, following all earlier phases of cementation. The much higher percentage volume of these late stage precipitates within cavities in the platform-top sediments exposed in Congost d'Erinya compared with those exposed in the Sant Corneli group of outcrops, therefore indicates that earlier cement generations were not as well developed in the platform-top sediments which outcrop in Congost d'Erinya than they were in the same facies sediments exposed in the group of outcrops in the region of the Santa Fe and Sant Corneli folds.

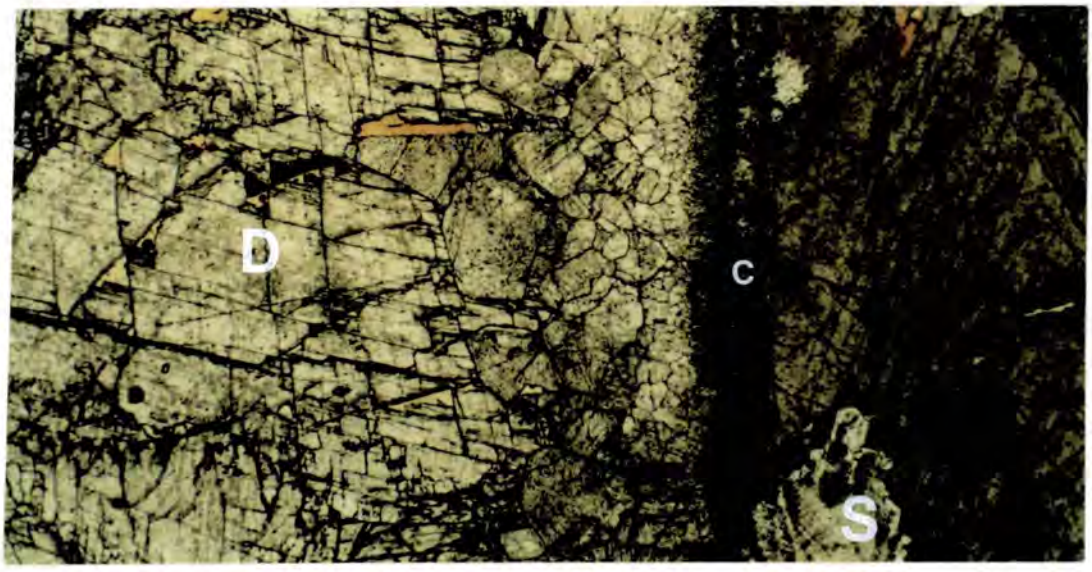


**Fig. 5.43.** Photomicrograph, showing the large area of an intraskeletal rudist cavity which has been occluded by late stage baroque dolomite (D). Note also the silicification (s) which has effected the outer calcite shell as well as the originally aragonitc internal shell layer (C). The baroque dolomite is identified by its high relief and curved crystal boundaries. Sample FB/21, Congost d'Erinya. Field of view 12 x 5mm.

## 5.6.7 The results of stable isotope analyses

### 5.6.7.1 Introduction

Where possible, during this diagenetic study of the platform-top sediments exposed in Congost d'Erinya, samples of particular interest have been analysed for their stable isotope composition. Samples for these analyses were taken from: 1) the outer low-Mg calcite layers of rudist shells; 2) areas of originally aragonitic rudist shell which have been neomorphically replaced; 3) calcite spar (both non-luminescent and zoned-luminescent) from within primary intraskeletal cavities; 4) the rectangular 'cement clasts' forming part of the infill to dissolution pipes; and 5) the calcite spar which surrounds the 'cement clasts' within the dissolution pipes. The results of these analyses are shown in Fig. 5.44. As discussed in section 5.4, the heaviest isotopic compositions of the calcite rudist shells are interpreted as a best estimate of the original composition of lagoonal carbonate against which all other isotopic compositions are compared.

### 5.6.7.2 Neomorphic spar

The samples of neomorphic spar from originally aragonitic shell areas can be seen to display a range of isotopic compositions. The heaviest values displayed by these samples, although slightly depleted in both $^{18}O$ and $^{13}C$ with respect to the best estimate of lagoonal carbonate composition, are similar to those of calcite rudist shells. The isotopically lightest sample possesses a $\delta^{18}O$ well within those predicted for precipitates from meteoric waters (see section 5.2.3.2), and shows a depletion in $^{13}C$, with respect to a best estimate of lagoonal carbonate compositon of 2.0‰ (PDB). The similarity in compositon of the isotopically lightest samples to that of calcite rudist shells suggests that some of the neomorphism may have occurred under the influence of lagoonal waters. The greater depletion in both $^{18}O$ and $^{13}C$ of the other samples, taken together with petrographic information, suggest that neomorphism occurred under the influence of organically charged meteoric waters. These interpretations of isotopic data suggest that some neomorphism of rudist aragonite may have occurred under the influence of lagoonal waters, while most probably took place under the influence of organically charged meteoric waters. This later conclusion is compatible with, and therefore substantiates, the conclusions which were derived from petrographic and cathodoluminescence studies (see section 5.6.4.2).

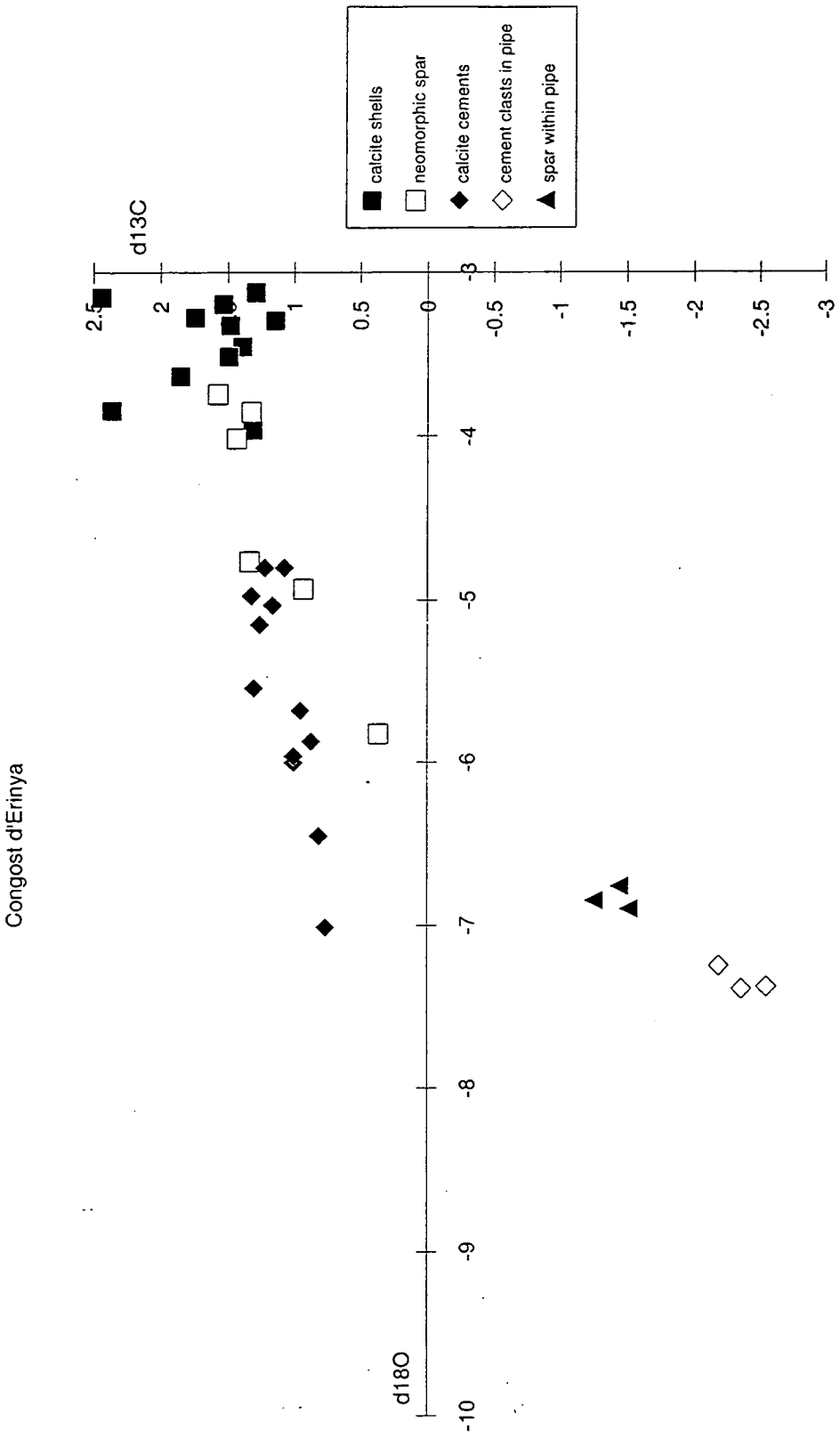


**Fig. 5.44.** Carbon and oxygen isotope cross-plot for shell, cement and neomorphic calcite samples from Congost d'Erinya.

The large variability in compositions of the neomorphic calcites should be noted, together with the fact that they are less depleted relative to the best estimate of lagoonal carbonate composition than the speleo-cements which infill the dissolution pipes. Since, like the precipitation of cements within dissolution pipes (see below and section 5.6.5.2), some of the neomorphism is interpreted to have taken place under the influence of organically charged meteoric waters, then this may be suggesting that the process of neomorphism operated as a semi-closed system.

### 5.6.7.3 Calcite spar cements within primary cavities

The calcite spar cement samples from within the primary intraskeletal cavities of rudists, also show a range of isotopic compositions. However, they show only a slight variation in their $\delta^{13}C$ compositions with the lightest being depleted by only 1.6 ‰(PDB) with respect to a best estimate of lagoonal carbonate composition. The $\delta^{18}O$ of these spar cements show a much greater variation with depletions of up to 3.8 ‰(PDB). A small number of these cement samples plot within the same compositional zone as the neomorphic spar, suggesting that some of these cements may have been precipitated within shallow environments under the influence of meteoric waters. However, the overall trend towards increasing depletion in $^{18}O$ suggests that many of these cements were precipitated under conditions of increasing temperature. This suggestion of precipitation under conditions of raised temperature is compatible with the interpretation from petrography and cathodoluminescence (see section 5.6.5.3), that many of the pore-filling cements in these platform-top sediments at Congost d'Erinya were precipitated during burial.

### 5.6.7.4 Calcite spar and 'cement clasts' from within karst pipes

The isotopic composition of both the 'cement clasts' and coarse spar from within the network of dissolution-enhanced pipes which mark the top of Congost platform sediments in Congost d'Erinya, is significantly depleted in both $^{18}O$ and $^{13}C$ with respect to all the rudist shell samples. The depletion in $^{13}C$ of between -3 and -5 ‰ (PDB), and the fact that $\delta^{18}O$ values are within the theoretical limits for calcite precipitated from meteoric waters at sedimentary temperatures (see section 5.2.3.2), together with the petrographic and outcrop features (see sections 4.4.6, 5.6.4.3 & 5.6.5.3) of these cements, strongly suggest that they precipitated from organically charged meteoric waters.

# 5.7 Summary

## 5.7.1 Introduction

The diagenetic features of the Congost platform-top sediments which are exposed in Congost d'Erinya and the Sant Corneli group of outcrops suggest that sediments from both sets of outcrops have undergone a broadly similar pattern of syn- and post-depositonal events. The broad pattern of events, interpreted to have effected these sediments has been set out in the previous sections; these events are briefly summarised below in section 5.7.2. However, there are some important differences between the diagenetic features displayed by the sediments in Congost d'Erinya and those displayed by the sediments from the Sant Corneli group of outcrops. The interpretation of these differences are discussed below in section 5.7.3.

## 5.7.2 Interpretation of the general succession of diagenetic events

The majority of these sediments are interpreted to have been deposited within a semi-protected lagoonal environment, under semi-tropical to tropical humid climatic conditions (see sections 4.2.4.3, 4.4.5, 4.4.5.4, 5.4.5 5.5.4, 5.5.5, 5.6.4 & 5.6.5). The isotopic composition of rudist shells suggests that the waters in this lagoonal environment, rather than being of typical marine composition were slightly brackish in nature (see section 5.4.5).

All the platform-top sediments have been subjected to micritisation and early marine cementation (see sections 5.5.2, 5.5.3, 5.6.2 & 5.6.3). In addition to the ubiquitous micritisation many rudists and corals show the effects of intensive boring activity. During these very early stages in their diagenetic history some of the aragonitic tabulae within rudists suffered neomorphic replacement, particularly at their edges (see sections 5.5.4.4, 5.5.4.5, 5.5.4.6 & 5.6.4.2). Some of this neomorphism appears to have taken place during the precipitation of cements from the lagoonal waters (see sections 5.5.4.6 & 5.6.7).

The next diagenetic processes to effect these sediments were extensive dissolution, neomorphism and cement precipitation, in the presence of organically charged and oxidised meteoric waters. There is evidence to suggest that these processes took place under a combination of vadose and phreatic conditions resulting from meteoric exposure under humid climatic conditions, with high rainfall causing periodic saturation (see sections 5.5.4, 5.5.5, 5.6.4, 5.6.5 & 5.6.7). Although there is no direct evidence to suggest that these features have resulted from numerous

exposure events of short duration, this is a likely scenario, bearing in mind the shallow nature of these lagoons (see sections 4.2.4.3, 4.4.5.3 & 4.4.5.4). This interpretation is also suggested by the fact that these features are observed, with the same characteristics, throughout the entire vertical succession of these platform-top sediments.

The last near surface diagenetic events to effect these sediments were the development of karst features, which mark the upper surface of Congost platform sediments at all localities and penetrate down into the platform-top strata (see sections 4.2.4.4, 4.3.3, 4.4.6, 5.5.4.7, 5.5.4.8 5.5.4.9, 5.5.4.10, 5.6.4.3). Differences exist between the karst features from the Sant Corneli group of outcrops and those in Congost d'Erinya. However, the features from both sets of outcrops are interpreted to have resulted from a process of dissolution enhanced fissuring during a prolonged period of relative sea-level fall, under humid climatic conditions. Cements within many of these pipes and cavities have been interpreted to have precipitated from oxidised, organically charged meteoric waters, which in some cases became stagnated as a result of total saturation brought about by high rainfall (see sections 5.5.4.7, 5.5.4.8, 5.5.4.10, 5.5.5.1, 5.6.5.2 & 5.6.7).

Diagenesis continued during shallow burial, with the precipitation of zoned-luminescent calcite spar within any remaining pore-space (see sections 5.5.5.2, 5.5.5.3, 5.6.5.3 & 5.6.7). The earliest zones of these cements are interpreted to have been precipitated in a shallow phreatic environment, which at first was subjected to sporadic recharge by fresh meteoric waters. The final cement zones were precipitated from wholly reducing pore-fluids, suggesting greater burial depths and possessed isotopic signatures suggesting increasing temperatures of precipitation. Some of the pipes and cavities, which developed during the period of karstification were not completely occluded by speleo-cements and appear to have provided conduits for these later burial fluids, resulting in some destruction and alteration of the cements within them (see section 5.5.4.9 & 5.5.4.10).

## 5.7.3 Significant diagenetic variations

The differences in diagenetic features between the platform-top sediments exposed in Congost d'Erinya and the same facies sediments exposed at the outcrops in the region of the Sant Corneli anticline and Santa Fe syncline have been discussed in previous sections. The aim of this short section is to briefly summarise these differences and provide some possible reasons for them.

The differences in marine cementation, namely the lack of any botryoidal type cements within the internal cavities of rudists from Congost d'Erinya, have been interpreted to suggest that there may have been slight differences in the pore-fluid flow regimes between the lagoonal environments represented by the two groups of outcrops (section 5.6.3).

When compared with the sediments from Congost d'Erinya, a much higher percentage of the pore-space (primary and secondary) within the sediments from the Sant Corneli group of outcrops has been occluded by cements interpreted to have precipitated from organically charged meteoric waters, under both vadose and shallow phreatic conditions (see sections 5.5.5 & 5.6.5.3). Taken together with the fact that rudist shells from the lagoonal sediments of the Sant Corneli group of outcrops appear to have suffered a higher degree of meteoric alteration than those from Congost d'Erinya (see section 5.4.4), this suggests that the sediments which are now exposed in the Sant Corneli group of outcrops were exposed to near surface meteoric fluids more frequently and for much longer periods of time than their counterparts which are now outcropping in Congost d'Erinya.

Conclusions drawn from geometrical and sedimentological features (see section 4.6), suggested that the Congost platform-top sediments from the Sant Corneli group of outcrops were deposited against a background of small-scale relative sea-level fluctuations which were superimposed on a background of little overall increase in accommodation space. By way of contrast, the platform-top sediments which outcrop in Congost d'Erinya, although also interpreted to have been effected by small-scale relative sea-level fluctuations were deposited against an overall background of increasing accommodation space. The interpretation that the sediments exposed in the Sant Corneli group of outcrops have been subjected to longer and perhaps more frequent periods of subaerial exposure than those outcropping in Congost d'Erinya is compatible with such conclusions. Such differing backgrounds of accommodation space change could also be deemed responsible for the slightly differing pore-fluid flow regimes, which are interpreted as responsible for the differences in marine cements between the platform-top sediments of these different groups of outcrop.

The well-developed karst features which penetrate down from the top of these sediments at all outcrops probably display the most striking differences. The Karstification which effected the sediments now outcropping in the region of the Sant Corneli and Santa Fe folds penetrated to a depth of up to 34 metres below their upper surface in places (see sections 4.2.4.4, 4.3.3, 5.5.4.7, 5.5.4.8, 5.5.4.9 & 5.5.4.10). The karst features present at the top of the outcrop in Congost d'Erinya (see sections 4.4.6, 5.6.4.3, 5.6.5.2 & 5.6.7) on the other hand, only penetrate down into the top few metres of platform-top sediments.

This marked difference in the depth of penetration of karst can be interpreted in two different ways:

One possibility is that the outcrops in the region of the Sant Corneli and Santa Fe folds, together with the outcrop in Congost d'Erinya represent different parts of the same platform, with the same diagenetic history; however, the marked difference in the depth of karst penetration has resulted from a variation in the depth to the ground water-table. Although, in a diffuse system where there is a relatively homogeneous pore network, the water table would be expected to be a subdued representation of the topographic relief. In fact the water table within modern carbonate platforms and shelf settings is generally very flat (Tucker & Wright, 1990).

Another possibile cause of these differences in the depth of karst penetration is that they result from the fall in relative sea-level, which caused the karstification, having had different relative magnitudes when compared to the different areas of platform-top represented by the two different groups of outcrop (see Fig. 5.45).

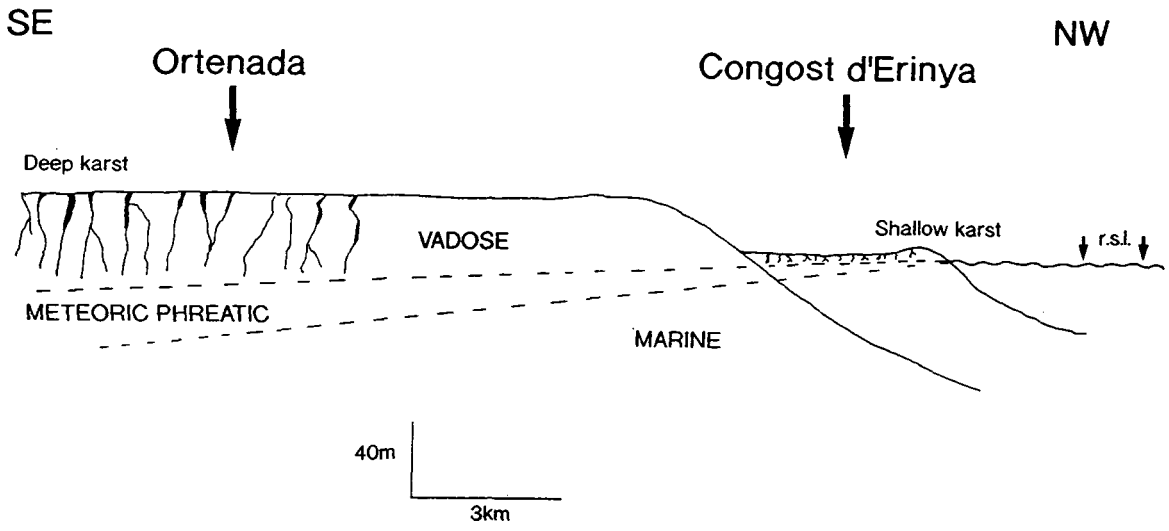


**Fig. 5.45.** Model to explain the differences in the depth of karst penetration between Ortenada and Congost d'Erinya. It is proposed that the outcrop in Congost d'Erinya represents a second phase of platform growth, which developed basinward and down slope of an earlier platform growth phase, as a result of a fall in relative sea-level. Continued relative sea-level fall caused karst development in the upper few metres of the sediments now exposed in Congost d'Erinya. Prolonged exposure and greater depth to the ground water zone within the sediments of the earlier progradational platform phase led to extensive and more deeply penetrating karst.

This second interpretation is compatible with the hypothesis in section 4.6, following an interpretation of geometrical and sedimentological features, which proposed that the outcrop in Congost d'Erinya represented a second phase in the development of the Congost platform which occurred during a period of forced regression. If as is suggested by this hypothesis, the outcrop in Congost d'Erinya does indeed represent some kind of forced regressive wedge which developed down the slope of the earlier phase of platform development; then, deeper karst penetration within the carbonates of earlier platform phase, represented by the outcrops in the region of the Sant Corneli and Santa Fe folds, would be expected as a result of: 1) A relatively longer period of subaerial exposure; and 2) their relatively higher topographic height. This hypothesis is explored further in chapter 7 where the Congost platform is considered within a sequence stratigraphic framework.

# Chapter 6
# The slope sediments at Sopiera

## 6.1 Introduction

Sopiera is a small village situated approximately 11km to the south of El Pont de Suert on the N.230. Exposed along the roadside and in the steep mountain slopes around Sopiera there is a complete stratigraphic section through over 1200 metres of Cenomanian to Santonian aged basinal and slope facies sediments. The area of the outcrop around Sopiera which contains Cenomanian aged slope facies sediments (slope facies of the Santa Fe platform) is shown as locality 6 on Fig. 3.1, whereas those of Coniacian age (deep slope equivalent of the Congost platform) is shown as locality 6 in Fig. 4.1.

Figure 6.1 shows a simplified geological map of the area around Sopiera, in which the Cenomanian to Santonian sediments have been divided into the lithological units that are described in the following sections. This map has been modified from fig. 9B in Simo (1992) and represents a sketch made from an aerial photograph, parts of which can be seen in Fig. 6.3. Following detailed biostratigraphic work by Esmeralda Caus, together with isotope geochemistry by Kate Soriano (Caus et al., 1993), it has been possible to correlate the basinal and slope facies sediments at Sopiera with corresponding platform facies sediments which are exposed farther to the south and east (see Fig. 3.9).

## 6.2 The Sopiera Marls

### 6.2.1 Brief description

The Sopiera Marls outcrop around and to the north of Sopiera and have a vertical thickness of approximately 350 metres (see Figs. 6.1 & 6.2). Caus et al (1993) provided a detailed description of a vertical section through the Sopiera Marls, with particular regard for their faunal content, and have divided them into 3 units:

The lowest unit comprises 130 metres of marls alternating with nodular limestone beds, which contain abundant benthic and planktonic foraminifera and show a marked upward decrease in grain size and skeletal fragment content. The

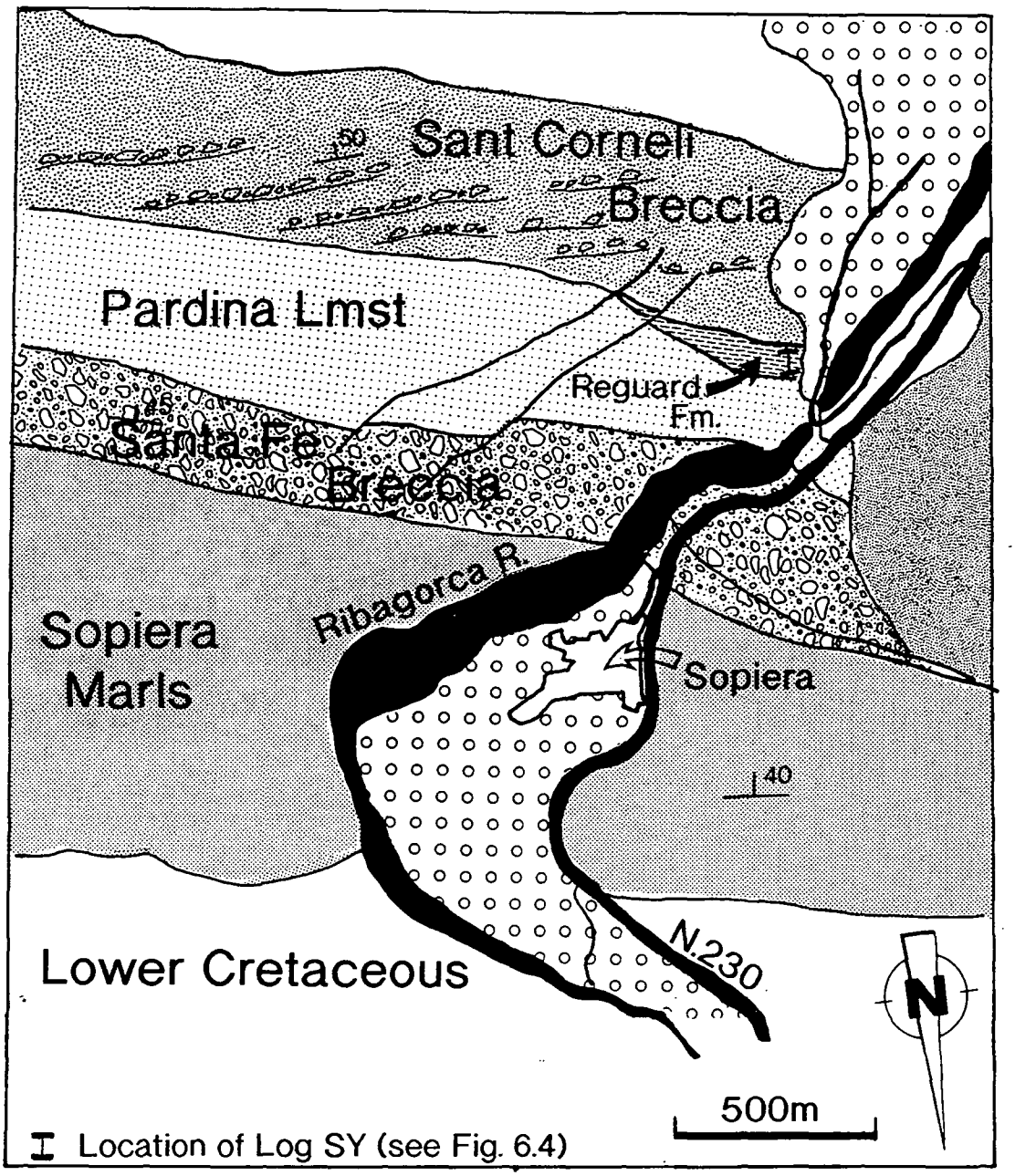


**Fig. 6.1.** Geological sketch map showing the major lithological units within the succession of Upper Cretaceous slope and basinal sediments which are exposed around the village of Sopiera. This sketch map has been modified from fig. 9B in Simo (1992) and represents a sketch made from an aerial photograph, parts of which can be seen in Figs. 6.3 & 6.9.

planktonic foraminiferal assemblages indicate a Lower Cenomanian age for this unit (Caus et al., 1993).

The middle unit is approximately 70 metres thick and consists of massive bioturbated marls with minor limestone beds rich in glauconite. Benthic foraminifera are rare in this middle unit, with the dominant grain types being calcispheres and diverse planktonic foraminifera. The planktonic foraminiferal assemblages indicate a Lower Cenomanian age for this unit (Caus et al., 1993), as do the ammonites (Martinez, 1982)

The upper unit is characterised by bedded limestones with occasional marly intervals which decrease in abundance up section. Calcispheres are abundant while planktonic foraminifera are rare. Benthic foraminifera, although scarce, show a marked increase in abundance up section. Both the ammonite and planktonic foraminiferal assemblages within this upper unit indicate a Middle Cenomanian age.

### 6.2.2 Brief interpretation

The Sopiera Marls are interpreted to represent a basinal facies which was accumulating during the development of the lower part of the Santa Fe platform (see Fig. 3.9). The decreasing skeletal debris content and increasing relative abundance of planktonic foraminifera up section through the lower and middle units, are interpreted to suggest that during the lower Cenomanian, conditions within the basin were becoming progressively deeper. The Middle Cenomanian-aged upper unit, on the other hand, with its increasing abundance of benthic foraminifera and decreasing marl content, is interpreted to represent a shallowing upward basinal succession (Caus et al., 1993).

## 6.3 The Santa Fe Breccia

### 6.3.1 Introduction

The Santa Fe Breccia forms a steep-sided ridge immediately to the south of Sopiera (see Figs. 6.1, 6.2 & 6.3) and represents the second lithological unit in this basinal succession. Ammonite and planktonic foraminiferal assemblages within the matrix of the Santa Fe Breccia indicate that they are of Upper Cenomanian age (Caus et al., 1993) and hence they can be interpreted as representing the basinal equivalent

of the upper part of the Cenomanian Santa Fe platform (see Fig. 3.9)(Mey et al., 1968; Simo & Puigdefabregas, 1985; Simo, 1986; Simo, 1989; Caus et al., 1993).

**Fig. 6.2.** View looking southeast from Sopiera. The steep cliff face which can be seen towards the right of the photograph is approximately 150 metres high. The thinly bedded easily weathered strata which can be seen outcropping below the scree slopes at the base of this cliff are the Sopiera Marls, while the main part of the cliff is composed of the Santa Fe Breccia, within which some of the larger blocks of Santa Fe platform margin material can be seen (arrowed). Note also the slightly chaotic bedding which can be seen in the central part of the cliff. The prominent cliff in the background on the left side of the photograph is the western edge of the Sierra de Sant Gervas and is composed of the in situ Santa Fe platform margin succession, which is separated from the Santa Fe Breccia by a thrust fault.

## 6.3.2 Lithology

The Santa Fe Breccia is so named because of the large quantity of irregular shaped blocks and numerous conglomeratic beds within it. Caus et al. (1993) divided the Santa Fe Breccia into three units. They described the lower two units as coarsening upward cycles and the upper one as a fining-upward cycle which grades upwards into the block-free Pardina Limestone.

The lower sections of each of these units are dominated by pelagic mudstones with channellised grainstones and conglomerates within which convoluted bedding is common, whereas the upper sections are even more chaotic and consist of

a matrix-supported megabreccia. The blocks within the breccias are very variable in size, with some of the largest having diameters in excess of 10 metres. Some of the larger blocks can be seen in Fig. 6.2 which shows an almost complete section through the Santa Fe Breccia as it outcrops in the steep-sided ridge to the south of Sopiera.

The blocks within these chaotic beds consist of a variety of lithologies, which include cemented skeletal grainstones, closely-packed rudist communities, coral boundstones and packstones with large rudist and coral fragments. All of these lithologies are typical of those found within the Santa Fe platform margin succession which is exposed along the Sierra de Sant Gervas (see sections 3.6, 3.7.2.2, 3.7.3 & 3.8). A Cenomanian age is confirmed for many of these blocks by the presence of the easily identifiable benthic foraminifera *Prealveolina,* which is very abundant within the platform facies of the Santa Fe Limestone (see sections, 3.2.2, 3.3.2, 3.4.2, 3.5.2 & 3.6.2 together with Figs. 3.5, 3.8a & 3.8b). Other common block lithologies include wackestones with calcispheres and fine-grained skeletal debris, similar to that which is found within the lower part of the coarsening-upward units and within the matrix which surrounds the blocks. Importantly none of the blocks within the Santa Fe Breccia which have been observed either during this study or those of other workers (Simo pers. com.; Drzewiecki pers. com.) show any evidence to suggest that they have suffered subaerial exposure prior to their deposition within these megabreccia units.

The matrix which surrounds and supports the blocks within these breccias consists mainly of wackestones and packstones together with smaller angular clasts of similar composition to the boulders. The wackestones and packstones contain calcispheres and rare planktonic foraminifera together with benthic foraminifera and an abundance of skeletal debris seemingly derived from the platform top.

The fining-upward unit towards the top of the Santa Fe Breccia contains grainstones, conglomerates and mudstones, which show some evidence of slumping but do not contain any of the large boulders. This unit passes vertically upward into the calcisphere and planktonic foraminifera-rich wackestones and packstones of the Pardina Limestone. The actual boundary between the two formations is difficult to define; however, stable isotope studies have revealed a 1 $^{o}/_{oo}$ enrichment in $^{13}C$ approximately 45-50 metres vertically up section from the last obviously conglomeratic bed. This isotopic anomaly can be correlated with that at the base of the Pardina Limestone in the inner platform (see Fig. 3.9 together with sections 3.2.4, 3.4.2, 3.7.3 & 3.8) (Soriano, 1992; Caus et al., 1993)

## 6.3.3 Geometrical relationships

Differences in the depositional dip between the Santa Fe Breccia and the underlying Sopiera Marls led Simo to interpret the lower boundary of the Santa Fe Breccia as a downlap surface (Simo & Puigdefabregas, 1985; Simo, 1986). Figure 6.3 shows an aerial photograph which as a result of the steep southerly tectonic dip in this area is an approximate representation of a vertical cross section through the succession. In this aerial photograph the downlap at the base of the Santa Fe Breccia can be clearly seen.


**Fig. 6.3.** Aerial photograph covering an area of approximately 1 x 0.5km in which the upper part of the Sopiera Marls (M), the Santa Fe Breccia (s) and the Pardina Limestone (p) can be seen (compare with Fig. 6.1). The village of Sopiera can be seen in the centre bottom of this photograph. Due to the steep tectonic dip of the strata this aerial photograph can be used as an approximate vertical cross-section through the succession. Note the difference in angle of dip between the Santa Fe Breccias (arrow) and the Sopiera Marls (dashed) which can be observed to the west of Sopiera and is interpreted to represent a downlap surface (after Simo & Puigdefabregas, 1985).

In the steep slopes to the south of Sopiera the Santa Fe breccias have a vertical thickness of approximately 150 metres (see Fig. 6.2); however, when they are traced eastwards towards the western edge of the Sierra de Sant Gervas a gradual decrease in thickness is observed, suggesting that this unit has an overall wedge-shaped geometry.

The prominent cliffs at the western end of the Sierra de Sant Gervas comprise a 150 metre thick succession through the coral and rudist rich bedded boundstones, grainstones and floatstones of the Santa Fe platform margin (see Figs.

3.8a, 3.8b & 6.2 together with sections 3.6, 3.7.2.2, 3.7.3 & 3.8). Unfortunately the Santa Fe Breccia cannot be traced laterally into the platform margin facies as the two are separated by a thrust fault which runs all the way along the southern margin of the Sierra de Sant Gervas. However, the amount of relative movement across the thrust is interpreted to have been slight (Simo pers. com.).

The overall geometry of the Santa Fe Breccia unit is interpreted to be that of a wedge shaped apron (after Mullins & Cook, 1986), which developed basinward of the Santa Fe platform margin and possessed an internal stratification which was dipping more steeply than the underlying basinal sediments to produce a downlap relationship along its base.

### 6.3.4 Further discussion and interpretation

The Santa Fe Breccia is interpreted as a platform talus facies which developed basinward of the Santa Fe platform margin, with the blocks and boulders having been derived through a process of platform margin collapse and submarine sliding. The basinward thickening geometry displayed by this prograding unit of platform talus (see section 6.3.3) suggests that prior to its deposition the pre-existing basin morphology included a significant slope. The presence of blocks consisting of slope facies wackestone within these breccia beds (see section 6.3.2) indicates that resedimentation of previously cemented slope sediments also took place during what must have been fairly catastrophic events of platform margin and slope failure. The matrix supported nature of the chaotic block rich units (see section 6.3.2) suggests that following collapse of the platform margin, large areas of unconsolidated upper slope sediment were also mobilised to create a debris flow in which the large blocks of both platform and consolidated slope sediments were transported down slope. Similar ancient carbonate debris flow beds, have been referred to as megabreccias (Cook et al., 1972; Mountjoy et al., 1972). The large blocks within such sheet like debris flows would have been supported by matrix strength and buoyancy, allowing them to travel large distances.

One possible mechanism which could have caused so much material to be shed from the platform margin in this way is seismic activity. Such seismic activity could have resulted from reactivation of the faults which developed during Albian rifting and now lie below the Upper Cretaceous succession. Seismic activity has been cited as the driving force behind many modern and ancient megabreccia deposits (eg. Labaume et al., 1987; Hine & Hallock, 1991; Mullins et al., 1991) Simo has suggested that the Santa Fe platform margin may have developed at the site of a

former fault scarp which he cited as the reason for the pronounced slope interpreted to have been present basinward of this very active platform margin (Simo & Puigdefabregas, 1985; Simo, 1986; Simo, 1989; Simo, 1992; Caus et al., 1993).

Another possible mechanism for this apparent massive platform margin collapse and slope failure is differential compaction. Differential compaction has been discussed previously, as a possible cause of the increased accommodation space at the platform margin which led to the much greater thickness of the platform margin succession compared with the lagoonal succession that accumulated farther to the south (see section 3.7.2.2). Apart from the possibility of differential compaction causing instability as a result of tilting, the increased accommodation space which compaction would create could have led to excessive aggradation and rapid deposition and hence an over-steepening of the platform margin which could eventually have led to instability and shedding events. As mentioned in section 3.7.2.2, the interpretation that this shedding may have been at least been partly driven by a process of differential compaction does not preclude the pre-existing fault scarp theory of Simo and Puigdefabregas (1985) and Simo (1986 & 1989) as such a mechanism requires the presence of a pre-existing basin morphology with a basinward dipping slope.

The presence of platform-derived skeletal debris within the packstones and wackestones which surround and support the blocks of cemented platform margin material suggests that the platform shedding events took place while the platform top was submerged (Caus et al., 1993). The fact that none of the re-sedimented blocks, which have been observed, show any evidence of subaerial exposure also suggests that they were shed from the platform margin prior to any exposure event. This is slightly surprising in view of the obvious Karst features present within the in-~~place~~ situ Santa Fe platform-margin sediments, which can be seen in the outcrop along the Sierra de Sant Gervas and are interpreted to be the result of a late Cenomanian exposure event which occurred prior to the deposition of the Pardina Limestone (see sections 3.6.2, 3.7.3 & 3.8). The presence of these karstic features within the platform margin succession at Sant Gervas, but not within the allochthonous blocks of platform material within the Santa Fe Breccia indicates that all the platform shedding which produced the Santa Fe Breccia took place prior to the exposure event in the Upper Cenomanian.

The hypothesis that platform shedding may have been driven by a mechanism of differential compaction and over-steepening of the platform margin is compatible with the suggestion that none of the re-sedimented blocks had suffered subaerial exposure prior to them having been shed from the platform. The increasing accommodation space which would be expected at the platform margin as a result of

differential compaction could have prevented any significant subaerial exposure. By way of contrast, a mechanism of fault reactivation could well have been expected to have caused some subaerial exposure of the platform margin through footwall uplift; this is especially as the Santa Fe platform is interpreted to have developed upon the up-thrown block of a former normal fault (Simo & Puigdefabregas, 1985; Simo, 1985; Simo, 1989) and the tectonic regime during the Cenomanian is thought to have been extensional (Puigdefabregas & Souquet, 1986).

## 6.4 The Pardina Limestone

### 6.4.1 Introduction

The Pardina Limestone outcrops to the south of Sopiera in the road cuttings and slopes around the dam which crosses the Ribagorca River and can be traced along the southern slopes of the prominent ridge to the south of Sopiera (see Figs. 6.1 & 6.3). In this basinal setting the Pardina Limestone has a vertical thickness of approximately 90 metres. The aerial extent of outcrop of the Pardina Limestone, as shown by Fig. 6.1, is slightly confusing, as at first glance it suggests that the Pardina Limestone has a greater vertical thickness than the underlying Santa Fe Breccia. However, as can be seen in Fig. 6.3 this apparent thickness is an exaggerated one as a result of the topographic slope on the southern side of the ridge to the south of Sopiera which dips steeply to the south at a similar angle to that of the southerly tectonic dip displayed by the sediments.

As mentioned previously in section 6.3.2, the base of the Pardina Limestone unit is difficult to define, as it is a transitional boundary, with conglomerate beds and skeletal debris becoming gradually less common towards the top of the underlying Santa Fe Breccia unit. However the isotopic anomaly (1 $^{o}/_{oo}$ enrichment in $^{13}C$) which occurs 45-50 metres vertically up section from the last obviously conglomeratic bed can be correlated with that which occurs at the base of the Pardina Limestone in the inner platform (see Fig. 3.9 together with sections 3.2.4, 3.4.2, 3.7.3 & 3.8) (Soriano, 1992; Caus et al., 1993)

### 6.4.2 Lithology

The lithology of the Pardina Limestone in this basinal section is very similar to that which is observed in the more landward outcrops (see sections 3.2.3, 3.3.3,

3.4.2, 3.5.2 & 3.6.2 together with Figs. 3.6a & 3.6b). The entire 90 metres or so of this unit consists of fine-grained calcisphere-rich packstones and wackestones with planktonic foraminifera.

Planktonic foraminiferal assemblages indicate that within this basinal succession the lower part of the Pardina belongs to the upper part of the *Rotalipora cushmani Zone* (Upper Cenomanian). The middle part, which displays the isotopic anomaly, was deposited during the *W. archaeocretacea zone* (Late Cenomanian - Early Turonian), although some key fauna are absent. The upper part belongs to the *H. helvetica* and *M. sigali* zones (Middle Turonian) (Caus et al., 1993).

### 6.4.3 Interpretation

As already discussed in sections 3.7.3, 3.7.4 & 3.8, the Pardina Limestone is interpreted to represent a deeper water facies which was deposited over the whole of the Santa Fe platform area as a result of a rise in relative sea-level (see Fig. 3.9). The positive δ13C isotope anomaly, which can be traced across the platform, is interpreted to indicate an increase in the preserved organic matter within the sediment, that resulted from a world-wide oceanic event which triggered a eutrophication event upon the Santa Fe platform top (see sections 3.7.3 & 3.8). The fact that certain key fauna appear to be missing from the planktonic foraminiferal assemblage in the sediments which display the isotopic anomaly may be a reflection of the proposed changes in oceanic conditions (Caus et al., 1993)

## 6.5 The Reguard Formation.

### 6.5.1 Introduction

There is no obvious lithological boundary to mark the top of the Pardina Limestone. However, detailed biostratigraphic work carried out by Esmeralda Caus (Universitat Autonoma de Barcelona) has shown planktonic foraminiferal assemblages belonging to the *Marginotruncana schneengasi* zone (Upper-Turonian to Early-Coniacian), to be present within a wedge-shaped unit of deep-water calcisphere-rich wackestones and channellised conglomerates which occur stratigraphically above the calcisphere-rich wackestones of the upper Pardina Limestone belonging to the *M. sigali* biozone (Mid-Turonian). The *Marginotruncana schneengasi* Zone is in fact the same biozone as that of the planktonic foraminiferal

assemblage within the Reguard Formation which lies stratigraphically above the Pardina Limestone in the outcrops further to the south and east (see sections 4.2.2, 4.4.4.1, 4.5.4 & 4.6). This together with the remarkably similar characteristics of this unit to those of the basal part of the Reguard Formation as it is exposed at Peracals (see section 6.5.3) are interpreted to indicate that this unit represents a small wedge-shaped package of the Reguard Formation.

The location of this wedge-shaped package of the Reguard Formation is shown in Fig. 6.1.

## 6.5.2 Field observations and petrography

### 6.5.2.1 Introduction

As described above, the lower boundary of this basinal wedge of the Reguard Formation is defined biostratigraphically but is difficult to pin-point in the field, as there are no obvious lithological differences between the calcisphere-rich wackestones at the base of the Reguard Formation and those in the upper part of the Pardina Limestone. The upper boundary of this unit is much better defined in the field as the fine-grained wackestones and packstones at the base of the overlying Sant Corneli Breccia unit possess a distinctive brown colouration and contain a small amount of silt-grade quartz (see section 6.6.2 together with Fig. 6.11), which contrast with the mostly grey-coloured and quartz-free wackestones within the Reguard Formation. At the western edge of the outcrop this wedge of the Reguard Formation has a vertical thickness of approximately 35 metres.

The stratigraphic log in Fig. 6.4 shows a section through the central part of this unit. The main lithology within this unit is heavily bioturbated wackestone containing abundant calcispheres together with planktonic foraminifera, sponge spicules, glauconite and small amounts of very fine grained skeletal debris (see Fig. 6.5). Other lithologies are present but only as allochthonous clasts within channellised conglomerates (see Figs. 6.6a, 6.6b & 6.6c)

### 6.5.2.2 Chaotic units separated by well-cemented beds

The convoluted bedding and numerous stratal truncations within this package of the Reguard Formation give it a very chaotic appearance. However, as can be seen in Fig. 6.4, it is possible to divide the measured stratigraphic section through this package of the Reguard Formation into several units of between 4 and 8 metres in

thickness which are capped by well-cemented beds that are resistant to erosion. These well-cemented beds are typically brown in colour and have abundant iron-oxide nodules and feeding traces on their upper surfaces (see Fig. 6.7). Unfortunately, exposure is poor and it is not possible to trace these well cemented horizons laterally for any great distance; however; the similarity in the internal characteristics between the units which these horizons define suggests that such a division of the succession is an acceptable one (see below).

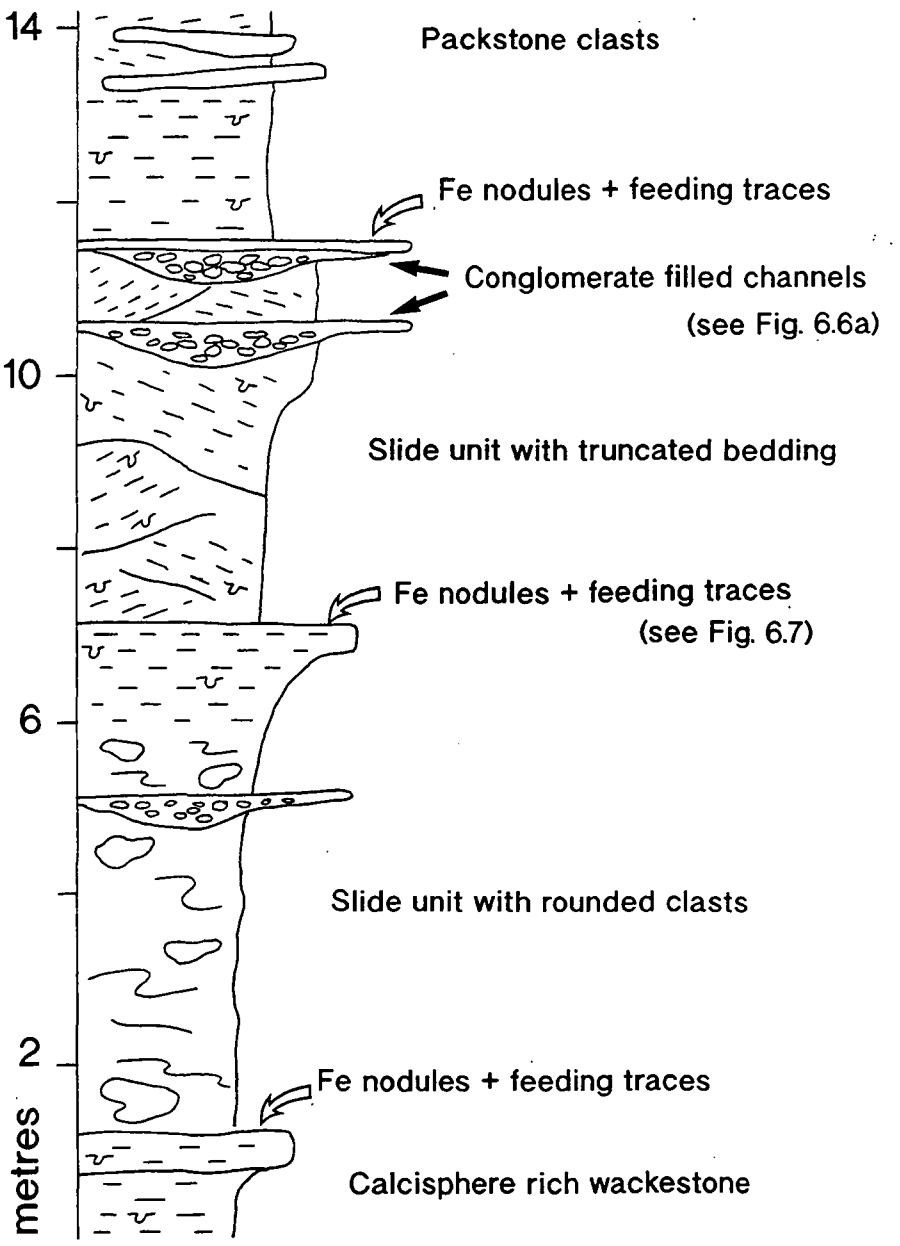


**Fig. 6.4.** Stratigraphic log SY, showing the central part of the Reguard Formation to the south of Sopiera. The location of this log is marked on Fig. 6.1.

**Fig. 6.5.** Photomicrograph showing some of the calcisphere rich wackestone which constitutes the main lithology within the slide units of the Reguard Formation at Sopiera. Sample SY/1, Reguard Formation, Sopiera. Field of view 3 x 2mm.

The main part of these units is somewhat chaotic and commonly displays either convoluted bedding together with rounded and locally folded clasts (eg. between 7 & 10m. in Fig. 6.4), or consists of metre-scale blocks of bedded wackestone which are arranged at varying angles to each other (eg. between 1 & 3m. in Fig. 6.4). The clasts which occur within the chaotic lower sections of these units consisting as they do of either fine-grained wackestone or packstone with abundant calcispheres, sponge spicules and planktonic foraminifera together with small amounts of shell debris and glauconite have the same lithology as the matrix which surrounds them. Most of the units possess a relatively thin upper section (1-2 metres) consisting of parallel and planar bedded, fine-grained wackestone containing abundant calcispheres, a small amount of echinoderm and other shell fragments together with trace amounts of glauconite.

#### 6.5.2.3 Channellised conglomerates

Towards the top of the chaotic lower sections of these units channel-shaped features are common (see Fig. 6.6a). These range in size from 2 to 5 metres in width and from approximately 0.5 to 2 metres in depth. They are well cemented and form prominent features against the easily eroded poorly cemented wackestones which surround them. The bases of these channel-shaped features cut down into and truncate laminae within the sediments of the slump units.

**Fig. 6.6a.** Photograph showing one of the channellised conglomerates within the Reguard Formation at Sopiera (see Fig. 6.4). Note the well-cemented nature of the channel compared to the easily-weathered, fine-grained wackestones which surround it. Note also the thin, clast-free layer at the top of the channel. 40cm long hammer for scale.

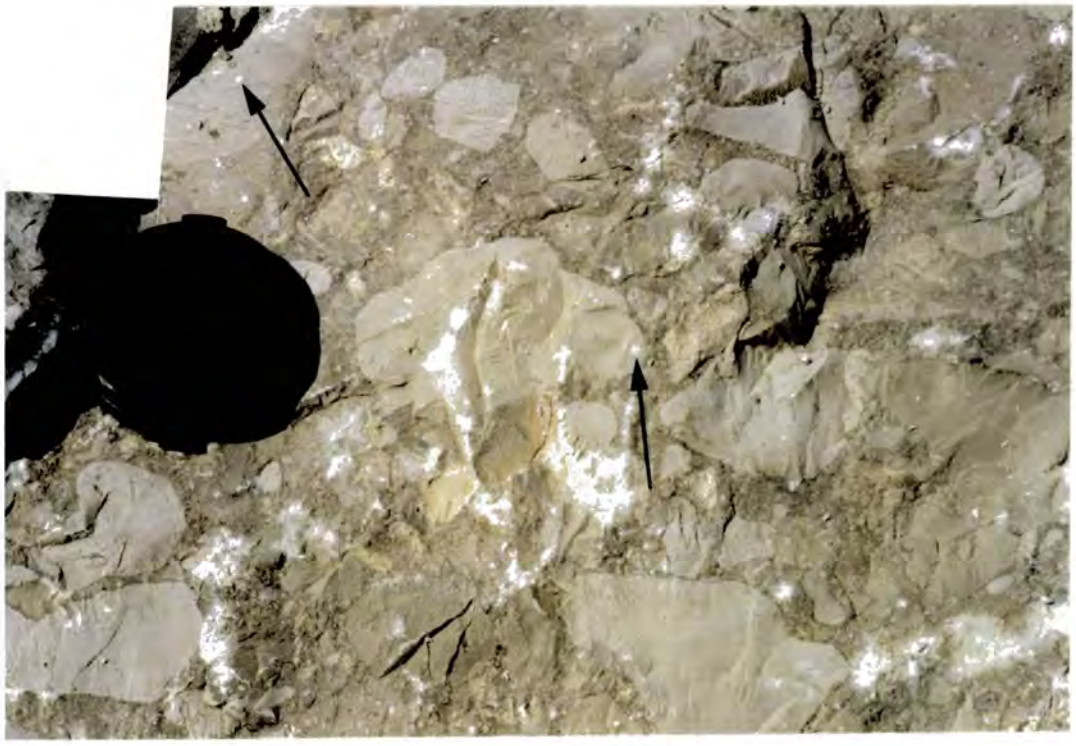

**Fig. 6.6b.** Close up of the channel which is shown in Fig. 6.6a. Note the subrounded nature and large variety of the clasts. Some of the clasts contain the benthic foraminifera *Prealveolina* (small white circles, arrowed). The slight green colouration of the matrix is due to the presence of glauconite. Reguard Formation, Sopiera. Lens cap for scale.

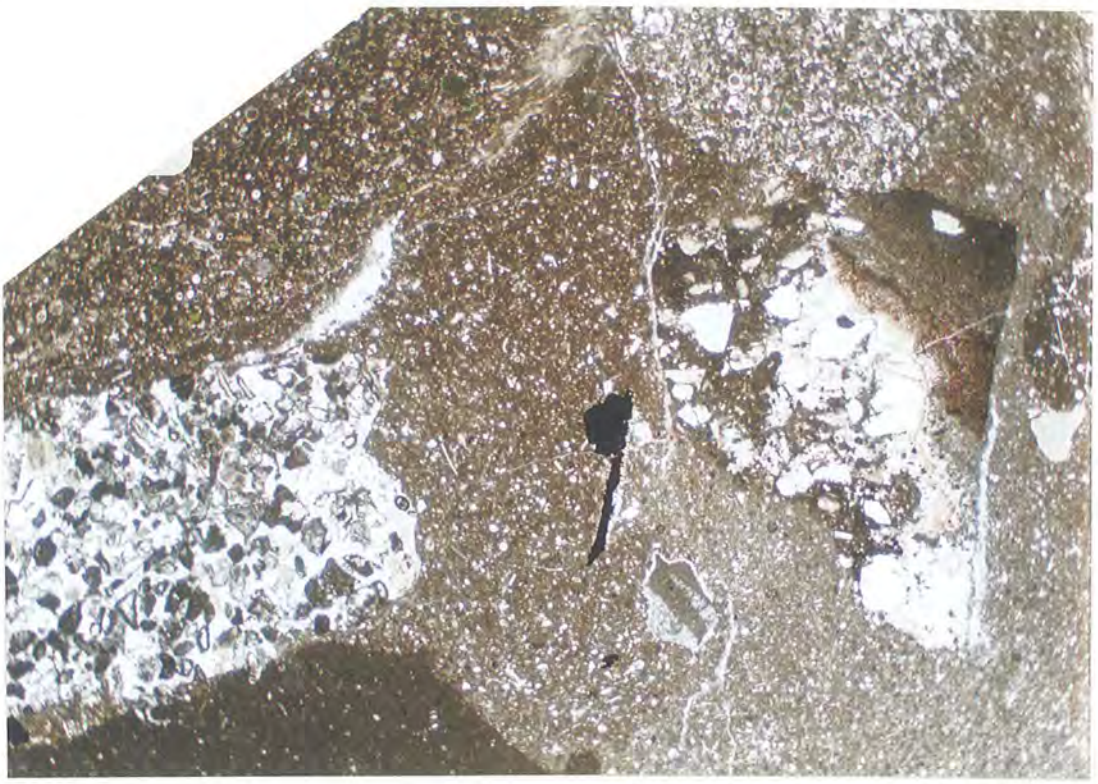

**Fig. 6.6c.** Photomicrograph showing a sample taken from one of the channellised conglomerates within the Reguard Formation at Sopiera. Note the subangular packstone clast towards the left of this photomicrograph which contains a dissolution cavity that has been filled with a fine grained slightly red coloured sediment. This clast together with the skeletal fragment rich grainstone are similar in character to in-situ carbonates of the Santa Fe platform margin in the outcrop along the Sierra de Sant Gervas (see section 3.6.2 together with Figs. 3.8a & 3.8b). Note also the clast of calcisphere rich wackestone with glauconite at the bottom right of this photomicrograph, which has very similar petrographic characteristics to the wackestone which is found at the base of the Reguard formation in many of the outcrops visited during this study (see sections 4.2.2.1 & 4.4.4.1 together with Figs. 4.3b(i) & 4.20c). Sample SY/2, Reguard Formation, Sopiera. Field of view 12 x 7mm.

The main part of these channels are filled by a sub-angular, poorly-sorted, clast-supported conglomerate, which contains a variety of small sub-angular limestone clasts (2mm-10cm diameter) surrounded by a matrix of fine grained calcisphere-rich wackestone with glauconite (see Figs. 6.6a, 6.6b & 6.6c). The clast supported conglomerates which infill the main part of the channels do not display any visible grainsize sorting; however, marking the top of all the channels there is a thin (15 cm or less) clast free layer (see Fig. 6.6a).


**Fig. 6.7.** Photograph showing the upper surface of one of the well-cemented beds within the Reguard Formation at Sopiera. Note the abundant feeding traces (f) and nodules of iron oxide (arrowed). The location of this photograph is shown on Fig. 6.4. Pen for scale.

In units which are entirely chaotic it is usual for the upper surface of a channel to correspond with the upper boundary of the unit and possess abundant iron-nodules and feeding traces.

In addition to being of a variety of sizes, the clasts within the channellised conglomerates are composed of many different lithologies (see Figs. 6.6b & 6.6c). Common clast lithologies include the following: 1) fine-grained wackestone with abundant calcispheres and glauconite together with planktonic foraminifera, echinoderm fragments and other fine-grained skeletal debris (see Fig. 6.6c); 2) fine grained packstone with abundant calcispheres, skeletal fragments, planktonic foraminifera and trace amounts of glauconite (some of these calcisphere-rich packstone clasts possess a distinctive red colouration); 3) medium-grained grainstone with peloids and sub-rounded skeletal fragments including those of echinoderms, rudists and other molluscs (see Fig. 6.6c); 4) coarse-grained, poorly-sorted packstone with angular rudist debris, peloids, other skeletal debris and benthic foraminifera including *Prealveolina*; importantly some of these clasts display cement and sediment filled dissolution cavities (see Fig. 6.6c); 5) medium grained peloidal packstone, with *Prealveolina*, miliolids, gastropods and skeletal debris (see Fig. 6.6c); 6) Poorly sorted wackestone, with angular echinoderm and rudist fragments together with miliolids and occasional *Prealveolina*.

## 6.5.3 Discussion and interpretation

### 6.5.3.1 The chaotic units bounded by well-cemented beds

The lower sections of each of the units within this package of the Reguard Formation display similar characteristics to that of the chaotic unit at the base of the Reguard Formation in the outcrop at Peracals and hence are interpreted in a similar way (see section 4.5.4 together with Figs. 4.30a, 4.30b, 4.30c, 4.31a & 4.31b).

The chaotic nature of the lower sections to each of the units (see Fig. 6.4) is interpreted to have resulted from large scale slope failure and submarine slide events. The convoluted bedding and locally folded clasts within some of these units suggest that the sediment was only poorly cemented prior to the slide events and hence was subjected to soft-sediment deformation during down-slope transportation. The units which consist of more coherent metre-scale blocks arranged at varying angles to each other can also be interpreted to have resulted from submarine sliding events; however, the sediment within them must have been relatively better cemented prior to the slide event and hence rather than having suffered plastic deformation it broke into blocks.

The calcisphere-rich wackestone or packstone with small amounts of fine grained skeletal debris, sponge spicules, glauconite and planktonic foraminifera of which both the clasts and matrix within the chaotic units are composed, can be interpreted as a slope facies (see Fig. 6.5). The similarity in the lithology between the upper part of the Pardina Limestone and the wackestone/packstone matrix within these chaotic units of the Reguard Formation at Sopiera means that without detailed biostratigraphic analysis of all the clasts it is impossible to ascertain whether they are all derived from the slope facies of the Reguard Formation or if some are derived from the previously deposited Pardina Limestone.

The upper sections which are present within some of these units and consist of parallel-bedded calcisphere-rich wackestones and packstones with small amounts of fine grained skeletal debris, planktonic foraminifera and glauconite are interpreted to represent periods when the background sediments within this slope environment were able to accumulate (see Fig. 6.4). The intensive bioturbation within these sediments probably reflects the slow sedimentation rates.

Slow sedimentation rates during the periods between slide events are also suggested by the presence of the well-cemented beds which have been used to define the upper boundaries of these slide units (see Figs. 6.4 & 6.7). This is because

seafloor cementation is related to sedimentation rate, seawater circulation, grainsize (permeability) and grain composition (Shinn, 1969; Glover & Pray, 1971); however, there is no obvious difference between the grainsize or grain content of the sediments within the well-cemented beds and that in the less well cemented sediments above or below them. The intensive bioturbation in the form of feeding traces and the abundant iron-oxide nodules which are a feature of these well cemented beds (see Fig. 6.7) are also indicative of low sedimentation rates.

### 6.5.3.2 Channellised conglomerates

#### i) General interpretation and discussion

As with the outcrop at Peracals (see section 4.5.4 together with Figs 4.30a, 4.30b, 4.30c, 4.31a & 4.31b) the presence of the channellised conglomerates towards the top of the chaotic units (see Figs. 6.4 & 6.6a) suggests that the final phase in these major slide events involved the development of channels which transported the finer grained debris. The lack of grading within the conglomerates which infill the channels (see Fig. 6.6a) suggests that they represent debris flows, where the larger clasts were supported by the cohesiveness of the finer clasts and sediment which surrounded them (Middleton & Hampton, 1976). The fact that the bases of these channels truncate laminae within the sediments of the slump units below them indicates that these channellised debris flows were erosive events.

The thin layer of clast-free sediment which forms a cap across the top of the channellised conglomerates (see Fig. 6.6a) is a common feature found at the top of many debris flow deposits from both modern and ancient carbonate slopes (Krause & Oldershaw, 1979; Davies, 1983; Mullins et al., 1984). This clast-free cap facies can be interpreted as a fine-grained turbiditic deposit which settled out of suspension following the passage of the channellised debris flow.

The fact that these channels form prominent features which stand proud of the easily eroded wackestones surrounding them (see Fig. 6.6a) suggests that they are much better cemented than the surrounding sediment. A possible explanation for this preferential cementation of the channellised conglomerates on the sea floor is that sea-water was able to circulate through them with relative ease due to the presence of coarse clasts which when rested against one another would protect the surrounding fine grained matrix from compaction.

As discussed above, the rounded clasts, convoluted beds and blocks which constitute the main part of the slump units all possess lithologies which are interpreted to have been derived from the slope. In contrast the clasts within the

channellised conglomerates represent a variety of facies which can be interpreted to have been derived from a variety of locations. The close association of the channellised conglomerates with the chaotic lower sections to the units within this package of the Reguard Formation (see Fig. 6.4) suggests that the channellised debris flows were triggered by the same event that caused the slope failure and sliding. However, the lithological differences between the clasts within the channels and those within the slide units indicates that they were sourced from different places.

**ii) Provenance of the most common channel clasts**

The fine-grained wackestone and packstone clasts which contain abundant calcispheres together with skeletal fragments, planktonic foraminifera and varying amounts of glauconite appear almost identical to those that occur within the channels at Peracals (see section 4.5.4 and compare Fig. 4.31b with 6.6c). Although biostratigraphic analysis of these clasts would be required in order to reveal their true provenance, the petrographic similarities that these clasts possess with sediments from both the upper part of the Pardina Limestone and the lower part of the Reguard Formation at outcrops to the south and east of Sopiera (see sections 3.3.3, 3.4.2, 3.5.2, 3.6.2, 4.2.2.1, 4.4.3.1, 4.4.4.1, 4.5.3.1 & 4.5.4.1 together with Figs. 3.4, 4.3b(i), 4.3b(ii), 4.20b, 4.20c & 4.28c) suggests that they represent a mixture of debris which has been derived from both these sources. The red coloured calcisphere rich packstone clasts are similar to those seen in the channellised conglomerates at Peracals (see section 4.5.4) and are similarly interpreted to have been derived from hardgrounds which developed locally at the top of the Pardina Limestone as a result of a prolonged period of sediment starvation linked to a transgressive event marking the base of the Reguard Formation.

The medium to coarse grained packstone and grainstone clasts which contain a variety of skeletal fragments including those of benthic foraminifera and rudists are interpreted to represent shallow-water platform top facies (some examples can be seen in Fig. 6.6c). The fact that some of these packstones and grainstones contain the benthic foraminifera *Prealveolina* is important as it identifies them as having been derived from the Cenomanian-aged Santa Fe platform. It is most likely these coarse grained skeletal packstone and grainstone clasts were derived from the platform margin area of the Santa Fe platform which is now exposed along the Sierra de Sant Gervas (see section 3.6.2 together with Figs. 3.8a, 3.8b & 3.9). The only other place that coarse skeletal grainstones and packstones with *Prealveolina* occur is in the inner platform succession of the Santa Fe platform which is now exposed in the Sierra del Montsec and had a palaeogeographic location in excess of 80km to the south of these

slope sediments (see sections 3.2.2 & 3.7.1 together with Figs. 3.2a & 3.9). The occurrence of cement and sediment-filled dissolution cavities within some of these clasts (see Fig. 6.6c) is interpreted to indicate that prior to their re-working, the Santa Fe platform had suffered a period of subaerial exposure. This is in agreement with the conclusion which was reached in section 3.7.3, that the Santa Fe platform margin succession suffered a period of subaerial exposure during the late Cenomanian to early Turonian prior to the deposition of the Pardina Limestone during the early to mid Turonian (see Fig. 3.9).

The clasts which consist of poorly-sorted wackestone, with angular echinoderm and rudist fragments can also be identified as having been derived from the Santa Fe platform. They possess almost identical characteristics to the lagoonal facies wackestones which typify the Santa Fe Limestone at all the localities examined during this study. However, it is most likely that these clasts were derived from the succession in the Santa Fe platform margin area for the following reasons: 1) the relative proximity of the Santa Fe platform margin to this slope area; and 2) the fact that no similar clasts were found within the channellised conglomerates at Peracals which had a palaeogeographic location southward, ie. landward, of the Santa Fe platform margin.

The varied provenance of the clasts within these channellised conglomerates is shown schematically in Fig. 6.21.

**iii) Further interpretation**

The fact that the channellised conglomerates which form part of this Upper Turonian to Lower Coniacian-aged succession of slope sediments contain clasts which have been derived from the Cenomanian-aged Santa Fe platform margin has interesting implications.

Evidence from all the outcrops to the south and east of Sopiera suggests that following a transgressive event at the base of the Turonian, the Cenomanian-aged carbonates of the Santa Fe platform were overlain by the deeper water facies Pardina Limestone which draped the entire platform (see sections 3.7.3, 3.7.4 & 3.8 together with Fig. 3.9). The fact that clasts have been re-worked from the Cenomanian-aged Santa Fe platform to become incorporated into channels within the Upper Turonian to Lower Coniacian-aged Reguard Formation which postdates the Turonian-aged Pardina Limestone indicates that the Santa Fe platform margin succession must have been exhumed from below the Pardina Limestone during the Upper Turonian to Lower Coniacian.

The most plausible explanation for the presence of debris from the Santa Fe platform margin within these Upper Turonian to Lower Coniacian-aged channels is that, as suggested in chapter 3 (see sections 3.7.2.2 & 3.8 together with Fig. 3.9) after Simo (Simo & Puigdefabregas, 1985; Simo, 1986; Simo, 1989), the Santa Fe platform margin succession developed at the site of a former fault scarp which remained active during the Upper Cretaceous. Such a hypothesis also provides an explanation for the seemingly episodic slope failure and slide events that produced the succession of slide units and conglomerates which are observed within the Reguard Formation at Sopiera and could have been triggered by seismic activity during times of movement along this fault.

The variety of clast types within the channellised conglomerates suggests that the debris flows developed at an intermediate source where a random collection of previously cemented debris from the Cenomanian-aged Santa Fe platform, the Turonian aged Pardina Limestone and the Upper Turonian to Lower Coniacian Reguard Formation had collected. Such a location could be envisaged at the base of the proposed fault scarp (see Fig. 6.8).

### 6.5.3.3 Depositional model

Figure 6.8 shows a schematic diagram to illustrate the depositional model for these Reguard Formation slope sediments which is outlined below.

The section through the Reguard Formation which has been described above is interpreted to represent a succession of lower slope facies sediments which developed upon a very active slope. It is proposed that higher up the slope a fault scarp was present which exposed Cenomanian through to Lower Coniacian strata. For the reasons outlined in section 6.5.3.2(iii), debris derived from the up-thrown block is thought to have accumulated as a talus apron at the foot of this fault scarp.

As outlined in section 6.5.3.1 the succession of Reguard Formation slope sediments is interpreted to record a series of slope failure and slide events, each of which was probably triggered by seismic activity. In addition to triggering slide events on the lower slope, the seismic events appear to have mobilised some of the debris which is proposed to have been collecting at the foot of the fault scarp towards the top of the slope (see section 6.5.3.2(iii)). The debris derived from the talus apron at the base of the fault scarp is interpreted to have travelled down slope as channellised debris flows which upon reaching the lower slope cut down into the newly deposited slide units (see section 6.5.3.2(i)). The clasts are interpreted to have become fragmented and rounded as a result of abrasion during their down-slope transport within the channellised debris flows. The parallel-bedded calcisphere-rich

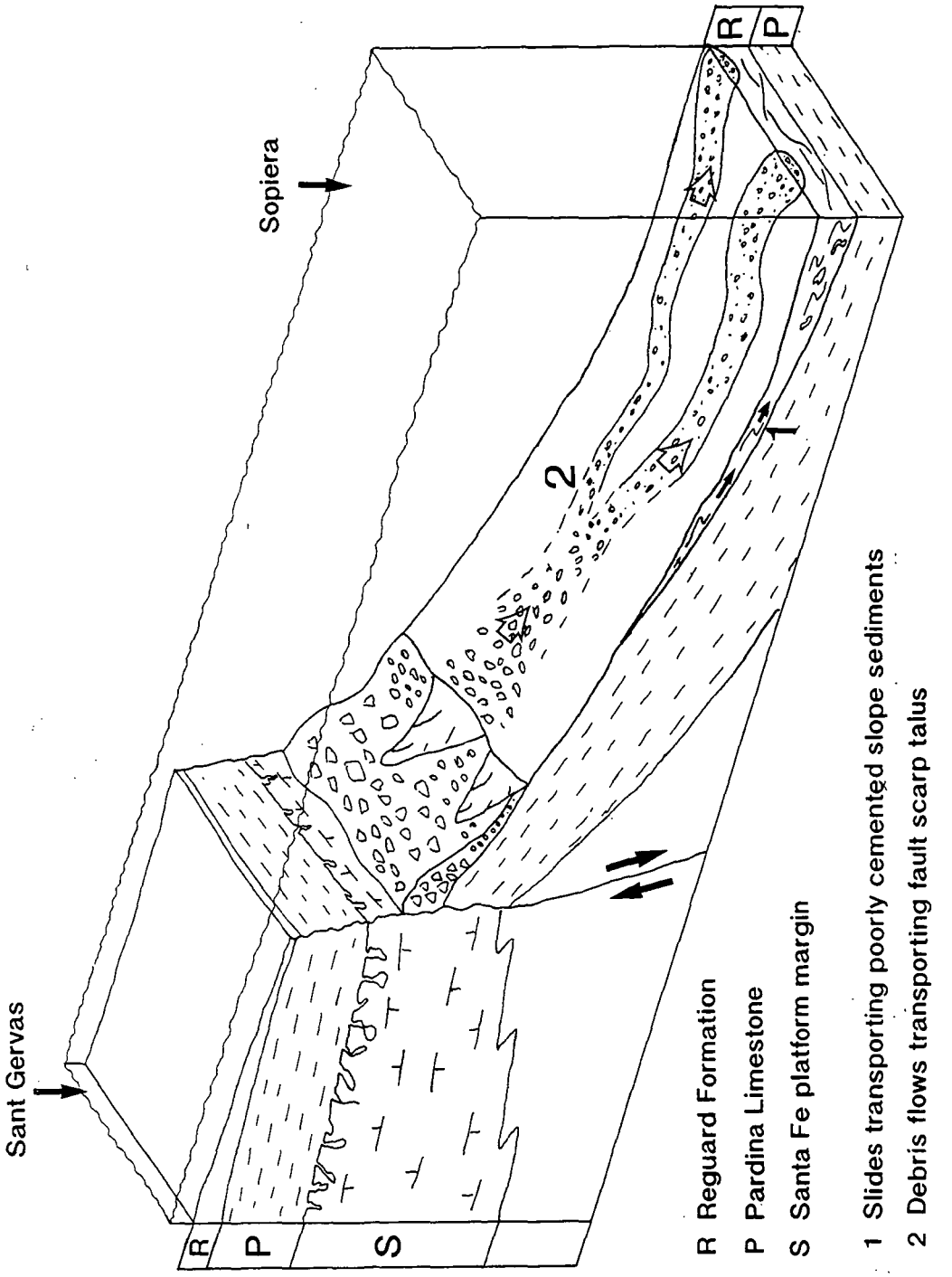


**Fig. 6.8.** Schematic diagram, illustrating the depositional model for the slide units and associated channellised conglomerates within the Reguard Formation at Sopiera. This model is based solely upon the information provided by the outcrop of the Reguard Formation at Sopiera and is not drawn to scale.

wackestones which form the upper section to some of the units within this basinal succession of the Reguard Formation suggest that during the periods between these major seismic-induced slope-failure events pelagic sedimentation continued (see section 6.5.3.1). The well-cemented beds which mark the top of the individual units within this succession display the effects of intensive bioturbation and contain abundant iron-oxide nodules and are therefore interpreted to indicate that during the intervening periods between seismic-induced slope failure sedimentation rates were low (see section 6.5.3.1). The fact that each of the units within this succession has been preserved suggests that these hardgrounds may have provided a protective cap to previous slide units and prevented them from being incorporated into the following slide which travelled down from higher up the slope as a result of the next seismic event.

## 6.6 The Sant Corneli Breccia

### 6.6.1 Introduction

For the purposes of this study the lithological unit which overlies both the Reguard Formation and the Pardina Limestone in the succession of slope sediments at Sopiera is named the Sant Corneli Breccia. The Sant Corneli Breccia, which outcrops on a northward facing slope, approximately 1 to 1.5km south of Sopiera (see Fig. 6.1), has been so-named for the following two reasons: 1) a series of breccia beds containing angular allochthonous debris of a variety of sizes, lithologies and stratigraphic age form prominent features within this unit; and 2) the slope sediments which are interbedded with the breccia beds have been shown by Gomez-Garrido (1987) and Caus (Universitat Autonoma de Barcelona) to possess assemblages of planktonic foraminifera belonging to the *Dicarinella concavata* biozone (Late Coniacian - Early Santonian); hence they can be considered to represent a deep slope equivalent of the Coniacian to Santonian-aged Sant Corneli platform (Simo, 1989).

### 6.6.2 Field observations and petrography

#### 6.6.2.1 Geometrical relationship with the underlying units

As described previously in section 6.5.2.1 the lower boundary of the Sant Corneli Breccia unit is fairly easy to identify in the field as the fine-grained

wackestones and packstones at its base possess a distinctive brown colouration and contain a small amount of silt-grade quartz (see Fig. 6.11); this contrasts with the mostly grey-coloured and quartz-free wackestones within the Reguard Formation. However, the geometrical nature of this boundary can only be seen from a distance and in fact is best viewed from the air.


**Fig. 6.9.** Aerial photograph covering an area of approximately 1Km$^2$ which lies just to the south of Sopiera. The Santa Fe Breccia (s) can be seen outcropping in shadow along the north side of the ridge, while the Pardina Limestone (p) forms the southerly dipping slope which is in the light. The prominent breccia beds within the Sant Corneli Breccia can be clearly seen within the upper part of this photograph. Due to the steep southerly tectonic dip this aerial photograph can be used as an approximate vertical cross-section through the succession. Note the difference in dip between the prominent breccia beds (arrowed) of the Sant Corneli Breccia and the bedding within the Pardina Limestone (dashed). This difference in dip between the two formations has led to the interpretation that the lower boundary of the Sant Corneli Breccia is an onlap surface (after Simo & Puigdefabregas, 1985).

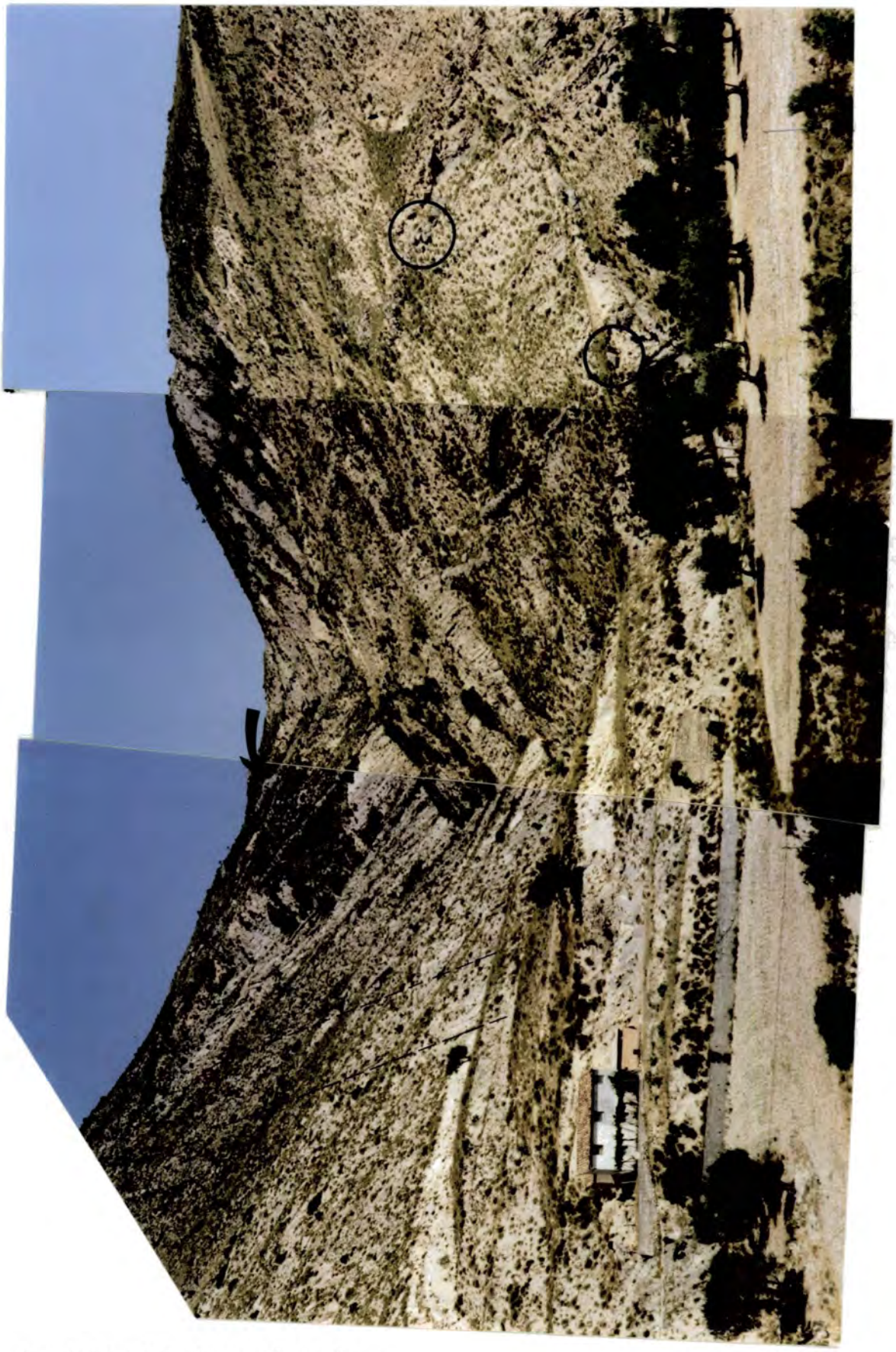

**Fig. 6.10** (see following page for caption)

**Fig. 6.10.** Panoramic view looking eastwards from the N230, along the base of the Sant Corneli Breccia. The steep slope on the left of the picture represents the upper part of the Pardina Limestone, while the Reguard Formation outcrops around the house and pinches out into the photograph. The approximate strike direction of the bedding within these two Formations is shown by the dashed line. The two prominent beds which can be seen on the right of the photograph are two of the breccia beds within the Sant Corneli Breccia (arrowed). Note that the strike of the two breccia beds can be seen to be different from that of the Pardina Limestone and that at their western ends (closest) these two beds become thinner and eventually terminate to be only present as the occasional block within the surrounding sediment (circled). See previous page.

Figure 6.9 shows an aerial photograph which covers an area approximately 1km east-west by 1.5km north-south, and roughly corresponds to the southeastern corner of the map in Fig. 6.1. Due to the steep tectonic dip of the strata in this area this aerial photograph is an approximate representation of a vertical cross section through the succession. The breccia beds within the Sant Corneli Breccia can be clearly seen within Fig. 6.9, as they form prominent features which stand out from the more easily weathered sediments around them. The difference in the strike directions of the breccia beds within the Sant Corneli Breccia and those of the beds within the underlying Pardina Limestone shows up clearly in the aerial photograph (see Fig. 6.9). The difference in strike direction between the Sant Corneli Breccias and the underlying Reguard Formation and Pardina Limestone can also be seen in Fig. 6.10, which shows a panoramic view looking eastward along the lower boundary of the Sant Corneli Breccias.

This obvious difference in strike direction between the Sant Corneli Breccia and the underlying units is interpreted to indicate that the lower boundary of the Sant Corneli Breccias is in fact an onlap surface. The onlapping nature of this unit was first described by Simo et al (1985) and Simo (1986); however, at that time this unit was considered to represent a deep slope equivalent of the Congost platform. Following the biostratigraphic information provided by Gomez-Garrido (1987)(see section 6.6.1), Simo (1989 & 1992) went on to describe this onlapping wedge as being the deep slope equivalent of the Sant Corneli platform. The onlapping nature of the breccia beds is shown schematically in Fig. 6.1.

### 6.6.2.2 Sedimentology and internal geometry

#### i) The units between the breccia beds

As can be seen in Figs 6.9 & 6.10, the prominent breccia beds from which the Sant Corneli Breccia gets its name are interbedded with much thicker units of more easily eroded sediments. In addition to them all being approximately 20 metres thick the units which lie between the breccia beds all contain similar lithologies and display similar internal geometries to one another.

Lithologicaly these units consist almost entirely of brown coloured, clay rich, packstones and wackestones with calcispheres, planktonic foraminifera, benthic foraminifera, sponge spicules, small amounts of fine-grained echinoderm and other skeletal debris together with varying amounts of silt-grade quartz (see Fig. 6.11).

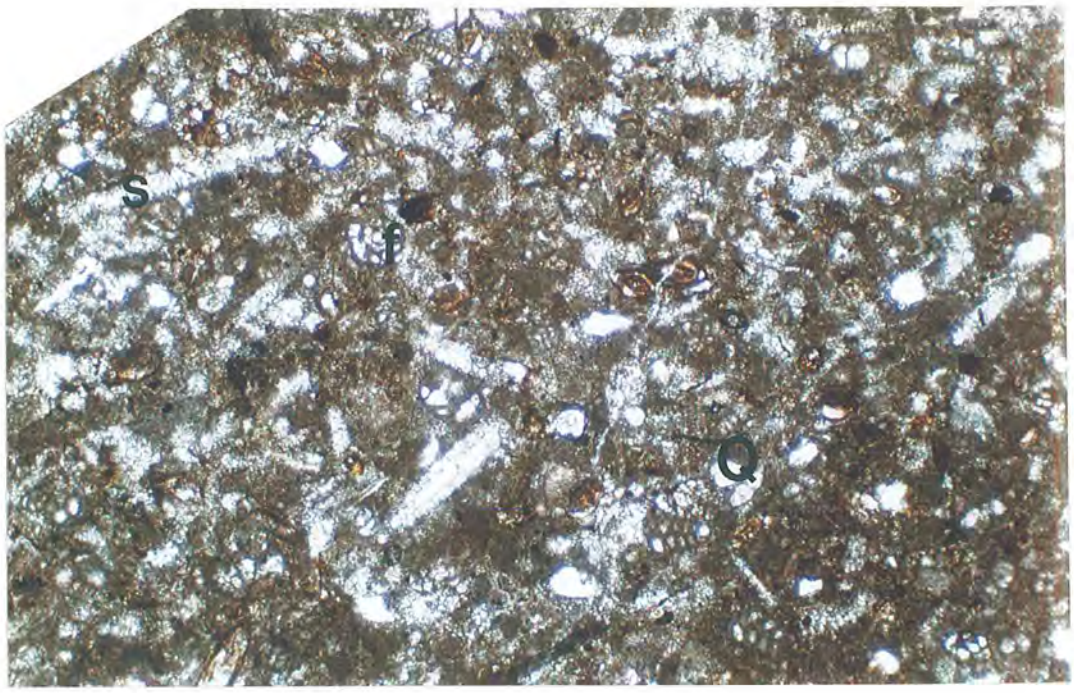


**Fig. 6.11** Photomicrograph showing a typical sample of the brown coloured, clay rich, packstone with calcispheres, both benthic and planktonic foraminifera (f), sponge spicules (s), fine grained skeletal debris and silt grade quartz (Q), which make up the slope facies units between the breccia beds of the Sant Corneli Breccia. Sample SB/6, Sant Corneli Breccia, Sopiera. Field of view 3 x 2mm.

**Fig. 6.12.** Photograph showing one of the many intraformational truncation surfaces within the pelagic slope facies sediments of the Sant Corneli Breccia at Sopiera. Note also the folded block which is present directly above the truncation surface (arrowed). Rucksack for scale.

**Fig. 6.13.** Photograph showing one of the many large folds which occur within the pelagic slope facies sediments of the Sant Corneli Breccia at Sopiera. Planar bedding both above and below this fold suggest that it was produced by soft sediment deformation. Rucksack for scale.

The bedding within these units, which is made obvious by the presence of abundant shaley horizons, is somewhat chaotic due to the presence of numerous discordant truncation surfaces (see Fig. 6.12) and folds (see Fig. 6.13). The axes of the smaller folds appear to be randomly orientated, whereas the larger folds, such as the one shown in Fig. 6.13, tend to have axes which plunge in a southerly direction. Bedding within these units is also disrupted by the occurrence of numerous rafted blocks which locally appear to have been folded. These rafted blocks are composed of the same lithology as that of the surrounding sediment and are most abundant directly above the numerous discordant truncation surfaces which cut through these units (see Fig. 6.12).

**ii) The breccia beds**

When viewed from a distance the breccia beds appear to possess an onlapping relationship with the underlying Reguard Formation and Pardina Limestone (see Figs. 6.1, 6.9 & 6.10). Unfortunately the actual surface of onlap cannot be observed in the field because the eastern ends of the breccia beds disappear below scree which has collected on the lower part of the slope in which the Pardina Limestone is outcropping.

At their eastern limits these beds are 8 to 10 metres thick and contain a variety of allochthonous debris that varies in size from small angular clasts with diameters of less than 1mm to large blocks with diameters in excess of 2m. At their eastern ends there is a tendency for the larger blocks to be concentrated towards the base of the beds (see Fig. 6.14), leaving the smaller clasts to form a cap facies along the upper surface (see Fig. 6.15).

As the breccia beds are traced westward they become gradually thinner and the grading becomes less obvious. Each of the breccia beds can be traced westward for approximately 700 metres until they eventually pinch out to be present only as an occasional allochthonous block within the bedded packstones which surround the breccia beds (see Fig. 6.10). At their most western ends the breccia beds contain relatively fewer small clasts and in some places they appear to consist almost entirely of 0.5-1 metre diameter blocks (see Fig. 6.16).

In addition to being of a variety of sizes, the clasts and blocks within these breccia beds are composed of many different lithologies, a selection of which are described below:

Many of the larger blocks consist of coarse skeletal packstones and grainstones with abundant rudist debris together with the benthic foraminifera *Prealveolina*. As can be seen in Fig. 6.16 much of the skeletal material which has

**Fig. 6.14.** Photograph taken towards the eastern end of the lowest breccia bed which can be seen in Fig. 6.10. The base of the bed is towards the left of the photograph. There is a large block with a diameter of approximately 3 metres at the base of the bed. Note that there is a rough sorting of clast size with the largest clasts tending to be in the lower part of the bed. Sant Corneli Breccia, Sopiera. Rucksacks for scale.

**Fig. 6.15.** Photograph showing the top surface of the lowest breccia bed which can be seen in Fig. 6.10. This photograph was taken towards the eastern end of this breccia bed and shows the smaller (< 30cm diameter) clasts and grainstone matrix which form the cap facies to the bed. Contrast this photograph with that of Fig. 6.16 which shows the top surface of the same breccia bed but was taken approximately 400 metres farther to the west. Sant Corneli Breccia, Sopiera. Baseball cap for scale.

**Fig. 6.16.** Photograph showing the top surface of the lowest breccia bed which can be seen in Fig. 6.10. This photograph was taken towards the western end of the same breccia bed that is shown in Fig. 6.15. Note that there are far fewer of the small clasts within this western end of the breccia bed than there are farther east (compare with Fig. 6.15). This western end of the breccia bed is almost entirely composed blocks with diameters between 1 and 2 metres. Note the brown colouration, which is due to silicification of the skeletal debris around the margins of the blocks. Sant Corneli Breccia, Sopiera. Rucksack for scale.

been exposed around the outer margins of these blocks has suffered silicification. It is common for such blocks to contain an interconnecting network of dissolution cavities (see Figs. 6.17a, 6.17b & 6.17c). These cavities can be either completely infilled with fine grained sediment (see Fig. 6.17a), or, as is more commonly the case, a combination of both sediment and coarse, bladed inclusion-rich calcite cement (see Figs. 6.17b, 6.17c & 6.17d). Where both sediment and cements infill the dissolution cavities it is common for there to have been more than one phase of sediment infill, as can be seen within sample SZ/7 which is shown in Figs. 6.17c & 6.17d. Figure 6.17d shows a polished slab of sample SZ/7 in which light brown and red coloured micritic sediment can be seen forming a geopetal infill at the base of a dissolution cavity, while inclusion-rich bladed calcite cements occlude the remaining space above the sediment. In Fig. 6.17d which shows a thin section from the same sample (SZ/7), a calcisphere-rich wackestone can be seen to post-date the bladed calcite cement and

**Fig. 6.17a.** Polished slab from one of the blocks of Santa Fe platform margin material within the breccia beds of the Sant Corneli Breccia. Note the dissolution cavity which has been infilled with sediment, together with a small amount of calcite cement. The host rock around the margins of the cavity display a marked brown colouration, suggesting they have suffered alteration. Note also the abundant *Prealveolina* (white circles, arrowed) within the host packstone. Sample SOP, Sant Corneli Breccia, Sopiera. Small divisions on scale are 1mm.

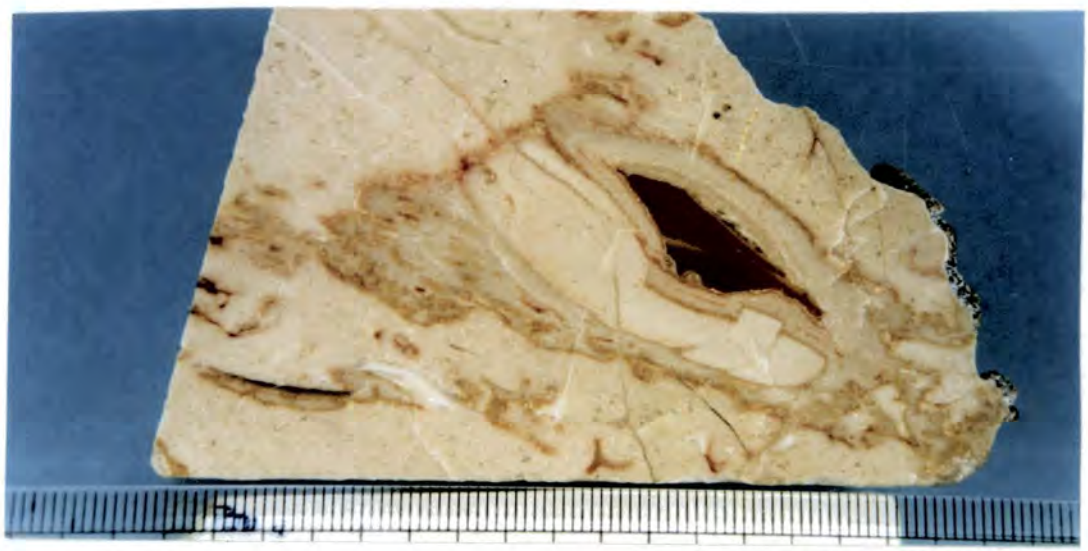

**Fig. 6.17b.** Polished slab cut from one of the blocks of Santa Fe platform margin material within the breccia beds of the Sant Corneli Breccia. Note the dissolution cavities which have been filled by alternating layers of isopachous cement and red-coloured, fine-grained sediment. Not also that the centre of the largest cavity has been filled with a laminated, deeper red coloured, fine-grained sediment. Sample SZ/5, Sant Corneli Breccia, Sopiera. Small divisions on scale are 1mm.


**Fig. 6.17c.** Polished slab cut from one of the blocks of Santa Fe platform margin material within the breccia beds of the Sant Corneli Breccia. Note the benthic foraminifera *Prealveolina* (arrowed). Note also the dissolution cavities which have been occluded by bladed isopachous cements which have developed polygonal compromise boundaries. Some of the dissolution cavities also contain laminated accumulations of red coloured, fine grained sediment. Sample SZ/7, Sant Corneli Breccia, Sopiera. Fine divisions on ruler = 1mm.

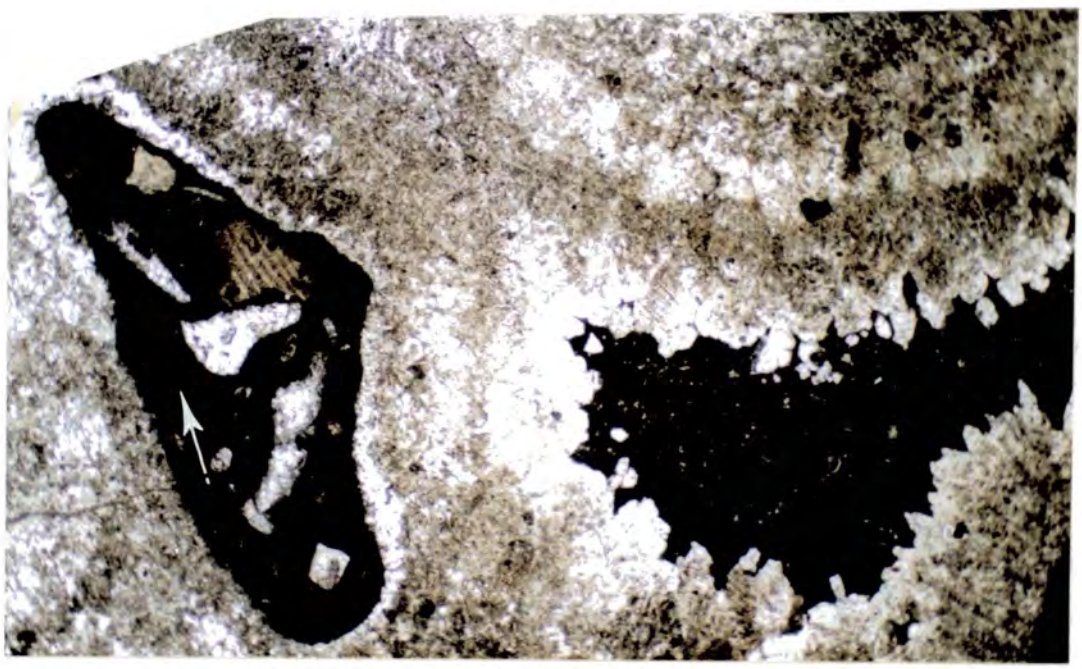

**Fig. 6.17d.** (see following page for caption)

**Fig. 6.17d.** Photomicrograph showing a thin section which has been cut from a sample of one of the large allochthonous blocks of skeletal debris rich packstone from within one of the Sant Corneli Breccia breccia beds. Note the large dissolution cavity which covers most of the area shown in this photomicrograph and has been almost totally occluded by coarse, bladed inclusion rich calcite cements. The remaining pore space at the centre of this dissolution cavity has been filled by wackestone containing calcispheres, fine grained skeletal debris and planktonic foraminifera. Note the presence of the benthic foraminifera *Prealveolina* (arrowed), within the skeletal debris packstone which forms the host rock to the network of cement filled dissolution cavities within this sample. The presence of *Prealveolina* within this allochthonous packstone block identifies it as having been derived from the Cenomanian-aged Santa Fe platform. Sample SZ/7, Sant Corneli Breccia, Sopiera. Field of view 12 x 7mm.

infill the remaining space at the centre of a dissolution cavity. Whole rock samples taken from immediately adjacent to the dissolution cavities, together with samples of the sediment and cements which infill the dissolution cavities within the examples of blocks that are shown in Figs. 6.17a, 6.17b & 6.17c were analysed for their stable isotopic compositions. The results of these stable isotope analyses are shown in Figs. 6.18a, 6.18b & 6.18c respectively.

Other common block lithologies include those which consist of earlier cemented breccia. These can either be breccias which contain clasts of the same lithology as in Fig. 6.19 or breccias which contain a variety of clast types. The angular clasts which can be seen within the sample shown in Fig. 6.19 consist of calcisphere-rich wackestone with abundant planktonic foraminifera and small amounts of fine-grained shell debris. Within this sample mineralisation can be seen to have occurred around the edges of the wackestone clasts, while the matrix which surrounds them is a very fine-grained wackestone containing a small number of calcispheres.

The finer grained debris which forms the matrix around the larger clasts and blocks within these breccia beds and represents the cap facies towards their eastern ends (see Fig. 6.15), has in most places a grainstone texture (see Figs. 6.20a & 6.20b). As can be seen in Fig. 6.20b, when micrite is present within the intergranular pore space it rests geopetally on top of the grains, causing there to be plenty of remaining calcite-cement-filled pore-space, in the form of shelter porosity below the larger grains. As can be seen in Figs. 6.20a & 6.20b the fine-grained matrix to the breccia beds contains abundant angular lithoclasts of a variety of different lithologies, along with shell fragments, foraminifera, other carbonate grains and glauconite. Common lithoclast lithologies include: calcisphere-rich wackestone with small amounts of fine-grained shell debris and varying amounts of glauconite; packstones with abundant

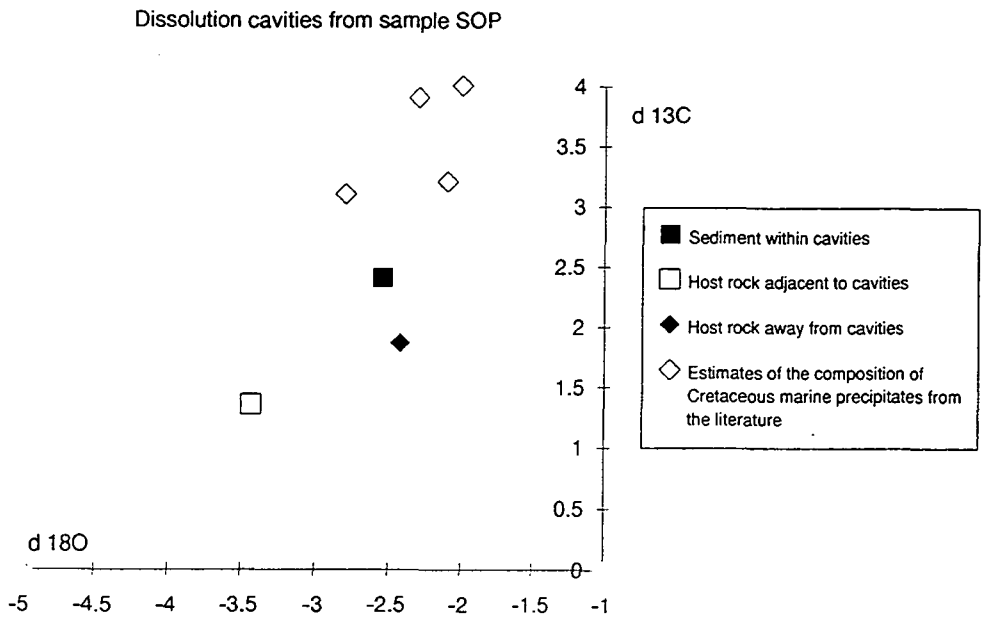


**Fig. 6.18a.** Carbon and oxygen isotope cross-plot in which samples drilled from specimen SOP (see Fig. 6.17a) have been compared with estimates of the composition of Cretaceous marine precipitates from the literature (Moldovanyi & Lohmann, 1984; Al Aasm & Veizer, 1986b & Enos, 1988).

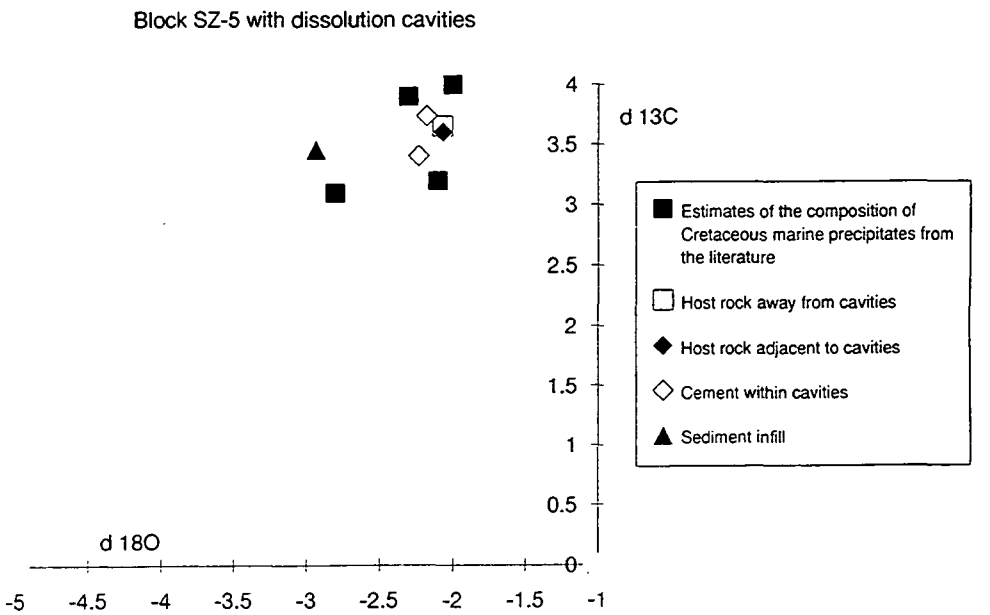


**Fig. 6.18b.** Carbon and oxygen isotope cross-plot in which samples drilled from specimen SZ/5 (see Fig. 6.17b) have been compared with estimates of the composition of Cretaceous marine precipitates from the literature (Moldovanyi & Lohmann, 1984; Al Aasm & Veizer, 1986b & Enos, 1988).

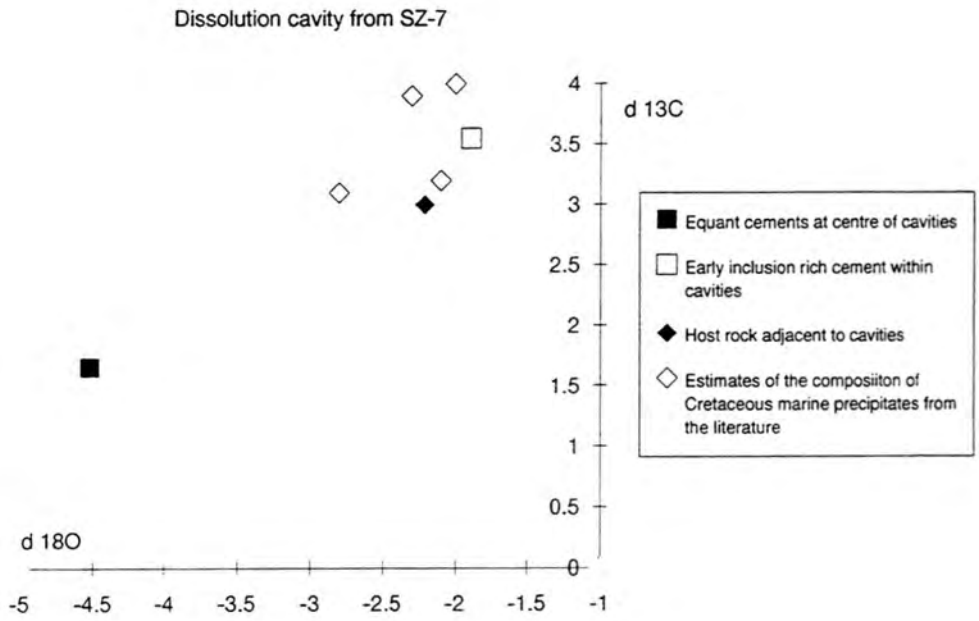


**Fig. 6.18c.** Carbon and oxygen isotope cross-plot in which samples drilled from specimen SZ/7 (see Fig. 6.17c) have been compared with estimates of the composition of Cretaceous marine precipitates from the literature (Moldovanyi & Lohmann, 1984; Al Aasm & Veizer, 1986b & Enos, 1988).

**Fig. 6.19.** Polished slab, cut from one of the blocks of previously cemented breccia which was found within the breccia beds of the Sant Corneli Breccia at Sopiera. Note the angular clasts of fine-grained, calcisphere-rich wackestone which have suffered mineralisation around their edges. The matrix within this breccia is also a fine-grained, calcisphere-rich wackestone. Sample SZ/9, Sant Corneli Breccia, Sopiera. Divisions on scale = 1mm.

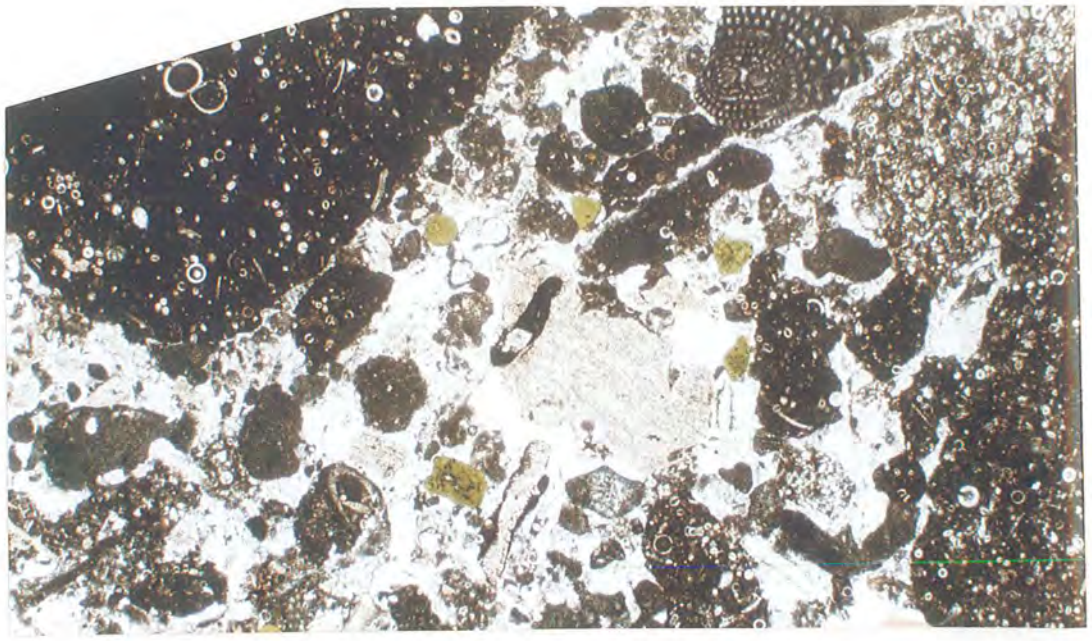

**Fig. 6.20a.** Photomicrograph showing a sample of the grainstone matrix within one of the Sant Corneli Breccia breccia beds. Note the abundant lithoclasts of a variety of different lithologies. Note also the glauconite grains, echinoderm fragments and *Prealveolina* fragment, which have all probably resulted from the mechanical breakdown of larger clasts during their transport. The presence of the *Prealveolina* indicates that some of the debris within this grainstone matrix has been derived from the Cenomanian-aged Santa Fe platform. The coarse calcite spar cement within this grainstone tends to display a poikilitic texture and is usually syntaxially associated with echinoderm fragments. Sample SC/7, Sant Corneli Breccia, Sopiera. field of view 6 x 4mm.

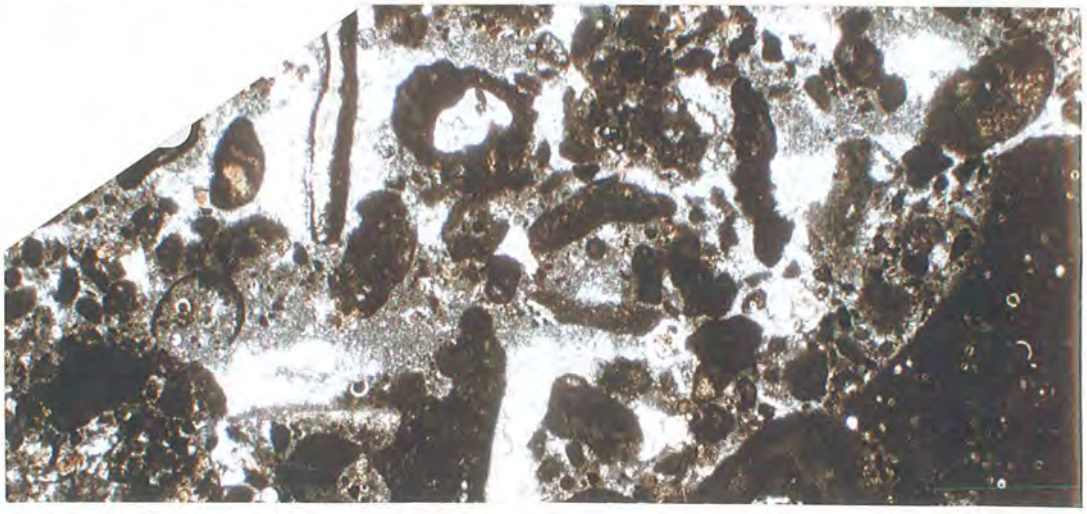

**Fig. 6.20b.** Photomicrograph showing a sample of the grainstone matrix within one of the Sant Corneli Breccia beds. Note that the micrite sized sediment which is present, rests geopetally upon the top of grains. As with Fig. 6.20a, the coarse calcite cement which infills the intergranular pore-space displays a poikilitc texture and is usually syntaxially associated with echinoderm fragments. Sample SC/1, Sant Corneli Breccia, Sopiera. Field of view 6 x 4mm.

calcispheres, fine-grained skeletal debris and glauconite; wackestones with angular skeletal debris along with miliolids and *Prealveolina*; skeletal debris and peloid-rich packstones; and skeletal debris rich grainstones, some of which contain *Prealveolina*. The cement which occludes the intergranular pore-space is a coarse, locally poikilotopic, calcite spar, which has commonly grown syntaxially around echinoderm fragments. When viewed under cathodoluminescence this calcite cement has a dull to bright orange luminescence.

## 6.6.3 Discussion and interpretation

### 6.6.3.1 Overall geometry and correlation

The Sant Corneli Breccias are interpreted as a wedge of allochthonous debris and slope sediments which onlap an unconformity and represent the deep slope equivalent of the late Coniacian to late Santonian-aged St Corneli platform (Simo et al., 1985; Simo, 1986; Gomez-Garrido, 1978; Simo, 1989 & Simo, 1992).

Observations made during this study would appear to substantiate this interpretation: The onlaping nature of the lower boundary to the Sant Corneli Breccias can be clearly seen in the aerial photograph and panoramic view shown in Figs. 6.9 and 6.10 respectively; and the brown-coloured, clay-rich, packstones and wackestones with calcispheres, planktonic foraminifera, sponge spicules, small amounts of fine-grained echinoderm and other skeletal debris, together with varying amounts of silt-grade quartz (see Fig. 6.11), which form the units between the breccia beds, are petrographicaly very similar to the Upper-Coniacian to Santonian-aged deep shelf facies of the Sant Corneli platform (Anserola Formation) which have been observed lying stratigraphically above the Conician-aged sediments of the Congost platform in the outcrops to the south and east of Sopiera (see sections 4.2.4.2, 4.2.4.3, 4.3.2.2, 4.3.2.3 & 4.4.6 together with Fig. 4.17c).

### 6.6.3.2 Units between the breccia beds

As mentioned above, petrographic similarities and biostratigraphic information suggest that the wackestones and packstones which form the units between the breccia beds can be correlated with the wackestones and packstones of the Anserola Formation, which represents the deep-shelf equivalent of the late Coniacian to late Santonian Sant Corneli carbonate platform. The small amounts of

platform-derived skeletal debris within these sediments at Sopiera suggest that they represent a fairly distal facies.

The chaotic nature of the bedding within these unit suggests that periodically these slope sediments suffered slide events which led to a certain amount of soft sediment deformation and this is taken to indicate that these sediments were deposited upon a slope. The intraformational truncation surfaces such as that shown in Fig. 6.12, which are a common feature within these sediments, are interpreted to represent slide scars, with the small overfolds and rafted blocks which are usually present immediately above these surfaces having resulted from soft-sediment deformation in the basal shear zone of the slides. Similar features have been described by Cook (1983) from the Permian, Bone Spring Formation of the Guadelupe Mountains, west Texas. Large open folds resulting from soft sediment deformation such as that shown in Fig. 6.13, are common features within the interior part of translational slides (see Cook & Mullins, 1983, for a summary of the internal characteristics of translational slides). The fact that there is a tendency for axes of the larger folds to plunge southwards suggests that the transport direction of these sediments during the slide events, relative to the present-day orientation of the outcrop at Sopiera, may well have been east-west.

#### 6.6.3.3 The breccia beds

##### i) Geometry and sedimentology

The general characteristics of these breccia beds suggests that they have resulted from catastrophic events which led to mass down-slope transport of previously-cemented debris under the influence of gravity. The rough grading of clast size within these beds (see Fig. 6.14) suggests that the mechanisms responsible for keeping the debris suspended during transportation were both the cohesive strength of the fine-grained matrix, and the upward component of fluid turbulence (Middleton & Hampton, 1976).

The gradual decreasing thickness of these breccia beds coupled with the decreasing relative abundance of finer-grained debris in a westward direction is interesting (see Fig. 6.10).

One possible explanation is that these breccia beds also thin in an eastward direction but lack of exposure prevents this from being observed. If this were the case then these breccia beds could be interpreted to represent channellised mass flow deposits which had a transport direction with an approximate north-south orientation relative to the present-day orientation of this outcrop. However, this interpretation

seems unlikely as there are at least 6 traceable breccia beds in this outcrop at Sopiera and none of them are observed to thin towards the east.

A more likely explanation for these features is that these breccia beds represent sheet-like, gravity driven, mass-flow deposits, which developed a tapering geometry as a result of increasing distance away from their source, which relative to their present-day orientation lay to the east. Such an interpretation suggests that these sediments were deposited on a submarine slope which was dipping to the west (relative to their present-day orientation). The presence of a westward dipping palaeoslope could also account for the orientation of the larger, soft sediment deformation folds within the units between the breccia beds. The fact that the relative abundance of finer-grained debris within the breccia beds decreases in the proposed down-slope direction, can be interpreted as a result of the greater momentum which would have been possessed by the larger blocks during such gravity-driven, down-slope, debris-flow events. Although produced within a subaerial environment and so lack some of the buoyancy forces which are associated with submarine mechanisms of gravity flow, similar depositional patterns can be observed within any mountainside scree slope today.

The grainstone texture which is observed within much of the fine-grained matrix to these breccia beds (see Figs. 6.20a & 6.20b) suggests that much of the micritic sediment must have been carried away in suspension, perhaps to be deposited farther down the slope. The geopetal nature of the micritic sediment which is present within the matrix of these beds (see Fig. 6.20b) suggests that it settled out from suspension after the passage of the debris flow, and this is another indication that the gravity-driven flows which produced these breccia beds did not behave like true debris flows. The zoned luminescence which is displayed by the poikilitopic cement within the matrix of these breccia beds suggests that most of the post debris flow cementation took place in the presence of reducing pore fluids, probably within the burial realm. The lack of any obvious early marine cements within the matrix of these breccia beds is probably to be expected; as sea-water circulation through these sediments is unlikely to have been high in their proposed deep slope setting. Such a setting would correspond to a 'stagnant marine phreatic zone' of Longman (1980).

The wide variety of clast lithologies within these breccia beds can be interpreted in a similar way to that of the channellised conglomerates within the Reguard Formation, although the much larger size and more angular nature of the blocks within the Sant Corneli Breccias (compare Figs. 6.6a & 6.6b with Figs. 6.14, 6.15 & 6.16) suggests that either the slope was much steeper or the source from which they were derived was much closer than for the Reguard conglomerates. The fact that the Sant Corneli Breccias form an onlapping wedge on top of the Reguard

Formation, indicates that tectonic movements may well have caused a steepening in the angle of slope towards the end of the middle Coniacian.

**ii) Clast and block provenance**

Although the clasts and blocks within these breccia beds are generally much larger and more angular than those within the channellised conglomerates of the Reguard Formation (compare Figs. 6.6a & 6.6b with Figs. 6.14, 6.15 & 6.6), they consist of very similar lithologies (see sections 6.5.2.3 & 6.6.2.2) and are similarly interpreted to have been derived from a mixture of: 1) the Santa Fe platform margin succession; 2) the Pardina Limestone; and 3) the Reguard Formation. The fact that the clasts and grain types which are present within the matrix of these breccia beds can all be found as constituents within the larger blocks suggests that the finer grained matrix is a product of the mechanical erosion of the larger blocks. The varied provenance of the blocks and clasts within these breccia beds is shown schematically in Fig. 6.21.

A number of the larger blocks within these breccia beds consist of lithologies typical of those found within the platform margin facies of the Cenomanian-aged Santa Fe platform and contain the benthic foraminifera *Prealveolina* (see section 3.6.2 together with Figs. 3.8a, 3.8b, 6.17a, 6.17c & 6.17d). As can be seen from the samples of such blocks which were described in section 6.6.2.2(ii), many of them contain dissolution cavities which have been infilled by a mixture of fine-grained sediment and cement (see Figs. 6.17a, 6.17b, 6.17c & 6.17d). The dissolution which produced such a network of smooth sided pipes and cavities within these blocks could only realistically have been produced by the action of meteoric waters. The red colouration of some of the very fine grained sediment which partly infills some of the dissolution cavities (see Figs. 6.17a, 6.17b & 6.17c) suggests that it may well represent 'terra rossa' type argillaceous material, which is considered a by-product of pedogenic processes and subaerial dissolution of limestones (Pye, 1983; Esteban & Klappa, 1983)

A meteoric influence during the development of these cavities is also suggested by the isotopic data collected from sample SOP (see Fig. 6.17a) which is shown in Fig. 6.18a. The whole rock sample from directly adjacent to a dissolution cavity shows depletions in both its $^{13}C$ and $^{18}O$ compositions, relative to the whole rock sample of the host rock away from the cavity, and to estimates of the composition of marine precipitates during the Cretaceous. The significant depletion in $^{13}C$ of between approximately 1.8 and 2.7 $^{o}/_{oo}$ together with the slight depletion in $^{18}O$ of between 0.6 and 1.3 $^{o}/_{oo}$ relative to estimates of Cretaceous marine carbonate

precipitates suggests that the host rock directly adjacent to the dissolution cavities may have suffered alteration in the presence of organically charged meteoric waters (see section 5.2.3). The alteration of the host rock adjacent to the dissolution cavities can be seen in Fig. 6.17a, where it shows up as a distinct zone of red/brown colouration. The fact that the whole rock samples taken from adjacent to the dissolution cavities in samples SZ/5 and SZ/7 do not show similar depletions (see Figs. 6.18b & 6.18c), does not discount this theory of meteoric dissolution, since, if the host rock had been well cemented prior to subaerial exposure then meteoric waters would not have been able to penetrate into the wall rock to cause any alteration.

Several lines of evidence strongly suggest that the cements within these dissolution cavities represent cements which were precipitated under marine conditions: the bladed habit displayed by the majority of the cements within these cavities, together with their inclusion-rich nature, non-luminescence and the fact that they have developed with equal thicknesses from all sides of the cavities, and in most cases completely occlude the available pore space by creating polygonal compromise boundaries (see Figs. 6.17c & 6.17d together with sections 5.1.2 & 5.5.3.2). The isotope data presented in Figs. 6.18b & 6.18c would appear to support such an interpretation, as the analyses of these inclusion-rich, bladed cements show similar isotopic values to those of estimates of Cretaceous marine carbonate precipitates. Isotopic information also suggests that the fine-grained sediments which partly infill many of these dissolution cavities were cemented in the presence of marine waters as they display isotopic compositions that are similar to estimates of Cretaceous marine precipitates (see Figs. 6.18a & 6.18b).

Some of the dissolution pipes and cavities within the blocks of Santa Fe platform margin material display evidence of complicated diagenetic histories. In some cases there appears to have been several phases of cementation within the dissolution cavities, separated by periods when red, fine grained sediment ('terra rossa'?) was deposited (see Fig. 6.17b). In many of these 'Santa Fe platform margin' blocks it is common for the deposition of red, fine-grained sediment ('terra rossa'?) to have been followed by bladed marine cements, which in turn has been followed by the deposition of calcisphere rich wackestone or packstone within the remaining pore-space towards the centre of the cavity (see Figs. 6.17c & 6.17d).

The samples which have been discussed here suggest that the Santa Fe platform margin suffered a prolonged period of subaerial exposure which resulted in the development of extensive karst networks. These same cement and sediment-filled karst networks can be seen in the Santa Fe platform margin outcrops at Sant Gervas (see sections 3.6.2 & 3.7.3 together with Figs. 3.8a & 3.8b). The presence of 'terra

rossa' like argillaceous sediment within the karstic cavities suggests that pedogenic processes were in operation at the surface during periods when the Santa Fe platform margin was subaerially exposed. When considered together with the seemingly extensive network of dissolution cavities this suggests that a fairly humid climate prevailed during this Upper Cenomanian subaerial exposure of the Santa Fe platform margin. This interpretation that the Tremp basin was experiencing a humid climate during the Upper Cenomanian agrees with the climatic conclusions which were reached during the study of Congost platform diagenesis in chapter 5 (see sections 5.1.3.2, 5.4.4, 5.5.4, 5.5.5, 5.6.4 & 5.6.5). The preservation of alternating isopachous marine cements and layers of 'terra rossa' like sediments within some of these dissolution cavities suggests that the proposed, prolonged period of subaerial exposure, may have been interrupted by a number of minor transgressive events which caused the active circulation of marine waters through the previously developed karst networks at the platform margin, and resulted in the precipitation of marine cements. The calcisphere-rich wackestones which are present as the final infill to many of the dissolution cavities within the blocks of Santa Fe platform margin material, display very similar lithologies to that of the Pardina Limestone and are hence interpreted to have been flushed into the karst networks during the major transgressive event which is proposed to have occurred during the early Turonian and resulted in the deposition of the deeper-water Pardina Limestone over the entire Santa Fe platform (see sections 3.7.3, 3.7.4 & 3.8 together with Fig. 3.9). The presence of what would appear to be sediment belonging to the Pardina Limestone Formation within these karstic cavities constrains the subaerial exposure event which produced them to have occurred during the late Cenomanian to early Turonian, prior to the deposition of the Pardina Limestone.

In the same way that the varied collection of clasts within the channellised conglomerates of the Reguard Formation was interpreted (see sections 6.5.3.2(ii), 6.5.3.2(iii) & 6.5.3.3), the variety of clast and block lithologies within the Sant Corneli Breccia beds suggests that the gravity-driven mass flows which deposited them, developed from an intermediate source, where a random collection of previously cemented debris from the Cenomanian-aged Santa Fe platform, the Turonian-aged Pardina Limestone and the Upper Turonian to Lower Coniacian Reguard Formation had collected. As proposed in sections 6.5.3.2(iii) and 6.5.3.3, such a location could be envisaged at the base of an active fault scarp which developed within the upper part of the slope (see Fig. 6.8). The presence of such blocks within the breccia beds of the Sant Corneli Breccia indicates that the fault which was proposed to have been responsible for exhuming the Santa Fe platform margin succession, the Pardina Limestone and the Reguard Formation during the

Upper Turonian to Coniacian in order to allow debris from each of these formations to have been included within the channellised conglomerates of the Reguard Formation slope sediments (see sections 6.5.3.2(iii) & 6.5.3.3 together with Fig. 6.8) must have remained active during the deposition of the Sant Corneli slope facies sediments during the Upper Coniacian to Santonian.

The many blocks within these breccia beds that are composed of a previously-cemented breccia, such as the one shown in Fig. 6.19, may in fact represent debris which became cemented while situated within the talus apron, which is thought to have existed at the base of the proposed upper slope fault scarp (see sections 6.5.3.2(iii) & 6.5.3.3 together with Fig. 6.8). Such blocks of previously cemented breccia provide the best evidence for the proposed former existence of a fault scarp talus apron. The mineralisation which can be seen to have occurred around the margins of the clasts within the sample of a previously cemented breccia block shown in Fig. 6.19, is interpreted to have occurred while the clasts rested within the talus apron at the base of the fault scarp, which, prior to the infiltration of fine grained sediment is likely to have had quite a high porosity. In thin section the mineralisation around the edges of the clasts within the breccia block shown in Fig. 6.19 can be seen to be associated with some form of colonial organism (now spar filled voids), the shape of which are suggestive of bacteria (Tucker, pers. com).

### 6.6.3.4 Brief summary and depositional model

The depositional model proposed for the Sant Corneli Breccia is very similar to that which was suggested in section 6.5.3.3 for the slope sediments of the Reguard Formation (see Fig. 6.8). Both these lithological units are thought to represent wedges of allochthonous debris and slope sediments which developed upon the lower part of a very active slope. It is proposed that higher up the slope a fault scarp was present which protruded above the sediment surface and exposed Cenomanian through to Lower Coniacian strata (see section 6.6.3.3(ii)). The type and variety of blocks and clasts within the breccia beds have led to the interpretation that debris derived from the up-thrown block accumulated as a talus apron at the foot of this fault scarp (see section 6.6.3.3(ii)).

The presence of basal truncation surfaces and evidence of soft sediment deformation within the units of deep slope facies sediments which lie between the breccia beds has led to the interpretation that these units record a series of slope failure and slide events, which like those within the Reguard Formation were probably triggered by seismic activity (see section 6.6.3.2). Seismic activity is also proposed to have been the trigger behind the mobilization of debris from the proposed

fault scarp talus apron which went on to form the gravity-driven down-slope mass flow events that produced the breccia beds (see sections 6.6.3.3(i) & 6.6.3.3(ii)).

The westward-tapering sheet-like geometry of the breccia beds, together with the westward decreasing abundance of smaller clasts and the lack of micritic material within their matrix is interpreted to have resulted from deposition upon a westward dipping slope, whereby the greater momentum of the larger blocks carried them farther down-slope than the finer debris, while all the fine-grained micritic material was carried farther basinward by the turbulence which would have been created during such events (see section 6.6.3.3(i)). The sheet-like geometries of the breccia beds within the Sant Corneli Breccia and their much coarser clast size compared with the channellised conglomerates of the Reguard Formation, are interpreted to indicate that the depositional slope upon which these sediments now exposed near Sopiera were deposited was steeper during the Upper Coniacian and Santonian than it was during Turonian to mid Coniacian times (see section 6.6.3.3(i)).

## 6.7 Summary

The main features of the accumulations of allochthonous debris within the succession of slope and basinal sediments that is exposed in the road cuttings and mountain slopes around the village of Sopiera are summarised in Fig. 6.21. Figure 6.22 shows an interpretive cross-section through the Cenomanian to Santonian-aged slope sediments in the Tremp basin which is based on the information provided by the outcrops around Sopiera.

Deposition of these Upper Cretaceous slope sediments began during the Lower to Middle Cenomanian with the accumulation of 350 metres of interbedded fine-grained marls and limestones which make up the Sopiera Marls (see section 6.2 together with Figs. 6.1 & 6.22). Variations in grainsize and skeletal fragment content are interpreted to indicate that the lower part of the Sopiera Marls represents a deepening-upward basinal succession, while the upper part represents a basinal succession which was shallowing upwards. The Lower to Middle Cenomanian-age of these sediments suggests that they represent the basinal equivalent of the lower part of the Santa Fe platform (see Fig. 3.9).

The next phase of sedimentation which is documented within the succession around Sopiera was the deposition of a basinward-thickening wedge of Upper Cenomanian-age, comprising chaotically-bedded pelagic mudstones, channellised conglomerates and megabreccia units which downlap onto the Sopiera Marls. This downlapping unit of slope facies sediments and allochthonous debris is the Santa Fe

| UNIT | ALLOCHTHONOUS DEBRIS GEOMETRY | TEXTURE | MICRITE IN MATRIX | CAP FACIES | CLAST PROVENANCE | KARSTED ST. FE DEBRIS ? |
|---|---|---|---|---|---|---|
| SANTA FE BRECCIA | Channels (5–10m wide) + Thick (>20m) megabreccia sheets | Matrix supported | Yes | None apparent | Santa Fe platform margin<br>Santa Fe slope | No |
| REGUARD FORMATION | (2 – 5m wide) Channels | Clast supported | Yes | Clast Free Layer | Santa Fe platform margin<br>Pardina Limestone<br>Reguard Formation | Yes |
| SANT CORNELI BRECCIA | Thin (<10m) tapered megabreccia sheets | Clast supported | No | Finer debris in east<br>None apparent in west | Santa Fe platform margin<br>Pardina Limestone<br>Reguard Formation<br>Anserola Formation | Yes |

**Fig. 6.21.** Table summarising the main features of allochthonous debris accumulations within the Cenomanian to Santonian-aged slope and basinal succession at Sopiera.

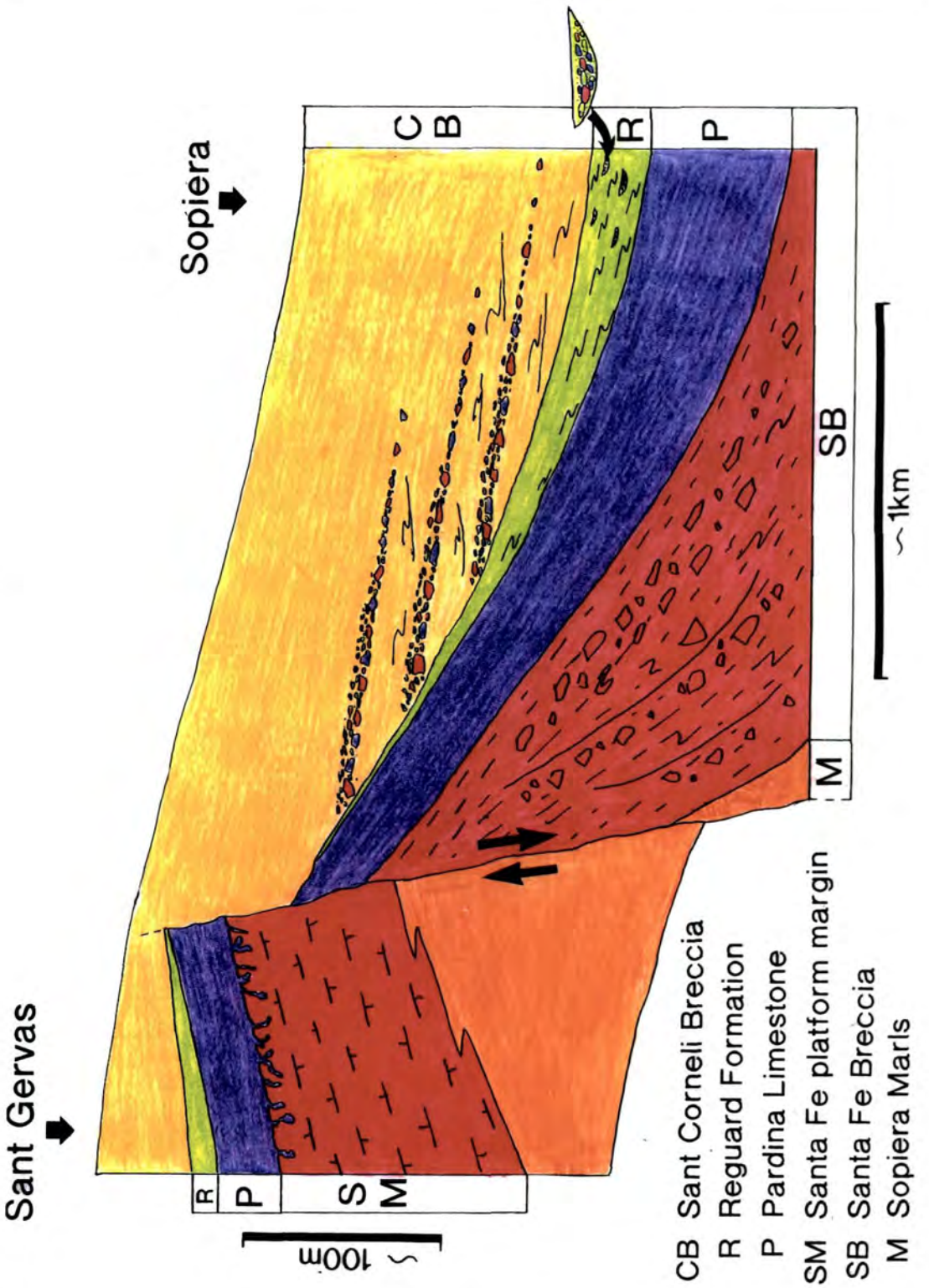


**Fig. 6.22.** Cross section through the Cenomanian to Santonian-aged slope sediments which are exposed around Sopiera. This cross section has been extended westwards on the basis of interpretation in order to include the fault scarp which is proposed to have been the source of allochthonous debris. The colour of the allochthonous debris within the slope sediments corresponds to that of the formation from which it was derived.

Breccia which is interpreted to represent the basinal equivalent of the upper part of the Santa Fe platform (see section 6.3 together with Figs. 3.9, 6.1, 6.2, 6.3 & 6.22). Many of the blocks within the megabreccia units can be identified as having been derived from the Santa Fe platform-margin succession (see Fig. 6.22). As none of these blocks display any evidence to suggest that they had suffered subaerial exposure prior to their deposition, they must have been shed from the Santa Fe platform margin prior to the subaerial exposure event which is proposed to have occurred towards the end of the Upper Cenomanian (see sections 3.7.3, 6.5.3.2(ii) & 6.6.3.3(ii)). Possible mechanisms which may have been responsible for the apparent massive platform margin collapse and slope failure which produced such a succession of allochthonous debris include seismic activity, associated with the fault which is proposed to have been present close to the site of the platform margin, and differential compaction, as the platform margin prograded out over the muddy and probably poorly-cemented basinal sediments (see section 6.3.4 together with Figs. 3.9 & 6.22).

The Pardina Limestone which overlies the Santa Fe breccia comprises an approximately 90 metre thick unit of Upper Cenomanian to Middle Turonian-aged wackestones and packstones rich in calcispheres and planktonic foraminifera (see section 6.4 together with Figs. 6.1 & 6.3). This low faunal diversity facies of the Pardina Limestone is observed to overlie the Cenomanian-aged sediments of the Santa Fe platform at all the localities which have been visited during this study and is interpreted to have been deposited over the entire Santa Fe platform as a result of a relative rise in sea-level (see sections 3.7.3, 3.7.4, 3.8 & 6.4 together with Fig. 3.9). The low faunal diversity of this unit is interpreted to be partly the result of a eutrophication of the platform top which occurred as a result of a world-wide oceanic event (see sections 3.7.3, 3.8 & 6.4.3).

Following the deposition of the Pardina Limestone the succession of slope sediments at Sopiera recorded a period of renewed down-slope slide events and influx of allochthonous debris via channellised debris flows during the deposition of the Upper Turonian to Lower Coniacian-aged Reguard Formation (see section 6.5 together with Figs. 6.1 & 6.4). This renewed activity upon the slope is interpreted to have been caused by seismic activity and resulted in the deposition of a series of slide units consisting of chaotically-bedded pelagic slope facies sediments which are capped by channellised conglomerates (see section 6.5.3). The presence of a mixture of clasts (some of which are karsted) within the channellised conglomerates which can be identified as having been derived from the Santa Fe platform margin, the Pardina Limestone and the Reguard Formation has led to the interpretation that the debris flows which resulted in the deposition of these channellised conglomerates developed as a result of the collapse of talus aprons which were accumulating at the

foot of an active fault scarp (or scarps), exposing the earlier deposited Cenomanian to Coniacian succession higher up the slope (see sections 6.5.3.2 & 6.5.3.3 together with Figs. 6.6a, 6.6b, 6.6c, 6.8 & 6.22).

The down-slope sliding and mass-flow events continued during the Upper Coniacian to Santonian and resulted in the deposition of the Sant Corneli Breccia which comprises an onlapping wedge of chaotically-bedded pelagic slope facies sediments together with tapered megabreccia sheets (see section 6.6 together with Figs. 6.1, 6.9, 6.10, 6.12, 6.13, 6.14, 6.15, 6.16 & 6.22). The tapering sheet-like geometry of the megabreccias together with their decreasing relative abundance of smaller clasts in a down-slope direction and grainstone texture, have led to the interpretation that they resulted from gravity-driven down-slope mass flow events, in which the larger blocks travelled farther than the smaller ones as a result of their relatively greater momentum while all the micritic material was carried away in suspension within the turbulent currents which would have been created by such events (see sections 6.6.2.2(ii) & 6.6.3.3 together with Figs. 6.10, 6.16, 6.20a & 6.20b). The fact that clasts within these megabreccia beds can be identified as having been derived from a mixture of the Santa Fe platform margin, the Pardina Limestone and the Reguard Formation, is interpreted to suggest that a similar 'active fault scarp and talus apron' system to that proposed to have been responsible for providing the constituents of the channellised debris flow deposits of the Reguard Formation, was in operation during the deposition of the Sant Corneli Breccia (see sections 6.6.2.2(ii), 6.6.3.3 & 6.6.3.4 together with Figs. 6.17a, 6.17b, 6.17c, 6.17d, 6.19, 6.20a, 6.20b & 6.22). The onlapping lower boundary of the Sant Corneli Breccia, together with the much coarser and more angular nature of the allochthonous debris within its sheet like mass flow deposits when compared to the channellised conglomerates of the Turonian to Lower Coniacian-aged Reguard Formation, are interpreted to indicate that there was an increase in the depositional palaeoslope between the Lower and Upper Coniacian (see sections 6.6.3.1, 6.6.3.3(i) & 6.6.3.4 together with Figs. 6.6a, 6.6b, 6.9, 6.10, 6.14, 6.15, 6.16 & 6.22) This increase in palaeoslope which appears to have occurred prior to the deposition of the Upper Cenomanian sediments at the base of the Sant Corneli Breccia is interpreted as a further expression of the tectonically active nature of the Tremp basin during the Upper Cretaceous.

# Chapter 7
# A sequence stratigraphic framework for the Congost platform

## 7.1 Introduction

Throughout this chapter it is assumed that the reader is familiar with the widely used sequence stratigraphic terminology of Mitchum (1977), Vail et al. (1977) and Van Wagoner et al. (1988).

As mentioned previously in chapter 2, a sequence stratigraphic framework for the Upper Cretaceous of the Tremp basin has been established by Simo (1992)(see also Simo, 1986; Simo, 1989 & Caus et al., 1993)(see section 2.5 together with Figs. 2.8a & 2.8b). In this sequence stratigraphic framework, the whole of the Upper Turonian to Coniacian-aged Congost platform, along with its associated slope and basinal sediments (the Reguard Formation) have been interpreted to represent one complete 3rd order depositional sequence. The purpose of this chapter is to utilise some of the information which has been provided in earlier parts of this thesis to build upon the sequence stratigraphic framework suggested for the Congost platform by Simo (1986, 1989 & 1992), and to discuss the possible mechanisms behind the proposed variations in accommodation space. As will be discussed in section 7.2.2, some of the conclusions which have been reached following the detailed studies presented earlier in this thesis suggest that it may be an oversimplification to include the whole of the Upper Turonian to Coniacian-aged Congost platform, along with its associated slope and basinal sediments (the Reguard Formation) within one 3rd order depositional sequence.

## 7.2 Background

### 7.2.1 The Congost sequence of Simo, 1992.

Figure 7.1 shows a schematic representation of the Congost sequence as proposed by Simo (1992). Simo (1992) defined the lower sequence boundary to the Congost sequence as the upper surface of the Pardina Limestone, which is mid-Turonian in age and can be correlated across the basin from the inner platform area, where it shows localised karsting, to the more basinal localities where accumulations

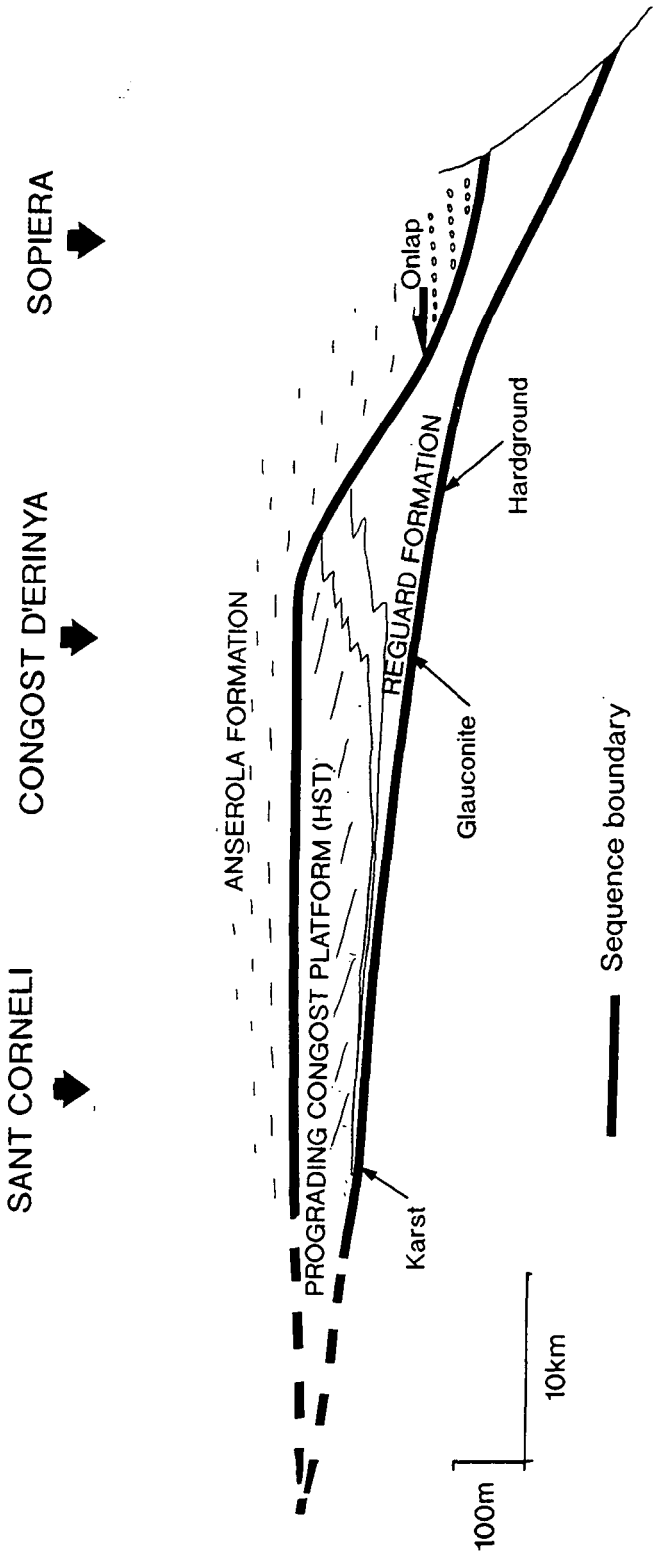


**Fig. 7.1.** A schematic representation of the mid-Turonian to mid-Coniacian-aged Congost depositional sequence proposed by Simo (1986; 1989 & 1992). After Simo (1989).

of glauconite and/or hardgrounds occur (see also Soriano, 1992 & Caus et al, 1993). The occurrence of localised hardgrounds and accumulations of glauconite at this correlatable boundary together with the presence of the pelagic Reguard Formation immediately above it, are interpreted to be indicative of a major transgressive event marking the base of the Congost sequence. Simo (1986; 1989; 1992) divided the Congost sequence into two units: (1) a lower transgressive wedge comprised of the early part of the Reguard Formation, and (2) an upper regressive package comprised of the prograding sediments of the Congost platform and slope. The mid-Coniacian sequence boundary, proposed as the upper boundary to the Congost sequence by Simo (1986, 1989 & 1992), corresponds to the upper surface of the Congost platform-top which he described as being characterised by local vadose diagenesis together with an abrupt change from shallow to deeper water facies, which can be correlated with submarine erosion in the basin.

The general characteristics of the Congost sequence boundaries (after Simo, 1992) are similar to all the others which have been recognised in the Upper Cretaceous strata of the Tremp basin by Simo (1986; 1989; 1992), where subaerial unconformities within the inner platform can be correlated with surfaces on the platform margin which show sharp transitions from shallow-water facies below to deeper-water facies above. These common features have been related to regional tectonic subsidence rates being much higher in the basin (50-100m/Ma) than they were in the inner platform area (20-30m/Ma)(Simo, 1989; 1992), since 3rd order global sea-level variations during the Upper Cretaceous were probably in the order of 30-45m/Ma (Haq et al., 1987), the inner platform areas would have been strongly effected by relative falls of sea-level, whereas the platform margins may not (Simo, 1989, 1992).

### 7.2.2 The forced regression model suggested by this study

In previous chapters of this thesis the sedimentology, diagenesis and depositional geometries of the Cenomanian to Coniacian carbonates of the Tremp basin have been discussed. Detailed investigation of the proposed mid-Turonian and mid-Coniacian sequence boundaries marking the lower and upper boundaries of the Congost sequence (after Simo, 1992) has revealed several features which lend support to the proposals of Simo (1986, 1989 & 1992)(see sections 7.3.2 & 7.3.5). However, conclusions drawn from both the geometrical and sedimentological study of the Congost platform in chapter 4 and the detailed diagenetic study of the Congost platform-top sediments in chapter 5 suggest that the Congost platform underwent two

separate phases of development which occurred under different regimes of accommodation space change (see sections 4.6 & 5.7.3). Sections 4.6 and 5.7.3 summarise the evidence for such a division of the Congost platform and discuss the important features of platform evolution during the two separate phases.

The interpretation that the two phases of Congost platform development occurred under different regimes of accommodation space change has important implications when they are considered within a sequence stratigraphic framework. As was proposed in sections 4.6 and 5.7.3, this together with the fact that well developed karst is seen to penetrate much deeper within the outcrops of the Congost platform associated with the first phase of its development than within those associated with the second suggests that the second phase of Congost platform development followed a forced regression which shifted platform productivity basinward, and down-slope of the previous platform margin (see Fig. 5.45). As discussed in section 4.6 the internal stacking patterns within the outcrop at Congost d'Erinya, which is interpreted to represent the second phase of Congost platform development, indicate that following the initial fall in relative sea-level which caused the proposed forced regression, there was a temporary increase in available accommodation space, which allowed this second phase of the platform to develop, prior to the continuation of the fall in relative sea-level which finally terminated the Congost platform and produced the karstification seen at Congost d'Erinya.

## 7.3 A new sequence stratigraphic framework

### 7.3.1 Introduction

The forced regression model, discussed above in section 7.2.2 (see also sections 4.6 & 5.7.3), which is proposed to explain the two separate phases of Congost platform development, necessitates certain modifications to the previous sequence stratigraphic framework for the Congost platform of Simo (1992)(see section 7.2.1). The forced regression model suggests that the Congost platform developed within two separate depositional sequences, albeit with one being on a much larger scale than the other. This section outlines a sequence stratigraphic framework for the Congost platform, which is compatible with the observations, interpretations and conclusions that have been provided by this thesis. As can be seen in Fig. 7.2, this new sequence stratigraphic framework for the Congost platform has two depositional sequences, an older Congost-A and a younger Congost-B sequence.

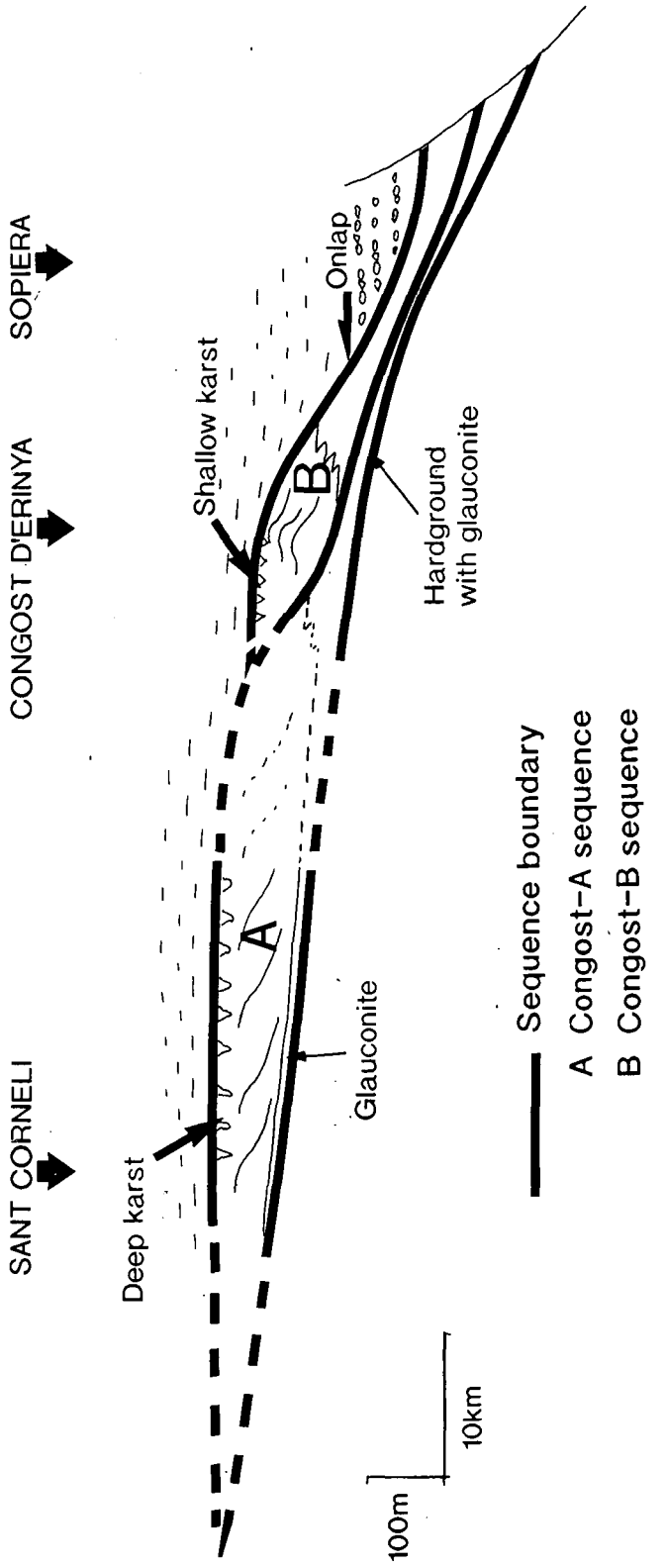


**Fig. 7.2.** A new sequence stratigraphic framework for the Congost platform which is compatible with the observations, interpretations and conclusions that have been provided by this thesis. See text for further explanation.

## 7.3.2 A mid-Turonian sequence boundary

### 7.3.2.1 Introduction

As mentioned in section 7.2.2, much evidence has been provided by the studies contained within this thesis to support the existence of the mid-Turonian sequence boundary as proposed by Simo (1986, 1989 & 1992). This mid-Turonian sequence boundary provided the transgressive surface ontop of which the Congost platform developed.

### 7.3.2.2 Evidence

In the Sierra del Montsec, which is the most southerly, ie landward, of the outcrops visited during this study, the upper part of the Pardina Limestone consists of a coarsening upward succession which is interpreted as a shoaling-upward succession that developed as a result of northward-directed platform progradation (see sections 3.2.3, 3.7.4 & 3.8 together with Fig. 3.2a)(after Soriano, 1992). This shoaling-upward succession is capped by a well-developed palaeosol (see sections 3.2.3, 3.7.4 & 3.8 together with Figs 3.2a, 3.3a, 3.3b & 3.3c).

Correlation of the upper surface of the Pardina Limestone across the basin has been made possible by the palaeontological studies of Gomez-Garrido (1981 & 1989), Caus and Gomez-Garrido (1989a & 1989b), Caus (pers. com.) and Gomez-Garrido (pers. com.). In the outcrops to the north of the Sierra del Montsec, ie basinward, the upper part of the Pardina is also interpreted to represent a shoaling-upward succession (see section 3.7.4). However, rather than being capped by a subaerial-exposure surface the top of the Pardina Limestone within these more distal locations is marked either by localised hardgrounds (see sections 3.4.2, 3.5.2, 4.4.3 & 4.5.3 together with Figs. 4.20a, 4.20b, 4.20c, 4.28a, 4.28b, 4.28c, 4.30a, 4.30b & 4.30c) and/or the occurrence of glauconite (see sections 3.3.3, 3.4.2, 4.4.3, 4.5.3, 4.5.4 & 4.6.1).

At all localities to the north of the Sierra del Montsec the Pardina Limestone is overlain by the Reguard Formation which is interpreted to represent a deeper-water facies (see sections 3.3.3, 3.7.4, 4.2.2, 4.4.4.1, 4.5.4.1 & 6.5).

### 7.3.2.3 Discussion and interpretation

As previously discussed in sections 3.7.4, 3.8, 4.4.3.3, 4.5.3.2 & 4.6, the localised hardgrounds and glauconite accumulations which mark the boundary

between the Pardina Limestone and Reguard Formation at many of the localities to the north of the Sierra del Montsec may well have resulted from a period of sediment starvation that was related to the subaerial exposure of the platform, as evidenced by the palaeosol in the Sierra del Montsec sections. The deposition of the deeper-water facies Reguard Formation above the Pardina Limestone at all localities to the north of the Sierrra del Montsec is interpreted to have resulted from a major transgressive event which would also have resulted in a certain amount of sediment starvation prior to the renewed platform progradation which followed.

The features which are displayed by the upper surface to the Pardina Limestone, in particular the localised subaerial-erosion surface and its correlatable conformity in the form of local hardgrounds and glauconite accumulations, together with the fact that it is overlain by a transgressive unit, suggest that this surface represents a depositional sequence boundary.

## 7.3.3 The Congost-A sequence

### 7.3.3.1 The lowstand and transgressive systems tracts

The Reguard Formation which overlies the mid-Turonian sequence boundary at the top of the Pardina Limestone on the shelf, is interpreted as a starved deeper-water facies which was being deposited basinward of the advancing Congost-platform (see section 4.2.2.2). As discussed above in section 7.3.2.3, glauconite accumulations and hardgrounds which are present at the boundary between the Pardina Limestone below and the Reguard Formation above (see also sections 3.3.3, 3.4.2, 3.5.2, 4.4.3, 4.5.3, 4.5.4 & 4.6.1 together with Figs. 4.20a, 4.20b, 4.20c, 4.28a, 4.28b, 4.28c, 4.30a, 4.30b & 4.30c) are interpreted to indicate a period of sediment starvation which resulted from the subaerial exposure of the inner shelf and following transgressive episode.

These observations suggest that following the development of the mid-Turonian sequence boundary significant sediment accumulation did not take place again until carbonate production recovered and the progradation of the Congost platform began. Hence, it would appear that the lowest part of the Reguard Formation represents the transgressive systems tract (TST) of the Congost-A sequence (see Fig. 7.2). In effect it is a condensed section and the transgressive surface coincides with the sequence boundary.

### 7.3.3.2 The highstand systems tract and upper sequence boundary

As discussed in section 4.6, the first major phase of Congost platform development was one of rapid progradation. This phase of rapid progradation covered a distance of at least 15km and is interpreted to have been brought to an end by the rapid migration of skeletal sands over the entire platform interior, which was in turn followed by a prolonged period of subaerial exposure. Although sedimentological and diagenetic features within this part of the platform suggest small-scale fluctuations in relative sea-level during the progradation, the large-scale geometry of this part of the platform suggest that the progradation occurred during a period when there was very little overall increase in accommodation space (see sections 4.2.3.5, 4.2.4.3, 4.2.4.4, 4.2.5, 4.3.3.1, 4.6 & 5.7.2).

The progradational nature of this phase in the development of the Congost platform and the fact that it is interpreted to have occurred after a major transgressive event, when there was very little overall increase in accommodation space suggest that in sequence stratigraphic terms it can be interpreted to represent the highstand systems tract (HST) of the Congost-A sequence (see Fig. 7.2).

As mentioned previously the karst which is observed to penetrate down into the top of this part of the Congost platform is interpreted to have been initiated by a fall in relative sea-level that caused a forced regression of the Congost platform. Hence, the subaerial exposure surface at the top of the part of the Congost platform which is exposed in the region of the Sant Corneli and Santa Fe folds is proposed to represent the upper sequence boundary to the Congost-A sequence. Following on from this forced regression model, this subaerial exposure is proposed to have a correlative conformity which runs underneath the lagoon and fringing reef complex of the Congost-B sequence which is exposed in Congost d'Erinya (see Fig. 7.2).

In an attempt to investigate the relative ages between the platform carbonates of the proposed Congost-A HST and those of the proposed Congost-B sequence, samples taken from the platform facies and deeper water facies of the Congost platform in the outcrops around the Sant Corneli anticline were compared biostratigraphically with samples collected from similar facies within the outcrop of the Congost platform in Congost d'Erinya (this biostratigraphic work was carried out by Esmeralda Caus of the Universitat Autonoma de Barcelona). Unfortunately the biostratigraphy based on foraminifera, is not sufficiently refined to be able to confirm that the Congost-A sequence is older than the Congost-B sequence.

### 7.3.4 The Congost-B sequence

The proposition that the outcrop of the Congost platform in Congost d'Erinya is part of a separate depositional sequence from the rest of the platform (see sections 7.2.2, 7.3.1) is slightly unfortunate as the Congost sequence of Simo (1986; 1989 & 1992) derives its name from the outcrop in Congost d'Erinya. However, as mentioned in section 7.3.1, for the purposes of this thesis and to avoid confusion the oldest of these proposed sequences which is interpreted to be represented by the transgressional Reguard Formation together with the overlying progradational phase of the Congost platform has been named the Congost-A sequence, while the sequence proposed to be represented by the outcrop in Congost d'Erinya, which is interpreted to have developed down slope from the previous platform margin as a result of a forced regression, has been named the Congost-B sequence (see Fig. 7.2).

The internal stacking patterns and exposure surfaces of the proposed Congost-B sequence are discussed in detail in sections 4.4.5, 4.6 and 5.7.3, where they are interpreted to indicate that following the initial fall in relative sea-level which ended the development of the proposed progradational HST of the Congost-A sequence, there was a period when accommodation space increased again to allow the development of the Congost-B sequence down slope from the margin of the exposed Congost-A sequence, prior to renewed relative sea-level fall which caused the demise of the Congost platform as a whole through further karstification (see Figs. 5.45 & 7.2).

### 7.3.5 An Upper Coniacian transgression

#### 7.3.5.1 Brief summary of evidence

At all localities visited during this study the upper boundary of the Congost platform-top is easily recognisable as light grey, lagoonal wackestones with rudists and corals, together with lens-shaped beds of skeletal grainstone which in places display well developed karst features. These contrast sharply with the brown-coloured, clay-rich packstones and wackestones containing calcispheres, fine-grained shell debris, planktonic foraminifera, sponge spicules, silt-grade quartz and localised accumulations of oyster fragments of the Anserola Formation (deep-shelf facies of the Sant Corneli platform) which overlie them (see sections 4.2.4.2, 4.2.4.3, 4.3.2.2 & 4.4.5.3).

In the succession of slope and basinal sediments at Sopiera, there is a pronounced difference between the strike direction of the Upper Coniacian to Santonian-aged Sant Corneli Breccia, which is the basinal equivalent of the Anserola Formation, and that of the underlying succession of Cenomanian to early-Coniacian sediments (Sant Corneli Breccia, Pardina Limestone and the Reguard Formation), which has been interpreted as an onlap surface (after Simo et al., 1985)(see section 6.6.2.1).

#### 7.3.5.2 Discussion and interpretation

The presence of the clay-rich, packstones and wackestones of the Anserola Formation, which are interpreted to represent the deep-shelf facies of the Upper Coniacian to Santonian-aged Sant Corneli platform, resting directly on top of the subaerial-exposure surface at the top of the Congost platform (see sections 4.2.4.2, 4.2.4.3, 4.3.2.2 & 4.4.5.3), is interpreted to indicate that, following the fall in relative sea-level which was responsible for the demise of the Congost platform, the Tremp basin experienced a major transgressive event during the early part of the Upper Coniacian. Hence, as proposed by Simo (1986, 1989 & 1992), the lower part of the Anserola Formation can be interpreted as the transgressive systems tract of an Upper Coniacian to Santonian-aged depositional sequence which overlies the Congost platform and its associated basinal succession (see Figs. 7.1 & 7.2).

### 7.3.6 Possible mechanisms of relative sea-level change: A discussion

#### 7.3.6.1 The mid-Turonian sequence boundary and transgression

As discussed earlier (section 7.2.1) the fact that the subaerial exposure associated with the mid-Turonian sequence boundary is limited to the inner shelf has been interpreted by Simo (1989 & 1992) to have been a result of the interplay between a 3rd-order eustatic fall in sea-level and variations in tectonic subsidence between the basin and the more stable areas of the inner shelf. However, the subaerial exposure of the inner shelf does not necessarily imply that there was a fall in eustatic sea-level.

The tectonically-active nature of the Tremp basin during the Upper Cretaceous (see sections 2.2 & 2.3), together with the evidence provided within the Upper Cretaceous stratigraphy of active normal faulting (see sections 3.7.2.2, 6.3.4, 6.5.3.2(iii), 6.5.3.3, 6.6.3.3, 6.6.3.4 & 6.7) suggest that the tilting and foot-wall uplift

associated with extensional block faulting could well have been a possible mechanism behind the lowering of relative sea-level within the inner platform area. It has also been suggested that some tectonic uplift of the inner platform area may have occurred due to the effects of diapirism of the underlying Triassic evaporites Van Hoorn (1970).

Several lines of evidence have been presented in earlier parts of this thesis to indicate that there was a strong tectonic influence either during or soon after the mid-Turonian transgressive event which deposited the relatively deeper-water facies of the early part of the Reguard Formation over the top of the Pardina Limestone on the shelf. These include: 1) the fact that the geometry of the Congost platform suggests that it prograded onto a sea-floor which was sloping in a basinward direction (see sections 4.2.3.2, 4.2.3.5 & 4.6), whereas, the underlying Pardina Limestone and lagoonal sediments of the Santa Fe platform-top are interpreted to have possessed relatively horizontal surfaces of deposition (see sections 3.7.2.1 & 3.7.4); 2) the evidence within the outcrop at Peracals of a major slope failure and down-slope slide event that occurred soon after the development of a hardground at the top of the Pardina Limestone (see sections 4.5.4.2 & 4.6); and 3) the outcrop of the Reguard Formation near Sopiera which shows evidence of an active fault scarp during the deposition of sediments immediately above the mid-Turonian sequence boundary (see section 6.5).

It would appear from the evidence provided by this study that the mechanism behind the formation of the mid-Turonian sequence boundary and the major transgressional episode which followed may well have been tectonic. However, modelling of thermal subsidence and its comparison to estimates of palaeo-water-depth, led Simo (1989) to suggest that tectonic subsidence alone could not account for the thickness of some of the Upper Cretaceous units and are attributed the additional space needed to eustatic sea-level movements.

### 7.3.6.2 The Congost-A and Congost-B depositional sequences

Evidence provided in earlier sections suggests that although there was very little variation in overall available accommodation space during the development of the HST of the Congost-A sequence, small-scale cyclic fluctuations in relative sea-level did occur (see sections 4.2.3.5, 4.2.4.3, 4.2.4.4, 4.2.5, 4.3.3.1, 4.6, 5.7.2, 7.3.3.2). The most likely explanation for such a cyclic variation in relative sea-level would be a variation in eustatic sea-level, as a tectonic mechanism is unlikely to have produced such a regular pattern. Such a small scale stratigraphic cyclicity has been recognised within many platform successions, in the form of parasequences which are

often considered to have been caused by perturbations of the Earth's orbit (Read & Goldhammer, 1988; Hinov & Goldhammer, 1988; Goldhammer et al., 1991). The shortest periodicity of such orbital cycles is considered to be approximately 18 - 21 ka.

The depth of karst penetration within the platform carbonates of the proposed HST to the Congost-A sequence indicates that the major fall in relative sea-level which is proposed to have been responsible for the development of the upper sequence boundary to the Congost-A sequence and the forced regression of the Congost platform must have had a magnitude of at least 40 metres (see sections 4.3.3.2, 4.6 & 5.7.3 together with Figs 5.45 & 7.2). Although there is no direct evidence to suggest whether this fluctuation in relative sea-level was caused by either local tectonics or global processes, it seems unlikely that a fall in relative sea-level of such magnitude, which effected the whole area of the platform top could have been instigated by the extensional tectonic regime that was operating in the southern Pyrenees during the Upper Cretaceous (see sections 2.2, 2.3 & 2.4). However, the short-lived increase in accommodation space which halted the major fall in relative sea-level and forced regression of the Congost platform (see sections 4.4.5 & 4.6), in order to allow the development of the Congost-B sequence, may well have been in response to tectonic activity.

As discussed in section 6.7 the onlapping lower boundary and sedimentological characteristics of the Upper Cenomanian to Santonian-aged Sant Corneli breccia, suggest that there was a significant increase in the depositional palaeoslope between the Lower and Upper Coniacian. This, together with the fact that certain sedimentological characteristics of the Sant Corneli Breccia suggest that the Tremp basin experienced active extensional faulting during the Upper Coniacian (see sections 6.6.3.3, 6.6.3.4 & 6.7) indicates that, as for the previous major transgressional episode during the mid-Turonian, the mid-Coniacian transgression which allowed the deposition of the deep-shelf facies of the Anserola Formation over the entire area of the previously exposed lower Coniacian shelf, may, at least in part, have been a result of regional extensional tectonic activity.

### 7.3.6.3 Summary

As would be expected within a tectonically-active basin, it would appear that the variations in available accommodation space which led to the sequence stratigraphic development of the Congost platform, were controlled by both local tectonic activity and global eustatic processes. It would also appear to be the case that the major transgressive events which are a distinctive feature of the Upper Cretaceous

stratigraphy within the Tremp basin, as they created a series of backsteping carbonate platforms, were controlled by major tectonic events.

## 7.4 Brief Summary

In this chapter it has been proposed that the two separate phases in the development of the Congost platform which were discussed in sections 4.6 and 5.7.3 represent two separate depositional sequences. These two depositional sequences form the basis of a new sequence stratigraphic framework for the Congost platform which is shown in Fig. 7.2.

Close consideration of sedimentological and geometrical evidence has led to the suggestion that the variations in available accommodation space which led to this sequence stratigraphic development of the Congost platform were controlled by a combination of local tectonic and global eustatic processes.

# Chapter 8
# General conclusions

## 8.1 The Santa Fe and Pardina Limestones

Upper Cretaceous deposition in the Tremp basin began with the development of the Cenomanian-aged Santa Fe platform, consisting of a wide low-energy lagoon that was protected from the open sea by a relatively narrow platform-margin belt of skeletal shoals and boundstones which developed at the site of an active fault scarp. The development of the Santa Fe platform appears to have been effected by fluctuations in both relative sea-level and global oceanic productivity.

The Pardina Limestone, with its dominantly wackestone texture and low faunal diversity, abundant calcispheres and planktonic foraminifera, overlies the Santa Fe Limestone both in the inner platform and at the platform margin, and is interpreted to represent a deeper-water facies which was deposited over the whole of the Santa Fe platform area as a result of a rise in relative sea-level. The deposition of the Pardina Limestone may in fact be a result of a continuation of the deepening event which is recorded by the upper Santa Fe Limestone. The upper section of the Pardina Limestone, with its increasing shell fragment and benthic faunal assemblage, is interpreted as a shoaling-upward succession representing platform recovery and progradation. Within the succession exposed in the most southerly outcrop, this shoaling-upward succession culminated in subaerial exposure, while farther to the north localised hardgrounds developed as a result of sediment starvation. It was upon this foundation that the Congost platform developed.

## 8.2 Congost platform evolution

It is proposed that the development of the Congost platform followed a period of major transgression, during or soon after which, basinward tilting of the sea-floor occurred.

Sedimentological and geometrical characteristics of the Congost platform suggest that its development can be divided into two phases. The first phase appears to have begun with the development of a shallow lagoon which developed at the edge of a gently sloping shelf and was semi-protected from the open sea by mobile skeletal sand shoals. It is postulated that skeletal debris derived from this shallow lagoon via

tidal channels and wind action began to prograde out onto the gently sloping shelf to form clinoforms. As this debris prograded it would have filled the available accommodation space and enabled the shallow lagoon and shoal system to move basinward. The platform continued to prograde basinward and gradually gained in height, as it filled the space provided by the increasing water depth above the sloping basin floor. The rate of clinoform progradation during this first phase of Congost platform development was very rapid compared to the accumulation rate of the pelagic Reguard Formation sediments which were being deposited away from the reaches of all but the finest wind-blown platform material.

This first phase of rapid progradation appears to have been a cyclic process, suggesting that the platform was effected by small-scale fluctuations in relative sea-level. These relative sea-level fluctuations also effected the shallow lagoons of the platform top. However, during the entire period of this rapid progradation there was very little increase in overall accommodation space. This phase of rapid progradation covered a distance of at least 15km and created a platform which was probably over 30km wide.

This first phase of platform progradation appears to have been brought to an end by the rapid migration of skeletal sands over the entire platform interior, indicating an increase in energy on the platform top. This would suggest that the rate of carbonate production had been exceeded by the rate of increase in accommodation space.

The final chapter in this first phase of Congost platform development, however, appears to have been a period of subaerial exposure related to a major fall in relative sea-level which had a magnitude of at least 40 metres. During this major fall in relative sea-level if the platform were to continue growing it would have been forced basinward. It is proposed that the results of this forced regression can be seen in the platforms most basinward outcrop at Congost d'Erinya.

Following the forced regression the second phase of Congost platform evolution involved the growth of coral reefs at the platform margin and the development of a geometry which shows aggradation as well as progradation. The geometry and stacking pattern of the reefs and associated lagoonal sediments indicate that aggradation decreased with time. This suggests that although this second phase of platform evolution occurred during a time of increasing accommodation space, the rate of increase in accommodation space was decreasing with time. In fact the erosional surface marking the top of the stacked reefs could be indicating that this decrease in the rate of accommodation space creation may have culminated in a period of platform exposure. The platform recovered again with the deposition of more shallow-water lagoonal sediments. However, the development of the Congost

platform finally came to an end during a period of subaerial exposure which produced an intersecting network of speleo-cement filled dissolution pipes and cavities marking the top of the lagoonal sediments at Congost d'Erinya.

## 8.3 Congost platform diagenesis

The diagenetic features of the Congost platform-top sediments suggest that the sediments from both phases in the development of the platform have undergone a broadly similar pattern of syn- and post-depositional events.

In their approximate order of occurrence, these events are: 1) micritisation and early marine cementation together with intense boring activity; 2) the neomorphic replacement of some aragonitic tabulae within rudists, particularly at their edges (some of which occurred during the precipitation of cements from the lagoonal waters); 3) extensive dissolution, neomorphism and cement precipitation, which occurred as a result of numerous short duration exposure events, under humid climatic conditions; 4) the development of karst features, which mark the upper surface of Congost platform sediments at all localities and penetrate down into the platform-top strata (characteristics of the cements within the karstic pipes suggest a palaeoclimate with high rainfall); 5) the precipitation of zoned-luminescent calcite spar within any remaining pore-space during shallow burial; and 6) the passage of burial fluids through conduits which were provided by some of the karstic pipes and cavities.

Differences in the early diagenesis between the Congost platform-top sediments from the outcrop at Congost d'Erinya and those from the outcrops in the region of the Sant Corneli and Santa Fe folds suggest that: 1) there may have been slight differences in the pore-fluid flow regimes between the lagoonal environments represented by the two groups of outcrops; and 2) the sediments which are now exposed in the Sant Corneli group of outcrops were exposed to near-surface meteoric fluids more frequently and for much longer periods of time than their counterparts which are now outcropping in Congost d'Erinya. These features together with the fact that the karstic pipes and cavities which occur along the top surface of the Congost platform penetrate much deeper into the sediments now outcropping in the region of the Sant Corneli and Santa Fe folds than they do into the sediments that outcrop in Congost d'Erinya, are considered as further evidence of the forced regression model proposed for the two phase development of the Congost platform.

## 8.4 The slope succession at Sopiera

Deposition of the Upper Cretaceous slope sediments began during the Lower to Middle Cenomanian with the accumulation of 350 metres of interbedded fine-grained marls and limestones which make up the Sopiera Marls. The Lower to Middle Cenomanian-age of these sediments suggests that they represent the basinal equivalent of the lower part of the Santa Fe platform (see Fig. 3.9).

The next phase of sedimentation which is documented within the succession around Sopiera was the deposition of the Santa Fe Breccia; a basinward-thickening wedge of Upper Cenomanian-age, comprising chaotically-bedded pelagic mudstones, channellised conglomerates and megabreccia units which represent the basinal equivalent of the upper part of the Santa Fe platform and downlap onto the Sopiera Marls. The allochthonous debris within the Santa Fe Breccia was shed from the Santa Fe platform margin prior to the subaerial exposure event which is proposed to have occurred towards the end of the Upper Cenomanian. Possible mechanisms which may have been responsible for the apparent massive platform-margin collapse and slope failure which produced such a succession of allochthonous debris include seismic activity, associated with the fault which is proposed to have been present close to the site of the platform margin, and differential compaction, as the platform margin prograded out over the muddy and probably poorly-cemented basinal sediments.

The Pardina Limestone which overlies the Santa Fe breccia comprises an approximately 90 metre thick unit of Upper Cenomanian to Middle Turonian-aged wackestones and packstones whose low faunal diversity is interpreted to be partly the result of a eutrophication of the platform top. This probably correlates with a world-wide oceanic event at this time.

Following the deposition of the Pardina Limestone the succession of slope sediments at Sopiera recorded a period of renewed down-slope slide events and influx of allochthonous debris via channellised debris flows during the deposition of the Upper Turonian to Lower Coniacian-aged Reguard Formation. This renewed activity upon the slope is interpreted to have been caused by seismic activity and resulted in the deposition of a series of slide units consisting of chaotically-bedded pelagic slope facies sediments which are capped by channellised conglomerates. The channellised conglomerates are interpreted to have resulted from the re-deposition of debris from talus aprons which were accumulating at the foot of an active fault scarp (or scarps), exposing the earlier deposited Cenomanian to Coniacian succession higher up the slope.

The down-slope sliding and mass-flow events continued during the Upper Coniacian to Santonian and resulted in the deposition of the Sant Corneli Breccia

which comprises an onlapping wedge of chaotically-bedded pelagic slope facies sediments together with tapered megabreccia sheets. Clast types within these breccia sheets suggest that a similar 'active fault scarp and talus apron' system to that proposed to have been responsible for providing the constituents of the channellised debris flow deposits of the Reguard Formation, was in operation during the deposition of the Sant Corneli Breccia. The onlapping lower boundary of the Sant Corneli Breccia, and its contrasting sedimentological features with the underlying Reguard Formation suggest that there was an increase in the depositional palaeoslope between the Lower and Upper Coniacian. This increase in palaeoslope is interpreted as a further expression of the tectonically-active nature of the Tremp basin during the Upper Cretaceous.

## 8.5 A sequence stratigraphic framework for the Congost platform

It has been proposed that the two separate phases in the development of the Congost platform represent two separate depositional sequences. These two depositional sequences form the basis of a new sequence stratigraphic framework for the Congost platform which is shown in Fig. 7.2.

Close consideration of sedimentological and geometrical evidence has led to the suggestion that the variations in available accommodation space which led to this sequence stratigraphic development of the Congost platform were controlled by a combination of local tectonic and global eustatic processes.

## 8.6 Final points

This study has shown that it is possible to interpret the geometry and evolution of carbonate platforms in terms of their response to variations in relative sea-level.

The study of Congost platform diagenesis has also shown that diagenesis is a useful tool for the identification of sequence boundaries.

During this study diagenesis has also been shown to be a useful aid for assessing the regime of accommodation space change under which particular packages of sediment were deposited. This fact indicates that, as was suggested by Tucker (1993), the diagenetic processes acting in the various systems tracts of a depositional sequence are different.

## 8.7 Future work

If the biostratigraphy for the Upper Cretaceous of the Tremp basin becomes further refined then possible future work could involve a detailed biostratigraphic analysis to assess the validity of the sequence stratigraphic model proposed for the Congost sequence during this study by determining the relative ages between the proposed Congost-A sequence and the proposed Congost-B sequence.

It would also be interesting to test further the usefulness of diagenesis as a predictive tool in sequence stratigraphy by studying the early diagenesis of some of the other carbonate platforms in the Tremp basin.

A much more detailed study of the Upper Cretaceous slope sediments at Sopiera would also be interesting, in particular the complicated diagenetic history of some of the allochthonous clasts, as this could provide further information as to the evolution of the Santa Fe platform margin and perhaps detail further the tectonic activity proposed to have been effecting slope deposition.

# Appendix 1
# Graphic logs and location of samples

During this study, numerous stratigraphic sections through the Cenomanian to Coniacian carbonates of the Tremp basin were measured and described in detail. The following are simplified versions of a selection of these logs, which have been marked to show the locations from which samples for petrographic, biostratigraphic and stable isotope study were collected.

The grid references (GR) given for each of these logs have been taken from the following 3 Cartografia Militar de Espana, serie L, 1:50,000 scale maps: 1) the Tremp sheet, 33-11 (252); 2) the Organya sheet, 34-11 (253); and 3) the Isona sheet, 33-12 (290). These maps are readily available in shops around the Tremp area.

**1) Logs AA, AZ and AY (locality 1c, Fig. 4.1)**

Located In the cliffs to the north of Abella de la Conca. The section runs up the southeastern corner of the prominent peak (height 1555m asl.) on the south side of the coll below Gallinove. This log shows the Santa Fe Limestone (0-10m), the Pardina Limestone (10-48m), the Reguard Formation (aprox. 48-52m) and the lower part of the Congost platform clinoform unit. GR 412711, Tremp sheet.

**2) Log M2 (locality 1e, Fig. 4.1)**

Located on the southwest side of Gallinove (height 1689m asl.). The section begins from the coll below Gallinove at a height of 1500m. This log shows the upper part of the Santa Fe Limestone (aprox. 0-8m), the Pardina Limestone (aprox. 8-38m) and the Congost platform clinoform unit. GR 410720, Tremp sheet.

**3) Log B2 (locality 1h, Fig. 4.1)**

Located in the cliffs to the north of Boixols. The section begins at the base of the cliff on the east side of the peak with a height of 1698 metres (asl.) which marks the western edge of the Sierra de San Juan. This log shows a section through part of the Congost platform clinoform unit. GR 508732, Organya sheet.

**4) Log AH (locality 1a, Fig. 4.1)**

Located in the small valley to the northeast of Casa Borrell. This log shows a section through the upper part of the Congost platform (0-19m) and the base of the Anserola Formation. GR 410701, Isona sheet.

**5) Log AX (locality1a, Fig. 4.1)**

Located in the small valley to the northeast of Casa Borrell. This log shows a section through the upper part of the Congost platform (0-14m) and the base of the Anserola Formation. GR 410701, Isona sheet.

**6) Log CA (locality 1f, Fig. 4.1)**

Located on the northern slopes of Gallinove. This log shows a section through the top few metres of the Congost platform (0-6m) and the base of the Anserola Formation. GR 410729, Tremp sheet.

**7) Log CB (locality 1f, Fig. 4.1)**

Located on the northern slopes of Gallinove. This log shows the upper part of the Congost platform (0-23m) and the base of the Anserola Formation. GR 412730, tremp sheet.

**8) Log OY (locality 2, Fig. 4.1)**

Located in a river valley (dry in summer) to the northwest of Ortenada. The river valley is reached via a small track from the village. This section begins in the river bed and shows an inverted section through the base of the Anserola Formation (0-24m) and the top part of the Congost platform. GR 385793, Tremp sheet.

**9) Log OZ (locality 2, Fig. 4.1)**

Located in a river valley (dry in summer) to the northwest of Ortenada. The river valley is reached via a small track from the village. This section begins at the base of the prominent cliff on the north side of the track as it winds down to the river and shows an inverted section through the upper part of the Congost platform. GR 384793.

**10) Logs F1, F2, F3 and F4 (locality 3, Fig. 4.1)**

Located along the west side of Congost d'Erinya, which is a deep gorge cut by the Flamicell River to the northwest of La Pobla de Segur. This section begins by the side of the C144 road at the northwestern end of the gorge. This log shows the top part of the Pardina Limestone (0-10m), the Reguard Formation (10-240m aprox.), the Congost platform (aprox. 240-420m) and the base of the Anserola Formation. GR 299848-300845, Tremp sheet.

**11) Log FZ (locality 3, Fig. 4.1)**

This section is located in the upper part of the cliff along the western side of Congost d'Erinya. This log shows a section through the upper part of the Congost platform (0-23m) and the base of the Anserola Formation. GR 300845, Tremp sheet.

**12) Log FSP (locality 3, Fig. 4.1)**

This section is located at the northwestern end of Congost d'Erinya. This section begins by the side of the C144 road and shows the Santa Fe Limestone (0-12m aprox.), the Pardina Limestone (aprox. 12-22m) and the basal part of the Reguard Formation. GR 299848, Tremp sheet.

**13) Log PA (locality 4, Fig. 4.1)**

This section is located on the western side of the small village of Peracals which is situated in the mountains, approximately 7km to the north of La Pobla de Segur. The section begins at the side of a goat track which leads westward from the village and shows the upper part of the Santa Fe Limestone (0-8m?), the Pardina Limestone (?8-17m) and the lower part of the Reguard Formation. GR 355860, Tremp sheet.

# Key for logs in appendix 1


Dissolution pipes and cavities


Bored hardground


Iron-oxide nodules


Rudists


Rudist fragments


Coral colonies


Brachiopods


Echinoderms


Gastropods


Coraline algae


Bivalves


Bryozoans


Sponge spicules


Peloids


Intraclasts


Calcispheres


Miliolids


Prealveolina


Other foraminifera


Silt grade quartz


Glauconite

Textural classification (Dunham, 1962)

M Mudstone

W Wackestone

P Packstone

G Grainstone

B Boundstone

Grain roundness (Pettijohn et al., 1973)

rnd. Rounded

sbrnd. Subrounded

sbang. Subangular

ang. Angular

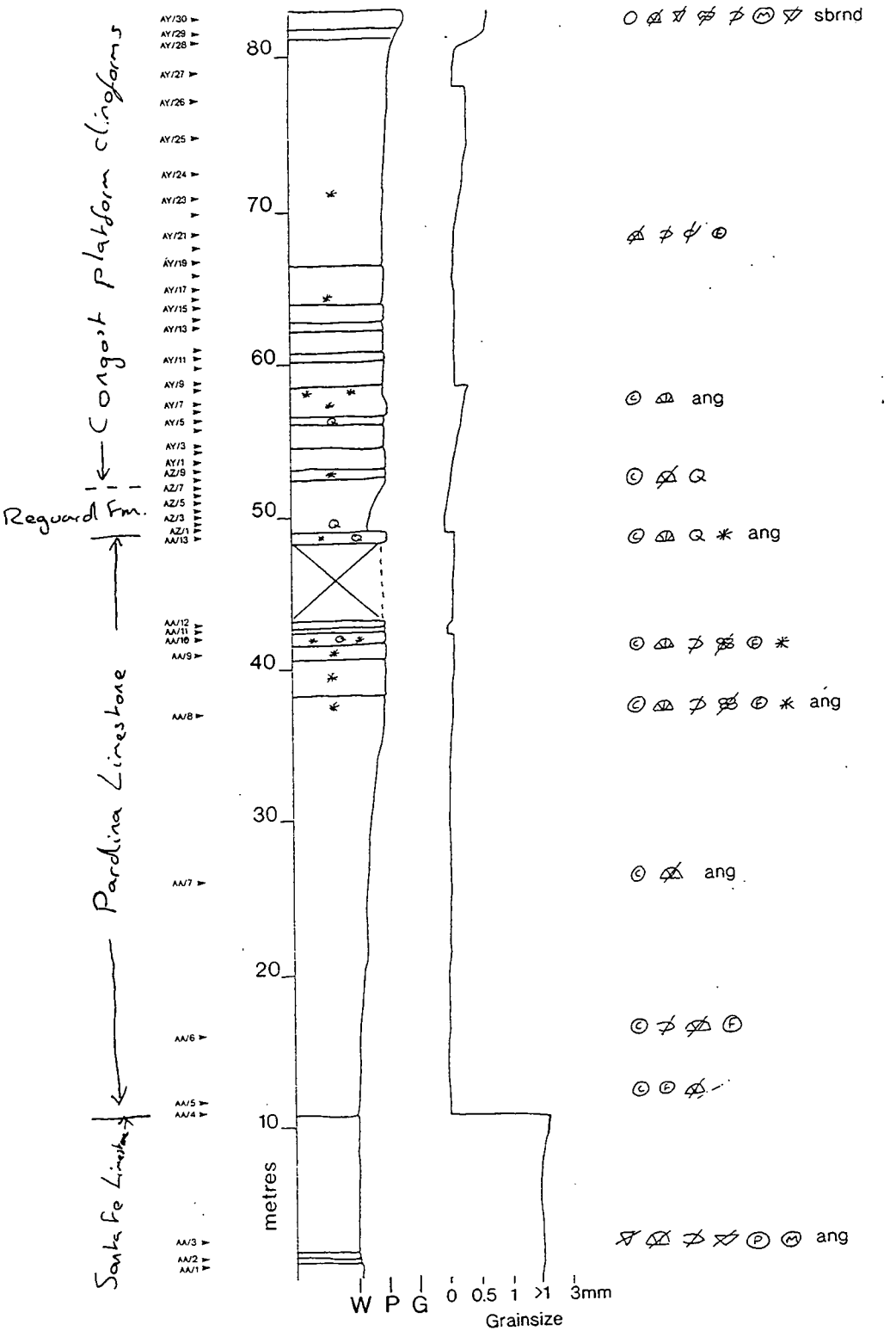


# 1) Logs AA, AZ and AY

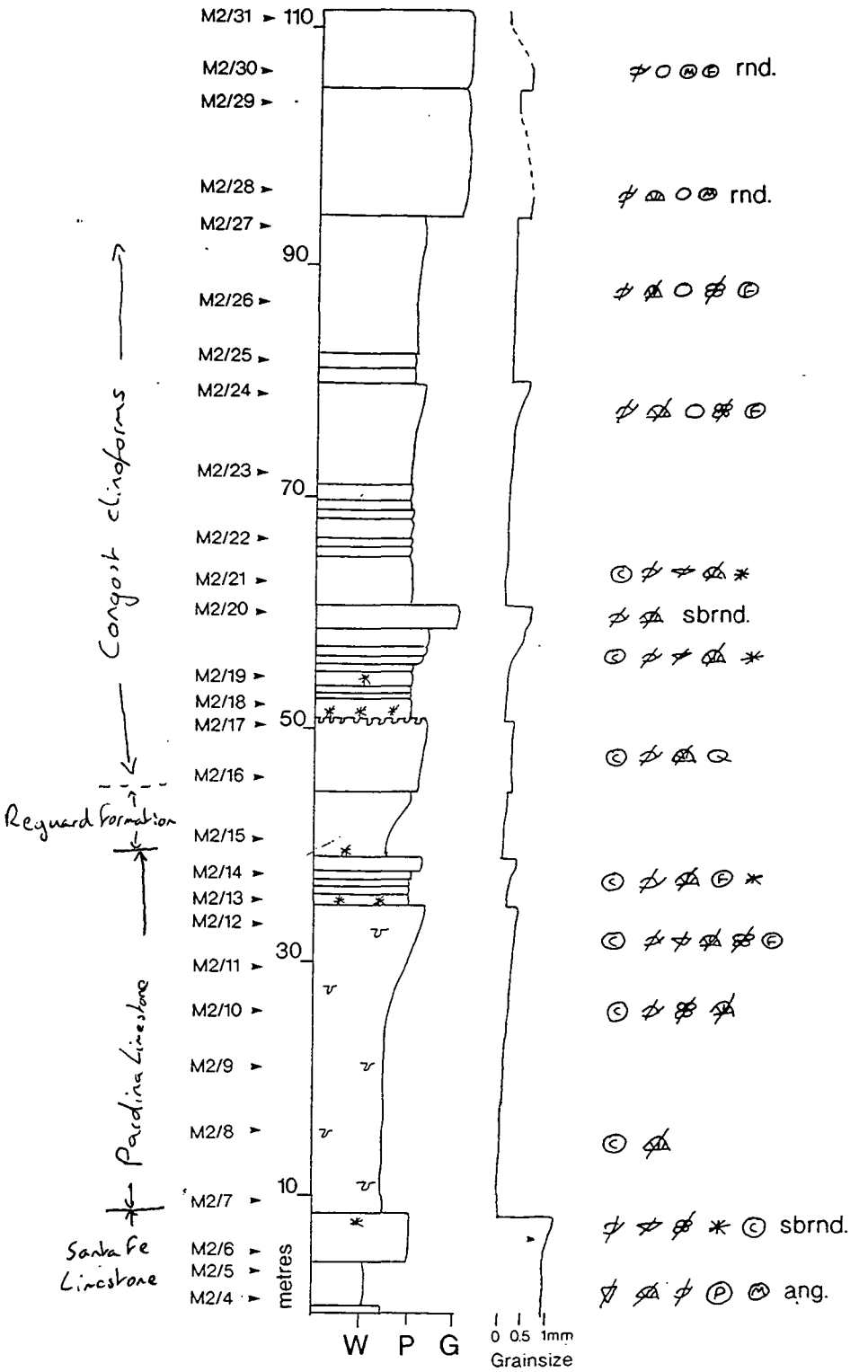
M2/31
M2/30
M2/29
M2/28
M2/27
M2/26
M2/25
M2/24
M2/23
M2/22
M2/21
M2/20
M2/19
M2/18
M2/17
M2/16
M2/15
M2/14
M2/13
M2/12
M2/11
M2/10
M2/9
M2/8
M2/7
M2/6
M2/5
M2/4
110
90
70
50
30
10
metres
Congost clinoforms
Regnard formation
Pardina Limestone
Santa Fe Limestone
W P G
0 0.5 1mm
Grainsize
rnd.
rnd.
sbrnd.
sbrnd.
ang.

## 2) Log M2

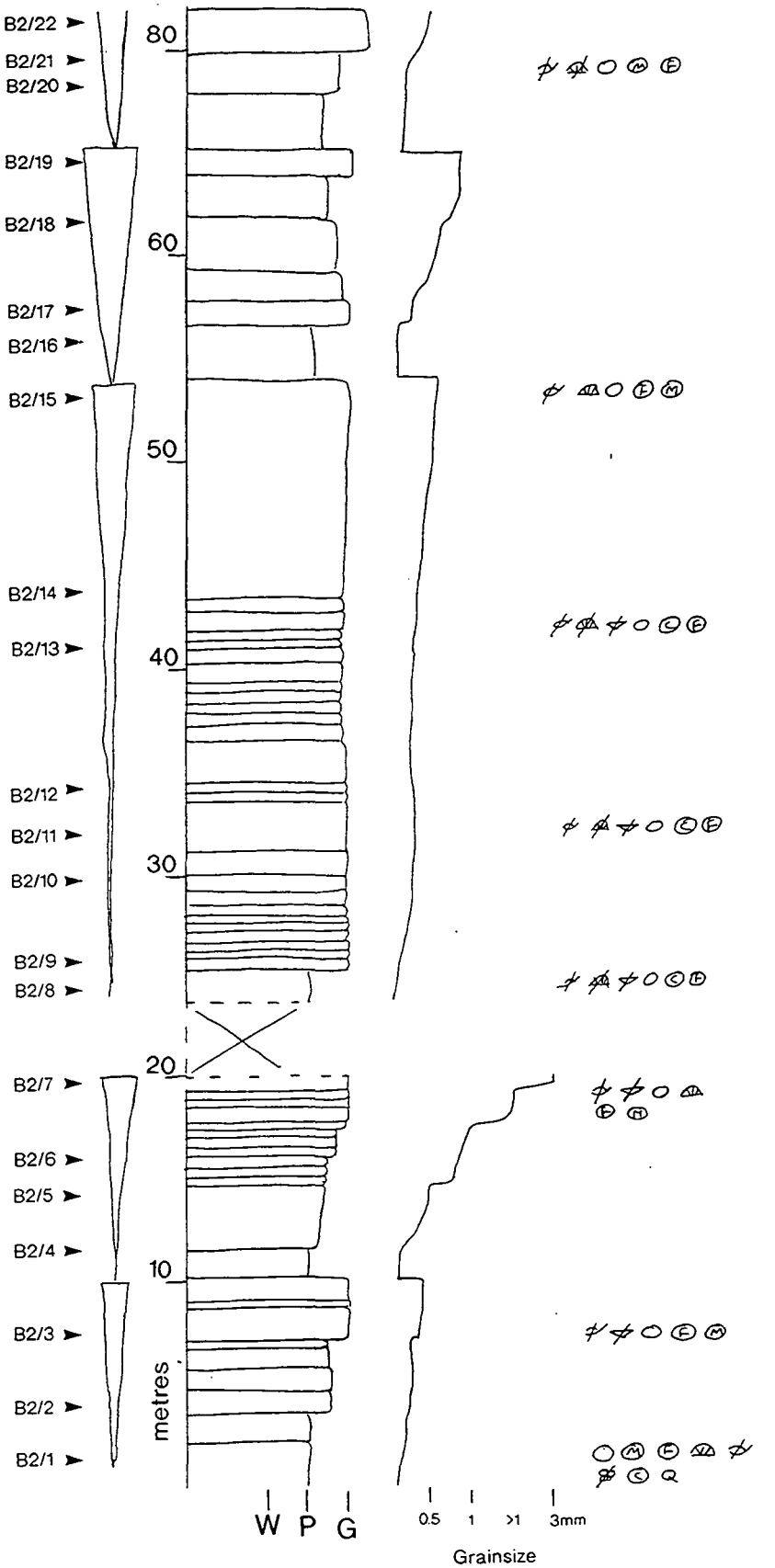
B2/22
B2/21
B2/20
B2/19
B2/18
B2/17
B2/16
B2/15
B2/14
B2/13
B2/12
B2/11
B2/10
B2/9
B2/8
B2/7
B2/6
B2/5
B2/4
B2/3
B2/2
B2/1
80
60
50
40
30
20
10
metres
W P G
0.5 1 >1 3mm
Grainsize

# 3) Log B2

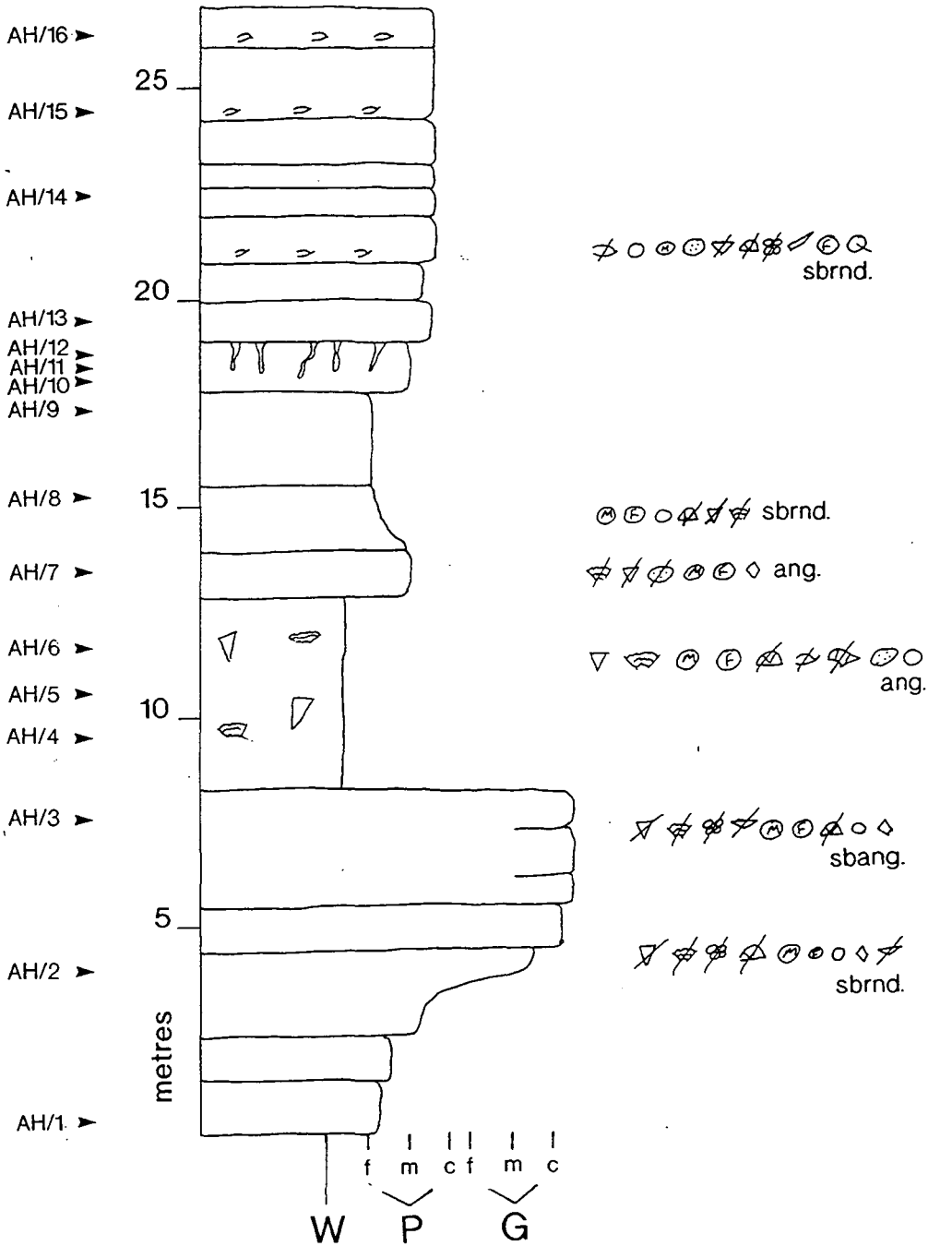
AH/16
AH/15
AH/14
AH/13
AH/12
AH/11
AH/10
AH/9
AH/8
AH/7
AH/6
AH/5
AH/4
AH/3
AH/2
AH/1
25
20
15
10
5
metres
sbrnd.
sbrnd.
ang.
ang.
sbang.
sbrnd.
f m c f m c
W P G

4) Log AH

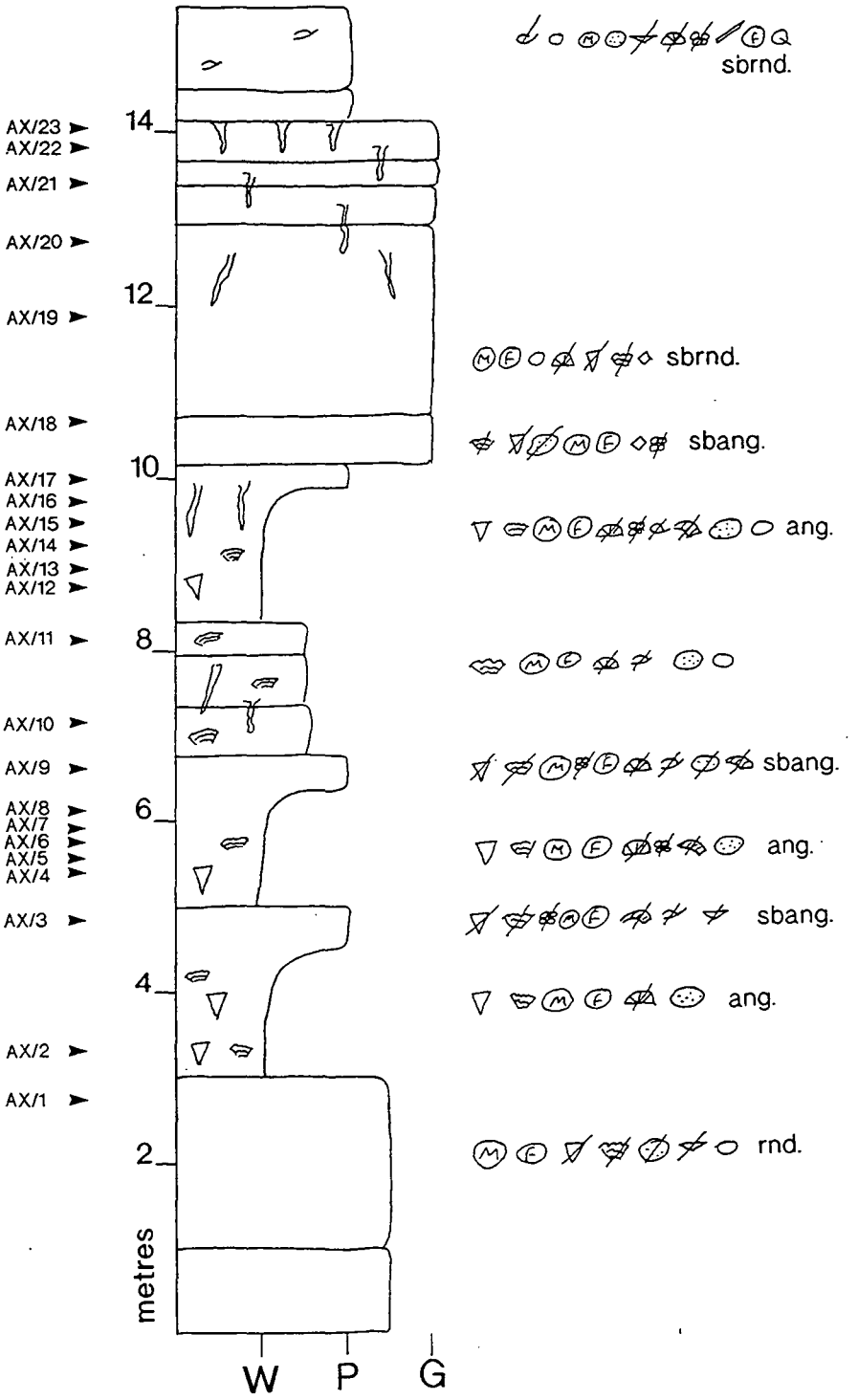
sbrnd.
sbrnd.
sbang.
ang.
sbang.
ang.
sbang.
ang.
rnd.
AX/23
AX/22
AX/21
AX/20
AX/19
AX/18
AX/17
AX/16
AX/15
AX/14
AX/13
AX/12
AX/11
AX/10
AX/9
AX/8
AX/7
AX/6
AX/5
AX/4
AX/3
AX/2
AX/1
14
12
10
8
6
4
2
metres
W
P
G

5) Log AX

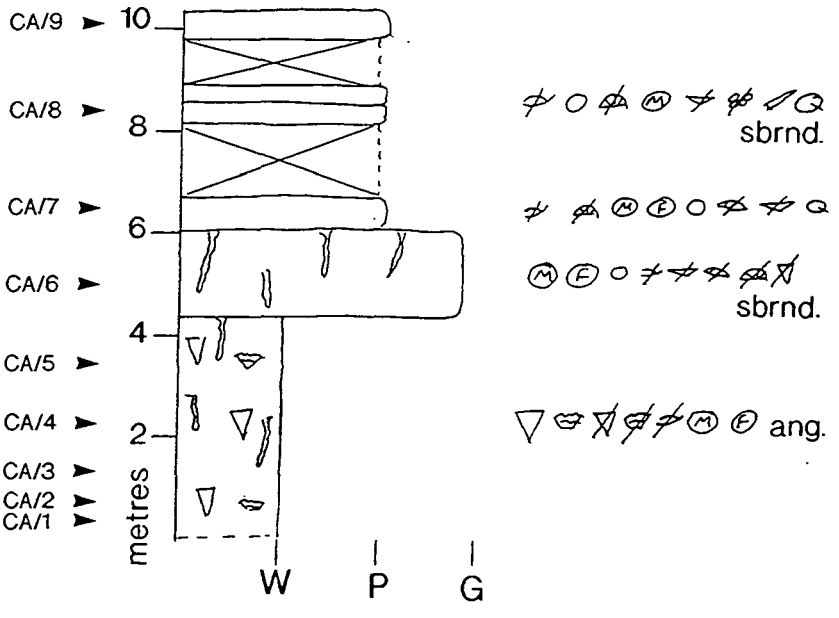
CA/9
CA/8
CA/7
CA/6
CA/5
CA/4
CA/3
CA/2
CA/1
10
8
6
4
2
metres
W
P
G
sbrnd.
sbrnd.
ang.

# 6) Log CA

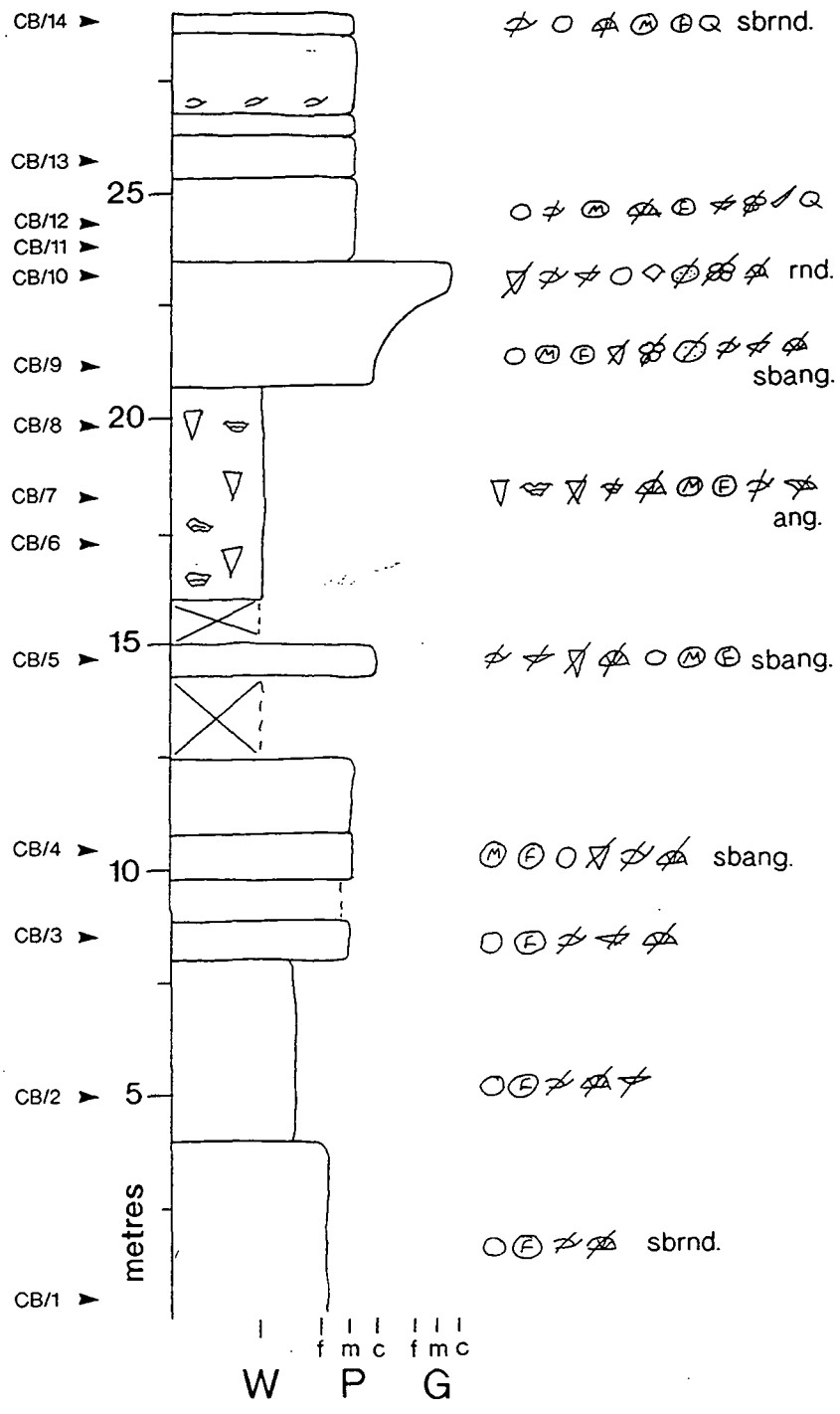
CB/14
CB/13
CB/12
CB/11
CB/10
CB/9
CB/8
CB/7
CB/6
CB/5
CB/4
CB/3
CB/2
CB/1
25
20
15
10
5
metres
sbrnd.
rnd.
sbang.
ang.
sbang.
sbang.
sbrnd.
f m c f m c
W P G

7) Log CB

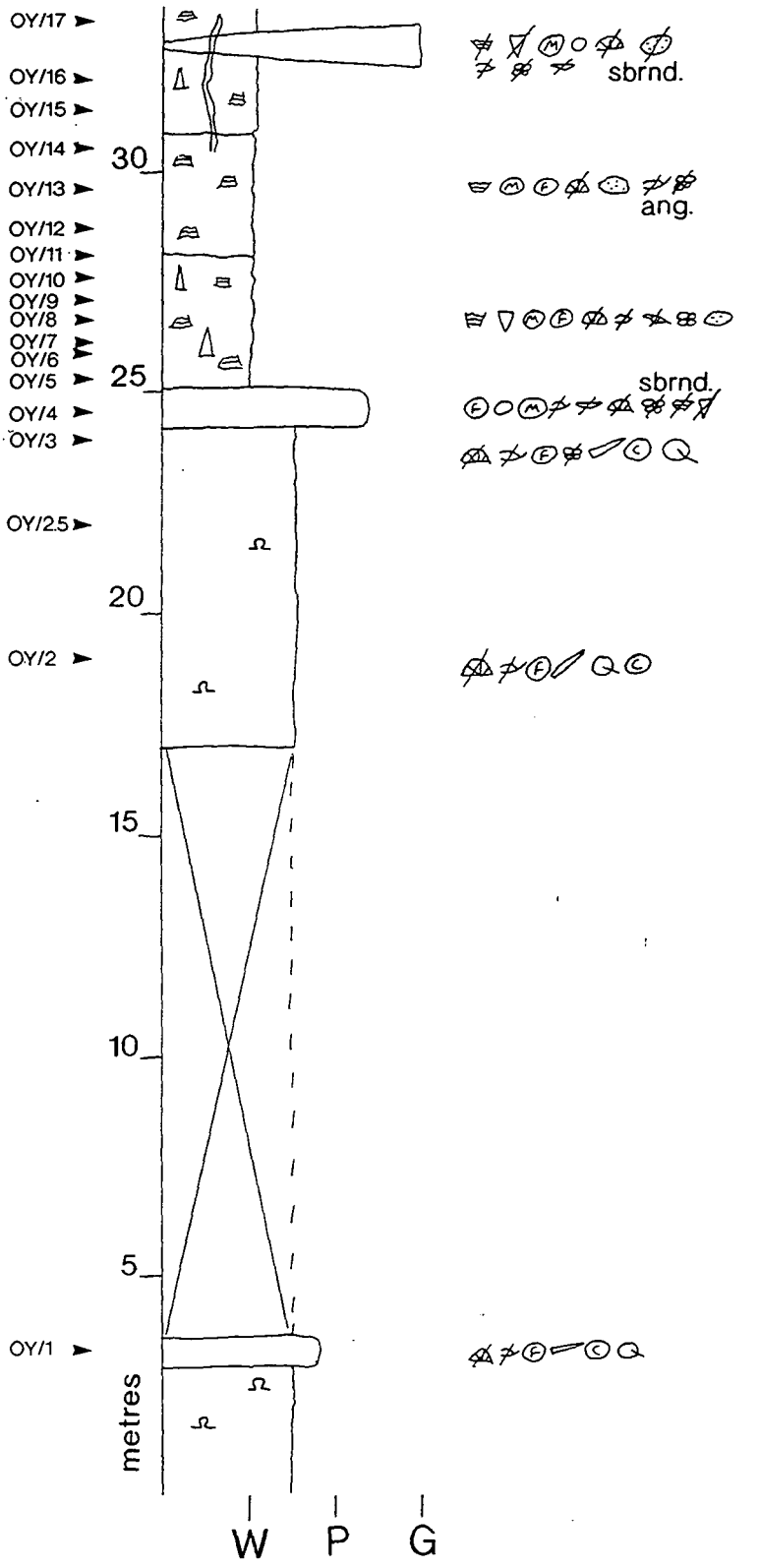
OY/17
OY/16
OY/15
OY/14
OY/13
OY/12
OY/11
OY/10
OY/9
OY/8
OY/7
OY/6
OY/5
OY/4
OY/3
OY/2.5
OY/2
OY/1
30
25
20
15
10
5
metres
sbrnd.
ang.
sbrnd.
W
P
G

8) Log OY

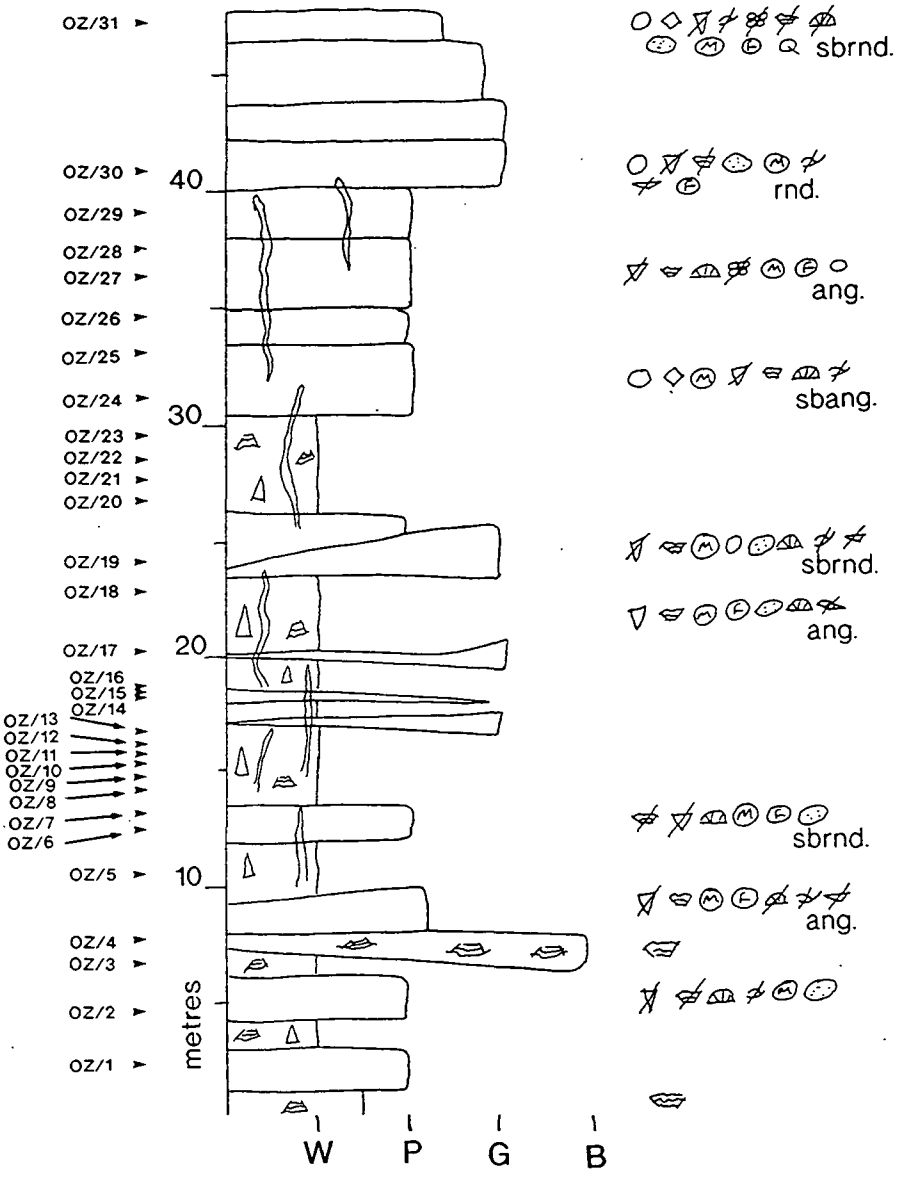
OZ/31
OZ/30
OZ/29
OZ/28
OZ/27
OZ/26
OZ/25
OZ/24
OZ/23
OZ/22
OZ/21
OZ/20
OZ/19
OZ/18
OZ/17
OZ/16
OZ/15
OZ/14
OZ/13
OZ/12
OZ/11
OZ/10
OZ/9
OZ/8
OZ/7
OZ/6
OZ/5
OZ/4
OZ/3
OZ/2
OZ/1
40
30
20
10
metres
W
P
G
B
sbrnd.
rnd.
ang.
sbang.
sbrnd.
ang.
sbrnd.
ang.

9) Log OZ

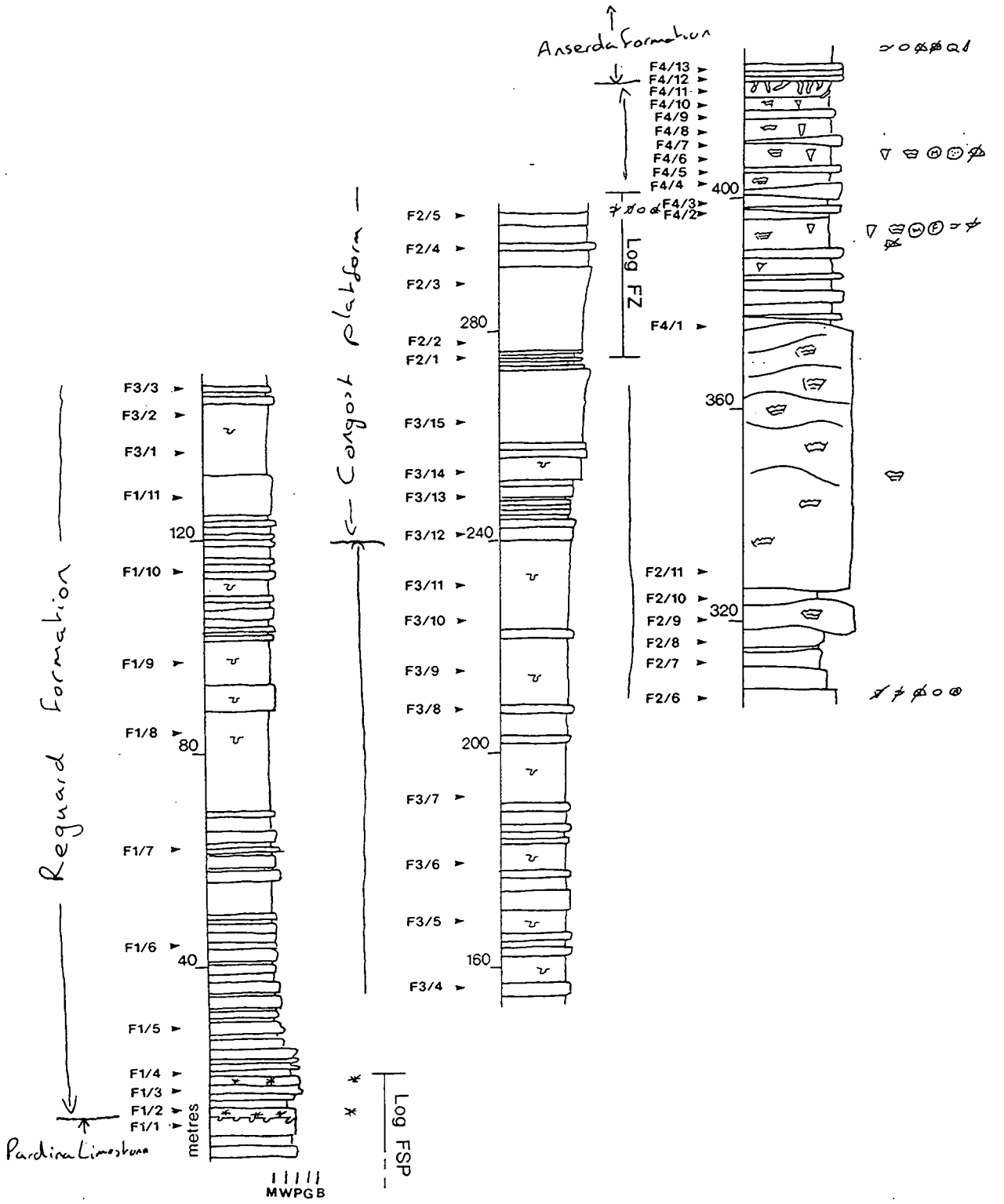


10) Logs F1, F2, F3 and F4

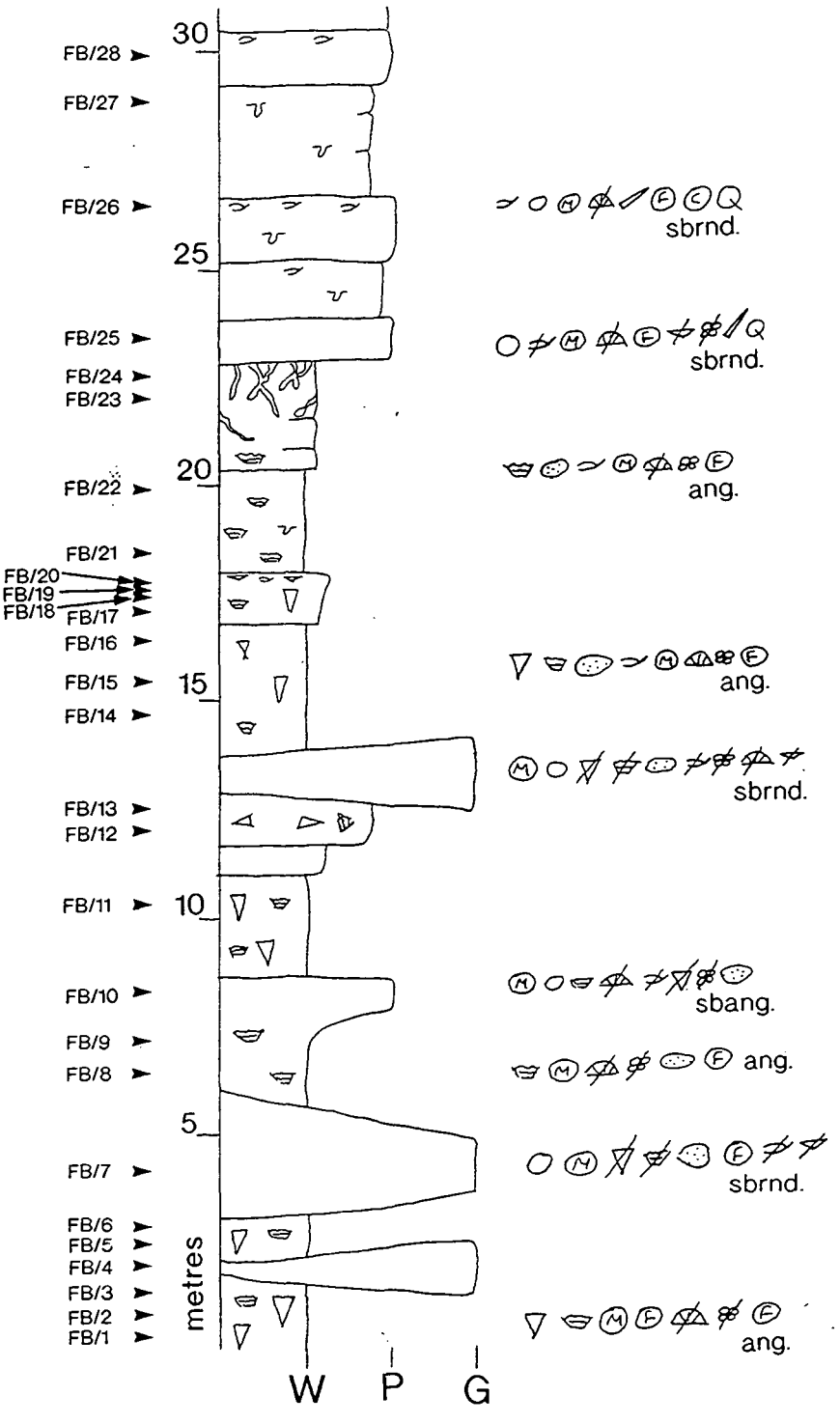
30
25
20
15
10
5
metres
FB/28
FB/27
FB/26
FB/25
FB/24
FB/23
FB/22
FB/21
FB/20
FB/19
FB/18
FB/17
FB/16
FB/15
FB/14
FB/13
FB/12
FB/11
FB/10
FB/9
FB/8
FB/7
FB/6
FB/5
FB/4
FB/3
FB/2
FB/1
sbrnd.
sbrnd.
ang.
ang.
sbrnd.
sbang.
ang.
sbrnd.
ang.
W
P
G

11) Log FB

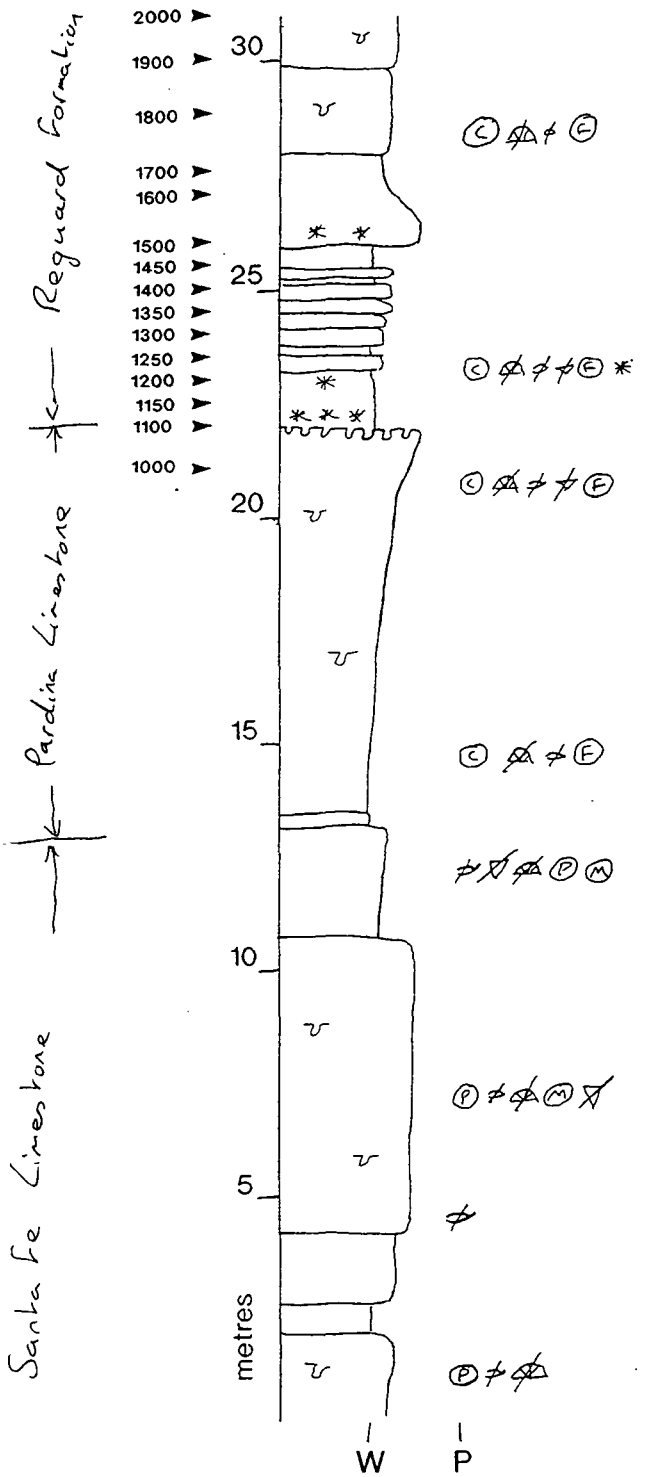
Reguard formation
Pardina Limestone
Santa Fe Limestone
2000
1900
1800
1700
1600
1500
1450
1400
1350
1300
1250
1200
1150
1100
1000
30
25
20
15
10
5
metres
W
P

12) Log FSP

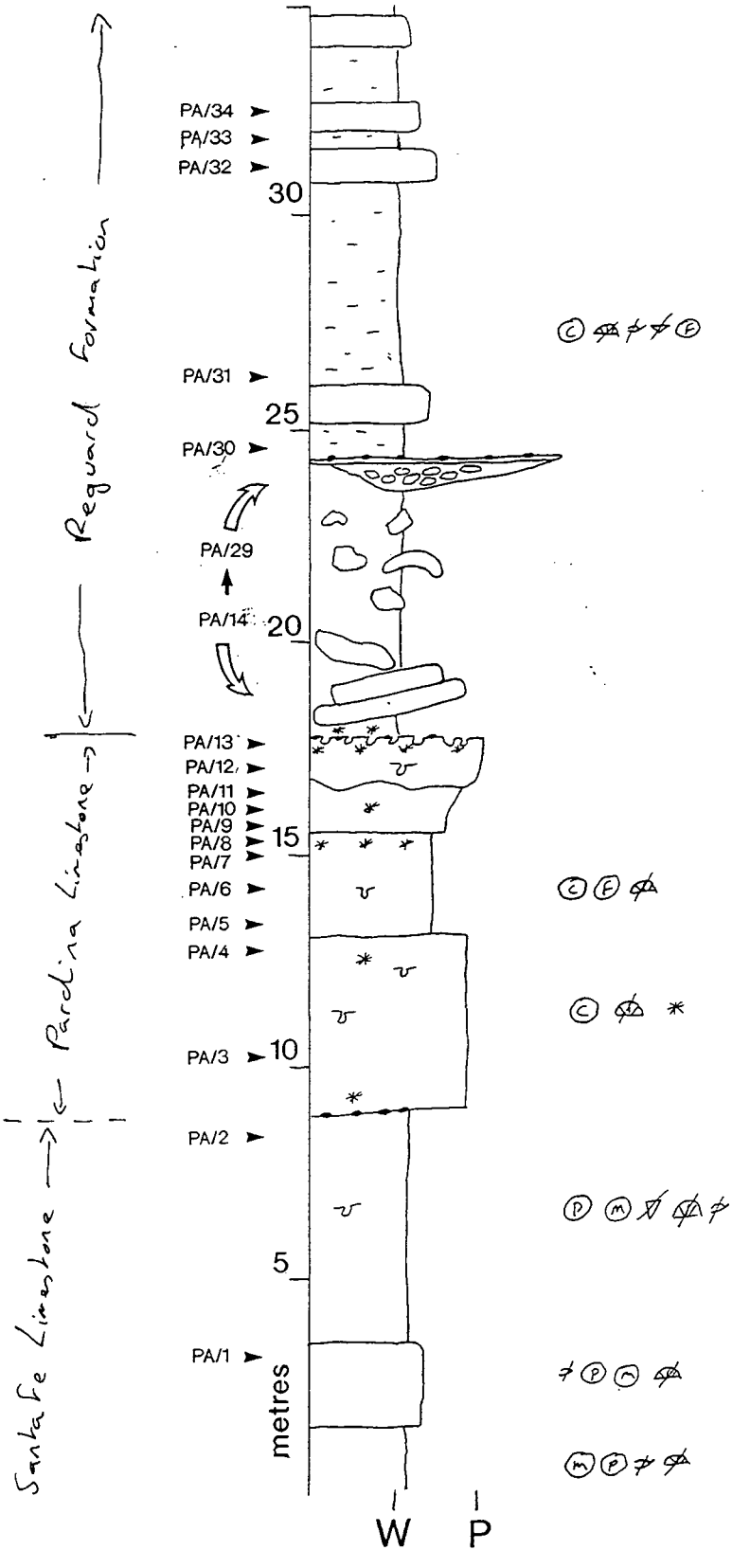
Reguard Formation
Pardina Limestone
Santa Fe Limestone
PA/34
PA/33
PA/32
PA/31
PA/30
PA/29
PA/14
PA/13
PA/12
PA/11
PA/10
PA/9
PA/8
PA/7
PA/6
PA/5
PA/4
PA/3
PA/2
PA/1
30
25
20
15
10
5
metres
W
P

13) Log PA

# Appendix 2
# Stable isotope data

### A.2.3 Stable isotope laboratory

All stable isotope analyses were performed at the NERC Isotope Geosciences Laboratory, in Keyworth, Nottingham.

### A.2.2 Notation

All carbon and oxygen isotopic compositions are reported relative to the PDB international standard in permil ($^{o}/_{oo}$) using the $\delta$ notation:

$$\delta(x) = \{ R(x) - R(std) \} / R(std) \times 1000$$

where $R(x) = {}^{13}C/{}^{12}C$ or ${}^{18}O/{}^{16}O$ sample

and $R(std) = {}^{13}C/{}^{12}C$ or ${}^{18}O/{}^{16}O$ standard (PDB)

Isotopic fractionation between two substances A and B during some physico-chemical process is expressed as a fractionation factor, $\alpha_{A-B}$

$$\alpha_{A-B} = R(A)/R(B) = \{ 1000 + d(A) \} / \{ 1000 + d(B) \}$$

### A.2.3 Sampling method

Isotopic analysis of carbonates was performed after petrographic study. Samples were produced by drilling from sawn and polished faces with a hand-held dentist drill (0.4 - 1.5mm tungsten carbide bit). In some cases it proved useful to view the sawn face through a binocular microscope while drilling.

### A.2.4 Analytical method

Approximately 10mg of the powdered calcite samples were left for over 15 hours to completely react under vacuum with 4ml of anhydrous 100% phosphoric acid in a temperature bath at 25°C.

The evolved carbon dioxide gas was collected and analysed on a VG Isogas SIRA 10 (series 2) mass spectrometer. The samples were generally run in batches of

fifteen unknowns, two duplicates from previous runs and 3 samples of laboratory standards (MCS 13).

Additional correction factors were required to correct for the temperature dependant fractionation for 18O during the acid reaction (see Fairchild et al., 1988). The factor used was:

$$\text{calcite } \alpha^{25} = 1.01025$$

which was applied using:

$$\delta 18O \text{ solid} = (\delta 18O \text{ gas, measured} + 1000) / \alpha - 1000$$

### A.2.5 Estimation of error

A random selection of eighteen MCS-13 (Magcobar Calcite) standards that were run during three visits to NIGL (Keyworth) with batches of calcite unknowns gave:

| | n | mean | S.D |
|---|---|---|---|
| δ13C | 18 | -0.7 | +/- 0.03 |
| δ18O | 18 | -9.18 | +/- 0.06 |

Sample duplicates were run in each batch and the average reproducibilty (based on 12 duplicate samples) is:

$$\delta 13C = +/- 0.10$$
$$\delta 18O = +/- 0.12$$

### A.2.5 Stable isotopic analysis results

The first part of the sample number, identifies the specimen from which it was drilled (These correspond to the sample numbers marked on the graphic logs in appendix 1).

# *Appendix 2*

| SAMPLE | d18O | d13C |
|---|---|---|
| WHOLE ROCK SAMPLES | | |
| AX1 | -5.79 | -0.54 |
| AX20 | -6.82 | -1.58 |
| AX19 | -6.79 | -1.03 |
| AX18 | -6.67 | -0.91 |
| | | |
| RUDIST SAMPLES | | |
| Calcite outer shell | | |
| AX2-T | -4.7 | 0.42 |
| Replaced tabulae + early cement | | |
| AX2-NSS | -7.8 | 0.28 |
| AX13-NSS | -4.12 | 1.67 |
| Equant calcite spar | | |
| AX2-S | -10.79 | -0.93 |
| AX13-S | -8.87 | 0.72 |
| | | |
| DISSOLUTION CAVITIES | | |
| Cement | | |
| AX23-S | -9.86 | -1.37 |
| AX22-S | -10.78 | -1.4 |
| AX0-S | -7.41 | -5.36 |
| AX15 | -9.9 | -3.35 |
| Wall rock | | |
| AX23-M1 | -4.86 | 0.83 |
| AX22-M1 | -6.93 | -1.78 |
| AX0-M1 | -6.24 | -0.59 |
| AX23-M2 | -4.67 | 0.69 |
| AX22-M2 | -5.77 | -2.06 |
| AX0-M2/B | -6.03 | -0.62 |
| AX0-M2/A | -6 | -0.5 |

| SAMPLE | d18O | d13C |
|---|---|---|
| RUDIST SAMPLES | | |
| Calcite outer shell | | |
| CA1-T | -5.03 | -0.33 |
| CA5-T | -3.33 | 1.25 |
| Replaced tabulae | | |
| CA1-NS | -5.91 | 0.33 |
| Inclusion rich early cement | | |
| CA1-IS | -6 | 0.35 |
| CA5-IS | -3.6 | 1.49 |
| Equant calcite spar | | |
| CA1-ES | -4.06 | 1.86 |
| CA5-ES | -5.31 | 1.39 |
| | | |
| DISSOLUTION CAVITY | | |
| Cement | | |
| CA4-S | -7.74 | 1.29 |
| Wall rock | | |
| CA4-M1 | -5.15 | 0.98 |
| CA4-M2 | -5.9 | 0.65 |

| SAMPLE | d18O | d13C |
|---|---|---|
| DISSOLUTION PIPE | | |
| Sediment infill | | |
| OZ16 - I | -4.15 | -1.02 |
| Wall rock | | |
| OZ16 - M1 | -4.22 | -1.73 |
| OZ16 - M2 | -6 | -0.5 |
| OZ16 - M3 | -2.08 | -4.1 |

| SAMPLE | d18O | d13C |
|---|---|---|
| DISSOLUTION CAVITY | | |
| Cement | | |
| CB10-S | -11.26 | 0.63 |
| CB10-S | -11.26 | 0.63 |
| Wall rock | | |
| CB10-M2/B | -5.44 | 1.31 |
| CB10-M2/A | -5.28 | 1.28 |
| CB10-M2/C | -5.44 | 1.31 |

| SAMPLE | d18O | d13C |
|---|---|---|
| RUDIST SAMPLES | | |
| Calcite outer shells | | |
| FA8-T | -3.15 | 2.44 |
| FB2-T | -3.19 | 1.53 |
| FB2-T/2 | -3.32 | 1.48 |
| FB20-T | -3.29 | 1.14 |
| F49X-T | -3.27 | 1.74 |
| FB22-T1 | -3.84 | 2.36 |
| FB22-T2 | -3.63 | 1.85 |
| FFT | -3.12 | 1.29 |
| FB3-T | -3.45 | 1.39 |
| FB5-T | -3.51 | 1.49 |
| FB16-T | -3.96 | 1.31 |
| Replaced tabulae | | |
| FF-N | -4.93 | 0.93 |
| FB5-N | -4.76 | 1.33 |
| FB16-NS | -3.85 | 1.32 |
| FT1-NSA | -5.82 | 0.36 |
| FB21-N | -4.01 | 1.43 |
| F49X-N | -3.74 | 1.57 |
| Cements | | |
| FF-S | -4.8 | 1.07 |
| FB5-S | -5.54 | 1.3 |
| FB16-S | -6 | 1 |
| FB16-S/2 | -5.96 | 1 |
| FT1-SA | -5.68 | 0.95 |
| FT1-SB | -4.97 | 1.32 |
| FT1-SC | -5.03 | 1.16 |
| FB2-S | -5.15 | 1.26 |
| FB2-S/2 | -5.87 | 0.87 |
| FB21-S | -4.8 | 1.22 |
| F49X-S | -6.45 | 0.81 |
| FB2-D | -7.01 | 0.86 |
| | | |
| KARST? | | |
| Cement clasts | | |
| FB23-C | -7.25 | -2.19 |
| FB24-C | -7.39 | -2.36 |
| FB24-C | -7.38 | -2.55 |
| Calcite spar | | |
| FB24-S | -6.76 | -1.44 |
| FB24-S | -6.9 | -1.51 |
| FB23-S | -6.85 | -1.25 |
| | | |
| LATE VEIN | | |
| FB23-V | -8.92 | 0.26 |

| SAMPLE | d18O | d13C |
|---|---|---|
| Whole rock | | |
| SOP-M1 | -3.43 | 1.35 |
| SZ5-M1 | -2.07 | 3.6 |
| SZ7-M1 | -2.21 | 3 |
| SZ9-M1/A | -1.57 | 2.86 |
| SZ9-M1/B | -1.61 | 2.9 |
| SOP-M2 | -2.42 | 1.86 |
| SZ5-M2 | -2.07 | 3.65 |
| SZ9-M2 | -1.35 | 3.03 |
| | | |
| Dissolution cavity infill | | |
| SOP-I | -2.54 | 2.4 |
| SZ5-I | -2.93 | 3.46 |
| | | |
| Calcite spar | | |
| SZ5-S2 | -2.23 | 3.41 |
| SZ5-S1 | -2.18 | 3.74 |
| SZ7-S2 | -4.52 | 1.65 |
| SZ7-S1 | -1.89 | 3.55 |

| SAMPLE | d 18O | d 13C |
|---|---|---|
| WHOLE ROCK | | |
| PA9 | -4.87 | 2.37 |
| PA10 | -4.78 | 2.23 |
| PA11 | -4.54 | 1.46 |
| PA12 | -5.08 | 1.65 |
| PA13 | -3.8 | 2.01 |

# References


**Aissaoui, D.M. 1985.** Botryoidal aragonite and its diagenesis. *Sedimentology*, 32, 345-361.

**Al Aasm, I.S. & Veizer, J. 1986a.** Diagenetic stabilization of aragonite and low-Mg calcite, 1. Trace elements in rudists. *Journal of Sedimentary Petrology*, 56, 138-152

**Al Aasm, I.S. & Veizer, J. 1986a.** Diagenetic stabilization of aragonite and low-Mg calcite, 2. Stable isotopes in rudists. *Journal of Sedimentary Petrology*, 56, 763-770.

**Alexanderson, T. 1972.** Intragranular growth of marine aragonite and Mg-calcite: Evidence of precipitation from supersaturated seawater. *Journal of Sedimentary Petrology*, 42, 441-460.

**Alexanderson, T. 1978.** Destructive diagenesis of carbonate sediments in the Eastern Skagerrak, North Sea: biochemical precipitation in under-saturated waters. *Journal of Sedimentary Petrology*, 44, 7-26.

**Allan, J.R. & Matthews, R.K. 1977.** Carbon and oxygen isotopes as diagenetic and stratigraphic tools: Surface and subsurface data, Barbados and West Indies. *Geology*, 5, 16-20.

**Allan, J.R. & Matthews, R.K. 1982.** Isotope signatures associated with early meteoric diagenesis. *Sedimentology*, 29, 797-817.

**Anderson, T.F. & Arthur, M.A. 1983.** Stable isotopes of oxygen and carbon and their application to sedimentological and paleoenvironmental problems. In: *Stable Isotopes in Sedimentary Geology*. M.A. Arthur & T.F. Anderson (eds). Soc. Econ. Paleo. Min. Short Course #10, Dallas, 1983.

**Arthur, M.A., Dean, W.E. & Pratt, L.M. 1988.** Geochemical and climatic effects of increased marine organic carbon burial at the Cenomanian/Turonian boundary, *Nature*, 335, 714-777.

**Banda, E. & Wickham, S. M. 1986 (eds).** The geological evolution of the Pyrenees. *Tectonophysics*, 129, 380p.

**Barron, E.J. 1986.** Modelling in paleooceanography. *Surveys in Geophysics*, 8, 1-23

**Bathurst, R.G.C. 1975.** *Carbonate sediments and their diagenesis*. Second edition, Elsevier, New York, 658pp.

**Bathurst, R.G.C. 1987.** Diagenetically enhanced bedding in argillaceous platform limestones: stratified cementation and selective compaction. *Sedimentology*, 34, 749-778.

**Berger, W.H. 1968.** Planktonic foraminifera: selective solution and paleoclimate interpretation: *Deep sea research*, 15, 31-43.

**Berger, W.H. 1978.** Deep-sea carbonate: pteropod distribution and the aragonite compensation depth: *Deep sea research*, 25, 447-452.

**Berner, R.A. 1981.** A new geochemical classification of sedimentary environments. *Journal of Sedimentary Petrology*, 51, 359-365.

**Bilotte, M. 1978.** Proposition pour une biozonation des series epicontinentales du Cenomanien Pyrenees. *Geologie Mediterranenne,* 5, 39-46.

**Bilotte, M. & Souquet, P. 1972.** Les biozones des foraminiferes benthiques du Cenomamien Pyreneen. *Comptes Rendus, Academie Science, Paris.*274, 3352-3355.

**Boillot, G. & Capdevila, R. 1977.** The Pyrenees: subduction and collision? *Earth and Planetary Science Letters,* 35, 151-160.

**Bosellini, A. 1984.** Progradation geometries of carbonate platforms: examples from the Triassic of the Dolomites, northern Italy. *Sedimentology* 20, 5-27.

**Bramlette, M.N. 1961.** Pelagic sediments. In: *Oceanography*, M. Sears (ed), American Assoc. for the Advancement of Science, Washington Publication, 67, 345-390.

**Buxton, T.M. & Sibley, D.F. 1981.** Pressure solution features in shallow buried limestone. *Journal of Sedimentary Petrology*, 51, 19-26.

**Calvet, F., Tucker, M.E. & Henton, J.M. 1990.** Middle Triassic carbonate ramp systems in the Catalan Basin, northeast Spain: facies, systems tracts, sequences and controls. In: *Carbonate Platforms,* M.E. Tucker, J.L. Wilson, P.D. Crevello, J.F. Sarg & J.F. Read (eds). Int. Assoc. Sediment. Spec. Publ. 9, 79-108.

**Caus, E. & Gomez-Garrido, A. 1989a.** Correlation of larger benthic and planktonic foraminifera of the Late Cretaceous in the South-Central Pyrenees. In: *Cretaceous of the Western Thethys.* J. Wiedmann (ed). *Proceedings of the 3rd International Cretaceous Symposium.* Tubingen 1987, 231-238.

**Caus, E. & Gomez-Garrido, A. 1989b.** Upper Cretaceous biostratigraphy of the South-Central pyrenees (Lleida, Spain). *Geodinamica Acta*, 3, 221-228.

**Caus, E., Gomez-Garrido, A., Simo, A. & Soriano, K. 1993.** Cenomanian-Turonian platform to basin integrated stratigraphy in the south Pyrenees (Spain). *Cretaceous Research*, 14, 531-551.

**Champ, D.R., Gulens, J. & Jackson, R.E. 1979.** Oxidation - reduction sequences in ground water flow systems. *Canadian Journal of Earth Sciences*, 16, 12-23.

**Choquette P.W. 1971.** Late ferroan dolomite cement, Mississippian carbonates, Illinois Basin, U.S.A. In: Bricker, O.P. (ed). *Carbonate Cements*. Baltimore, The John Hopkins Univ. Press, 339-346.

**Choquette P.W. & James, N.P. 1987**. Diagenesis in limestones, 3. The deep burial environment. *Geoscience Canada*, 14, 3.35.

**Choukroune, P. 1969.** Sur la presence, le style et l'age des tectoniques superposees dans la Cretace nord pyrenean de la region de Lourdes (Hautes Pyrenees). *Bull. Bur. Rech. geol. min. Fr.* 2, 11-20.

**Choukroune, P. 1976a.** Strain patterns in the Pyrenean Chain. *Phil. Trans. R. Soc. London,* 283, 271-280.

**Choukroune, P. 1976b.** Structure et evolution tectonique de la zone Nord-Pyreneenne. *Mem. Soc. Geol. Fr.* 127, 1-116.

**Choukroune, P. & Seguret, M. 1973.** Tectonics of the Pyrenees, role of gravity and compression. In: De Jong, K. H. & Schollen, R. (eds). *Gravity and Tectonics.* Wiley, New York. 141.

**Cook, H.E. 1983.** Ancient Carbonate platform margins, slopes, and basins. In: H.E. Cook, A.C. Hine & H.T. Mullins (eds), *Platform Margins and Deep Water Carbonates,*Soc. Econ. Palaeont. Miner. Short Course No. 12. Tulsa, Oklahoma 5/1-5/189

**Cook, H.E., McDanial, P.N., Mountjoy, E.W. & Pray, L.C. 1972.** Allochthonous carbonate debris flows at Devonian bank ('reef') margins, Alberta Canada. *Bull. Can. Petrol. Geol.* 20, 439-497.

**Czerniakowski, L.A., Lohmann, K.C. & Wilson, J.L. 1984.** Close system marine burial diagenesis: isotopic data from the Austin chalk and its components. *Sedimentology*, 31, 863-877.

**Daignieres, M., Gallart, J., Banda, E. & HIrn, A. 1982.** Implications of the seismic structure for the orogenic evolution of the Pyrenean range. *Earth and Planetary Letters,* 57, 88-100.

**Davies, G.R. 1977.** Former magnesian calcite and aragonite submarine cements in Upper Paleozoic reefs of the Canadian Arctic: a summary. *Geology*, 5, 11-15.

**Davies, R.A. 1983.** Sediment gravity flow deposition on a modern carbonate slope apron: Northern Little Bahama Bank. *Bulletin of the American Association of Petroleum Geologists,* 67, 447.

**Dansgaard, W. 1964.** Stable isotopes in precipitation. *Tellus*, 16, 436-468.

**Deramond, J., Graham, R.H., Hossack, J.R., Baby, P. & Crouzet, G. 1985.** Noveau modele de la chaine des Pyrenees. *C. R. Acad. Sci. Paris,* 303, II, 16, 1213-1216.

**Desrochers, A. & James, N.P. 1988.** Early Paleozoic Surface and Subsurface Paleokarst: Middle Ordovician Carbonates, Mingan Islands, Quebec. In: *Paleokarst.* N.P. James & P.W. Choquette (eds), Springler-Verlag, New York, 183-210.

**Dickson, J.A.D. 1965.** A modified staining technique for carbonates in thin section. *Nature*, 205, 587

**Dickson, J.A.D. 1966.** Carbonate identification and genesis as revealed by staining. *Journal of Sedimentary Petrology*, 36, 491-505.

**Dorobek, S.L. 1987.** Petrography, geochemistry and origin of burial diagenetic facies, Siluro-Devonian Helderberg group (Carbonate rocks), Central Appalachians. *American Association of Petroleum Geologists Bulletin*, 71, #5, 492-514.

**Dunham, R.J. 1962.** Classification of carbonate rocks according to depositional texture. In: W.E Ham (ed), *Classification of carbonate rocks. Am. Assoc. Petrol. Geol. Mem.* 1, 62-84.

**Dunham, R.J. 1969.** Early vadose silt in Townsend mound (reef), New Mexico. In: *Depositional environments in carbonate rocks*, G.M. Friedman (ed), Soc. Econ. Paleontologists and Mineralogists Spec. Publ. 14, 139-181.

**ECORS Pyrenees Team. 1988.** The ECORS deep reflection seismic survey across the Pyrenees. *Nature*.331, 508-511.

**Enos, P. 1986.** Diagenesis of mid-Cretaceous rudist reefs, Valles platform, Mexico. In: *Reef Diagenesis*. J.H. Schroeder & B.H. Purser (eds), Springer-verlag, Berlin, 160-185.

**Enos, P. 1988.** Evolution of pore space in the Poza Rica trend (mid-Cretaceous) Mexico. *Sedimentology*, 35, 287-325.

**Esteban, M. 1974.** Caliche textures and *Microcodium*: *Soc. Geol. Italiana Bull. (supp.)*. 92, 105-125.

**Esteban, M. & Klappa, C.F. 1983.** Subaerial exposure environment. In: *Carbonate Depositional Environments*. P.A. Scholle, D.G. Bebout & C.H. Moore (eds). *American Association of Petroleum Geologists Memoir* 33, 1-54. Tulsa, Oklahoma, U.S.A.

**Fagerstrom, J.A. 1987.** *The Evolution of Reef Communities*. J. Wiley and Sons. New York.

**Farrell, S.G., Williams, G.D., & Atkinson, C.D. 1987.** Constraints on the age of movement of the Montsech and Cotiella thrusts, south central Pyrenees, Spain, *Journal of the Geological Society, London,* 144, 907-914.

**Fischer, A.G. 1981.** Climatic oscillations in the biosphere. In: M.H. Nitecki (ed), *Biotic Crises in Ecological and Evolutionary Time.* Academic Press, New York, N.Y. 103-131.

**Fischer, A.G. 1982.** Long-term climatic oscillations recorded in stratigraphy. In: W.H. Berger & J.C. Crowell (eds), *Climate in Earths History.* National Academic Press, Washington, D.C. 97-104.

**Fischer, A.G. 1984a.** The two Phanerozoic supercycles. In: W.A. Bergren & J.A. van Couvering (eds), *Catastrophies and Earth History* . Princeton Univ. Press, Princeton, N.J. 129-150.

**Fischer, A.G. 1984b.** Biological innovations and the sedimentary record. In: H.D. Holland & A.F. Trendall (eds), *Dahlem Conferenzen 1984.* Springler - Verlag, Berlin, 145-157.

**Fischer, A.G. & Arthur, M.A. 1977.** Secular variations in the pelagic realm. In: Cook, H.E. & Enos, P., (eds), *Deep-water carbonate environments, S.E.P.M. Spec. Publ.*25, 19-50.

**Fischer, M.W. 1984.** *Structural studies in the French Pyrenees. Unpublished* Phd. thesis, University of Wales.

**Folk, R.L. 1965.** Some aspects of recrystallisation in ancient limestones. In: *Dolomitization and Limestone diagenesis.* L.C. Pray & R.C. Murray (eds), Spec. Publ. Soc. Econ. Paleont. Miner. 13, 14-48.

**Fondecave, M. J. 1975.** Essai de biozonation par les foraminiferes pelagiques du Senonien sud-Pyreneen: Description d'une nouvelle espece " *Hedebergella aubertae* n. sp.". *Geologie Mediterraneenne,* 2, 5-10.

**Frank, J.R., Carpenter, A.B. & Oglesby, T.W. 1982.** Cathodoluminescence and composition of calcite cement in the Taum Sauk Limestone (upper Cambrian), Southeast Missouri. *Journal of Sedimentary Petrology,* 52, 631_638.

**Gallemi, J., Martinez, R. & Pons, J.M. 1983.** Coniacian - Maastrichtian of the Tremp area (south central pyrenees). *Newsletter Stratigraphy,* 12, 1-17.

**Garrido-Mejias, A. 1973.** *Estudio geologico y relacion entre tectonica y sedimentacion del Secundario y Terciario de la vertiente meridional pirenaica en su zona central (provinca de Huesca y Lerida).* Unpublished PhD. thesis, University of Grenada, Spain. 395p.

**Ginsburg, R.N. & Schroeder, J.H. 1973.** Growth and submarine fossilization of algal cup reefs, Bermuda. *Sedimentology,* 20, 575-614.

**Given, R.K. & Lohmann, K.C. 1985.** Derivation of original isotopic composition of Permian marine cements. *Journal of Sedimentary Petrology*, 55, 430-439.

**Glover, E.D. & Pray, L.C. 1971.** High-magnesium calcite and aragonite cementation within modern subtidal carbonate cement grains. In: *Carbonate Cements*. O.P. Bricker (ed). Johns Hopkins Press, Baltimore, MD. 180-187.

**Goldhammer, R.K., Lehmann, P.J., Todd, R.G., Wilson, J.L., Ward, W.C. & Johnson, C.R. 1991.** Sequence stratigraphy and cyclostratigraphy of the Mesozoic of the Sierra Madre Oriental, Northeast Mexico, a field guidebook. *Gulf Coast Sect. Soc. Econ. Palaentol. Mineral. Foundation, 86pp.*

**Goldsmith, I.R. & King, P. 1987.** Hydrodynamic modelling of cementation patterns in modern reefs. In: *Diagenesis of sedimentary sequences*. J.D. Marshall (ed), Spec. Publ. Geol. Soc. London, 36, 1-13.

**Gomez-Garrido, A. 1981.** *Foraminiferos planktonicos de La Formation Reguard (Turoniense) en el Valle del Flamicell (Prepirenio de Lerida).* Publications de Geologia, Universitat Autonoma de Barcelona, Spain. No. 16, 48pp.

**Gomez-Garrido, A. 1987.** *Foraminiferos planktonicos del Cretacico superior del Surpirineo central.* Unpubl PhD thesis, Universitat Autonoma de Barcelona, Spain, 184pp.

**Gomez-Garrido, A. 1989.** Biostratigrafia (foraminiferos planktonicos) del Cretacico superior del supirineo central (Espana). *Revista Espanola de Micropaleontologia*, 21, 145-171.

**Grimaud, S., Boillot, G., Collete, B.J., Mauffret, A., Miles, P.R. & Roberts, D.G. 1982.** Western extension of the Iberia-European plate boundary during early Cenozoic (Pyrenean) convergence: A new model. *Marine Geology,* 45, 63-77.

**Gross, M.G. 1964.** Variations in the $^{18}O/^{16}O$ and $^{13}C/^{12}C$ ratios of diageneticaly altered limestones in the Bermuda Islands. *Journal of Geology*, 72, 170-194.

**Grover, G. Jr. & Read, J.F. 1983.** Paleoaquifer and deep burial related cements defined by regional cathodoluminescent patterns, Middle Ordovician carbonates, Virginia. *American Association of Petroleum Geologists*, 67, 1275-1303.

**Hallam, A. 1977.** Secular changes in marine inundation of USSR and North America through the Phanerozoic. *Nature*, 269, 769-772.

**Hallock, P. & Hansen, H.J. 1979.** Depth adaptation in Amphistegina: change in lamellar thickness. *Bull. Geol. Soc. Denmark,* 27, 99-104. Kopenhagen.

**Haq, B.U., Hardenbol, J., & Vail, P.R. 1987.** Chronology of fluctuating sea-levels since the Triassic. *Science,* 235, 1156-1167.

**Haq, B.U., Hardenbol, J. & vail, P.R. 1988.** Mesozoic and Cenozoic chronostratigraphy and cycles of sea-level change. In: *Sea-level changes: an Integrated Approach,* C.K. Wilgus, B.S. Hastings, C.G.St.C. Kendall, H.W. Posamentier, C.A. Ross & J.C. Van-Wagoner (eds). Spec. Publ. Soc. Econ. Palaeont. Mineral. 42, 71-108.

**Harrison, R.S. 1977.** Caliche profiles, indicators of near-surface subaerial diagenesis, Barbados, West Indies: Canadian Petroleum Geol. Bull., 25, 123-173.

**Hays, P.D. & Grossman, E.L. 1991.** Oxygen isotope in meteoric calcite cements as indicators of continental palaeoclimate. *Geology*, 19, 441-444.

**Heckel, P.H. 1983.** Diagenetic model for carbonate rocks in mid-continent Pennsylvanian eustatic cyclothems. *Journal of Sedimentary Petrology*, 53, 733-759.

**Hine, A.C. & Hallock, P. 1991.** Tectonic controls on carbonate platforms of the Nicaraguan Rise, Carribean Sea (abstract). *Dolomieu Conference on Carbonate platforms and Dolomitization, Abstracts*, Ortisei, Italy, September 16-21, p110.

**Hinnov, L.A. & Goldhammer, R.K. 1991.** Spectral analysis of the Middle Triassic Latemar Limestone. *Journal of Sedimentary Petrology,* 61, 1173-1192.

**Hispanoil, 1985.** Unpublished cross section of the South Pyrenean Zone.

**Hudson, J.D. 1962.** Pseudo-pleochroic calcite in recrystalised shell limestones. *Geol. Mag.* 99, 492-500.

**Hudson, J.D. 1977.** Isotopes and limestone lithification. *Journal of the Geological Society of London,* 133, 637-670.

**Hunt. D.W. 1992.** *Application of Sequence Stratigraphic Concepts to the Cretaceous Urgonian Carbonate Platform, Southeast France.* Unpublished PhD thesis, University of Durham.

**Hunt. D.W. & Tucker, M.E. 1993.** Sequence stratigraphy of Carbonate shelves with an example from the mid-Cretaceous (Urgonian) of southeast France. In: *Sequence Stratigraphy and Facies Associations* , H.W. Posamentier, C.P. Summerhayes, B.U. Haq & G.P. Allen. Spec. Publs. Int. Ass. Sediment. 18, 307-341.

**Institut Cartographic de Catalunya. 1990.** *Mapa geologic de Catalunya (1:250,000).*Institut Cartographic de Catalunya, Balmes 209-211, 08006 Barcelona, Catalunya, Spain.

**James, N.P. 1974.** Diagenesis of Sclerectinian corals in the subaerial vadose environment. *Journal of Sedimentary Petrology*, 44, 785-799.

**James, N.P. 1983.** Reefs. In: *Carbonate Depositional Environments,* P.A Scholle, D.G. Bebout & C.H. Moore (eds). Mem. Am. Ass. Petrol. Geol. 33, 345-462.

**James, N.P. 1984.** Reefs. In: *facies models*, R.G. Walker (ed). Geoscience Canada. 229-244. Geological Association of Canada. Toronto.

**James N.P. & Choquette, P.W. 1983.** Diagenesis 6. Limestones - the sea-floor diagenetic environment. *Geoscience Canada*, 10, 162 - 180.

**James N.P. & Choquette, P.W. 1984.** Diagenesis 9. Limestones - the meteoric diagenetic environment. *Geoscience Canada*, 11, 161 - 194.

**James, N.P. & Ginsburg, R.N. 1979.** The seaward margin of Belize barrier and atoll reefs. *Spec. Publ. International Association of Sedimentology*, 3, 191.

**James, N.P., Ginsburg, R.N., Marszalek, D.S. & Choquette, P.W. 1976.** Facies and fabric specificity of early subsea cements in shallow Belize (British Honduras) reefs. *Journal of Sedimentary Petrology*, 46, 523-544.

**James, N.P. & Klappa, C.F. 1983.** Petrogenesis of early Cambrian reef limestones, Labrador, Canada. *Journal of Sedimentary Petrology*, 53, 1051-1096.

**Jenkyns, H.C. 1980.** Cretaceous anoxic events: from continents to oceans. *J. Geol. Soc.* 137, 171-188.

**Kahle, C.F. 1988.** Surface and subsurface paleokarst, Silurian Lockport, and Peebles Dolomites, Western Ohio. In: *Paleokarst.* N.P. James & P.W. Choquette (eds), Springler-Verlag, New York, 229-255.

**Kauffman, E.G. & Johnson, C.C. 1988.** The morphological and ecological evolution of middle and upper Cretaceous reef-building rudistids. *Palaios*, 3 (Reefs Issue), 194-216.

**Kendall, A.C. 1985.** Radiaxial fibrous cements: a reappraisal. In: *Carbonate Cements.* N. Schneidermann & P.M. Harris (eds), Spec. Publ. Soc. Econ. Paleont. Miner. 36, 59-77.

**Kendall, A.C. & Tucker, M.E. 1973.** Radiaxial fibrous calcite: a replacement after acicular carbonate. *Sedimentology*, 20, 365-389.

**Kenter, J.A. 1990.** Carbonate platform flanks: slope angle and sediment fabric. *Sedimentology*, 37, 777-794.

**Kennedy, W.J. & Taylor, J.D. 1968.** Aragonite in rudists. *Proceedings of the Geological Society of London*, 1645, 325-331.

**Kinsman, D.J.J. 1969.** Interpretation of $Sr^{2+}$ concentrations in carbonate minerals and rocks. *Journal of Sedimentary Petrology*, 39, 486-508.

**Kobluk, D.R. & Risk, M.J. 1977.** Micritisation and carbonate grain binding by endolithic algae. *American Association of Petroleum Geologists Bulletin*, 61, 1069-1082.

**Krause, F.F. & Oldershaw, A.E. 1979.** Submarine carbonate breccia beds - a depositional model for two-layer sediment gravity flows from the Sekwi Formation (Lower Cambrian), Mackenzie Mountains, Northwest Territories, Canada. *Can. J. Earth Sci.* 16, 189-199.

**Labaume, P., Mutti, E. & Seguret, M. 1987.** Megaturbidites: A depositional model from the Eocene of the SW-Pyrenean foreland basin, Spain. *Geo-Marine Letters,* 7, 91-101.

**Land, L.S. & Goreau, T.F. 1970.** Submarine lithification of Jamaican reefs. *Journal of Sedimentary Petrology*, 40, 457-462.

**Le Pichon, X., Bonnin, J. & Sibuet, J.C. 1970.** La faille transformante liee a l'ouverture du Golfe de Gascogne. *Comptes Rendus academie de Science de Paris.* 1941-4.

**Liebau, A. 1973.** El Maastrichtiense lagunar (Garumniense) de Isona. *Coloquio Europeo de Micropaleontologia, Espana,* 87-111.

**Lohmann, K.C. 1988.** Geochemical patterns of meteoric diagenetic systems and their application to studies of paleokarst. In: *Paleokarst.* N.P. James & P.W. Choquette (eds), Springler-Verlag, New York, 58-80.

**Lohmann, K.C., & Meyers, W.J. 1977.** Microdolomite inclusions in cloudy prismatic calcites - a proposed criterion for former high magnesian calcites. *Journal of Sedimentary Petrology*, 47, 1078-1088.

**Longman, M.W. 1980.** Carbonate diagenetic textures from nearshore diagenetic environments. *American Association of Petroleum Geologists Bulletin*, 64, 461-487.

**Longstaffe, F.J. 1987.** Stable isotope studies of diagenetic processes. In: A Short Course in Stable Isotope Geochemistry of Low Temperature Fluids. K.T. Kyser (ed), Saskatoon, May, 1987. *Min. Assoc. Canada,* 13, 187-257.

**Loucks, R.G. & Folk, R.L. 1976.** Fan-like rays of former aragonite in Permian Capitan Reef pisolite. *Journal of Sedimentary Petrology*, 46, 483-485.

**Macintyre, I.G., Mountjoy, E.W. & D'Anglejan, B.F. 1968.** An occurrence of submarine cementation of carbonate sediments of the west coast of Barbados, WI. *Journal of Sedimentary Petrology,* 38, 660-664.

**Manabe, S. & Bryan, K. 1985.** $CO_2$ - induced change in a coupled ocean-atmosphere model and its palaeoclimatic implications. *Journal of Geophysical Research*, 90, 11689-11707.

**Manze, U. & Richter, D.K. 1979.** Die Veranderung des $^{13}C/^{12}C$ - Verhaltnisser in seeigelcoronen die der Umwandlung von Mg-Calcit in Calcit unter meteorisch-vadosen Bedingungen. *Neues Jb. Geol. Palaont.* Abh. 158, 334-345.

**Marlowe, J.I. 1971.** Dolomite, phosphorite and carbonate diagenesis on a Carribbean seamount. *Journal of Sedimentary Petrology*, 41, 809 - 827.

**Martinez, R. 1982.** Ammonoideos cretacicos del Prepireneo de la provincia de Llieda. *Publicaciones de Geologia* 17, 1-193.

**Masson, D.G. & Miles, P.R. 1984.** Mesozoic seafloor spreading between Iberia, Europe, and North America. *Marine Geology,* 56, 279-287.

**Mathis, R.L. 1978.** *Carbonate sedimentation and diagenesis of reef and associated shoal-water facies, Sligo Formation (Aptian), Black Lake Field, Natchitoches Parish, Louisiana.* (Unpub. M.S. thesis). Troy, NY, Rensselaer Polytechnic Institute, 214p.

**Mattauer, M. 1968.** Les traits structuraux essentiels de la Chaine Pyreneenne. *Revue de Geographie Physique et de Geologie Dynamique,*10, 3-11.

**May, J.A. & Perkins, R.D. 1979.** Endolithic infestation of carbonate substrates below the sediment -water interface. *Journal of Sedimentary Petrology*, 49, 357-377.

**Mazzullo, S.J. 1980.** Calcite pseodospar replacive of marine acicular aragonite, and implications for aragonite cement diagenesis. *Journal of Sedimentary Petrology*, 50, 409-422.

**Mazzullo, S.J. & Harris, P.M. 1992.** Mesogenetic dissolution: Its role in porosity development in carbonate reservoirs. *American Association of Petroleum Geologists Bulletin*, 76, 607-620.

**McCaig, A.M. 1988.** Deep geology of the Pyrenees. *Nature, 331, 480-481.*

**McIlreath, I.A. & Morrow, D.W. (eds). 1990.** *Diagenesis.* Geosci. Can. Rep. Ser. 4.

**Mey, P.H.W., Nagtegaal, P.J.C., Roberti, K.J. & Hartevelt, J.J.A. 1968.** Lithostratigraphic subdivision of post-Hercynian deposits in the south-central Pyrenees. *Leidse Geologische Mededelingen*, 41, 221-228.

**Meyers, W.J. 1974.** Carbonate cement stratigraphy of the Lake Valley Formation (Mississippian), Sacramento Mountains, New Mexico. *Journal of Sedimentary Petrology*, 44, 837-861.

**Meyers, W.J. 1988.** Paleokarstic features on Mississippian Limestones, New Mexico. In: *Paleokarst.* N.P. James & P.W. Choquette (eds), Springler-Verlag, New York, 306-328.

**Mitchum, R.M. 1977.** Seismic stratigraphy and global changes of sea level, Part 1: glossary of terms used in seismic stratigraphy. In: Payton, C.E. (ed), *Seismic Stratigraphy - Applications to Hydrocarbon Exploration.* American Association of Petroleum geologists Memoir 26, 53-62.

**Moldovanyi, E.V. & Lohmann, K.C. 1984.** Isotopic and petrographic record of phreatic diagenesis: lower Cretaceous Sligo and Cupid formations. *Journal of Sedimentary Petrology*, 54, 972-985.

**Moore, C.H. 1989.** *Carbonate Diagenesis and Porosity.* Elsevier, 338pp.

**Moss, S.J. 1992.** *Burial Diagenesis, Organic Maturation and Tectonic Loading in the French Subalpine Chains, S.E. France.* Unpublished PhD thesis, University of Durham.

**Mountjoy, E.W., Cook, H.E, Pray, L.C. & McDaniel, P.N. 1972.** Allochthonous carbonate debris flows - worldwide indicators of reef complexes, banks or shelf margins. *24th International Geological Congress Montreal Sect.* 6, 172-189.

**Mullins, H.T., Heath, K.C., Van Buren, H.M. & Newton, C.R. 1984.** Anatomy of a modern open-ocean carbonate slope: northern Little Bahama Bank. *Sedimentology,* 31, 141-168.

**Mullins, H.T., Dolan, J., Breen, N., Anderson, B., Gaylord, M., Petruccione, J.L., Wellner, R.W., Melillo, A.J. & Jugens, A.D. 1991.** Carbonate platforms: Response to tectonic processes. *Geology,* 19, 1089-1092.

**Munoz, J.A. 1985.** *Estructura Alpina i Herciniana a la vora sud de la zona axial del Pirineu oriental.* Unpublished PhD. thesis, Universidad de Barcelona.

**Mussman, W.J., Montanez, I.P. & Read, J.F. 1988.** Ordovician Knox Paleokarst Unconformity, Appalachians. In: *Paleokarst.* N.P. James & P.W. Choquette (eds), Springler-Verlag, New York, 211-228

**Mullins, H.T. & Cook, H.E. 1986.** Carbonate apron models: alternatives to the submarine fan model for palaeoenvironmental analysis and hydrocarbon exploration. *Sedimentary Geology,* 48, 37-79.

**Nagtegaal, P.J.C. 1972.** Depositional history and clay minerals of the Upper Cretaceous basin in the south-central Pyrenees, Spain. *Leidse Geologische Mededelingen*, 47, 251-275.

**Niemann, J.C. & Read, J.F. 1988.** Regional cementation from unconformity-recharged aquifer and burial fluids, Mississippian Newman Limestone, Kentucky. *Journal of Sedimentary Petrology*, 58, 688-705.

**Odin, G.S. & Matter, A. 1981.** De glauconiarium origine. *Sedimentology*, 28, 611-641.

**Owen, H.G. 1983.** *Atlas of Continental Displacement, 200 million years to present,* Cambridge University Press, Cambridge.

**Palmer, T.J., Hudson, J.D., & Wilson, M.A. 1988.** Paleoecological evidence for early aragonite dissolution in ancient calcite seas. *Nature*, 335, 809-810.

**Pedersen, T.F. & Calvert, S.E. 1990.** Anoxia vs. productivity: what controls the formation of organic-carbon-rich sediments and sedimentary rocks? *The American Association of Petroleum Geologists Bulletin,* 74, no. 4, 454-466.

**Pettijohn, F.J., Potter, P.E. & Siever, R. 1973.** *Sand and Sandstone,* Springer, Berlin.

**Pingitore, N.E. 1976.** Vadose and phreatic diagenesis: processes, products and their recognition in corals. *Journal of Sedimentary Petrology,* 46, 785-1006.

**Popp, B.N., Anderson, T.F. & Sandberg, P.A. 1986.** textural, elemental and isotopic variations among constituents in Middle Devonian limestones. *Journal of Sedimentary Petrology,* 56, 715-727.

**Prezbindowski, D.R. 1985,** Burial cementation - is it important? A case study, Stuart City trend, south-central Texas. In: *Carbonate Cements.* Schneidermann, N. & Harris, P.M. (eds), *Spec. Publi. Soc. Econ. Paleont. Miner.* 36, 241-264.

**Puigdefabregas, C & Souquet, P. 1986.** Tecto-sedimentary cycles and depositional sequences of the Mesozoic and Tertiary from the Pyrenees. *Tectonophysics,* 129, 173-203.

**Pye, K. 1983.** Red beds. In: A.S. Goudie (ed). *Chemical sediments and geomorphology: precipitates and residua in the near-surface environment.* London, Academic Press. 227-263.

**Radke, B.M. & Mathis, R.L. 1980.** On the formation and occurrence of saddle dolomite. *Journal of Sedimentary Geology,* 50, 1149-1168.

**Read, J.F. & Goldhammer, R.K. 1988.** Use of Fischer plots to define third-order sea-level curves in Ordovician peritidal cyclic carbonates, Appalachians. *Geology,* 16, 895-899.

**Reiss, Z. & Hottinger, L. 1984.** The Gulf of Aqaba. *Ecological studies,* 50, 1-345. Springer, Berlin.

**Rosell, J. 1967.** estudio geologico del sector del Pireneo comprendido entre los rios Segre y Noguera Ribagorzana (provincia de Lerida). *Pireneos,* 21, 9-214.

**Rosell, j., Obrador, A. & Pons, J.M. 1972.** Significacion sedimentologia y palaeogeographica del nivel arcilloso con corales del Senomiense superior de los alrededores de Pobla de Segur (provincia de Lerida). *Acta Geologica Hispanica,* 7, 7-11.

**Ross, D.G. 1989.** *Facies analysis and diagenesis of Tethyan Rudist Reef Complexes.* Unpub. PhD. thesis, University of Wales, 206pp.

**Ross, D.G. 1991.** Botryoidal high-Mg calcite marine cements from the Upper Cretaceous of the Mediterranean region. *Journal of Sedimentary Petrology*, 61, 349-353.

**Ross, D.G. & Skelton, P.W. 1993.** Rudist formations of the Cretaceous: a palaeoecological, sedimentological and stratigraphic review. In: *Sedimentology Review /1*, V.P. Wright (ed). Blackwell Scientific Publications, Oxford. 73-91.

**Sandberg, P.A. 1983.** An oscillating trend in Phanerozoic non-skeletal carbonate mineralogy. *Nature*, 305, 19-22.

**Sandberg, P.A. 1985.** Aragonite cements and their occurrence in ancient limestones. In: *Carbonate Cements*, Schneidermann, N. & Harris, P.M. (eds). *Soc. Econ. Paleont. Miner. Spec. Publ.* 36.

**Sandberg, P.A., Schneidermann, N. & Wunder, S.J. 1973.** Aragonitic ultrastructural relics in calcite-replaced Pleistocene skeletons: *Nature Physical Science*, 245, 133-134.

**Sarg, J.F. 1988.** Carbonate sequence stratigraphy. In: *Sea-level changes: an Integrated Approach,* C.K. Wilgus, B.S. Hastings, C.G.St.C. Kendall, H.W. Posamentier, C.A. Ross & J.C. Van-Wagoner (eds). Spec. Publ. Soc. Econ. Palaeont. Mineral. 42, 155-181.

**Scholle, P.A. & Arthur, M.A. 1980.** carbon-isotope fluctuations in Cretaceous pelagic limestones: potential stratigraphic and petroleum exploration tool. *Bulletin of the American Association of Petroleum Geologists*, 64, 67-87.

**Schlager, W. 1991.** Depositional bias and environmental change - important factors in sequence stratigraphy. *Sedimentary Geology,* 70, 109-130.

**Schlager, W. 1992.** *Sedimentology and sequence stratigraphy of reefs and carbonate platforms, a short course.* Educ. Course Note Ser. Am. Assoc. Pet. Geol., 34, 71pp.

**Schlager, W. 1993.** Accommodation and supply - a dual control on stratigraphic sequences. *Sedimentary Geology,* 86, 111-136.

**Schlager, W. 1994.** Reefs and carbonate platforms in sequence stratigraphy. In: *High Resolution Sequence Stratigraphy: Innovations and Applications* (Conference Abstract Volume). S.D. Johnson (ed). Dept. of Earth Sciences, University of Liverpool, Liverpool. 143-153.

**Schlanger, S.O., Arthur, M.A., Jenkyns, H.C. & Scholle, P.A. 1987.** The Cenomanian - Turonian oceanic anoxic event, 1; Stratigraphy and distribution of organic-carbon-rich beds and the marine $^{13}C$ excursion. In: Brooks, J. & Fleet, A.J., (eds), *Marine and petroleum source rocks, Geological Society of London Special Publication*26, 371-399.

**Schlanger, S.O. & Jenkyns, H.C. 1976.** Cretaceous oceanic anoxic events; causes and consequences, *Geologie en Mijnbouw,* 55, 179-184.

**Scholle, P.A. & Arthur, M.A. 1980.** Carbon isotope fluctuations in Cretaceous pelagic limestones: potential stratigraphic and petroleum exploration tool. *The American Association of Petroleum Geologists Bulletin,* 64, no. 1, 67-87.

**Schroeder, J.H. 1972.** Fabrics and sequences of submarine carbonate cements in Holocene Bermuda cup reefs. *Geol. Rundsch.* 61, 708-730.

**Scott, R.W. 1988.** Evolution of Late Jurassic and Early Cretaceous reef biotas. *Palaois*, 3, 184-193

**Scott, R.W., Fernandez-Mendiola, P.A., Gili, E. & Simo, A. 1990.** Persistence of coral-rudist reefs into the Late Cretaceous. *Palaios*, 5, 98-110.

**Seguret, M. & Daignieres, M. 1986.** Crustal balanced cross-sections of the Pyrenees; discussion. *Tectonophysics,* 129, 303-318.

**Sellwood, B.W. 1978.** Shallow-water carbonate environments. In: H.G. Reading (Ed), *Sedimentary Environments and Facies.* Blackwell Oxford. 259-312.

**Shinn, E.A. 1969**. Submarine lithification of Holocene carbonate sediments in the Persian Gulf. *Sedimentology*, 12, 109-144.

**Simo, A. 1986.** Carbonate platform depositional sequences, Upper Cretaceous, south central Pyrenees (Spain). *Tectonophysics* 129, 205-231.

**Simo, A. 1989.** Upper Cretaceous platform-to-basin depositional sequence development, Tremp basin, south-central Pyrenees, Spain. In: *Controls on Carbonate Platform and Basin Development, SEPM Spec. Publ.*44, 365-377.

**Simo, A. 1992.** *Upper Cretaceous Depositional Sequences, Sequence Boundaries and Carbonate Platforms, South-Central Pyrenees.* Conference Field Guidebook, La Seu, Spain, August 31 - September 3, 1992. Dept. of Geology and Geophysics, University of Wisconsin, Madison.

**Simo, A. 1993.** Cretaceous Carbonate platforms and Stratigraphic sequences, South-Central pyrenees, Spain. In: Simo, A. & Scott, R.W. (eds), *Cretaceous Carbonate Platforms. Am. Ass. Petrol. Geol. Studies in Geology.* 325- 341.

**Simo, A. & Puigdefabregas, C. 1985.** Transition from shelf to basin on an active slope, Upper Cretaceous Tremp area, southern Pyrenees. In: *6th European Regional Meeting Excursion Guide-book.* Mila, M.D. & Rosell, J. (eds). 63-108.

**Skelton, P.W. 1978.** The evolution of functional design in rudists (Hippuritacea) and its taxonomic implications. *Phil. Trans. R. Soc. Lond. B.* 284, 305-318.

**Skelton, P.W. 1985.** Preadaptation and evolutionary innovation in rudist bivalves. *Spec. Paps. Paleont.*, 33, 159-173.

**Skelton, P.W. & Gili, E. 1991.** Palaeoecological classification of rudist morphotypes. In: *First International Conference on Rudists, October 1988, Proceedings.* M. Sladic-Trifunovic (ed). 71-86. Serbian Geological Society: Belgrade.

**Smart, P.L., Palmer, R.J., Whitaker, F. & Wright, V.P. 1988.** Neptunian dykes and fissure fills: An overview and account of some modern examples. In: *Paleokarst.* N.P. James & P.W. Choquette (eds), Springler-Verlag, New York, 149-166.

**Sole-Sugranes, L. 1978.** Gravity and compressive nappes in the central southern Pyrenees (Spain). *Am. J. Sci.* 278, 609-657.

**Soriano, K. 1992.** *Stratigraphy and Sedimentology of Cenomanian-Santonian Carbonate Platforms, Montsec Mountains, South-Central Pyrenees, Spain.* Unpubl. Msc. thesis, University of Wisconsin-Madison, 201pp.

**Souquet, P. 1967.** *Le Cretace superieur sud-Pyrenees en Catalogne, Aragon et Navarra.* Unpubl. PhD. thesis, University of Toulouse, 329pp.

**Souquet, P. 1984.** Les cycles majeurs du Cretace de la paleomarge iberique dans les Pyrenees. *Strata,* Universite de Toulouse III, France. 1, 47-70.

**Takahashi, T. 1975.** Carbonate chemistry of seawater and the calcite compensation depths in the oceans: In: W.V. Sliter, A.W.H. Be & W.H. Berger (eds). *Cusman Foundation Foraminifera Resources Special Publication*, 13, 11-26.

**Towe, K.M. & Hembleben, K.M. 1976.** Diagenesis of magnesian calcite: evidence from miliolacean foraminifera. *Geology*, 4, 337-339.

**Tucker, M.E. 1991.** *Sedimentary Petrology: an Introduction to the Origin of Sedimentary rocks.* Blackwell Scientific Publications, Oxford.

**Tucker, M.E. 1993.** Carbonate diagenesis and sequence stratigraphy. In: *Sedimentology Review /1*, V.P. Wright (ed). Blackwell Scientific Publications, Oxford. 51-72.

**Tucker, M.E. & Bathurst, R.G.C. (eds). 1990.** *Carbonate diagenesis.* Reprint Series, Int. Ass. Sedimentologists, 1.

**Tucker, M.E. & Hollingworth, N.T.J. 1986.** The Upper Permian Reef Complex (EZ) of North East England: Diagenesis in a marine to evaporitic setting. In: *Reef Diagenesis.* J.H. Schroeder & B.H. Purser (eds), 270-290. Sringler-Verlag, Berlin.

**Tucker, M.E. & Wright, V.P. 1990.** *Carbonate Sedimentology.* Blackwell Scientific Publications, Oxford.

**Tucker, M.E., Calvet, F. & Hunt, D. 1993.** Sequence stratigraphy of carbonate ramps: systems tracts, models and application to the Muschelkalk carbonate platforms of eastern Spain. In: *Sequence Stratigraphy and Facies Associations,* H.W. Posamentier, C.P. Summerhayes, B.U. Haq & G.P. Allen. Spec. Publs. Int. Ass. Sediment. 18, 397-415.

**Turner, F.T. & Patrick Jnr, W.H. 1968.** Chemical changes in water-logged soils as a result of oxygen depletion: *Ninth International Congress of Soil Science Transactions*, 4, 53-65.

**Vail, P.R., Mitchum, R.M. & Thompson, S. 1977.** Seismic stratigraphy and global changes of sea-level, part 4: global cycles of relative change of sea-level. *Mem. Ass. Petrol. Geol.* 26, 83-97.

**Van-Hoorn, B. 1970.** Sedimentology and palaeogeography of an Upper Cretaceous turbidite basin in the south-central Pyrenees, Spain. *Leidse Geologische Mededelingen,* 45, 73-154.

**Van-Wagoner, J.C., Posamentier, H.W., Mitchum, R.M.Jr., Sarg, J.F., Loutit, T.S. & Hardenbol, J. 1988.** The key definitions of sequence stratigraphy. In: Wilgus, C.K., Hastings, B.S., Kendall, G.St.C., Posamentier, H.W., Ross, C.A. & Van-Wagoner, J.C. (eds). *Sea-Level Changes: An Integrated Approach.* Special Publication of the Society of Economic Palaeontologists and Mineralogists, 42, 39-45.

**Van-Wagoner, J.C., Mitchum, R.M., Campion, K.M. & Rahmanian, V.D. 1990.** *Siliciclastic Sequence Stratigraphy in Well Logs, Cores and Outcrops.* Am. Assoc. Petrol. Geol. Methods in exploration Series, No 7, pp. 45.

**Veevers, J.J. 1990.** Tectonic - climatic supercycle in the billion-year plate-tectonic eon: Permian Pangean icehouse alternates with Cretaceous dispersed-continents greenhouse. *Sedimentary Geology*, 68, 1-16.

**Vera, J.A., Ruiz-Ortiz, P.A., Garcia-Hernandez, & Molina, J.M. 1988.** Paleokarst and related pelagic sediments in the Jurassic of the Subbetic Zone, Southern Spain. In: *Paleokarst.* N.P. James & P.W. Choquette (eds), Springler-Verlag, New York, 364-384.

**Verges, J. & Munoz, J.A. 1990.** Thrust sequences in the southern central Pyrenees. *Bull. Soc. Geol. France,* VI, No 2, 265-271.

**Walls, R.A., Mountjoy, E.W. & Fritz, P. 1979.** Isotopic composition and diagenetic history of carbonate cements in Devonian Golden Spike reef, Alberta, Canada. *Bull. Geol. Soc. Am.* 90, 963-982.

**Wilkinson, B.H., Smith, A.L. & Lohmann, K.C. 1985.** Sparry calcite marine cement in Upper Jurrasic limestones of southeastern Wyoming. In: *Carbonate Cements.* Schneidermann, N. & Harris, P.M. (eds), Spec. Publi. Soc. Econ. Paleont. Miner. 36, 169-184.

**Williams, G.D. 1985.** Thrust tectonics in the south-central Pyrenees. *Journal of Structural Geology.* 7, 11-17.

**Williams, G.D. & Fischer, M.W. 1984.** A balanced cross section across the Pyrenean orogenic belt. *Tectonics,* 3, 773-780.

**Wilson, J.L. 1975.** *Carbonate Facies in Geological History,* pp471. Springer-Verlag, Berlin.

**Wilson, J.L., Wilkinson, B.H., Lohmann, K.C. & Hurley, N.F. 1983.** *New ideas and methods for exploration for carbonate reservoirs - a short course.* Dallas Geological Society, American Association of Petroleum Geologists Annual meeting.

**Winland, H.D. 1969**, Stability of calcium carbonate polymorphs in warm, shallow seawater. *Journal of Sedimentary Petrology*, 39, 1579-1587.

**Woo, K.S. 1986.** *Isotopic-textural-chemical studies of mid-Cretaceous limestones: implications for carbonate diagenesis and palaeoceanography.* Unpubl. phD thesis, University of Illinois at Urbana-Champaign.

**Woronick, R.E. & Land, L.S. 1985**. Late burial diagenesis, Lower Cretaceous Pearsall and lower Glen Rose formations, South Texas. In: *Carbonate Cements.* Schneidermann, N. & Harris, P.M. (eds), Spec. Publi. Soc. Econ. Paleont. Miner. 36, 265-275.

**Wright, V.P. 1988.** Palaeokarsts and palaeosols as indicators of palaeoclimate and porosity evolution: A case study from the Carboniferous of South Wales. In: *Paleokarst.* N.P. James & P.W. Choquette (eds), Springler-Verlag, New York, 329-341.

**Yurtsever, Y., & Gat, J.R. 1981.** Atmospheric waters. In: J.R. Gat & R. Gonfiantini (eds), *Stable isotope hydrology: Deuterium and oxygen-18 in the water cycle*: Vienna, International Atomic Energy Agency, 103-142.